Application of Mineral Magnetic Measurements as a Pollution Proxy for Urban Road Deposited Sediment.

CHRISTOPHER JAMES CROSBY
BSc (Hons) (University of Wolverhampton)

A thesis submitted in partial fulfilment of the
requirements of the University of Wolverhampton
for the degree of Doctor of Philosophy

September 2012

This work or any part thereof has not previously been presented in any form to the University or to any other body whether for the purposes of assessment, publication or for any other purpose (unless previously indicated). Save for any express acknowledgements, references and/or bibliographies cited in the work, I confirm that the intellectual content of the work is the result of my own efforts and of no other person.

Signature

Date 10/ 09 /2012

Abstract

Application of mineral magnetic measurements as a pollution proxy for urban road deposited sediment

Road Deposited Sediment (RDS) is an important pathway of pollution material in the urban environment. Traditional particulate matter (PM) monitoring methods are typically expensive and time consuming. To date, urban sediment studies have not fully explored the application of mineral magnetic technologies as an alternative to characterise RDS or, perhaps more importantly, their use as particle size proxy. Therefore, this study addresses these issues by determining the extent of any linkages between magnetic properties and the physio-chemical concentrations of RDS. Investigations have focussed on a spatial temporal study (2008-10) of RDS from the City of Wolverhampton (n = 546) and a similar 'snap-shot' study of eight selected town and cities across the UK (n = 306), plus a comparison investigation linked to regional monitoring of air sampling units (ASU) (n = 208). A suite of analytical approaches, namely mineral magnetism, laser diffraction, X-Ray Fluorescence spectroscopy (XRF), Scanning Electron Microscopy (SEM) and Loss on Ignition (LOI), were employed to characterize sample properties. Data interrogation identified mainly weak correlations exist between most mineral magnetic parameters and particle size classes (i.e. sand, silt and clay) and respiratory health-related size classes (i.e. PM_{10}, $PM_{2.5}$ and $PM_{1.0}$). The few strongest correlations (p <0.001) were found between mineral magnetic concentration and <PM_{10} parameters. In Wolverhampton this occurred for samples collected during the spring months (March and May), indicating possible seasonal influences on RDS dynamics and sources. Elsewhere in the UK, and at ASU stations, results revealed mainly limited or insignificant (p >0.05) correlations exist between mineral magnetic parameters and particle size. However, for some locations (most notably, London and Scunthorpe), results exhibit signatures perceived to be associated with environmental factors. Detailed multivariate Factor Analysis plots and Geographical Information System (GIS) images have been used to explore these findings further. These illustrate RDS properties of road types (arterial and residential) display significantly different characteristics, with raised mineral magnetic concentrations for arterial roads, compared to lesser concentrations for residential roads, which corresponds to traffic flow data. This is supported by SEM analyses that reveal elevated concentrations of iron oxide spheres in samples collected from arterial roads, which are indicative of inputs from anthropogenic combustion sources. Contextualising these findings within the framework of existing knowledge, a conceptual approach has been presented that explores factors (i.e. sampling area, topography, land use, sediment source and potential mixing), which influence the reliability of using mineral magnetic techniques a particle size proxy. This demonstrates that any increase in the complexity of these factors (sampling area dynamics) can be used to predict the likelihood of being able to employ mineral magnetic measurements as a proxy. To surmise the work overall, despite mineral magnetic technologies offering an inexpensive and rapid means of analysing RDS, its use as a proxy measure for particulate matter appears to be limited by a series of site-related factors but the technique seems to offer valuable insights for pollution source studies.

Acknowledgements

This research has been part-funded by the University of Wolverhampton, to whom I am most grateful for this opportunity. I would like to thank all of my supervisory team; Dr David Searle, Dr Jamal Khatib, and Professor Annie Worsley for their expert advice, help and guidance. Special thanks go to Dr Colin Booth and Professor Mike Fullen who's belief in me, support and advice has been greatly appreciated. I also thank everyone who provided me with technical support during this research, especially David Townrow for hours of XRF analysis, David Luckhurst for imparting his knowledge of GIS, and Barbara for tutoring me through the hours of SEM analysis. Thanks also go to Keith Jones for his mineral magnetism expertise and Andy Black for allowing me use of laboratory equipment. Thanks to Patricia Osborne and Lulu van Greuning for allowing me to use the school office as my own.

I gratefully acknowledge Professor Roy Harrison and Aleina Stark of University of Birmingham for allowing me to use their laboratory and equipment. Thanks to Dr Tom Dijkstra and Professor Neil Dixon of Loughborough University for their patience help and support.

A debt of thanks goes to my family who has supported me through my academic career, Elizabeth and Antony Crosby who have shown invaluable support over the last seven years, my sister Caroline who put me up for a year of my study and during the time gave birth to my nephews Lennon and Harry. My extended furry family Tilly and Evie for keeping me otherwise occupied when I was supposed to be working. Mike Freebury for introducing me to new avenues of research and Jill for making Sundays worthwhile and feeding me excessive amounts of dinner, trifle and cake.

Thanks go out to my good friends and colleagues, Mozz Baker for introducing me to new and challenging work opportunities, Peter Harris, Danen Appasamy, Mark Duffield and Martin, Cheryl and Hayden for being good friends.

Finally extra special gratitude goes to the love of my life, Emma Louise Sandy Isla was has been the greatest support in the final stages of my work. I owe Emma a great debt as she has put up with moody behaviour, strops and my ever reluctant shopping face. This work is dedicated to Emma and my daughter Amélie Isla for whom I am striving to provide a better future.

To all I have not mentioned, I thank you. Each has contributed towards making my research possible and I thank you all.

CONTENTS

List of Figures

Chapter 1

Chapter 2

Chapter 3

Chapter 4

Chapter 5

Chapter 6

List of Tables

Chapter 1

Chapter 2

Chapter 3

Chapter 4

Chapter 5

Chapter 6

For Emma and Amélie.

List of Abbreviations

AAS	Automatic Absorption Spectrometry
AQEG	Air Quality Expert Group
AQMA	Air Quality Management Area
ARM	Anhysteretic Remanent Magnetization
ASU	Air Sampling Unit
AURN	Automatic Urban and Rural Network
CBD	Central Business District
COMEAP	Committee on Medical Effects of Air pollution
DEFRA	Department of the Environment, Food and Rural Affairs
GIS	Geographical Information System
ICP-MS	Inductively Coupled Plasma Mass Spectrometry
LOI	Loss on Ignition
MD	Multidomain
OSGB	Ordnance Survey Great Britain
PAH	Polycyclic aromatic hydrocarbons
PM	Particulate Matter
PS	Particle size
PTFE	Polytetrafluoroethylene
RDS	Road Deposited Sediment
SEM	Scanning Electron Microscopy
SIRM	Saturation Isothermal Remanent Magnetization
SP	Superparamagnetic
SSD	Single-Stable-Domain
SW	Steel works
TEOM	Tapered Element Oscillating Microbalance
TSP	Total Suspended Particles
XRF	X-Ray Fluorescence

CO	Carbon Monoxide
CO_2	Carbon Dioxide
Fe_2O_3	Hematite
Fe_3O_4	Magnetite
H_2O	Water
N_2	Nitrogen
NH_3	Ammonia
NO_x	Nitrogen Dioxide
SiO_2	Silicon Dioxide (Quartz)
SO_2	Sulphur Dioxide

Al	Aluminium
Ca	Calcium
Cd	Cadmium
Cu	Copper
Cr	Chromium
Fe	Iron
K	Potassium
Mn	Manganese
Mg	Magnesium
Ni	Nickel
Pb	Lead
S	Sulphur
Ti	Titanium
Zn	Zinc

Chapter 1
Introduction, aims and objectives

1.1 Overview

Road Deposited Sediment (RDS) is an important pathway of pollution material in the urban environment, acting as a sink for vehicle exhaust, weathered material, soil and as a source of atmospheric particulate matter (PM) (Perry and Taylor, 2007). There is growing interest in the study of PM because of its potential acute and chronic human health implications (Harrison *et al*., 2004; COMEAP, 2010; DEFRA, 2012). PM emissions are monitored in areas of concern, but traditional monitoring methods are static, expensive and time consuming (AQEG, 2005). Therefore, this study investigates the use of a rapid and inexpensive magnetic method to determine PM and geochemical concentrations in RDS.

1.2 Particulate Matter

Particulate matter has long been cause for concern to the air quality management community, because of its wide-ranging effects. These include health problems (Dockery *et al.,* 1993; Seaton *et al.,* 1995; COMEAP, 2010; DEFRA, 2012), impacts on crops and soils (Chameides *et al*., 1999; Mitra *et al*., 2002; Luo *et al*., 2011), effects on visibility (Jacobson, 1997; Chen and Xie, 2012), buildings and water bodies (Peters *et al.,* 2002; González and Aristizábal, 2012), atmospheric heat transfer rates and the formation of precipitation (Ricci *et al*., 1996).

Airborne particulate matter is made up of a collection of solid and/or liquid materials of various sizes that range from a few nanometres in diameter to ~100 μm, originating from both anthropogenic and natural sources. Particulate material is classified by size. PM_{10} identifies particles <10 μm diameter; similarly, $PM_{2.5}$ describes the concentration of particles <2.5 μm diameter. An older, but still useful method, measures blackness of particulate matter and is termed black smoke. Particulate matter consists of primary and secondary components (Table 1.1). Primary components are released directly from source into the atmosphere, and secondary are formed in the atmosphere by chemical reactions. Primary and secondary particles with linkages to sources are shown in Table 1.1. Primary sources of particulate matter can be divided into natural and anthropogenic sources. Natural sources include wind-blown soil, sea spray, plant pollen and spores. Anthropogenic sources are highly varied and include motor vehicle emissions, road dust re-suspension and industrial emissions (Table 1.2).

1.3 Particle size

Atmospheric particles vary greatly in size. For example, pollen can be <10 μm, clay particles in soil are <2 μm, tobacco smoke is <0.01 μm, and smog (primarily resulting from automobile combustion) <0.001 μm. The particle size distribution of total suspended particles (TSP) is trimodal, including coarse particles (comminution mode), fine particles (accumulation mode) and ultrafine (nucleation mode) particles (Table 1.3).

Table 1.1 Components of particulate matter. Primary and secondary particles with corresponding source

Primary Particles	Sources
Sodium chloride	Sea salt.
Elemental carbon	Black carbon (soot) is formed during high temperature combustion of fossil fuels, such as coal, natural gas and oil (diesel and petrol), and biomass fuels, such as wood chips.
Trace metals	These metals are present at very low concentrations and include lead, cadmium, nickel, chromium, zinc and manganese. They are generated by metallurgical processes, such as steel making, or by impurities found in or additives mixed into fuels used by industry. Metals in particles are also derived from mechanical abrasion processes, e.g. during vehicle motion and break and tyre wear.
Mineral components	These minerals are found in coarse dusts from quarrying, construction and demolition work and from wind-driven dusts. They include aluminium, silicon, iron and calcium.
Secondary Particles	**Sources**
Sulphate	Formed by the oxidation of sulphur dioxide (SO_2) in the atmosphere to form sulphuric acid, this can react with ammonia (NH_3) to give ammonium sulphate.
Nitrate	Formed by the oxidation of nitrogen oxides (NOx – which consists of nitric oxide (nitrogen monoxide, NO) and nitrogen dioxide (NO_2) in the atmosphere) to form nitric acid, which can react with NH_3 to give ammonium nitrate. Also present as sodium nitrate.
Water	Some components of aerosols, such as ammonium sulphates and ammonium nitrates, take up water from the atmosphere.
Primary and Secondary Components	**Sources**
Organic Carbon	Primary organic carbon comes from traffic or industrial combustion sources. Secondary organic carbon comes from the oxidation of volatile organic compounds (VOCs). There may be several hundred individual components. Some of these trace organic compounds, such as certain polycyclic aromatic hydrocarbons, are highly toxic.

Table 1.2 Typical sources and composition of PM_{10} divided into particle diameter ranges (Source: Harrison *et al*., 1997; Cyrys *et al.,* 2003; D'Alessandro *et al*., 2003)

PM Classification	Composition	Examples of source
PM_{10}	Minerals	Soil, road dust, industrial dust
	Trace Metals	Soil, oil and coal combustion
Coarse particles	Organic Carbon	Tyre rubber and asphalt wear
(2.5 µm–10 µm)	Bioaerosols	Animals, plant, fungi, bacteria
	Aqueous droplets	Fogs, water sprays
	Associated gases	Ammonia, sulphur dioxide (SO_2), hydrogen sulphide (H_2S), carbon dioxide (CO_2)
$PM_{2.5}$	Minerals	Oil, road dust, industrial dust
	Trace metals	Oil and coal combustion, machinery wear, industrial processes (e.g. smelting, welding)
Fine (<2.5 µm)	Carbonaceous	Wildfires, liquid fuel, soild fuel and waste combustion, cooking, engine exhaust, tyre wear
	Sulphates and nitrates	Volcanoes, oceans, oxidation of SO_2 and nitrogen oxides (NO_x), fires, engine exhaust
	Ammonium compounds	Reactions of ammonia produced by animals, sewage, fertilizers and engine exhaust
	Bioaerosols	Viruses and bacteria
	Associated gases	Formaldehyde, SO_2, NO_x, ozone (O_3), carbon monoxide (CO)
$PM_{0.1}$	Trace metals	Incombustible constituents of fuel
	Organics	Condensation of volatile emissions from complex plants, microbes, fuel combustion
Ultrafine	Carbon	Fuel combustion
(<0.1 µm)	Miscellaneous	Gas-to-particle conversion reactions

Table 1.3 Particle size distribution of Total Suspended Particles (TSP)

Total (TSP)	Total amount of airborne particles (TSP) is defined as the part of the dust which can be suspended in the air for a longer period of time (Figure 1.1), and are particles with, aerodynamic diameter <75-100 µm. Particles above this size are named 'dust downfall' because they will sediment relatively rapidly (i.e close to the source). The TSP was defined by the design of the high volume sampler (Wilson and Suh, 1997).
Respirable **100 µm**	PM_{10} represents the standard measure for respirable (thoracic) particles used to describe ambient air particulates. It is the mass of particles having a 50% cut-off for particles with an aerodynamic diameter of 100 µm. Respirable dust is airborne PM which can penetrate to the gas-exchange region in the lungs (alveoli). In occupational settings it is defined as $PM_{4.0}$ which is the mass of particles present in the air having a 50% cut-off for particles with an aerodynamic >4 µm. Particles <4 µm impact onto the surface of the upper respiratory tract and cannot reach the lungs. It is usually meant PM_{10} when ambient airborne particles is referred to, since this is the fraction for which limit values are set in connection to requirements for ambient air quality. Approximately 9-10% of TSP is <10 µm (Wilson and Suh, 1997; Chen *et al.,* 2007).
Coarse $PM_{10-2.5}$	The coarse part, $PM_{10-2.5}$, contains mainly mechanically-generated and emission particles (Schwartz *et al*., 1996). According to Wilson and Suh (1997) *"fine and coarse particles are separate classes of pollutants and should be measured separately in research*". Some authors describe particles >1 µm as course e.g. (Wilson and Suh, 1997; Claiborn *et al*., 2000).
Fine $PM_{2.5}$	The fine mode $PM_{2.5}$ is formed mainly by chemical reactions predominantly from combustion processes, nucleation, and condensation of gases and coagulation of smaller particles, and is the mass of particles having a 50% cut-off for particles with an aerodynamic diameter of 2.5 µm. These particles are very numerous and represent large surface areas compared to mass. Fine particles produced by combustion processes are usually <1 µm. Schwartz *et al*. (1996) and Claiborn *et al*. (2000), therefore, proposed that the cut point be 1 µm to avoid bias during wind-blown dust storms.
Ultrafine $PM_{0.1}$	Ultrafine particles ($PM_{0.1}$) are particles <0.1 µm. The number of particles and total surface area are large compared to mass. Ultrafine particles are mainly produced by combustion processes and the probability for production of ultrafine particles by road abrasion is very low (Dybing *et al*., 2005). The atmospheric lifetime of these particles in high concentrations is very short. Concentrations observed in urban air can be a few hours (Katsouyanni *et al*., 2005). This makes exposure assessment for them more demanding than for accumulation mode particles.
Nanoparticles $PM_{0.001}$	Nanoparticles ($PM_{0.001}$) are particles <0.001 µm (= 1 nm), and they are generated mostly from combustion processes (road traffic). Some of these particles are likely to originate from rubber in tyres (Dahl *et al*., 2006). Humans inhale airborne particulate matter while breathing. An adult breathes ~10 000 litres of air every day, and air quality is therefore important for human health. Figure 1.2 illustrates inhalability of particles as a function of particle size, ~75% of 10 µm particles can be inhaled, and ~90% of particles 2.5 µm are inhalable.

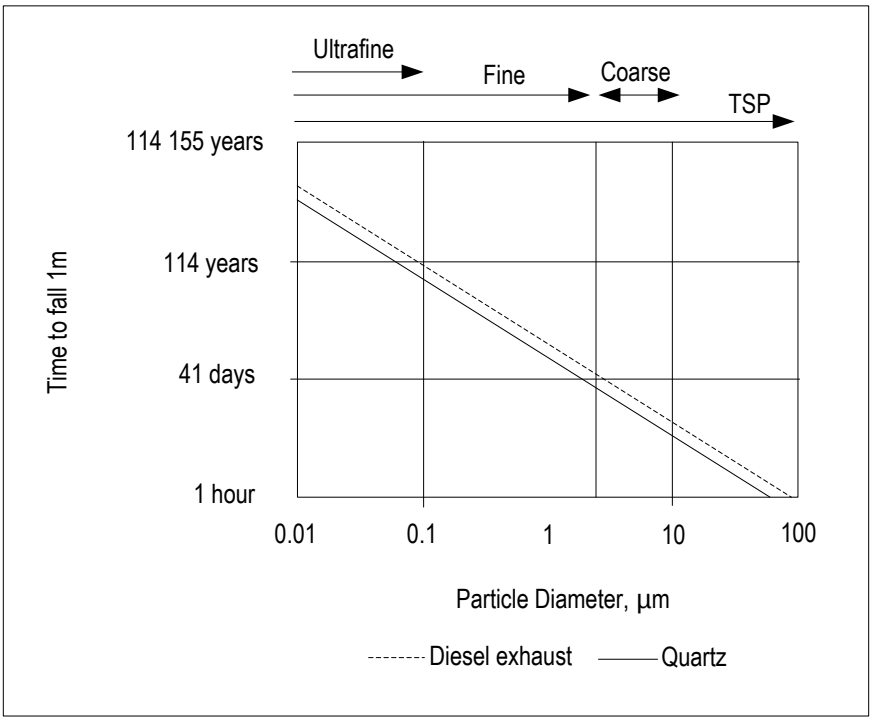

Figure 1.1 Calculated time for particles to fall 1 m in stagnant air as a function of size and origin (Source: Corn *et al.,* 1971).

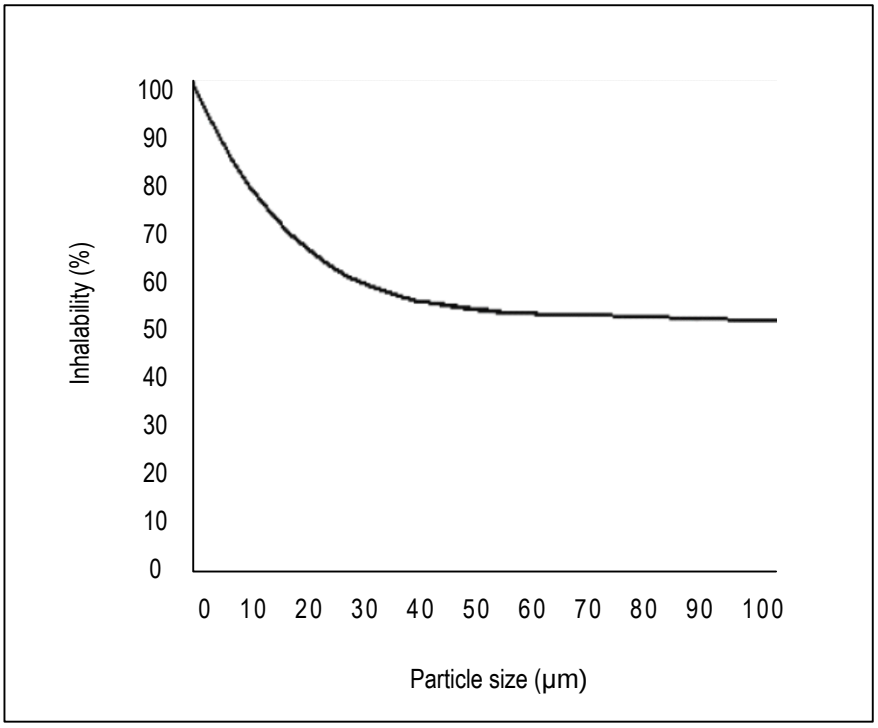

Figure 1.2 Inhalability as a function of particle size, illustrating the smaller particle size, the greater chance of inhalation (Schwartz *et al*., 2004).

In general, particle diameter implies a diameter of a sphere, but for non-spherical particles, there is no unique diameter. According to Matsuyama and Yamamoto (2004) a certain basis will be defined and on that basis some reading relating to particle size will be measured. Particle size is often defined by the aerodynamic diameter, which is determined by the actual particle size, the particle density, and an aerodynamic shape factor. The aerodynamic diameter is a theoretical diameter to a spherical particle with density 1 g/cm^3, which will have the same falling velocity in air as the real particle (Stein *et al*., 1969; DeCarlo *et al*., 2004). It is somewhat different from the geometric diameter; different densities give different aerodynamic diameters of particles which are alike geometrically. For comparison of deposition probabilities for particles with various sizes, shapes and densities, the aerodynamic diameter is used (Skaug, 2001). Airborne particles are defined based on their size as PM (Skaug, 2001; Schwartz *et al*., 2004).

1.4 Particle shape

The particle shape is an important factor with regard to particle motion and deposition probabilities. It is often assumed that the particles are spherical, but ambient air particles are seldom so. Urban particles have large daily variations in the frequency of occurrence of different particle shapes (Stein *et al*., 1969). Three different but related properties determine particle shape: form, roundness and surface texture. Particle form is the overall shape of particles, typically defined in terms of the relative lengths of the longest, shortest and intermediate axes. Particles can be cubic, spherical, elliptical, elongated, flat, tubular, platy or needle shaped (Dodds, 2003). The global shape or form of a particle is determined during formation, and is later affected by weathering.

Weathering mechanisms are related to mineral cleavage. Weathering changes roundness and roughness. Roundness or angularity is a measure of the large-scale smoothness of particles, while surface texture defines local roughness features (Barrett, 1980). Particle roughness is environmentally determined, as specific surface textures are characteristic of specific environments (Dodds, 2003). Fourier analysis is often used for defining particle shape, since it captures the shape of a particle at many different scales.

Freshly crushed mineral particles are more angular with a rougher surface texture and usually flakier and more elongated compared with particles which have been eroded for some considerable time. The roundness of rock particles normally increases through abrasion, and can change greatly without much effect on form (Barrett, 1980). The hardness, micro-cracks and structure of minerals will influence the particle shape after crushing. The fracture strength and the specific fracture energy of most minerals increase with the decrease of their size in the range of ~10 μm to 120 mm. However, <10 μm, the fracture strength decreases with decreasing particle size (Ryu and Saito, 1991). More energy is required to break particles into smaller units, which establishes a lower limit of 1 μm for coarse particles (mechanically generated) (Wilson and Suh, 1997).

1.5 Particles in the atmosphere

The behaviour of particles in the atmosphere is determined largely by their physical properties, which strongly depend on particle size. Figure 1.3 shows in schematic form, the typical size distribution of airborne particles. Sizes range over several orders of magnitude. The smallest, freshly nucleated particles are only 1–2 nm in diameter and contain only tens of molecules. At the other extreme, particles may be ≤100 μm in diameter, particles as large as this rapidly settle out from the air. Once aerosol is suspended in the atmosphere it is altered, removed or destroyed. It cannot stay in the atmosphere indefinitely, and average lifetimes are in the order of a few days to one week. The lifetime of any particular particle depends on its size and location. Larger aerosol settle out of the atmosphere very quickly under gravity, and some surfaces are more efficient at capturing aerosols than others.

i. Nucleation

Nucleation mode particles occur within <50 nm and are newly formed particles by means of homogeneous nucleation in the atmosphere or by nucleation processes that occur within the emissions from high temperature sources. These lead to the emission of primary nucleation mode particles. Harrison and Jones (1995) described the smallest particles, <10 nm, as the nucleation mode and the particles falling between 10-50 nm as the Aitken mode. The nucleation mode in urban areas often contains comparatively few particles. Very close to local sources significant numbers may be found, but in urban areas there is generally adequate supply of species to rapidly condense onto small aerosols, moving them into the accumulation mode. Further accumulation mode concentrations tend to be very high, so that available precursor gases will condense onto those particles without the need to nucleate fresh particles, in most circumstances.

ii. Coagulation

Coagulation is the sticking together of two particles which collide and coalesce together. It is the result of particles coming into contact due to Brownian diffusion or some force (electrostatic, phoretic effects). Contact does not necessarily lead to coagulation, but must happen as a pre-requisite. This happens more quickly for nucleation mode particles (Aitken mode) with large aerosols than for coagulation of two nucleation mode particles (Seinfeld and Pandis, 1998). Coagulation is also enhanced in shearing or turbulent flows, as these induce relatively rapid particle motion.

iii. Accumulation / Condensation mode

Growth of nucleation mode particles, primarily by vapour condensation but also as a result of coagulation processes, leads to the formation of accumulation mode particles. These particles are typically between 50 nm and 1 μm. Such particles are too large to be subject to rapid Brownian motion and too small to settle from the air rapidly under gravity. Their further growth is inhibited because they do not coagulate rapidly as fine and coarse particles. There are also diffusion barriers to their growth by condensation.

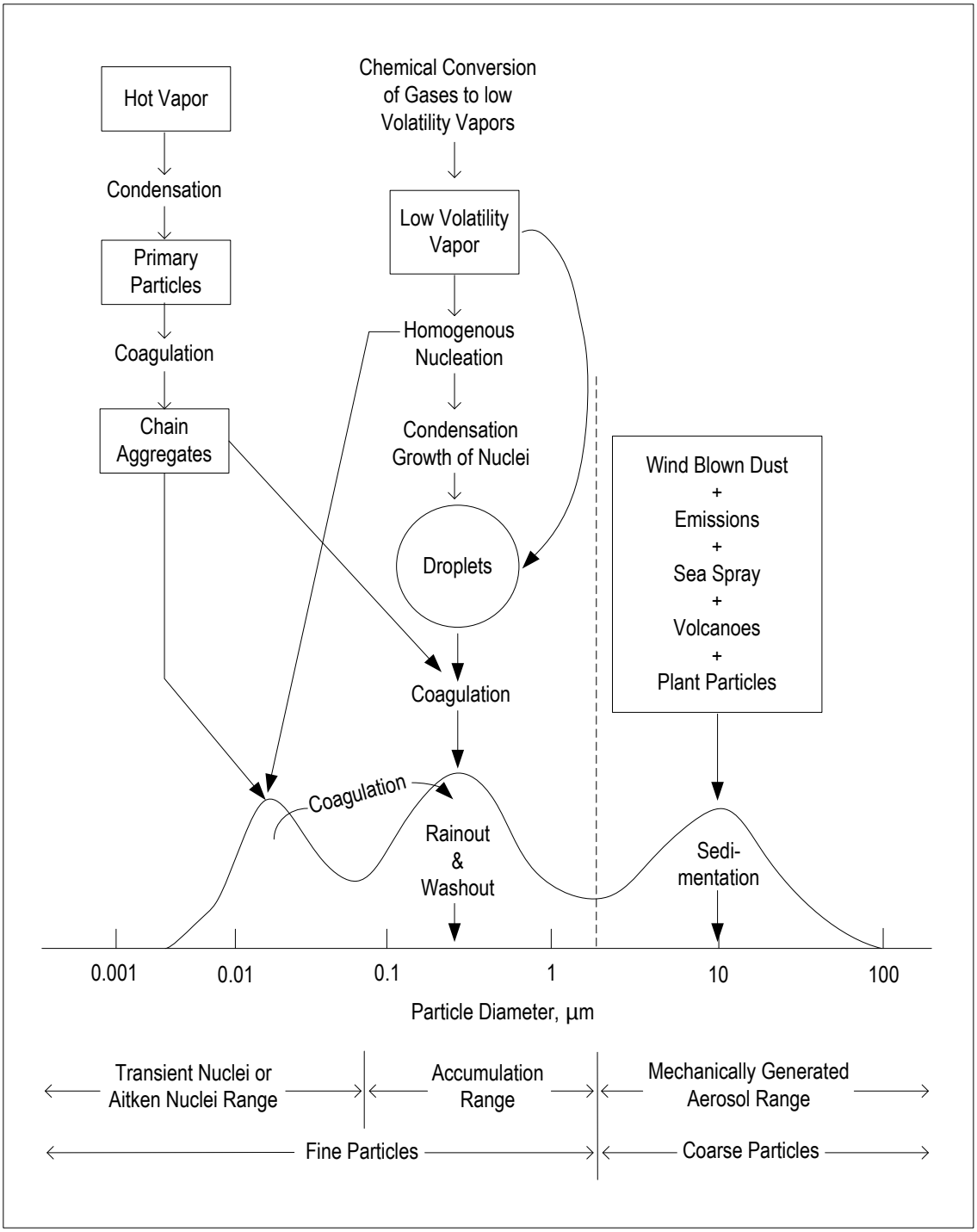

Figure. 1.3 The behaviour of particles in the atmosphere with the typical size distribution of airborne particles (Source: AQEG, 2005).

Particulate size, emission source, meteorological and topographical conditions influence the ambient concentrations, transport and deposition of PM (Wu *et al*., 2006). Due to greater settling velocities PM >10 µm are effectively removed from the atmosphere under gravity and therefore deposit close to source (~10 km) (Alloway and Ayres, 1997; Morwaska and Zhang, 2002; Phalen, 2002; AQEG, 2005; Zheng *et al*., 2010). Although airborne particulates can also be removed via wet deposition (Alloway and Ayres, 1997), finer PMs (<10 µm) remain suspended in the atmosphere for longer periods (days to months) and, therefore, can be transported great distances from source (hundreds to thousands of km) (Phalen, 2002; Harrison, 2004; AQEG, 2005). Particles <1 µm are even less effectively removed from the atmosphere and have longer residency times and are therefore subject to long-range (trans-boundary) transport (ApSimon *et al.,* 2001). Coarse particles tend to be mechanically generated, but are composed of materials such as tyre dust, sea salt and certain dust. Fine particles (accumulation and nucleation mode) tend to be produced either directly from combustion sources, or by gas to particle conversion involving reaction products of sulphates, nitrates, ammonium and organics.

The falling velocity of particles is important for evaluating the retention time of particles in air. According to Stokes Law the falling velocity (v_{Stokes}) in stagnant air for a spherical particle is shown and explained (Eq 1.1). The estimated time for particles to fall 1m is shown in Figure 1.1. The result from the calculation shows that the ultrafine and fine fractions of the dust take much longer to fall and settle, even in stagnant air. However, in urban areas the air is usually turbulent and suspension time of particles can be longer. Table 1.4 links particle size with deposition, time and potential health impacts.

Climatic and seasonal conditions are important for the amount of atmospheric dust. When pavements are wet, dust is bound by water. Harrison *et al*. (1997) found differences between PM concentrations and adjacent seasons. In winter months $PM_{2.5}$ comprised ~80% of PM_{10} and was strongly correlated with NO_x indicating the importance of road traffic as a source. In summer months, fine particles ($PM_{1.0}$-$PM_{2.5}$) account for ~50% of PM_{10} and the influence of re-suspended surface dusts and soils and of secondary particulate matter was evident. Other processes influence particle counts, such as rain and melting water from ice and snow can flow onto the pavement binding dust and reducing particle counts. Dry pavements increase dust raised by vehicles and dispersed in the air more easily. Salt has a similar effect as water, and is often used as a dust binding measure to prevent high dust concentrations. The hygroscopic properties of salt contribute to keeping pavements wet. However, salting can lead to wear of pavement surfaces and an enhanced need for cleaning, since moist pavements are worn 2-6 times faster than dry pavements (Harrison *et al*., 2004).

VStokes = d2g (pparticle – pair) / η (air)

Where:

d = diameter of the particle (µm)

g = gravitational constant (9.80665 m/s^2)

ρ = density (µg)

η = viscosity (18.6 µPa s for air)

Stoke's Law can be used to estimate the time needed by particles of different size to fall 1 m. The following particle densities are employed:

ρparticle = 2.65 g/cm^3 for quartz (Hinds, 1999).

ρparticle = 1.1-1.2 g/cm^3 for diesel exhaust particles (Virtanen *et al,* 2002).

ρair = 0.0012 g/cm^3 for air (Hinds, 1999).

Eq. 1.1 Stokes Law equation of the falling velocity in stagnant air for a spherical particle (Hinds, 1999; Virtanen *et al,* 2002).

Table 1.4 Size classifications and physical behaviour of PM (Alloway and Ayres, 1997; Morawska and Zhang, 2002; Harrison, 2004; Kingham *et al*., 2005)

PM size	Aerodynamic diameter (µm)	Transport and deposition	Time to deposition	Health Impacts
Total suspended particulates (TSP)	<100	Settle quickly from the atmosphere and therefore deposit close to source: <10 km	Hours	Filtered by the nasal tract
PM_{10} (Coarse)	<10	Remain suspended in the atmosphere and therefore can deposit hundreds to thousands of km from source	Days	Penetrate the lower respiratory system
$PM_{2.5}$ (Fine)	<2.5	Less effectively removed from the atmosphere and therefore subject to long-range transport	Months	Deposit deep in the lung (gas-exchange portions).
PM_1 (Fine)	<1.0		Years	
$PM_{0.1}$ (Ultrafine)	<0.1			

1.6 Particulate matter in the urban environment

Composition of urban air in large cities consist mostly of organic particles from combustion processes (Dockery *et al.,* 1993; Harrison., *et al.,* 2000; Parekh *et al*., 2001; Curtis *et al*., 2006; Husain *et al*., 2007), anthropogenic emissions are more numerous than natural sources and add more particulate matter to the atmosphere (Alloway and Ayres, 1997; Harrison and Grieken, 1998; Morwaska and Zhang, 2002; Phalen, 2002; Artiola and Warrick, 2004; COMEAP, 2012).

The general interactions are shown in Figure 1.4. $PM_{2.5}$ and PM_{10} are closely related to urban sites but not to rural, due to the close proximity and traffic density of urban areas (Chen, 2007). In urban areas spatial distributions of finer particles ($PM_{1.0}$ to $PM_{2.5}$) are relatively more uniformly distributed than coarser particles (Monn, 2001; Wilson and Suh, 1997). In addition to spatial variation, particle concentrations fluctuate over time (Chow *et al.,* 1994; Ito *et al.,* 1995; Adgate *et al*., 2002; Bari *et al.,* 2003; Brimblecombe, 2011). Many urban areas experience diurnal cycles of air pollution concentrations, as anthropogenic sources contribute most pollution (Chow *et al*., 2002). Over short sampling durations (hourly or daily), concentrations between sites in a city will usually differ to a greater degree than measurements averaged over longer periods (annually) (Monn, 2001). It is important to note that there are major differences between total emissions of pollutants and local air quality.

In concentration calculations, the amount of particles available for inhalation is considered and the altitude for emission is essential (i.e. particles from wood burning for heating purposes are more diluted when they reach inhalation altitude since they are emitted higher up than e.g. exhaust from vehicles). Road traffic contributes to emissions affecting local air quality and concentrations of airborne PM (Harrison *et al.,* 1997; Abu-Allaban *et al.,* 2003; Harrison *et al.,* 2003*;* Li *et al*., 2004; Kumar and Britter, 2005; Fuller and Green, 2006; Kittleson *et al.,* 2006; Perry and Taylor, 2007; Thorpe and Harrison, 2008).

1.7 Road deposited sediment

Compared with sediment in natural environments, RDS has a wide and diverse range of sources (Figure 1.5). Sources are either intrinsic to the road surface, which are predominantly anthropogenic in nature, or extrinsic, which are predominantly naturally derived. Intrinsic sources include vehicle exhaust emissions, vehicle tyre, brake and body wear, building and construction material, road salt, road paint and pedestrian debris (Table 1.5). Extrinsic sources are soil material, plant and leaf litter and atmospheric deposition. RDS is an important pathway of pollution in the urban environment and is subject to constant disturbance and re-suspension from vehicle traffic and weather events (Apeagyei *et al*., 2011). Health related PM are components of RDS from anthropogenic and natural source deposition (Harrison *et al.,* 2004) and are prone to re-suspend in populated areas (Chen, 2007).

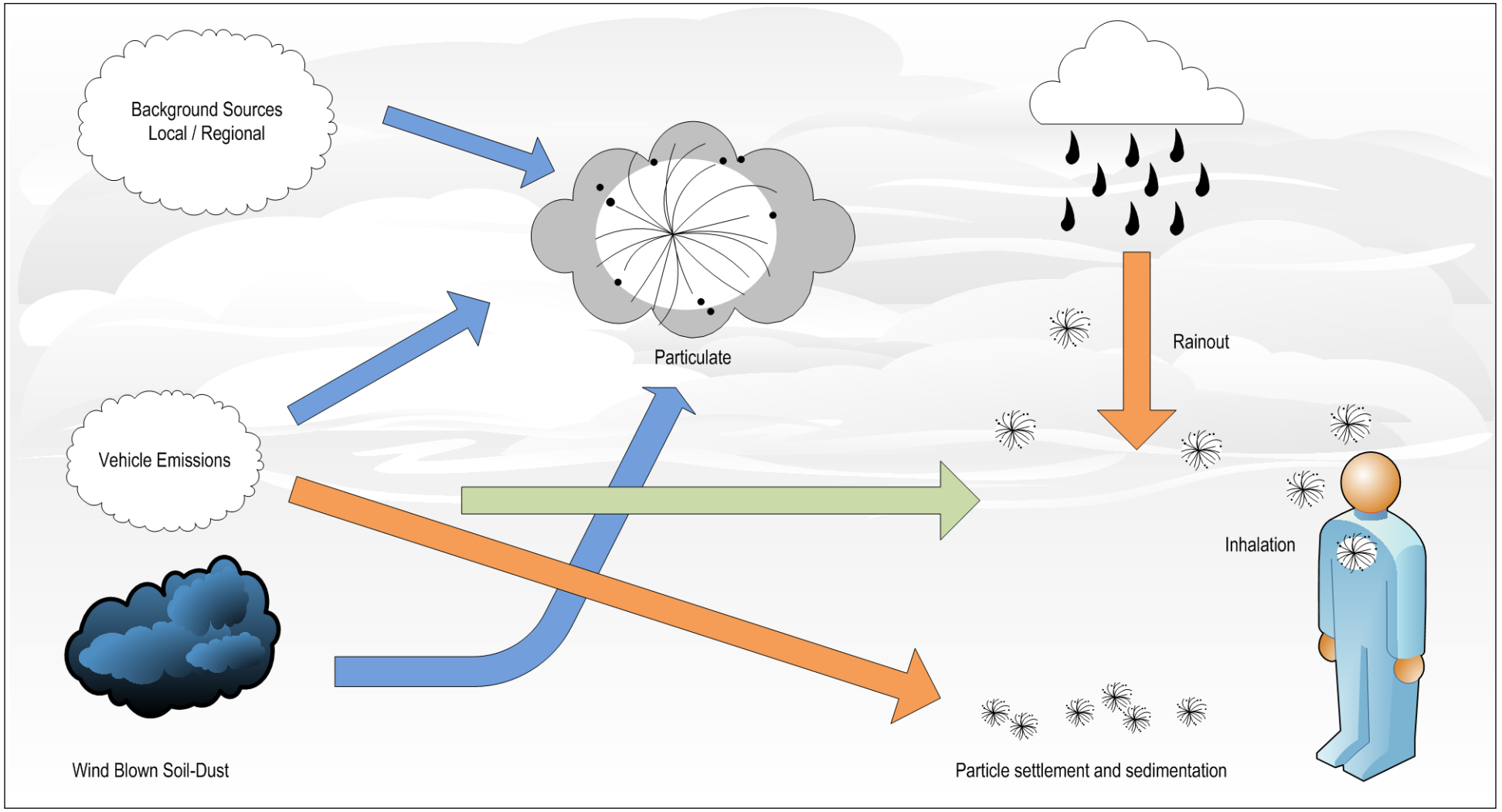

Figure 1.4 Diagram of primary sources of particulate matter (Source: adapted from Harrison, 1997)

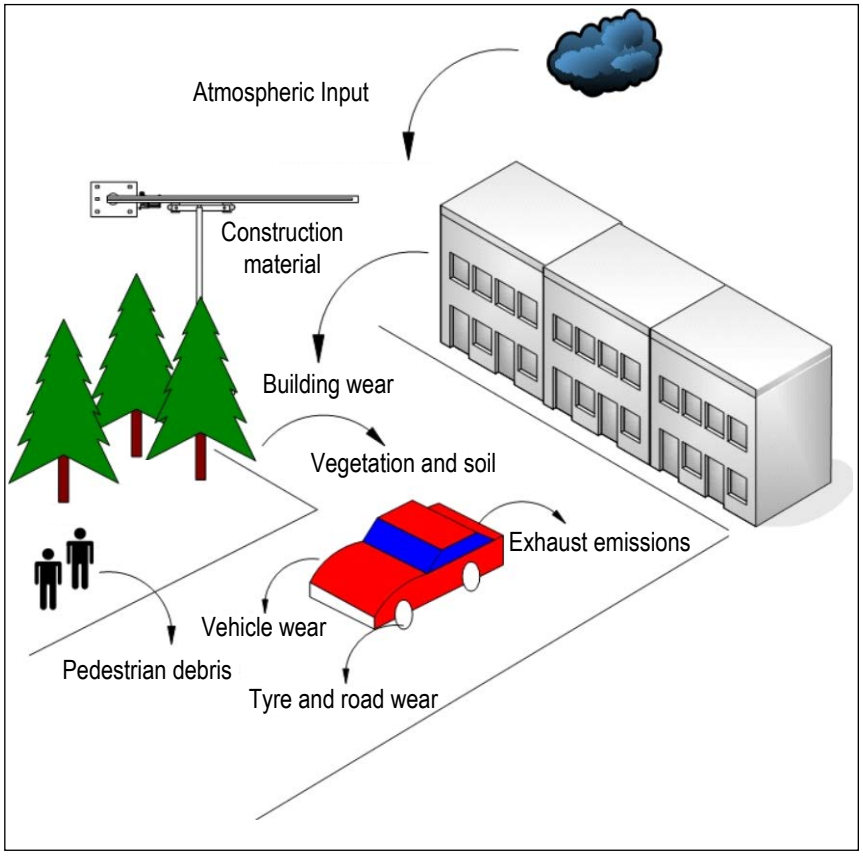

Figure 1.5 Sources of sediment comprising road-deposited sediment; (Source: adapted from Perry and Taylor, 2007)

Table 1.5 Contaminant sources of road-deposited sediment (Source: Perry and Taylor, 2007)

Contaminant	Source
Pb	Petrol combustion, paint, smelters, coal combustion
Zn, Cd	Tyre wear, galvanised roofs, abrasion of vehicles, lubricating oils, alloys
Cu	Brake linings, alloys, metal industry
Fe	Car exhaust particulates, corrosion of vehicle body work, background geology
Mn	Tyre wear, brake linings, background geology
Cr	Engine wear, vehicle plating and alloys, road surface wear
Ni	Engine wear, metal industry, background geology
Asbestos	Brake clutch linings
Cl, Na	Road salt
PGEs (Pt, Pd, Os)	Catalytic convertors
Pesticides / herbicides	Garden application
PAHs	Biomass burning, petroleum combustion
PCBs	Petroleum combustion, industry
Bacteria	Sewage treatment works, animal faeces
Pharmaceutical compounds	Sewage treatment works

1.8 Health implications

PM can affect our health and particle size is considered to be a primary concern in terms of health effects (COMEAP, 2009). Decreasing PM particle size generally creates greater probability of inhalation and deep penetration of the lungs (Figure 1.2). It is when the smallest particles enter the sensitive lung areas that a secondary concern becomes apparent over time, with composition and toxicity of particles (AQEG, 2005; COMEAP, 2009). Available evidence suggests that it is the fine components of PM, which have a diameter <2.5 μm and are formed by combustion, that are the main cause of the harmful effects of PM (AQEG, 2005; COMEAP, 2009) causing triggering mechanisms linked to respiratory problems (such as asthma) (Hetland *et* al., 2001; Perera, 2008). These fine particles consist of carbon, trace metals (such as Cu and Zn) and organic compounds, which are potentially toxic and pose a greater risk to health with decreasing particle size (Dockery *et al*., 1993; Kelly and Fussell, 2012). Studies in the USA (Dockery *et al.*, 1993; Pope *et al.*, 1995) showed that individuals living in less air polluted cities live longer than those living in more air polluted cities. In the UK, the London smog of December 1952 proved a turning point in the history of air pollution and attempts at its control. As a result of a dense fog lasting nearly a week, when black smoke reached a daily average concentration of 4000 μg/m^3 and sulphur dioxide concentrations (daily mean) reached 3000-4000 μg/m^3, at least 4000 deaths occurred in excess of those expected in a two week period. All age groups were affected, although infants and the elderly were found to be most at risk. The main causes of death were respiratory and cardiac disease. Recent analyses have stressed that the effects of the smog on health persisted longer than two weeks and that the total number of deaths may have significantly exceeded 4000. As a direct consequence of this event, the UK Clean Air Act (1956) aimed to control both industrial and domestic emissions. It was very effective: the mean urban black smoke concentration in the UK fell from >200 μg/m^3 in the 1950s to 20 μg/m^3 in 1980 (Department of the Environment, 1997).

There is less evidence to connect secondary inorganic PM (such as sulphates and nitrates) or larger particles with adverse health effects, although they cannot be eliminated as probable causes. Particles cause the most serious health problems among those susceptible groups with pre-existing lung or heart disease and/or the elderly and children. There is evidence that short and long-term exposure to particulate matter cause respiratory and cardiovascular illness and even death. It is likely that the most severe effects on health are caused by exposure to particles over long periods of time. However, UK estimates indicate that short-term exposure to the levels of PM_{10} that we experienced in 2002 led to 6,500 deaths and 6,400 hospital admissions being brought forward that year, although it is not possible to know by what length of time those deaths were brought forward (COMEAP, 2001). Studies conducted by the Committee on Medical Effects of Air Pollution (COMEAP) found for every 1 μg/m^3 decrease in $PM_{2.5}$ over the lifetime of the current population of England and Wales, between 0.2-0.5 million years of life will be gained (COMEAP, 2010). This is equivalent, on average, to 1.5–3.5 days for every individual in England and Wales. The effect is unlikely to be evenly spread across the population, however, and some people will gain much more. Due to these effects in 2003, the UK Government set strict limits for fine particle concentrations, as discussed in section 1.9.

1.9 Current regulation/legislation

PM emissions and concentrations are subject to several national and international agreements and initiatives. EU directives relate directly to PM emissions and concentrations[1].

i. The First Air Quality Daughter Directive (1993/30/EC) sets limit values for 24 hours and annual average PM_{10} that had to be achieved throughout the European Community (EC) by 1 January 2005 (Table 1.6). The Directive also contained Stage II limit values for both 24 hour and annual average PM_{10} to be achieved by 1 January 2010 (Table 1.7). This Directive is more commonly known as the The National Air Quality Objectives (Air Quality Strategy V1, 2007).

ii. The Auto-Oil Programme set a stringent series of emission and fuel quality standards (Euro III) to apply to all new cars and light vans sold from January 2000 and to all new heavy duty vehicles from October 2001. This included the ban on the general sale of leaded petrol from 1 January 2000. Tighter standards were further introduced for cars, vans and heavy duty vehicles, in January 2006.

iii. The Large Combustion Plant Directive (2001/80/EC) established controls on emissions from particulates and the secondary particle precursors sulphur dioxide and nitrogen oxides. This controlled emissions from large combustion plants, power stations, oil refineries and large energy producers within industry.

iv. The Integrated Pollution Prevention and Control (IPPC) Directive (96/61/EC). This Directive takes into consideration the location and state of the local environment so individual industrial plants take the necessary measures to comply with any relevant EC legislation (AQEG, 2005).

Current EU legislation only controls the mass concentration of particles with a diameter <10 µm (PM_{10}) in ambient air (Council Directive, 1999/30/EC). Until recently this is implemented by imposing two health-based limit values: (i) a 24 hour mean concentration of 50 µg/m^3 not to be exceeded more than 35 times during a calendar year; and (ii) an annual mean concentration of 40 µg/m^3. Currently (post 2010) stringent PM_{10} objectives have been achieved by most EU countries: (i) a 24 hour mean concentration of 50 µg/m^3 not to be exceeded seven times during a calendar year; and (ii) an annual mean concentration of 20 µg/m^3.

To protect health in the UK, the Department for Environment Food and Rural Affairs (DEFRA) and the Devolved Administrations of the UK, have set two air quality objectives for PM_{10} in their Air Quality Strategies:

[1]This thesis concentrates mainly on the first EU Directive (1993/30/EC).

Table 1.6 The First Air Quality Daughter Directive (1993/30/EC) limit values 24 hour and annual average PM_{10} that had to be achieved throughout the UK by 1 January 2005 (Air Quality Strategy V1, 2007)

	Objective	Measured as	UK Target	EU Target
Particles (PM_{10}) (gravimetric) All authorities	50 μg/m³ Not to be exceeded more than 35 times per year	24 hour Mean	31 December 2004	1 January 2005
	40 μg/m³	Annual Mean	31 December 2004	1 January 2005
Particles (PM_{10}) Authorities in Scotland only	50 μg/m³ Not to be exceeded more than 7 times per year	24 hour Mean	31 December 2004	1 January 2005
	18 μg/m³	Annual Mean	31 December 2004	1 January 2005

Table 1.7 The First Air Quality Daughter Directive (1993/30/EC) limit values 24-h and annual average PM_{10} for UK regions (Air Quality Strategy V1, 2007)

Region	Objective	Measured as	To be achieved by
Greater London	50 μg/m³ not to be exceeded >10 times per year	24 hour Mean	31 December 2010
Greater London	23 μg/m³	Annual Mean	31 December 2010
Greater London	20 μg/m³	Annual Mean	31 December 2015
Rest of England, Wales and Northern Ireland	50 μg/m³ not to be exceeded >7 times per year	24 hour Mean	1 January 2010
Rest of England, Wales and Northern Ireland	20 μg/m³	Annual Mean	1 January 2010

1. The 24-hourly objective, which is the concentration of PM_{10} in the air averaged over 24 hours, is designed to ensure that we are not exposed to high concentrations of PM_{10} for short periods of time. High concentrations can arise during pollution episodes, which are short periods of high levels of pollution that are usually associated with particular weather conditions.

2. The annual objective, which is the concentration of PM_{10} in the air averaged over one year, aims to protect us from being exposed to PM_{10} over prolonged periods.

The EU also recommended implementing stricter limit values from 1 January 2010. These plans involved a reduction of the number of allowed exceedences of the 24 hourly limit value from 35 to seven and a decrease in the annual limit value from 40 to 20 µg/m^3. EU Directive 2008/50/EC member states that are having difficulty complying with these values (including the UK) a postponement date limit of January 2015. Member states will be subject to further assessment and discussion by experts and policy-makers before a decision is made on whether to adopt them. In its Addendum to the Air Quality Strategy, the UK Government and local Administrations are striving to adopt these stricter indicative limit values as provisional objectives to be achieved in the UK by January 2015 (European Commission, 2012).

Currently, the main source of airborne fine particulates in the UK is road traffic emissions (AQEG, 2005). Road traffic is responsible for 41% of particles <2.5 µm in urban areas (Greenwood *et al*., 1996; Allen *et al*., 2001). However, it is estimated that road transport emissions of fine particles will fall by two-thirds of those a decade ago. Moreover, the European Commission has proposed that the legislation on particulate matter should be supplemented by setting a limit value of 35 µg/m^3 for $PM_{2.5}$ particles and an interim reduction target of 20% to be attained between 2010–2020. The UK has been unable to attain these limits (as of mid-2011) and have notified (24 April 2009) to the European Commission to secure additional time to meet the limit values (DEFRA, 2011). Assessment of the extent and severity of urban dust concentrations requires thorough investigation before 'Air Quality Management Plans' and remediation can be instigated, which means that there is scope for new PM monitoring technologies.

1.10 UK monitoring of airborne particulate matter

There are over 1500 monitoring sites across the UK, which monitor air quality. Due to the stringent legislations on PM concentrations, the UK currently has a network of 64 automatic monitoring sites and an additional seven gravimetric analysers[2] that measure PM. These sites use a Tapered Element Oscillating Microbalance (TEOM) filter baser gravimetric method and sequential gravimetric analyser (Partisol) or ß-attenuation monitor to measure PM. The networks form the Automatic Urban and Rural Network (AURN), operated by DEFRA. As well as PM_{10} the monitoring sites also observe $PM_{2.5}$, particulate nitrate, particulate sulphate, elemental and organic carbon, polycyclic aromatic hydrocarbons (PAHs), 'black smoke', heavy

[2] www.uk-air.defra.gov.uk/networks/network-info?view=aurn

metals and particle numbers. The collective measurements of the automatic monitoring sites provide a valuable resource of temporal and spatial variations of PM, extending over 10 years of monitoring (AQEG, 2005).

Although road traffic emissions are a major source of particulate matter near roads, the regional contribution to PM is substantial. Controlling background particulate matter must, therefore, be a central part of any UK strategy to control exposure to particulate matter. In addition, because there is no known safe level for exposure to PM, it is not appropriate to rely solely on the use of air quality objectives. They focus attention on 'hotspots' for example close to busy roads, but where relatively few people tend to reside (AQEG, 2005). Static TEOM systems record reliable data for busy roads and hotspots, but can be unreliable recording PM concentrations for larger areas due to interference from weather systems and long range transport of particulates (AQEG, 2005). This limitation potentially leaves populated areas unchecked, and exposed to uncertain PM concentrations.

1.11 Scope of this research

It is timely for innovative PM technologies to be considered as an alternative, or in tandem, to those already employed to determine $PM_{2.5}$ and PM_{10} concentrations. Moreover, ideally, they need to be rapid, reliable, dynamic and inexpensive. However, to assess the suitability of any analytical technique as an efficient particle size proxy, it is necessary that the nature of the relationship between the proposed parameters and particle size follow predictable patterns.

It is well documented that particle size plays a significant role in controlling pollution concentrations in sediments; whereby, concentrations tend to increase with declining particle size (Rae, 1997). Magnetic concentrations have been used for the normalization and identification of heavy metal concentrations and particle size effects in several environments (Booth *et al.,* 2005; Zhang *et al.,* 2007). A recent pilot investigation between magnetic and particulate matter parameters within urban settings (Booth, 2007) has already identified significant relationships ($r = 0.701$; $p < 0.001$; $n = 50$). These associations indicate mineral magnetic measurements have considerable potential as a particle size proxy for determining urban roadside particulate matter concentrations.

Anthropogenic Particles in urban settings display distinctive magnetic properties such as magnetic enhancement (Thompson and Oldfield, 1986), some studies have found strong relationships between certain magnetic properties (magnetic susceptibility χ) and heavy metal concentrations (Clifton *et al*., 1999; Petrovský and Ellwood, 1999; Xie *et al*., 2001). Despite these advances, the approach of using mineral magnetic properties in the study of environmental pollution has not been fully explored.

Booth *et al*. (2005) suggested if a particle size proxy could be measured in an efficient fashion, with shorter analysis time, lower cost, and following a universal pattern of relationship, it would offer potential advantages. Compared with other geochemical techniques, mineral magnetic

methods are relatively quick and simple to prepare and analyse (Walden, 1990). Measurements of magnetic susceptibility (χ_{LF}) can be made in ~1 minute, within either a laboratory or field environment (Booth *et al*., 2005). This allows relatively large data sets to be acquired, adding statistical weight to any data collected (Walden, 1990). Initial costs of magnetic susceptibility (χ_{LF}) instrumentation are low (Bartington MS2 susceptibility meter and sensor £3,960 (Bartington, 2011, 2012 (Appendix 7.4))) when compared to XRF and ICP-MS. TEOM systems operated by the AURN, cost tens of thousands of pounds to operate and maintain (Appendix 7.5).

Given the speed, low-cost, sensitivity and application range of mineral magnetic measurements, magnetic techniques can potentially be used as an alternative and/or complementary exploratory technology for particulate pollution investigations. Furthermore, in certain instances, mineral magnetic methods could potentially examine linkages between respiratory health, PM size, composition and anthropogenic emissions.

1.12 Aims and objectives

Mineral magnetic measurements as a PM particle size proxy is the primary interest of this study (Aim 1). PM properties associated with size, shape and surface area can cause acute health problems. Essentially, the probability of PM penetrating deep into the lungs increases with decreasing particle size. As a result, the finer fraction of PM can potentially trigger respiratory problems in sensitive and vulnerable groups (children, elderly). As a secondary strand to this research, geochemical composition is also addressed due to chronic health incidences associated with particle composition when particles are inhaled deep into the lungs over time (Aim 2). Therefore the aims and objectives of this research are:

Aim 1: Investigate the extent to which mineral magnetic concentration parameters can be used as a proxy for indicating RDS PM particle size.

Objectives:

- To conduct an extensive literature review on PM it's health effects and mineral magnetic methods to determine proxy potential.
- To devise a sampling strategy based on previous research and actual existing database of PM levels, traffic counts, multiple land uses and health data.
- Generate a wide range of new data for areas in the West Midlands and UK.
- Perform laboratory experiments including mineral magnetic, SEM, particle size, and organic loss on ignition.
- Thoroughly characterise the RDS and determine the state in which mineral magnetic methods can be used as a PM proxy for RDS by using statistical and GIS methods.
- Assess the reliability of using mineral magnetic methods as a proxy for particle size

Aim 2: Investigate the extent to which mineral magnetic concentration parameters can be used as a proxy for geochemical composition of RDS at local, and national scales within the UK, and whether these data associations follow the predictable trends of other studies.

Objectives:

- Investigate elemental concentrations in RDS using XRF and SEM-EDX for roadside, city and national scales.
- Compare results of mineral magnetic and geochemical data with previous studies conducted on RDS.
- Determine from data whether mineral magnetic methods can be used reliably as a proxy for geochemical composition at different spatial scales.

This work will develop from previous research in the following ways:

- By establishing mineral magnetic and particle size associations over time and at varying spatial scales (road, city, regional and national) as a review of literature suggests that previous research has not fully explored urban RDS relationships and only concentrates on small sampling areas.

- Investigating linkages of roadside particle size, airborne PM (through ASU data) and mineral magnetic associations, as there is a lack of research and available data in this area.

- Compare geochemical parameters to infer influencing factors and sources, but at various spatial scales as previous research has only concentrated on hot spots and small scales.

- Establishing and investigating the reliability of mineral magnetic measurements as an urban geochemical pollution indicator within RDS at a number of spatial scales, as only small scales have been investigated in previous research.

- Investigate the factors that influence the reliability of mineral magnetic methods as a particle size proxy, as a lack of research and data have failed to provide explanations for the success or failure of these methods.

1.13 Thesis Overview

Chapter 1 outlined the overall rationale for research and the scope of research undertaken. Chapter 2 reports the outcome of previous research on health effects, sources and methods for measuring PM and RDS. Previous work highlights the potential advantages over established techniques and limited scope of work already conducted using mineral magnetic methods. Chapter 3 outlines the practical methodologies used in the field and laboratory. Data confidence is explored as a pilot study investigating reliability of the proposed methods for RDS analysis and potential limitations.

Chapter 4 presents the main results from the experiments used in this research and a statistical treatment of the data for the temporal, local and regional viewpoint. Chapter 5 presents results for the larger UK spatial study with an investigation of towns and Cities in the UK. Data is explored in terms of spatial application and introduces geochemical data.

Chapter 6 discusses the results and compares to previous research further developing the findings, evaluating the application and implications of the methods. Chapter 7 relates the aims of the work to the results and success/failure of the methods. Limitations of the study are discussed, and recommendations are stated for future work.

Chapter 2

Health effects, proxy measurements and mineral magnetic methods

This chapter details the health issues associated with PM and the rationale for this research which aims to investigate mineral magnetism as a quick, cost effective alternative PM proxy method.

2.1 Health effects of particulate matter

Airborne particulate matter is receiving world-wide attention due to its impact on air quality, with cases of particulate matter exposure linked with respiratory illness, diabetes and other health problems (COMEAP, 2010; DEFRA, 2012). Airborne particulate matter affects human health in different ways and it is important to identify how and why these particles can be harmful. According to Pope and Dockery (2006), four factors affect the toxicity of PM hence the risk of developing disease:

1) Amount of dust retained in the lung.
2) Duration and intensity of exposure.
3) Individual sensitivity.
4) Dust properties.

Several studies (Oberdörster *et al*., 1994; Fubini, 1997; Harrison and Yin, 2000; Hetland *et al*., 2000; Hetland *et al*., 2001; Skaug, 2001; Muhle and Mangelsdorf, 2003; Moreno *et al*., 2004; Nygaard *et al*., 2004; Brunekreef and Forsberg, 2005; Dybing *et al*., 2005; Perry and Taylor, 2007) indicate that the most important characteristics of particles are:

a) Particle size, shape, surface area and number of particles.
b) Particle composition, substances attached and solubility of particles.

2.2 Particle mass and number exposure

Fine particles have a much higher total surface area compared to coarser particles at a given dose in mass. Biological effects of particles are believed to depend on how much of the particles are in direct contact with human cells (Klemm *et al*., 2000; Hetland *et al*., 2001). Some particles are smooth and the geometric surface area can be calculated from the size distribution. With indented particles the true exposed surface may be evaluated only by means of physical adsorption of gases (BET).

Findings indicate that toxic effects of particles have a higher correlation with the particle number or surface area concentration than with the mass concentration (Granum *et al*., 2001; Katsouyanni *et al.,* 2005). Particle exposure has traditionally been monitored as mass concentration of PM_{10}. However, mass concentration is strongly influenced by large particles. Therefore mass concentration is a poor measure for characterizing the fine, and possibly more biologically potent particles (Nygaard *et al*., 2004). Studies in Sweden show 70-80% of total particle number concentration in a large city is caused by local sources compared to only 30-

40% for PM_{10} (mass concentration) (Johansson *et al*., 2007). Johansson *et al*. (2007) also found particle number concentration is highly correlated with vehicle exhaust particles. Figure 2.1 illustrates the ratio between a coarse, fine and ultrafine particle, and Table 2.1 shows relative surface area and relative number of particles for a given mass of spherical particles. There is an enormous difference in the total number of particles (one million ultrafine particles compared to one individual coarse particle for the same mass), but also the relative surface area is much larger for small particles (Figure 2.2). On the surface of some particles, especially with large specific surface area, such as carbon particles from combustion processes, allergic agents, gases, fungal spores and endotoxins can become attached (Schwartz *et al*., 2004). These compounds can potentially have triggering effects, where the body reacts to the particles. Human cells will not recognize what is inside an insoluble particle, but only react with the molecules according to their structure at the particle surface. Donaldson and Borm (1998) and Fubini *et al*. (1997) studied impurities on silica particles, especially iron and aluminum which is the most commonly found metal ion contaminants on these specimens. These impurities can enhance or decrease the intensity of pathogenic responses, and the reactive surface can be inactivated by various common minerals e.g. aluminum salts.

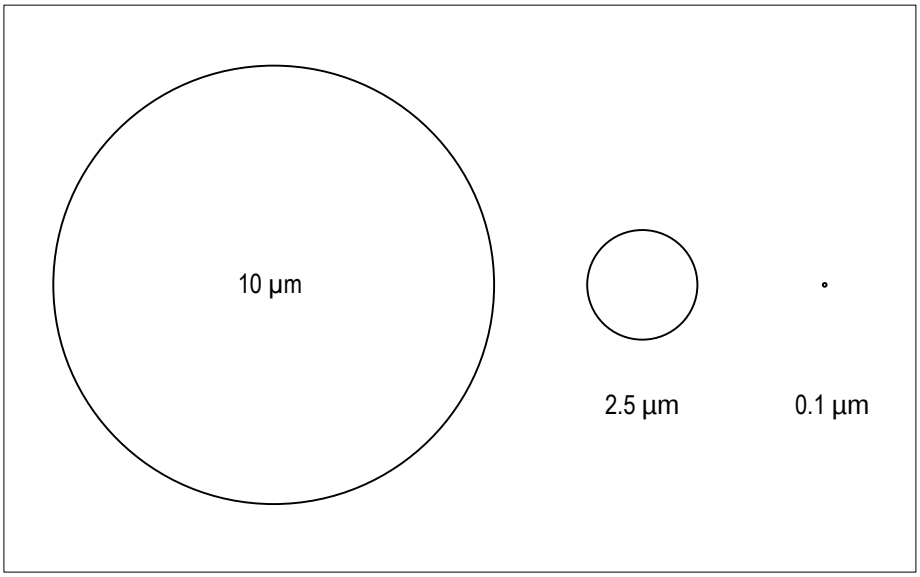

Figure 2.1 Ratio between a particle with diameter 0.1 µm (e.g. a diesel particle), 2.5 µm and 10 µm (e.g. mineral particle).

Table 2.1 Relative surface area and number of particles for a given mass of spherical particles with different diameter (Source: Kittleson, 1998)

Particle diameter	Mass	Relative surface area	Relative number
0.1	1	100	1 000 000
1.0	1	10	1 000
2.5	1	4	64
10.0	1	1	1

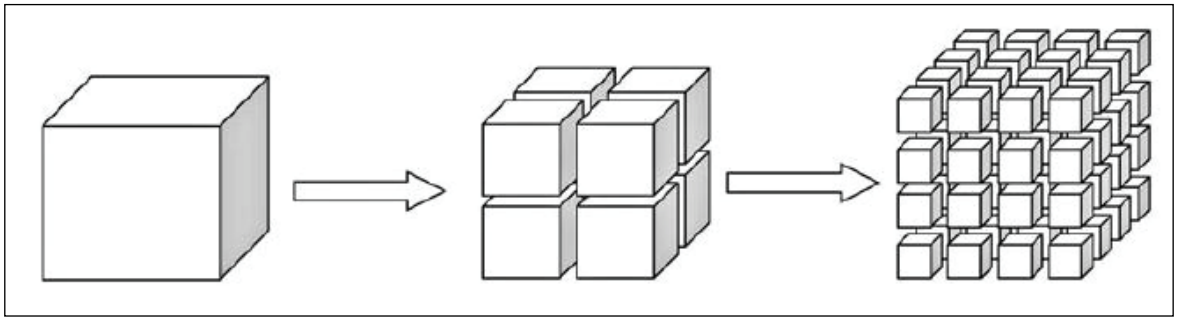

Figure 2.2 Illustration of surface area and number of particles with same total mass (Source: Kittleson, 1998).

Aerosols have integral properties that depend upon the concentration and size distribution of the particles (Figure 2.3):

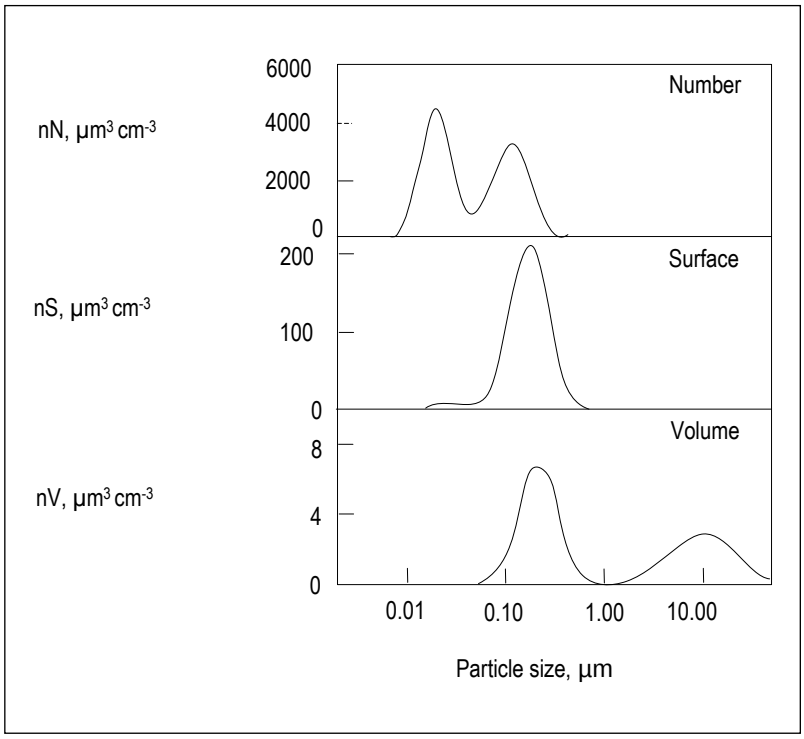

Figure 2.3 Typical urban aerosol number, surface and volume distributions (Source: Seinfeld and Pandis, 2006).

- Number concentration, which is the total number of airborne particles per unit volume of air, without size distinction.

- Surface concentration, which is the total external surface area of all particles in the aerosol, may be of interest when surface catalysis or gas adsorption processes are of concern. Aerosol surface is one factor affecting light-scatter and atmospheric visibility reductions.

- Mass concentration (volume), which is the total mass of all particles in the aerosol, is frequently of interest. The mass of a particle is the product of its volume and density. If all particles have the same density, the total mass concentration is simply the volume concentration times the density. In some cases, such as respirable, thoracic and inhalable dust sampling, the parameter of interest is the mass concentration over a restricted range of particle sizes.

According to Nygaard *et al*. (2004) the particle number concentration mainly reflects the amount of ultrafine particles (<0.1 µm), the surface area best reflects the particles between 0.1-1 µm, whereas the particle mass reflects particles >0.1 µm. Small particles have a larger total surface area compared to the same volume of larger particles. This means more substances can adhere to the particles and can be transported into the human body. A high volume of particles inside macrophages, blockading further phagocytosis and allowing particles to interact with the epithelium, was believed to be the mechanism of overload (Donaldson and Tran, 2002). More recently work has emphasized the role of particle surface area in the initiation of overload. By experiments on rats, one can confirm this by testing same mass deposition of different particulate substances in the lungs with respect to adjustment to same surface area of the particles deposited (Donaldson and Tran, 2002). A single response to surface area was evident, while the inflammatory response was different for the substances. Donaldson and Tran (2002) concluded, that a mass burden of ultrafine particles is more likely to cause overload than the same mass burden of larger particles of the same material. The smaller the particle size, the lower the mass of particles needed to initiate overload. Cardiovascular causes and lung cancer seemed to have threshold effects, while chronic obstructive pulmonary disorder (COPD) appeared to have linear effects (Næss *et al*., 2006).

2.3 Particle size effects on health

The primary aim of this work investigates particle size due to acute health effects. The amount of dust retained in the lung depends on the physico-chemical properties of the dust (particle size, shape, density and solubility) and where in the respiratory tract the particles are deposited (Raabe and Yeh, 1976; Schwartz *et al*., 2004). Figure 2.4 presents the structure of the human respiratory tract. The way of breathing (nasal/oral, breathing frequency and volume), physical activity, possible existing diseases and particle properties determine the location in the respiratory system of particle deposition (Schwartz *et al*., 2004). The potential for health risk depends on if, and how rapidly the particles are removed from the respiratory system. The human respiratory tract can be considered as a series of filters starting with the nose or mouth, via the various diameters of airways to the alveoli, Figure 2.5 presents deposition efficiency in the airways as a function of particle diameter. Efficiency is related to particle mass inhaled. According to Dybing *et al*. (2005), three mechanisms determine deposition in the respiratory tract: (1) sedimentation by gravitational forces acting on particles >0.5 µm in aerodynamic diameter; (2) impaction caused by their inertial mass in branching airways acting on particles >1.5 µm; and (3) diffusional motion of particles <0.5 µm by thermal motion of air molecules.

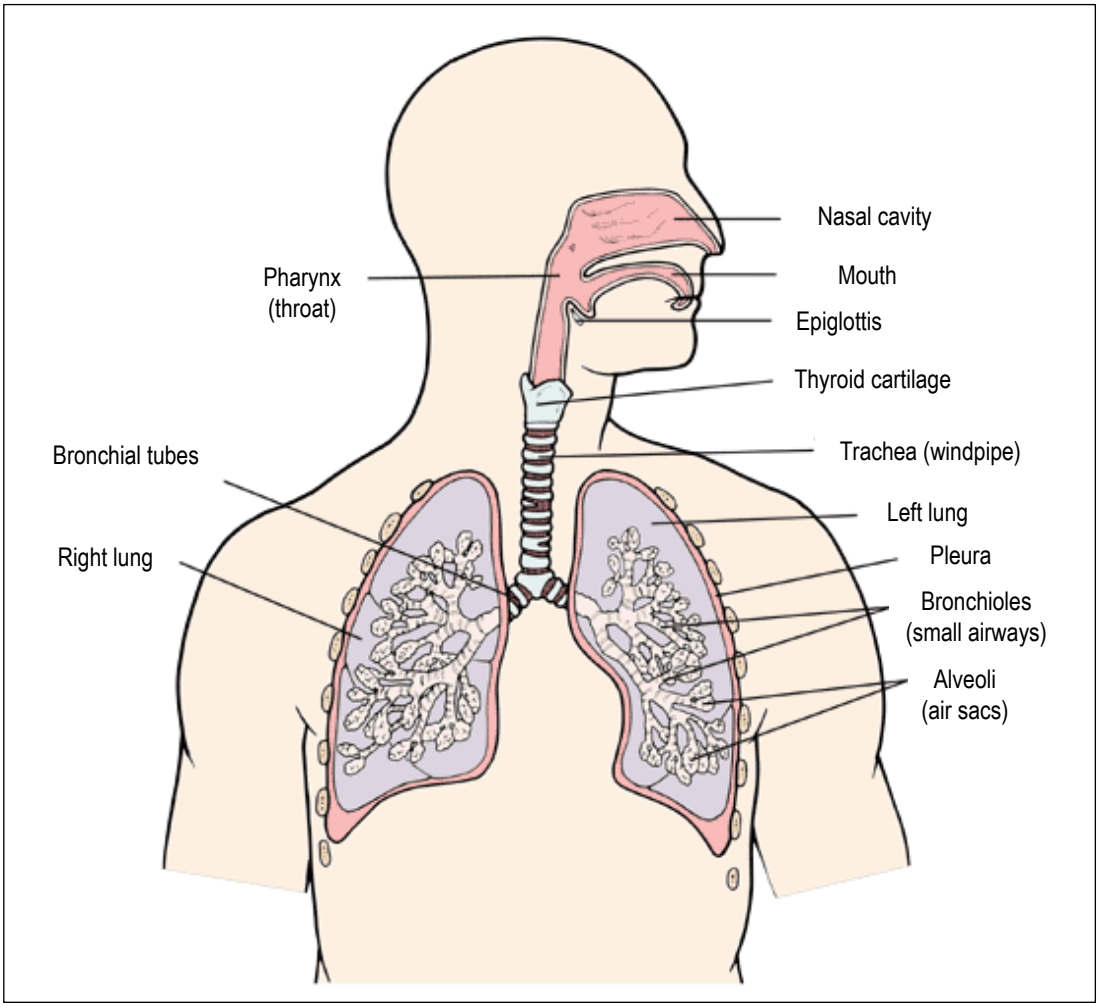

Figure 2.4 Diagram of the human respiratory tract (Source: National Health Service, 2009).

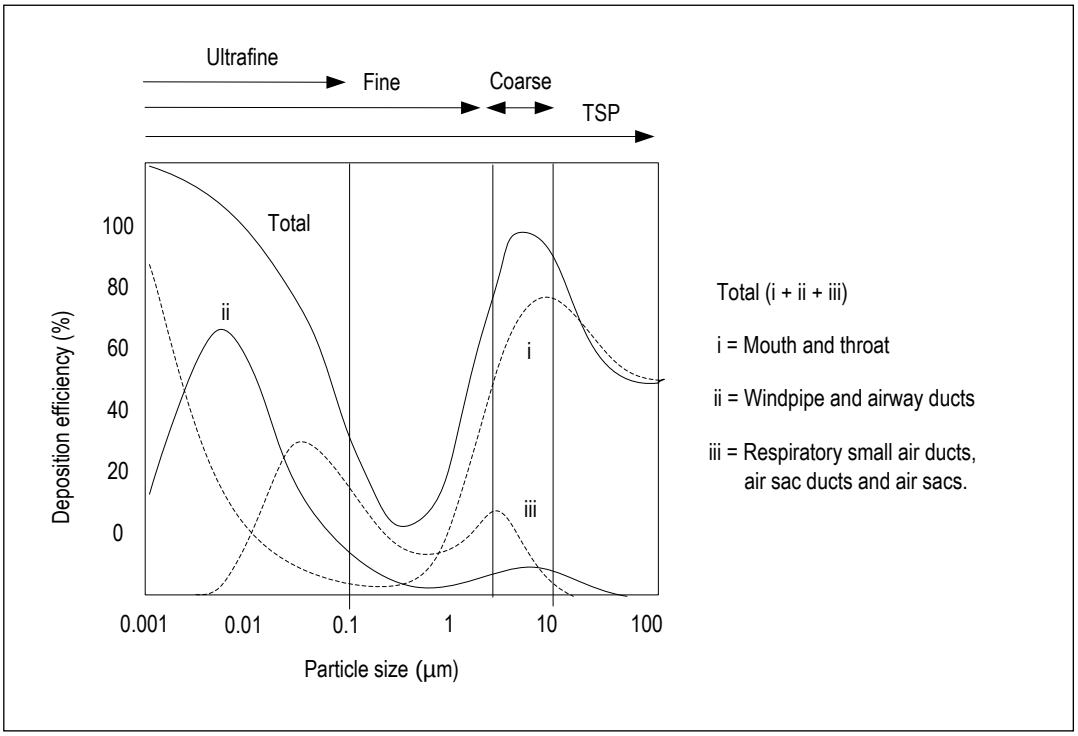

Figure 2.5 Deposition of particles in the airways (Source: Schwartz *et al*., 2004).

These mechanisms work through three important components during breathing: (a) particle dynamics, including the size and shape and its possible dynamic change during breathing; (b) geometry of the branching airways and alveolar structures; and (c) breathing pattern determining airflow velocity and the residence time in the respiratory tract, including breathing through the nose compared with breathing through the mouth. Different cells with various properties exist in our respiratory system and air sacs (Schwartz *et al.,* 2004):

- Some cells produce mucus and secrete compounds to counteract effects of particles and other foreign matter. The thickness of the mucus layer (lining fluid) is least in the deep lung (air sacs, terminal airways and small air ducts). If sufficient foreign matter reaches the lungs, cells will send out signaling substances which summon other cells (i.e. different types of leucocytes such as granulocytes and lymphocytes) that create inflammation to render the foreign matter harmless. Inflammation is important to block infections by destroying foreign matter, but can also result in injury to adjacent tissue. Strong and persistent inflammatory reaction may lead to cell damage and create areas sensitive to illness in the lungs.

- Other cells are covered with cilium and are involved in the transport of mucus to the gullet. In this way, particles, microbes and other foreign matter can be transported away from the respiratory system.

- Specialized cells (macrophages) take up and break down foreign matter in the gas exchange areas of air sacs.

2.3.1 Particles inhaled and absorbed by the body

Particles can be divided into three categories, depending on their solubility (Schwartz *et al*., 2004); soluble, partly soluble and low solubility. The main part of urban airborne PM is partly soluble. Particle size is important for removal of the low solubility fraction. Particles of different size are removed in different ways and the place of deposition also determines in what way the particles are removed. Particles deposited in the upper and middle part of the respiratory tract are removed relatively fast (hours, days), while it may take much longer (months, years) for particles deposited in the lower part. Deposited particles are removed in different ways, depending on solubility and where they are deposited in the respiratory tract (Schwartz *et al*., 2004):

- Soluble particles or components are removed fast. A protecting liquid layer covers the surface of the respiratory system and has different composition in different parts of the respiratory tract. Soluble particles or components attached can be partly or completely dissolved, and the components may reach blood vessels often via the lymphatic system. This may cause effects far from the place they were deposited.

- Coarse low solubility particles >5 μm which are deposited in the upper part of the respiratory tract are removed by coughing, sneezing or by muccociliary clearance to the gullet, where the particles can reach the gastrointestinal tract. They are either secreted with excrements or taken up in the gut. The muccociliary transport is slower and particles are deposited further down in the respiratory tract. Low solubility particles with size between 5-0.1 μm can be taken up by macrophages. Ultrafine particles (<0.1 μm) can enter into the blood stream and reach other organs, but the effect of these particles is not yet established.

The activation state of the target lung in terms of the response to particle exposure reflects an important issue. Differences in the activation state of the macrophages dictate the extent of their pro-inflammatory response (Salvi *et al.,* 1999; Donaldson and Tran, 2002). The sequence of effects in lungs after exposure to low solubility particles is inflammation, fibrosis and then cancer (Muhle and Mangelsdorf, 2003). Inflammation is crucial to the development of adverse health effects associated with particle exposure. There are several implications for health connected to inhalation of airborne PM. The particles can affect the heart and blood vessel system. The heart is the organ that receives the blood stream from the respiratory system first. According to Dybing *et al*. (2005), air pollution may result in diminished oxygen supply, increased blood coagulation and possible clot formation in the vessels supplying the heart muscle, with deleterious heart rhythm effects (Gold *et al*., 2000). Ultrafine particles can be found in the liver, spleen, kidneys, brain and nerves (Dybing *et al*., 2005). Lung inflammation, heart variability, changes in blood viscosity and oxygen deprivation can result in exacerbating the symptoms of pre-existing lung disease, such as asthma, as well as heart and blood vessel disease and probably induction of lung cancer (Dybing *et al*., 2005; Katsouyanni *et al*., 2005).

2.3.2 Duration and intensity of exposure

The length and intensity of exposure to PM are important factors that influence effects on health. Both short-term (hours, days) and long-term (weeks, months, years) exposure to PM can enhance existing disease in a population. Long-term exposure can directly contribute to the development of disease and subjects living in cities with higher long-term average PM_{10}/$PM_{2.5}$ concentrations die earlier than subjects living in cities with low air pollution. Short-term exposure has been linked to increased daily mortality and numbers hospitalized due to respiratory and cardiovascular diseases (Harrison *et al*., 1996; Katsouyanni *et al*., 2005; COMEAP, 2009).

Relatively few studies have documented effect of long-term exposure on local air pollution on health (Pope and Dockery, 2006; COMEAP, 2009). However, it is documented that the relative risk due to long-term exposure is greater than short term exposure (Seaton *et al*., 1995; Soloman *et al.,* 2003; Pope and Dockery, 2006). Studies on effects of outdoor air pollutants on human health have included both epidemiological and toxicological studies. Toxicology aims to understand the processes of how pollutants affect people's health and to identify the factors influencing those processes, while epidemiology identifies disease by studying its occurrence in a population and employs statistical methods to assess whether exposure and disease are

related. The AIRNET network project on air pollution and health (2002-2005) founded by the EU, has tried to create a foundation for public health policy that can improve European air quality (Dybing *et al*., 2005; Katsouyanni *et al*., 2005).

Epidemiological studies show a connection between short-term exposure to PM_{10} and acute health effects. An increase in PM_{10} of 10 µg/m^3 resulted in an increase in relative risk of 0.6% for all causes of death, and 0.9% and 1.3% for death by cardiovascular and respiratory diseases, respectively (Soloman *et al.,* 2003). There is also evidence of cardiac infarction in response to very short changes (hours) in PM_{10} concentration (Gold *et al.,* 2000; Zanobetti and Schwartz, 2007). It is difficult to separate health effects of PM_{10} from short and long-term exposures. However, for long-term exposure an increase in $PM_{2.5}$ of 10 µg/m^3 resulted in an increase in relative risk of 4% for all causes of death, and 6% and 8% for death by cardiovascular disease and lung cancer respectively (Soloman *et al.,* 2003). The risk for developing health effects increases linearly even at very low concentrations of air pollution in general and PM in particular, and it was not possible to establish a level of concentration beyond which there is no health effect (Schwartz *et al*., 2004). There are different opinions on whether a threshold level for exposure to airborne PM exists (de Kok *et al*., 2006). Donaldson and Tran (2002) assumed all particles have a threshold effect level where the lung can deal with them, while Dybing *et al*. (2005), Katsouyanni *et al*. (2005) and de Kok *et al*. (2006) reported no support for general thresholds for PM-induced adverse health effects at a population level, even though general toxicology understanding makes thresholds for individuals biologically plausible.

2.3.3 Individual sensitivity

Individual sensitivity towards the actual dust is important for evaluation of health effects from PM air pollution. Risk or susceptibility depends on the specific health end point being evaluated and the level and length of exposure (Pope and Dockery, 2006). Some groups of the population are particularly susceptible to PM. Fetuses, children, elderly people and groups with chronic diseases (respiratory disorders like asthma, allergy and chronic obstructive pulmonary disorder (COPD), cardiovascular disease, cancer and diabetes) are more susceptible than healthy people (Soloman *et al*., 2003; Schwartz *et al*., 2004; Næss *et al*., 2006; Pope and Dockery 2006; Kelly and Fussell, 2012). There is also evidence of increased infant mortality rates and various birth defects because of particle exposure (Pope and Dockery, 2006). In addition, risk for worsening of asthma and allergy because of air pollution is larger for children than adults (Perera, 2008). Age is an important factor when evaluating individual sensitivity. Children have narrower bronchia and different breathing patterns compared to adults, which may result in different places of deposition for inhaled particles (Heinrich and Slama, 2007). Increased sensitivity with elderly people may be caused by diseases as a consequence of age and not age itself. Characteristics that have been shown to influence susceptibility include pre-existing respiratory or cardiovascular disease, diabetes, medication use, age, gender, race, socio-economic status, health care availability, educational attainment, housing characteristics and genetic differences (Pope and Dockery, 2006). Geographical and socio-economic variation magnify these effects within susceptible groups, for instance, children living alongside main

roads are more likely to develop asthma (Duran-Tauleria and Rona, 1999; Edwards *et al.,* 1994; Oosterlee *et al*., 1996; Wilkinson *et al.,* 1999). Poverty is also linked with child asthma and urban areas (Duran-Tauleria and Rona, 1999). But gaps in knowledge still exist for who is most at risk or susceptible to PM. The number of those susceptible to less serious health effects may be larger than the risk of dying or hospitalization. For most people those effects are likely to be small, transient and largely unnoticed (Pope and Dockery, 2006).

2.4 Particle composition effects on health

The secondary aim of this work investigates particle composition and is secondary due to potential chronic health effects of particles. Urban dust generally causes more health effects than rural dusts. Emissions produced by motor vehicles appear to be most dangerous to human health (Kelly and Fussell, 2012). Health issues are primarily due to particle size effects and secondary long-term effects of geochemical composition and potential toxicity of particles (Katsouyanni *et al*., 2005; Molfino *et al.,*1991; Sandstrom, 1995; Kelly and Fussell, 2012). In urban air the fine fraction (<2.5 μm) mainly consist of organic components, such as sulphur aerosols and soot particles, while the coarse fraction (2.5-10 μm) is predominantly composed of inorganic mineral matter such as silicates (Harrison and Yin, 2000; Granum *et al*., 2001; Dybing *et al.,* 2005).

Mineral particles can be divided into crystalline and non-crystalline (amorphous) forms. In crystalline phases, the molecules make a three-dimensional repeating pattern forming the mineral structure. Amorphous minerals have no such pattern; the molecules are arranged randomly. Crystallinity seems to be an important factor in the toxicity of mineral particles (Øvrevik, 2006). Studies of mineral particles have demonstrated that toxic and carcinogenic effects are often related to the surface area of inhaled particles and their surface activity (Fubini 1997; Donaldson and Borm, 1998; Donaldson *et al*., 1998, 2006; Harrison and Yin, 2000). Particle surface characteristics are key factors in the generation of free radicals and reactive oxygen species formation and in the development of fibrosis and cancer by quartz (crystalline silica) (Fubini, 1997).

Particles are capable of generating or inducing generation of free radicals in humans, thereby leading to increased oxidative stress (Sørensen *et al*., 2003). Oxidative stress may damage cells and important molecules (Donaldson and Tran 2002; Dybing *et al*., 2005). Donaldson and Borm (1998) emphasized the ability of quartz to generate free radicals causing oxidative stress, modifying a range of substances that affect quartz surfaces in the process. Transition metals contribute to this reactive oxygen species generation through the Fenton reaction, thus enhancing particle toxicity (Fubini, 1999). In an experiment on human epithelial lung cells, Hetland *et al*. (2000) reported that the most potent particle samples exhibited a relatively high content of transition metals, such as iron. In this study the size distribution on different materials was the same, but the mineral content and metal composition differed. In the same experiment it was concluded that exposure to identical masses or surface areas resulted in the same order of potency among the different particle samples. Donaldson and Borm (1998) argued that it is

only the surface layer that interacts with lung cells and fluids. A change in chemistry of the layer could alter particle reactivity, but might impact only minimally on the bulk chemistry of the quartz. Experiments with external agents not in the dust have shown that such agents may coat the quartz surfaces and decrease its toxicity (Donaldson and Borm, 1998). Metals need only be present in trace amounts to generate inflammation via receptor mediated cell activation or via oxidative stress pathways (Donaldson and Tran, 2002).

The mineral particle itself needs not to be harmful to human health, but may act as a transporter of other substances into the body via inhalation (Gomes and Silva, 2007; COMEAP, 2010). These substances attached on the mineral particles can be endotoxins, metals and other substances, such as polycyclic aromatic hydrocarbons (PAH) from combustion processes, pollen and fungi. The chemical composition of the coarse PM is likely to vary spatially and temporally in addition to climate and time of day (Harrison and Yin, 2000; Brunekreef and Forsberg 2005, Wilson *et al.,* 2005). Both the particle core, organic and inorganic substances on the particles, particle composition and biosolubility have shown to affect allergic sensitization (Nygaard *et al*., 2004). Specific chemicals present in PM such as metals and polycyclic aromatic hydrocarbons (PAH) and their derivates, largely determine the toxic potency of PM (de Kok *et al*., 2006).

Airborne particles are recognized as important carriers of metals, and in urban areas road traffic is an important source both for particles and certain metals (Sternbeck *et al*., 2002; de Kok *et al*., 2006). The vehicle itself (e.g. wear products from brake linings, tyres, coach and combustion products from fuel and oil) and the pavement wear contribute to the composition. Resuspension processes have major effects on the presence of many metals and larger particles in air close to roads (Berube *et al.,* 1997; QUARG, 1996; Sternbeck *et al*., 2002). Transition metals contribute to particle-induced reactive oxygen species (ROS) through the Fenton reaction (Hetland, 2001).

Specific heavy metals attribute to the toxicity of PM as seen in many recent studies. These studies provide evidence that particle-associated metals contribute to health effects of PM (Armistead and Brunkreef, 2009; Donaldson and Borm, 2010; Lipman, 2010). Heavy metals are considered toxic components of PM and they are responsible for a variety of pathological changes in living organism (Donaldson and Borm, 2010). Particles inhaled or ingested pose a substantial threat with potential of releasing accumulated heavy metals into the bloodstream and distributed within the body.

Research has linked lead, cadmium, nickel and arsenic in consequence of their toxicity and potential adverse health effects to an exposed population (Armistead and Brunkreef, 2009; Donaldson and Borm, 2010; Lipman, 2010). Exposure to such metals has been linked to substantial health risk in terms of their carcinogenic effects. Risks of developing cancer due to PM has become one of the most serious and relevant issues in air pollution health risk assessment (WHO, 2007; Sadovska, 2012). Lead exposure has been linked to possible source of tumors, developmental and neuro-behavioural effects on fetuses, infants and children, there

is also evidence of elevated blood pressure in adults (WHO, 2007). Cadmium is recognized as one of the most noxious pollutants in the environment (Yu, 2001). Toxicity of Cadmium leads to accumulation in soft tissues (liver and kidneys) and mineralizing tissues (bones). Key health endpoints include kidney, bone damage and cancer. Chronic exposure from inhalation can also cause chronic pulmonary effects (Kampa and Castanas, 2008; Donaldson and Borm, 2010). Effects of nickel Inhalation may lead to nasal and pulmonary tumors (Donaldson and Borm, 2010).

2.5 Airborne particulate matter

This study concentrates on anthropogenic sources of particles released into the atmosphere due to the potential health effects discussed. Several stationary and mobile sources can be attributed to this with the major mobile source being road transport (Greenwood *et al*., 1996; Allen *et al*., 2001; Kumar and Britter 2005). The other main sources are from burning of fuels for industrial, commercial and domestic purposes. Anthropogenic activities related to construction and quarrying also produce high concentrations of particulate matter. Natural contributions of particulate are produced from sea spray, volcanic activity, forest fires and dust from the Sahara Desert travelling vast distances (Namdeo and Colls, 1996). These particles tend to be coarse compared to finer anthropogenic-formed particles. Secondary particulate matter is formed from chemical reactions of the gases NH_3, SO_2 and NO_x released into the atmosphere (Phalen, 2002; Wilson *et al*., 2004). The chemical composition includes sulphates, nitrates, ammonium, sodium chloride, elemental and organic carbon, magnetic spherules and several minerals (Allen *et al*., 2001; Phalen, 2002; Kukier *et al*., 2003; Matthias, 2007).

The composition of atmospheric particles is influenced by a balance between sources, chemical transformations in the atmosphere, long-range transport effects and removal processes (Harrison *et al*., 1997; Morwaska and Zhang, 2002; Celis *et al*., 2004; Schmeling, 2004). Particulate pollution episodes are influenced in several ways with strong traffic related emissions regularly attributed to pollution episodes in urban environments (Charron, 2007). This combined with poor atmospheric conditions (e.g. calm winds and temperature inversions); and natural sources of particles (e.g. wind-blown dust, sea salt) can further increase particle concentration levels (Deacon *et al.,* 1997; Smith *et al.,* 2001; Vardoulakis, 2008; Mugica *et al*., 2009).

2.5.1 Anthropogenic sources of particulate matter

All combustion and metallurgical processes and many other industrial operations lead to the emission of particles into the atmosphere. Road traffic contributes on average 25% of total PM_{10} concentrations in the UK. However, with a marked increase in high traffic density in urban areas, concentrations can reach 80% (AEAT / NETC, 2004). $PM_{2.5}$ and PM_{10} have also been closely related to urban sites, but not to rural due to the close proximity and traffic density of urban areas (Chen, 2007). Stationary sources can be classed as industrial, commercial and domestic processes, these include power stations, refineries, iron, steel, oil and gas industries. High temperature metallurgical processes, coal burning and refuse incineration cause the

formation of fine metal-rich particles by the condensation of cooling vapours. The inorganic ash spheres are amorphous, comprising mostly of aluminsilicate glass and containing calcium, iron, magnesium and alkali metals. Within this matrix, there are mineral phases, consisting of high temperature phases of quartz (SiO_2), magnetite (Fe_3O_4), hematite (Fe_2O_3) and maghemite (γFe_2O_3) (Fly Ash Resources Centre, 1999). Despite the best efforts of arrestment plants, a small proportion of such particles inevitably enter the atmosphere (AQEG, 2011). Construction activities and weathering of building material within urban areas contributes quartz sand, concrete and cement particles to PM. In urban areas undergoing extensive development, the volume of building material of PM can be large, and may have important consequences for air quality (Perry and Taylor, 2007). AQEG (2005) identified road traffic emissions as the main primary contributor of PM_{10} in urban areas and will be discussed further.

2.5.2 Road traffic contribution

Road transport is the major contributor of PM in urban areas (Quarg, 1996; COMEAP, 2012). Forming 25% of PM nationally, it should be noted that this is a national average, and in urban areas, high traffic density can increase this value to <80%. Diesel fuel combustion is the single most significant contributor of fine particulate material to urban areas (Berube *et al*., 1997). Diesel engines are of particular significance as they emit particulates at a far greater rate than petrol or spark ignition engines, with typical emissions being 10-100 times greater than comparable petrol engines (Sagai and Ichinose, 1994; Kittleson, 1998). The combustion of hydrocarbons is ideally represented by the conversion of fuel primarily to CO_2 and H_2O (Bockhorn, 1995). However, combustion is often incomplete due to insufficient oxygen to convert all available fuel, which leads to the formation of by-products such as hydrogen, carbon monoxide and particulates. Haywood (1988) described particle formation beginning with the creation of carbonaceous material (soot) in the cylinder. In addition, several studies show that almost 100% of diesel particulates are <10 µm in diameter (Kleeman *et al*., 2000). Figure 2.6 illustrates the typical sources and types of PM from road traffic.

Although the efficiency of diesel is well noted with higher calorific values during combustion, particulate emissions from diesel engines are high due to incomplete combustion, when there is insufficient oxygen to completely burn a droplet of fuel. This typically only happens at full power or heavy load conditions. The outside of the fuel droplet starts to burn but then oxygen levels inside the engine drop to the point that the inside of the droplet forms into a tiny lump of carbon rather than being burnt. A cloud of these lumps of carbon coming from the tailpipe then constitutes diesel smoke. The EU have implemented regulations to control diesel emissions (EU 715/2007), which regulates the fitting of catalytic converters and particle filters and controls emissions of PM to 0.005 g/km for passenger vehicles (Figure 2.7).

Condensation reactions of gas-phase species, such as unsaturated hydrocarbons and PAHs, lead to the appearance of the first recognizable solid material (soot spheres) at combustion temperatures of 730–2530^{o}C. A phase of particle growth then follows inside the cylinder that includes surface growth of spherules by absorption of gas-phase components.

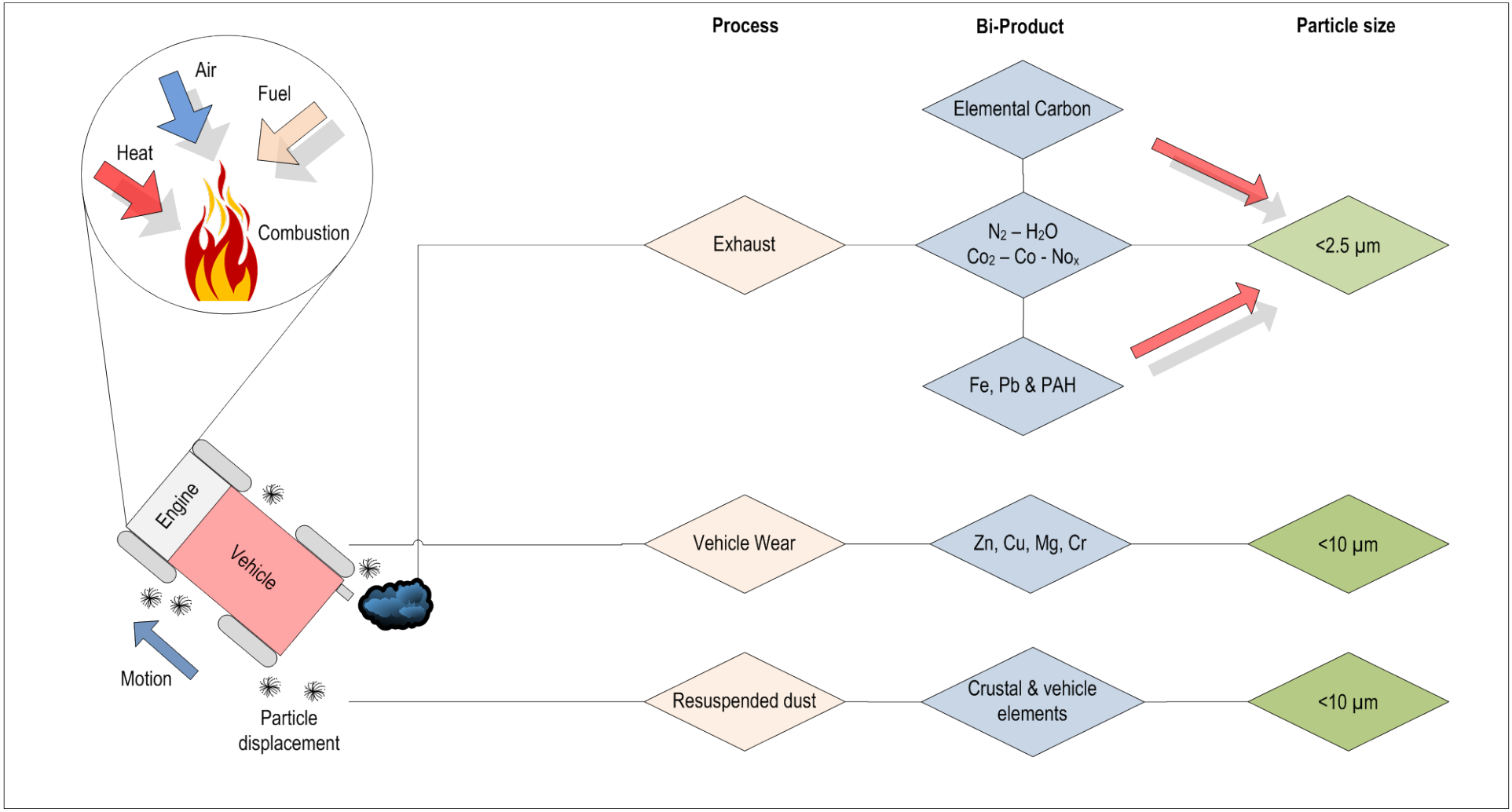

Figure 2.6 Diagram of sources of particulate matter from road traffic (Source: adapted from Bockhorn, 1995; Harrison, 1995).

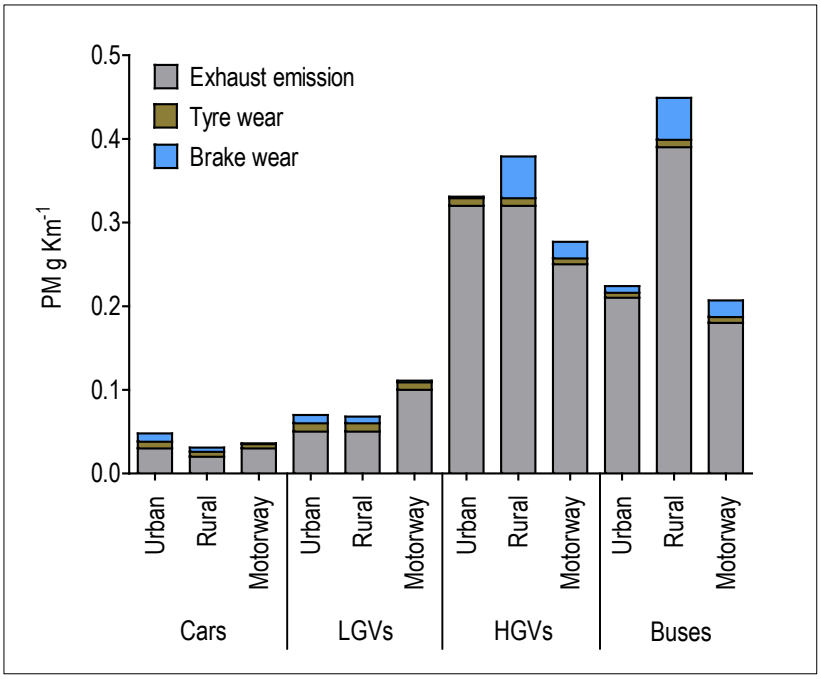

Figure 2.7 Mean PM_{10} emission factors for exhaust, tyre and brake wear in the UK (Source: AQEG, 2005).

At temperatures of 500°C particles are principally clusters of spherules with individual diameters of 15–30 nm. Once these clusters have left the cylinder they are then subject to a further mass addition process as the exhaust gases cool. As temperatures fall <500°C, particles become coated with absorbed and condensed high-molecular weight organic compounds. A part by-product of particulate matter are polycyclic aromatic hydrocarbons (PAH) and are a major health concern, with several PAHs known to be carcinogenic and capable of forming more toxic compounds when metabolised (Riddle, 2007). Harrison (1995) described four primary pollutants from motor vehicles:

1. Carbon monoxide.
2. Oxides of nitrogen (NO and NO_2).
3. Particulate matter.
4. Volatile organic compounds (e.g. benzene, 1-3-butadiene).

Road traffic emissions generally emit particles in the PM_{10} size range of which 25% are <10 µm, 38% <1.0 µm and 52% <1.0 µm (by volume). Most (>90%) particulates emitted from diesel engines are in the <1 µm particle size fraction (McClellan, 1989). Most mass is in the 0.1–1.0 µm "accumulation" size fraction, while most particles are in the <0.1 µm "ultrafine" or "nanoparticle" fraction (Kittelson, 1998). A given mass of very small particles contains more particles with a corresponding larger surface area, than an equivalent mass of larger particles. Consequently, a given mass of ultrafine particles will impact a larger surface area of lung tissue than will an equal mass of larger particles, leading to more extensive exposure of lung tissue (Oberdörster, 1995).

The following factors affect the final physico-chemical characteristics of diesel engine particulate (DEP) (Bartlett *et al*., 1992):

i. Chemical composition of fuel and lubricating oil.
ii. Operating conditions of the engine (i.e. engine revolutions and load).
iii. Engine design and wear.

Automobiles also produce particulates through tyre and brake wear. Particles are produced mechanically due to the rolling shear of the tyre on the road surface. Tyre tread which wears to produce dust, is normally composed of co-polymers of natural rubbers, polyisoprene rubber, butadiene rubber and styrene-butadiene rubber. The composition is obviously one of the main determinants of the chemical composition of road particulates. The type of rubber or the blend of rubbers used in manufacture of the tyre depends on factors such as the physical strength and wear resistance required by the vehicle. The quantity of particulate generated is highly dependent upon several factors, including driving conditions (e.g. acceleration, average speed, braking), tyre conditions (pressure, age of tyres,) and type of road surface (asphalt or concrete) (Abu-Allaban *et al*., 2003). Several authors have attempted to quantify the amount of particulates generated by tyre wear. The Air Quality Expert Group (AQEG, 2005) gives values for PM_{10} emissions from car tyres as 0.00874g km^{-1} (Figure 2.7), whilst values as high as 0.09 g km^{-1} have been reported (Wolfgang *et al*., 1993). Nicholson (2000) estimated a mean PM_{10} emission factor of 40 mg km^{-1} for the UK, based on the current UK mix of vehicles. In general it is believed that particulates produced from tyre wear are unlikely to be <2.5µm diameter due to the physical nature of the mechanisms leading to their generation. Brake lining dust is produced under forced deceleration, vehicle brake linings are subject to large frictional heat generation and associated wear. This mechanical process generates particles from both brake linings and brake surfaces. Because brake manufacturers use many different materials for the manufacture of brake linings, the dust may contain various contaminants. AQEG (2005) attempted to quantify emissions from brake linings and suggested a value for cars of 0.0177 g km^{-1}.

2.6 RDS in the urban environment

PM_{10} and $PM_{2.5}$ have been measured extensively in urban air, and a major component of these particles, especially those >2.5 µm, can be derived from road deposited sediment (RDS) (Hosiokangas *et al*., 1996; Allen *et al*., 2001). RDS is composed of a wide range of sediment grains, which are typically dominated by quartz, clay and carbonates, due mainly to underlying parent material (Perry and Taylor, 2007). In addition, abundant anthropogenic grains are present, including glass particles from industrial processes and high temperature combustion, metal slags, cement grains, metallic fragments and iron oxide particles (Perry and Taylor, 2007).

Road deposited sediments are characterized by short residence times, although they may contain substantial metal concentrations, RDS represent only rather recent accumulation of pollutants (Harrison *et al*., 1981). Allott *et al*. (1990) computed residence times of <250 days for street dusts in Barrow-in-Furness, UK, and statement that residence times *"will be site specific*

due to variations in the local processes''. However, material constituting street dust includes eroded urban soils, which may have historical associated metal pollution.

Currently, there is limited understanding of pathways that sediments take from their source to receiving water bodies, rate of transport and the location of short and long term sinks. The movement of sediment through the urban environment can be represented by the *'urban sediment cascade'* (Figure 2.8) (Charlesworth and Lees, 1999). The urban sediment cascade is a dynamic system which recognizes relationships between sediment sources, transport mechanisms and sediment deposition. The bulk of sediment transport in the urban environment occurs through the action of water, but local distribution upon street surfaces may also occur by wind (Perry and Taylor, 2007).

RDS characteristically exhibits high metal concentrations, in most cases significantly above average natural background levels, an aspect of which most research has been directed (Harrison, 1979; Beckwith *et al*., 1986; Leharne *et al*., 1992; De Miguel *et al*., 1997; Kim *et al*., 1998; Robinson *et al*., 2000; Charlesworth *et al*. 2003; Robertson *et al*., 2003; Sutherland, 2000; Shi *et al*., 2008; Fujiwara *et al*., 2011; Trang and Lee, 2011). These metals consist of iron rich combustion particles (mostly iron-oxides), lead, copper, zinc and other trace metals (Please refer to Table 1.5). Studies show clear spatial distributions of metal concentrations in RDS (De Miguel *et al*., 1997; Charlesworth *et al*. 2003; Robertson *et al*., 2003). Spatially metal concentrations are higher in inner city sites compared to outer city, with different hotspot locations for different metals, reflecting the contrasting levels of vehicular activity (Nageotte and Day, 1998; Charlesworth *et al*., 2003; Robertson *et al*., 2003; Perry and Taylor, 2007; COMEAP, 2012). RDS also has the potential to reflect historical episodes of anthropogenic activity, as well as current traffic movements, industrial and urban processes.

The correlation of Fe, Pb, Zn, Cu and Ni are good indicators of anthropogenic sources within RDS (Robertson *et al*., 2003; Harrison *et al*., 2004). These elements contribute to RDS from combustion sources and mechanical abrasion (Perry and Taylor, 2007). In most cases, enhanced geochemical concentrations compared to background levels indicate anthropogenic influences. However, it is not necessarily high values that indicate anthropogenic influences, but the comparative ratios of elements. Correlations between geochemical concentration parameters can be used in urban studies to establish influencing factors (Harrison *et al*., 2003; Robertson *et al*., 2003). Due to the abundance and ease of collecting RDS, it is considered an ideal medium when investigating urban pollution.

2.6.1 Techniques used in RDS studies

Various techniques have been used to determine characteristics and provenance of RDS. Measurements of soil, street dust and sediments have been used to map areas polluted by industrial emissions, such as coal-burning power plants, lead ore smelters, and roadside pollution due to automotive traffic and other atmospheric pollution.

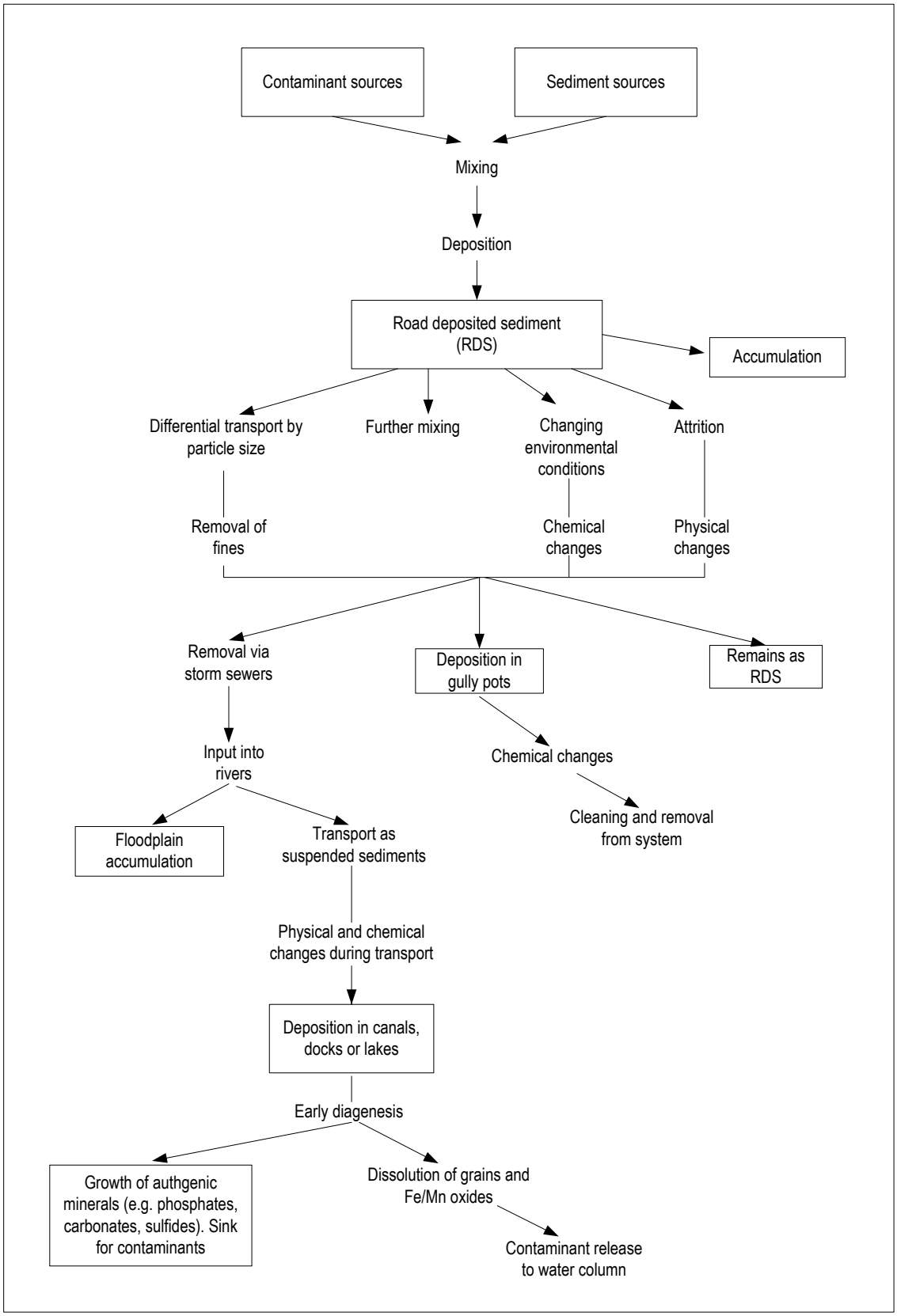

Figure 2.8 The urban sediment cascade, showing the pathways of, and change in, urban sediment particulates from sources to sink (Source: Charlesworth and Lees, 1999).

The most widely used techniques are: Inductively Coupled Plasma-Mass Spectroscopy (ICP-MS) (Amato *et al*., 2009; Anagnostopoulo and Day, 2006; Ferreira-Baptisa and Miguel, 2005; Herngren *et al*., 2006; Manno *et al*., 2006; De Miguel, 1997). Inductively Coupled Plasma-Atomic Emission Spectroscopy (ICP-AES) (Murakami *et al.,* 2007; Al-Khashmann, 2004; Sutherland and Tolosa, 2000), Scanning Electron Microscope (SEM) techniques (Abu-Allaban *et al*., 2003; Robertson *et al.,* 2003), sequential extraction methods (Kartal *et al.,* 2006; Tessier *et al*., 1979; Charlesworth *et al*., 2003; Robertson *et al.,* 2003), Graphite Furnace Atomic Absorption Spectrometry GFAAS (Anagnostopoulou and Day, 2006), Flame Atomic Absorption Spectrometry (FAAS) (Kartal *et al.,* 2006) and X-Ray Fluorescence (XRF) spectrometry (Abu-Allaban *et al.,* 2003; Amato *et al.,* 2009; Han *et al.,* 2008; Xie *et al.,* 2001). The results from a wide range of studies which investigated the geochemical composition of RDS are shown in Appendix 2.1. These studies successfully revealed heavy metal concentrations in soil and RDS, with a range of intensities indicating local and regional pollution. However, traditional geochemical methods (e.g. AAS, ICP-MS) are relatively complex, time-consuming and expensive due to the expensive instrumentation and additional expertise to operate. These instruments are bound to static locations and require specific laboratory environments and are therefore unsuitable for mapping or monitoring of large-scale pollution. Magnetic methods have also been used within similar investigations with success.

2.7 Proxy methods

A proxy method is an alternative approach that overcomes many of the problems associated with prospective studies. The advantages in urban sediment studies would be an alternative method which follows a universal trend, takes shorter analysis time, costs less and could be used non-destructively. Urban pollution detection using environmental magnetism may be a suitable tool for such studies, due to its ability to identify magnetic particles produced from anthropogenic processes. The use of mineral magnetic measurements follows some of the main advantages required for a reliable proxy, requiring short analysis time and being non-destructive and inexpensive.

Sediment-related analytical data can be strongly affected by particle size effects. Sediment contamination by heavy metals, radionuclides or persistant organic pollutants, can influence particle size effects and give false readings (Forstner and Salomons, 1980; Alloway, 1990). It is necessary, therefore, to first remove this influence by either normalizing data relative to the abundance of a specific particle size interval or fractioning samples.

Generally the finer a sediment, the greater its concentration of both natural and anthropogenic pollutants (Forstner and Salomons, 1980). This is typically due to finer grained sediments possessing larger specific surface areas, surface charges and cation exchange capacities, which enhance the extent of their preferential chemical absorption (Forstner and Salomons 1980). Because of the non-uniform distribution of pollutants over the range of sediment sizes, this causes variations in the chemical composition of sediments and thus the samples need to be corrected.

A range of processes have been developed to minimise these effects. The most accepted method is to normalize data, either relative to the abundance of a specific particle class or to conduct the analyses on a specifically separated particle size fraction e.g. <16 μm (Klamer *et al.* 1990), <20 μm (Ackerman *et al.* 1983), <50 μm (Aston and Stanner, 1982), <60 μm (Ackermann, 1980), <63 μm (Araujo *et al*. 1988), <75 μm (Clifton and Hamilton, 1982), <100 μm (Langston, 1986), <150 μm (Jones and Turki, 1997) or <250 μm (Hornung *et al*. 1989). Although these methods are considered reliable, they require additional, and in the case of fractioning samples into specific size ranges, time-consuming laboratory work.

Other techniques have also been adopted involving comparison with 'conservative' elements (such as aluminium (de Groot *et al*., 1982; Ergin *et al*., 1996), iron (Lapp and Balzer, 1993), caesium (Ackermann, 1980), rubidium (Middleton and Grant, 1990), or titanium (Forstner and Wittman, 1979)) or a correction factor for inert or organic material (Williams *et al.,* 1978). In general these approaches employ extrapolation from regression curves or a mathematical formulation of correcting particle size effects after analysis of bulk samples (de Groot *et al*., 1982; Covelli and Fontolan, 1997; Szava-Kovats, 2002).

Where a particle size proxy can be measured efficiently (that is, shorter analysis time or lower cost), it can offer potential advantages. However, to assess the suitability of an efficient particle size proxy, it is necessary that the nature of the relationship between the proposed parameters and particle size follow predictable patterns (like those of trace metals, radionuclides and BCPs with particle size).

Recently a magnetic approach has been suggested (Oldfield *et al*., 1993; Oldfield and Yu, 1994; Clifton *et al*., 1999; Booth *et al*., 2005; Zhang *et al*., 2007) for particle size proxy purposes. In the study of coastal sediments (Oldfield *et al*., 1993), marine, estuarine and fluvial sediments (Booth *et al*., 2005, Zhang *et al*., 2007), soil (Schmidt *et al*., 2005), road deposited sediments (Booth *et al.,* 2007) and roadside dust on tree leaves (Power *et al.,* 2006), mineral magnetic methods have been used as indicators of particle size and pollution. Although magnetic methods are simple, quick and non-destructive, such studies are relatively sparse (Zhang *et al*., 2007) with findings in current and other areas of study remaining to be validated.

2.8 Mineral magnetic techniques

Magnetic particles produced from anthropogenic processes have increased in abundance within the environment since the industrial revolution (*circa* 19th century), primarily from the combustion of fossil fuels (Petrovský and Ellwood, 1999; Dekkers, 1997; Dearing, 1999). Iron occurs as an impurity in fossil fuels which unburned, has low magnetization (Flanders, 1994). However, on combustion (industrial, domestic, vehicular) carbon and organic material are lost by oxidation and highly magnetic iron oxide (magnetite and haematite) spherules are produced (Kukier *et al.,* 2003; Muxworthy *et al.,* 2003; Petrovský and Ellwood, 1999). Combustion temperature and fuel type determines the magnetic grain size, mineralogy and concentration of these particulates (Flanders, 1984; Robertson *et al.,* 2003; Matzka and Maher, 1999). The

magnetic signature of anthropogenic combustion particulates can be separated from natural inputs within road deposited sediment to produce a pollution 'signal' (Locke and Bertine, 1986; Oldfield, 1991; Hay *et al.,*1997; Dearing, 1999; Rose *et al.,* 2004; Shilton *et al.,* 2005; Manno *et al.,* 2006; Booth *et al.,* 2005, 2007).

2.8.1 Magnetic minerals

Iron oxides are abundant in RDS and mineral magnetic analysis has been applied to study source apportionment in these sediments. Road deposited sediments receive a range of mineral magnetic grains originating from:

- Subaerial: detrial material originating from erosion of bedrock, subsoil and topsoil (Oldfield, 1999b; Hay *et al*., 1997; Xie *et al*., 1999b).

- Atmospheric: direct atmospheric fall-out of particulates from natural sources such as volcanic activity (Haberle and Lumley, 1998; Hallett *et al*., 2001), cosmic sources (Thompson *et al*., 1980; Taylor *et al*., 1996) and dust from storms (Dinarès-Turell *et al*., 2003). In addition there are anthropogenic pollutants from burning fossil fuels (Hunt *et al*., 1984; Oldfield *et al*., 1983; Oldfield and Richardson, 1990; Charlesworth and Lees, 1999; Xie *et al*., 2001).

- Authegenic (*in situ)* magnetic formation: subsequent to deposition of magnetic minerals, post-depositional diagenetic processes can alter magnetic assemblages, e.g. bacterial magnetosomes (Oldfield, 1999; Bazylinski, 1996; Snowball, 1994).

The application of environmental magnetic techniques can discriminate between these sources, by investigating mineral assemblages within sediments. The application of particularly heavy mineral analysis in road deposited sediments has enabled determination of anthropogenic contributions (Xie *et al* 1999; Charlesworth and Lees, 2001; Kim *et al*., 2009) and explored relationships of heavy minerals to source areas and their influence on urban sediments (Beckwith *et al*., 1986; Charlesworth and Lees, 2001). In the absence of other influences, the assemblage of minerals (and their magnetic behaviour) within a sediment represents a mix of all the source components from which it is derived. As such, it should be possible to use the magnetic character of sediment to relate it to its source or sources. In a similar manner, it should be possible to correlate sediments that are separated spatially but derived from the same source.

Mineral magnetic methods of sediment correlation or provenance determination use the same underlying principle as other geochemical or petrological approaches. Some measurable mineralogical or elemental property of the sediment is compared to an equivalent sediment for correlation purposes, or compared to potential source components to establish provenance (Walden, 1990). The expansion of geophysical technology for measuring the magnetic

remanence of rocks has enabled a series of techniques to evolve, which has allowed the magnetic properties of minerals to be interrogated. This advance in analysis of geological materials means that mineral magnetic studies can be used in other contexts. These include forensic techniques for examining diverse sedimentary environments (e.g. urban, desert, glacial, lakes, fluvial, coastal and estuarine. All geological substances possess magnetic properties, and it is the compositional characteristics of these materials that environmental magnetic measurements attempt to classify. With appropriate instrumentation these properties can be measured. Different mineral types have distinct magnetic properties, allowing identification and differentiation of rock and sediment types based purely on their magnetic characteristics (Thompson and Oldfield, 1986).

Figure 2.9 shows the sources of magnetic minerals in the terrestrial environment. Mineral magnetic analysis (Thompson and Oldfield, 1986; Oldfield, 1991; Walden *et al*., 1999) has now become established as a means of characterizing sediment samples and recent rapid growth has occurred in the application of mineral magnetic measurements as a means of studying environmental processes (Walden *et al.,* 1999).

2.8.2 Types of magnetic behaviour

The magnetic characteristics of rocks and minerals are extensively detailed in several applied physics texts (e.g. Nagata, 1961; Stacey and Banerjee, 1974; McElhinny, 1973; O'Reilly, 1976, 1984; Dunlop and Özdemir, 1997). Therefore, the aim of this section is to outline the types of physical magnetic behaviour possessed by geological materials.

The origins of the magnetic properties in any 'natural' substance are held within its constituent atoms. The behaviour of the electrons enables them to orbit the nucleus of an atom and to spin on their own axes. Both of these 'spins' produce magnetic moments (Smith, 1999). This magnetic phenomenon which occurs at the atomic-scale, is responsible for regimenting the entire magnetic behaviour of any natural material. As a result, the assorted combinations of atoms that compose the crystallographic structure of each mineral species promote distinct magnetic properties. These magnetic properties of individual minerals contribute to the overall magnetic properties of a sediment.

Three types of magnetic behaviour have been recognized: diamagnetic; paramagnetic and ferromagnetic (which includes anti-ferromagnetic, ferrimagnetic and canted anti-ferromagnetic). Summaries of the types of magnetic behaviour are presented in Table 2.2, together with examples of some of the mineral species that are indicative of each particular type of magnetic behaviour. These atomic and crystallographic structures exert only partial controls on the existence and behaviour of magnetic materials, as ferromagnets are also controlled by magnetic domains. These are regions of parallel atomic magnetic moment in a crystal (Smith, 1999). Essentially, this means that magnetic domains represent areas inside the crystal structure of materials, which can be magnetized in a particular direction. Consequently, magnetic domains are influenced by the *size* and *shape* of the magnetic domains within a crystal and by the *boundaries* (walls) between neighbouring magnetic domains in any particular assemblage.

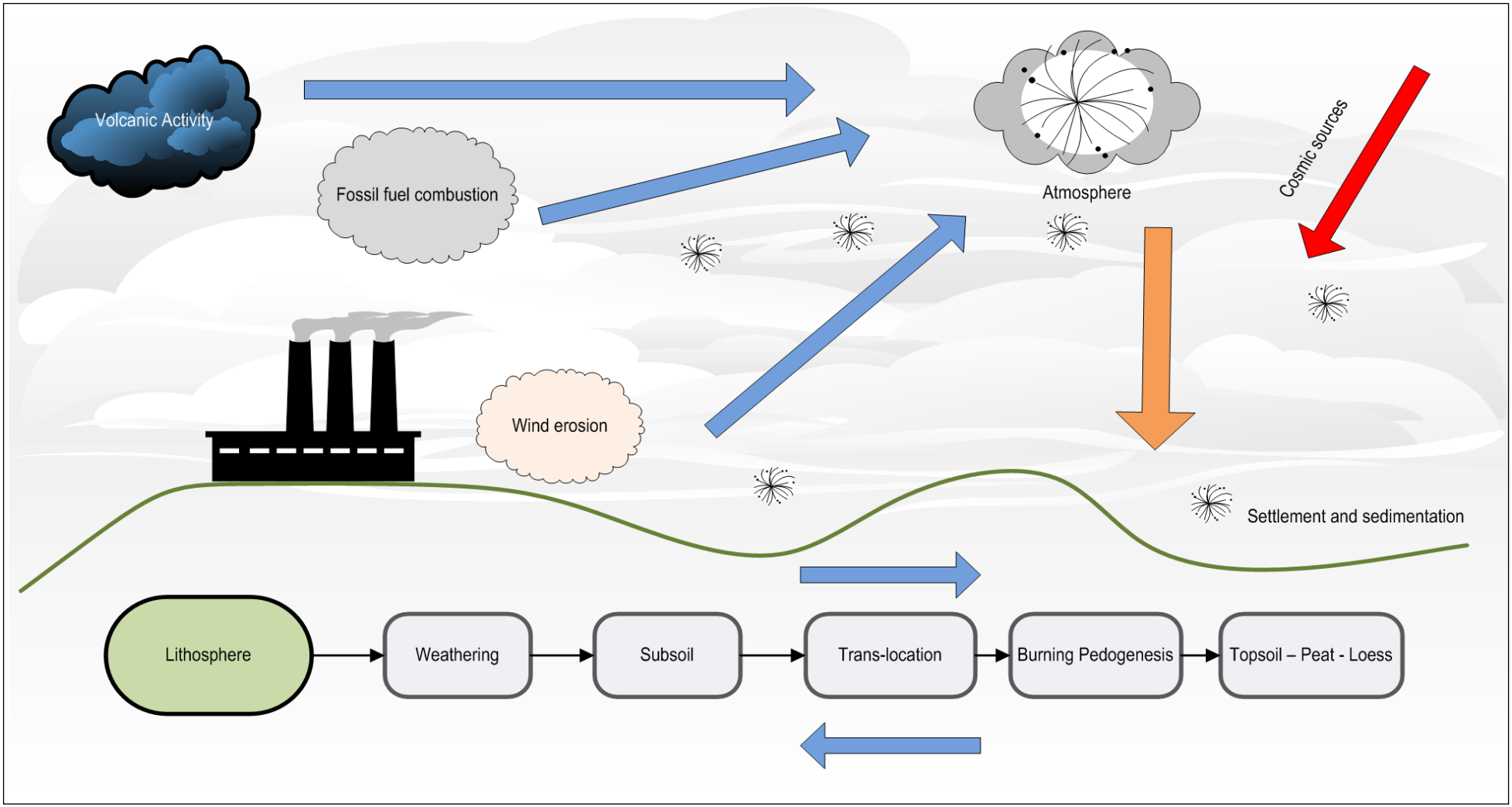

Figure 2.9 The variety of natural and anthropogenic sources of magnetic minerals (Source: Walden 1999).

Table 2.2 Explanation of types of magnetic behaviour (after Smith, 1999)

Type of magnetic behaviour	Explanation	Examples of mineral exhibiting behaviour.
Diamagnetism	Diamagnetism is exhibited by substances with no unpaired electrons in the various electron shells of their constituent atoms. Diamagnetic behaviour is only exhibited when an external (natural or artificial) magnetic field is applied; under such conditions the electron orbits become aligned so as to oppose the external field. This alignment of orbital planes, which would otherwise cancel, therefore produces a magnetic moment. When the field is removed this induced moment is lost and electron orbits precess, effectively at random, to positions giving no net moment. This type of magnetic behaviour is fundamental to all substances, but is weak and negative (relative to the direction of the applied field), and becomes masked if other types of magnetic behaviour are present.	Quartz, alkali-feldspar, calcite, halite, kaolinite.
Paramagnetism	Paramagnetism is a phenomenon produced where a substance has some atoms with unpaired electrons, so that a net magnetic moment exists (from both the electron spin and orbit). The interaction of these atomic magnetic moments with each other is very small because the distances between atoms with unpaired electrons within the substances are relatively large and, with no externally applied field, the magnetic moment of a paramagnetic substance is zero because of the random orientation of such magnetic moments. Within an applied field, the magnetic moments tend to align in the same direction as the applied field. On removing the field, the alignment disappears and no net moment remains. The paramagnetic effect is generally one or two orders of magnitude greater than the diamagnetic effect, but is still weak compared with the magnetic behaviour of an equivalent amount of ferromagnetic substance as described below.	Olivine, ilmenite, siderite, pyroxene, garnet, biotite, chamosite, amphibole, epidote, pyrite, illite, bentonite, smectite, chalcopyrite, dolomite.
Ferromagnetism	Ferromagnetism is a collective term for a group of related magnetic phenomena found in substances with unpaired electrons in atoms that are closely and regularly spaced and where, as a consequence, strong interaction (coupling) between unpaired electron spins occur. These crystalline substances are normally compounds of the transition metals (especially iron, cobalt or nickel). Unlike other forms of magnetic behaviour, the relationship of one atom to another is important and ferromagnetism is therefore a co-operative phenomenon (Nagata, 1961). Because of the interaction of forces between unpaired electrons in adjacent atoms, their spins become aligned, even in the absence of an externally applied field. This behaviour is called 'spontaneous magnetization'. It can occur in a small single ferromagnetic crystal, but would not be measurable in a sediment with randomly orientated grains where the net moment would be zero. In a crystal where atoms are organized in fixed geometrical relationships, the spontaneous magnetization normally forms in one particular direction with respect to the crystallographic axes; giving the so-called 'easy direction' of magnetization. This preferred orientation of magnetization leads to what is called magnetocrystalline anisotropy. The difference between the magnetization energy of the easy direction and that of the most difficult is known as the magnetocrystalline anisotropy energy. Different forms of ferromagnetic behaviour result from the arrangement of atoms in the crystal lattice and four conditions can be defined. In the case of (ferromagnetic) metals and their alloys, parallel coupling of all unpaired electrons may take place and this results in the development of strong magnetization. Such behaviour is known as 'ferromagnetism' (*senso stricto*)). In the oxides of these metals, because the coupling occurs via an intermediate oxygen atom, alternate layers of the crystal lattice become magnetised in opposite directions (anti-parallel). If these alternate layers or sub-lattices have equal numbers of unpaired electron sites, then the substance has no overall ferromagnetic behaviour. However, if the atomic magnetic moments of the two sub-lattices are unequal, then there is a net spontaneous magnetization. This behaviour is known as 'ferrimagnetism'. For various reasons, the sub-lattices in an otherwise anti-ferromagnetic arrangement may not be perfectly anti-parallel and a small residual spontaneous magnetization exists. This behaviour is called 'canted', 'non-colinear' or 'imperfect' anti-ferromagnetism. These contrasts between the magnetic properties of ferrimagnetic minerals (e.g. magnetite) and canted antiferromagnetc minerals (e.g. haematite) provides one of the key ways in which environmental magnetic measurements can be diagnostic of the iron oxide assemblage within a rock, sediment or soil. When a sample of a ferromagnetic substance, of any type, is placed in, or removed from, an externally applied magnetic field, complex patterns of behaviour are exhibited and these are related to the fact that ferromagnetic behaviour is not just controlled by a crystal form but by the presence of magnetic 'domains'.	Iron, cobalt, nickel. Magnetite, maghaematite, titanomagnetite, pyrrhotite, titanohaematite, greigite. Haematite, goethite.

There are three principal forms of magnetic domains in ferromagnetic materials: multidomain (MD), stable-single-domain (SSD) and superparamagnetic (SP). Summaries of the types of magnetic domains are presented in Table 2.3. Detailed explanations of magnetic domains are provided by Nagata (1961), Thompson and Oldfield (1986), Jiles (1991), Butler (1992), Lees (1994) and Smith (1999).

2.8.3 Mineral magnetic parameters

Those variables used in this study to characterise the mineral magnetic properties of environmental materials and an explanation of their interpretation are presented in Table 2.4.

2.8.4 Mineral magnetic methods as an indicator of particle size.

Relationships between mineral magnetic measurements and sediment properties have been explored, and studies have identified mineral magnetic measurements as a suitable tool for determining sediment provenance (Oldfield and Yu, 1994; Booth *et al*., 2005), sediment transport pathways (Lepland and Stevens, 1996), and as proxies for geochemical, radioactivity, organic matter content and particle size data (Bonnett *et al.,* 1988; Oldfield *et al.,* 1993; Hutchinson and Prandle, 1994; Clifton *et al*., 1997, 1999; Xie *et al.,* 1999, 2000, 2001; Zhang *et al.,* 2001, 2007; Shilton *et al.,* 2005; Power *et al*., 2006; Booth *et al.,* 2005, 2007; Pye *et al.,* 2007).

An association has been found between different sediment sizes and magnetic concentrations. Anhysteretic remanent magnetization (ARM) identifies fine grained magnetite (<0.1 μm) in clay and χ_{LF} measurements identify coarser multi-domain magnetite (<1.0 μm) in sands and coarse silts (Oldfield *et al.,* 1993). Clifton *et al.* (1999) investigated the relationship between χ_{LF} and sediments and found a close relationship between sand, medium silts and $\chi_{LF.}$ Susceptibility of anhysteretic remanent magnetization (χ_{ARM}) was strongly linked with clay and fine silts. Saturated isothermal remanent magnetisation (SIRM) was strongly associated with fine to medium silts (Table 2.5).

Booth *et al*. (2005) demonstrated an association between high magnetic concentration measurements and fine grained sediments (Table 2.6a). Zhang *et al*. (2007) found that χ_{ARM} and other mineral magnetic parameters could be used very effectively to normalise intertidal sediments for particle size effects (Table 2.7). Studies of Carmarthan Bay, the Gwendraeth Estuary and the Rivers Gwendraeth Fach and Fawr found that mineral magnetic data could be used as a particle size proxy (Booth *et al.,* 2005). However, its recommended the methods are used with caution, as the relationship between magnetic parameters ($\chi_{LF,}$ $\chi_{ARM,}$ and SIRM) and particle size was not strictly universal between different environmental settings (Table 2.6b). Research conducted on an investigation of mineral magnetic properties and soil; suggested magnetic measurements are unsuitable as a proxy for particle size normalization (Booth *et al.,* 2008). The unsuitability was attributed to mineral magnetic concentration measurements and textural property differences for particular sedimentary environments, even if the sample has been taken within the same sedimentary system.

Table 2.3 Explanations of the three principal forms of magnetic domains (after Lees, 1994)

Type of magnetic domain	Explanation	Identification characteristics
Multidomain	Multidomain behaviour is controlled by the movement of domain walls. On the application of a strong field, the domain with a magnetization in the direction of the field will grow at the expense of other domains. Similarly due to magnetization, initial changes will be reversible, while in stronger field changes in the positions of the domain walls will reach a new equilibrium for that field. On removal of the applied field the domains may remain in their magnetised position, thus causing the remanence to be held by the material. The material is 'saturated' when all the domains are aligned in the direction of the applied fields.	Low values of SIRM/χ and ARM/χ ratios, and high values of SIRM/ARM ratio.
Single-Stable-Domain	Single domain behaviour cannot be explained by the movement of domain walls since there are no domain boundaries. The single domain grain has an axis of easy magnetization when a field is applied. The direction of magnetization is forced into alignment with the field. The field required to do this may have to be very strong. The hysteresis properties of the grains will depend on the angle that the axis of easy magnetization makes with the field. Once the field is removed the magnetization returns to its original axis direction. An assemblage of single domain grains will then add or oppose each other in terms of magnetization (for reversible changes at low fields).	High values of SIRM/χ and ARM/χ ratios, and low values of SIRM/ARM ratio.
Superparamagnetic	As grains become smaller, their magnetic properties become time dependent and changes in remanence occur in minutes and seconds; these grains are superparamagnetic or viscous. Such small grains have a thermal energy that can be as great as their magnetic energy; they are magnetically unstable and do not exhibit hysteresis or any remanence property. The thermal energy can also overcome an applied magnetic field that causes serious implications for measurements. However, this time dependency can be used to advantage. Many of the affected grains are of secondary magnetite size and can be detected when making high frequency susceptibility field measurements. Whilst in an applied field the grains exhibit alignment to the field, upon removal thermal agitations destroy this alignment. The property of the grains is similar to the overall property of paramagnetism, but is stronger. Superparamagnetic grains have a greater effect on the magnetic susceptibility of a material than both multidomain and single domain grains. A phenomenon that causes many problems in the interpretation of magnetic results, especially in superparamagnetic grains, is that of magnetostatic interaction. This occurs because of grains lying close to each other may interact leading to demagnetization causing reduction of the overall magnetic moment.	Zero values of SIRM and ARM, with a disproportionately high χ value.

Table 2.4 Mineral magnetic variables used in this research and their basic interpretations (after Banerjee *et al*., 1981; King *et al*., 1982; Maher, 1988; Yu and Oldfield, 1989; Hutchinson, 1995; Walden *et al*., 1999)

Magnetic variables	Interpretations
χ	Mass specific *Magnetic Susceptibility* (χ): This is measured within a small magnetic field and is reversible (no remanence is induced). Its value is roughly proportional to the concentration of ferrimagnetic minerals within the sample, although in materials with little or no ferrimagnetic component and a relatively large antiferromagnetic component, the latter may dominate the signal (Walden *et al*., 1999).
$\chi_{FD\%}$	Frequency dependent χ is a measure of occurrence of very fine magnetic domains on the superparamagnetic (SP) to stable single domain (SSD) boundary (Table 2.9).
ARM	Mass specific *Anhysteretic Remanent Magnetization* (ARM): For this work ARM was induced in the samples by combining a peak AF field of 100mT with a DC biasing field of 0.04mT (Yu and Oldfield, 1989). It is particularly sensitive to the concentration of magnetic grains of SSD size (Banerjee *et al*., 1981; King *et al*., 1982), e.g. ~0.03-0.06µm (Maher, 1988).
χ_{ARM}	A more accurate parameter than ARM as corrected by the biasing field. This ratio is "highly selective of true stable single domain ferromagnetic grains in the 0.02-0.4µm range" (Walden *et al.,* 1999). Values drop dramatically with the presence of ferromagnetic grains above and below this size range.
SIRM	Mass specific *Saturation Isothermal Remanent Magnetization* (SIRM): This is the highest amount of magnetic remanence that can be produced in a sample by applying a large magnetic field. It is measured on a mass specific basis. In this study a saturating field of 0.8T has been used and will produce saturation in most mineral types. However, some antiferromagnetic minerals may not be saturated in this field (e.g. goethite) and therefore this parameter is often called IRM_{800mT}. The value of SIRM is related to concentrations of all remanence-carrying minerals in the sample, but is also dependent upon the assemblage of mineral types and their magnetic grain size (Walden *et al*., 1999).
Magnetisation variables (forward field ratios) i.e. %soft and %hard	It is instructive to calculate the percentage of the final SIRM acquired at selected, increasing field strengths. Forward field ratios are shown against a horizontal scale of percentage saturation at 20mT ($100(IRM_{+20mT}/SIRM)$) and 300mT ($100(IRM_{+300mT}/SIRM)$). These values help discriminate between ferrimagnetic and imperfect antiferromagnetic mineral types, since the latter are likely to be the main contributors to remanence acquired above the second field (Hutchinson, 1995). The amount of remanence acquired in an initially demagnetised sample after it has experienced a field of 20mT. At such low fields, the magnetically 'hard' canted antiferromagnetic minerals such as haematite or geothite are unlikely to contribute to the IRM, even at fine grain sizes. The value is therefore approximately proportional to the concentration of the magnetically 'softer' ferrimagnetic minerals (e.g. magnetite) within the sample, although also grain size dependent. At high fields of 300mT, the magnetically 'soft' ferrimagnetic minerals are likely to have been saturated and any subsequent growth of IRM will be due to magnetically 'harder' canted antiferromagnetic component within the sample. The value is approximately proportional to the concentration of canted antiferromagnetic minerals (e.g. haematite and geothite) within the sample.
Backfield Ratios i.e. S-ratio (IRM_{-100mT})	Various demagnetization parameters can be obtained by applying one or more reversed magnetic fields to a previously saturated sample. The loss of magnetization at each backfield can be expressed as a ratio of $IRM_{backfield}$/SIRM, and therefore gives a result between +1 and -1 normalized for concentration. Such ratios can be used to discriminate between ferrimagnetic and canted antiferromagnetic mineral types. For example, using the 100mT backfield ratio, minerals which are relatively easy to demagnetise (e.g. magnetite) have relatively low values (referred to as 'soft' magnetic behaviour). Minerals that show a stronger resistance to demagnetization (e.g. haematite) show relatively high 100mT backfield ratios (referred to as 'hard' magnetic behaviour) (Walden *et al*., 1999).
ARM / χ	The ratio of these variables can indicate the concentration of ferrimagnetic grain size variations (e.g. a high ratio indicates the presence of SSD grains).
SIRM / ARM	In samples dominated by ferrimagnetic minerals, the ratio of these variables is indicative of relative magnetic grain size variations (e.g. a low ratio indicates the presence of SSD grains).
SIRM / χ	The ratio of these variables can be diagnostic of either magnetic mineralogy (e.g. a low ratio might indicate paramagnetic minerals, and a high ratio might indicate the importance of haematite or geothite) or where samples have similar mineral types and concentrations, it can be diagnostic of magnetic grain size variations (e.g. a high ratio indicates SSD ferrimagnetic grains, and a low ratio indicates the importance of superparamagnetic (SP) or multidomain (MD) grains).

Table 2.5 Significant particle size and mineral magnetic concentration associations found by Oldfield *et al.,* (1993) and Clifton *et al.,* (1999)

	χ_{LF}	$\chi_{ARM,}$	SIRM
Clay (<2μm)	×	✓	×
Silt (2-63μm)	✓	✓	✓
Sand (63-2000μm)	✓	×	×

Table 2.6 Significant particle size and mineral magnetic concentration associations found in marine, estuarine (a) and fluvial environments (b) (Booth *et al*., 2005)

(a)	χ_{LF}	$\chi_{ARM,}$	SIRM
Clay (<2μm)	✓	✓	✓
Silt (2-63μm)	✓	✓	✓
Sand (>63μm)	✓	✓	✓

(b)	χ_{LF}	$\chi_{ARM,}$	SIRM
Clay (<2μm)	×	×	×
Silt (2-63μm)	×	×	×
Sand (>63μm)	×	×	×

Table 2.7 Significant particle size and mineral magnetic concentration associations found in intertidal sediments by Zhang *et al.,* (2007)

	χ_{LF}	$\chi_{ARM,}$	SIRM
Clay (<2μm)	×	✓	✓
Silt (2-63μm)	✓	✓	✓
Sand (>63μm)	×	✓	✓

Mineral magnetic methods can become unsuitable as a particle size proxy depending on the nature of the environment. However, the relationship between magnetic and textural properties should be fully explored within differing sedimentary environments and field settings, and models should be further supported by fractionated samples and geochemical evidence before use as a proxy for particle size (Booth *et al.,* 2005).

Few studies have investigated the particle size and mineral magnetic associations in RDS. Mineral magnetic and particle size associations have been investigated on a small scale using RDS in the town of Southport (UK) (Booth *et al.*, 2007). A pilot study was conducted (n = 50 samples) where χ_{LF} had the strongest associations with RDS class sizes (Table 2.8). Power *et al*. (2006) used a novel approach by collecting particles from tree leaves. This proved a successful way of determining pollution concentrations along busy roads and analysing mineral magnetic and particle size associations (Table 2.9). Although initial studies proved successful, Booth *et al*. (2005, 2007, 2008) identified the need for further research in different sedimentary environments to check the consistency of the relationships.

Table 2.8 Particle size and mineral magnetic concentration associations found in RDS by Booth *et al*., (2007)

(a)	χ_{LF}	$\chi_{ARM,}$	SIRM
Clay (<2µm)	✓	✓	✓
Silt (2-63µm)	✓	✓	×
Sand (63-2000µm)	✓	✓	×
$PM_{1.0}$	✓	✓	✓
$PM_{2.5}$	✓	✓	✓
PM_{10}	✓	×	×

Table 2.9 Significant particle size and mineral magnetic concentration associations found on tree leaves (*Tilia europaea*) by a roadside by Power *et al*. (2006)

	χ_{LF}	$\chi_{ARM,}$	SIRM
PM_{10}	✓	✓	✓

To assess the appropriateness of mineral magnetic methods as an efficient particle size proxy it is necessary that the nature of the relationship between the proposed parameters and particle size follow a universal pattern. To date most work has not examined the extent to which mineral magnetic parameters could be used as a soil and road-sediment indicator of texture, which in-turn could possibly be linked as an airborne indicator of ambient PM. If associations are found and can be linked to airborne PM by ground collection methods, this could suggest the use of mineral magnetic measurements as a particle size proxy method. This would enable PM measurements to be taken with shorter analysis time, non-destructively and costing less than current methods. Therefore, this study addresses the primary issue of whether particle size-mineral magnetic associations exist within urban RDS over time and at different spatial scales.

2.8.5 Mineral magnetic methods as an indicator of composition.

As geochemical composition is also an important issue in regards to health, this study demonstrates an additional proxy addressing mineral magnetic and geochemical (heavy metal) associations. Correlations between mineral magnetic and geochemical concentration parameters have previously been used effectively as a proxy for heavy metal pollution and anthropogenic source in RDS (Guatam *et al.,* 2005; Kim *et* al., 2007; Yang *et al*., 2010) (Table 2.10).

In recent years the use of magnetic parameters as proxies for quantifying the contents of certain contaminants such as heavy metals in street dust, atmospheric particles or soil have been demonstrated on relatively small scales (road – inner city) (Shu *et al*., 2001; Robertson *et al*., 2003; Kim *et al*., 2007, 2009; Duan *et al*., 2010). Strong correlations were found between heavy metals and magnetic concentration parameters for topsoil, stream and marine sediments (Chan *et al*., 2001; Wang and Qin, 2006; Lu *et al*., 2006, 2008, 2009; Yang *et al*., 2007; Chaparro *et al*., 2008; Canbay *et al*., 2010). Robertson *et al.* (2003) studied the geochemical

and mineral magnetic characteristics of Manchester (UK) where he found high concentrations of heavy metals at road sides linked with ferromagnetic multi-domain (MD) mineral magnetic composition. These results also exhibited a clear spatial trend, whereby concentrations are enhanced in inner city samples. Table 2.11 shows typical χ_{LF} and SIRM concentrations found in urban areas.

Other studies have shown similar results where MD ferromagnetic characteristics are linked with urban RDS samples (Xie *et al*., 1999, 2001; Gautam *et al.,* 2005; Kim *et al*., 2007; Blundell *et al*., 2009; Yang *et al*., 2010). These MD characteristics are indicative of anthropogenic sources and are a consequence of the initial formation of particles during combustion. These studies prove that quantified relationships between magnetic parameters and heavy metals can be constructed based on appropriate indexes, but is an area of research that has not been fully explored. The reliability of mineral magnetic methods as an additional geochemical proxy has shown potential at small scales but must therefore be investigated at larger scales to access the suitability of wider spatial investigations. Advantages of further study will benefit the understanding of larger catchment characteristics and RDS dynamics. Proxy measurements could also provide vital pollution indexes of larger areas. This study will investigate the application of mineral magnetism to develop further associations with geochemical relationships at city wide, national and smaller localized spatial scales

Table 2.10 Mineral magnetic concentration and geochemistry correlations found in previous studies. (**p* <0.05; ***p* <0.01; ****p* <0.001)

Location (χ)	Fe	Mn	Zn	Cu	Pb	Ni	Author
Kathmandu (Nepal)	0.84***	0.76***	0.86***	0.74***	0.64**	0.60**	Gautam *et al*. (2005)
Seoul (Korea)	0.72***	0.41*	0.90***	0.79***	0.09	/	Kim *et al.* (2007)
Wuhan (China)	0.740**	0.349*	0.106	0.486*	0.035	0.351*	Yang *et al*. (2010)

Table 2.11 Mineral magnetic concentrations found in selected UK urban areas.

Location	χ_{LF} x $10^{-7}m^3kg^{-1}$	SIRM x $10^{-4}Am^2kg^{-1}$	Author
London	34.5 – 72.8	510	Beckwith *et al*, (1986)
Liverpool	50.28	/	Xie *et al*, (2001)
Manchester	27.1	286	Robertson *et al*, (2003)
Wolverhampton	58.83	595	Booth *et al*, (2005)
Southport	27.95	/	Booth *et al*, (2007)

Chapter 3
Methodology

Chapter 3 introduces details of the research, and methodological framework. Materials and analytical methods used during the project are presented. The sections are described in sequential order of completion, beginning with initial desktop urban environment determinations, followed by field sampling techniques, laboratory analyses, both statistical and geographical information (GIS) computation and subsequent modelling. Laboratory procedures were conducted at the University of Wolverhampton (UK) with random samples tested against known standard values at Birmingham University (UK) and Edge Hill University (UK). All techniques and procedures used for the duration of this work followed standard field and laboratory practises.

3.1 Site description and rationale for selecting Wolverhampton as main study area.

Wolverhampton is located to the north of the West Midlands conurbation, and lies on the edge of the Black Country, some 25km from the regional centre of Birmingham. Wolverhampton functions as a major centre within the Black Country and the northern part of the West Midlands, with an estimated population of 239,100 (Wolverhampton.gov.uk, 2012). The City benefits from good communication links, with access to the national motorway network provided by the M6 to the east, the M54 to the north, and the newly completed M6 Toll, which runs around the northern and eastern edges of the conurbation. Wolverhampton also has a mainline railway station which provides direct trains to Birmingham, London, the West Country and the north. Proposals are currently underway to introduce improvements to the railway station and its environment through the City Interchange Project. The Midland Metro a light railway system, currently connects Wolverhampton to Birmingham Snow Hill station. The City of Wolverhampton consists of the traditional central business district containing a portion of commercial industries. This central area is surrounded by the major road network which connects all surrounding areas. Surrounding the CBD are major residential areas which consist of pre-1900s housing and was originally housing for the engineering industries within the central city. Historically Wolverhampton's economy has been dominated by engineering and manufacturing industries but has now been replaced by the service sector, and is one of the main retail sectors within the West Midlands region.

Housing within the City centre mainly consists of terraced properties with frontages on the main walkways and roads. It is noted that the residential areas within the City are closely packed areas along main roads. Away from the central city area, the housing changes to semi-detached and detached housing with front gardens, including more spacious and pre-planned residential areas. Due to previous research, it has been noted that residents housed along and close to main roads are more susceptible to health complaints due to urban pollution (Edwards *et al*., 1994; Oosterlee *et al*., 1996; Wilkinson *et al.,* 1999). Since 1998, the City Council has completed periodic 'Review and Assessment' reports of air quality in Wolverhampton. This process has culminated in the decision of the Council to declare the whole City an ‘Air Quality

Management Area (AQMA)'. These reports are available on the Wolverhampton MBCs own Web site at: http://www.wolverhampton.gov.uk/ environment/pollution/air/quality/default.htm

The Environment Act (1995) provides local authorities (in Part IV) with duties in respect of local air quality management. District councils are required to periodically review and assess local air quality against the standards specified in national objectives, and where necessary, to declare air quality management areas (AQMA). In 1998 Wolverhampton City Council started a review of air quality in conjunction with the six partner Authorities in the former West Midlands County Area. The purpose of the review was to determine if the air quality objectives set out in the Government's Air Quality Strategy were being met. The third stage of the Review and Assessment (July 2001) concluded that '*there were no significant sources of benzene, 1,3-butadiene, carbon monoxide, and lead in Wolverhampton*'. Levels of these pollutants already meet the air quality objectives. The review completing the First Review and Assessment, concluded that there were significant sources of nitrogen dioxide, particles and sulphur dioxide within Wolverhampton.

The Assessment of Air Quality report in May 2004 featured a comprehensive assessment of air quality in Wolverhampton, using a combination of real-time continuous analysers and sophisticated dispersion modelling techniques. The report states '*The findings of the detailed assessment have confirmed that the objectives for PM_{10} and nitrogen dioxide were not being met at Lichfield Street Wolverhampton (City centre) and surrounding areas, and was deemed therefore necessary to declare this part of the City Centre an Air Quality Management Area (AQMA)*'. The Detailed Assessment also established that the PM_{10} objectives are being met at the junctions of Birmingham Road/Parkfield Road and Willenhall Road/Neachells Lane. The area studied (in the Detailed Assessment of Air Quality 2004) included Lichfield Street, Broad Street, Stafford Street, Princess Square, Princes Street and Queen Street within the City Centre. Lichfield Street is the City's main access route into the bus station with some 4000 bus movements per day and is included in the area to be affected by the City Interchange Project. The surrounding roads are also subject to high numbers of bus movements, as well as local shopping traffic using the many routes of the City. A comprehensive network of nitrogen dioxide diffusion tubes was established in this area for the first Review and Assessment. In addition, a further automatic monitoring station was located in Lichfield Street in order to undertake the Detailed Assessment of nitrogen dioxide (NO_2) and particles (PM_{10}).

The Detailed Assessment concluded that the annual EU 1999/30/EC NO2 objective was exceeded at the diffusion tube intensive survey areas (ISAs) along Lichfield Street, Princess Street and Queen Street. The EU 1999/30/EC 24hr PM_{10} objective was exceeded at the Lichfield Street automatic monitoring site. On the basis of this conclusion, an air quality management area, to comprise at least this area of the City, was required. The City Council also acts as a Local Site Operator for DEFRA in respect of the urban background site at St. Peter's Square, Wolverhampton (which contributes to the UK Automatic Urban and Rural Network,) and maintains further sites at the road junctions of Stafford Road (A449) and Church

Road, Bushbury; and Penn Road (A4039) and Goldthorn Hill, Penn Fields. With the exception of 2003 (exceptionally adverse weather conditions being responsible for poor air quality) these sites have continually shown compliance with air quality objectives. The 2008 Annual Progress Report (on air quality in Wolverhampton (Appendix 7.1)) confirmed potential exceedences of the annual nitrogen dioxide and PM_{10} objective at the Birmingham New Road, Stafford Road, St Peters Square and Lichfield Street. These additional areas are incorporated into the declaration of the whole City as an Air Quality Management Area (AQMA).

With the introduction of stricter legislation from EU 2008/50/EC, existing levels of $PM_{10,}$ nitrogen dioxide and sulphur dioxide reach upper limits and in some areas (Lichfield Street) have exceeded the new EU 2008/50/EC objectives for pollution. Within the City of Wolverhampton, as with most urban environments (including much of the West Midlands conurbation), the principal source of these air pollutants is transport. Whilst, in recent years, there has been increasing use of emissions control technology in vehicles (for example catalytic converters,) the number of vehicles on roads is continually increasing. In short, technological improvements only partially mitigate the effects of increased road traffic.

The study area chosen for this work has taken into account areas noted for air quality within Wolverhampton. This work will assess the appropriateness for using mineral magnetic techniques to determine particle size associations within RDS, developing an insight into the characteristics and linkages of RDS in Wolverhampton and the potential use of mineral magnetic measurements as a particle size proxy.

3.1.1 Sample design

As discussed in Chapter 2, RDS consists of a wide range of sources and can reflect land use and traffic intensity (Zhao, 2010; Chen *et al*., 2010). To address the potential mineral magnetic–particle size and geochemical relationships within urban areas, a strategy is used that incorporates a representative mix of land uses and traffic conditions.

Previous research shows spatial variability of mineral magnetic and geochemical concentrations within urban RDS environments. Several studies have used spatial design to identify sites of specific interest, Booth *et al.,* (2006) used city roads to contrast with rural roads, and examples by Yin *et al.* (2005), Banerjee, (2003) and Yang *et al*. (2010) used industrial and residential areas to analyse differences in RDS within unique environments. Some studies have investigated high volume traffic areas to develop a study area, with sampling taking place along busy urban roads (Abu-Allaban *et al.,* 2003; Giugliano *et al.,* 2005; Harrison *et al.,* 1981; Kim *et al.,* 2007), city centres (Charlesworth *et al.,* 2003; Anagnostopoulou and Day, 2006; Haugland *et al.,* 2007) and urban street canyons (Kumar and Britter, 2005). In addition to urban sampling design there have been numerous studies involving specific sites, such as schools, day care centres, parks and hospital gardens, which have been incorporated into sampling strategies (Anagnostopoulou and Day, 2006; Haugland *et al.,* 2007). Gautam *et al.* (2005) used arterial and inner roads as a focus within urban areas, while Sutherland and Tolosa (2000) based their strategy on a representative mix of traffic conditions.

Various sampling strategies and techniques have been employed when collecting RDS, some of the most common methods have utilized grid networks over an area, with the mid-point of each grid being used as the exact sampling point. Grid techniques have been used in various ways. Charlesworth *et al.* (2003) used a grid network to collect RDS from Coventry City centre, but also used specific points to further build on their data set. Ferreira-Baptista and De Miguel (2005) used a grid system, but sampled randomly within the grid squares (Figure 3.1); whereas, Hanesch *et al.* (2003), McIntosh *et al.* (2007) and Shah and Shaheen (2007) used a grid centre specific approach (Figure 3.2).

3.1.2 Sampling strategy selected in this work.

The sampling strategy used in this study included a combination of design features that have shown to work successfully in other studies (Sutherland and Tolosa, 2000; Banerjee, 2003; Charlesworth *et al.,* 2003; Gautam *et al.,* 2005; Yin *et al.,* 2005; Anagnostopoulou and Day, 2006; Booth *et al.,* 2006; Haugland *et al.,* 2007, and Yang *et al*. 2010). The urban area has been considered, with a mix of industrial, commercial and residential areas (Appendix 3.1). Traffic volumes and vehicle movements within the study area have also been considered, where influencing factors found in other studies (Sutherland and Tolosa, 2000; Haugland *et al.,* 2007), show spatial and diurnal traffic patterns.

Spatial and diurnal variation of traffic has been investigated as part of the sampling methodology for this study (Figure 3.3 Appendix 3.2). The data for traffic counts in Wolverhampton shows distinct areas of high and low activity, diurnally and spatially. Figure 3.3 shows high levels of traffic on the main arterial routes of the city. To the north and east, roads have high levels of traffic and suggest that these are the main entry routes into the city. In comparison most of the side roads display low vehicle numbers and suggests considerably quieter traffic conditions. The data suggest that most side roads in Wolverhampton are access routes to homes and that most vehicle traffic comes in from outside of the city.

Strategies involving grid techniques were explored but failed to provide sample points across all roads and areas of interest. Figures 3.1-3.2 show these sample arrangements with land use for Wolverhampton (Appendix 3.1). To include a representative mix of roads with differing traffic conditions a radial system was developed, using the city-hall as the centre point, and then incorporating the arterial road network leading out of a city or town to pinpoint sample sites. The system used takes into account the ‘in’ and ‘out’ traffic routes, which are seen within the traffic data. A radius increment of 500 m – to – 1 km – to – 2 km from the city centre was used and sample points were plotted at intersection points with main roads. This system enables all major road networks within the study area to be identified and studied. It also enables a system where a road could be monitored along its length over time, this successfully incorporated all arterial highways and, thus, supplied an even number of sample points along each of the roads. In-between the main road network a series of sample points were plotted, these were located as near to central in-between the main roads. The in-between points provided a series of low traffic urban roads to be included within the study area (Figure 3.4).

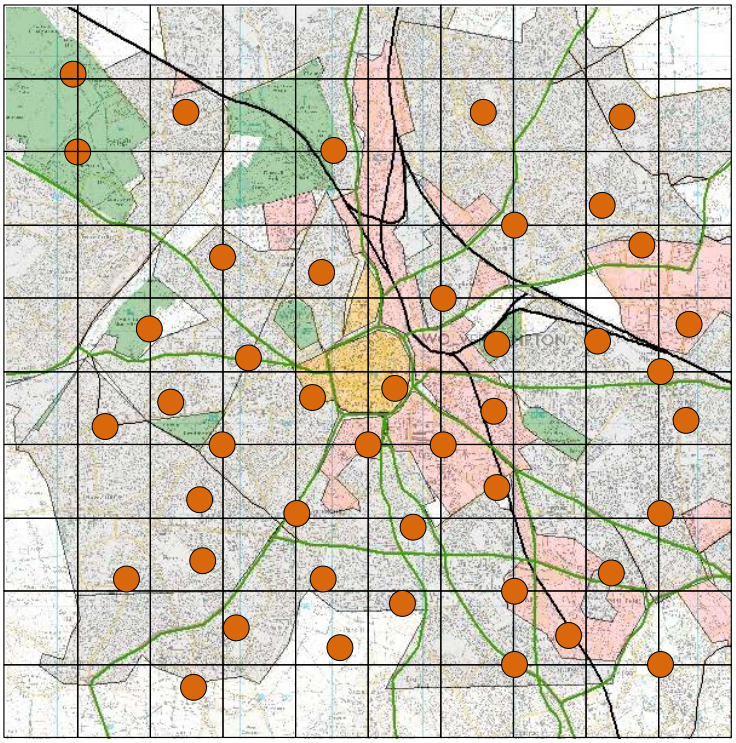

Sample point

Figure 3.1 Random grid technique used for spatial sampling (as used by Ferreira-Baptista and De Miguel, 2005).

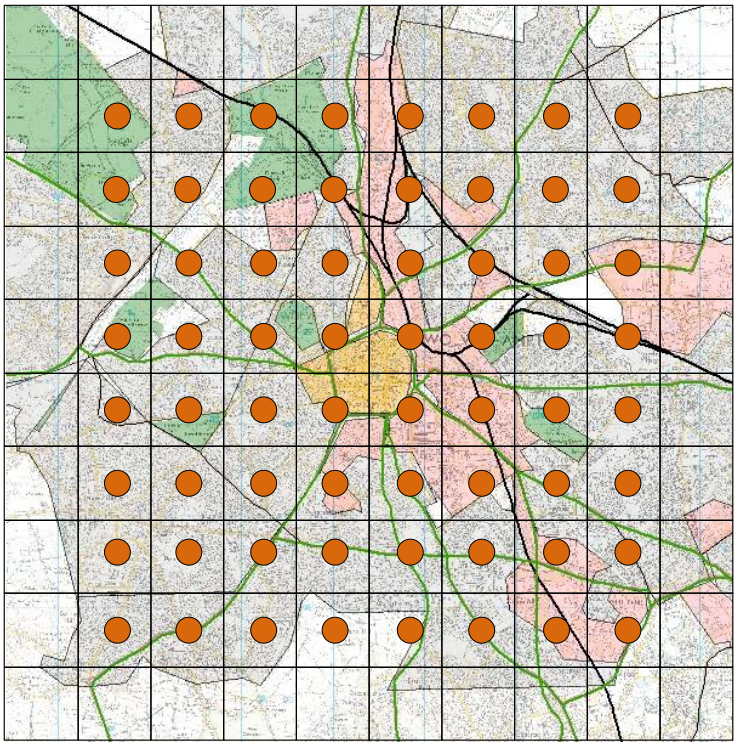

Sample point

Figure 3.2 Central specific grid technique used for spatial sampling (as used by Charlesworth *et al*., 2004).

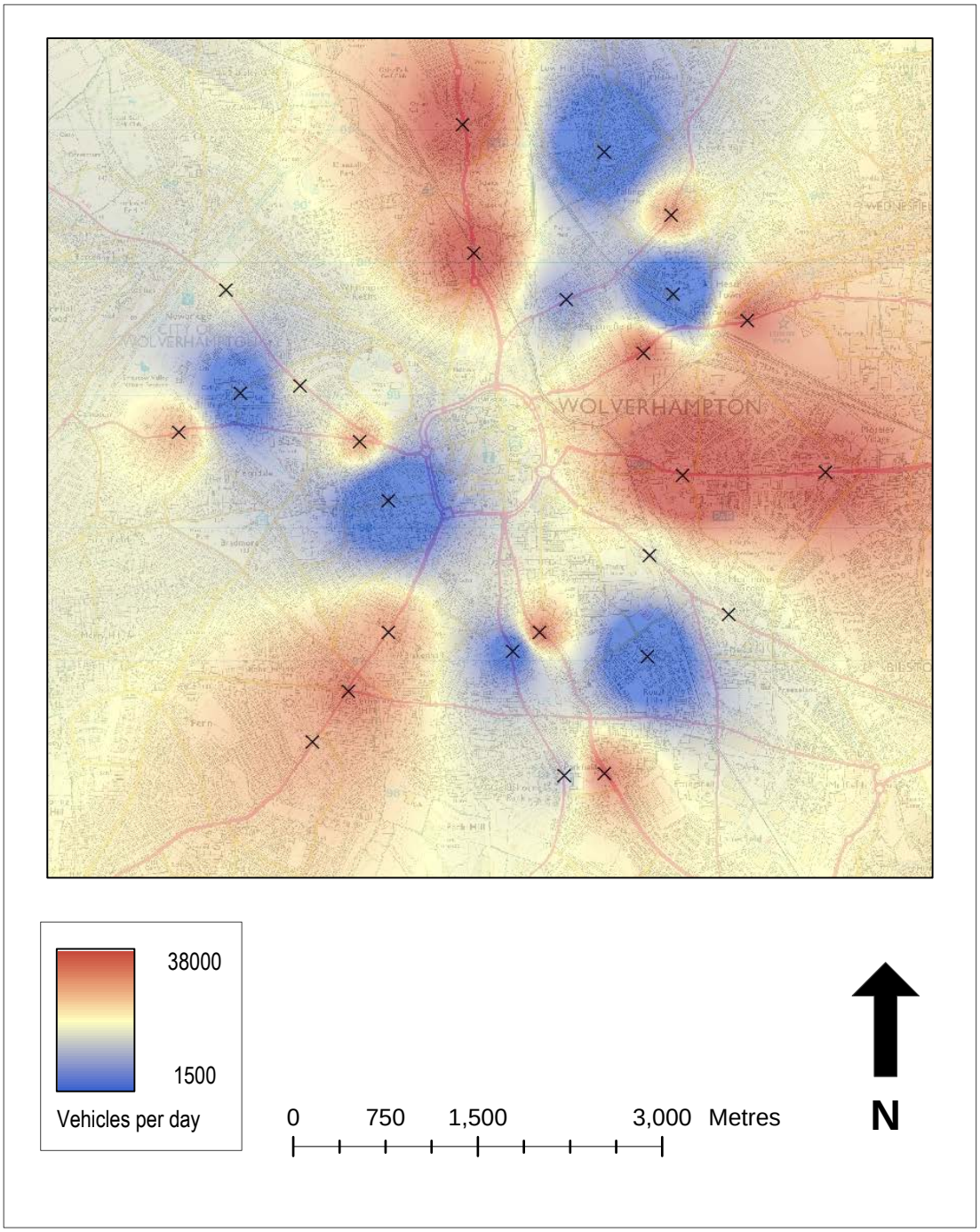

Figure 3.3 Spatial distributions of vehicle numbers per day (approx) in Wolverhampton during May 2007 (Data: Wolverhampton MBC 2008).

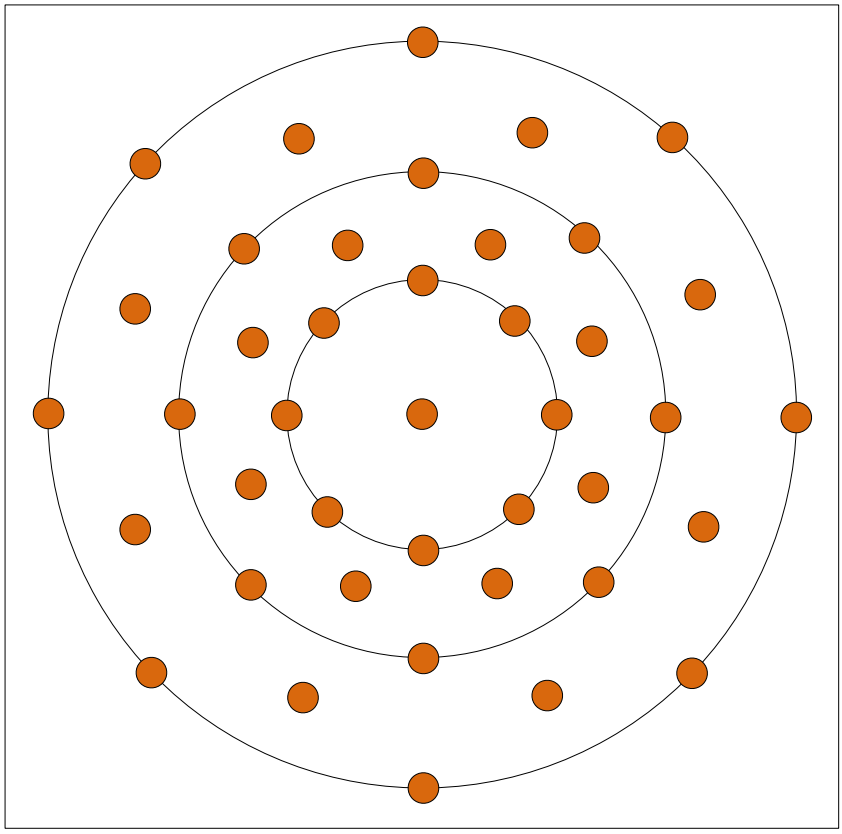

Sample point

Figure 3.4 Radial sampling technique utilized in this research investigation.

3.1.3 Sample collection methods

High and low volume sequential samplers (Figure 3.5) have been used extensively to study airborne particles. Traditionally pollutants and particulate levels have been monitored and measured using specialist equipment, Tapered Element Oscillating Microbalance (TEOM is a registered trademark of Rupprecht and Patashnick, Inc.) filter baser gravimetric method and sequential gravimetric analysers (Partisol) or ß-attenuation monitors are used to measure PM. Table 3.1 shows the location and monitoring capabilities of monitoring stations in Wolverhampton.

Table 3.1 Air sampling unit information for Wolverhampton (West Midlands Air Quality Group, 2009)

Area	ASU	Grid Reference	Pollutants Measured	Station type
Wolverhampton	Lichfield Street	391641 - 298785	PM_{10}, NO_x.	Roadside
	Penn Road	390375 - 302200	PM_{10}, NO_x, SO_2	Roadside
	Stafford Road	391259 - 298785	PM_{10}, NO_x, SO_2	Roadside
	Pendeford	390724 - 302697	PM_{10}	Background

(a) (b)

Figure 3.5 Air sampling units in Wolverhampton; (a) Site 41, Stafford Road, Wolverhampton, SO 391261 – 302206 (17/06/08); and (b) location of sampling point highlighted (red arrow), Site 42, Penn Road, Wolverhampton, SO 390379 – 296772 (13/05/08).

The TEOM is a gravimetric-based method for near-continuous measuring of PM_{10} or $PM_{2.5}$ concentrations. For this reason, it is also frequently used in epidemiological studies when daily or hourly concentrations are needed for the assessment of health effects of PM. The TEOM method measures the mass collected on an exchangeable filter cartridge by monitoring the corresponding frequency changes of a tapered element. The sample flow passes through the filter, where particulate matter is collected. As more mass collects on the exchangeable filter, the tube's natural frequency of oscillation decreases. A direct relationship exists between the tube's change in frequency and mass on the filter. Complete details of the TEOM method operation are available (Patashnick and Rupprecht, 1991). These are static sites which are used to monitor areas for long periods. However, these systems are costly due to initial equipment outlay, sensor arrays, power supply and air conditioning of the units, telephone connection for data links and service and maintenance contracts. Appendix 7.5 highlights the cost of operating such systems and is dependant on different factors which include, location, range of pollutants monitored and duration of operation.

More versatile and mobile methods have been used to study particulates and atmospheric pollution levels. High volume air samplers (GMWL-2000H, USA) (Shah *et al.,* 2004; Shah and Shaheen, 2007) have been used to analyse atmospheric trace metals in particulate fractions. The air sampler is statically placed on top of a building, but could be relocated if necessary. The use of microbalances have been used to determine $PM_{2.5}$ and PM_{10} mass in city centres utilizing Whatman PTFE filters using Rupprecht and Pataschnick Dichotomous Partisol-Plus Model (2025) Sequential Air samplers at ground level (1.0-2.0 m) (Yin *et al.* 2005). Abu-Allaban *et al.* (2003) used a Sierra-Anderson 254 PM_{10} inlet-cyclone to determine size fractions using sampling protocols as described by Watson *et al*. (1994). Various techniques have been employed when collecting sediment samples linked with anthropogenic pollution. Methods range from collection of top soils (Hay *et al.,* 1997; Haugland *et al.,* 2007) and bio-monitoring by use of dust settlement on vegetation (Lehndorff and Schwark, 2004; Hanesch *et al.,* 2003; McIntosh *et al.,* 2007). Beckwith *et al.* (1986) used a combination of vacuum and sweeping techniques, and the most effective method was road sweeping (Harrison *et al.,* 1981) (Table 3.2). Road sweeping techniques have been used successfully due to the ease and cost effectiveness of collecting RDS. However, there are some limitations in respect to collection due to the loss and re-suspension of small particles when sweeping. Although there is some loss of material, this is a negligible amount within the bulk sample. The method is a quick and adaptable approach, due to the availability of material at ground level. Therefore, RDS can be collected easily and efficiently at any location where particles settle.

3.1.4 Sample collection method selected in this work.

Sweeping techniques have been applied in this study, due to speed, cost and non-destructive methods that had been used in previous studies (Table 3.2). Typically road surface dust samples of 10-50g representing the net accumulation (Figure 3.6) (irrespective of weather conditions and foot traffic during the month), were collected by brushing with a small paint brush inside a 1 m^2 quadrat. RDS was transferred to clean, pre-labeled, self-seal, airtight plastic bags.

Table 3.2 Road deposited sediment, collection methodology of previous studies

Author	Method	Sampling	Location
Harrison (1981)	Dust pan and Brush	Edge of road	Cumbria (UK)
Fergusson (1984)	Dust pan and Brush	Footpath or gutter	London (UK) New York (USA) Halifax (Canada) Kingston (Jamaica) Christchurch (New Zealand)
Leharne *et al.* (1992)	Dust pan and brush	Gutter	London (UK)
Akhter and Madany (1993)	Dust pan and brush	Gutter	Bahrain
De Miguel *et al.* (1997)	Dust pan and brush	Path, road and gutter	Madrid (Spain)
Charlesworth and Lees (1999)	Dust pan and brush	Pavement and gutter	Coventry (UK)
Sutherland and Tolosa (2000)	Nalgene (Plastic) scoop	Gutter	Honolulu (Hawaii)
Xie *et al*. (2000)	Dust pan and brush	Pavement and gutter	Liverpool (UK)
Charlesworth *et al*.(2003)	Dust pan and brush	Pavement and gutter	Birmingham (UK)
Banerjee (2003)	Dust pan and brush	Road	Delhi (India)
Goddu *et al.* (2004)	Dust pan and brush	Gutter	Visakhapatnam (India)
Al-Khashman (2004)	Dust pan and brush	Kerb	Jordan
Ferrerira and de Miguel (2005)	Dust pan and brush	Road, pavement and gutter	Luanda (Angola)
Shilton *et al*. (2006)	Dust pan and brush	Unknown	Wolverhampton (UK)
Anagnostopoulou and Day (2006)	Scraping	Road	Athens (Greece)
Booth *et al*.(2006)	Dust pan and brush	Pavement	Wolverhampton and Dudley (UK)
Booth *et al.(*2007)	Dust pan and brush	Pavement	Southport (UK)
Han *et al.* (2008)	Dust pan and brush	Unknown	Xi'an (China)
Christoforidis and Stamatis (2009)	Dust pan and brush	Pavement	Kavala (Greece)
Taylor (2009)	Dust pan and brush	Gutter and road	Manchester (UK)
Lu *et al.* (2010)	Dust pan and brush	Pavement edge	Baoji (China)
Yang *et al.* (2010)	Dust pan and brush	Road	Wuhan (China)
Fujiwara *et al.* (2011)	Dust pan and brush	Pavement edge	Buenos Aires (Argentina)

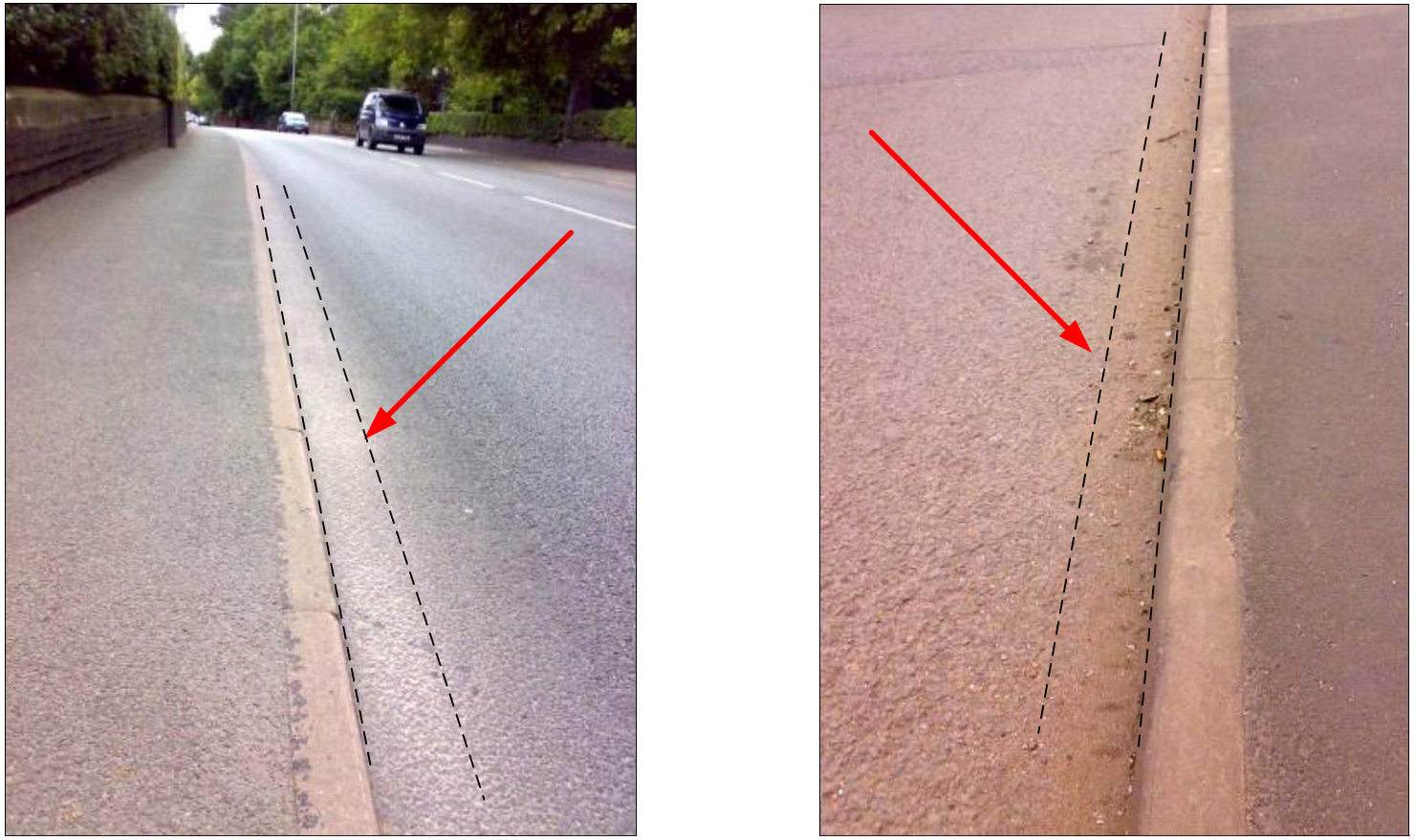

(a) (b)

Figure 3.6 RDS accumulation is shown. (a) Site 17, RDS accumulated by kerbside and shown as lighter area along kerb-stone. Penn Road Wolverhampton, SO 390685–297213, (14/07/08); and (b) Site 30, RDS accumulated along kerbside and shown as a darker conglomerate of a range of particles and debris. Thornton Road, Wolverhampton, SO 393809–298060, (14/07/08).

RDS was collected on a bi-monthly basis for two years (January 2008–January 2010 (n = 504 samples)), and followed the Construction Industry Research and Information Association guidelines (Butler and Clark, 1995). These guidelines state that the build-up of sediment on road surfaces reaches a maximum within 6-8 weeks, where sediment supply to road surfaces reaches an equilibrium state of sediment loss equaling sediment influx.

3.1.5 Wolverhampton study area

Sample collection within Wolverhampton City (West Midlands, UK) (specific sample sites are shown in Chapter 4, Figure 4.2; Appendix 3.3)) was undertaken on dry days throughout the study period (2007-09), following Xie *et al.* (1999). To ensure a constant and reliable collection method, it was necessary to collect after a minimum of two days of dry weather. This allowed time for accumulation of solids at ground level. Local meteorology was recorded at the University of Wolverhampton urban meteorological station located at Compton Horticultural Unit, so meteorological conditions could be included if appropriate in the final analyses.

3.1.6 West Midlands air sampling unit study area

Road Deposited Sediment (RDS) was collected from four Air Sampling Units (ASU) (Figure 3.7) within the West Midlands area (UK). Wolverhampton, Birmingham, Coventry and Leamington Spa were chosen due to their spatial location and PM_{10} monitoring capabilities (Table 3.3). Accessibility was important so that all samples could be taken within a 4-hour period, and ensured consistency of collection under environmental conditions. Four samples were taken from within close proximity of each site, ensuring a good cross section of material from the area, and represent the particulate fallout around the ASU. Sediment was collected at two-month intervals over a two year period using the same methods used in the Wolverhampton study. Published data for each ASU was also collected to form part of the data set (www.wmair.org).

Table 3.3 Air Sampling Unit Information for West Midland towns and cities (Source: Veritas, 2008)

ASU	Grid Reference	Pollutants Measured	Station type
Wolverhampton	SP916987	PM_{10}, NO_x.	Urban Centre
Birmingham	SP063869	$PM_{10,}$ NO_x, SO_2, CO, O_3.	Urban Centre
Coventry	SP328773	$PM_{10,}$ NO_x, CO, O_3.	Urban Background
Leamington Spa	SP319657	$PM_{10,}$ NO_x, CO.	Urban Background

3.1.7 Selected towns and places in the UK

Seven separate study areas were chosen within the UK (Figure 3.8) to investigate wider spatial patterns. Each site has either high, medium or low potential of PM concentrations (Figure 3.9, appendix 3.4), PM exceedences (Figure 3.10, Appendix 3.4 (Directive 1993/30/EC Table 1.6-1.7)), hospital admissions (asthma, cardiovascular diseases) (Figure 3.11), any other previously noted problem areas and the availability of data for the area, was also taken into consideration.

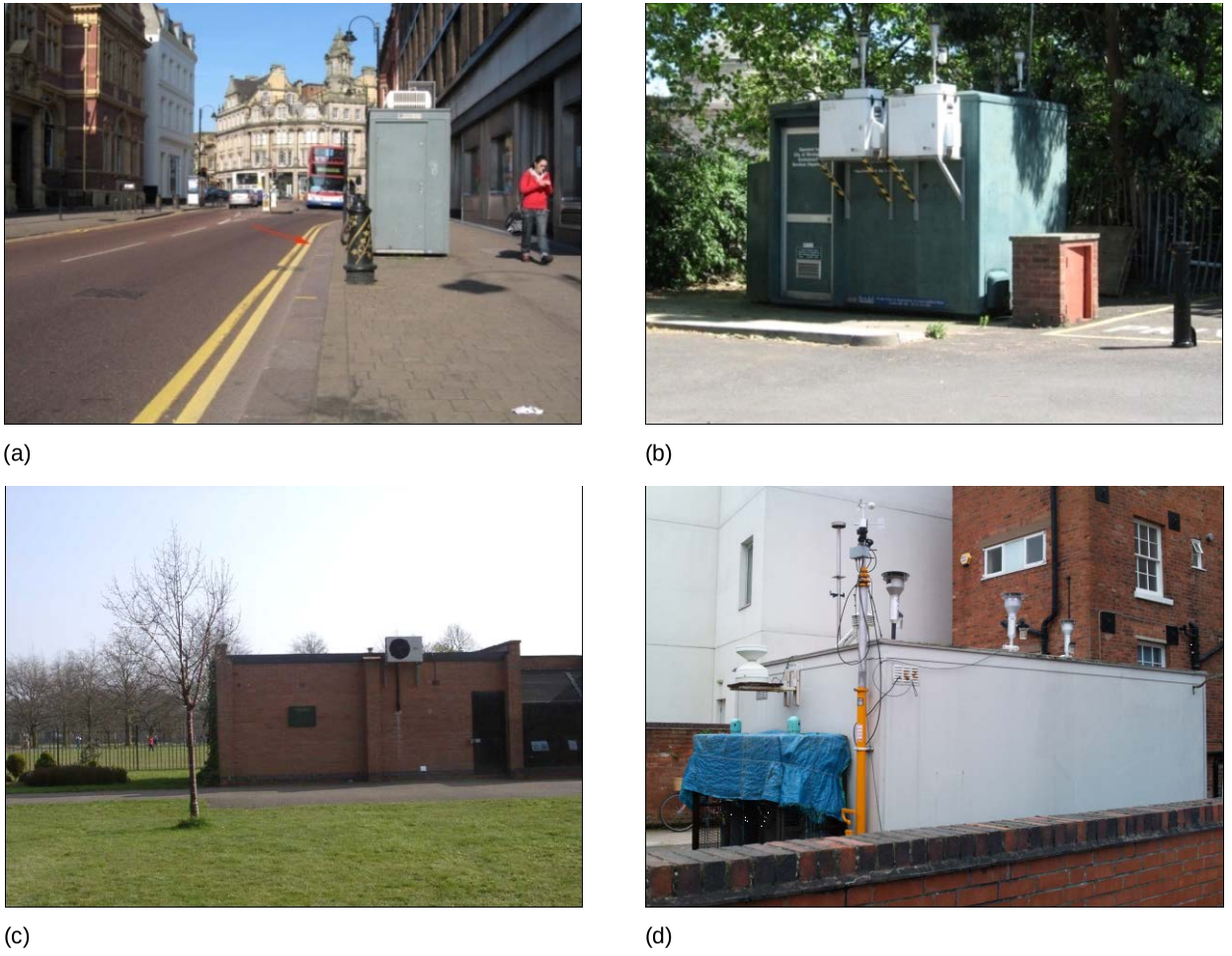

(a) (b)

(c) (d)

Figure 3.7 Air sampling units in the West Midlands; (a) Lichfield Street Wolverhampton City Centre, SO 391641 298785, (13/05/2008); (b) Birmingham City Centre, SO 406341 286859, (10/06/08); (c) Coventry Memorial Park, SO 432787 277474, (10/06/08); and (d) Leamington Spa Centre, SO 431941 265731, (10/06/08).

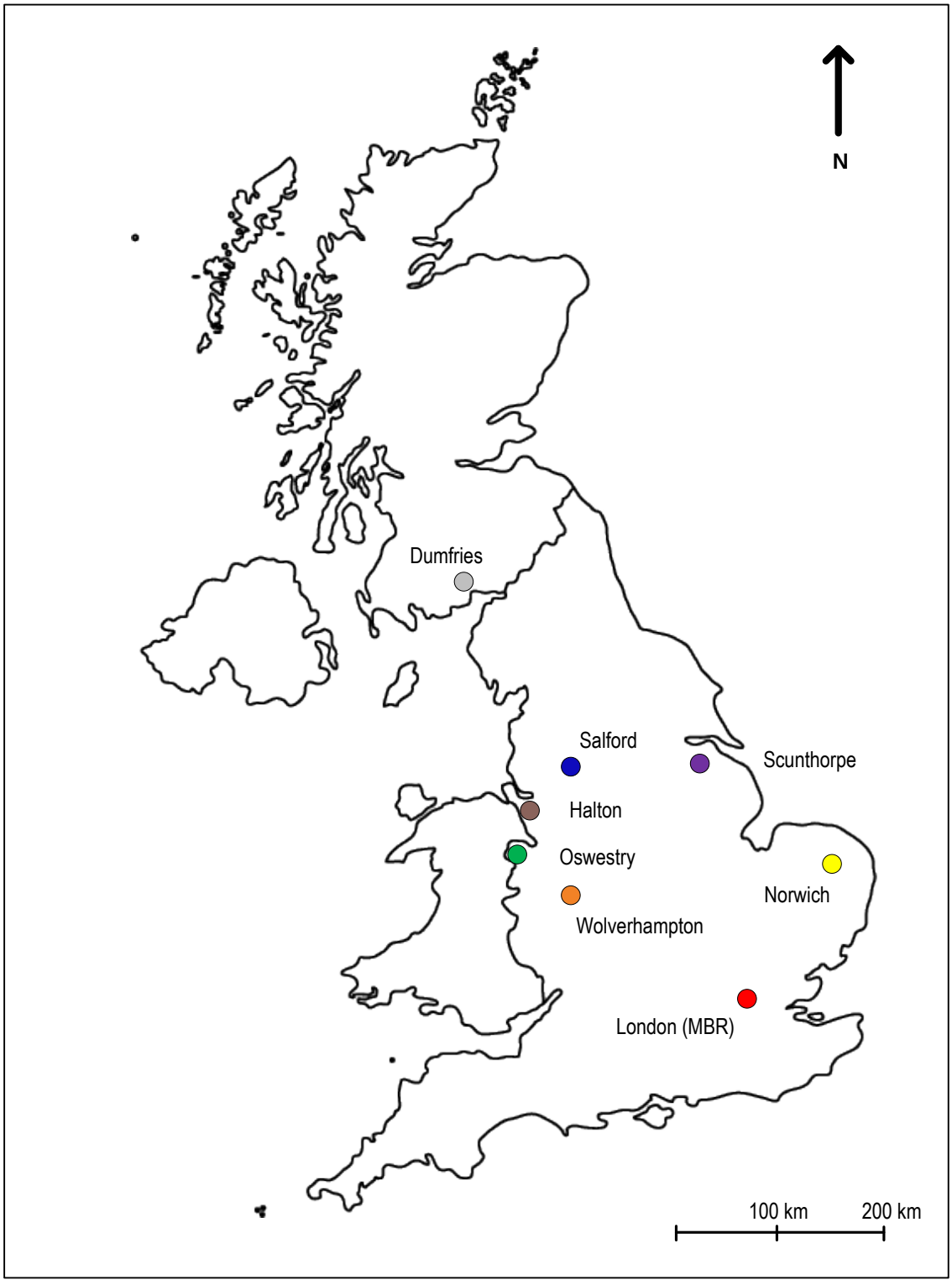

Figure 3.8 UK map of towns and places sampled in this study[1]. Grid references (a) NX 29 57; (b) SJ 34 37; (c) TQ 52 18; (d) TG 62 30; (e) SO 32 32; (f) SD 37 39; (g) TA 48 10; (h) SO 38 29.

Dumfries Halton London (MBR) Norwich
Oswestry Salford Scunthorpe Wolverhampton

[1]Colours link to towns and places throughout the thesis.

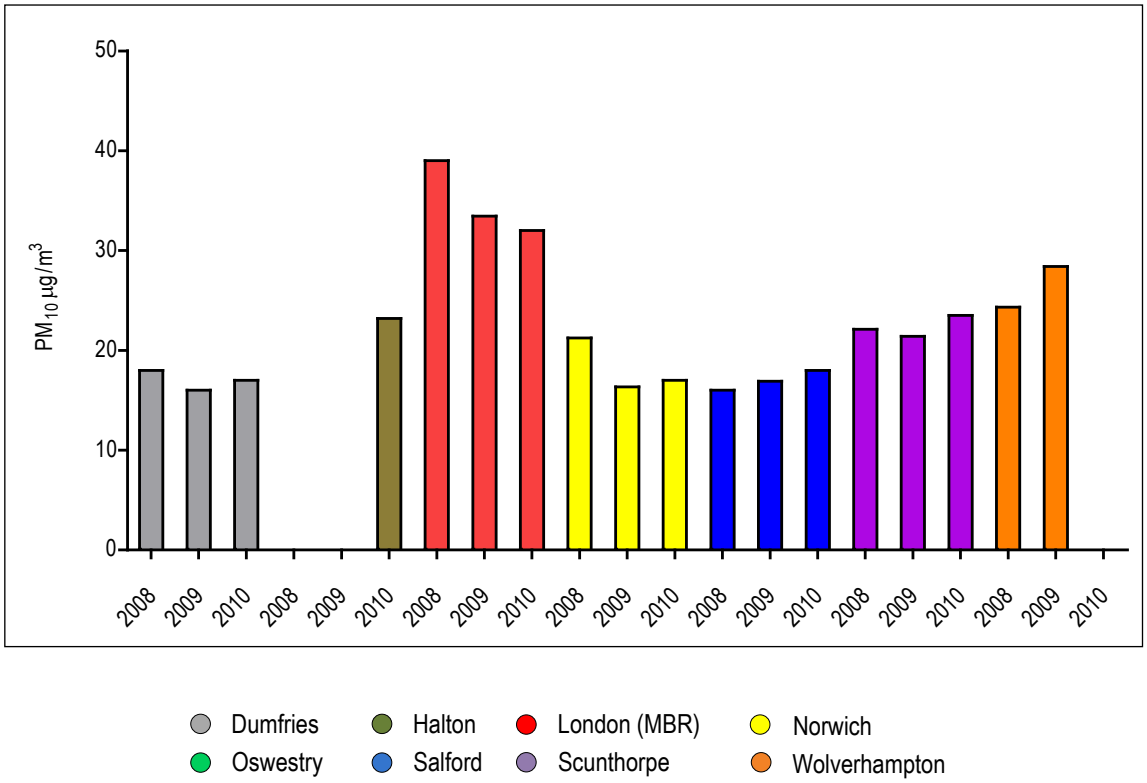

Figure 3.9 Annual mean hourly measured PM_{10} µg $m^3$for UK study area (Source: AEA, 2008).

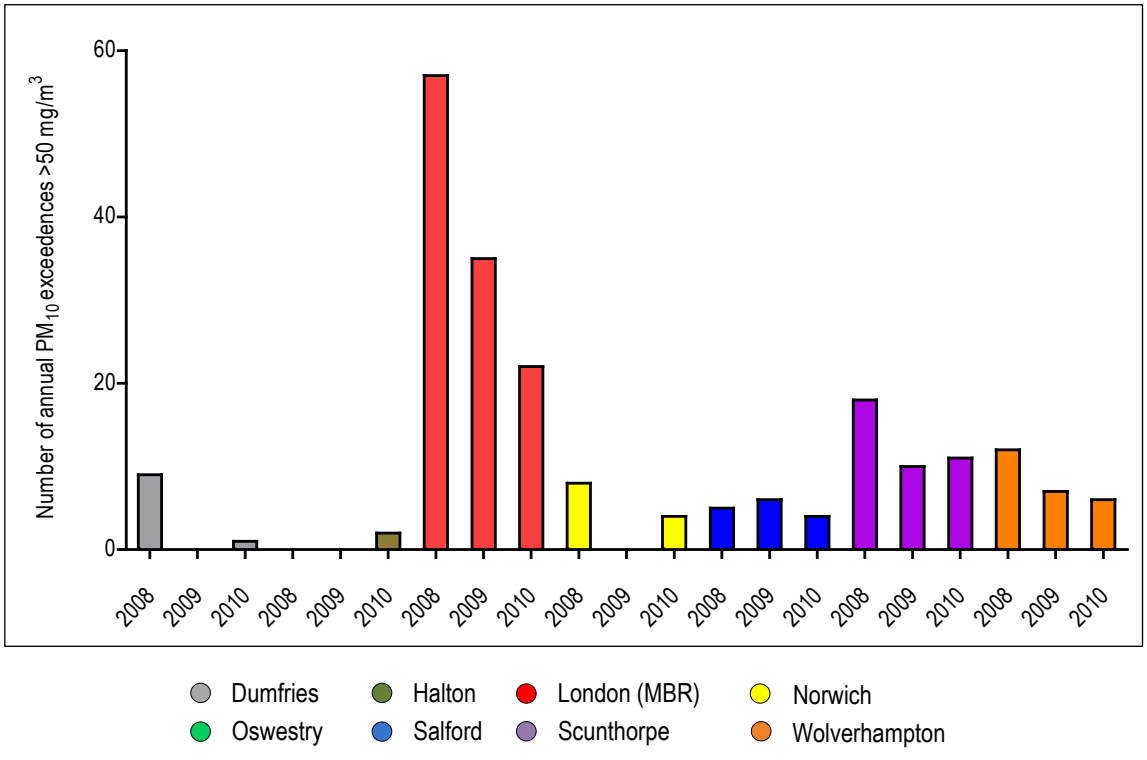

Figure 3.10 Air quality strategy standard (PM_{10}) daily mean >50 µg m^3 for UK study area (Source: AEA, 2008).

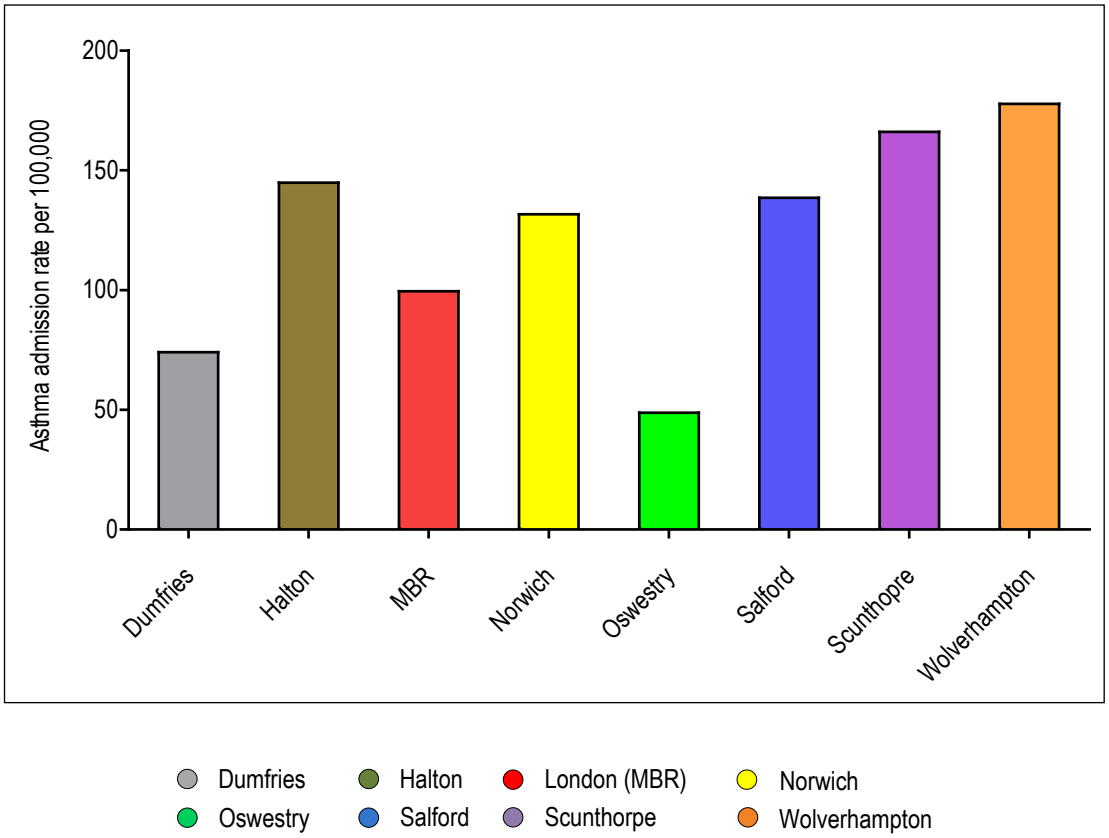

Figure 3.11 Asthma admission to hospitals per 100,000 population, 1998-2003 for UK study area (Source: Goldacre *et al.,* 2005).

Street dust was collected at 30-40 spaced locations (Appendix 5.5), using the same methodology as the Wolverhampton sampling. The number of samples depended on the size of the town. Consistent spacing of samples was used in all towns using the radial approach, this resulted in larger towns-cities having more sampling points due to area size. This ensured that all major land-use areas (centre, inner and outer fringes – commercial, industrial and residential), were accounted for within the sampling area. This approach was true for all but Marylebone Road, where a specific area was chosen to reflect a localised sample area in a known pollution hotspot.

3.2 Laboratory methods

All samples were subjected to the same techniques throughout the study period. All laboratory equipment and experimentation was undertaken at the University of Wolverhampton during the period January 2008-February 2010.

3.2.1 Sample preparation

Walden *et al.* (1999) recommends samples awaiting analyses are not kept in long-term storage, as some workers observed significant changes in sediment properties with time (Snowball and Thompson, 1988; Hilton and Lishman, 1985; Oldfield *et al.,* 1992). In the laboratory, samples were visibly screened to remove macroscopic traces of hair, animal and plant matter, to ensure that material analysed was not contaminated with foreign material. Appendix 3.5 shows typical

RDS collected with evident differences of material between each of the samples, colour and grain sizes. Each sample was oven dried at 40^{o}C for 72h so not to thermally alter the magnetic properties. Samples were then dried-out, sieved to separate the <1000 µm fraction from the bulk material, stones, glass, organic matter and other similar large debris (Banerjee, 2003).

3.2.2 Procedure for mineral magnetic analysis

Each sample was separately packed into pre-weighed 10 cc styrene pot (Appendix 3.5) and then re-weighed to calculate mass specific values. All weights were measured on pre-calibrated balances, to three decimal places. This yielded samples of ~8–5 g dry weight. Walden *et al.* (1999) suggested that a larger sample weight, such as those used in this study, generally improve the resulting data quality during analysis. Each sample was subjected to a series of routine mineral magnetic analyses (Thompson and Oldfield, 1986; Walden *et al.,* 1999). Figure 3.12 shows a flow diagram to illustrate the stages and order of mineral magnetic measurements.

3.2.3 Susceptibility measurements

Single sample mass specific magnetic susceptibility (χ) measurements were made using a Bartington MS2 magnetic susceptibility meter connected to a Bartington MS2B dual frequency susceptibility sensor (Appendix 3.6.1). Measurements were taken at low frequency (0.47 kHz; (χ_{LF})) and high frequency (4.65 kHz; (χ_{HF})). Both low and high frequency susceptibilities were measured (χ_{LF} and χ_{HF}) to allow frequency dependent susceptibility to be calculated ($\chi_{FD\%}$).

3.2.4 Remanence measurements

The instruments used included a Molspin alternating field demagnetiser with an Anhysteretic Remanent Magnetization (ARM) attachment; a Molspin ‘small-field’ pulse magnetizer; a Molspin ‘large-field’ pulse magnetizer; and a Molspin magnetometer (Appendix 3.6.2) connected to a personal computer, which is controlled by Winspin software supplied to the University of Wolverhampton by John Walden, University of St. Andrews. The use of each instrument is discussed by Thompson and Oldfield, (1986) and Walden *et al.* (1999).

An ARM was induced in the samples (Appendix 3.6.1), using steady biasing 0.04 mT field, and the resultant remanence measured by the magnetometer, as were all subsequent remanence measurements. The samples were then exposed to a demagnetization field in order to remove induced ARM. Samples were then placed into pulse magnetizers and exposed to successively increasing sizes of ‘forward’ magnetic fields (20, 40, 300, 500 and 1000 mT) until a total saturation field of 1000 mT was generated. This field was chosen to represent the Saturation Isothermal Remanent Magnetisation ($SIRM_{1000}$ mT), as it was the largest magnetic field that could be produced on the ‘large’ pulse magnetizer. Once saturation had been obtained a reverse field (-100 mT) was applied, which destroyed the saturation effect on the sample. After each forward and reverse field, Isothermal Remanent Magnetisation (IRM) was measured.

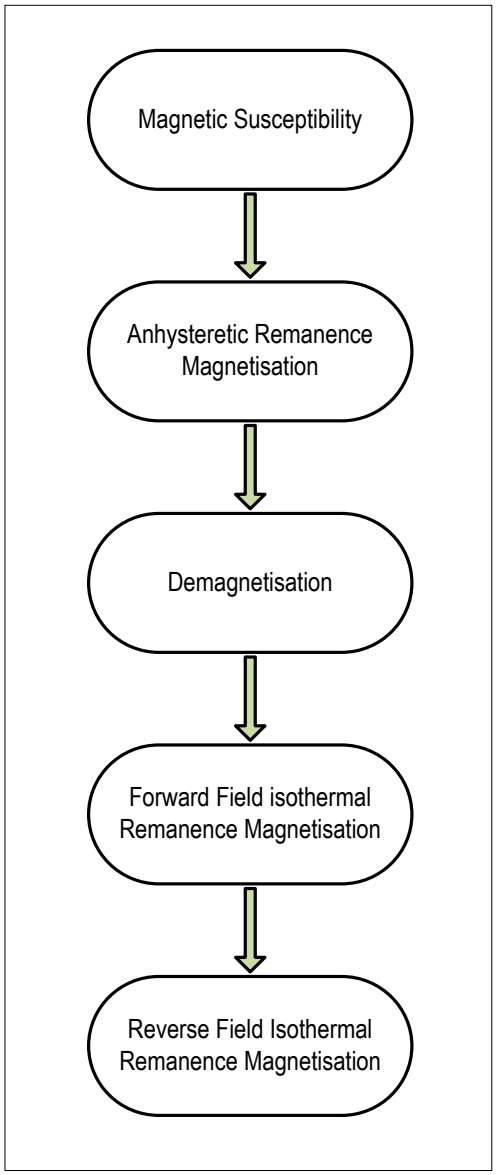

Figure 3.12 Flow-chart outlining the stages of the mineral magnetic procedures used for analysing the magnetic properties of sediments.

3.2.5 Textural analysis techniques

As discussed in section 3.1.3 methods used by the AURN include the Tapered Element Oscillating Microbalance (TEOM) filter baser gravimetric method and sequential gravimetric analyser (Partisol) or ß-attenuation monitor to measure PM. This method generally gives a bulk reading of a particular particle size, but limitations of the equipment prove problematic when data for specific particle size fractions are needed.

The technological development of laser diffraction has developed techniques which can be used quickly and precisely to measure all particles in the size range 0.1–2000 μm. The method employed for determining the textural properties of sediments in this study was laser diffraction analysis (Syvitski, 1991; Tucker, 1991), or more precisely, Low Angle Laser Light scattering (LALLS). Traditionally more classical techniques (i.e. sieves, sedimentation, electrozone sensing and microscopy) have been used to analyse the textural properties of sediments.

Laser diffraction and sieving can provide similar results when characterizing spherical or semi-spherical particles. However, significant differences can be observed for non-spherical particles due to the different particle properties measured by each technique. The reason for the difference between the two techniques can be shown by assuming that both are used to measure a rectangular particle with dimensions of 100 x 100 x 200 µm. During the sieve analysis a 110 µm sieve is used. The particle will fall through this sieve, because the particle is classified according to its second largest dimension (100 µm). Laser diffraction will however, report a spherical equivalent size relating to the volume of the particle. In this case the diameter of the sphere that has the same volume as the particle being measured is 156 µm (Malvern, 2008). Figure 3.13 shows the distribution comparison of sieving and laser diffraction.

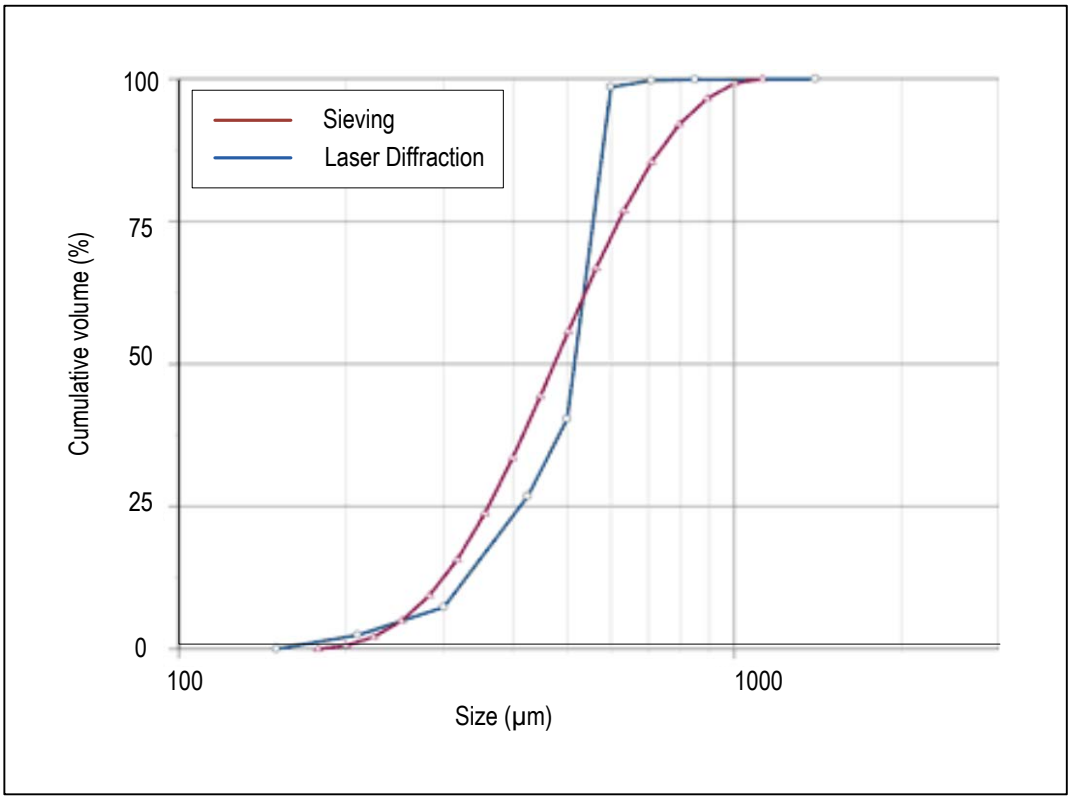

Figure 3.13 Typical comparison between laser diffraction and sieving showing how different properties measured by each technique changes the reported size distribution (Source: Malvern, 2008).

3.2.6 Textural measurements

The laser diffraction instrument used to analyse sediments was a Malvern Mastersizer Long-bed X with a MSX17 sample presentation unit (Appendix 3.6), connected to a PC governed by Malvern v1.2 software. Malvern Instruments' laser diffraction systems meet or exceed the requirements in ISO13320, which conform to international standards for laser diffraction measurements. The technique is based on the principle that, as a particle passes through a laser, light is diffracted and the diffraction angle is inversely proportional to particle size. A schematic diagram shows the arrangement of the internal hardware of the Malvern Mastersizer (Figure 3.14). This set-up is based on Fourier-optics and involves a laser light passing through

cell windows that receive a constant flow of dilute sediment suspension. As the suspended particles travel through the laser beam, they cause light to be diffracted, with the resulting diffraction pattern being focused onto a series of detectors. The diffraction patterns received by the detectors are then averaged over a fixed time period and deconvolved into particle size values. These values are then arranged into discrete size ranges, given by the size of the detector areas. Unfortunately, this approach (using Fraunhofer theory) assumes that all sizes of particles scatter with equal efficiencies, and that all particles are opaque and transmit no light (Bohren and Huffman, 1988; Lehner *et al.,* 1998).

Since these assumptions are not always correct, the latest Malvern instrumentation and software has been designed to compensate for these influences and (using Mie theory (Bohren and Huffman, 1988; Lehner *et al.,* 1998)) allows the refractive index of materials to be taken into account when calculating particle size values.

Mie Theory predicts the primary scattering response observed from the particle surface, with the intensity predicted by the refractive index difference between the particle and the dispersion medium. It also predicts how the particle's absorption affects the secondary scattering signal caused by light refraction within the particle. This is especially important for particles <50 µm in diameter and is extremely important when the particle is transparent, as stated in the international standard for laser diffraction measurements (ISO13320-1, 1999; ISO, 2008; Malvern, 2008). The procedure used for performing laser diffraction measurements is shown as a flow-chart in Figure 3.15.

Sample analysis initially involves configuration of the appropriate Mastersizer hardware, followed by laser alignment, and then recording the background reading of water. Macroscopic traces of organic matter were removed from representative sub-samples before being dampened by the drop wise addition of a standard chemical solution (40 g/l solution of sodium hexametaphosphate ($(NaPO_3)_6$) in distilled water) to disperse aggregates. The sub-sample slurry was then added to the water chamber of the sample presentation unit. The sample was stirred and particles pumped past the laser-beam, causing beam scatter. The diffraction pattern was received by a series of detectors, which enabled the computer to calculate particle sizes, and generate a distribution graph with descriptive statistics (Median Particle size (PS), Mean-PS, Mode-PS, Sorting, Skewness and Kurtosis) for each sediment sample.

3.2.7 Textural parameters

Variables used to characterize the textural properties of sediments and an explanation of their interpretation is presented in Table 3.4. To ensure reliable results over the sampling period, samples were subject to regular re-runs and the Malvern instrumentation was regularly calibrated using latex beads of known size.

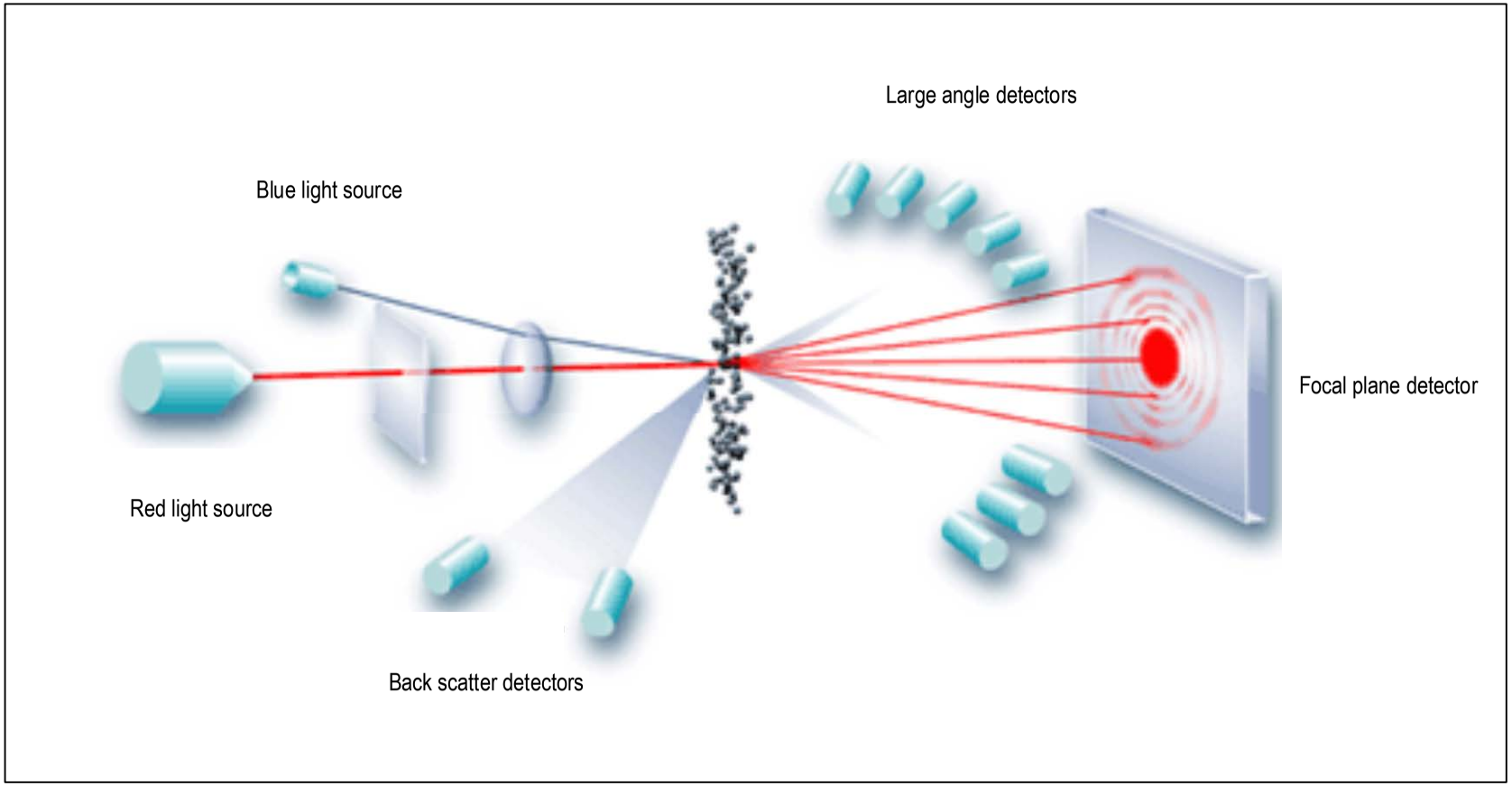

Figure 3.14 The technique of laser diffraction is based on the principle that particles passing through a laser beam will scatter light at an angle that is directly related to their size. As the particle size decreases, the observed scattering angle increases logarithmically. The observed scattering intensity also depends on particle sizes and diminishes, to a good approximation, in relation to the particle's cross-sectional area. Large particles therefore scatter light at narrow angles with high intensity, whereas small particles scatter at wider angles but with low intensity (Source: Malvern, 2008).

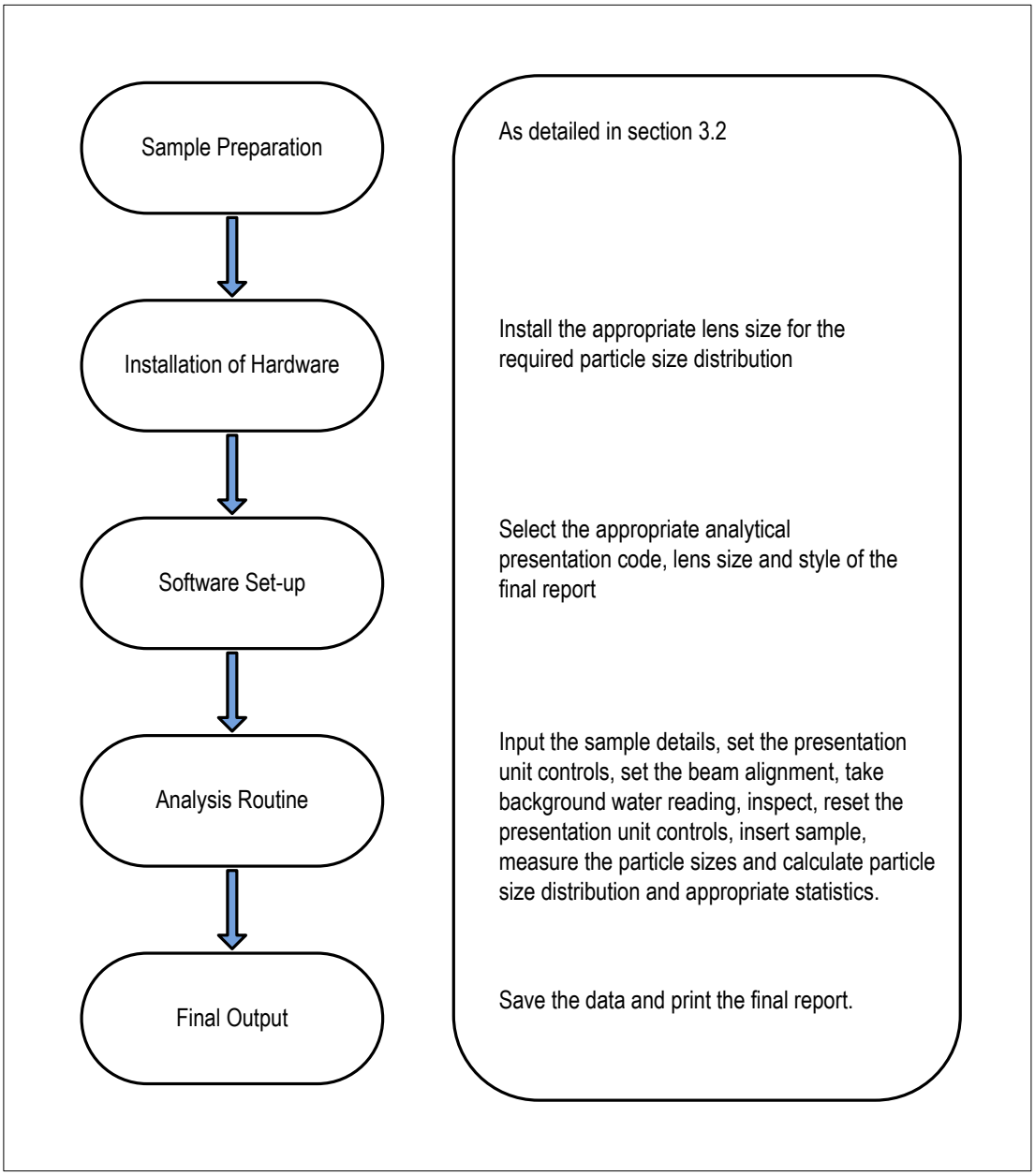

Figure 3.15 Flow-chart outlining the stages of laser diffraction procedure used for analysing the texture of sediments.

3.2.8 Organic matter

Sequential loss-on-ignition (LOI) is a common and widely used method to estimate the organic content of sediments (Ball, 1964; Dean, 1974; Xie *et al.,* 2000; Shilton *et al.,* 2005; Heiri *et al.,* 2001). Igniting samples at high temperatures oxidizes organic carbon to carbon dioxide and ash; therefore, organic matter is calculated by measuring weight loss. Dean (1974) evaluated the method and concluded that LOI provides a fast and inexpensive means of determining the carbonate and organic contents of sediments. Depending on the ignition temperature, various losses of volatile salts, structural water and inorganic carbon may occur (Dean, 1974; Ball, 1964). Using temperatures >375^{o}C showed that most weight loss was due to water loss from clay minerals and below this temperature removed appreciably less carbonaceous matter and was therefore unsuitable.

Table 3.4 (a) shows those textural variables used in this research (after Tucker, 1991); (b) shows descriptive terms applied to size values (after Friedman and Sanders, 1978); (c) shows descriptive terms applied to Sorting values (after Folk and Ward, 1957); (d) shows descriptive terms applied to Skewness values (after Folk and Ward, 1957); and (e) shows descriptive terms applied to Kurtosis values (after Folk and Ward, 1957). All textural results referred in this thesis are expressed to three decimal places. This is done for consistency of the work, rather than an indication of the detection limits of the instruments employed or the variables used

(a) Textural variables	Interpretation
Median-PS	The median particle size is when half of the grains are coarser and half finer than the median diameter, whose size is most readily determined from the 50% line of the cumulative distribution curve. Although useful for many unimodal sediments, in polymodal distributions the median may fall in the tails of two sub-populations of grains, in a size fraction that is scarce. A listing of the size descriptions for the values obtained are presented in Table 3.5b.
Mean-PS	The mean particle size in the best measure of average grain size, the mean is computed from sizes of particles spread through a range of percentile values. A listing of the size descriptions for the values obtained are presented in Table 3.5b.
Mode-PS	The modal particle size is the size class on a size frequency histogram in which the greatest percentage of grains is represented. Alternatively, on a size frequency distribution plot the highest point on the curve provides the modal value. The modal size is, therefore, the commonest grain size in a distribution. A listing of the size descriptions for the values obtained are presented in Table 3.5b.
Sorting	In many forms of analysis the full range of sizes present is of relevance. However, it is rarely possible to define the size of the largest or the smallest particles precisely in a size distribution. Of more importance is an assessment of the spread of particles about the average, to define the dispersion or sorting of the sediment, as represented by the breadth of the frequency curve or the shape of the cumulative frequency distribution. A listing of the descriptions for the values obtained are presented in Table 3.5c.
Skewness	In a normal distribution with a bell-shaped frequency curve the median and mean values coincide. Any tendency for a distribution to lean to one side, i.e. to deviate from normality, leads to differences between the median and mean values. These differences are used to characterize the asymmetry or skewness of the curve. The skewness has a positive or negative value when more fine or coarse materials are present than in a normal distribution, seen as tails to the right or left respectively on frequency distribution plots. Again, although skewness may be computed for the central segment of the distribution, for most purposes broader spreads are used. Effectively skewness is determined from the value of the mean less the median, all divided by the range used in defining the mean. A listing of the descriptions for the values obtained are presented in Table 3.5d.
Kurtosis	The kurtosis is related to both the dispersion and the normality of the distribution. Very flat curves of poorly sorted sediments or those with bimodal frequency curves are platykurtic, whereas very strongly peaked curves, in which there is exceptionally good sorting of the central part of the distribution, are leptokurtic. A listing of the descriptions for the values obtained are presented in Table 3.5e.

(b) Size description	Size scale
PM 0.1	<0.1 μm
PM 1.0	<1.0 μm
PM 2.5	<2.5 μm
PM 10	<10μm
PM 100	<100 μm
Clay	<2 μm
Fine Silt	2 – 6 μm
Medium Silt	6 – 20 μm
Coarse Silt	20 – 60 μm
Silt	2 – 60 μm
Fine sand	60 – 200 μm

(c) Sorting description	Sorting σ_1 scale
Very well sorted	<0.35
Well sorted	0.35 to 0.50
Moderately well sorted	0.50 to 0.70
Moderately sorted	0.70 to 1.00
Poorly sorted	1.00 to 2.00
Very poorly sorted	2.00 to 4.00
Extremely poorly sorted	>4.00

(d) Skewness description	Skewness SK_1 scale
Very positively skewed	+0.3 to +1.0
Positively skewed	+0.1 to +0.3
Symmetrical	+0.1 to -0.1
Negatively skewed	-0.1 to -0.3
Very negatively skewed	-0.3 to -1.0

(e) Kurtosis description	Kurtosis K_G scale
Very platykurtic	<0.67
Platykurtic	0.67 to 0.90
Mesokurtic	0.90 to 1.11
Leptokurtic	1.11 to 1.50
Very leptokurtic	1.50 to 3.00
Extremely leptokurtic	>3.00

It has been demonstrated that to avoid losses of clay structural water an optimum temperature of 375^{o}C for 16 hours was needed to remove >90% of carbonaceous material without loss of structural water (Keeling, 1962). Ball (1964) further supported this theory concluding that the 375^{o}C 16h method was of greater accuracy compared to higher temperature shorter period methods. Therefore, LOI at 375^{o}C as applied to street dust by Xie *et al.* (2000); and Shilton *et al.* (2005) was used. LOI values compliment magnetic measurements, by allowing data normalization for the diluting effects of organic content on the magnetic signal (Maher *et al*., 1999). LOI data are also required for determining X-ray fluorescence spectrometry (XRF) values in order to understand sample composition, and to calculate effects of mass attenuation (process of absorption of fluoresced x-rays) by samples during XRF measurements.

3.2.9 Loss on Ignition technique

Ceramic crucibles were labelled, weighed and filled with a 0.5 mg–1 g subsample of sediment and re-weighed (W1). To assure result consistency, the same analytical balance was used for all measurements. Sample were then oven-dried overnight (105^{o}C), in order to remove any moisture. Following this, samples were allowed to cool in a dessicator at room temperature, to prevent absorption of atmospheric moisture, and then re-weighed (W2). Samples were then placed in a muffle furnace and ignited at 375^{o}C for 16 hours. Samples were then cooled in the dessicator and re-weighed (W3). Organic matter content was then calculated for each sample (Eq.3.1).

Eq.3.1: $LOI\% = 100 \times (W2 - W3) / W2$

3.2.10 Geochemical and X-Ray Fluorescence Spectrometry techniques

RDS geochemical composition can be analysed in several ways and have been discussed in section 2.6.1. The technique used in this study is X-Ray Fluorescence (XRF) and is a widely used technique for both qualitative and quantitative analysis, particularly for solid samples, and is a popular choice often because of the limited sample preparation required and rapid rate of analysis (Adams and Allen, 1998). The technique exhibits wide elemental coverage, good detection limits (typically mg kg^{-1}) and an extensive working range (to high percentage of pure materials). XRF is a good method used for characterizing the elemental composition of sediments and can reveal natural and anthropogenic inputs (Xie *et al*., 2001; Lu *et al*., 2010). Elevated levels beyond natural background concentrations and accumulation rates can also be calculated, to assess the impact of pollution (Allen and Rae, 1986; Xie *et al*., 2001; Abu-Allaban *et al*., 2003; Dearing and Jones, 2003; Lu *et al*., 2010). Furthermore, the elemental composition of particulate pollution is an important factor in understanding the impact of particulate pollution on health (Harrison, 2004; Johnson *et al.,* 2005; Xie *et al.,* 2001).

Energy dispersive radioisotope-source X-Ray Fluorescence (XRF-ED) has been used to characterize the elemental composition of road-deposited sediment (RDS). XRF analysis is based on the photoelectric fluorescence of secondary x-rays generated within a sample by irradiation. The secondary x-rays produced are characteristic of source elements within the

sample, and the emission rates are a function of concentration (Boyle, 2000). Therefore, elemental composition can be determined directly by allowing for instrument geometry, detector efficiency, fluorescence yield of elements and absorption of radiation by samples (Boyle, 2000). XRF analysis has been widely applied to sediments, to interpret elemental characteristics of pollution and temporal contamination trends (Versteeg *et al.,* 1995; Lee and Cundy, 2001; Xie *et al*., 2001; Abu-Allaban *et al*., 2003; Robertson *et al*., 2003; Canepari *et al*., 2009; Lu *et al.,* 2010).

XRF-ED is a highly precise, reliable and rapid (~70 samples per day) method for total elemental sediment analysis of bulk samples (Al-Merey *et al*., 2005). Compared to alternative techniques (for example, energy dispersive x-ray spectrometry), XRF-ED has higher detection limits; however, for many elements, observed levels are above this detection limit (Boyle, 2000). Analysis was undertaken at the University of Wolverhampton using an ARL 8410 XRF spectrometer. XRF is non-destructive and there is minimal handling of samples. Prior to measurements, the instrument was calibrated using a range of reference materials, which contain certified levels of element concentrations (Boyle, 2000).

3.2.11 Scanning electron microscopy

Scanning electron microscopy (SEM) is a common and effective technique which can be used to examine particle and geochemical characteristics of sediments and PM, it was therefore chosen (SEM observations were carried out at magnifications <x1500) with the aid of an energy dispersive X-ray spectroscopy (SEM-EDAX), to identify particles of specific interest.

The physical characteristics of PM can be analysed in conjunction with particle counts and compared to known particles from similar environments, where SEM analysis has been used in several mineral magnetic studies on RDS (Pina *et al.,* 1999; Robertson *et al.,* 2003; Kim *et al* 2007). Figure 3.16a-c shows SEM micrographs of typical Fe oxide particles found within urban sediments in Manchester. The spherical Fe oxide particles observed within the Manchester RDS have been identified as being probably derived from high temperature combustion processes. Robertson *et al*. (2003) supported this by mineral magnetic data from the Manchester RDS samples, which characterized magnetic particulates as being of multi-domain ferrimagnetic mineralogy, therefore, resulting from high temperature combustion processes. This association has been found in other studies (Pina *et al.,* 1999; Kim *et al*., 2007) where mineral magnetic concentrations and the use of SEM micrographs and particle counts have identified anthropogenic sources.

3.3 Statistical analysis

Descriptive statistics were calculated using Microsoft Excel (2007) and Graph Pad Prism 5.03 (2009) software. The Anderson- Darling normality test was performed on all data, the outcome of which was usually non-normally distributed data. Therefore, non-parametric data analyses were performed. Using MINITAB PC (version 15), sample comparisons were determined by Spearman's rank.

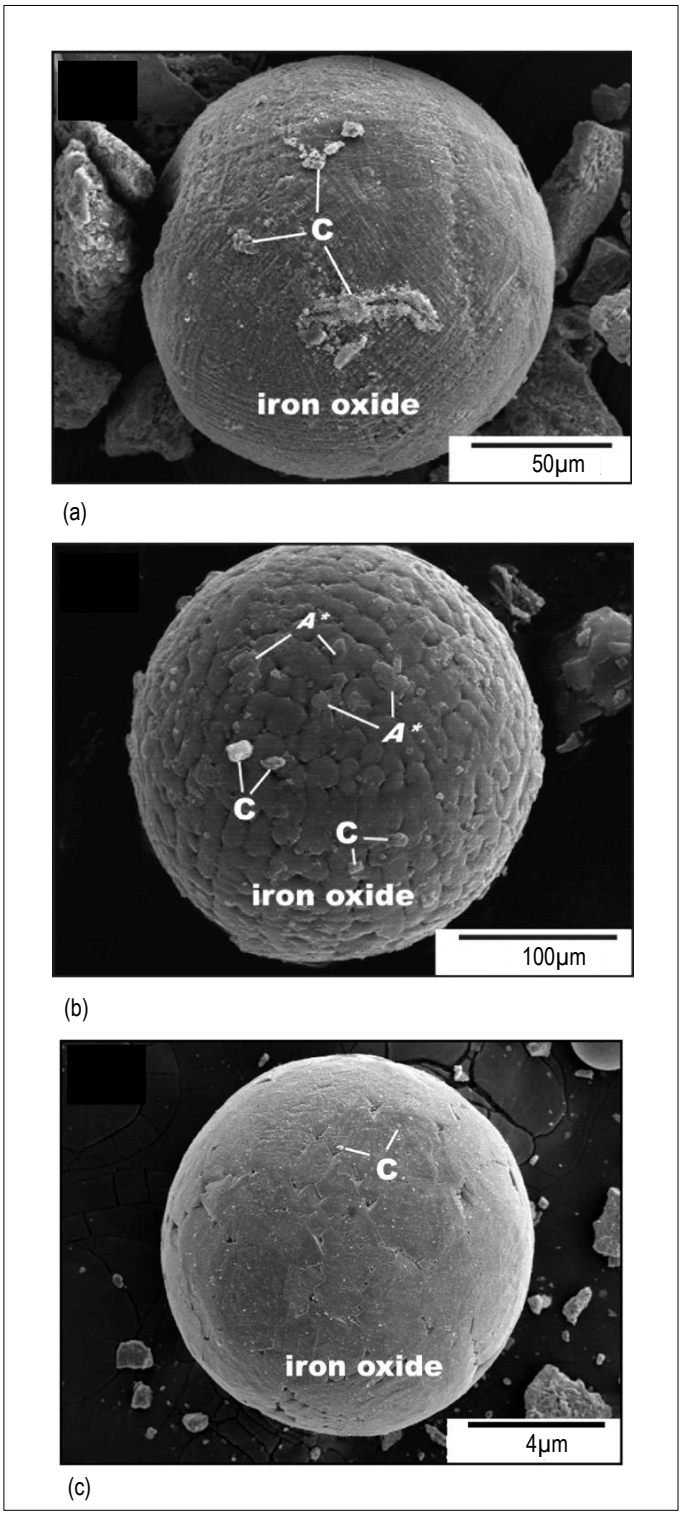

Figure 3.16 SEM micrographs of typical Fe oxide combustion particles originating from urban RDS.

The statistical approaches, including Mann-Whitney and Kruskal-Wallis tests, are routine for random samples and are presented in Table 3.5. Thorough explanations are available in standard texts (e.g. Ebdon, 1978; Davis, 1986; Stuttard, 1994). Some techniques that have been adopted in this thesis are less common and therefore merit further discussion.

3.3.1 Box-plots

To graphically demonstrate the degree of statistical variation in the distribution of any variable, many measurements used in this study have been replicated, either as field samples, laboratory sub-samples or as analytical measurements. When this information is expressed graphically, it is common practise to plot the data, using standard deviation whiskers above and below the sample mean. However, this style of plot fails to show whether a distribution is skewed or the position of minimum and maximum values. A box-plot can be used to summarize these distributions, with each individual sample-set represented by a rectangular box with whiskers (Figure 3.17). The horizontal lines that define the top and bottom of the box portray the ranges of the upper and lower inter-quartile limits, while the median value is shown by a line that is positioned within the box. The extreme values are shown by the upper and lower point of termination of the vertical whisker lines, which extend above and below each box. A useful alternative is to add notches (Figure 3.18) these are calculations of data confidence. If the notches of the boxes do not overlap, this offers evidence of statistically significant differences between medians (Wessa, 2011).

3.3.2 Multivariate statistics: simultaneous R- and Q-mode factor analysis

The data-sets produced by the mineral magnetic and laser diffraction techniques are multivariate (i.e. each observational unit is characterized by several variables). For provenance purposes, this means that data-sets could be explored on a univariate basis using repeated F-tests. However, this simple approach does not give a visual perception of the relationships between groups, and can fail to indicate the more complex or subtle relationships that may simultaneously exist within several groups of variables.

Multivariate methods can alternatively be used for this type of data examination, such that data are simplified and major trends become emphasized and minor variations ignored (Kovach, 1995).The nature of multivariate data is usually a two-dimensional matrix, of *n* samples by *m* variables (Johnson, 1980; Manly, 1994; Walden and Smith, 1995), which can be visualized as scatter-plots. In scatter-plots the data can either be viewed in 'variable space' or 'sample space'. In 'variable space' points on a diagram represent the samples and the axes correspond to the variables. The opposite scenario is observed in 'sample space'.

As the number of samples and variables increase, so do the number of axes, making it increasingly difficult to visualize any increase in the dimensions involved. In some instances, these problems can be overcome by multivariate methods, particularly factor analysis.

Table 3.5 Description of each statistical data test performed in this thesis (Source: Minitab (version 15))

Statistical test used	Description of statistical test
Anderson-Darling	A one-sample hypothesis test determines whether the same sample population is non-normal. The null hypothesis for a normality test states that the population is normal. The alternative hypothesis states that the population is non-normal. Anderson-Darling compares the empirical cumulative distribution function of the sample data with the distribution expected if the data were normal. If this observed difference is sufficiently large, the test will reject the null hypothesis of population normality, which means that non-parametric statistical tests are required.
Spearman's Rank correlation	Spearman's Rank correlation measures the degree of dependence between two variables. The number of raw scores are converted into ranks. Then the differences between the ranks of each observation on the two variables are calculated. The correlation coefficient assumes a value between -1 and +1. If one variable tends to increase as the other decreases, the correlation coefficient is negative. Conversely, if the two variables tend to increase together the correlation coefficient is positive.
Mann-Whitney	A 2-sample rank test of the equality of two population medians, calculating the corresponding point estimate and confidence interval. This test assumes that the data are independant random samples from the two populations and whose variance are equal and a scale that is continuous or ordinal (possesses natural ordering) if discrete. The 2-sample rank test is slightly less powerful (the confidence interval is usually wider) than the 2-sample test with pooled sample variance when the populations are normal and considerably more powerful (confidence interval is usually narrower) for many other populations.
Kruskal-Wallis	Tests the equality of medians for two or more populations, by ranks. This test is a generalization of the procedure used by Mann-Whitney test and offers a non-parametric alternative to one-way Analysis of Variance. An assumption for this test is that the samples from the different populations are independent random samples from continuous distributions.
Multivariate Factor Analysis	Factor analysis, a parametric statistical analysis, like Principal Component Analysis summarizes the data covariance structure in a few dimensions of the data. However, the emphasis in factor analysis is the identification of underlying "factors" that might explain the dimensions associated with large data variability.

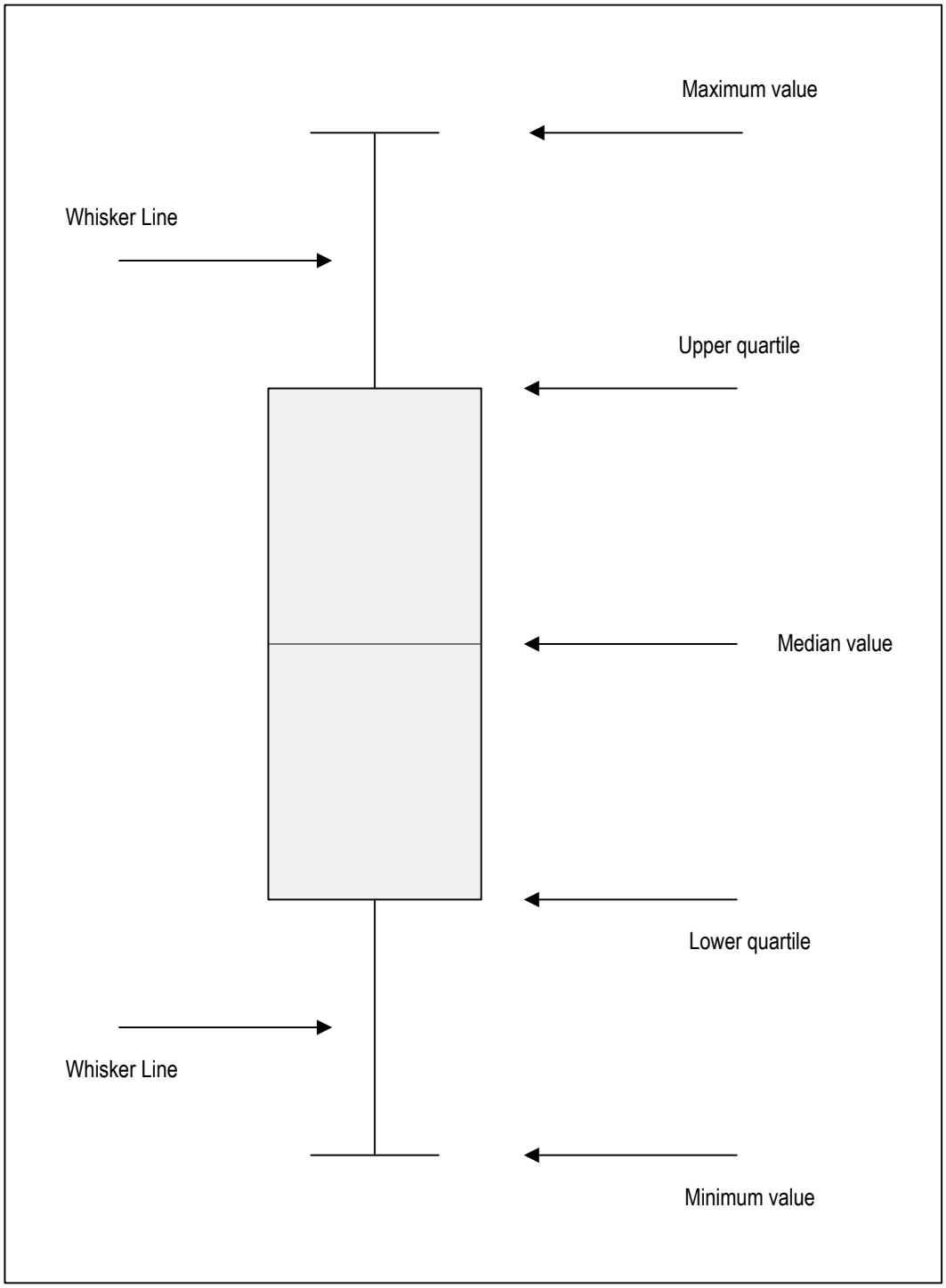

Figure 3.17 An example box-plot to accompany the explanatory text in Section 3.3.1 (after Tukey, 1977; McGill *et al.,* 1978; Walden, 1990).

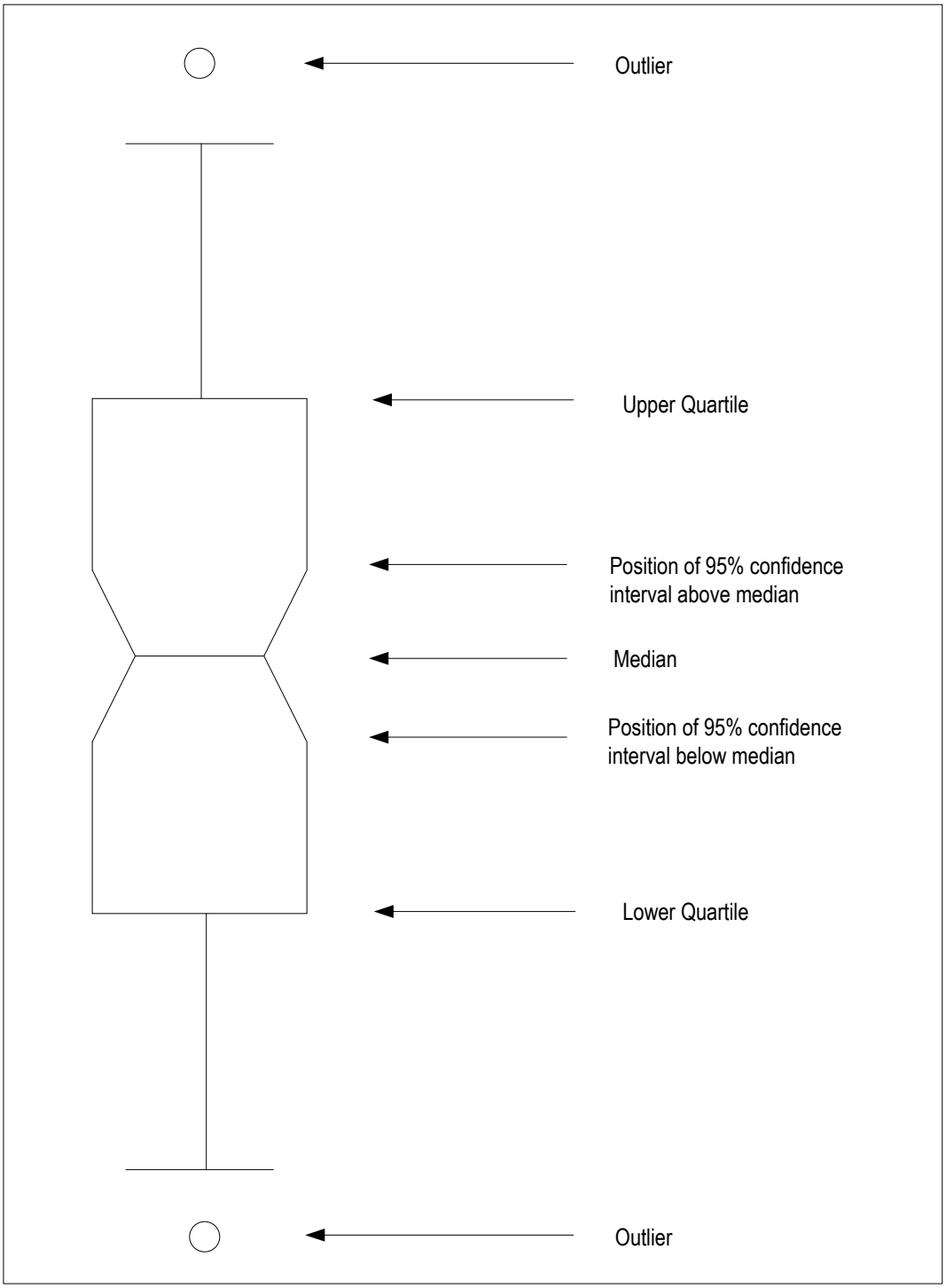

Figure 3.18 An example notched box-plot (after McGill, 1978; Walden, 1990).

These are widely used in geological literature (Klovan, 1966; Allen *et al*., 1972; Temple, 1978; Johnson, 1980; Zhou *et al*., 1983; Shaw and Wheeler, 1985; Oldfield and Clark, 1990; Walden, 1990; Walden *et al*., 1992, 1997; Walden and Smith, 1995; Booth *et al*., 2005, 2006; Lu *et al*., 2010). They were described by Kovach (1995) as being 'invaluable' for studying complex systems, while Davis (1986), referred to them as being an 'extremely powerful' method, that allows researchers to manipulate more variables than they can assimilate by themselves.

Multivariate methods and factor analysis have been applied to several environmental media including RDS (Tahri *et al*., 2005; Booth *et al*., 2005, 2006; Han *et al*., 2006; Kartal, *et al*., 2006; Tokahoğlu and Kartal, 2006; Al-Khashman *et al*., 2007; Lu *et al*., 2010). Booth *et al*. (2005, 2006) used multivariate analysis to differentiate between RDS in the West Midlands, which successfully aided interpretation of dust variations and simplified inter-relationships between magnetic parameters. Lu *et al*. (2010) successfully used correlation coefficient analysis and multivariate methods to identify possible sources of heavy metals in RDS.

The main function of simultaneous R- and Q-mode factor analysis is to reduce the dimensionality of data by extracting the common factors, so that the remaining variance can be attributed to error (Davis, 1986). The R-mode analysis is very similar to Principal Components Analysis (PCA), except the factors are chosen to maximize the correlation between the original variables rather than to maximize variance (Kovach, 1995; Walden and Smith, 1995; Schneeweiss and Mathes, 1995). Q-mode analysis is very similar to cluster analysis in that it locates groups of samples, but in numerical terms is similar to PCA (Kovach, 1995; Walden and Smith, 1995).

Both R- and Q-mode factor analysis are based on eigenvector methods and can be performed separately. R-mode factor analysis detects interrelations between variables, whereas Q-mode factor analysis attempts to identify patterns or groupings of the samples within their arrangement in 'multivariate space' (Walden, 1990) or 'multidimensional factor space' (Walden and Smith, 1995). Table 3.6 shows the mathematical steps of the procedure (Walden and Smith, 1995; Davis, 1986, 2002), involving a range of basic matrix algebra operations on the original raw data matrix (of n samples by m parameters).

In this case, analysis is carried out using MINITAB PC (version 15). However, because this technique is mathematical and not statistical, the results are not subjected to any significance testing. Factor analysis cannot quantify the relative proportions of each variable, as it only shows changes in the balance between sources.

Figure 3.19 (Table 3.7) shows a hypothetical factor plot to illustrate how factor analysis results can be interpreted in an environmental situation. In this example, factor analysis was performed on a multivariate dataset of 12 parameters, which were measured on five sample populations (AE) each containing different numbers of samples (perhaps representing RDS samples from different road side environments). The parameter and sample loadings for the first two factors

Table 3.6 Procedure for simultaneous R- and Q-mode factor analysis (after Davis, 1986, 2002; Walden and Smith, 1995)

Step	Procedure
1	Compile a raw data matrix of n samples (rows) by m parameters (columns) denoted by [x], as in convential matrix algebra.
2	[x] is standardized to give [w]. Each element of [x] has its column (parameter) mean subtracted from it. It is then divided by the product of the column (parameter) standard deviation (s) and the square root of n.
3	[W]' is created by transposing [W]. This involves turning the rows of [W] into the columns of [W]' and the columns into rows.
4	[R] is created by matrix manipulation of [W]' · [W]. The matrix [R] represents a correlation matrix between parameters.
5	Eigenvectors and eigenvalues (distinct properties of the matrix) are extracted from [R]. The eigenvectors are used to form a matrix [U]. The eigenvalues can be used to compute the percentage of the total variance in the original data set explained by the new 'underlying' factors.
6	The square roots of the eigenvalues are placed in the top left to bottom right diagonal elements of a matrix are set to zero.
7	$[A^R]$ is computed by multiplication from [U] · [^]. The matrix $[A^R]$ contains the R-mode (parameter) factor loadings. Each column represents the loadings of the original parameters on an individual factor (e.g. column 1 on factor 1). These values are used when plotting the parameters in 'factor space' in the form of scatter diagrams.
8	$[A^Q]$ is computed by multiplication from [W] · [U]. The matrix $[A^Q]$ contains the Q-mode (sample) factor loadings. Each column represents the loadings of the original parameters on an individual factor (e.g. column 1 on factor 1). These are the values used when plotting the samples in 'factor space' in the form of scatter diagrams.

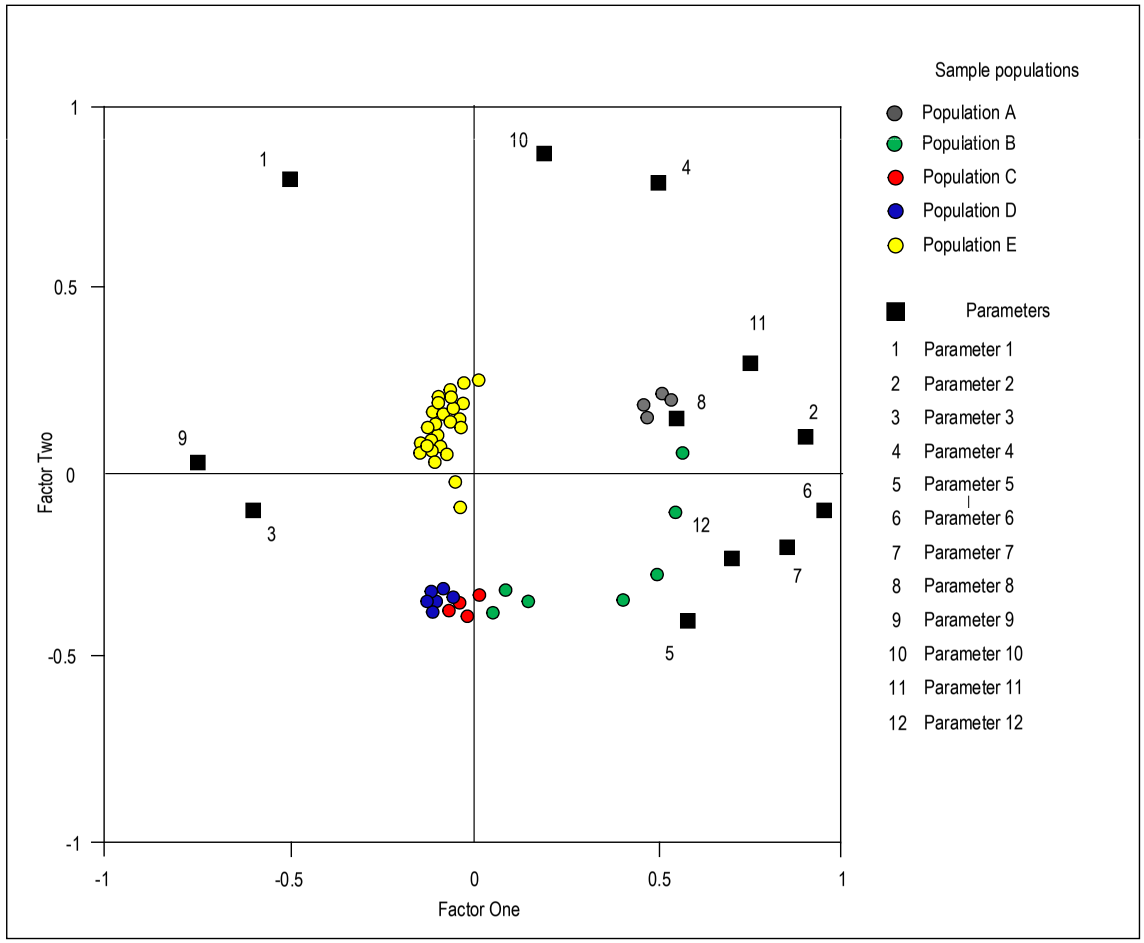

Figure 3.19 Hypothetical example of a simultaneous R- and Q-mode factor analysis plot of Factor 1 versus Factor 2, based on 12 hypothetical parameters.

Table 3.7 Hypothetical summary results from a factor analysis using 12 parameters

Factors	Eigenvalues	Total variance (%)	Cumulative eigenvalues	Cumulative total variance (%)
1	6.595	54.955	6.595	54.955
2	2.321	19.338	8.195	74.294
3	0.959	7.992	9.874	82.286
4	0.834	6.950	10.708	89.235
5	0.463	3.857	11.171	93.093
6	0.358	2.981	11.529	96.074
7	0.192	1.600	11.721	97.673
8	0.126	1.051	11.847	98.724
9	0.068	0.568	11.915	99.293
10	0.052	0.434	11.967	99.726
11	0.020	0.165	11.987	99.893
12	0.013	0.107	12.000	100.000

extracted from analysis (Factor 1 and Factor 2) have been used to generate the factor plot. Attempts are made at identifying underlying causes to, subsequently, 'label' or 'name' each factor (expressed in brackets after the factor is first mentioned in the text).

Table 3.7 shows that the first two factors extracted explain 74.29% of variation in the parameters. Factor 1 ('name' (e.g. representing distance from kerb)) has broadly separated the sample populations C, D and E from sample populations A and B. This indicates that Factor 1 (distance) provides a means of discriminating these groups, suggesting that those sample populations negatively loaded on Factor 1 have different characteristics to those positively loaded on Factor 1. The spread of sample loadings along Factor 2 ('name' (e.g. representing road type)) separates sample population A from sample populations C and D. This indicates that Factor 2 (road type) provides an effective means of discriminating between these groups, suggesting that those sample populations negatively loaded on Factor 2 have different characteristics to the group positively loaded on Factor 2. However, Factor 2 has failed to separate sample populations B and E, which have both positive and negative Factor 2 loadings.

The distribution of parameter loadings shows that the parameters are influenced by Factors 1 and 2. Parameters 2, 3, 5, 6, 7, 8, 9, 11 and 12 are influenced by Factor 1, while parameters 1, 4 and 10 are influenced by Factor 2. This suggests that Parameters 2, 3, 6, 7 and 9 provide the strongest means of discriminating between sample populations. As parameters 9 and 3 have plotted close together, this suggests that the sample populations are responding to these two variables in a similar manner (i.e. they are strongly positively correlated). Parameter 2 plots opposite parameter 3, suggesting parameter 2 has a negative correlation with parameter 3.

Theoretically, if sample population A represented a main arterial road sediment and sample population D represented a residential road sediment, the factor plot could be applied as a semi-quantitative approach for assigning such road types to another sample population (F). In these circumstances, any population F samples plotted amongst population A samples are probably dominated by RDS characteristics associated with main arterial roads and any population F samples plotting amongst population D samples are more probably dominated by residential road characteristics. Any population F samples plotting between populations A and D represent a mixture of characteristics.

3.3.3 Geographical information systems

A Geographic Information System (GIS) is a computer-assisted system for the acquisition, storage, analysis and presentation of geographic data (Tomlin, 1990). In this study the software program Arcview GIS, ESRI V10 (2010) was used for spatial modelling of mineral magnetic and textural data. Essentially, IDRISI consists of two components, a spatial database and an attribute database, which are combined into a single entity. Around this main database are sequences of software components that allow selected constituents of the database to be used for map production. A georeferenced base map (using a co-ordinate system, in this case, OSGB)) for given sampling areas was created, and the constituents of the spatial database

plotted on the base map as points. A software routine was then performed to allow attribute values for the selected variable to be attached to each of the points. From this, an interpolated surface of the specific variable was created. The generated image, in raster format, was then overlaid by a mask, so as to display only the sample area. Finally, a text layer was applied to depict individual localities on each GIS map.

3.4 Data confidence

Prior to experimentation and analysis, it is useful to be aware of the limitations in the data collected. Any researcher needs to be able to demonstrate the extent to which confidence can be shown in any interpretations that are derived from their data. However, in most mineral magnetic studies, the reliability of the environmental magnetic data is not formally stated (Booth *et al*., 2004). The most obvious sources of uncertainty are likely to be due to:

1. Failure of the field sampling strategy to account for natural spatial variability in the material being sampled. Such variability may occur at a range of spatial scales.
2. Sub-sampling of bulk field samples within the laboratory during the sample preparation stage.
3. Instrument error, particularly in terms of calibration accuracy.
4. Operator error in using analytical equipment.

Lees (1994, 1999) provided a thorough examination of (1) at the large and intermediate spatial scales and Booth *et al.* (2004) at the (2) sub-sampling of bulk field samples. The work focused on the spatial variability of sediment samples when used to characterize the environmental magnetic properties of particular sediment types as part of a catchment-scale sediment-source study. Lees (1994) demonstrated that considerable spatial variability can exist in the magnetic properties of a single sediment type over scales of several 100 m to ~10 m, whereas Booth *et al.* (2004) demonstrated variability within individual samples. Lees (1994, 1997) and Booth *et al* (2004) proposed a comprehensive field sampling strategy in order to fully quantify this variability but, to date, few published studies have adopted such a rigorous approach.

This investigation focuses on the first three of the above sources of uncertainty. As Lees (1994, 1997) provided an excellent analysis of: (1) large and intermediate scales and Booth *et* al. (2004) investigated (2) small scales. Only intermediate scale spatial variability (i.e. at the scale of the individual sampling location) is considered here. Operator error within the laboratory (4) is likely to be reduced with experience, as inconsistencies or problems with the data are more likely to be identified as data are obtained.

Samples were collected from five field sites within the Wolverhampton area (Figure 3.20; Step 1). Sites were selected to include contrasting traffic and sedimentological conditions. At each individual field site, five field samples were collected, taken from the four corners (10 m corner to corner) and centre of the road (Figure 3.20; Step 2), using the methods detailed in section 3.2 and stored, as described in section 3.2.

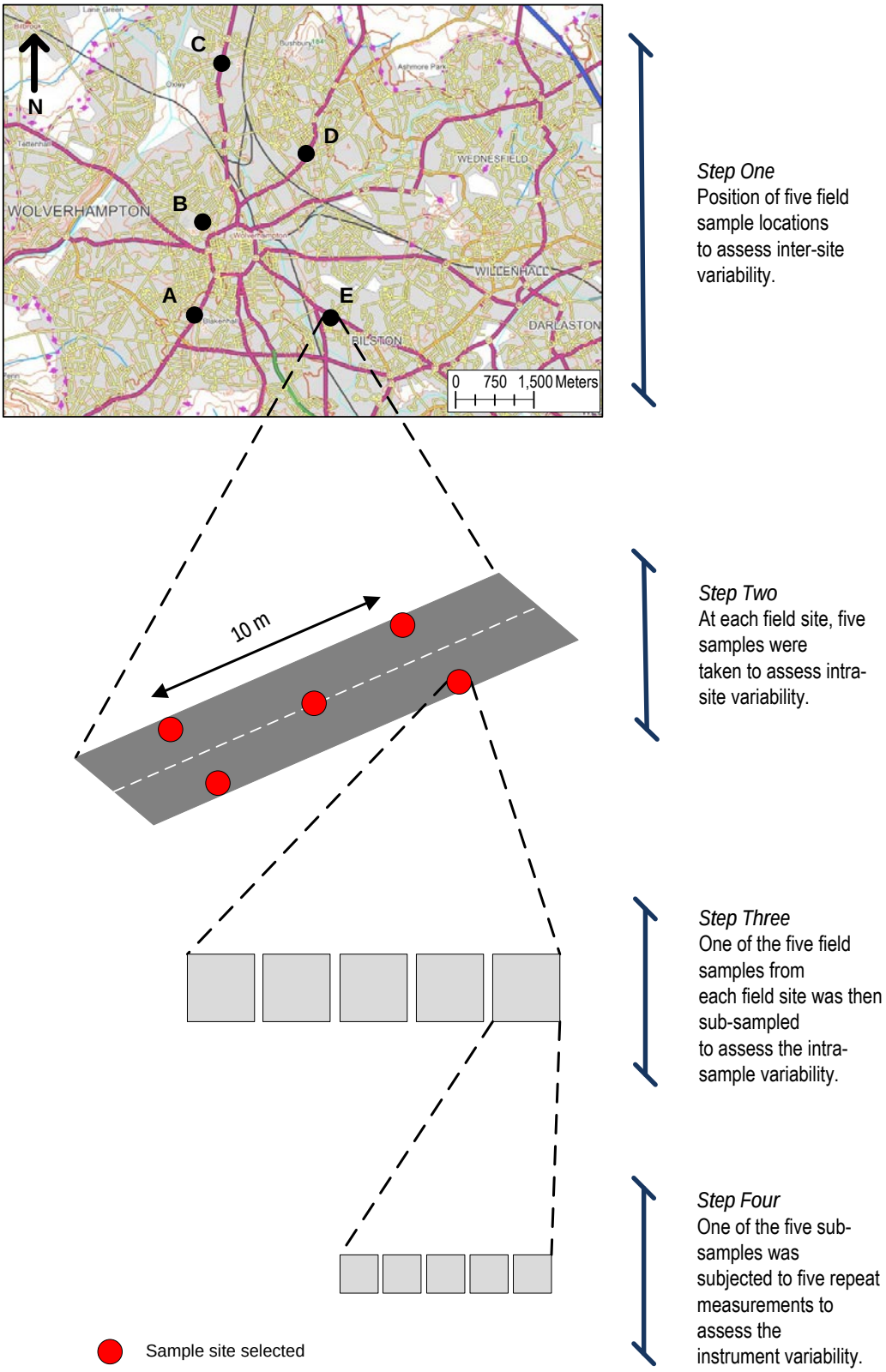

Figure 3.20 An explanation of how the field (step two), sub-samples (step three) and machine (step four) variations were established in this study. Grid references (A) SO 390685 297213; (B) SO 390941 299175; (C) SO 391261 296772; (D) SO 392870 300359; and (E) SO 393314 297346.

In addition, to assess intra-sample variability, five sub-samples were taken from one of the field samples from each of the five field sites (Figure 3.20; step 3). Finally, one of these sub-samples from each of the five field locations was selected for repeat measurements (Figure 3.20; step 4) to assess instrument error. The resulting 25 bulk field samples were then analysed using procedures detailed in section 3.2.

There are several statistical approaches used to highlight data variability. Such analyses are particularly important, as it is possible for two data sets to have identical mean values, but extremely different data distributions. The simplest approach is to quote the data range (i.e. the minimum and maximum values). However, a more conventional approach is to quote the standard deviation and/or the standard error and/or the 95% confidence limits. Alternatively, the data can be displayed graphically using the mean values as data points with their standard deviation or standard error or the 95% confidence limits as distribution bars, or simply by plotting all the data as boxplots.

For brevity, only selected mineral magnetic variables (χ_{LF} and SIRM) and textural variables (Mean-PS and PM_{10}) are reported. Figure 3.21 indicates that the mineral magnetic and textural characteristics of the sediments throughout the urban environment are more diverse than the characteristics of the sediments at any one-sample site. There is clearly a measurable degree of compositional variability over spatial areas <1 m^2 at each field sampling site. While in these samples, this intra-site variability is of a smaller magnitude than inter-site variability, comparisons between some individual samples between sites demonstrates the problems that may occur if a single field sample is taken as representative for each sampling location. For example, while the mean magnetic properties from sample site B and sample site C are statistically different, taking the individual field samples with the most extreme magnetic properties from each 1 m^2 quadrat sample, grids would suggest these two locations had very similar χ_{LF} (Figure 3.20a) and SIRM (Figure 3.20b) values.

Figures 3.22–3.25 suggest that the degree of intra-sample variability (Stage 3) is somewhat less than the intra-site variability, although this is not so in all cases (i.e.χ_{LF}) values for sample site E). Again, failure to homogenize an individual field sample prior to sub-sampling for analysis could lead to errors of a similar magnitude to those resulting from use of an individual field sample to represent the magnetic properties of a field site.

Figures 3.22-3.25 also suggest that, for these magnetic and textural variables at least, error due to instrument variability is low (i.e. the level of repeatability of the measurements for individual samples seem to be high) compared to both intra-sample and intra-site variability. The relatively high inter-site, as opposed to intra-site, variability displayed by these data suggests that any environmental magnetic variations and subsequent interpretations of the sediments within this particular field setting can be identified with confidence. Inter-site variations are likely to represent ‘real’ differences between sample sites and are unlikely to be due to intra-site variations.

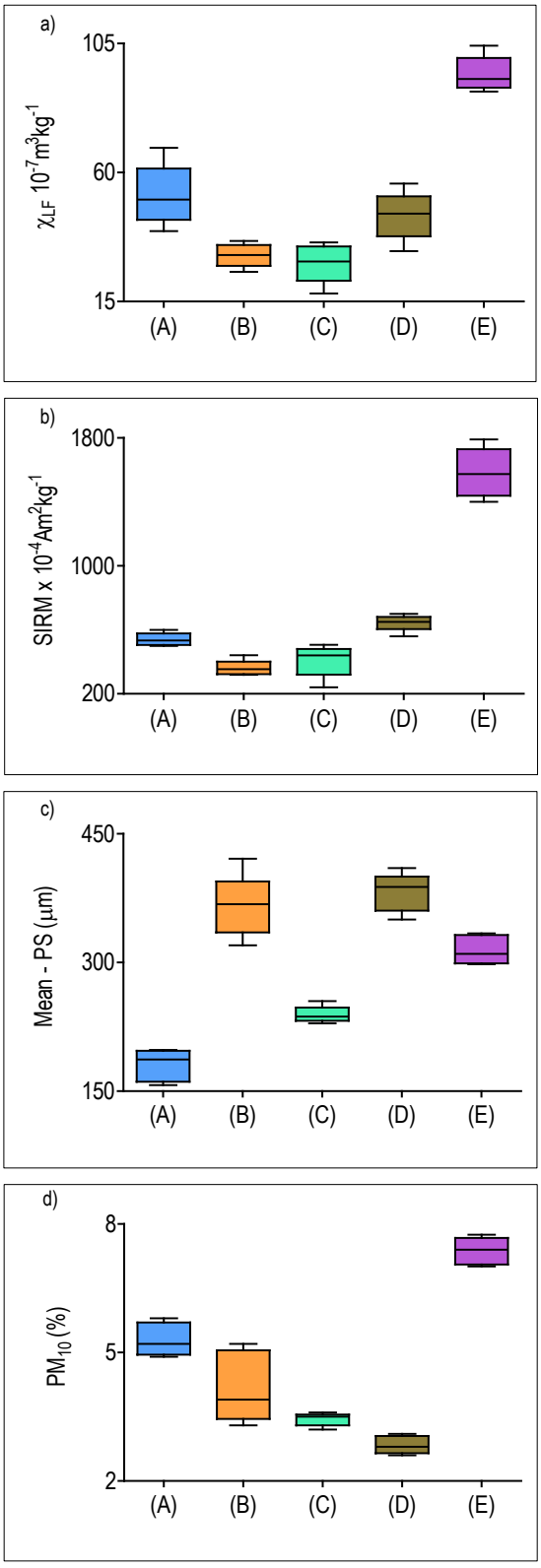

Figure 3.21 Boxplots of the quadrat variations for each of the five locations in Wolverhampton. (A) SO 390685 297213; (B) SO 390941 299175; (C) SO 391261 296772; (D) SO 392870 300359; and (E) SO 393314 297346. (a) boxplots of the χ_{LF} variable; (b) boxplots of the SIRM variable; (c) boxplots of the mean-PS variable; and (d) boxplots of the PM_{10} variable.

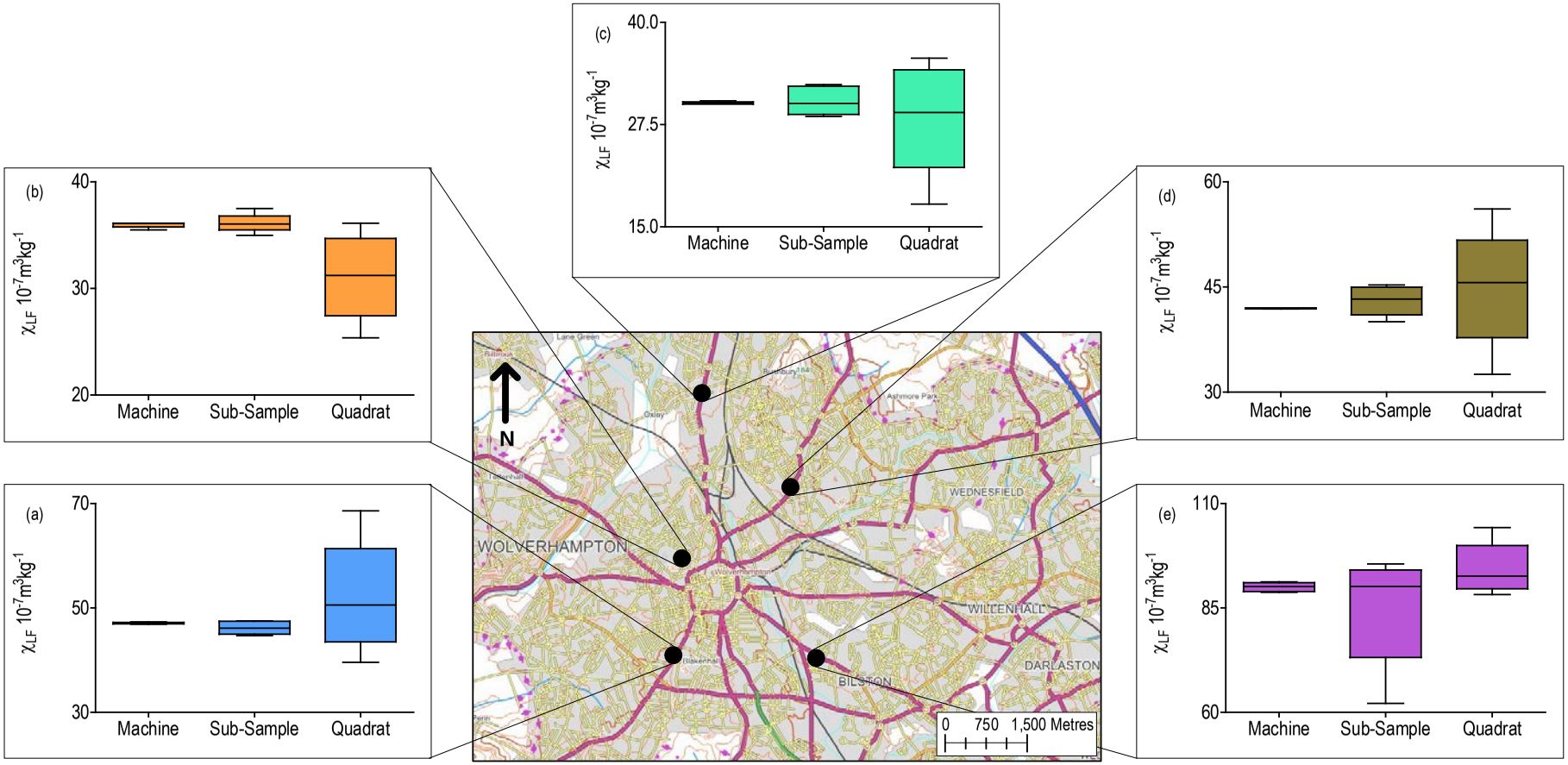

Figure 3.22 χ_{LF} ($10^{-7}m^3kg^{-1}$) variation between replicate analytical instrument measurements, sub-samples, and quadrat samples from five locations in Wolverhampton. (A) SO 390685 297213; (B) SO 390941 299175; (C) SO 391261 296772; (D) SO 392870 300359; and (E) SO 393314 297346.

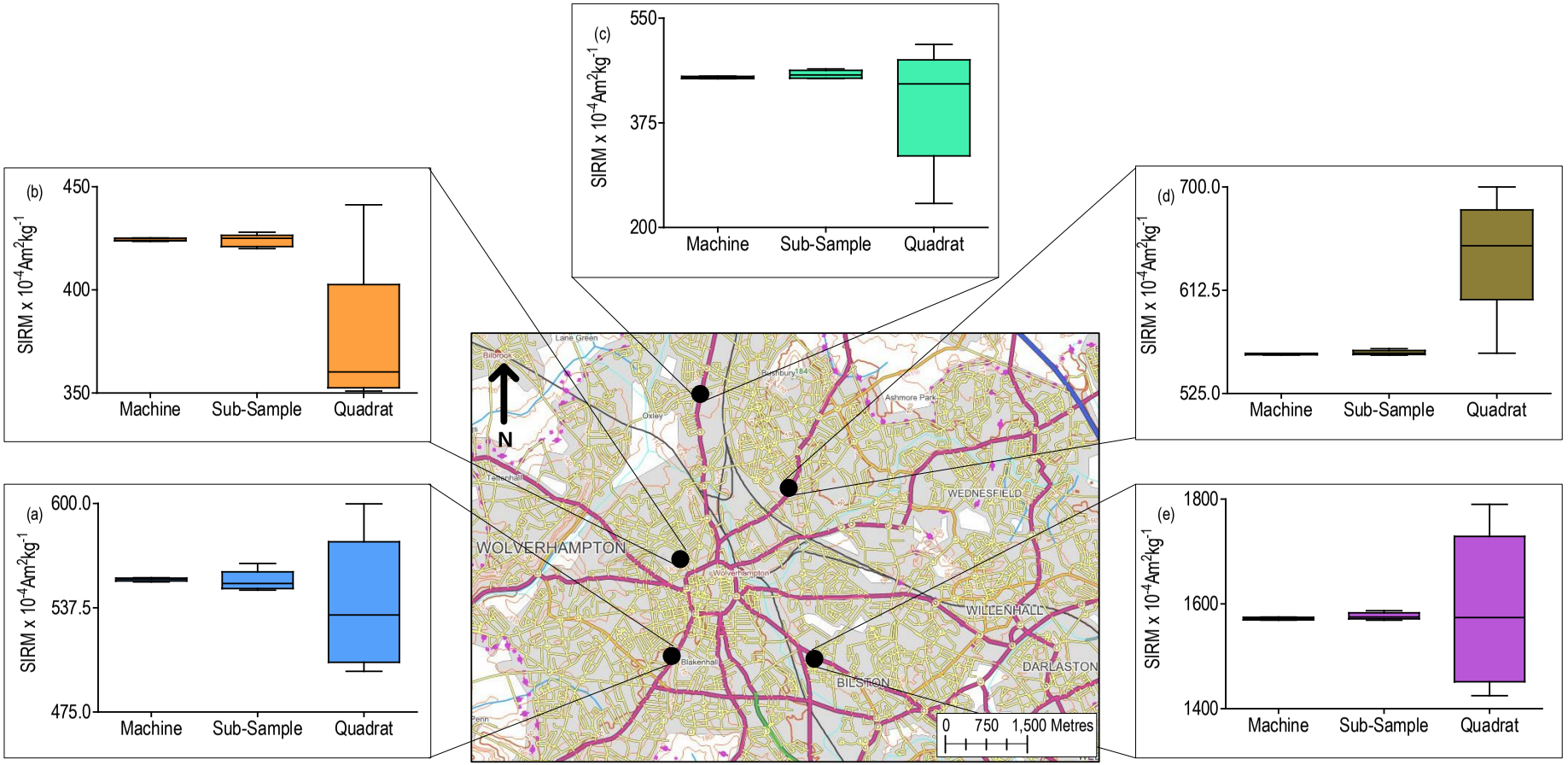

Figure 3.23 SIRM ($10^{-4}Am^2kg^{-1}$) variation between replicate analytical instrument measurements, sub-samples, and quadrat samples from five locations in Wolverhampton. (A) SO 390685 297213; (B) SO 390941 299175; (C) SO 391261 296772; (D) SO 392870 300359; and (E) SO 393314 297346.

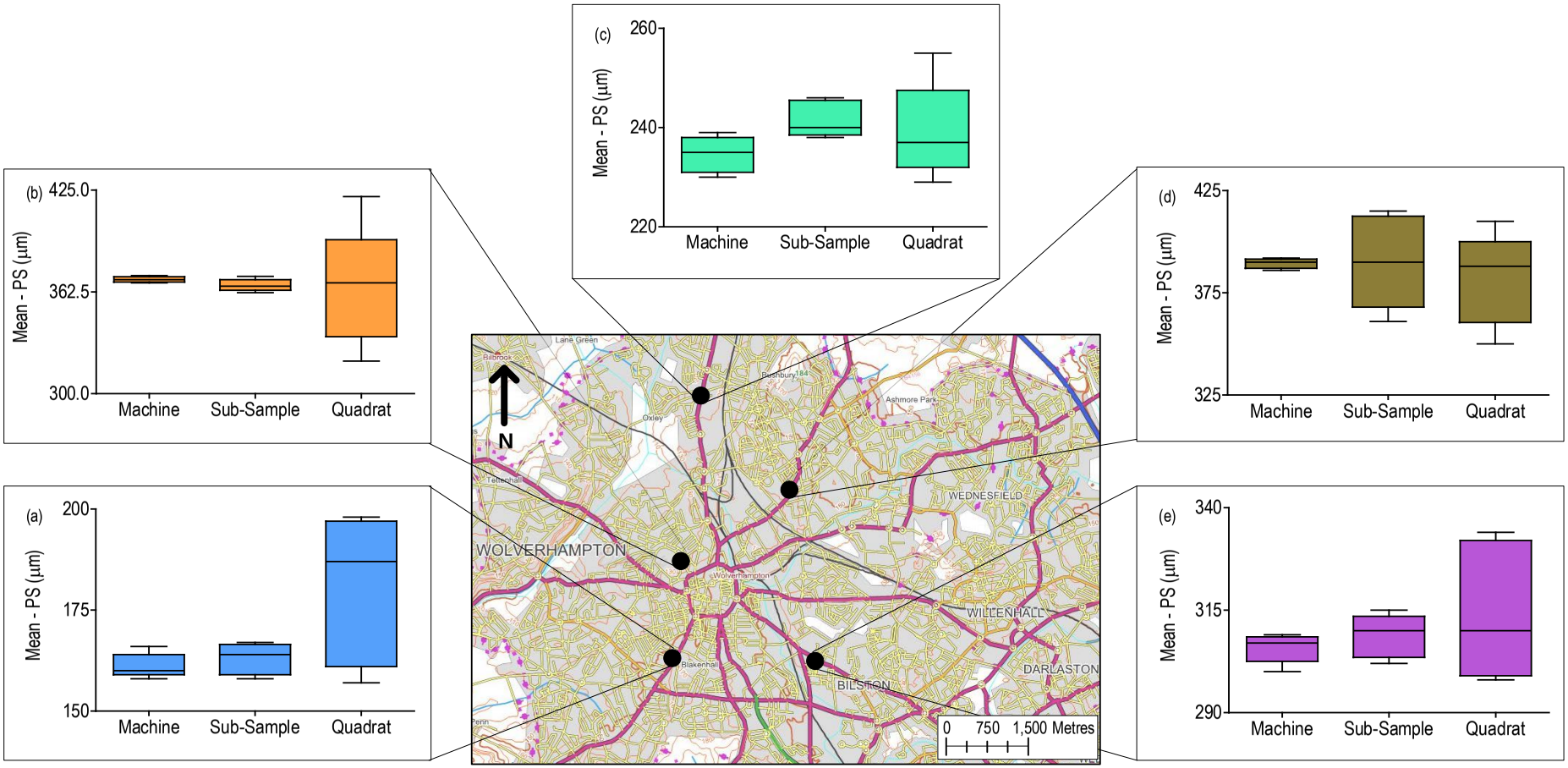

Figure 3.24 Mean-PS (µm) variation between replicate analytical instrument measurements, sub-samples, and quadrat samples from five locations in Wolverhampton. (A) SO 390685 297213; (B) SO 390941 299175; (C) SO 391261 296772; (D) SO 392870 300359; and (E) SO 393314 297346.

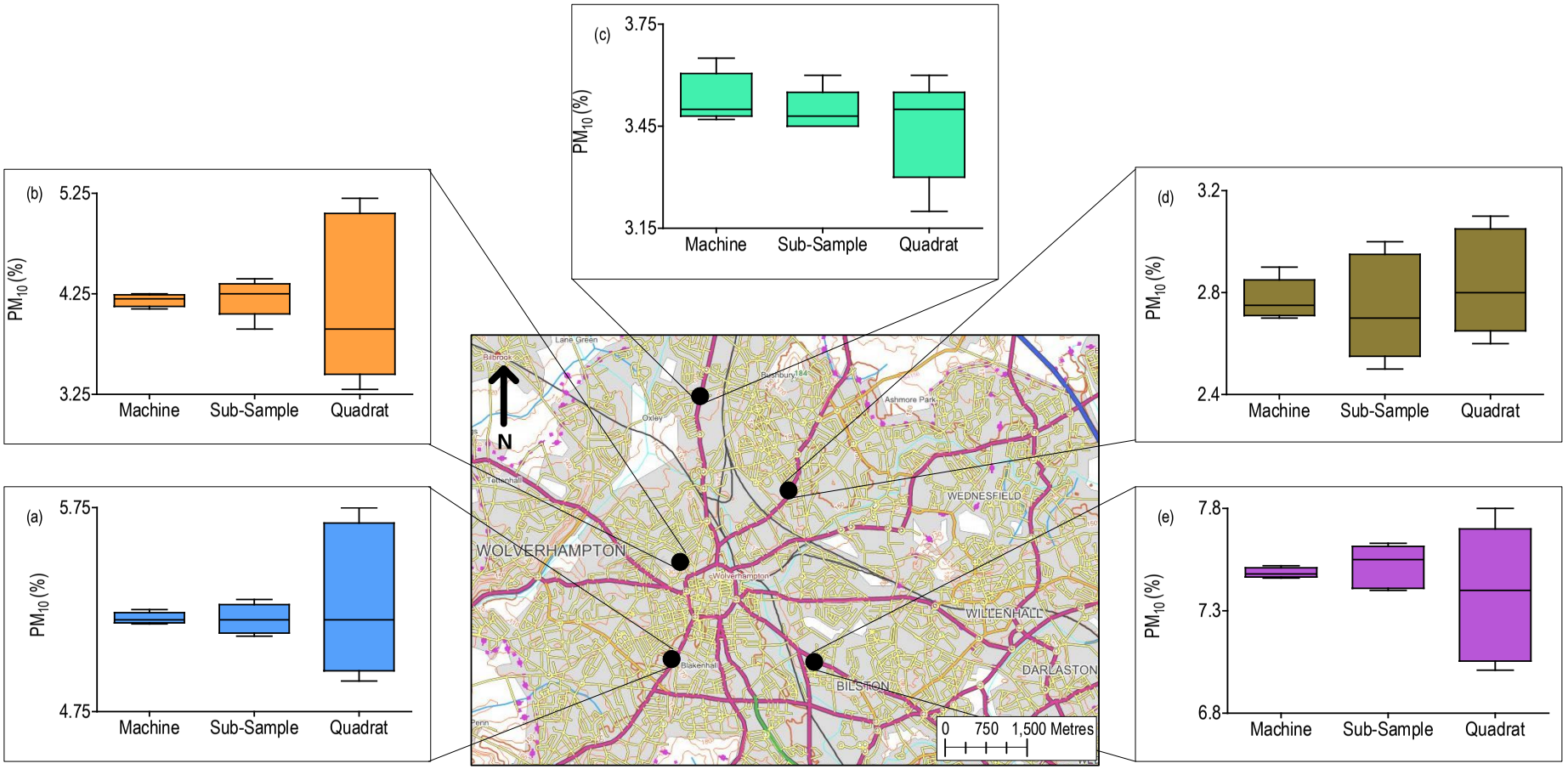

Figure 3.25 PM_{10} variation between replicate analytical instrument measurements, sub-samples, and quadrat samples from five locations in Wolverhampton. (A) SO 390685 297213; (B) SO 390941 299175; (C) SO 391261 296772; (D) SO 392870 300359; and (E) SO 393314 297346.

The degree of intra-site variability shown by these samples could, of course, be a more significant problem in other field contexts. This level of intra-site variability could be large enough to mask inter-site variability in a sediment system with more subtle inter-site magnetic variations. Lees (1994, 1997) outlined methods to ensure that the degree of inter-site variability is fully assessed at scales from 100s to a few 10s of metres. The current data demonstrate that care must also be exercised at a smaller spatial scale appropriate to the individual field-sampling site. Combining multiple samples taken over a small area (~1 m^2) is likely to prove more representative of the sediment body being sampled than a single sample taken from a specific point.

These data also demonstrate the need for care in sub-sampling field samples in the laboratory. Again, where inter-site variability in a sediment system is relatively low, the magnitude of intra-sample variability may become significant. Thorough mixing of field samples prior to sub-sampling and correct use of a sample splitter is therefore required to reduce such possible sources of error. For these samples, the degree of machine error is relatively low.

Nevertheless, to have confidence in data collected and subsequent interpretations, it seems highly desirable that standard practise should include regular replicate sub-samples and re-runs of samples to ensure that both representative and accurate data are obtained (Lees, 1994; 1999; Booth *et al*., 2004).

Three general conclusions can be drawn from the analysis.

I. Levels of intra-site variability should be assessed routinely in sampling sediments for environmental magnetic analysis, particularly where relatively low inter-site variability exists (preferably established using the rigorous approach of Lees (1994; 1999).

II. Field samples need to be thoroughly homogenized within the laboratory prior to extracting sub-samples for analysis, as intra-sample variability can be as great as small scale (~1 m^2) intra-site variability (Booth *et al*., 2004).

III. For environmental magnetic measurements made on the types of equipment used here, the level of instrument variability seems relatively small. Even so, good practise should include regular duplicate measurements of samples to ensure confidence in the final data.

In light of these conclusions, to have confidence in the data collected throughout the duration of this work, it was considered necessary to generate frequent replicate sub-samples and re-runs of samples to ensure precision.

Chapter 4

Mineral magnetic and textural characteristics of Road Deposited Sediment (RDS) from Wolverhampton (UK)

4.1 Introducing road deposited sediment results for the City of Wolverhampton

Chapter 4 characterizes the mineral magnetic and textural properties of RDS collected from the City of Wolverhampton (n = 546 samples). Figure 4.1 maps the framework for this investigation and highlights the fundamental principles of this methodology by examining proxy methods temporally and spatially. The use of statistical and graphical techniques has determined the mineral magnetic properties of RDS and the possible influence of texture on characteristics. From these linkages the use of mineral magnetic measurements for PM identification in Wolverhampton will be assessed for its suitability as a PM particle size proxy.

4.2 Characteristics of RDS in Wolverhampton

RDS was collected from 42 pre-selected sampling points (Figure 4.2, Appendix 3.3) in Wolverhampton on 13 occasions over a period of two years (2008-2010, n = 546). The material collected consists a mixture of organic matter, soil and building material consisting of sand, silt and clay particles, which was collected from a wide range of differing environments (urban, industrial, commercial, residential, urban-rural). Initial RDS characteristics for Wolverhampton are presented in Table 4.1 and consist of (a) mineral magnetic and (b) textural data. The data presented are discussed in this chapter, with the potential use of mineral magnetic methods for PM particle size proxy purposes.

4.2.1 Mineral magnetic data of RDS in Wolverhampton

Magnetic concentration-dependent parameters indicate Wolverhampton RDS contains a moderate to high concentration of magnetic minerals ((mean values χ_{LF} 43.999 x $10^{-7}m^3kg^{-1}$; χ_{ARM} 0.094 x 10^{-5} m^3kg^{-1}; SIRM 689.830 x $10^{-4}Am^2kg^{-1}$) when compared to other studies (Table 2.11 (Xie *et al.,* 2001*;* Booth *et al.,* 2007)). When these results are compared to published values for other environmental materials (Dearing, 1999), they indicate that the magnetic properties of sediments are similar to intermediate igneous rocks, basic/ultra-basic rocks and ferromagnetic minerals. The SIRM values indicate relatively high variation between sites (57.575-6045.963 x $10^{-4}Am^2kg^{-1}$).

The Soft ($_{IRM20mT}$) parameter, indicating the content of ferrimagnetic 'magnetite-type' minerals (low coercivity), range from 1.674-41.155%, and the Hard ($_{IRM300mT}$) parameter, indicating the content of canted antiferromagnetic 'hematite-type' minerals (high coercivity), range from 1.095-27.459%. These values Indicate that most samples have a greater influence of magnetically-soft minerals (e.g. magnetite (Fe_3O_4) and maghaemite (γFe_2O_3)), than magnetically-hard minerals (e.g. hematite (αFe_2O_3) and goethite (αFeOOH)), but do contain mixed magnetic mineralogy's of both soft and hard types of minerals.

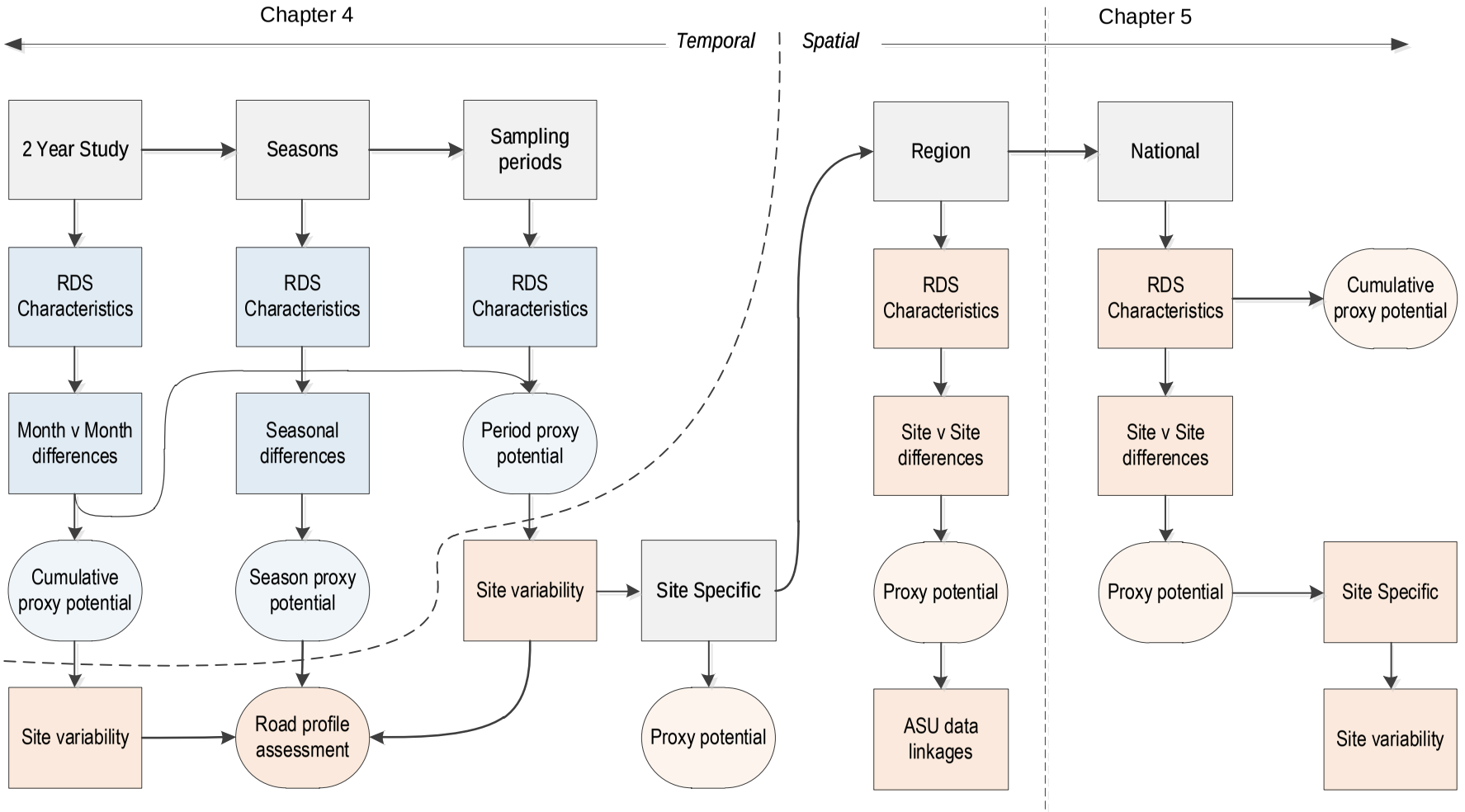

Figure 4.1 Framework and principal methods reported in Chapters 4 and 5.

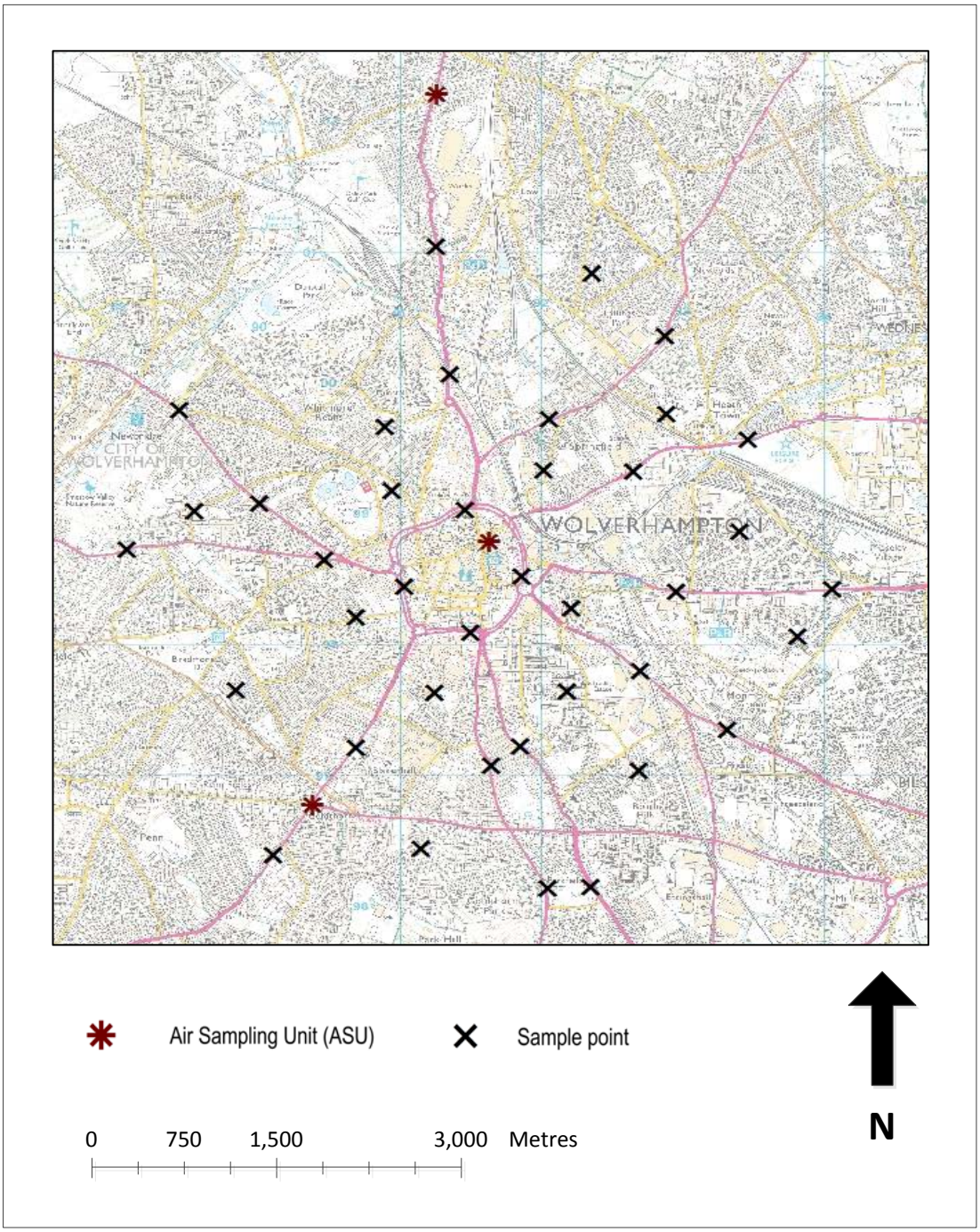

Figure 4.2 Map of the Wolverhampton sampling area. Each of the 42 points were sampled on 13 occasions between January 2008 and January 2010. ASU locations are shown and formed part of the 42 points.

Table 4.1 Summary RDS analytical data* for Wolverhampton (January 2008–January 2010) (n = 546)

	Parameters	Units	Mean	Median	SD	CV (%)	Min	Max	Range
(a)	χ_{LF}	$10^{-7}m^3kg^{-1}$	43.999	39.704	22.104	50.236	5.403	131.240	125.837
	χ_{FD}	%	1.270	1.221	0.750	59.044	0.053	4.930	4.877
	χ_{ARM}	$10^{-5}m^3kg^{-1}$	0.094	0.074	0.086	91.491	0.012	0.824	0.812
	SIRM	$10^{-4}Am^2kg^{-1}$	689.830	543.314	624.961	90.596	57.575	6045.963	5988.388
	S-Ratio	Dimensionless	-0.799	-0.797	0.059	-7.431	-0.979	-0.593	0.386
	$SOFT_{\%20mT}$	%	17.415	16.781	4.017	23.065	1.674	41.155	39.481
	$SOFT_{\%40mT}$	%	41.906	41.589	5.087	12.139	5.060	89.953	84.894
	$HARD_{\%300mT}$	%	9.421	8.898	3.901	41.406	1.095	27.459	26.364
	$HARD_{\%500mT}$	%	4.502	3.875	3.075	68.307	0.007	21.105	21.097
	$SOFT_{IRM20mT}$	$10^{-4}Am^2kg^{-1}$	117.516	89.494	114.105	97.097	8.166	1324.087	1315.921
	$SOFT_{IRM40mT}$	$10^{-4}Am^2kg^{-1}$	288.451	221.955	321.366	111.411	25.635	5438.547	5412.912
	$HARD_{IRM300mT}$	$10^{-4}Am^2kg^{-1}$	65.598	46.501	74.391	113.405	3.327	836.084	832.757
	$HARD_{IRM500mT}$	$10^{-4}Am^2kg^{-1}$	30.196	20.444	41.192	136.416	0.084	606.889	606.804
	ARM/χ	$10^{-1}Am^{-1}$	0.685	0.593	0.463	67.629	0.113	5.369	5.256
	χ_{ARM}/SIRM	$10^{-3}Am^2kg^{-1}$	0.152	0.133	0.113	74.463	0.011	1.467	1.457
	SIRM/ARM	Dimensionless	251.027	235.806	155.024	61.756	21.404	2956.467	2935.063
	SIRM/χ	$10^{-1}Am^{-1}$	15.230	13.797	10.391	68.231	1.668	197.360	195.692
(b)	Mean - PS	μm	293.801	295.259	88.701	30.191	44.747	594.311	549.564
	Median - PS	μm	358.015	358.442	88.833	24.813	119.033	801.405	682.372
	Sorting	σ_1	2.153	2.136	0.395	18.362	1.168	3.178	2.010
	Skewness	SK_1	0.459	0.464	0.136	29.617	-0.065	0.784	0.849
	Kurtosis	K_G	1.390	1.299	0.596	42.904	0.721	10.020	9.299
	Sand	%	77.879	78.831	7.627	9.793	42.714	93.596	50.882
	Silt	%	19.412	18.407	7.450	38.380	5.085	54.618	49.533
	Clay	%	2.709	2.297	1.313	48.464	0.061	7.668	7.607
	$PM_{1.0}$	%	1.631	1.330	0.946	58.018	0.000	6.137	6.137
	$PM_{2.5}$	%	3.158	2.709	1.477	46.768	0.567	8.192	7.625
	PM_{10}	%	7.866	7.213	3.393	43.136	1.643	18.716	17.073
	PM_{100}	%	25.578	24.067	8.841	34.564	10.791	67.762	56.971
	LOI	%	1.080	1.063	0.090	8.371	2.041	0.816	1.225

SD = Standard Deviation; CV = Percentage coefficient of variation; Min = Minimum value; Max = maximum value. Values are shown to 3 decimal places for consistency, not accuracy.

This is further supported by the S-ratio parameter, which shows values ranging from -0.979 to -0.593. Given that most S-ratio values are >-0.7, they are described by Robinson (1986) as intermediate values (~-0.4 to -0.6), and therefore, indicate that some samples contain either magnetically soft minerals with a fine magnetic grain size or an assemblage with a small canted antiferromagnetic component, or both. However, samples with low negative S-ratio values (<-0.7) may be dominated by magnetically soft minerals with a coarse magnetic grain size.

The ARM/χ values range from high to low (0.113-5.369 x $10^{-1}Am^{-1}$), indicating a predominately coarse grained magnetic material (mean 0.685 x $10^{-1}Am^{-1}$). The SIRM/ARM values range from 21.40-2956 (SD 155.024; mean 251.027) and are high compared to other environmental materials (Yu and Oldfield, 1993). This supports the ARM/χ values, by indicating a coarse magnetic grain size. SIRM/χ values are low (mean 15.23 x $10^{-1}Am^{-1}$), with a wide range (1.668-1973.60 $10^{-1}Am^{-1}$). High SIRM/χ values suggest the presence of fine grained magnetic material.

4.2.2 Textural data for RDS in Wolverhampton

Results indicate that RDS are moderately sorted (mean 293.801 µm; 2.153 σ_1), with moderate to high sand concentrations (77.879%), smaller silt concentrations (19.412%), and low clay concentrations (2.709%) (Table 4.1b). The RDS particle size data also suggests a moderate level of sediment beneath the PM_{100} boundary (25.578%), with lesser PM_{10} concentrations (7.866%), low concentrations of $PM_{2.5}$ (3.158%) and $PM_{1.0}$ (1.631%). The LOI values are typically low ((mean 1.080%), Xie *et al.,* 2001) (range 2.041-0.816%; SD 0.090).

4.2.3 Relationships between mineral magnetic and textural parameters

To determine mineral magnetic methods as a particle size proxy, statistical tests were carried out on the Wolverhampton RDS samples. Relationships between mineral magnetic and textural parameters were examined. The data set was interrogated by correlation statistics (Spearman Rank) and graphically displayed with bivariate plots. Table 4.2 displays correlation values for every possible pairing of parameters.

Table 4.2 summarizes correlation statistics between the mineral magnetic parameters and textural parameters for Wolverhampton and shows some relationships between the mineral magnetic and textural parameters. Although there is some indication of inter-parameter linkages, these relationships are relatively weak (i.e. most correlation of coefficient values are *ca.* r =≤-0.001–0.182 and not significant). This suggests that texture of RDS has very limited control on the mineral magnetic assemblages in Wolverhampton. However, the stronger relationships appear related to magnetic concentration and mineralogy (χ_{LF} versus $PM_{1.0}$ – PM_{100}, r = 0.109-0.125; χ_{ARM}/χ versus $PM_{1.0}$–$PM_{10,}$ r = -0.193- -0.232 and $PM_{100,}$ r = -0.144; S-ratio versus $PM_{1.0}$–$PM_{100,}$ r = -0.162-0.135 (p <0.05 to <0.001)). The relationships shown between these parameters are weak (p <0.05) with χ_{LF} versus $PM_{1.0}$ (Figure 4.3a (r = 0.109; p <0.05)) and SIRM versus $PM_{1.0}$ (Figure 4.3b (r = 0.120; p <0.01)).

Table 4.2 Statistical relationships between the mineral magnetic and textural parameters for Wolverhampton (January 2008–January 2010) (**bold** text is significant (*p <0.05; **p <0.01; ***p <0.001)) (n = 546)

Parameters	Median-PS	Mean-PS	Sorting	Skewness	Kurtosis	Sand	Silt	Clay	$PM_{1.0}$	$PM_{2.5}$	PM_{10}	PM_{100}	LOI
χ_{LF}	-0.140**	-0.080	0.070	-0.081	-0.078	-0.102*	0.071	0.125**	0.109*	0.109*	0.096*	0.125**	0.205***
$\chi_{FD\%}$	-0.078	-0.057	0.085	-0.016	-0.151***	-0.134**	0.139**	-0.023	-0.043	-0.015	0.080	0.147***	-0.124*
χ_{ARM}	-0.084	-0.009	0.043	-0.088*	-0.091*	-0.053	0.036	0.068	0.065	0.055	0.030	0.088*	0.148**
SIRM	-0.135**	-0.076	0.036	-0.096*	-0.048	-0.067	0.036	0.120**	0.103*	0.099*	0.067	0.090*	0.260***
Soft $_{\%20mT}$	-0.100*	-0.046	-0.045	-0.117**	-0.122**	-0.039	0.052	-0.086	-0.090*	-0.075	-0.086	0.093*	-0.089
Soft $_{\%40mT}$	-0.001	0.053	-0.040	-0.089*	-0.054	-0.032	0.062	-0.105	-0.117**	-0.096*	-0.064	0.062	-0.021
Hard $_{\%300mT}$	-0.070	-0.128**	-0.146***	-0.060	0.097*	0.118	-0.133	-0.004	-0.023	-0.020	-0.079	-0.088*	0.122*
Hard $_{\%500mT}$	0.030	-0.031	-0.021	0.062	0.071	0.052	-0.070	0.060	0.048	0.066	0.048	-0.065	0.073
Soft $_{IRM20mt}$	-0.178***	-0.101*	0.001	-0.154***	-0.091*	-0.068	0.044	0.066	0.053	0.052	0.018	0.115**	0.190***
Soft $_{IRM40mT}$	-0.126**	-0.060	0.030	-0.106*	-0.056	-0.071	0.044	0.106*	0.089*	0.086	0.060	0.095*	0.248***
Hard $_{IRM300mT}$	-0.157***	-0.130**	-0.037	-0.120**	-0.010	-0.010	-0.024	0.098*	0.069	0.075	0.019	0.044	0.279***
Hard $_{IRM500mT}$	-0.075	-0.073	0.005	-0.036	0.005	-0.012	-0.021	0.112	0.098*	0.104*	0.069	0.020	0.212***
S-ratio	-0.066	-0.014	0.058	-0.045	-0.185***	-0.125**	0.155***	-0.175***	-0.162***	-0.159***	-0.011	0.135**	-0.375***
ARM/χ	-0.001	-0.006	-0.214***	-0.114**	0.083	0.182***	-0.158***	-0.159***	-0.193***	-0.181***	-0.232***	-0.114**	-0.021
SIRM/ARM	-0.094*	-0.131**	-0.058	-0.049	0.094*	0.006	-0.032	0.091	0.084	0.076	0.028	-0.017	0.209***
SIRM/χ	0.033	0.035	-0.033	-0.009	0.065	0.052	-0.065	0.060	0.053	0.043	-0.014	-0.060	0.269***
χ_{ARM} /SIRM	-0.137**	-0.138**	-0.224***	-0.190**	-0.023	0.087*	-0.062	-0.162***	-0.215***	-0.190***	-0.223***	-0.005	-0.044

The Hypothesis tested was:-

Null Hypothesis (H_0)	There are no significant correlations between mineral magnetic and textural parameters.
Alternative Hypothesis (H_1)	There are significant correlations between mineral magnetic and textural parameters

The strongest correlations are between the S-ratio and RDS fraction (((PM$_{1.0}$ and PM$_{2.5}$) r = -0.163 to -0.159; p <0.001), Figure 4.3c-d) with S-ratio decreasing with increasing PM$_{1.0.}$ This suggests that a decrease in hard magnetic minerals is associated with a corresponding decrease in PM$_{1.0}$. At p <0.05 the statistical tests indicate a weak significant correlation exists between the mineral magnetic and textural parameters. The data suggests that mineral magnetic measurements are unlikely to be useful at this scale for particle size proxy purposes.

4.2.4 Relationships between the mineral magnetic parameters

To assess whether relationships exist between the mineral magnetic parameters, the data set was interrogated by correlation statistics (Spearman Rank). The results are summarized in Table 4.3. The results for the Wolverhampton samples show that most of the mineral magnetic parameters exhibit strong and significant correlation values, which are statistically significant at the p <0.05-0.001 confidence level (Table 4.3). The strongest correlation coefficients exist between each of the magnetic concentration dependent parameters (r = 0.768-0.907; p <0.001), with χ_{LF} and SIRM being strongest (r = 0.907; p <0.001).

Figure 4.4a, shows χ_{LF} versus SIRM, an exceptionally strong positive correlation exists between these parameters. Increases in χ_{LF} values are associated with corresponding increases in SIRM values. This indicates that the mineral magnetic signals of the sediment samples in Wolverhampton are dominated by remanence type of magnetism (ferrimagnetic and/or canted-antiferromagnetic). Since, none of the data-points have high SIRM values and corresponding low χ_{LF} values, canted-antiferromagnetic behaviour is considered insignificant in these sediment samples, and the main type of magnetic remanence is ferrimagnetism.

Figure 4.4b and c shows χ_{ARM} versus χ_{LF} and χ_{ARM} versus SIRM (Table 4.3). Strong positive correlations (r = 0.768-0.783; p <0.001) exist between these parameters. Any increases in χ_{ARM} values are associated with corresponding increases in SIRM and χ_{LF} values. This further confirms that the mineral magnetic signals of the Wolverhampton sediment samples are dominantly ferrimagnetic and their magnetic grain sizes are predominantly ultrafine. Figure 4.4d, shows, χ_{LF} and $\chi_{FD\%}$ plots, which have been used in several studies (Dearing *et al.,* 1996; Walden *et al*., 1999) to demonstrate the domain size of the magnetic material within a sample. The plot indicates that samples are predominantly coarse grained material, with very little or no SP grains present. The weakest correlation coefficient values are associated with correlation between the χ_{ARM}/χ parameters and most other mineral magnetic parameters (r = -0.285-0.218). All other parameters are quite strongly correlated, with most correlation coefficient values being r = ≤0.5–0.8.

4.2.5 Mineral magnetic and textural data for sampled months

Magnetic properties of the individual sampling months have distinct differences, with relative highs and lows of magnetic material present temporally (Figures 4.5 and 4.6).

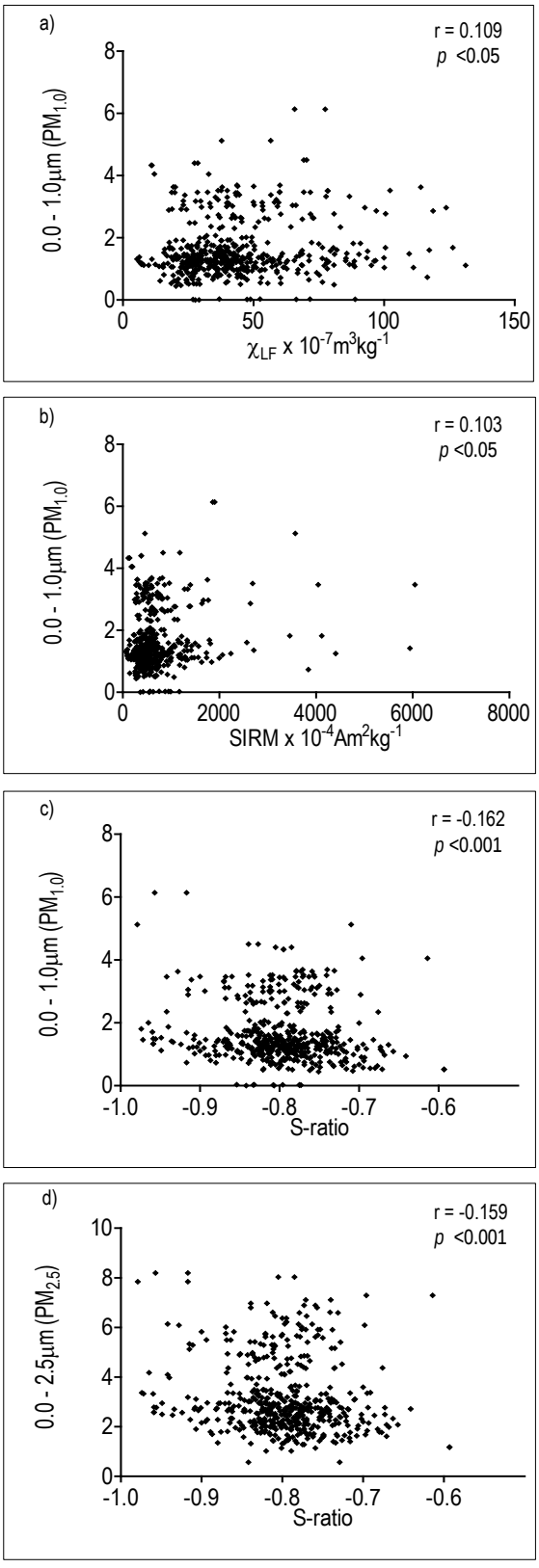

Figure 4.3 Bivariate plots of selected mineral magnetic and textural parameters for Wolverhampton RDS samples (n = 546).

Table 4.3 Statistical relationships between the mineral magnetic parameters Wolverhampton (January 2008-January2010) (**bold** text is significant (*p <0.05; **p <0.01; ***p <0.001)) (n = 546)

Parameters	χ_{LF}	$\chi_{FD\%}$	χ_{ARM}	SIRM	Soft $_{\%\ 20mT}$	Soft $_{\%40mT}$	Hard $_{\%300mT}$	Hard $_{\%500mT}$	Soft $_{IRM20mT}$	Soft $_{IRM40mT}$	Hard $_{IRM\ 300mT}$	Hard $_{IRM\ 500mT}$	S-ratio	χ_{ARM}/χ	SIRM/ $_{ARM}$	SIRM/χ
$\chi_{FD\%}$	0.226***															
χ_{ARM}	0.769***	0.166***														
SIRM	0.907***	0.173***	0.783***													
Soft $_{\%20mT}$	-0.008	-0.028	-0.015	-0.081												
Soft $_{\%40mT}$	-0.011	-0.023	-0.023	-0.073	0.472***											
Hard $_{\%300mT}$	-0.002	-0.047	-0.016	0.082	-0.248***	-0.428***										
Hard $_{\%500mT}$	-0.103*	-0.034	-0.133**	-0.039	-0.148***	-0.320***	0.599***									
Soft $_{IRM20mt}$	0.856***	0.163***	0.725***	0.885***	0.311***	0.117**	-0.025	-0.103*								
Soft $_{IRM40mT}$	0.909***	0.172***	0.781***	0.962***	0.014	0.123**	-0.008	-0.109*	0.913***							
Hard $_{IRM300mT}$	0.674***	0.149***	0.595***	0.785***	-0.183***	-0.297***	0.629***	0.316***	0.643***	0.706***						
Hard $_{IRM500mT}$	0.443***	-0.113*	0.370***	0.551***	-0.156***	-0.313***	0.518***	0.763***	0.432***	0.473***	0.742***					
S-ratio	0.362***	0.278***	0.232***	0.349***	0.021	-0.104*	0.026	0.097*	-0.344***	-0.372***	-0.241***	-0.122**				
ARM/χ	-0.102*	0.003	0.217***	0.027	0.057	0.032	0.218***	-0.004	0.036	0.033	0.148***	0.039	-0.032			
SIRM/ARM	0.239***	-0.022	0.223***	0.340***	-0.113*	-0.100*	0.196***	0.173***	0.277***	0.306***	0.348***	0.327***	0.169***	0.285***		
SIRM/χ	-0.027	0.056	0.109*	0.273***	-0.163***	-0.144**	0.288***	0.180***	0.187***	0.236***	0.366***	0.331***	-0.109*	0.281***	0.256***	
χ_{ARM} /SIRM	0.139**	0.074	0.160***	0.114**	0.107*	0.036	0.034*	-0.100*	0.172***	0.139**	0.116**	0.011	-0.027	0.077	-0.060	-0.013

Interpretation of 'p' values

The 'p' value is a measure of the level of significance at which the null (or alternative) hypothesis must be accepted. For example, if the 'p' value is equal to or less than the level of significance being used, the null hypothesis can be rejected. Thus using a probability level of p<0.05 (0.95), the null hypothesis would be rejected if 'p' value = <0.05 (Walden, 1990).

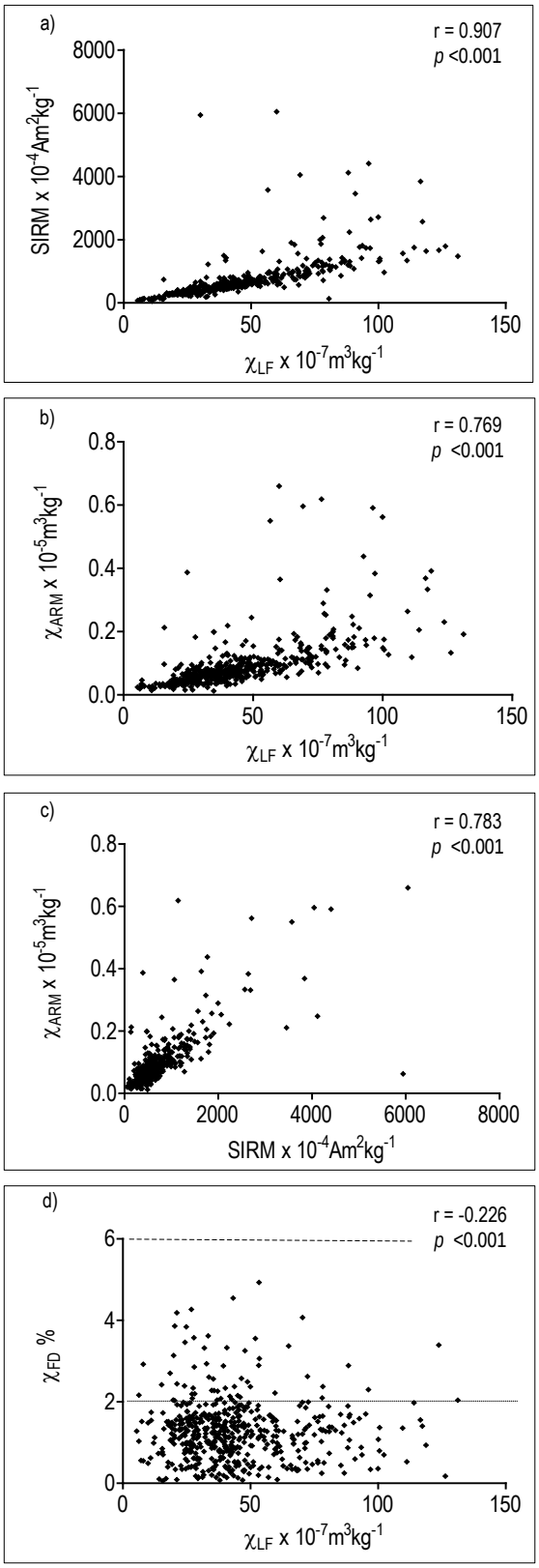

Figure 4.4 Bivariate plots of selected mineral magnetic parameters for Wolverhampton RDS samples (n = 546).

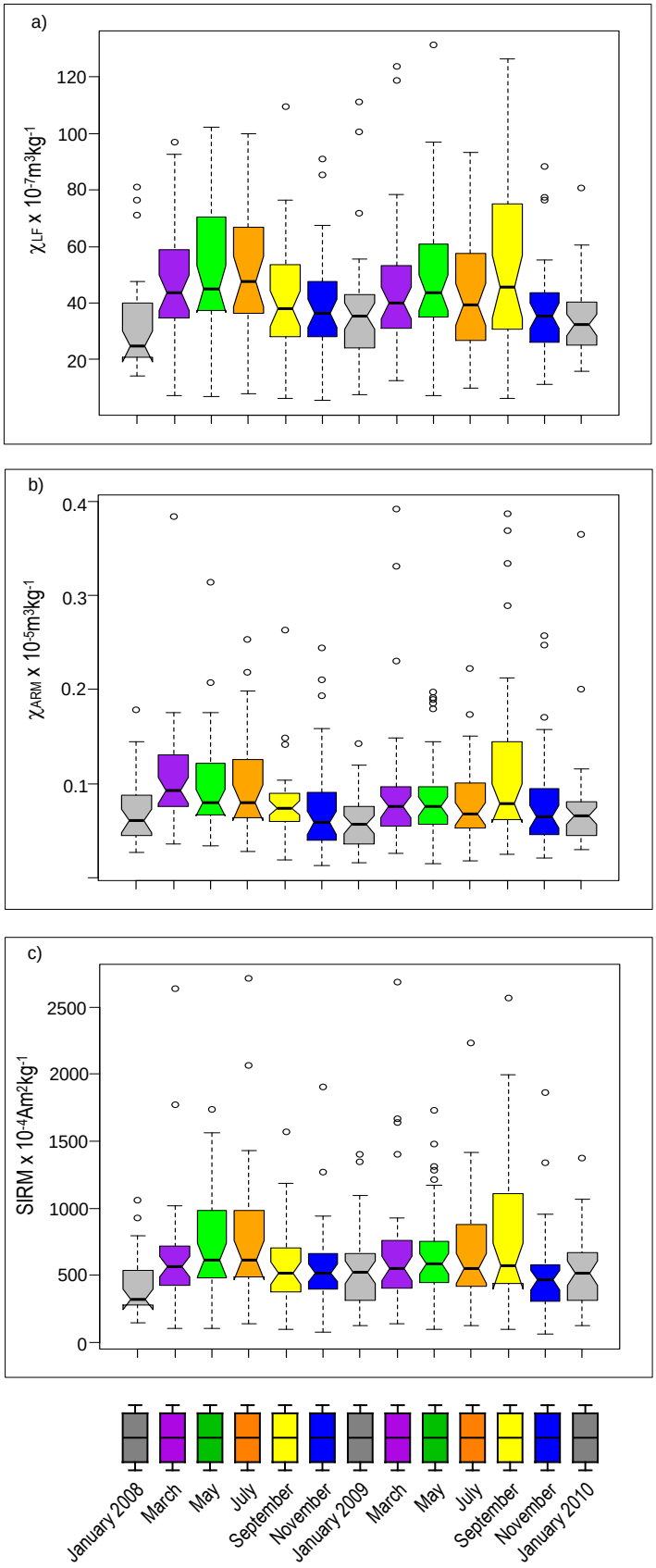

Figure 4.5 Box plots of RDS sample population distributions for selected mineral magnetic parameters for Wolverhampton, January 2008–January 2010.

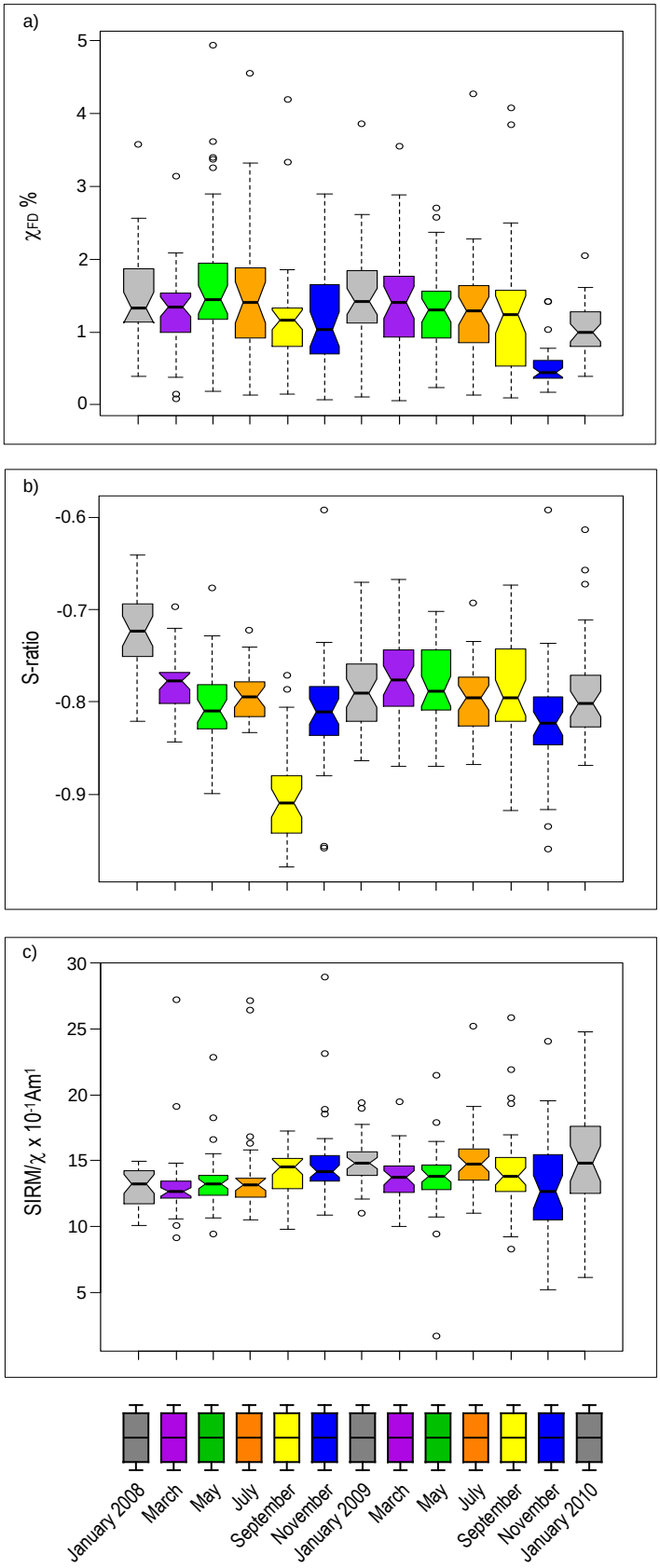

Figure 4.6 Box plots of RDS sample population distributions for selected mineral magnetic parameters for Wolverhampton, January 2008–January 2010.

The magnetic concentration parameters for January and November are relatively low compared to other months (Figure 4.5 a,b,c) and are moderate compared to other urban RDS (χ_{LF} 31.980-39.250 x $10^{-7}m^3kg^{-1}$; χ_{ARM} 0.057-0.20094 x $10^{-5}m^3kg^{-1}$; and SIRM 419.000-662.995 x $10^{-5}Am^2kg^{-1}$). May and July 2008 display high concentrations of χ_{LF} (52.410-53.050 x $10^{-7}m^3kg^{-1}$) with other months showing relatively consistent mean values. High variation exists over the sampling area in all months.

Figure 4.5b shows concentrations of χ_{ARM} to be relatively consistent in all months but with high variation in most months apart from January 2008 and January 2009. Moderate variations exist for July 2009. Figure 4.5c shows SIRM values were relatively consistent over the sampling period, with high levels of variation during May 2008, July 2008, September and November 2008 and again in May, September and November 2009. Low variability existed during January 2008, 2009 and 2010, with moderate levels of variation over the sampling areas during the months March 2008, 2009 and July 2009.

Figure 4.6a shows relative consistency in mineral magnetic grain size and suggests a predominantly multi-domain characteristic, with little to no SP grains present. Some variation exists with all months with November 2009 showing least variation. Some months display differences with the S-ratio parameters (Figure 4.6b), but all months suggest the dominance of soft ferromagnetic material within RDS. The S-ratio variance suggests a mixture of soft and hard minerals within RDS, whereas September 2009 displays elevated soft concentrations of mineralogy. SIRM/χ (Figure 4.6c)) values display relatively consistent levels across the sampled months. High variation existed over the sampling areas during May 2008, 2009, July 2008, September 2008 and November 2008 and 2009, with low variation during January 2008 and 2009. The steady levels of multi domain, soft magnetic minerals suggest a consistent source of magnetic material.

Figure 4.7 and 4.8 shows the textural box plots for the sampled periods. Figure 4.7a shows the mean values and variation over the sampling periods. Each pairing of months display similar results with a relative pattern between the months that is also evident in Figure 4.7b. Particle size classes $PM_{1.0}$ (Figure 4.7c), $PM_{2.5}$ (Figure 4.8a), PM_{10} (Figure 4.8b) and PM_{100} (Figure 4.8c) varied over the sampling periods, with March 2008 and March 2009 displaying high readings of $PM_{2.5}$ and January 2008, May 2008 and May 2009 displaying low levels (Figure 4.8a). March 2008 also displayed high PM_{10} levels with decreased levels during January and May 2008 (Figure 4.8b). September and November 2008 show lower levels of PM_{100} compared to other months. All sampling periods showed moderate to high variation across the sampling areas.

4.2.6 Distinguishing sampling periods using Wolverhampton RDS characteristics

Statistical and graphical techniques indicate significant variations in physical characteristics of Wolverhampton RDS. However, visually there are obvious relationships between months. Statistical analysis using Kruskal Wallis and Mann Whitney U tests determined possible cross linkages of sampling periods.

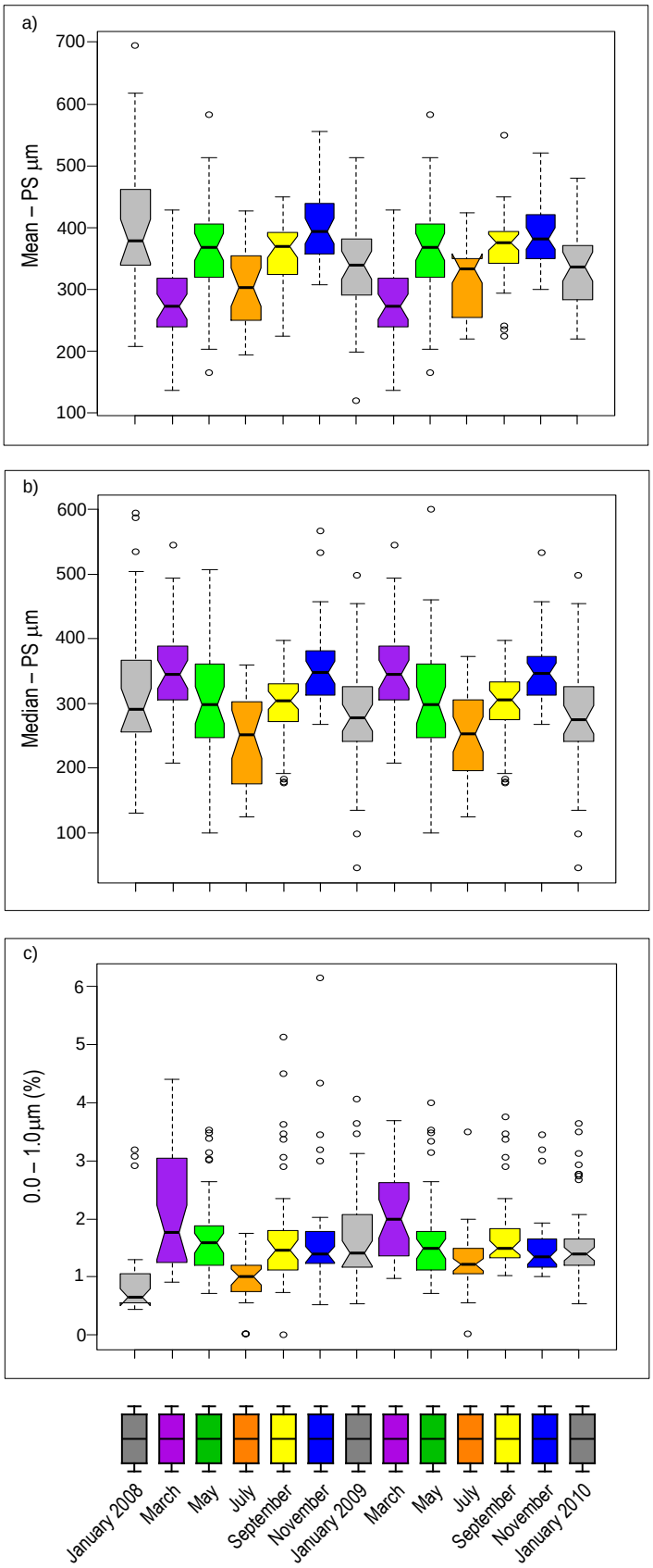

Figure 4.7 Box plots of RDS sample population distributions for selected textural parameters for Wolverhampton, January 2008–January 2010.

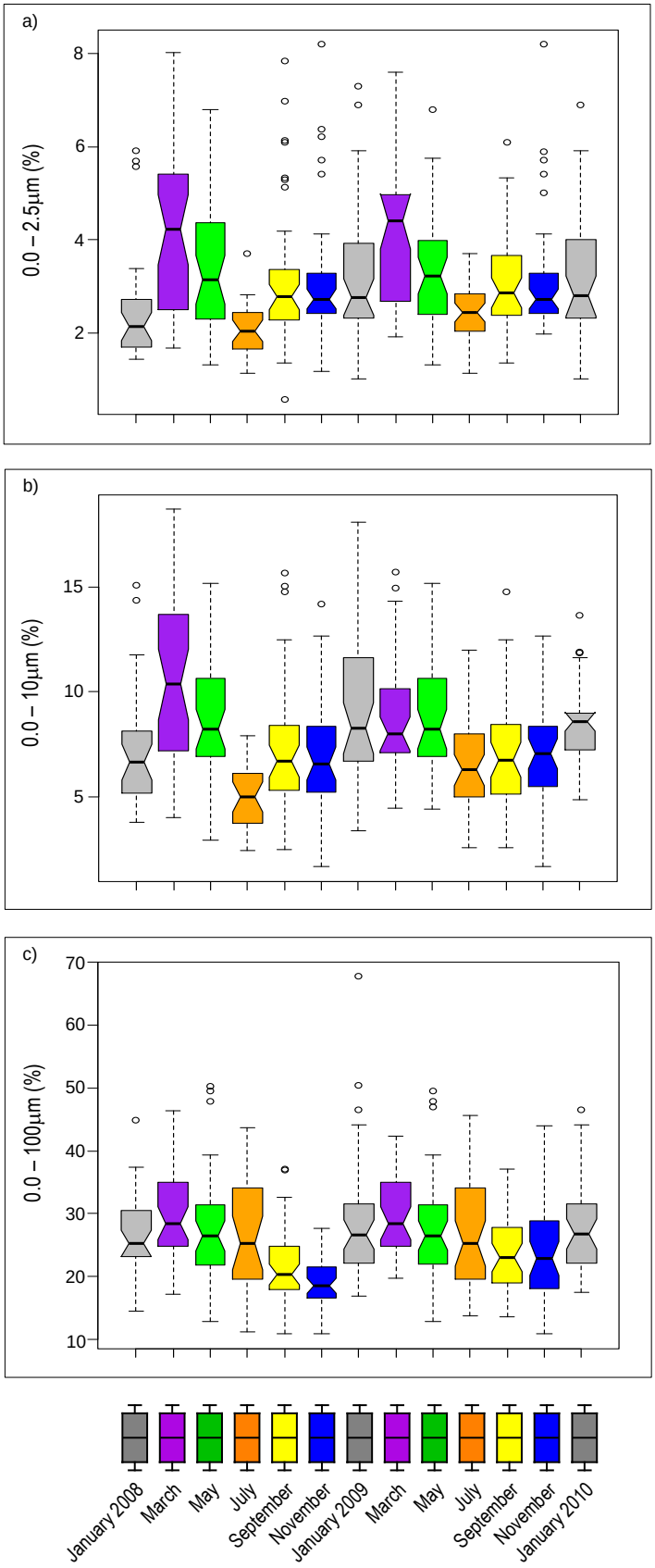

Figure 4.8 Box plots of RDS sample population distributions for selected textural parameters for Wolverhampton, January 2008–January 2010.

Tested Hypotheses

Null Hypothesis (H_0)	There are significant differences between the parameters during sampling periods.
Alternative Hypothesis (H_1)	There are no significant differences between the parameters during sampling periods.

Summary data for the physical characteristics of each of the Wolverhampton sampling periods are described and both null (H_0) and alternative (H_1) hypotheses are tested. The result of the non-parametric Kruskal-Wallis tests (data not presented) show differences between more than two of the Wolverhampton sampling periods RDS sample populations for each parameter, independent of each other (H_0). Non-parametric Mann-Whitney U tests (Appendix 4.2.1-4.2.5) compared difference of the medians of each of the Wolverhampton sampling periods RDS sample populations for each parameter.

4.2.7 Distinguishing sampling periods using mineral magnetic characteristics

The mineral magnetic characteristics for RDS in Wolverhampton over the sampling period 2008–2010 (n = 13) display significant differences (H_0). Mineral magnetic concentration parameters (Appendix 4.2.1-4.2.2 (χ_{LF}, χ_{ARM}, SIRM and $\chi_{FD\%}$)) are significantly different over several months. χ_{LF} January 2008 (Figure 4.5-4.6) is significantly different (p <0.001) for months March to September but the same for November and respective January months. March 2008 was different from November 2009 (p <0.05) and January 2008, 2009 and 2010 (p <0.01), but similar to other months. May and July is significantly different to September, November and January (p <0.05-<0.001). During September significant differences were found between and January, November and May (p <0.05-<0.001). χ_{ARM} (Figure 4.5b) has significant differences between the months of May, September, November and January. Similar relationships were found with $\chi_{FD\%}$ (Figure 4.6a) and May with November and January being significantly different to May (p <0.05-<0.001).

January months were found to be significantly different (p <0.001) to March 2008, May 2008, July 2008 and May 2009, July 2009, and September 2009 (p <0.05-<0.001). July months are significantly different (p <0.05-0.001) to September 2008, November 2008, January 2008 and November, January 2009 (p <0.05-<0.01). SIRM (Figure 4.5c) had very similar linkages, most notably May and July months being significantly different (p <0.05-<0.01) to September 2008, November 2008, January 2009 and November 2009 and January 2010 (p <0.001). January also displays very strong difference with months (March-September 2008 (p <0.01-<0.001) and March-September 2009 (p <0.001)).

These observations show distinct groups of months which have differences and suggest linkages with time of year and possibly weather conditions when compared to weather data (Appendix 4.3a-d). January is significantly different to months March-September and suggests a

possible seasonal influence. This is supported by the warm months of May and July being significantly different to the cooler months of November and January (χ_{LF}, χ_{ARM} and SIRM). The use of interrogating the data via Mann Whitney tests has showed the potential to distinguish differences and relationships between months, sampling periods and possible seasons. This will now enable the investigation to analyse possible effects of mineral magnetic concentrations on seasonality.

4.2.8 Distinguishing sampling periods using textural characteristics

Textural characteristics display significant differences (Appendix 4.2.3-4.2.5 (p <0.05-<0.001)) over a range of months and parameters (H_0). Mean and median particle size (Appendix 4.2.3 and Figure 4.7 a-b) shows significant differences (p <0.05-<0.001) with January compared to March, July and September. July is significantly different (p <0.01-<0.001) to September and November 2008 and 2009. November is consistently different (p <0.05-<0.001) to all months during the sampling period. Selected separate particle sizes (Appendix 4.2.4-4.2.5 ($PM_{1.0}$ $PM_{2.5}$, PM_{10}, and PM_{100})) display significant differences throughout the sampling period. Particle class size $PM_{1.0}$ (Figure 4.7c) and $PM_{2.5}$ (Figure 4.8a) during January months and July 2009 months had significant differences (p <0.05-<0.001) within all months, except July 2008. Particle class size PM_{10} (Figure 4.8b) during March and May show significant differences (p <0.05-<0.001) with July, September and November. Particle class size PM_{100} (Figure 4.8c) during September and November show significant differences (p <0.05-<0.001) to all other months over the sampling period. The textural parameters display similar behaviour to mineral magnetic data, with groupings of months associated with each other, again indicating a possible seasonal influence on RDS in Wolverhampton.

4.2.9 Factor analysis using selected parameters

To further clarify temporal relationships, multivariate factor analysis was used. In each case, parameter and sample loadings extracted from Factors 1 and 2 were used to generate factor plots.

Factor analysis was initially performed using all mineral magnetic and textural parameters; however the resultant plot (not presented) was chaotic and did not appear to show clear patterns. Factor analysis was reapplied to relevant parameters (mineral magnetic and textural) to distinguish between parameters and sample groupings. The resultant plot (Figure 4.9) includes the main parameters and displays loadings. The first two factors extracted explain 32.20% of variation. Factor 1 explains 25.56% of variation in parameters, while Factor 2 explains 6.64%. The spread of parameter loadings along Factor 1 indicate mineral magnetic concentration parameters are the major influencing factor, with some particle size influence with PM_{10} closely linked. The spread of parameter loadings along Factor 2 suggests textural parameters are the main influencing factor. Sample loadings in its present form appear chaotic.

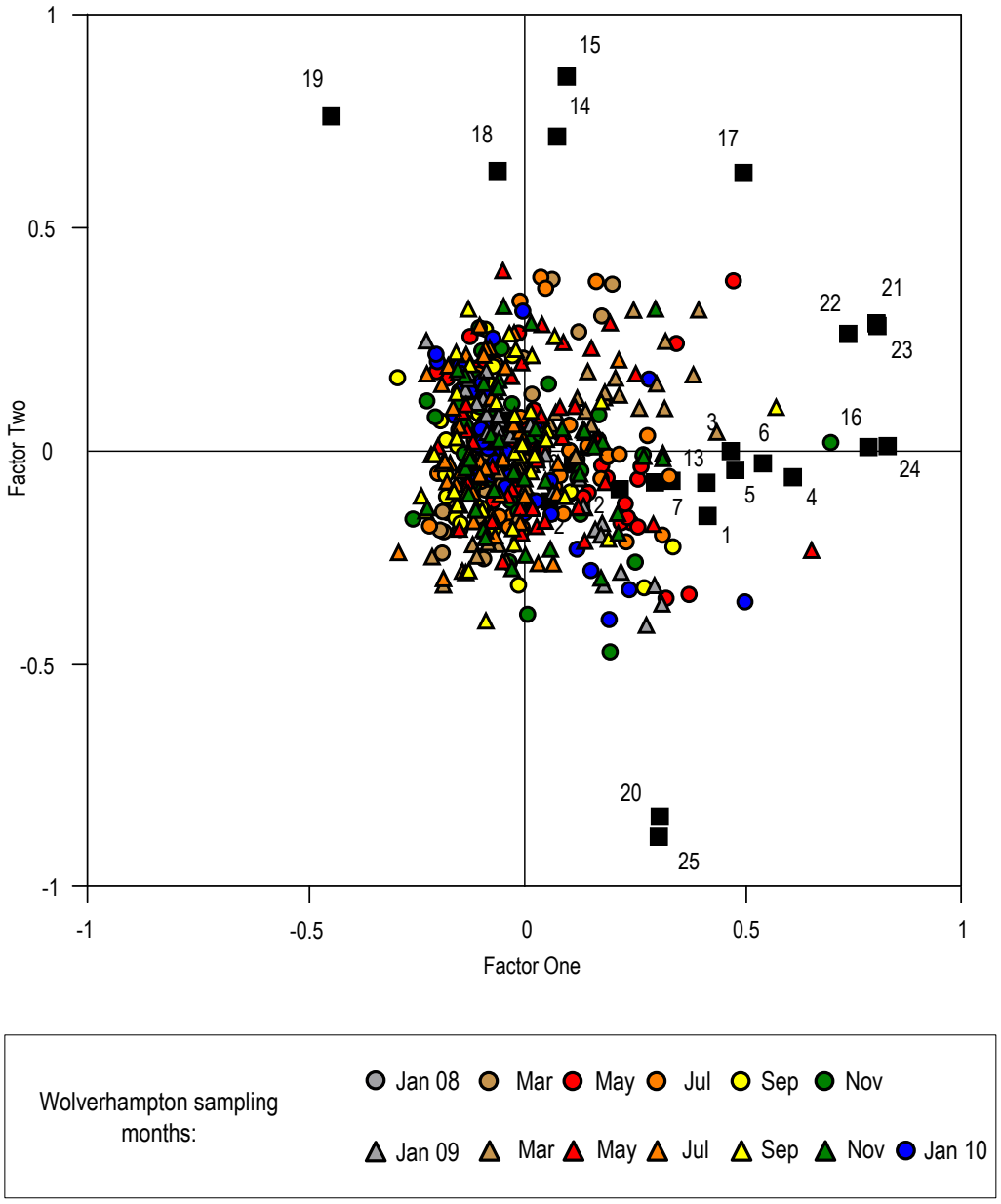

	Parameters								
1	χ_{LF}	6	$Soft_{IRM40mT}$	11	χ_{ARM}/SIRM	16	Sorting	21	Clay
2	χ_{FD}	7	$Hard_{IRM300mT}$	12	SIRM/ARM	17	Skewness	22	$PM_{1.0}$
3	χ_{ARM}	8	$Hard_{IRM500T}$	13	SIRM/χ	18	Kurtosis	23	$PM_{2.5}$
4	SIRM	9	S-ratio	14	Mean	19	Sand	24	PM_{10}
5	$Soft_{IRM20mT}$	10	ARM/χ	15	Median	20	Silt	25	PM_{100}

Figure 4.9 Simultaneous R- and Q mode factor analysis plots of Factor 1 versus Factor 2, based on characteristics and cumulative Wolverhampton parameters.

4.2.10 Spatial characterization of mineral magnetic concentration characteristics using Arcview GIS (version 10)

Statistical and graphical techniques indicate significant variations in physical characteristics of Wolverhampton RDS. However, bivariate plots and Mann-Whitney U tests used thus far failed to show geographical relationships between adjacent samples. Therefore, the mineral magnetic concentration data (χ_{LF}, χ_{ARM} and SIRM) was used to generate GIS images, determining the nature of spatial variations. Baseline maps were created in Arcview GIS (version 10). The masked boundary excludes unsampled areas. Figure 4.10a shows mean χ_{LF} to vary across the sampling area.

There are several high concentration of χ_{LF} directly associated with the main road system and these have been highlighted by an outlined circle (Figure 4.10a). To the north, east and south-east of the sampling area there are high concentrations of magnetic material (χ_{LF} 95.148-102.310 x $10^{-7}m^3kg^{-1}$) and these high concentrations are directly related to the main road network entering the City. To the west of the City centre there are several lower concentrations of magnetic minerals (χ_{LF} 6.856-18.493 x $10^{-7}m^3kg^{-1}$) which can be directly associated with residential side roads. This pattern can be observed throughout the concentration parameters (Figure 4.10b,c) for the sampling period with main roads displaying higher readings than the side road networks. These concentrations reveal similar patterns to the road traffic data (Figure 3.3, Appendix 3.2.1) when compared.

Spatial distributions of χ_{ARM} (Figure 4.10b) highlight the main arterial road network to the north, south and east of the City. This association also corresponds well with traffic levels at these locations (Figure 3.3, Appendix 3.1). Figure 4.10d shows the S-ratio and the relative even distribution of soft ferrimagnetic minerals across the sampling area. Towards the south there are high levels of mineral magnetic concentrations. When compared to land use maps (Appendix 3.1) the areas appear to be linked to heightened anthropogenic activity due to local industry. When comparing χ_{LF} values (Figure 4.10) to road traffic and land use data (Appendix 3.1) there appears to be distinct visual similarities with corresponding highs and lows. This observation suggests road traffic and land use as an influencing factor to mineral magnetic concentrations in Wolverhampton.

4.2.11 Further assessment of road profiles using mineral magnetic bivariate plots of Wolverhampton Cumulative RDS

Bivariate plots were used to determine relationships or patterns between the arterial and residential road systems, as observed within Figure 4.10. Figure 4.11 (a-d) show groupings of similar readings, which are associated with residential roads and arterial road networks. There is little mixing throughout the graphs and remain consistent with the relationships found. The sample points highlighted in Figure 4.11 (a-d) display a narrow band of similar concentrations (highlighted area) of mineral magnetic material, whereas the main road systems display a broad band of concentrations which are spread throughout the range.

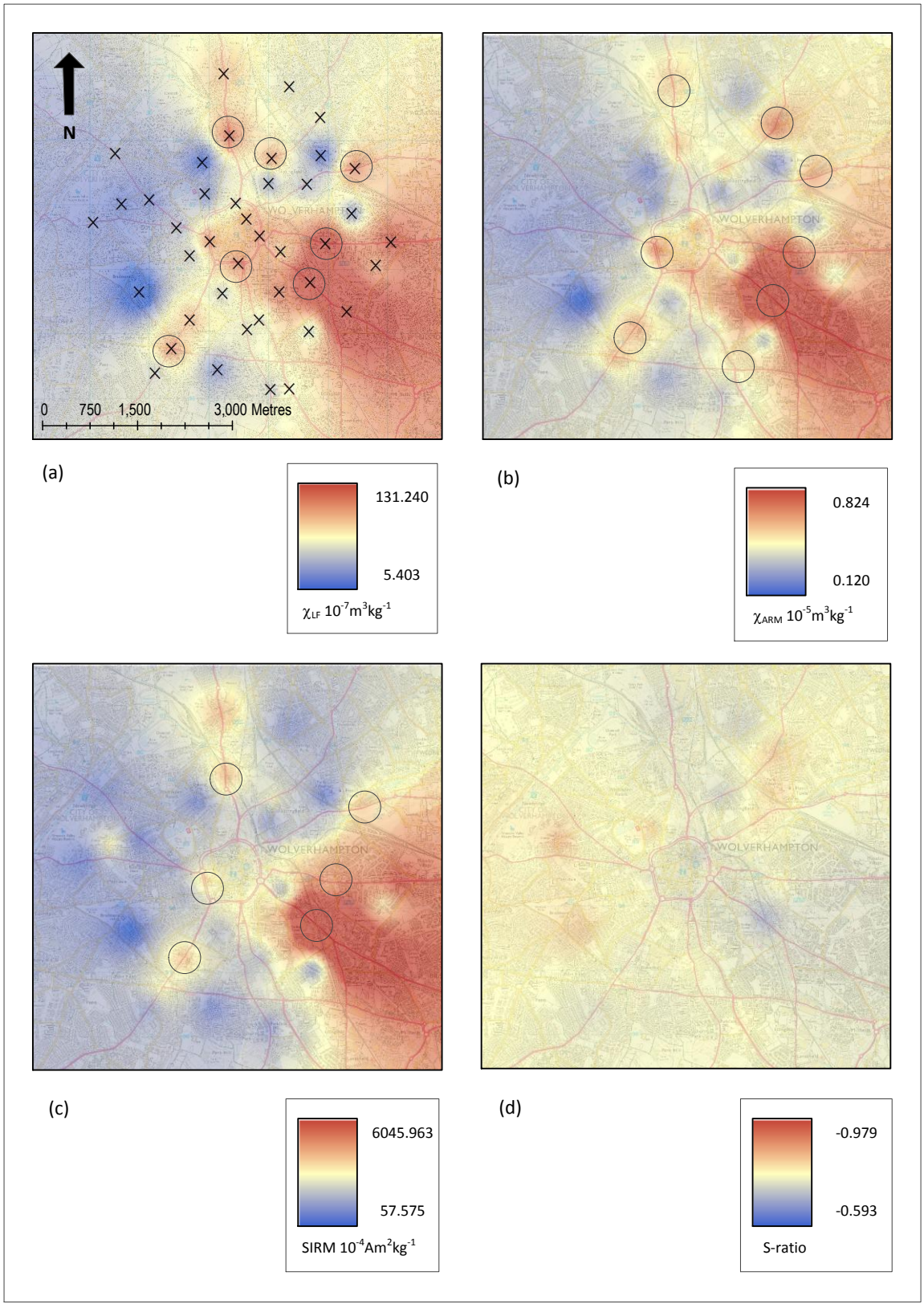

Figure 4.10 Spatial distributions of the Wolverhampton RDS mean value mineral magnetic concentrations ((a, χ_{LF}; b, $\chi/_{ARM}$; c, SIRM and d, S-ratio). Highlighted circles indicate areas of high mineral magnetic concentrations).

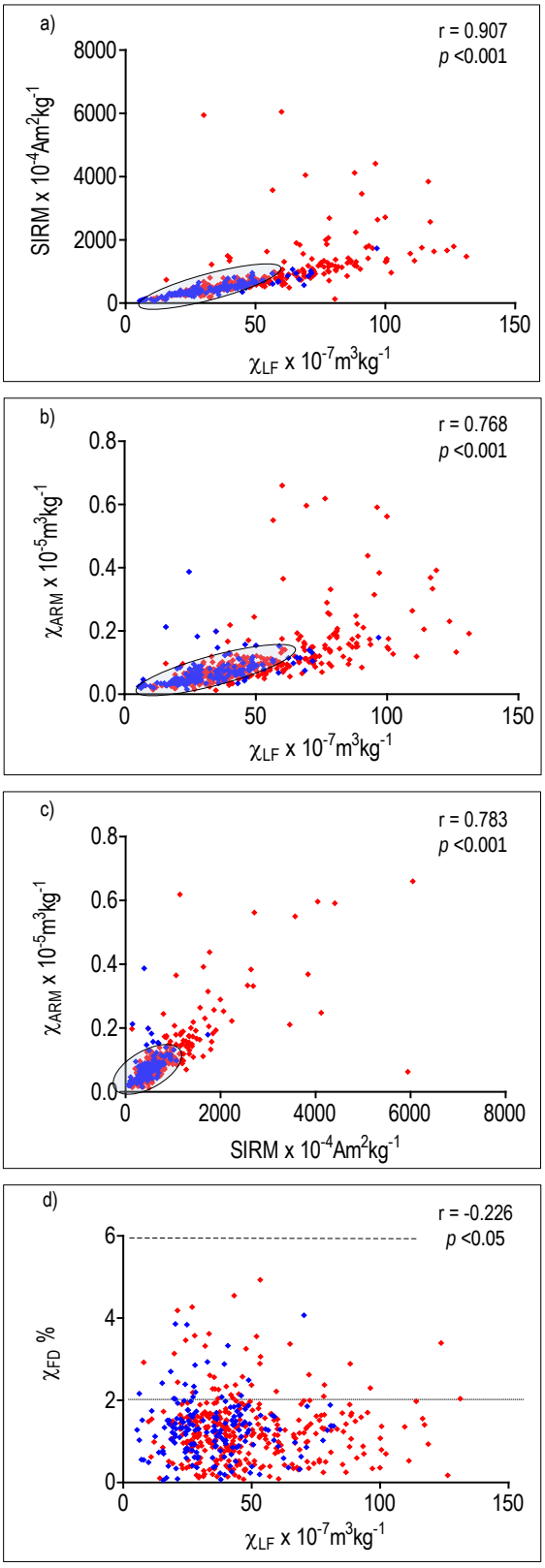

Figure 4.11 Bivariate plots of selected mineral magnetic parameters for Wolverhampton cumulative RDS samples (n = 546), with road types identified (red points are arterial and blue points are residential roads). Areas of highlighted rings identify sample groups.

Results are reflected by traffic volumes with lower mineral magnetic concentrations associated with side roads. Main roads have a combination of high and low concentrations of mineral magnetic behaviour and are possibly a result of higher concentrations of vehicles inputting combustion and mechanical abrasion particulates. Figure 4.11d further supports the suggestion that main road RDS is dominated by MD ferromagnetic mineralogy.

4.2.12 Further investigation of the Wolverhampton samples

Statistical and graphical techniques indicate significant variation between the sampling intervals of Wolverhampton RDS. Results presented suggest some limited relationships exist between the mineral magnetic and textural parameters and require further investigation. Section 4.3–4.5 will break down the data into component parts (seasons and separate sampling intervals) to further explore temporal relationships.

4.3 Seasonal Characteristics of Wolverhampton RDS (Summer, Autumn, Winter, Spring)

A complete series of relationships between the mineral magnetic and textural parameters has not been evident so far from the cumulative Wolverhampton samples. Mann-Whitney U test investigations into individual months (Appendix 4.2) suggested possible linkages between groups of months. This has suggested that seasonality may play a part in distinguishing Wolverhampton RDS relationships. Therefore, to distinguish potential relationships, seasonal data have been combined using specific months to determine characteristics. The Roman calendar has been used to determine which month belonged to each season (***Summer:*** June, July, August; ***Autumn;*** September, October, November; ***Winter;*** December, January, February; ***Spring;*** March, April, May) which is the most commonly used seasonal system. Kim *et al.* (2009) utilized a similar approach to assess the magnetic properties of urban road dust during seasons. Kruskal Wallis and Mann-Whitney U tests were applied to these specific month combinations (Table 4.4-4.5) to assess the potential for using grouped months in this study.

4.3.1 Distinguishing seasons using mineral magnetic characteristics

Mann Whitney U and Kruskal Wallis tests were carried out to determine if any of the sampling seasons were different. The tests were applied to the mineral magnetic and textural data. Summary data for the physical characteristics of each of the Wolverhampton seasonal periods are described and both null (H_0) and alternative (H_1) hypotheses are tested.

Tested Hypotheses

Null Hypothesis (H_0)	There are significant differences between parameters during seasons.
Alternative Hypothesis (H_1)	There are no significant differences between parameters during seasons.

To determine whether the variations between the sources are statistically significant, non-parametric Kruskal-Wallis tests were performed on the four seasonal groups for each of the magnetic and textural parameters (Table 4.4). P-values show that for each of the parameters the alternative hypothesis is rejected and, therefore, the medians of each of the seasonal populations are significantly different (H_0). Non-parametric Mann-Whitney U tests (Table 4.5) compared the difference of the medians of each of the Wolverhampton sampling season RDS sample populations for each parameter. Seasonal samples for Wolverhampton are also presented as box-plots (Figure 4.12-4.13) and readings suggest a close consistency for all parameters throughout the seasons, with some overlap.

By comparing the box-plots (Figures 4.12-4.13) for each selected magnetic and textural parameter, it is clear that there is some variation. This suggests that the characteristic properties of the seasons are dissimilar. For most other cases, only the whiskers overlap between seasons. This indicates differences between seasons, except for a few samples which possess similar values.

Using Mann Whitney U value tests the mineral magnetic concentration parameters (χ_{LF}, χ_{ARM} and SIRM) display fairly consistent relationships throughout the seasons (Table 4.5), with significant differences (p <0.05-<0.001) between spring and autumn-winter months. χ_{LF} parameters (Figure 4.12a) during summer are significantly different to winter (p <0.001) whereas spring is significantly different to autumn and winter (p <0.001). This relationship is replicated with the χ_{ARM} (Figure 4.12b) SIRM (Figure 4.12c) and S-ratio (Figure 4.12d) (p <0.05-<0.001) parameters.

Table 4.4 Kruskal Wallis '*p*' values for Wolverhampton RDS seasons

Parameters	P Value
χ_{LF}	<0.001
$\chi_{FD\%}$	<0.001
χ_{ARM}	<0.001
SIRM	<0.001
S-Ratio	<0.001
SOFT $_{IRM20mT}$	<0.001
SOFT $_{IRM40mT}$	<0.001
HARD $_{IRM300mT}$	<0.001
HARD $_{IRM500mT}$	<0.05
SIRM/χ	<0.05
Mean - PS	<0.001
Median - PS	<0.001
$PM_{1.0}$	<0.001
$PM_{2.5}$	<0.001
PM_{10}	<0.001
PM_{100}	<0.001

Table 4.5 Mann-Whitney U test '*p*' values for mineral magnetic seasonal data for Wolverhampton RDS (January 2008–January 2010)

χ_{LF}		Spring	Summer	Autumn
	Summer	0.649		
	Autumn	<0.001	0.053	
	Winter	<0.001	<0.001	<0.001

$\chi_{FD\%}$		Spring	Summer	Autumn
	Summer	0.526		
	Autumn	<0.001	<0.001	
	Winter	0.453	0.948	<0.001

χ_{ARM}		Spring	Summer	Autumn
	Summer	0.450		
	Autumn	<0.05	0.208	
	Winter	<0.001	<0.001	<0.01

SIRM		Spring	Summer	Autumn
	Summer	0.490		
	Autumn	<0.05	<0.05	
	Winter	<0.001	<0.001	<0.01

Soft $_{IRM20mT}$		Spring	Summer	Autumn
	Summer	0.348		
	Autumn	<0.01	<0.001	
	Winter	<0.001	<0.001	<0.05

Soft $_{IRM40mT}$		Spring	Summer	Autumn
	Summer	0.867		
	Autumn	<0.01	<0.05	
	Winter	<0.001	<0.001	<0.05

Hard $_{IRM300mT}$		Spring	Summer	Autumn
	Summer	<0.001		
	Autumn	0.944	<0.001	
	Winter	0.702	<0.001	0.817

Hard $_{IRM500mT}$		Spring	Summer	Autumn
	Summer	0.118		
	Autumn	0.103	0.958	
	Winter	<0.01	0.244	0.175

S-ratio		Spring	Summer	Autumn
	Summer	<0.05		
	Autumn	<0.001	<0.001	
	Winter	0.080	<0.01	<0.001

SIRM/χ		Spring	Summer	Autumn
	Summer	<0.01		
	Autumn	<0.01	0.534	
	Winter	<0.01	0.747	0.774

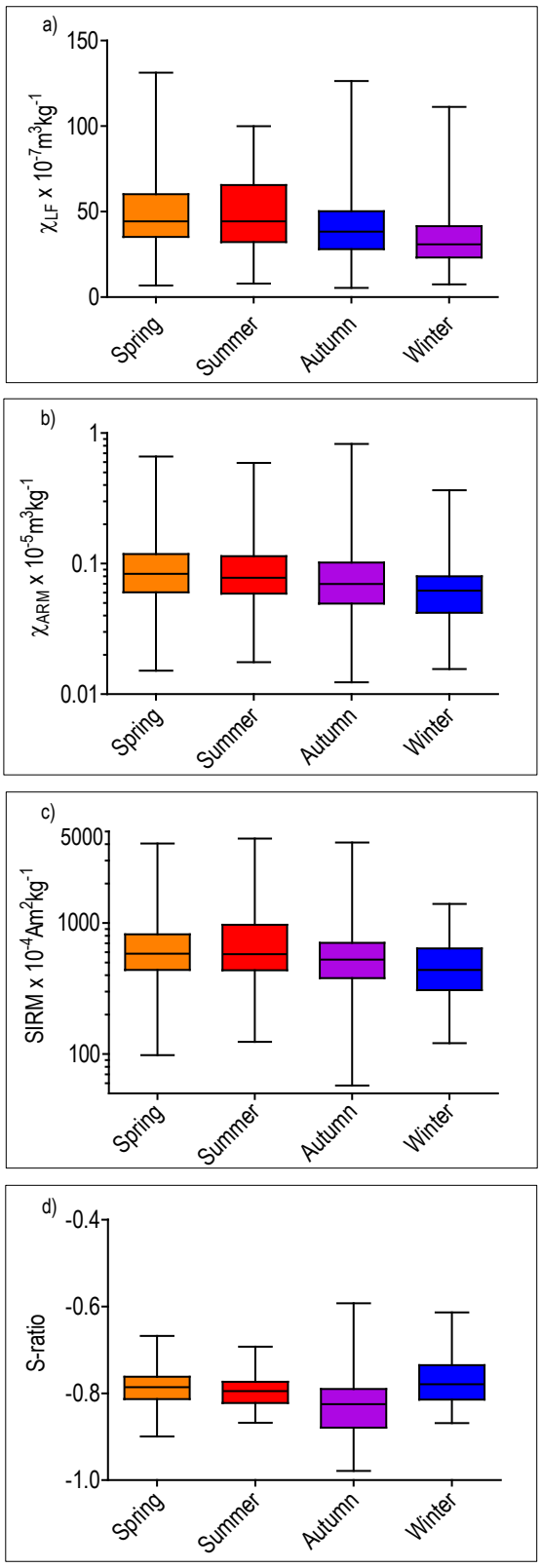

Figure 4.12 Box plots of RDS seasonal sample population distributions for selected mineral magnetic parameters for Wolverhampton.

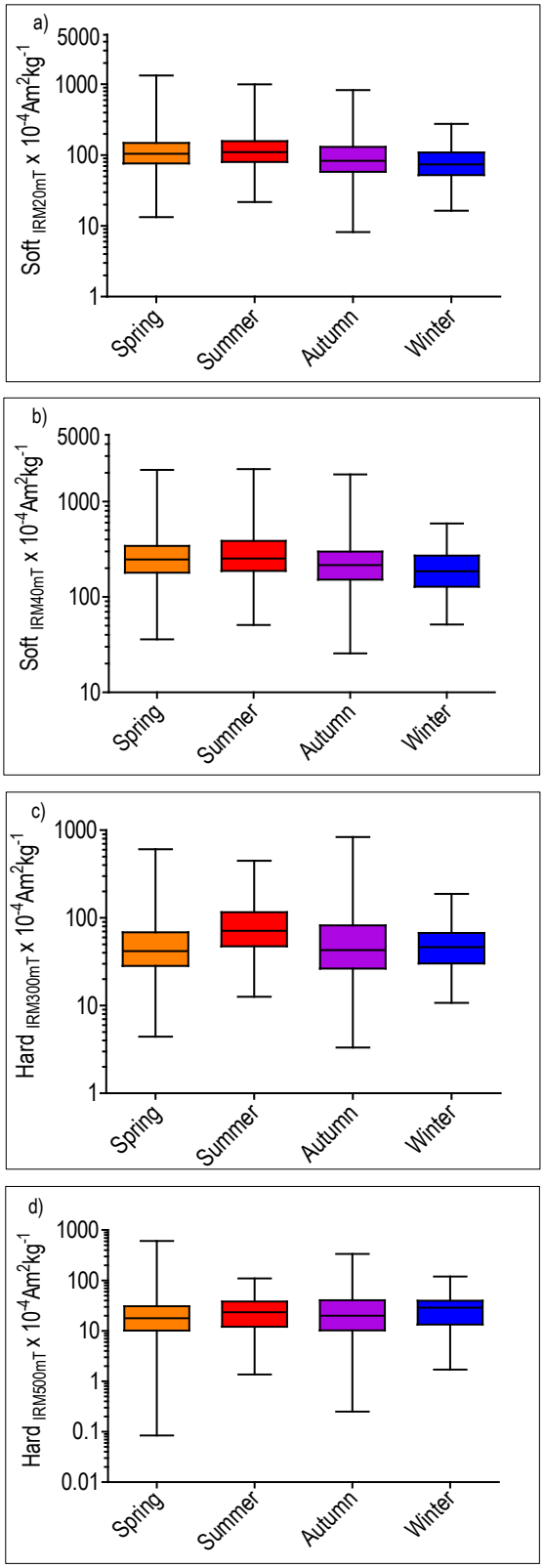

Figure 4.13 Box plots of RDS seasonal sample population distributions for selected mineral magnetic parameters for Wolverhampton.

Significant differences are evident for autumn and winter compared to spring within the $Soft_{IRM20/40mT}$ (Figure 4.13a-b) magnetic characteristic (p <0.01-<0.001). $Hard_{IRM300mT}$ parameters (Figure 4.13c) show that months are the same, apart from spring and summer months (p <0.001). $Hard_{IRM500mT}$ (Figure 4.13d) display significant differences between spring and winter (p <0.01). Other seasons have significant relationships (H_1).

The Mann-Whitney U test results for seasons showed that there are differences between all parameters. Opposite seasons (spring, autumn and summer, winter) are significantly different in various mineral magnetic parameters, whereas some seasons have shown similarities within certain parameters (spring and summer with χ_{LF}, χ_{ARM} and SIRM).

Seasonal variability suggests conditions may be responsible for the different values. The mean daily rainfall and overall rainfall patterns over the sampling periods influence mineral magnetic concentrations of RDS (Appendix 4.3a). However the results for mean temperature and χ_{LF} (Appendix 4.3b) also appear to influence the mineral magnetic characteristics of RDS. These results suggest that weather conditions play an important role in concentration parameters.

The contribution of magnetic material from road and industry generally does not fluctuate over seasons (Kulshrestha, 2009) whereas concentrations of crustal material can be affected by weather due to the weathering contributing to RDS loads during these periods. The contribution of weathered crustal material potentially has a diluting and mixing effect, thus weakening the magnetic signal during seasons with increased weather activity (Appendix 4.3).

4.3.2 Further assessment using multivariate factor analysis plots

Results of Mann-Whitney U tests identified two-dimensional key seasonal characteristic associations with each of the mineral magnetic parameters. However, these data cannot identify the role of each mineral magnetic parameter within the seasonal characteristics.

To achieve this, multivariate factor analysis was used to provide multi-dimensional details on seasonal changes in mineral magnetic behaviour. The main advantage of using multivariate factor analysis, over Mann Whitney U tests, is the reduction of parameters, by combining two or more variables into one single factor to identify hidden dimensions that would not have been apparent from direct analysis. The resultant plot identifies groups of inter-related parameters. Factor analysis is used to estimate how much variability between parameters is due to common factors. In each case, parameter and sample loadings extracted from Factors 1 and 2 were used to generate factor plots.

4.3.3 Factor analysis of the mineral magnetic data to classify seasons

Figure 4.14 is split into five factor plots. Each display key mineral magnetic parameters for all seasons during the sample period (January 2008–January 2010). The first two factors extracted explain 41.40% of variation. Factor 1 explains 23.34% of variation in parameters, while factor 2 explains 18.06%. The spread of parameter loadings along Factor 1 indicate

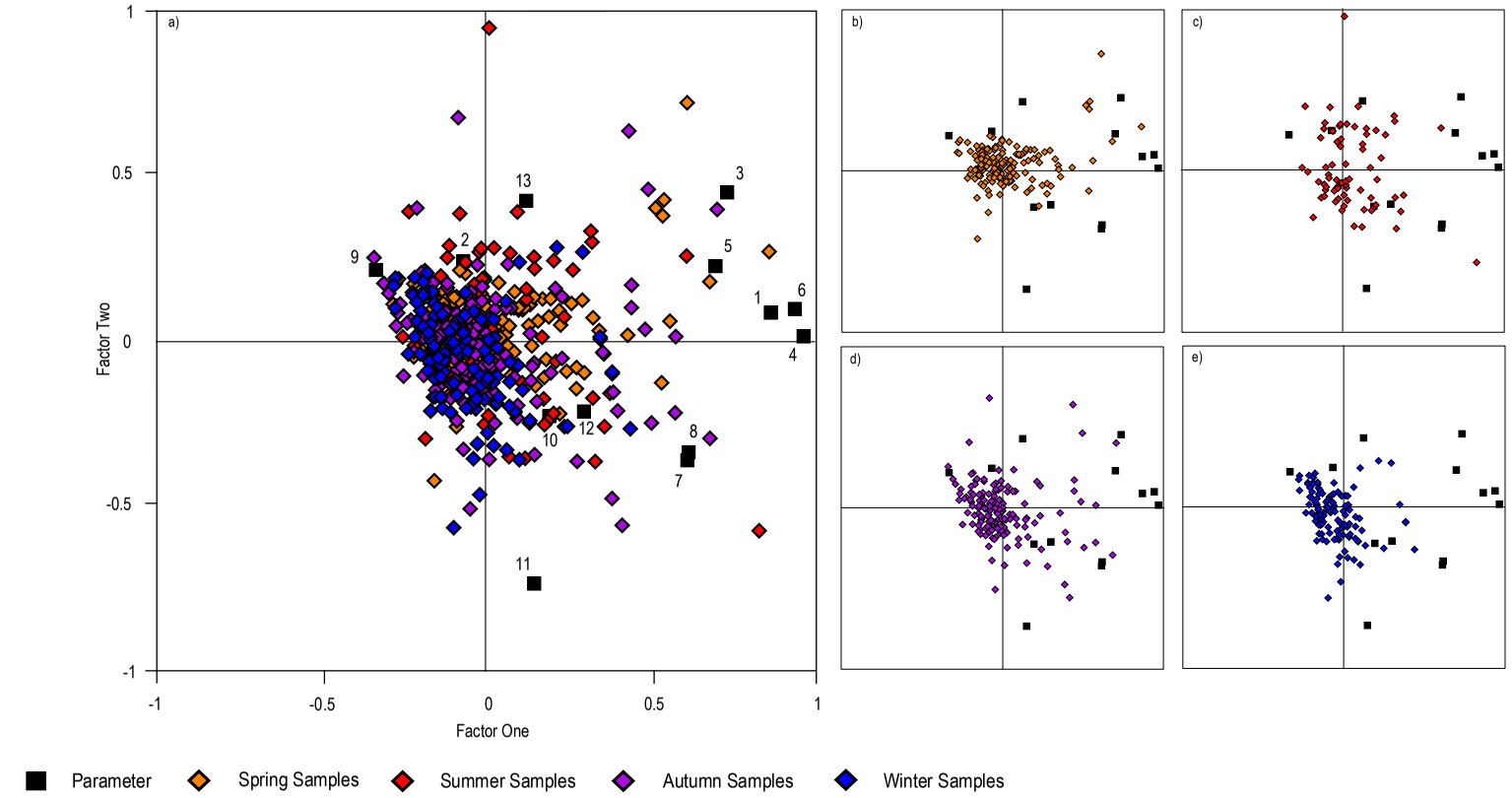

	Parameters							
1	χ_{LF}	4	SIRM	7	Hard $_{IRM20mT}$	10	ARM/χ
2	χ_{FD}	5	Soft $_{IRM20mT}$	8	Hard $_{IRM40mT}$	11	χ_{ARM}/SIRM
3	χ_{ARM}	6	Soft $_{IRM40mT}$	9	S-ratio	12	SIRM/ARM
						13	SIRM/χ

Figure 4.14 Simultaneous R- and Q mode factor analysis plots of Factor 1 versus Factor 2, based on characteristics and cumulative Wolverhampton parameters.

magnetic concentration parameters as the major influencing factors, with $\chi_{FD\%}$ displaying limited influence. Factor 2 shows the spread of loadings influenced by magnetic domain size. Figure 4.14(b) displays the sample loadings for the spring season. Most samples are fairly compacted and spread along a positive Factor 2 with cross over into Factor 1. There is indication of influence from mineral magnetic concentration and domain size parameters in the resultant plot. Figure 4.14(c) displays the sample loadings for summer. The sample loading are spread evenly across all factors with no apparent pattern or behaviour. Figure 4.14(d) displays sample loadings for autumn, with a wide spread of loadings over both Factors 1 and 2, and some mineral magnetic domain size influence is apparent. Figure 4.14(e) displays sample loadings for winter which show uniform patterns indicating mineral magnetic domain size influences.

4.3.4 Factor analysis of selected mineral magnetic and textural data to classify seasons

Figure 4.15 is split in to five factor plots, each displaying key mineral magnetic and textural parameters for all seasons during the sampling period. The first two factors extracted explain 50.80% of variation. Factor 1 explains 29.72%, while Factor 2 explains 21.08%. The spread of parameter loadings along Factor 1 indicate textural parameter influences. Factor 2 shows the spread of loadings being influenced more by mineral magnetic characteristics.

Figure 4.15(b) displays the sample loadings for spring. Most samples are spread along a positive Factor 2 with some cross over into Factor 1. The sample spread indicates the influence of particle size. Figure 4.15(c) displays sample loadings for summer. The sample loading are spread across negative Factor 1, indicating mineral magnetic concentration influence. Figure 4.15(d) displays sample loadings for autumn, with a wide spread of loadings over Factor 2, the spread of samples indicate textural and limited mineral magnetic influence. Figure 4.15(e) displays sample loadings for winter with a wide spread of loadings over Factor 2. The spread of samples indicate textural and limited mineral magnetic influences.

4.3.5 Characteristics and linkages of separate seasons

Use of statistical and graphical techniques has enabled a basic understanding of seasonal characteristics and proves to be effective in discriminating seasonal factors, with clear differences between the seasons Identified. Relationships between land use, traffic and weather conditions appear to influence the concentrations of magnetic minerals found in RDS temporally and spatially. Seasonal linkages between mineral magnetic, textural parameters and particle size proxy potential will now be explored.

4.3.6 Seasonal mineral magnetic and textural relationships

The cumulative Wolverhampton RDS samples show limited success in accessing linkages between mineral magnetic and textural parameters. The seasonal arrangement has been subjected to identical interrogation with each season checked for linkages. Selected relationships are shown in Table 4.6.

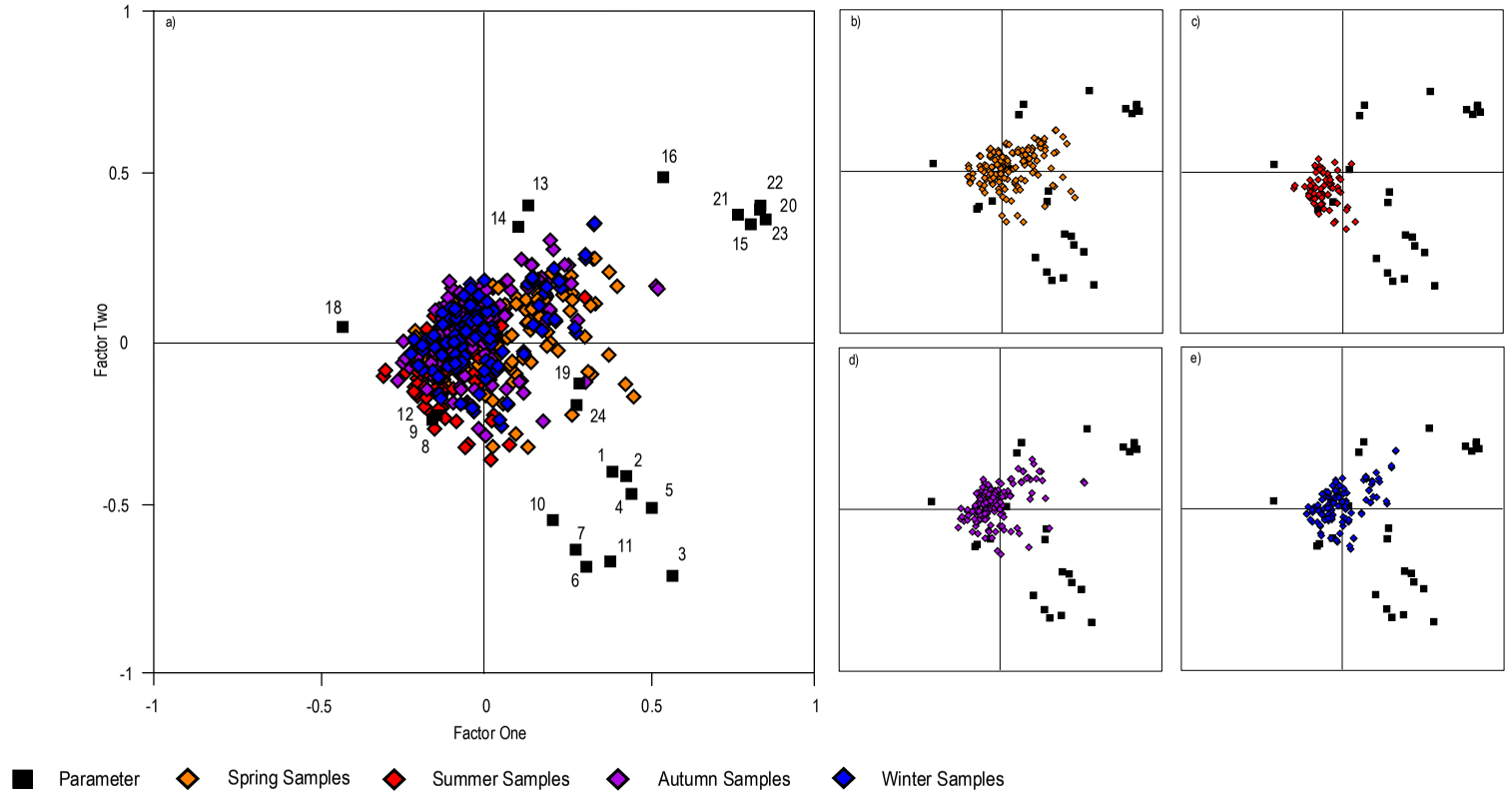

	Parameters								
1	χ_{LF}	6	Soft $_{IRM40mT}$	11	χ_{ARM}/SIRM	16	Sorting	21	Clay
2	χ_{FD}	7	Hard $_{IRM20mT}$	12	SIRM/ARM	17	Skewness	22	$PM_{1.0}$
3	χ_{ARM}	8	Hard $_{IRM40mT}$	13	SIRM/χ	18	Kurtosis	23	$PM_{2.5}$
4	SIRM	9	S-ratio	14	Mean	19	Sand	24	PM_{10}
5	Soft $_{IRM20mT}$	10	ARM/χ	15	Median	20	Silt	25	PM_{100}

Figure 4.15 Simultaneous R- and Q mode factor analysis plots of Factor 1 versus Factor 2, based on characteristics and cumulative Wolverhampton parameters.

Table 4.6 Summary mineral magnetic concentration (χ, $\chi_{ARM,}$ and SIRM and textural (<PM_{10}) parameter spearman rank correlation relationships for all seasons (**bold** text is significant (*p <0.05; **p <0.01; ***p <0.001 (n =546))).

Parameters	Clay	$PM_{1.0}$	$PM_{2.5}$	PM_{10}
χ_{LF}	0.353***	0.330***	0.356***	0.376***
χ_{ARM}	0.312***	0.298***	0.311***	0.316***
SIRM	0.387***	0.371***	0.387***	0.371***
χ_{LF}	0.172	0.086	0.173	0.192
χ_{ARM}	0.109	0.083	0.098	0.107
SIRM	0.257*	0.158*	0.246*	0.079
χ_{LF}	0.001	-0.035	-0.003	-0.003
χ_{ARM}	-0.113	-0.104	-0.121	-0.151
SIRM	0.005	-0.041	-0.003	-0.067
χ_{LF}	-0.098	-0.020	-0.110	-0.036
χ_{ARM}	-0.153	-0.149	-0.140	-0.040
SIRM	-0.107	-0.005	-0.124	-0.066

Spring | Summer | Autumn | Winter

The results show that during autumn and winter there are no significant relationships between the mineral magnetic and textural parameters, with no potential for particle size proxy purposes. Few linkages are found during summer, with SIRM and <$PM_{2.5}$ values (p <0.05) showing weak relationships. The strongest linkages are found between the mineral magnetic and textural parameters during spring (p <0.001) with <PM_{10} and all magnetic concentration parameters (χ_{LF} , $\chi_{ARM,}$ and SIRM) showing a consistent pattern with all particle size fractions. When compared to all other seasons results for spring have shown the greatest potential for particle size determination. However, these results are still weak and display the limited particle size proxy potential, over these periods and at these scales.

4.4 Detailed investigation of potential proxy season (Wolverhampton Spring samples)

Spring samples are further discussed, due to the consistent linkages between mineral magnetic and particle size parameters. Results for the Wolverhampton spring months are presented (Table 4.7 and Figures 4.12-4.13) with summary data of RDS sample physical characteristics during this period (n = 168).

Table 4.7 Summary RDS analytical data* for Wolverhampton (spring) (n = 168)

	Parameters	Units	Mean	Median	SD	CV (%)	Min	Max	Range
(a)	χ_{LF}	$10^{-7}m^3kg^{-1}$	50.563	44.593	23.736	46.943	6.856	131.240	124.384
	χ_{FD}	%	1.438	1.354	0.780	54.248	0.191	4.930	4.739
	χ_{ARM}	$10^{-5}m^3kg^{-1}$	0.104	0.079	0.091	87.722	0.015	0.660	0.645
	SIRM	$10^{-4}Am^2kg^{-1}$	782.979	594.770	706.396	90.219	98.135	6045.963	5947.828
	S-Ratio	Dimensionless	-0.789	-0.789	0.044	-5.569	-0.900	-0.668	0.232
	$SOFT\%_{20mT}$	%	21.091	18.369	22.075	104.665	9.922	197.887	187.965
	$SOFT\%_{40mT}$	%	46.344	43.108	32.332	69.766	33.192	389.261	356.069
	$HARD\%_{300mT}$	%	7.436	7.031	2.583	34.740	1.925	18.337	16.412
	$HARD\%_{500mT}$	%	3.305	2.786	2.278	68.911	0.000	14.359	14.359
	$SOFT_{IRM20mT}$	$10^{-4}Am^2kg^{-1}$	158.303	110.543	213.868	135.100	13.248	1791.693	1778.445
	$SOFT_{IRM40mT}$	$10^{-4}Am^2kg^{-1}$	366.021	257.799	526.420	143.822	39.852	5438.547	5398.695
	$HARD_{IRM300mT}$	$10^{-4}Am^2kg^{-1}$	7.436	7.031	2.583	34.740	1.925	18.337	16.412
	$HARD_{IRM500mT}$	$10^{-4}Am^2kg^{-1}$	28.583	17.949	57.606	201.536	1.021	606.889	605.868
	ARM/χ	$10^{-1}Am^{-1}$	0.002	0.002	0.001	60.368	0.001	0.011	0.010
	χ_{ARM}/SIRM	$10^{-3}Am^2kg^{-1}$	0.000	0.000	0.000	87.699	0.000	0.001	0.001
	SIRM/ARM	Dimensionless	248.116	240.339	77.681	31.308	21.404	716.667	695.262
	SIRM/χ	$10^{-1}Am^{-1}$	15.195	13.645	9.805	64.532	1.668	100.645	98.977
(b)	Mean - PS	μm	291.050	293.796	93.876	32.254	87.141	507.135	419.994
	Median - PS	μm	358.960	359.539	87.704	24.433	165.742	582.702	416.960
	Sorting	σ_1	2.306	2.272	0.341	14.795	1.507	3.178	1.671
	Skewness	SK_1	0.477	0.510	0.136	28.475	0.137	0.702	0.565
	Kurtosis	K_G	1.265	1.139	0.393	31.065	0.759	2.246	1.487
	Sand	%	75.034	75.665	7.240	9.649	56.717	88.334	31.617
	Silt	%	21.964	21.198	7.213	32.839	10.318	40.990	30.672
	Clay	%	3.002	2.645	1.306	43.517	1.127	6.965	5.838
	$PM_{1.0}$	%	1.857	1.592	0.877	47.226	0.719	4.404	3.685
	$PM_{2.5}$	%	3.509	3.139	1.483	42.266	1.316	8.027	6.711
	PM_{10}	%	9.128	8.445	3.179	34.827	2.921	16.825	13.904
	PM_{100}	%	28.154	27.304	8.912	31.655	12.763	53.277	40.514

*SD = Standard Deviation; CV = Percentage coefficient of variation; Min = Minimum value; Max = maximum value.

4.4.1 Wolverhampton Spring RDS mineral magnetic data

Magnetic concentration parameters indicate RDS contains high concentrations of magnetic minerals (mean χ_{LF} 50.563 x $10^{-7}m^3kg^{-1}$; χ_{ARM} 0.104 x $10^{-7}m^3kg^{-1}$; SIRM 782.979 x $10^{-4}Am^2kg^{-1}$). When these results are compared to published values for other environmental materials (Dearing, 1999), they indicate that the magnetic properties of the sediments are similar to intermediate igneous rocks, basic/ultra-basic rocks and ferromagnetic minerals. SIRM values indicate high variation between sites (98.135-6045.963 x $10^{-4}Am^2kg^{-1}$). The ARM/χ values range from high to low (0.001-0.011 x $10^{-1}Am^{-1}$), indicating a predominately coarse grained magnetic material (mean 0.002 x $10^{-1}Am^{-1}$). SIRM/ARM values range from 21.404-716.667 (SD 77.681; mean 248.116) and are high compared to other environmental materials (Yu and Oldfield, 1993). This supports the ARM/χ values, by indicating a coarse magnetic grain size. SIRM/χ values are also low (mean 15.195 x $10^{-1}Am^{-1}$), with a range of values (1.668-100.645 x $10^{-1}Am^{-1}$). The high SIRM/χ values suggest the presence of fine grained magnetic material.

4.4.2 Wolverhampton Spring RDS textural data

Results of descriptive statistics (Table 4.7b) have identified key particle size parameters, indicating that RDS contains moderately sorted sediment (2.306 σ_1; mean 291.050 µm), with moderate to high concentrations of sand (75.034%), moderate concentrations of silt (21.964%), and low concentrations of clay (3.002%). The RDS particle size data for Wolverhampton also suggests a moderate level of sediment within the PM_{100} boundary (28.154%), with lesser PM_{10} concentrations (9.128%), low concentrations of $PM_{2.5}$ (3.509%) and minimal concentrations of $PM_{1.0}$ (1.857%).

4.4.3 Relationships between mineral magnetic and textural variables

Table 4.8 summarizes correlation statistics between the mineral magnetic variables and textural variables for the Wolverhampton spring samples. Almost all mineral magnetic concentration and textural variables show some relationships (i.e. most correlation of coefficient values are r = ≤0.330-0.376 (p <0.05). This suggests that RDS texture may have some influence on mineral magnetic assemblages in Wolverhampton during spring months. The statistical tests indicate that a weak significant relationship exists between mineral magnetic and textural variables. $\chi_{LF,}$ χ_{ARM} and SIRM all display strong relationships (p <0.001) with PM_{10}.

Figures 4.16 a-d show magnetic concentration dependent parameters versus selected textural parameters (χ_{LF}, SIRM versus $PM_{2.5,}$ PM_{10}). The graphs display a wide spread of sample points across the plot area, but does show patterns which can then be verified via statistical analysis. The patterns are consistent throughout the graphs and suggest that, increases in magnetic concentration values (χ_{LF} and SIRM) are associated with corresponding increases in the amount of $PM_{1.0}$ to PM_{10}. This suggests that there is a relationship between the mineral magnetic concentration and textural parameters, although weak, which could relate to inter parameter dependencies. However, the relationship is not strong enough to infer that the methods could be used as a proxy for PM particle size during this time period.

Table 4.8 Statistical relationships between mineral magnetic and textural parameters for Wolverhampton (Spring) (**bold** text is significant (*p <0.05; **p <0.01; ***p <0.001)) (n = 168)

Parameters	Median	Mean	Sorting	Skewness	Kurtosis	Sand	Silt	Clay	$PM_{1.0}$	$PM_{2.5}$	PM_{10}	PM_{100}	LOI
χ_{LF}	-0.110	-0.073	**0.276*** **	0.059	-0.051	**-0.186***	0.128	**0.353*** **	**0.330*** **	**0.355*** **	**0.376*** **	0.153	**0.331****
$\chi_{FD\%}$	0.034	0.022	0.029	0.037	0.049	0.045	-0.049	0.021	0.024	0.021	0.031	-0.042	0.047
$\chi/_{ARM}$	-0.035	-0.012	**0.240*** **	0.087	-0.048	-0.132	0.083	**0.312*** **	**0.298*** **	**0.311*** **	**0.316*** **	0.102	**0.306****
SIRM	-0.061	-0.032	**0.290*** **	0.120	0.008	-0.149	0.083	**0.387*** **	**0.371*** **	**0.387*** **	**0.371*** **	0.115	**0.398*** **
Soft $\%_{20mT}$	0.025	0.045	-0.041	-0.027	-0.034	0.013	-0.009	-0.088	-0.089	-0.090	-0.103	-0.005	-0.068
Soft $\%_{40mT}$	0.060	0.038	-0.136	-0.048	0.041	0.072	-0.044	-0.113	-0.105	-0.115	-0.122	-0.049	0.015
Hard $\%_{300mT}$	-0.037	-0.009	0.064	-0.031	0.034	-0.012	-0.007	0.098	0.098	0.102	0.085	0.007	0.114
Hard $\%_{500mT}$	0.042	0.050	0.029	0.010	0.045	-0.008	-0.020	0.065	0.065	0.066	0.041	-0.022	0.027
Soft $_{IRM20mt}$	-0.054	-0.017	**0.230****	0.075	0.012	-0.108	0.053	**0.304*** **	**0.291*** **	**0.303*** **	**0.282*** **	0.083	**0.277***
Soft $_{IRM40mT}$	-0.046	-0.023	**0.238****	0.098	0.023	-0.112	0.059	**0.336*** **	**0.323*** **	**0.335*** **	**0.323*** **	0.086	**0.360****
Hard $_{IRM300mT}$	-0.084	-0.029	**0.285*** **	0.042	-0.027	**-0.169***	0.113	**0.349*** **	**0.332*** **	**0.352*** **	**0.350*** **	0.143	**0.446*** **
Hard $_{IRM500mT}$	-0.012	0.028	**0.215****	0.055	0.014	-0.127	0.063	**0.278*** **	**0.266*** **	**0.277*** **	**0.259****	0.080	**0.344****
S-ratio	0.006	0.036	**-0.166***	-0.097	0.015	0.071	-0.045	**-0.180***	**-0.165***	**-0.185***	**-0.205****	-0.046	**-0.334****
ARM/χ	0.110	0.087	-0.083	0.048	0.092	0.100	-0.077	-0.061	-0.042	-0.068	-0.097	-0.090	-0.023
SIRM/ARM	-0.034	-0.018	0.024	-0.004	**0.162***	0.034	-0.065	0.100	0.101	0.102	0.066	-0.029	0.208
SIRM/χ	**0.187***	**0.193***	0.075	**0.158***	**0.166***	0.106	-0.140	0.125	**0.157***	0.118	0.052	-0.123	0.084
χ_{ARM} /SIRM	0.033	0.017	-0.024	0.003	**-0.163***	-0.034	0.066	-0.102	-0.103	-0.104	-0.068	0.030	-0.210

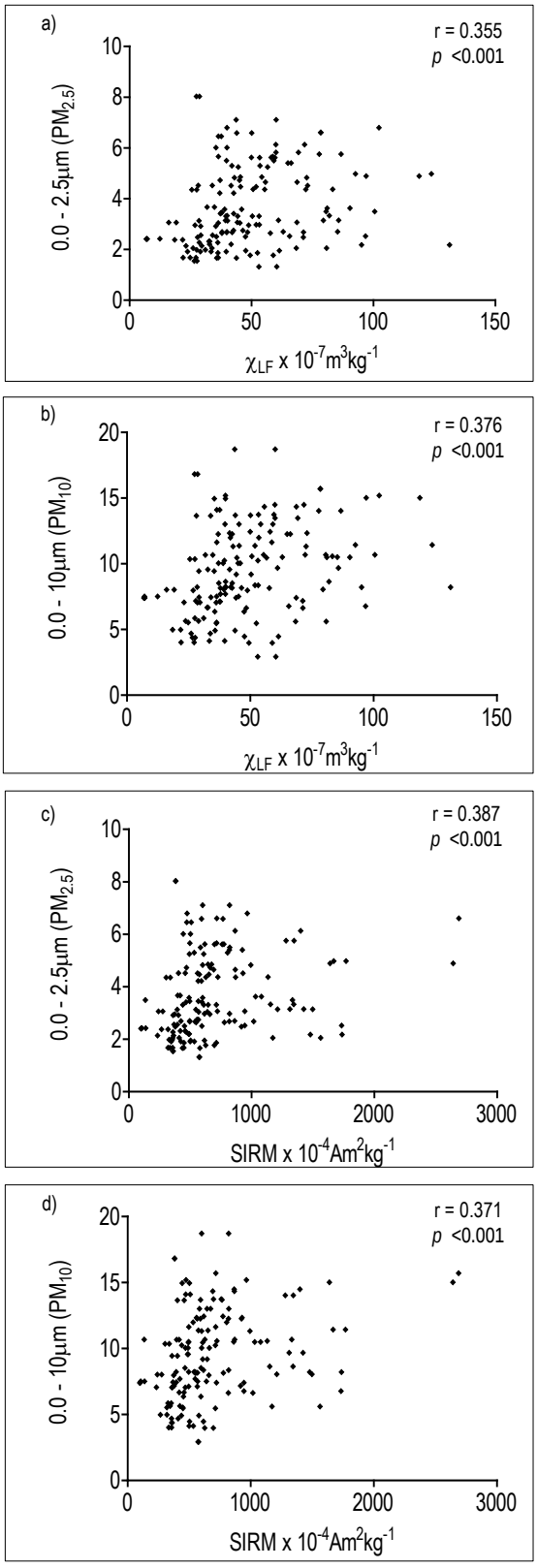

Figure 4.16 Bivariate plots of selected mineral magnetic and textural parameters for Wolverhampton Spring RDS samples (n = 168).

4.4.4 Factor analysis using mineral magnetic and textural parameters

To further clarify environmental relationships, multivariate factor analysis was used. In each case, parameter and sample loadings extracted from Factors 1 and 2 were used to generate factor plots. Factor analysis of key Spring characteristics is used to distinguish inter-parameter and sample loading relationships.

Figure 4.17(a) is the resultant factor plot for Spring key mineral magnetic and textural parameters. The first two factors extracted explain 49.47% of variation. Factor 1 explains 28.77% of variation in parameters, while Factor 2 explains 20.70%. The spread of parameter loadings along Factor 1 indicate magnetic concentration, domain size and some textural parameters as major influencing factors, with $\chi_{FD\%}$ displaying limited influence. Factor 2 shows the spread of loadings influenced by larger sized textural properties (sand and silt). Figure 4.17(a) displays sample loadings for Spring. Most samples are quite compacted and spread within both factors. There is some indication of influence of textural parameters from the resultant plot.

4.4.5 Factor analysis using mineral magnetic parameters

Figure 4.17(b) is the resultant factor plot for Spring key mineral magnetic parameters. The first two factors extracted explain 33.41% of variation. Factor 1 explains 25.90% of variation in parameters, while Factor 2 explains 7.51%. The spread of parameter loadings along Factor 1 indicate magnetic concentration parameters as the major influencing factors. Factor 2 shows the spread of loadings being influenced by magnetic domain size. The distribution of samples indicate that magnetic domain size is the main influence and, to a lesser extent, mineral magnetic concentration parameters.

4.4.6 Re-analysis data with additional factors

To further expand the understanding of RDS during seasons it was necessary to further investigate the data. With the use of GIS and traffic data, mineral magnetic concentrations have been analysed according to road types (Figure 3.3 and 4.10). Figure 4.18 displays the road types and samples used for the additional analysis.

4.4.7 Bivariate plots utilizing road type data

Figure 4.19 shows the bivariate plots with data sorted into two key groups, classified in terms of daily use and traffic numbers. Figure 4.19a distinguishes between road types, with a clear grouping of residential roads within the $PM_{2.5}$ <3% and χ_{LF} ~<50 x $10^{-7}m^3kg^{-1}$. Figure 4.19b displays a grouping of residential road samples associated with lower concentrations of SIRM, whereas arterial roads are associated with a mix of high and low concentrations. The bivariate plots for χ_{LF} and SIRM parameters show that residential roads have relatively low concentrations (Figure 4.19c,d). There is some mixing throughout the graphs, but they are fairly consistent with low concentration residential and medium to high concentration arterial.

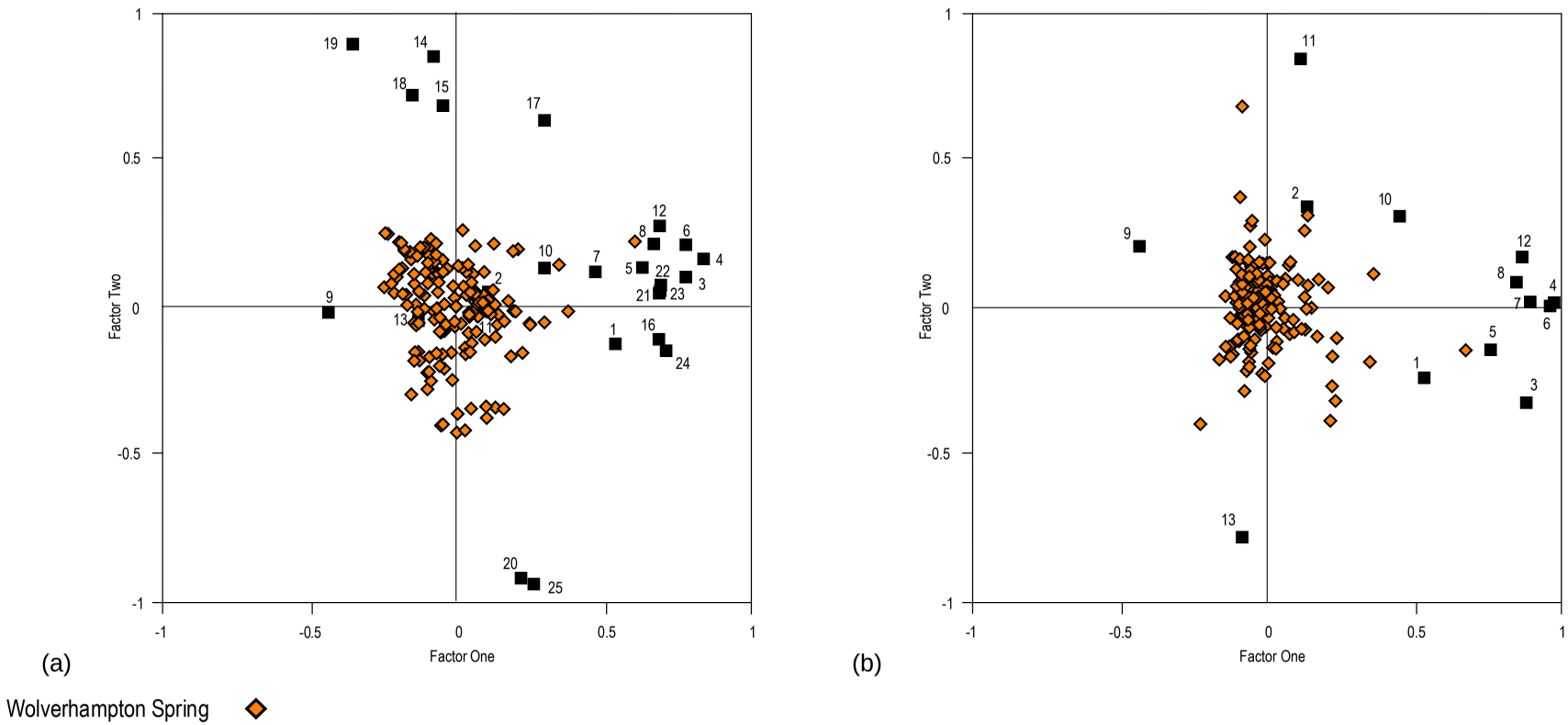

	Parameters								
1	χ_{LF}	6	Soft $_{IRM40mT}$	11	χ_{ARM}/SIRM	16	Sorting	21	Clay
2	χ_{FD}	7	Hard $_{IRM20mT}$	12	SIRM/ARM	17	Skewness	22	$PM_{1.0}$
3	χ_{ARM}	8	Hard $_{IRM40mT}$	13	SIRM/χ	18	Kurtosis	23	$PM_{2.5}$
4	SIRM	9	S-ratio	14	Mean	19	Sand	24	PM_{10}
5	Soft $_{IRM20mT}$	10	ARM/χ	15	Median	20	Silt	25	PM_{100}

Figure 4.17 Simultaneous R- and Q mode factor analysis plots of Factor 1 versus Factor 2, based on characteristics and Spring season Wolverhampton parameters.

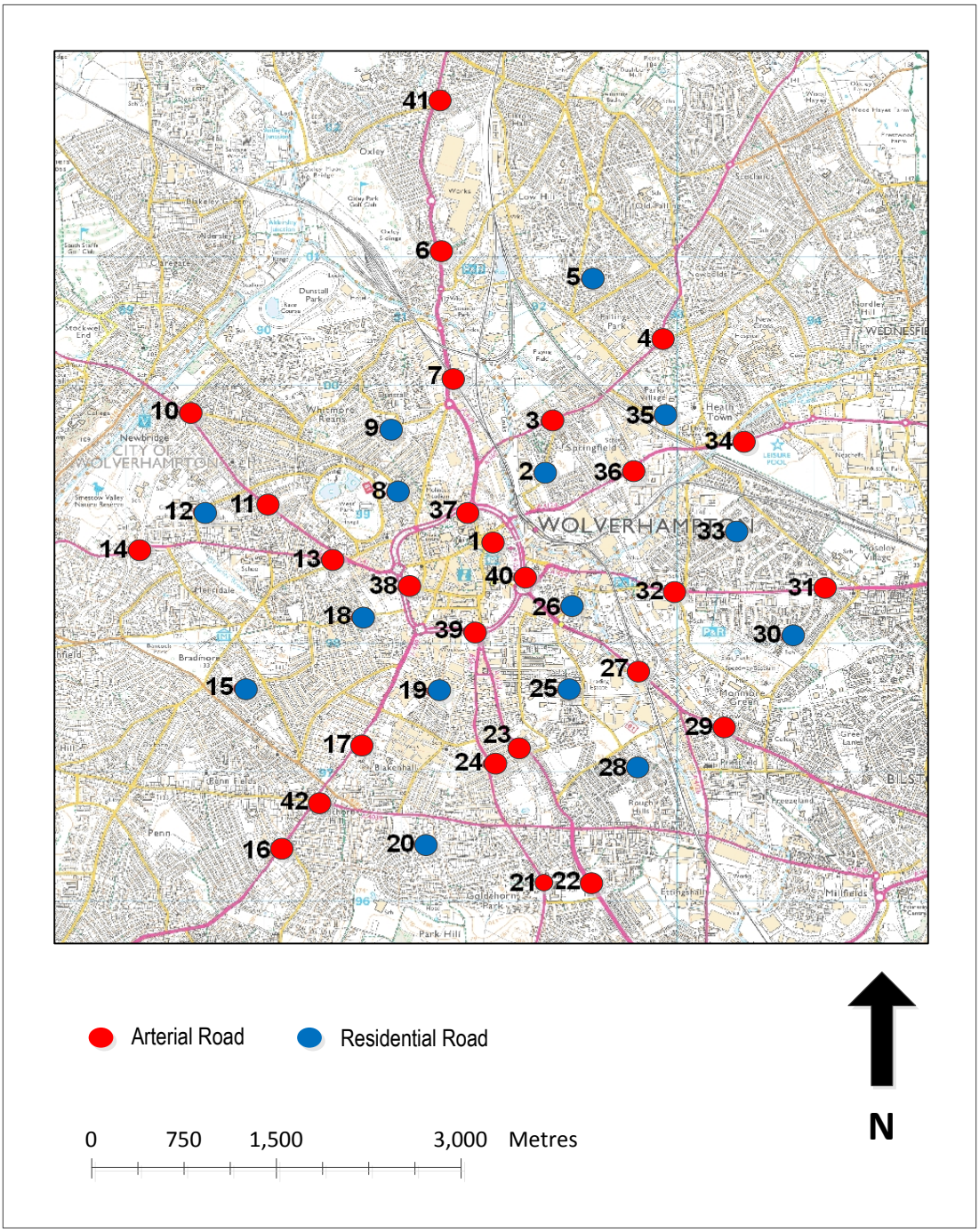

Figure 4.18 Sample map of Wolverhampton showing road types (red markers represent arterial roads and blue markers represent residential roads).

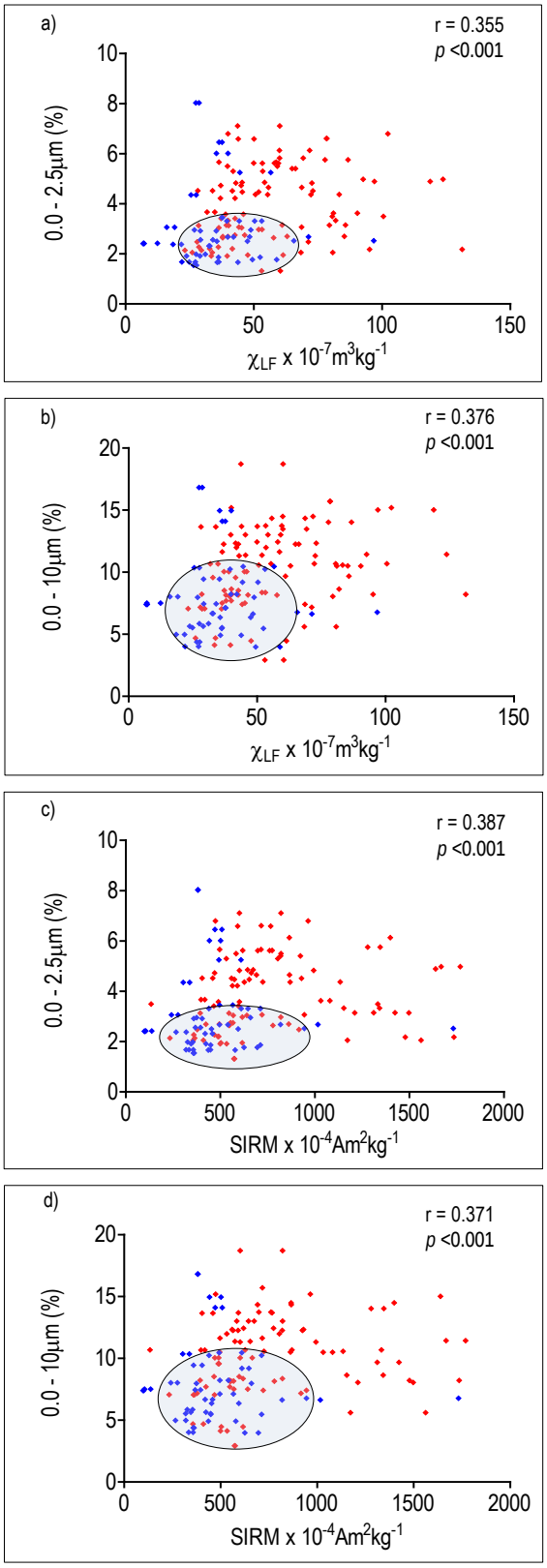

Figure 4.19 Bivariate plots of selected mineral magnetic and textural parameters for Wolverhampton Spring RDS samples (n=168), with road types identified (red points are arterial and blue points are residential roads). Highlighted rings identify sample groups.

The sample points highlighted in Figure 4.19(a-d) display a narrow band of similar concentrations of mineral magnetic material, whereas the arterial road systems display a broad band of concentrations which are spread throughout the range. Results suggest that low mineral magnetic concentrations are associated with residential roads, whereas arterial roads have a variation of values which is a combination of high and low concentrations of magnetic minerals.

4.4.8 Distinguishing Wolverhampton Spring road profiles using RDS characteristics

Table 4.9 compares the medians of each mineral magnetic component of the road populations for each parameter; while, Figures 4.20 and 4.21 (box-plots) presents population distributions for selected mineral magnetic and textural parameters. To distinguish road profiles, both null (H_0) and alternative (H_1) hypotheses were tested. Non-parametric Mann-Whitney U tests are used to compare the differences of these medians.

Tested Hypotheses

Null Hypothesis (H_0)	There are significant differences between the road types.
Alternative Hypothesis (H_1)	There are no significant differences between the road types.

4.4.9 Distinguishing road profiles using mineral magnetic and textural characteristics

By comparing boxplots (Figures 4.20-4.21) for each selected variable, it is clear that road types overlap. This indicates that the characteristic properties of road types are dissimilar (H_0). To determine whether the variations between road types are statistically significant, non-parametric Mann-Whitney tests were performed on arterial and residential roads for each of the magnetic and textural variables (Table 4.9). The '*p*' values show that for each variable the alternative hypothesis has been rejected and, therefore, the medians of each road type population are significantly different (Table 4.9 (p <0.001)). Using Mann Whitney U value tests the mineral magnetic concentration parameters (Figure 4.20 (χ_{LF}, χ_{ARM} and SIRM/χ)) display consistent relationships throughout the seasons (Table 4.9), with significant differences (p <0.001) between road systems. There are significant associations (H_1) for $\chi_{FD\%}$ (p =0.842) and SIRM/χ (p =0.372), which indicate consistency of multi-domain ferromagnetic grains between road types. All mineral magnetic concentration parameters on residential roads are significantly different to arterial roads (p <0.001), with high concentrations associated with main roads and low concentrations with residential roads. Textural parameters (Figure 4.21) display coarser particle sizes associated with arterial roads. These results further support the correlations within the mineral magnetic and textural data. Differences were not significant between mineralogical parameters ($\chi_{FD\%}$, SIRM/χ and S-ratio), which suggests that mineralogy across road types is fairly consistent.

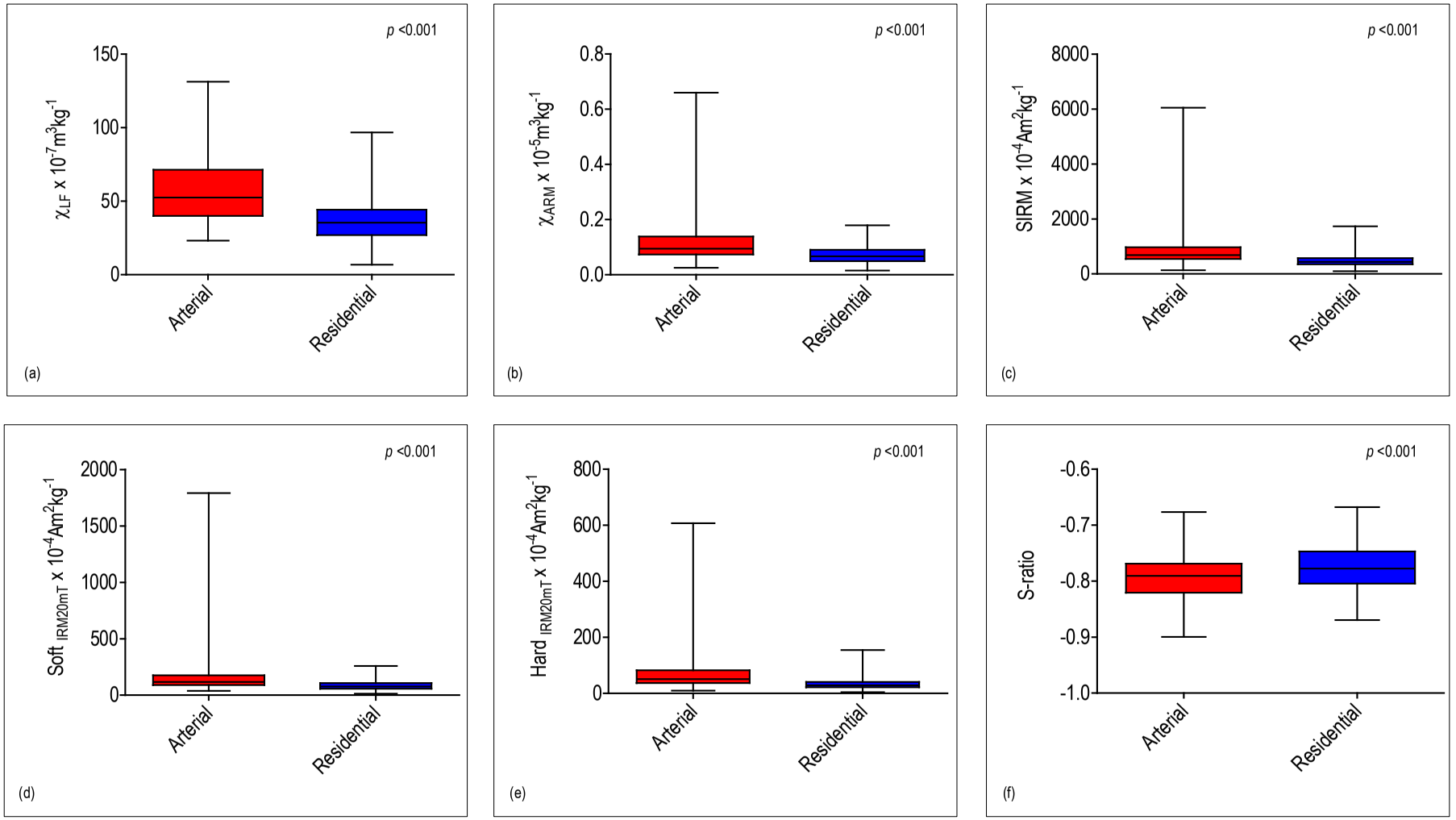

Figure 4.20 Boxplots Identifying the range of concentrations for mineral magnetic parameters for Wolverhampton spring RDS samples (red plots for arterial roads and blue plots for residential roads).

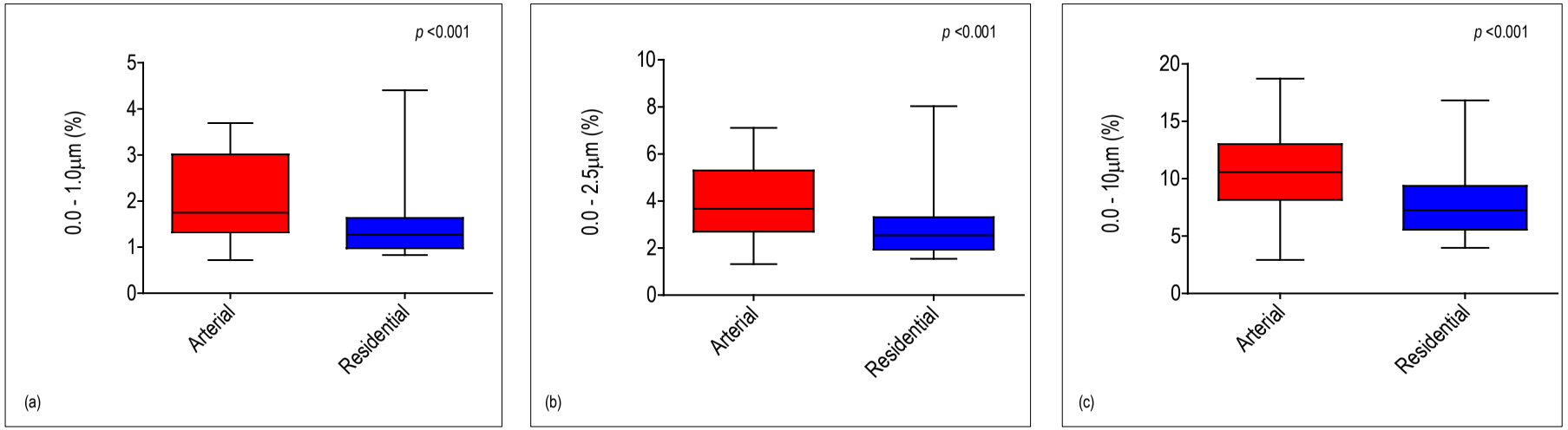

Figure 4.21 Boxplots Identifying the range of concentrations for textural parameters for Wolverhampton Spring RDS samples (red plots for arterial roads and blue plots for residential roads).

Table 4.9 Mann-Whitney U test '*p*' values for Spring Wolverhampton arterial and residential road parameters (**bold** text is significant).

Parameters											
χ_{LF}	<0.001	Soft $_{IRM20mt}$	<0.001	SIRM/ARM	<0.001	Mean - PS	<0.001	Sand	<0.001	$PM_{1.0}$	<0.001
$\chi_{FD\%}$	0.842	Soft $_{IRM40mT}$	<0.001	SIRM/χ	0.372	Median - PS	<0.001	Silt	<0.001	$PM_{2.5}$	<0.001
χ_{ARM}	<0.001	Hard $_{IRM300mT}$	<0.001	χ_{ARM} /SIRM	<0.001	Sorting	<0.001	Clay	<0.001	PM_{10}	<0.001
SIRM	<0.001	Hard $_{IRM500mT}$	<0.001			Skewness	<0.001			PM_{100}	<0.001
S-ratio	<0.001	ARM /χ	<0.001			Kurtosis	<0.001				

4.4.10 Distinguishing road profiles during all seasons

The results for all other seasons (data not shown (Summer, Autumn and Winter)) showed relationships consistent with those found with Spring samples, with significant differences between road types (H_0). The results suggest that although concentrations vary throughout the year, the mineralogy ($\chi_{FD\%}$, SIRM/χ) between road types remain fairly consistent (H_1).

4.4.11 Mineral magnetic and particle size relationships of arterial and residential roads for Spring months

To further investigate the potential for particle size determination by mineral magnetic measurements, Spearman rank correlation tests were applied to the arterial and residential road data. Results (Table 4.10) show that the mixed road samples display strong relationships throughout the particle size range, whereas on independent road types there is a significant loss in relationships (all parameters) on residential roads. Mineral magnetic and textural parameters on arterial roads remain fairly consistent, with slight loss in associations (r) across all parameters.

The results suggest that mineral magnetic concentration parameters have a stronger influence on arterial, than residential roads. Table 4.10a,b show χ_{LF} and χ_{ARM} linkages to be consistent, showing a moderate to weak relationship (r = 0.247-0.318;*p* <0.05-<0.01), whereas SIRM (Table 4.10c) displays the highest r values (r = 0.324-0.345;*p* <0.001) and is consistently higher than other parameters when road types are mixed. The greater potential for a particle size proxy shown on arterial roads, suggests the greater concentration of magnetic material may be an influencing factor. Although there are some significant relationships, the results are weak and thus inappropriate for particle size proxy purposes.

Table 4.10 Summary mineral magnetic concentration (χ_{LF}, χ_{ARM}, SIRM and textural (<PM_{10})) parameter spearman rank correlation relationships for Wolverhampton road types (Mixed, n = 168; Arterial, n = 108; Residential, n = 60) during Spring (**bold** text is significant (**p* <0.05; ***p* <0.01; ****p* <0.001)

(a) χ_{LF}	Clay	$PM_{1.0}$	$PM_{2.5}$	PM_{10}
Mixed	0.353***	0.329***	0.356***	0.376***
Arterial	0.274**	0.247*	0.270**	0.318**
Residential	0.202	0.159	0.197	0.078

(b) χ_{ARM}	Clay	$PM_{1.0}$	$PM_{2.5}$	PM_{10}
Mixed	0.311***	0.298***	0.310***	0.316***
Arterial	0.261**	0.252*	0.257**	0.285**
Residential	0.125	0.090	0.124	0.025

(c) SIRM	Clay	$PM_{1.0}$	$PM_{2.5}$	PM_{10}
Mixed	0.386***	0.370***	0.386***	0.370***
Arterial	0.345***	0.329***	0.340***	0.324***
Residential	0.196	0.170	0.190	0.047

4.5 Relationships between the mineral magnetic and textural variables for individual months.

The seasonal data suggest weak relationships exist between mineral magnetic and textural parameters during specific periods. With Spring and Summer months displaying limited proxy potential, further investigation into individual months (Appendix 4.4.1-4.4.12) have explored intra-month associations to determine which periods offer the greatest proxy potential. This further analysis will establish limitations/success for mineral magnetic particle size proxy use over time in Wolverhampton. Table 4.11 presents linkages of separate months for selected mineral magnetic and textural parameters.

Spearman rank correlation tests conducted on all sampling months show limited success (Table 4.11). Results for January, July and November have no linkages between parameters, whereas September displays some weak relationships with χ_{LF} versus $PM_{1.0}$ ($r = 0.452$; $(n = 42)$ $p < 0.001$ (Table 4.11a)), χ_{ARM} versus $PM_{1.0}$ ($r = 0.671$; $(n = 42)$ $p < 0.001$ (Table 4.11b)) and SIRM versus $PM_{1.0}$ ($r = 0.910$; $(n = 42)$ $p < 0.001$ (Table 4.11c)). The best parameter linkages are shown through March and May with χ_{LF} versus textural variables $<PM_{10}$ (Table 4.11a) displaying moderately strong relationships (May $r = 0.118$-0.560; $p < 0.05$-<0.01, and March $r = 0.338$-429; $p < 0.05$-<0.01). Linkages between parameters and months of May and March reflect the relationships found within the spring investigation, this has shown that the combined months contribute to the individual spring linkages. When the monthly data is compared to weather data for the periods (Appendix 4.3) relationships appear to improve during warm, dry periods (stable conditions). Increased temperatures and decreased rainfall also shows an increase in magnetic material in Wolverhampton RDS during these periods. This observation appears to indicate that stable conditions and accumulation of magnetic material improve mineral magnetic-particle size proxy potential.

4.5.1 Detailed investigation of May 2008 RDS Wolverhampton samples

Table 4.12 presents summary data for the physical characteristics of Wolverhampton RDS samples ($n = 42$). The magnetic concentration parameters are considered high compared to urban topsoils (Dearing, 1999), and moderate compared to other urban road deposited sediments (Charlesworth, 2003; Robertson, 2003; Booth, 2006; Kim , 2009), with relatively high values of magnetically soft minerals (Soft $_{IRM20mT,}$ 167.645 x $10^{-4}Am^2kg^{-1}$; Soft $_{IRM40mT,}$ 494.383 x $10^{-4}Am^2kg^{-1}$).

4.5.2 Relationships between mineral magnetic and textural variables

Table 4.13 summarizes correlation statistics between mineral magnetic and textural variables for Wolverhampton during May 2008. Magnetic concentration parameters show relatively weak positive correlation. Figure 4.22a shows a strong relationship between χ_{LF} versus clay. This relationship is also evident within the finer textural size fractions ($PM_{1.0}$–PM_{10}) with consistent strengthening of the relationships as the particle size increases (χ_{LF}, $r = 0.341$-0.560; $p < 0.01$ (Figure 4.22b,c,d)) and weakening of the relationship with χ_{ARM} ($r = 0.354$-0.707; $p < 0.01$) and SIRM ($r = 0.374$-0.627; $p < 0.01$).

Table 4.11 Summary Wolverhampton RDS mineral magnetic concentration ((a) χ_{LF}, (b) $\chi_{ARM,}$ and (c) SIRM and textural (<PM_{10})) parameter Spearman rank correlation relationships for all months sampled (**bold** text is significant (*p <0.05; **p <0.01; ***p <0.001 (n = 42)))

(a) χ_{LF}	Clay	$PM_{1.0}$	$PM_{2.5}$	PM_{10}
January 2008	x	x	x	x
March	0.324*	0.338*	x	x
May (a)	0.443*	0.341**	0.457*	0.560**
July	x	x	x	x
September	x	0.452***	x	x
November	x	x	x	x
January 2009	x	x	x	x
March (b)	0.429**	0.420**	0.420**	0.408*
May	0.308*	x	x	0.381*
July	x	x	x	x
September	x	x	x	x
November	x	x	x	x
January 2010	x	x	x	x

(b) χ_{ARM}	Clay	$PM_{1.0}$	$PM_{2.5}$	PM_{10}
January 2008	x	x	x	x
March	x	x	x	x
May (a)	0.334*	0.707***	0.328*	0.354*
July	x	x	x	x
September	x	0.671***	x	x
November	x	x	x	x
January 2009	x	x	x	x
March (b)	0.382*	0.382*	0.371*	0.406*
May	0.295*	x	0.284*	0.285*
July	x	x	x	x
September	x	x	x	x
November	x	x	x	x
January 2010	x	x	x	x

(c) SIRM	Clay	$PM_{1.0}$	$PM_{2.5}$	PM_{10}
January 2008	x	x	x	x
March	0.332*	0.347*	x	x
May (a)	0.372*	0.627**	0.364*	0.374*
July	x	x	x	x
September	x	0.910***	x	x
November	x	x	x	x
January 2009	x	x	x	x
March (b)	0.501**	0.503**	0.492**	0.459**
May	<0.05*	<0.05*	<0.05*	<0.05*
July	x	x	x	x
September	x	x	x	x
November	x	x	x	x
January 2010	x	x	x	x

Months presented	May	March

Table 4.12 Summary RDS analytical data* for Wolverhampton May 2008 (a) (n = 42)

	Parameters	Units	Mean	Median	SD	CV (%)	Min	Max	Range
(a)	χ_{LF}	$10^{-7}m^3kg^{-1}$	53.050	45.370	22.860	43.100	6.860	102.310	95.450
	χ_{FD}	%	3.110	1.510	9.300	299.400	0.270	6.850	6.120
	χ_{ARM}	$10^{-5}m^3kg^{-1}$	0.113	0.080	0.103	91.360	0.034	0.660	0.626
	SIRM	$10^{-4}Am^2kg^{-1}$	873.000	610.000	832.000	95.290	102.000	5439.000	5337.000
	S-Ratio	Dimensionless	-0.807	-0.811	0.044	-5.455	-0.900	-0.676	0.223
	$SOFT\%_{20mT}$	%	17.577	16.084	3.888	22.119	11.872	25.514	13.642
	$SOFT\%_{40mT}$	%	46.984	44.751	8.308	17.683	37.636	89.953	52.318
	$HARD\%_{300mT}$	%	6.763	6.494	1.765	26.092	3.585	11.088	7.504
	$HARD\%_{500mT}$	%	2.640	2.229	1.732	65.611	0.391	10.038	9.647
	$SOFT_{IRM20mT}$	$10^{-4}Am^2kg^{-1}$	167.645	113.131	212.841	126.959	13.248	1324.087	1310.839
	$SOFT_{IRM40mT}$	$10^{-4}Am^2kg^{-1}$	494.383	287.036	869.604	175.897	42.343	5438.547	5396.204
	$HARD_{IRM300mT}$	$10^{-4}Am^2kg^{-1}$	66.328	39.392	97.897	147.595	7.013	607.055	600.042
	$HARD_{IRM500mT}$	$10^{-4}Am^2kg^{-1}$	34.070	15.660	99.045	290.707	3.233	606.889	603.656
	ARM/χ	$10^{-1}Am^{-1}$	0.696	0.554	0.514	73.870	0.282	3.498	3.217
	χ_{ARM}/SIRM	$10^{-3}Am^2kg^{-1}$	0.138	0.131	0.044	31.680	0.077	0.332	0.255
	SIRM/ARM	Dimensionless	244.600	239.450	61.720	25.230	94.720	409.500	314.780
	SIRM/χ	$10^{-1}Am^{-1}$	16.360	13.490	13.050	79.760	7.860	90.540	82.680
(b)	Mean - PS	μm	295.300	294.300	101.800	34.460	87.100	507.100	420.000
	Median - PS	μm	362.200	364.100	93.000	25.690	165.700	582.700	417.000
	Sorting	σ_1	2.274	2.266	0.318	13.990	1.507	2.902	1.395
	Skewness	SK_1	0.471	0.510	0.149	31.620	0.137	0.702	0.565
	Kurtosis	K_G	1.300	1.153	0.417	32.050	0.759	2.246	1.487
	Sand	%	75.430	76.660	7.430	9.860	57.160	88.330	31.170
	Silt	%	21.710	20.610	7.550	34.750	10.320	40.990	30.670
	Clay	%	2.856	2.621	1.209	42.320	1.127	5.787	4.660
	$PM_{1.0}$	%	1.760	1.598	0.816	161.526	0.719	3.520	2.801
	$PM_{2.5}$	%	3.344	3.132	1.370	40.964	1.316	6.792	5.476
	PM_{10}	%	8.789	8.224	2.836	32.265	2.921	15.190	12.269
	PM_{100}	%	27.863	27.116	9.490	34.058	12.763	53.277	40.514
	LOI	%	1.012	1.050	0.330	-32.591	1.168	1.035	2.203

*SD = Standard Deviation; CV = Percentage coefficient of variation; Min = Minimum value; Max = maximum value.

Table 4.13 Statistical relationships between mineral magnetic and textural parameters for Wolverhampton (May 2008) (**bold** text is significant (*p <0.05; **p <0.01; ***p <0.001)) (n = 42)

Parameters	Median	Mean	Sorting	Skewness	Kurtosis	Sand	Silt	Clay	$PM_{1.0}$	$PM_{2.5}$	PM_{10}	PM_{100}	LOI
χ_{LF}	-0.093	-0.049	**0.484****	0.054	-0.168	-0.298	0.222	**0.443****	**0.341****	**0.457****	**0.560****	0.224	0.104
$\chi_{FD\%}$	-0.054	-0.005	0.167	-0.051	0.045	-0.085	0.066	0.106	0.147	0.105	0.168	0.077	0.054
$\chi/_{ARM}$	0.013	0.007	**0.371****	0.127	-0.138	-0.157	0.101	**0.334***	**0.707****	**0.328***	**0.354****	0.116	-0.055
SIRM	0.034	0.034	**0.392****	0.142	-0.125	-0.127	0.066	**0.372****	**0.627****	**0.364****	**0.374****	0.099	-0.029
Soft $\%_{20mT}$	-0.003	0.005	0.129	0.093	-0.109	-0.025	0.017	0.048	**0.807***	0.059	0.107	-0.002	-0.020
Soft $\%_{40mT}$	0.079	0.024	0.279	0.199	-0.039	0.001	-0.054	0.325	**0.459***	0.309	0.247	-0.003	-0.030
Hard $\%_{300mT}$	0.070	0.084	0.248	0.117	-0.001	-0.026	-0.011	0.227	-0.058	0.228	0.242	-0.002	0.227
Hard $\%_{500mT}$	0.108	0.159	0.120	0.008	-0.048	0.035	-0.057	0.138	**0.244***	0.129	0.141	-0.012	0.245
Soft $_{IRM\ 20mt}$	0.017	0.019	**0.318****	0.153	-0.161	-0.093	0.053	**0.242***	**0.253***	**0.246***	**0.292***	0.056	-0.028
Soft $_{IRM\ 40mT}$	0.068	0.052	**0.345****	0.169	-0.092	-0.065	0.008	**0.346***	**0.601****	**0.335***	**0.324***	0.047	-0.018
Hard $_{IRM\ 300mT}$	0.088	0.081	**0.421****	0.204	-0.090	-0.074	0.009	**0.400****	**0.550****	**0.391****	**0.393****	0.042	0.008
Hard $_{IRM\ 500mT}$	0.100	0.084	0.321	0.177	-0.061	-0.021	-0.031	0.327	**0.564***	0.315	0.304	0.010	0.015
S-ratio	0.124	0.234	-0.175	-0.030	-0.040	0.160	-0.110	-0.295	**-0.212***	-0.293	**-0.360****	-0.155	**-0.296***
χ_{ARM}/χ	0.083	0.040	0.196	0.178	-0.105	-0.009	-0.016	0.154	0.558	0.145	0.124	-0.007	-0.109
$SIRM/_{ARM}$	-0.048	0.026	0.200	-0.054	0.006	-0.080	0.048	0.193	-0.082	0.194	0.205	0.092	0.129
$SIRM/\chi$	0.080	0.063	0.249	0.152	-0.076	-0.011	-0.029	0.246	0.543	0.234	0.201	0.008	-0.063
χ_{ARM} /SIRM	0.015	-0.056	-0.143	0.087	-0.066	0.044	-0.008	-0.218	0.074	-0.212	-0.195	-0.069	-0.130

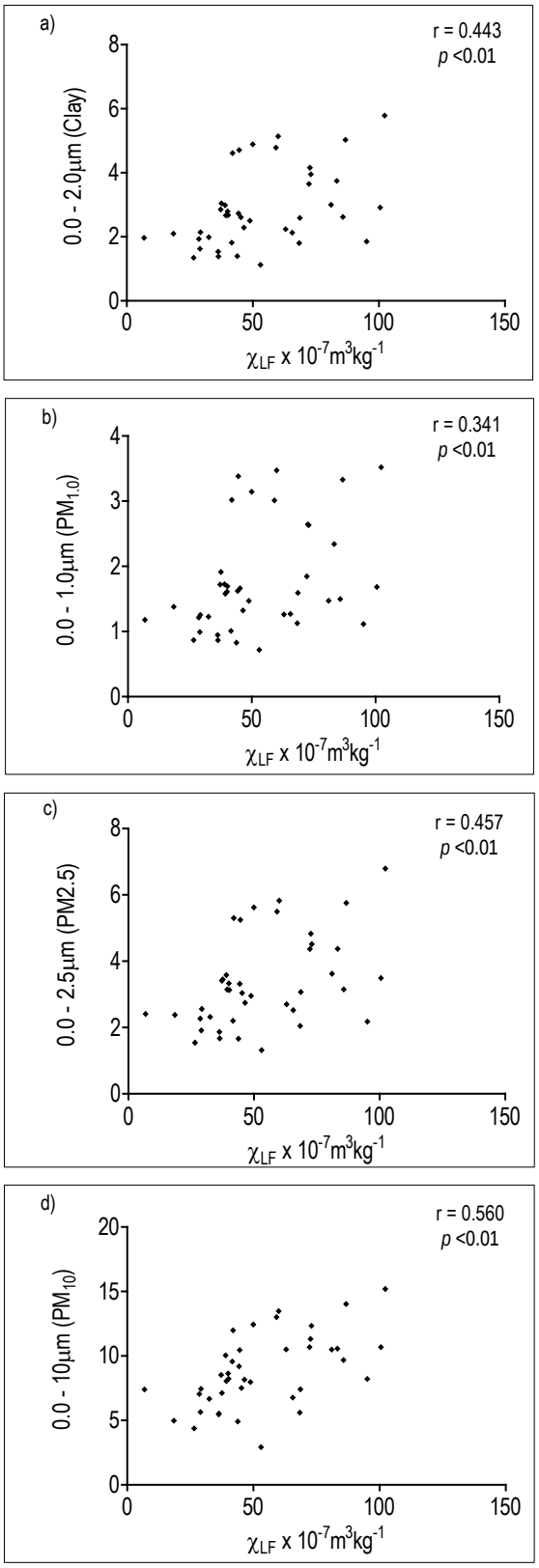

Figure 4.22 Bivariate plots of selected mineral magnetic and textural parameters for Wolverhampton May 2008 (a) samples (n = 42).

Associations were found within some of the mineralogical parameters and the fractions ($PM_{1.0}$), (Soft $_{IRM\ 20mT}$ and $_{40mT}$, Hard $_{IRM\ 20mT}$ and $_{40mT}$ (r = 0.550-0.601; *p* <0.01). Almost all other mineral magnetic and textural parameters weakly correlated (i.e. most correlation coefficients are *ca* r= 0.106–0.234 (*p* >0.05). Results suggest that mineral magnetic concentration parameters have some influence on finer sediment fractions in Wolverhampton during May.

Correlation between concentration measurements and finer particle size fractions ($PM_{1.0}$-PM_{10}) suggests consistent correlations through the particle size range, whereas an increase in magnetic concentration is associated with an increase in particle size concentration (%).χ_{LF}, χ_{ARM} and SIRM also show relatively weak positive correlations with finer fractions of RDS ($PM_{1.0}$-PM_{10}) (χ_{LF} shown in bivariate graphs). Plots show a distinct relationship, which is consistent through the particle size range, whereas an increase in magnetic concentration is associated with an increase in particle size concentration (%). Moderate correlations (r = ≤0.560; *p* <0.01) exist between these parameters. This pattern is consistent with all other concentration parameters (χ_{ARM} and SIRM,) with any increase (Table 4.13) in magnetic concentration associated with a corresponding increase in $PM_{1.0}$ - PM_{10}. Mineral magnetic measurements have limited potential as a particle size proxy at these scales.

4.5.3 Spatial characterization of mineral magnetic and textural data

The coefficient of variation ((CV) = standard deviation (SD) / mean)) is used to analyse spatial variation between parameters. So far, it has been demonstrated 'how' the samples vary, in terms of their mineral magnetic and textural properties over time, and that some variation is associated with differences in sedimentary environments. However, geographical relationships between adjacent samples have not been addressed, nor has an environmental explanation for 'why' variations exist. Therefore, selected GIS images are used to analyse spatial variations.

4.5.4 Spatial characterization of physical-characteristics using Arcview GIS (v 10)

χ_{LF} values are used to generate the GIS images due to the potential use in field conditions. The quick and easy application of susceptibility measurements has clearly shown the potential to map areas of interest (Figure 4.10a), highlighting potential hot-spots for RDS investigation.

Figure 4.23 shows χ_{LF} variation across the sampling area, with several high concentrations of χ_{LF} directly associated with the arterial road system (Table 4.14). To the north and east of the sampling area there are high concentrations of magnetic material (χ_{LF} 95.148-102.310 x $10^{-7}m^3kg^{-1}$) and these high concentrations are directly associated with the arterial roads. To the west of the City centre there are several lower concentrations of magnetic minerals (χ_{LF} 6.856-18.493 x $10^{-7}m^3kg^{-1}$) which appear to be directly associated with residential side roads. This pattern can be observed throughout the map, with main roads displaying higher readings than side roads. When compared to road traffic data (Figure 3.3, Appendix 3.2.1) there appears to be similarities between traffic volumes and χ_{LF} concentrations as previously observed in section 4.2.10. Land use also simulates the previously observed patterns (Appendix 3.1) with high χ_{LF} concentrations to the east suggesting links to industrial sources and low concentration to the west suggesting natural background and anthropogenic sources.

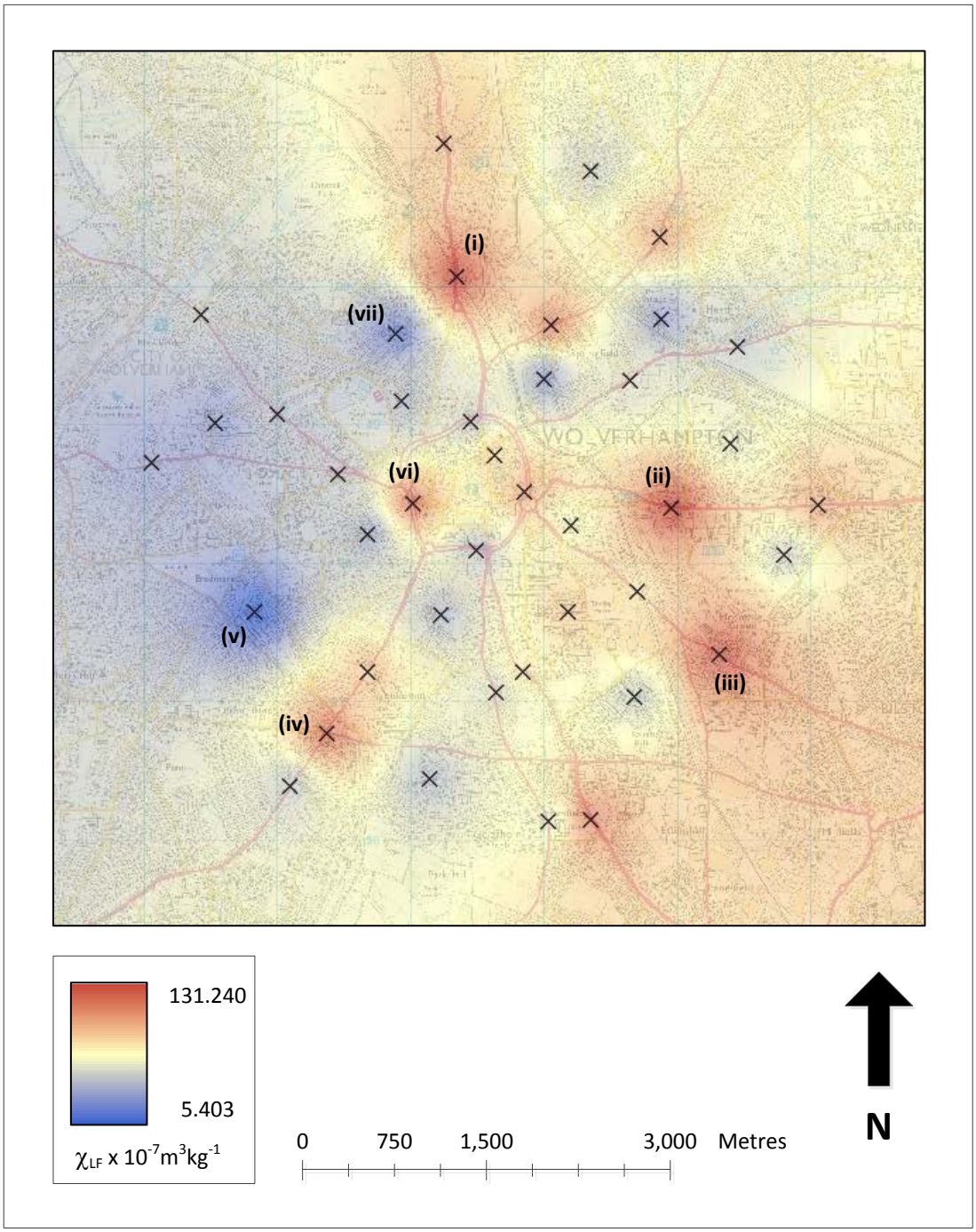

Figure 4.23 Spatial distributions of χ_{LF} in Wolverhampton during May 2008.

Table 4.14 Selected parameters for specific sites in Wolverhampton during May 2008.

	Sample	χ_{LF}		Sample	χ_{LF}
i	7	100.507	v	15	6.856
ii	32	102.310	vi	38	85.734
iii	29	95.148	vii	9	18.493
Iv	42	86.764			

4.5.5 Further assessment using bivariate plots

Bivariate plots were again used to analyse spatial patterns between the arterial and residential road systems (Figure 4.23). Figure 4.24(a-d) show groupings of similar readings (highlighted circle) which are associated with residential roads and arterial road networks. There is some mixing, but they remain fairly consistent with groups of data. The sample points highlighted in Figure 4.24(a-d) display a narrow band of similar concentrations (highlighted area) of mineral magnetic material, whereas the arterial road systems display a broad band of concentrations, spread throughout the range. Results suggest that lower mineral magnetic concentrations are associated with residential roads, whereas arterial roads have a combination of both high and low concentrations.

4.5.6 Distinguishing road profiles using RDS characteristics

Table 4.15 compares the medians of each mineral magnetic component of the road populations for each parameter; while, Figures 4.25 and 4.26 presents population distributions for selected parameters.

Tested Hypotheses

Null Hypothesis (H_0)	There are significant differences between road types.
Alternative Hypothesis (H_1)	There are no significant differences between road types.

4.5.7 Distinguishing road profiles using mineral magnetic parameters

By comparing boxplots (Figure 4.25 – 4.26) for each magnetic and textural parameter, it is clear that road types overlap (H_0). To determine whether the variations between the road types are significant, non-parametric Mann Whitney U tests were used.

Selected mineral magnetic parameters of main and side roads are significantly different (Table 4.15 (p <0.001)). Using Mann Whitney U tests, the mineral magnetic concentration parameters (χ_{LF}, χ_{ARM} and SIRM) and fine particle class parameters display significant differences (p <0.001) between the road systems. All mineral magnetic concentration parameters on residential roads are significantly different to arterial roads (p <0.001), with higher concentrations associated with arterial roads and lower concentrations associated with residential roads (Figure 4.25). Textural parameters display limited differences with some particle sizes showing no differences (sand, silt and PM_{100} (Figure 4.26)). SIRM/χ results suggest that road types have similar mineralogy with a weak $\chi_{FD\%}$ relationship.

4.5.8 Road type magnetic grain size

Bivariate plots (Figure 4.27) show χ_{LF} versus $\chi_{FD\%,}$ indicating arterial and residential roads in May are dominated by multi-domain magnetic grain sizes. Mann Whitney U tests indicate differences, which are evident within the bivariate plots.

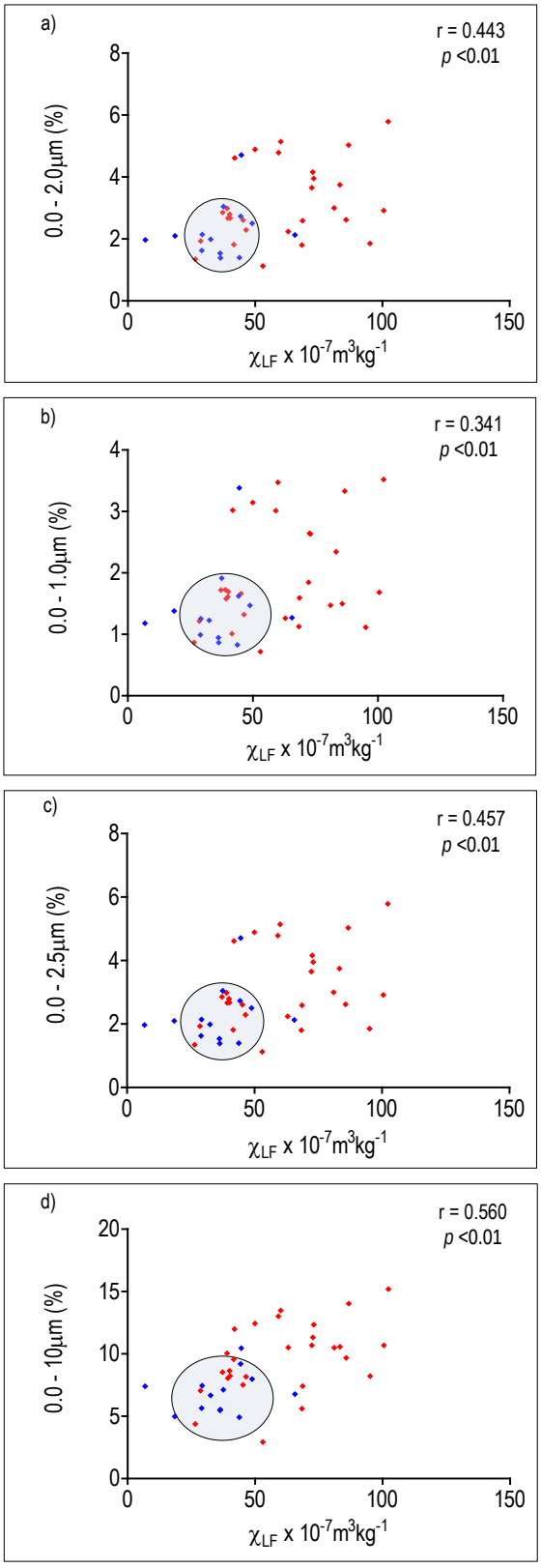

Figure 4.24 Bivariate plots of indicated road types. χ_{LF} versus $PM_{1.0}$ to PM_{10}, of Wolverhampton in May 2008 RDS samples (n = 42). (Red points are arterial and blue points are residential roads). Areas of highlighted rings identify sample groups.

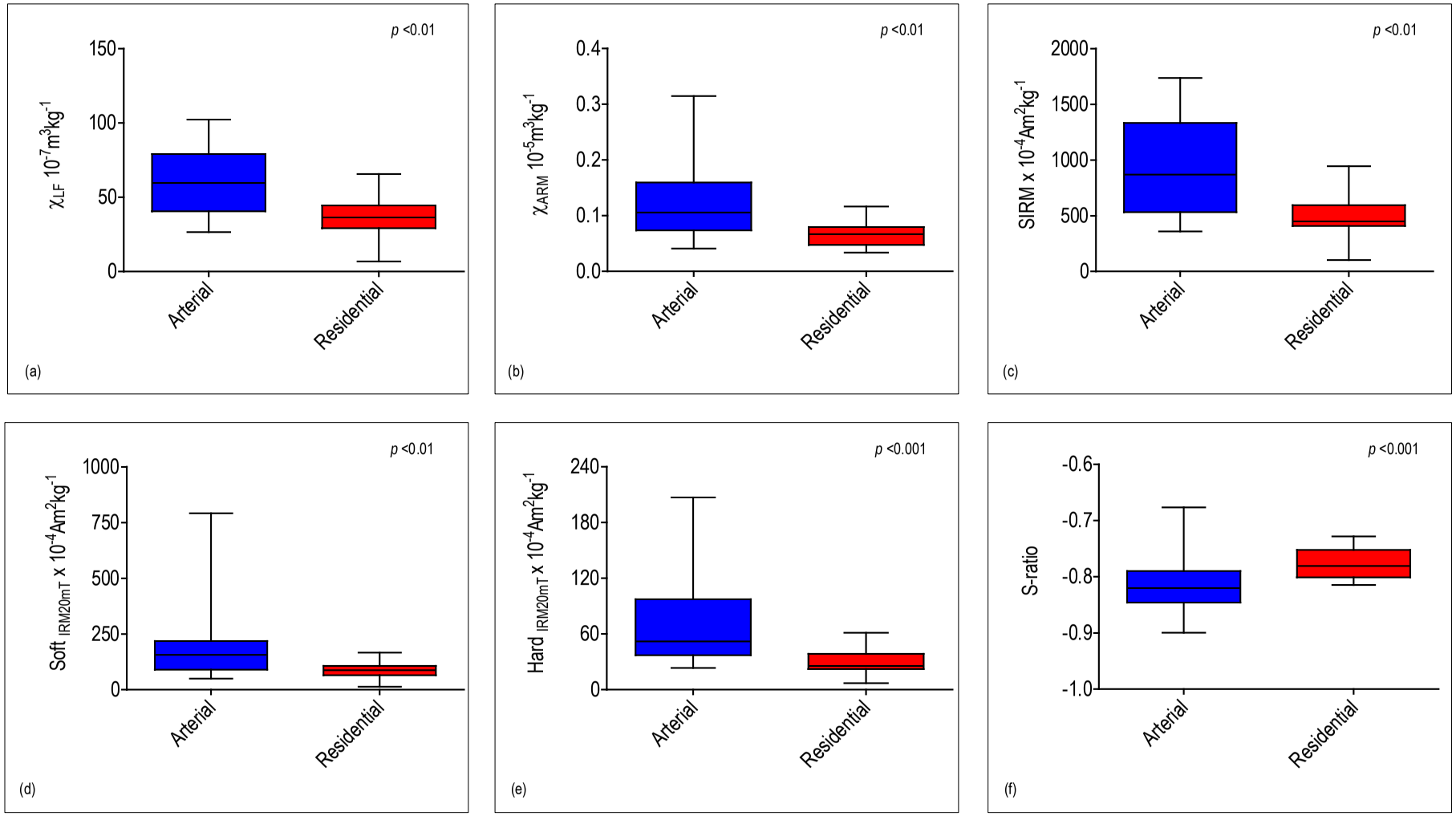

Figure 4.25 Boxplots identifying the range of concentrations for mineral magnetic parameters for Wolverhampton May 2008 RDS samples (red plots for arterial roads and blue plots for residential roads).

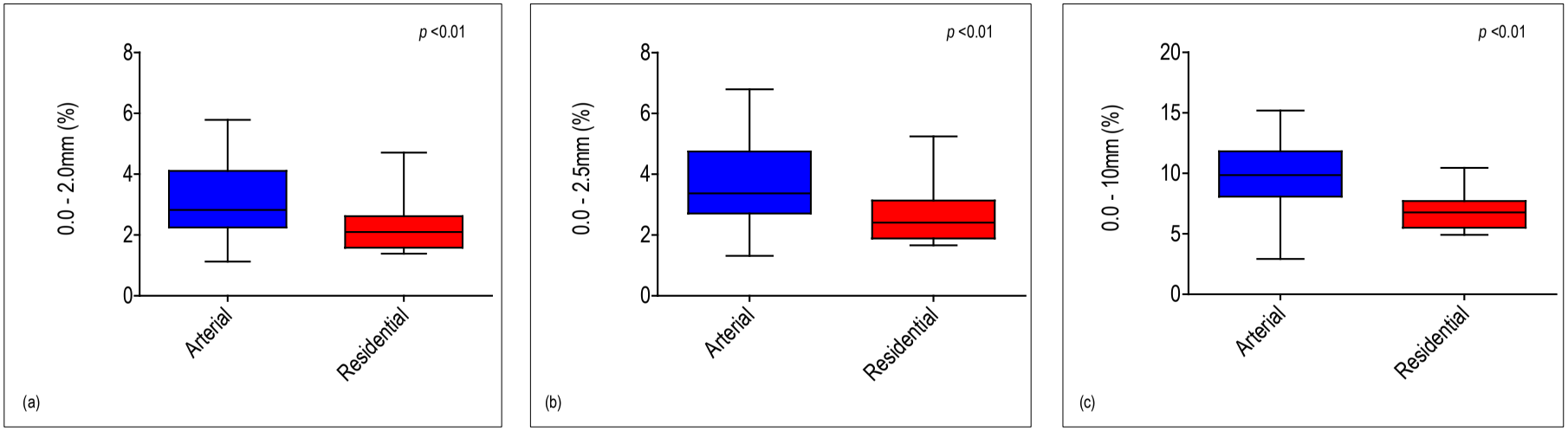

Figure 4.26 Boxplots identifying the range of concentrations for textural parameters for Wolverhampton May 2008 RDS samples (red plots for arterial roads and blue plots for residential roads).

Table 4.15 Mann-Whitney U test '*p*' values for Wolverhampton May 2008 arterial and residential road parameters. (**bold** text is significant).

Parameters											
χ_{LF}	<0.01	Soft $_{IRM\ 20mt}$	<0.01	SIRM/ARM	0.337	Mean - PS	0.855	Sand	0.424	$PM_{1.0}$	<0.05
$\chi_{FD\%}$	0.183	Soft $_{IRM\ 40mT}$	<0.01	SIRM/χ	0.664	Median - PS	0.726	Silt	0.877	$PM_{2.5}$	<0.05
χ_{ARM}	<0.01	Hard $_{IRM\ 20mT}$	<0.001	χ_{ARM} /SIRM	0.400	Sorting	0.051	Clay	<0.05	PM_{10}	<0.001
SIRM	<0.01	Hard $_{IRM\ 40mT}$	0.053			Skewness	0.643			PM_{100}	0.694
S-ratio	<0.001	ARM/χ	0.674			Kurtosis	0.921				

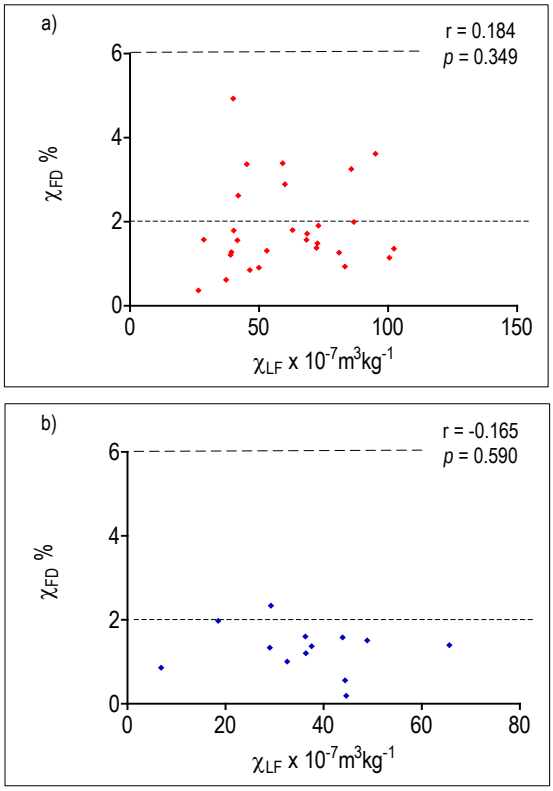

Figure 4.27 Bivariate plots for Wolverhampton May 2008 RDS; χ_{LF} versus $\chi_{FD\%}$ of road type (a) arterial road (n = 27) (b) residential road (n = 15)) samples, indicating magnetic grain size.

Arterial road samples (Figure 4.27a) include some SSD/PSD or coarse and fine ferrimagnets. Figure 4.27b suggests that residential roads contain a consistently low ratio and are dominated by multi-domain grain sizes. The bivariate plots suggest that within the road type samples, there is little to no presence of SP ferrimagnets. This further validates the Mann Whitney results which show a relatively weak $\chi_{FD\%}$ relationship due to the influence of SSD grains (Figure 4.27a).

4.5.9 Further assessment using factor analysis plots

To further clarify environmental inter-relationships, multivariate factor analysis was used. In each case, parameter and sample loadings extracted from Factors 1 and 2 were used to generate factor plots. Factor analysis was performed initially using all parameters. However, the resultant plot (not shown) did not appear to show any clear patterns. Factor analysis was re-applied to various parameter combinations until sample groupings and separations became apparent.

4.5.10 Factor analysis using selected key parameters

Simultaneous R- and Q-mode factor analysis was performed using selected mineral magnetic parameters. Factors 1 and 2 explain 30 and 9% respectively of the variation in all 13 original magnetic parameters. Parameter and sample loadings extracted from Factors 1 and 2 were used to generate a factor plot (Figure 4.28a).

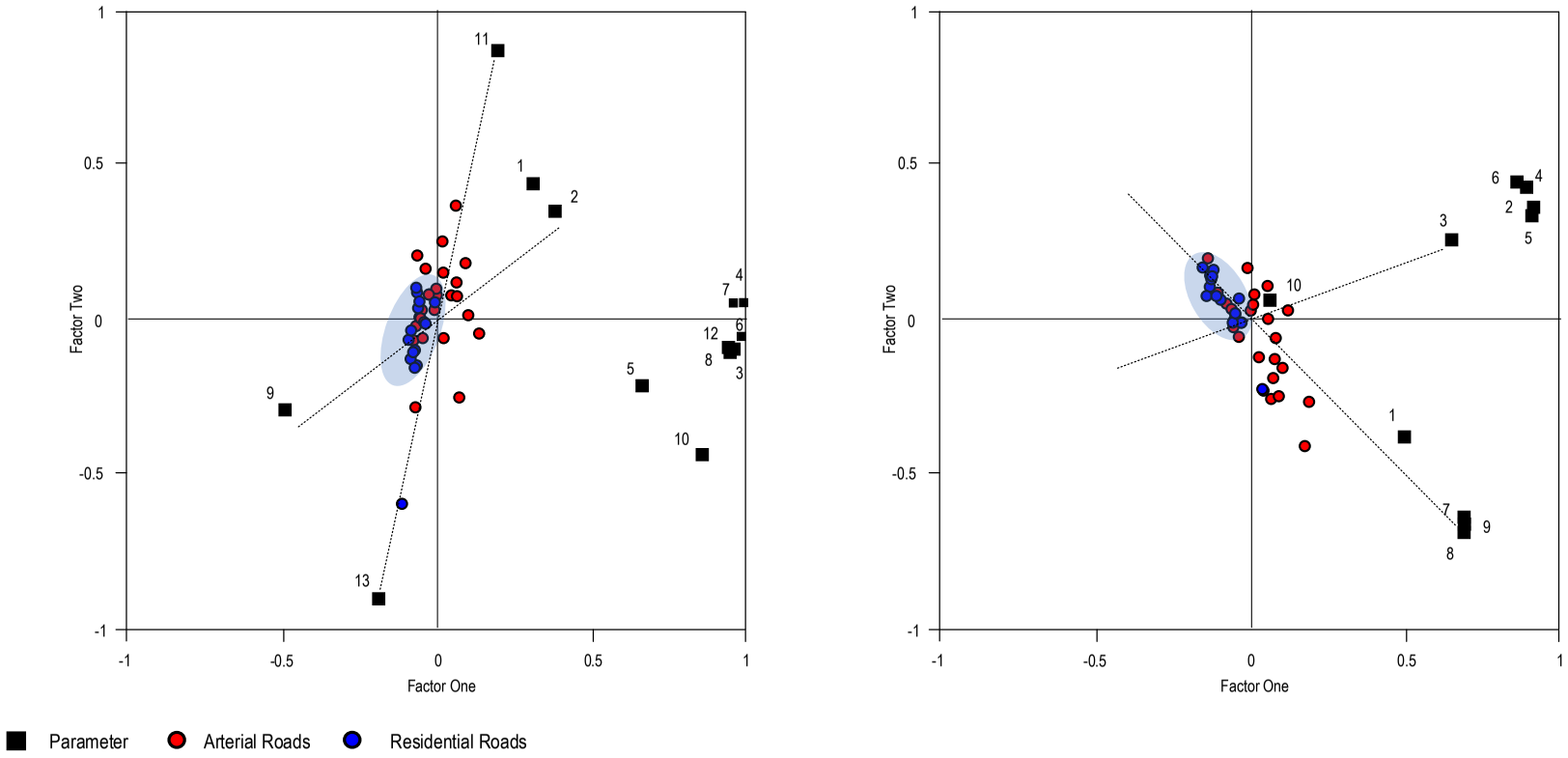

(a)	Parameters				
1	χ_{LF}	6	$Soft_{IRM40mT}$	11	χ_{ARM}/SIRM
2	$\chi_{FD\%}$	7	$Hard_{IRM20mT}$	12	SIRM/ARM
3	χ_{ARM}	8	$Hard_{IRM40mT}$	13	SIRM/χ
4	SIRM	9	S-ratio		
5	$Soft_{IRM20mT}$	10	ARM/χ		

(b)	Parameters		
1	χ_{LF}	6	$Hard_{IRM40mT}$
2	SIRM	7	$PM_{1.0}$
3	$Soft_{IRM20mT}$	8	$PM_{2.5}$
4	$Soft_{IRM40mT}$	9	PM_{10}
5	$Hard_{IRM20mT}$	10	PM_{100}

Figure 4.28 Simultaneous R- and Q mode factor analysis plots of Factor 1 versus Factor 2, based on magnetic parameters (a) and selected key parameters (b) for Wolverhampton May 2008RDS.

The χ_{LF}, $\chi_{FD\%}$, SIRM and χ_{ARM}/SIRM parameters have positive loadings on Factor 1. The S-ratio and SIRM/χ parameters have negative loadings on Factor 2. These relationships suggest that a combination of Factors 1 and 2 are influenced by a magnetic concentration gradient (top right to bottom left, Figure 4.28a) and magnetic mineralogy gradient (top right to bottom left, Figure 4.28a).

Sample loadings suggest samples are influenced by Factors 1 and 2. Distributions of samples indicates similar magnetic properties between samples. Sample groupings are identified by indication of road types and geographical location (Figure 4.28a). Arterial road samples show some overlap with residential road samples, with samples grouped predominantly and influenced negatively within Factor 2. Residential road samples suggest an influence from magnetic mineralogy and concentration parameters. Arterial road samples are positively influenced within Factor 1 by concentration (χ_{LF}, $\chi_{FD\%}$) and mineralogy (χ_{ARM}/SIRM)gradients.

4.5.11 Road factor plots of selected key mineral magnetic and textural parameters

Simultaneous R- and Q-mode factor analysis was performed by reducing the parameters further and using selected mineral magnetic and textural parameters. Factors 1 and 2 explain 21 and 9%, respectively of the variation in all 10 original magnetic and textural parameters. Parameter and sample loadings extracted from Factors 1 and 2 were used to generate a factor plot (Figure 4.28b).

The χ_{LF}, and SIRM parameters and textural properties have positive loadings on Factor 1. These relationships suggest that Factor 1 influences the magnetic concentration and textural gradient (top right to bottom right, Figure 4.28b). From the spread of sample loadings, the samples are influenced mainly by Factor 1. The distribution of sample points indicates similarities of magnetic properties between samples. Sample groupings are identified by road types and geographical location (Figure 4.28b). The main arterial road samples (highlighted in red) do overlap with residential road samples, but do show a cluster (highlighted in blue) of samples.

4.5.12 Further investigation using SEM

Figure 4.29a shows a spherical Fe oxide particle observed in the arterial road samples and is likely to have been derived from high temperature combustion. Note the orange peel texture which is typical of combustion particles. Residential road samples contain almost identical Fe oxide particles and size ranges (<60 µm). Figure 4.29b shows a typical spherical Fe oxide particle with a non-uniform surface texture. Particle counts have shown that samples taken from arterial roads are more likely to have higher counts of these glassy iron spherules (Figure 4.30 (For help interpreting figure 4.30 please refer to appendix 3.6.3)). In some sample locations, arterial sample particle counts are two to three times that of residential roads. The types and frequency of particles suggest that they derive from traffic and industrial combustion processes. Figure 4.30 shows a higher contribution of particles <20 µm on arterial roads compared to residential roads, which suggests that the higher traffic numbers could be responsible for higher particle counts.

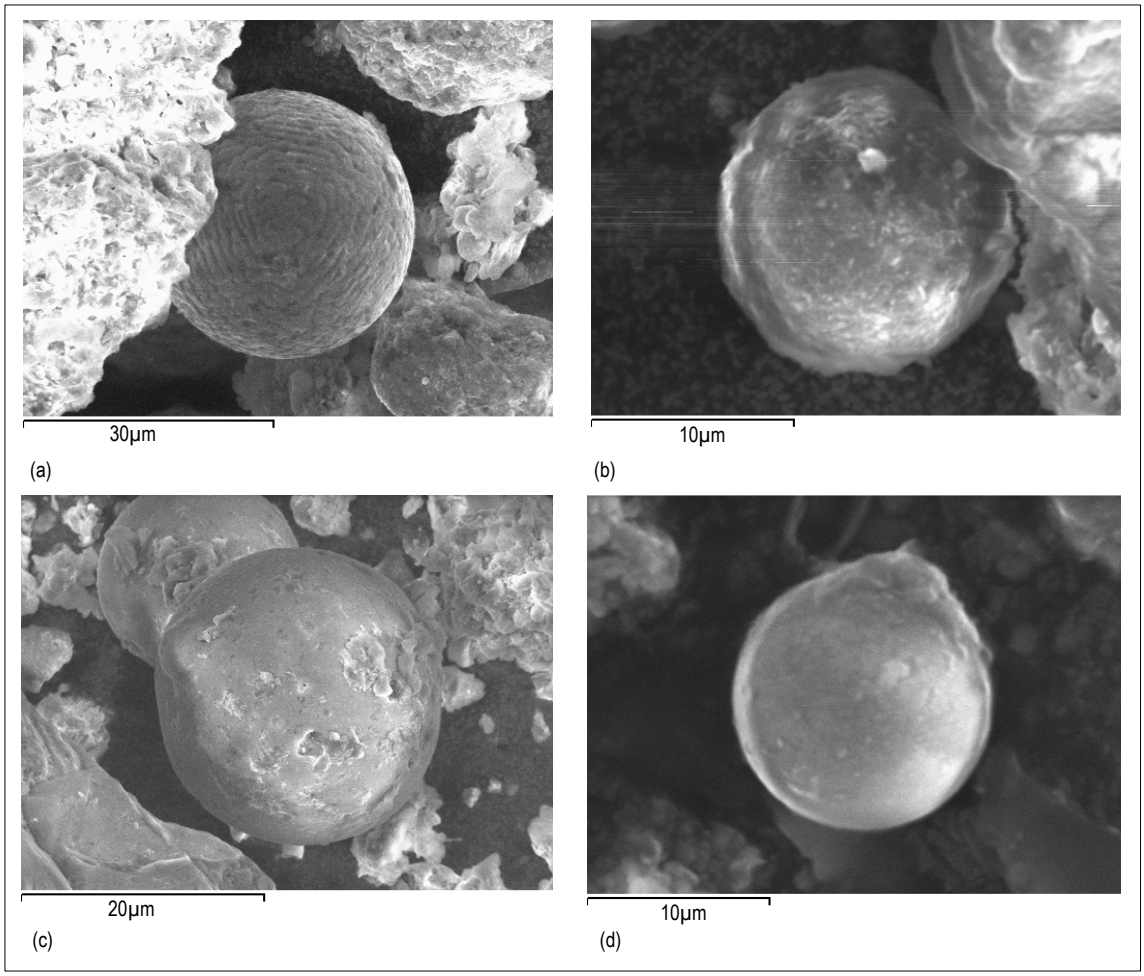

Figure 4.29 SEM micrographs of Wolverhampton RDS. Typical spherical particles found within RDS (Fe oxide glassy spheres a-d).

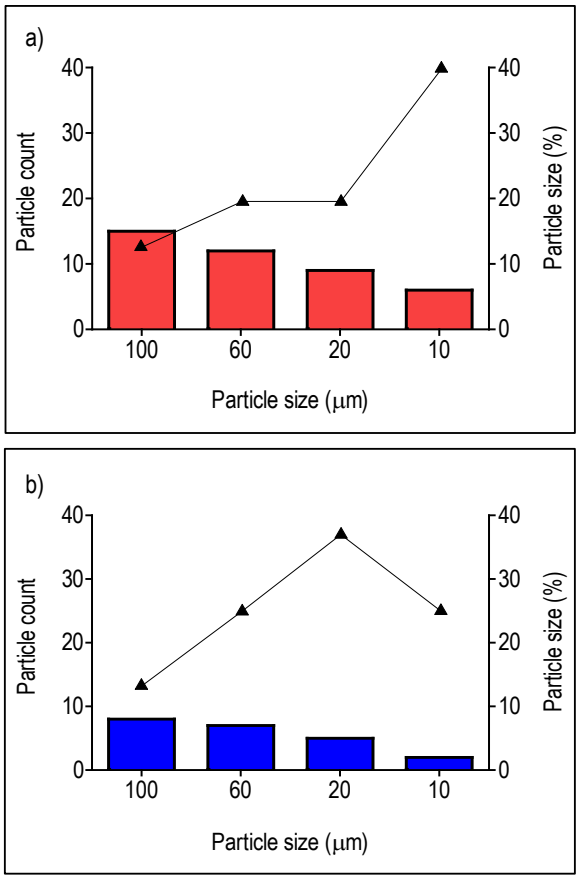

Figure 4.30 SEM particle counts and particle size (%) for (a) arterial roads and (b) residential roads.

This assertion is supported by the mineral magnetic data which shows elevated concentrations at high volume traffic areas, and is characterized as multi-domain ferrimagnetic mineralogy. Figure 4.29c shows a double sphere within the <20 μm size range. Figure 4.29d shows a typical smooth small (<10 μm) Fe oxide particle most likely derived from vehicle combustion. Differences in surface texture are evident from the variation of particles found here and later on in this work. Surface texture can be attributed to conditions when the particles are formed, so no particle is ever the same. Combustion temperature, pressure, cooling and solidification rates all influence the appearance of the Fe oxide particles (Kim *et al*., 2007). Conditions in each combustion process is never identical (petrol, diesel, compression ratios, engine size, age of engine and time run are some of the many variables), hence differing appearances of particles.

4.5.13 Mineral magnetic and particle size relationships of arterial and residential roads

To investigate the potential for particle size determination by mineral magnetic measurements, Spearman rank correlation tests were applied to arterial and residential road data sets. Results (Table 4.16) show that the mixed road samples display strong relationships through the particle size range, whereas when road types are split into two groups there is a significant loss in the relationship (χ_{LF} , χ_{ARM} and SIRM versus clay and $PM_{2.5}$) across both road types.

Table 4.16 Summary mineral magnetic concentration (χ_{LF}, χ_{ARM} and SIRM and textural (<PM_{10})) parameter Spearman rank correlation relationships for Wolverhampton road types (Mixed, n = 42; Arterial, n = 27; Residential, n = 15) during May 2008 (**bold** text is significant (*p <0.05; **p <0.01; ***p <0.001))

(a) χ_{LF}	Clay	$PM_{1.0}$	$PM_{2.5}$	PM_{10}
Mixed	0.443**	0.341**	0.457**	0.560**
Arterial	0.350	0.573**	0.363	0.490**
Residential	0.418	0.907***	0.379	0.363

(b) χ_{ARM}	Clay	$PM_{1.0}$	$PM_{2.5}$	PM_{10}
Mixed	0.334*	0.707**	0.318*	0.354**
Arterial	0.286	0.887***	0.290	0.234
Residential	0.055	0.764**	0.049	0.165

(c) SIRM	Clay	$PM_{1.0}$	$PM_{2.5}$	PM_{10}
Mixed	0.372**	0.627**	0.364**	0.374**
Arterial	0.262	0.864***	0.269	0.238
Residential	0.313	0.852***	0.269	0.225

Arterial road relationships remain consistent with $PM_{1.0}$ through all mineral magnetic parameters, with some strengthening associated with χ_{ARM} (a) and SIRM (b). This is further supported by Figure 4.28b, in which arterial roads appear to be influenced by mineral magnetic and fine-fraction particles. This suggests that $PM_{1.0}$ and mineral magnetic concentration parameters have strong influences on arterial roads. Residential road relationships decrease through the coarser particle size range, but have strong relationships with the finer fraction ($PM_{1.0}$) of RDS.

4.5.14 Cumulative, season and individual month summary of Wolverhampton RDS

The characteristics of Wolverhampton RDS show a wide range of variation over time with significant variation between the sample months. The characteristics and relationships for Wolverhampton RDS can be summarized as:

- Magnetic properties of RDS in Wolverhampton are predominantly ferromagnetic.
- Mineral magnetic grain size remains consistently multi-domain within the study area.
- Mineral magnetic concentration parameters vary over time but also display significant relationships for similar time periods (May-May; March-March).
- Seasonal weather patterns appear to influence the mineral magnetic concentrations and mineral magnetic-particle size proxy potential during warm-dry periods.
- Road types display clear differences in concentrations, but remain multi-domain in nature.
- Road traffic conditions and land use appears to be an additional influencing factor of mineral magnetic concentrations.
- No proxy potential is found during the time at the city-wide scale for Wolverhampton.

4.6 Investigation of Wolverhampton sample sites

Individual samples sites have been investigated to assess the mineral magnetic–particle size proxy potential over time at small scale specific sites. All 42 Wolverhampton sample sites have been investigated using methods previously discussed over 24 months. Results have shown limited potential for particle size proxy purposes. The site with the greatest potential is further discussed (site 15).

4.6.1 Detailed investigation of Wolverhampton sites (site 15)

Sample point 15 is located in south Wolverhampton (SO389297). The area is within a small residential cul-de-sac surrounded by 1920s semi-detached and detached housing and forms part of the Bradmore area. There are no thoroughfares through to main roads and, as a result, the road only experiences local traffic. The main road is ~140 m north-west of the sample point. The road network is an enclosed system with no evidence of considerable input of material from outside areas. There is no significant history to the area other than residential housing (1880–present) and was previously agricultural land. Figure 4.31 shows the site profile. Site 15 displayed significantly lower concentrations of magnetic material within the study period and was thus chosen to investigate differences in sample point characteristics. Figure 4.31 shows the GIS profile graph for the study period for location 1. There are relatively consistent concentrations of χ_{LF}. Table 4.17 presents the summary data for the physical characteristics of Wolverhampton site 1 RDS samples (n = 13). The magnetic concentration parameters are high compared to urban topsoils, with relatively high values of magnetically soft minerals (Soft $_{IRM20mT,}$ 158.303 x $10^{-4}Am^2kg^{-1}$; Soft $_{IRM40mT,}$ 366.021 x $10^{-4}Am^2kg^{-1}$). Figure 4.31 shows site variations of χ_{LF} over the sampling period.

4.6.2 Wolverhampton site mineral magnetic data

Mineral magnetic data for the Wolverhampton Site (WLV 15) samples is summarized in Table 4.17a. Magnetic concentration-dependent parameters indicate RDS contain low to moderate concentrations of magnetic minerals and a predictable signature compared to other sampling points in Wolverhampton (mean values χ_{LF} 9.493 x $10^{-7}m^3kg^{-1}$; χ_{ARM} 0.031 x $10^{-7}m^3kg^{-1}$; SIRM 117.664 x $10^{-4}Am^2kg^{-1}$). Compared to published values for other environmental materials (Dearing, 1999), they indicate that the magnetic properties of the sediments are similar to intermediate igneous rocks, basic/ultra-basic rocks and ferromagnetic minerals. SIRM values indicate some variation over time (57.575-261.061 x $10^{-4}Am^2kg^{-1}$; SD 48.955). ARM/χ values range from high to low (0.184-2.544 x $10^{-1}Am^{-1}$), indicating a predominately coarse grained magnetic material (mean 0.725 x $10^{-1}Am^{-1}$). SIRM/ARM values range from 132.291-443.387 (mean 254.443; SD 96.156) and are high compared to other environmental materials (Yu and Oldfield, 1993). This supports the ARM/χ values, indicating a coarse magnetic grain size. SIRM/χ values are also high (mean 12.859 x $10^{-1}Am^{-1}$, 5.178-16.813 x $10^{-1}Am^{-1}$). The high SIRM/χ values suggest the presence of fine-grained magnetic material.

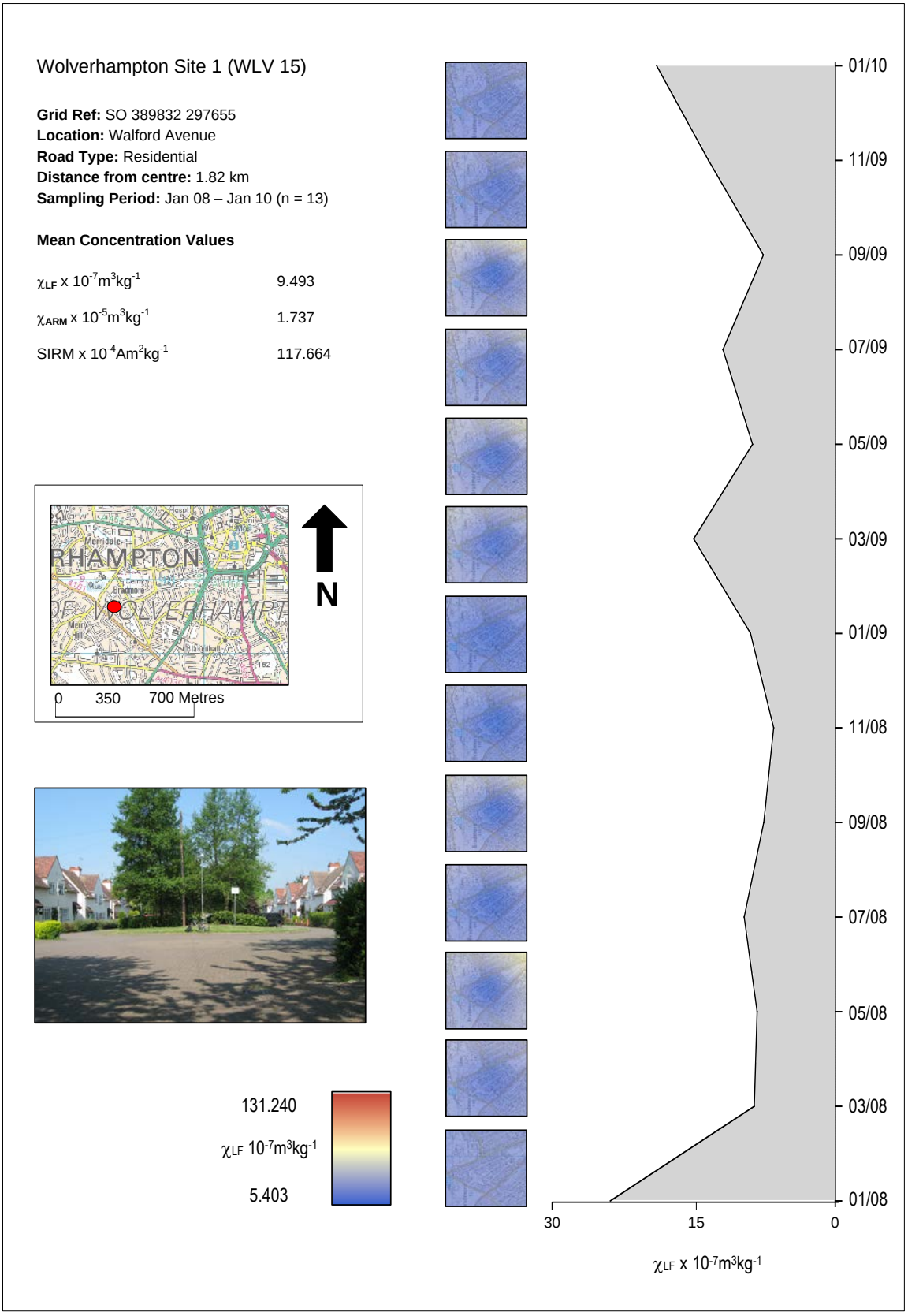

Figure 4.31 Wolverhampton site 1 time-series profile showing mean χ_{LF} concentrations over the sampling period, map and photograph of sampling location.

Table 4.17 Summary RDS analytical data* for Wolverhampton (WLV 15) (n = 13)

	Parameters	Units	Mean	Median	SD	CV (%)	Min	Max	Range
(a)	χ_{LF}	$10^{-7}m^3kg^{-1}$	9.493	7.440	4.239	44.652	5.403	19.730	14.327
	χ_{FD}	%	1.737	1.758	0.561	32.308	0.858	2.881	2.023
	χ_{ARM}	$10^{-5}m^3kg^{-1}$	0.031	0.028	0.010	31.234	0.019	0.052	0.033
	SIRM	$10^{-4}Am^2kg^{-1}$	117.664	105.428	48.955	41.606	57.575	261.061	203.486
	S-Ratio	Dimensionless	-0.742	-0.741	0.044	-0.059	-0.809	-0.673	0.136
	$SOFT\%_{20mT}$	%	16.350	15.705	3.071	18.783	12.970	23.337	10.409
	$SOFT\%_{40mT}$	%	41.193	41.676	2.886	7.005	34.115	44.524	9.844
	$HARD\%_{300mT}$	%	8.907	8.977	3.076	34.530	4.512	14.356	10.522
	$HARD\%_{500mT}$	%	3.941	3.182	3.008	76.342	0.072	10.594	38.152
	$SOFT_{IRM20mT}$	$10^{-4}Am^2kg^{-1}$	19.668	16.370	10.080	51.251	8.166	46.318	86.371
	$SOFT_{IRM40mT}$	$10^{-4}Am^2kg^{-1}$	48.516	42.343	21.387	44.082	25.635	112.006	13.692
	$HARD_{IRM300mT}$	$10^{-4}Am^2kg^{-1}$	10.086	8.409	4.238	42.021	4.428	18.120	13.272
	$HARD_{IRM500mT}$	$10^{-4}Am^2kg^{-1}$	4.297	3.618	3.499	81.431	0.099	13.371	0.136
	ARM/χ	$10^{-1}Am^{-1}$	0.511	0.356	0.618	1.209	0.184	2.544	2.360
	χ_{ARM}/SIRM	$10^{-3}Am^2kg^{-1}$	1.849	0.261	5.689	3.077	0.131	20.780	20.649
	SIRM/ARM	Dimensionless	120.673	120.403	29.324	24.300	71.641	156.463	84.822
	SIRM/χ	$10^{-1}Am^{-1}$	12.859	13.518	3.255	25.310	5.178	16.813	11.635
(b)	Mean - PS	μm	325.809	305.831	65.096	19.980	250.941	419.250	168.309
	Median - PS	μm	364.297	329.336	53.375	14.652	316.716	441.820	125.104
	Sorting	σ_1	2.115	2.134	0.171	8.110	1.851	2.309	0.458
	Skewness	SK_1	0.547	0.557	0.073	13.332	0.406	0.632	0.226
	Kurtosis	K_G	1.376	1.307	0.348	25.312	0.903	1.864	0.961
	Sand	%	78.721	79.679	3.778	4.799	72.539	83.508	10.969
	Silt	%	19.220	18.644	3.848	20.020	14.362	25.492	11.130
	Clay	%	2.059	2.056	0.239	11.611	1.381	2.332	0.951
	$PM_{1.0}$	%	1.158	1.157	0.183	15.785	0.617	1.381	0.764
	$PM_{2.5}$	%	2.448	2.419	0.281	11.461	1.627	2.764	1.137
	PM_{10}	%	7.014	7.399	1.209	17.232	3.939	8.522	4.583
	PM_{100}	%	23.825	24.562	3.886	16.310	18.560	29.735	11.175

*SD = Standard Deviation; CV = Percentage coefficient of variation; Min = Minimum value; Max = maximum value.

4.6.3 Wolverhampton site textural data

Textural data for the Wolverhampton Site (15) samples is summarized in Table 4.17b. Particle size parameters indicate that RDS contains moderately sorted sediment (2.115 σ_1; mean 325.809 µm), with high concentrations of sand (78.721%), moderate concentrations of silt (19.220%) and low concentrations of clay (2.059%). The RDS particle size data also suggest a moderate amount of sediment beneath the PM_{100} boundary (23.825%) with lesser PM_{10} concentrations (7.014%) and low concentrations of $PM_{2.5}$ (2.448%) and $PM_{1.0}$ (1.158%). LOI values are low (mean 1.084%; range 0.816-1.547; SD 0.123).

4.6.4 Relationships between the mineral magnetic and textural parameters

Table 4.18 summarizes correlation statistics between mineral magnetic and textural parameters for Wolverhampton sample site 15. Most all mineral magnetic and textural parameters are weakly correlated (i.e. most correlation coefficients are *ca*. r = -0.050–0.333), with the exception of mineral magnetic concentration parameters (χ_{LF}, χ_{ARM} and SIRM) and fine textural properties (<10µm) which are statistically significant (r = -0.581-0.911 *p* <0.05-<0.001). This suggests that mineral magnetic concentration parameters and fine texture of RDS does have some potential for proxy purposes.

Overall, statistical tests indicate a weak significant relationship between mineral magnetic and textural parameters (*p* <0.05). However, only strong correlation coefficients have been selected for further study through bivariate plot analysis. Figures 4.32a-d show the spread of the sample points for each set of bivariate data and show magnetic concentration dependent parameters versus selected textural parameters. Figure 4.32a shows a moderate negative correlation between χ_{LF} versus $PM_{1.0}$ (r = -0.656; *p* <0.05, n = 13) with a strong correlation between SIRM versus $PM_{1.0}$ (r = -0.894; *p* <0.01, n = 13 (Figure 4.32b)). Figure 4.32c shows the moderate negative correlation between SIRM and $PM_{2.0}$ (r = -0.582; *p* <0.01, n = 13) with also a strong correlation between SIRM versus PM_{10} (r = -0.715; *p* <0.01, n = 13 (Figure 4.33d)). χ_{LF} and SIRM have strong negative correlations with the finer fractions of RDS ($PM_{2.5}$–$PM_{1.0}$) (χ_{LF} and SIRM shown in bivariate graphs (Figure 4.32a-d)). The plots show a distinct strong correlation (r = ≤-0.894; *p* <0.01) existing between these parameters (Table 4.18). The patterns are consistent with all other concentration parameters (χ_{ARM} and SIRM), with any increase in magnetic concentration values being associated with a corresponding decrease in $PM_{1.0,}$ $PM_{2.5}$ and $PM_{10.}$ Mineral magnetic concentrations show strong relationships with the finer fraction of PM and indicate that SIRM could potentially be used as a size proxy for $PM_{1.0}$.

4.6.5 Site specific potential for particle size proxy purposes

Few sites have shown potential for particle size proxy purposes. The sites that do have potential are relatively isolated in terms of location and influencing factors. Mineral magnetic concentrations are unique to each site and reflect local environmental and anthropogenic conditions. The concentrations show a consistent pattern through the time period of observation, with highs and lows corresponding to time of year (Figure 4.31). The site results showing variation in proxy potential illustrate the need for further study to establish reliability.

Table 4.18 Correlation coefficients between mineral magnetic and textural parameters for Wolverhampton site 15 (**bold** text is significant (*p <0.05; **p <0.01; ***p <0.001)) (n =13)

Parameters	Median-PS	Mean-PS	Sand	Silt	Clay	$PM_{1.0}$	$PM_{2.5}$	PM_{10}	PM_{100}
χ_{LF}	0.177	0.266	0.083	0.000	-0.449	-0.656**	-0.751**	-0.675**	-0.083
$\chi_{FD\%}$	0.155	0.454	-0.017	-0.011	0.371	0.174	0.582*	0.404	0.017
χ_{ARM}	-0.031	0.058	-0.461	0.669**	-0.911***	-0.675**	-0.650**	-0.581*	0.461
SIRM	-0.100	0.116	-0.011	0.127	-0.582*	-0.894***	-0.715**	-0.656**	0.011
Soft $\%_{20mT}$	-0.030	0.219	0.280	-0.008	-0.235	-0.515	-0.424	-0.335	-0.280
Soft $\%_{40mT}$	0.490	0.335	0.163	-0.125	-0.058	0.116	0.042	0.186	-0.163
Hard $\%_{300mT}$	0.147	0.186	0.324	-0.562*	0.629**	0.166	0.363	0.175	-0.324
Hard $\%_{500mT}$	0.518	0.368	0.108	-0.280	0.269	0.149	0.269	0.457	-0.108
Soft $_{IRM20mt}$	-0.166	0.094	0.105	0.078	-0.527	-0.884***	-0.727**	-0.283	-0.105
Soft $_{IRM40mT}$	-0.255	-0.094	-0.083	0.133	-0.527	-0.751**	-0.638**	-0.172	0.083
Hard $_{IRM300mT}$	-0.191	0.069	0.169	-0.269	0.008	-0.556*	-0.235	-0.058	-0.169
Hard $_{IRM500mT}$	0.344	0.316	0.194	-0.310	0.017	-0.268	-0.094	0.238	-0.194
S-ratio	0.017	0.133	-0.230	0.133	-0.036	-0.143	0.158	0.336	0.230
ARM/χ	-0.370	-0.591*	-0.092	0.016	-0.061	0.045	-0.225	-0.344	0.092
SIRM/ARM	-0.482	-0.244	0.360	-0.416	0.094	-0.382	-0.249	-0.493	-0.360
SIRM/χ	-0.069	-0.091	-0.053	0.042	-0.125	-0.119	-0.224	-0.047	0.053
χ_{ARM} /SIRM	-0.039	-0.039	0.428	-0.428	0.117	-0.350	-0.350	-0.350	-0.428

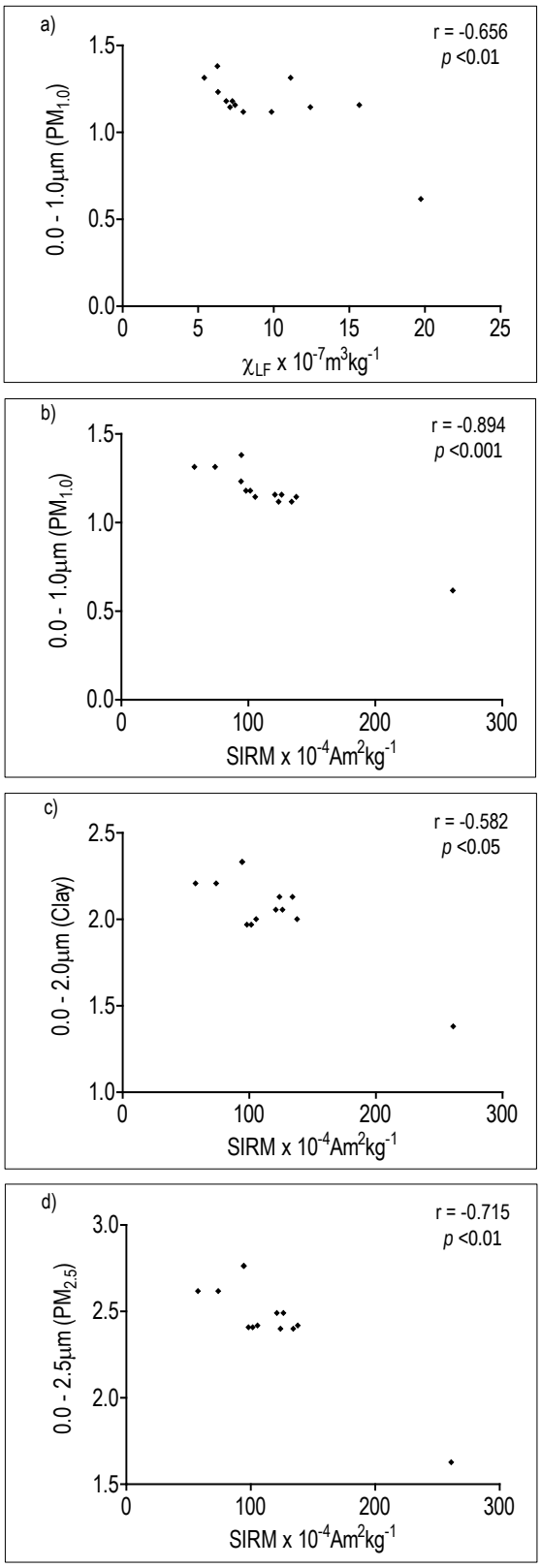

Figure 4.32 Bivariate plots of selected mineral magnetic and textural parameters for Wolverhampton site 15 (n = 13).

4.7 Site specific West Midlands (UK) Monitoring station sites (Regional analysis)

Air sampling monitoring sites (Air Sampling Unit: ASU) have been investigated. Four sites (summary results presented) were sampled, but only one is presented. This shows potential firstly for mineral magnetic and textural relationships and secondly for mineral magnetic and recorded PM data linkages at site and regional scales. The sites investigated were monitored over 24 months. The method for sampling air sampling monitoring stations is discussed in Chapter 3.1.6, with an overview of the air sampling monitoring station capabilities in Table 3.3.

4.7.1 Description of the Wolverhampton ASU site (a)

Wolverhampton ASU is located north of Wolverhampton City centre (Grid ref SO 391 261 302206). The area is open, within a mix of residential and commercial properties and forms part of the Oxley area. To the immediate west of the monitoring station (~5 m) is a busy main road (A449: Stafford Road (dual carriageway) which experiences ~30,000 vehicles per day. The main carriageway serves Wolverhampton to the south (~3 km) and the main motorway network to the north (M54–M6), which links the north, west and south of England. The ASU (Figure 3.5a) is housed within a self-contained, air conditioned cabin on the west corner of a junction situated on the main road. The height of the particle inlet is ~3.5 m above ground level and is the input for ambient PM levels.

4.7.2 Description of the Birmingham ASU site (b)

Birmingham ASU is located to the north west of Birmingham City centre near the A456 (Broad Street). The monitoring station (Figure 3.7b) is within a self-contained, air conditioned housing located within a pedestrianized area of the City centre. The nearest road is ~10 metres (Cambridge Street) away and is used for access to the adjacent car park. The nearest heavily trafficked urban road (A456) is ~60 metres from the ASU. The particle inlet is 3.5 metres above ground level. The surrounding area is generally open and comprises the International Convention Centre (ICC), Symphony Hall and the Birmingham Reparatory Theatre. Trees and vegetation occur within 2 metres of the monitoring station.

4.7.3 Description of the Coventry ASU site (c)

Coventry ASU is located within Memorial Park which is 1.6km south of Coventry City centre. Memorial Park is predominantly open parkland with large trees, shrubs and vegetation and surround the park. The ASU site is situated within an aviary building (Figure 3.7c). The height of the particle inlet is ~3.5 m above ground level and is the input for ambient PM levels. The site is close to two major roads, Kenilworth Road (150m) with a traffic flow of 22058 vehicles per 24 hours and Leamington Road (250m) with a mean traffic flow of 12,990 vehicles per 24 hours (wmair.org, 2012).

4.7.4 Description of the Leamington Spa ASU site (d)

Leamington Spa ASU is located within a self-contained, air conditioned housing located at the rear of a three-storey regency terrace near the town centre (Figure 3.7d). The nearest road is used for access to nearby office and public buildings car park. The nearest urban road is ~50 m

from the station and is generally free flowing. There are no trees within 50 m from the monitoring station. The surrounding area is generally built up, with commercial and residential properties. At the time of sampling, construction and demolition activities were taking place ~80 m from the ASU, which have affected recorded PM data.

4.7.5 Detailed investigation of West Midlands (ASU) sites (a-d)

Selected West Midlands ASU sites have been investigated to reveal a spatial perspective of RDS characteristics and mineral magnetic–particle size proxy potential within the region. Results for the West Midlands (ASU) sites (Wolverhampton (a), Birmingham (b), Coventry (c) and Leamington Spa (d)) (Figure 3.7) are presented. Table 4.19 and Figures 4.33–4.34 presents summary data for the physical characteristics of West Midlands (ASU) sites. The magnetic concentration parameters are high compared to urban topsoils, with relatively high values of magnetically soft minerals (Soft $_{IRM20mT,}$ Table 4.19 (a) 114.243; (b)156.773; (c) 211.025; (d) 243.297 x $10^{-4}Am^2kg^{-1}$ and Soft $_{IRM40mT.}$ Table 4.19 (a) 332.087; (b) 469.091; (c) 501.493; (d) 529.931 x $10^{-4}Am^2kg^{-1}$).

4.7.6 West Midlands (ASU) site mineral magnetic data

Mineral magnetic data for the West Midlands site is summarized in Table 4.19a. Magnetic concentration-dependent parameters indicate RDS contain a high concentration of magnetic minerals (mean values χ_{LF} 25.790 x $10^{-7}m^3kg^{-1}$; χ_{ARM} 0.139 x $10^{-7}m^3kg^{-1}$; SIRM 246.300 x $10^{-4}Am^2kg^{-1}$). Mineral magnetic values show large differences over the sample area (Figure 4.33), with Wolverhampton samples showing greatest concentrations (χ_{LF} 41.880 x $10^{-7}m^3kg^{-1}$) compared to other sites (mean over b, c and d, χ_{LF} 16.72 x $10^{-7}m^3kg^{-1}$(Figure 4.33 a)). Site a displays high concentrations when results are compared to values for other environmental materials (Dearing, 1999), site b, c and d display moderate concentrations. The samples indicate that magnetic properties are similar to intermediate igneous rocks, basic/ultra-basic rocks and ferromagnetic minerals. SIRM values indicate some variation with sites (Figure 4.33b (117.212–481.678 x $10^{-4}Am^2kg^{-1}$). The S ratio values remain fairly consistent (Figure 4.33c (-0.706-0.797)) indicating a predominately magnetically soft material. SIRM/ARM values range from 152.527-292.411 (mean 201.525) and are high compared to other environmental materials (Yu and Oldfield, 1993). This supports the ARM/χ values, indicating a coarse magnetic grain size. SIRM/χ values are also high (mean 46.764 x $10^{-1}Am^{-1}$, range 15.596-69.568 x $10^{-1}Am^{-1}$; SD 2.833). The high SIRM/χ suggests the presence of fine-grained magnetic material.

West Midland sites display inter-site variation, with Wolverhampton displaying higher mineral magnetic concentrations than Birmingham, Coventry and Leamington Spa. Wolverhampton also displays typical multi-domain coarse grained characteristics derived from anthropogenic sources with low $\chi_{FD\%}$ and SIRM/χ values. In comparison Birmingham, Coventry and Leamington Spa display similar $\chi_{FD\%}$ but relatively higher SIRM/χ values, indicating the presence of fine grained magnetic material, which is usually derived from naturally occurring magnetic sources. When comparing site locations the proximity to roads and surrounding environments suggest influences to mineral magnetic concentrations.

Table 4.19 Summary mean RDS analytical data for West Midlands (ASU) RDS (n = 208)

	Parameters	Units	Wolverhampton (a)	Birmingham (b)	Coventry (c)	Leamington Spa (d)
(a)	χ_{LF}	$10^{-7}m^3kg^{-1}$	41.880	11.376	16.193	22.592
	$\chi_{FD\%}$	%	1.150	1.924	1.630	1.127
	χ_{ARM}	$10^{-5}m^3kg^{-1}$	0.162	0.086	0.148	0.160
	SIRM	$10^{-4}Am^2kg^{-1}$	481.678	210.324	117.212	176.100
	S ratio	Dimensionless	-0.791	-0.746	-0.797	-0.763
	SOFT $_{IRM20mT}$	$10^{-4}Am^2kg^{-1}$	243.297	156.773	211.025	114.234
	SOFT $_{IRM40mT}$	$10^{-4}Am^2kg^{-1}$	529.931	469.091	501.453	332.087
	HARD $_{IRM20mT}$	$10^{-4}Am^2kg^{-1}$	86.190	57.832	36.844	93.639
	HARD $_{IRM40mT}$	$10^{-4}Am^2kg^{-1}$	45.439	35.552	17.811	33.590
	ARM/χ	$10^{-1}Am^{-1}$	0.165	0.103	0.995	0.685
	χ_{ARM}/SIRM	$10^{-3}Am^2kg^{-1}$	1.648	0.530	1.250	2.115
	SIRM/ARM	Dimensionless	292.411	157.233	152.527	203.932
	SIRM/χ	$10^{-1}Am^{-1}$	15.596	69.568	49.682	52.212
(b)	Mean - PS	μm	168.313	290.147	265.478	253.674
	Sand	%	72.332	72.620	77.243	71.264
	Silt	%	26.085	24.454	18.846	24.169
	Clay	%	1.583	2.926	3.911	4.567
	$PM_{1.0}$	%	1.181	1.832	2.097	1.965
	$PM_{2.5}$	%	2.301	3.292	3.981	3.778
	PM_{10}	%	7.027	7.471	12.137	5.278
	PM_{100}	%	36.598	19.014	25.193	17.546
(c)	PM_{10} Mean 2	μg m^3	16.340	22.310	22.465	24.101
	1 month	μg m^3	16.080	13.560	14.564	22.193
	1 Week	μg m^3	16.358	20.280	20.631	19.197
	3 Day	μg m^3	16.940	26.341	25.697	25.231
	2 Day	μg m^3	16.620	26.075	23.409	22.224
	1 Day	μg m^3	16.011	22.341	22.345	22.0833
	Hour	μg m^3	16.270	19.854	20.114	21.078
	PM_{10} Median 2	μg m^3	15.166	13.542	15.921	22.116
	1 month	μg m^3	15.002	11.212	12.001	21.017
	1 Week	μg m^3	15.189	18.257	20.675	17.952
	3 Day	μg m^3	15.582	23.333	25.991	25.542
	2 Day	μg m^3	15.600	22.752	23.552	23.693
	1 Day	μg m^3	15.641	21.850	21.597	23.639
	Hour	μg m^3	16.320	15.647	23.112	15.991

*SD = Standard Deviation; CV = Percentage coefficient of variation; Min = Minimum value; Max = maximum value.PM_{10} Mean/Median 2 = 2 month

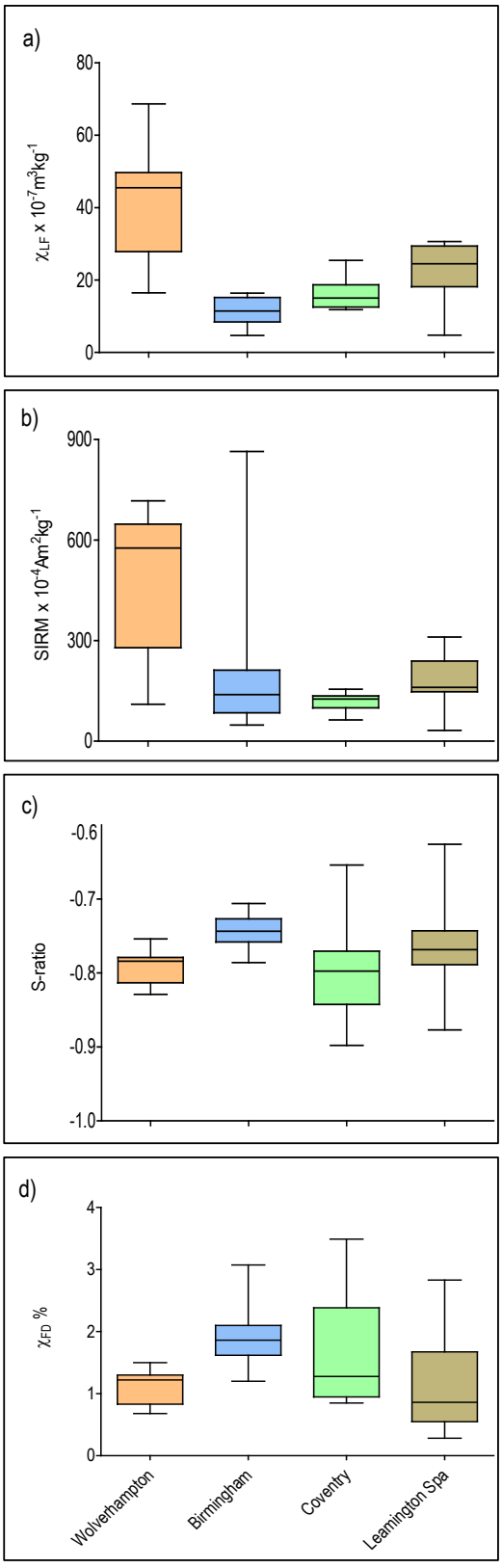

Figure 4.33 Box plots of West Midlands ASU-RDS for selected mineral magnetic parameters.

4.7.7 West Midlands (ASU) site textural data

Textural data for the West Midlands site samples is presented in Figure 4.34 and Table 4.19b. Particle size parameters indicate RDS contains moderate sand concentrations (71.264-80.631%), moderate silt concentrations (17.538-26.085%), and low clay concentrations (1.583-4.567%). Particle size data for the RDS West Midlands (ASU) sites also suggests a high level of sediment within the PM_{100} boundary (17.546-36.598%), with mean values of PM_{10} concentrations of 7.970% and low mean concentrations of $PM_{2.5}$ (3.338%) and $PM_{1.0}$ (1.768%). All sites display consistent textural distributions, with the exception of the clay content in Leamington Spa, which is slightly higher than the mean (4.567%, clay mean 3.246%).

4.7.8 West Midlands PM_{10} (ASU) data

Air sampling monitoring PM_{10} data for Wolverhampton, Birmingham, Coventry and Leamington Spa is summarized in Table 4.19c. Data has been collected from the West Midlands Air Monitoring Group website (wmair.org), which records and publishes hourly PM_{10} data for air monitoring stations in the West Midlands. Mean, median, maximum and minimum values were recorded for the 2 months, 1 month, 3, 2 and 1 days and hour prior to sampling. Mean PM_{10} values for the sampling period were low (18.32 µg m^{-3}) (index 1) compared to the air pollution index (Tables 4.20 and 4.21) and remains consistent over the sampling period (SD 3.900). Some variation exists between the ASU sites, but do not deviate from the low levels as reported in Tables 4.20 and 4.21 (UK National Air Quality Archive, 2012). Table 4.22 shows recommendations when experiencing effects to corresponding pollution bands.

Table 4.20 Boundaries between index points for PM_{10} (Source: UK National Air Quality Archive, 2012)

Band	Index	PM_{10} µg m^{-3} Running 24 hr mean
Low	1	0-16
	2	17-33
	3	34-49
Moderate	4	50-58
	5	59-66
	6	67-74
High	7	75-83
	8	84-91
	9	92-99
Very High	10	>100

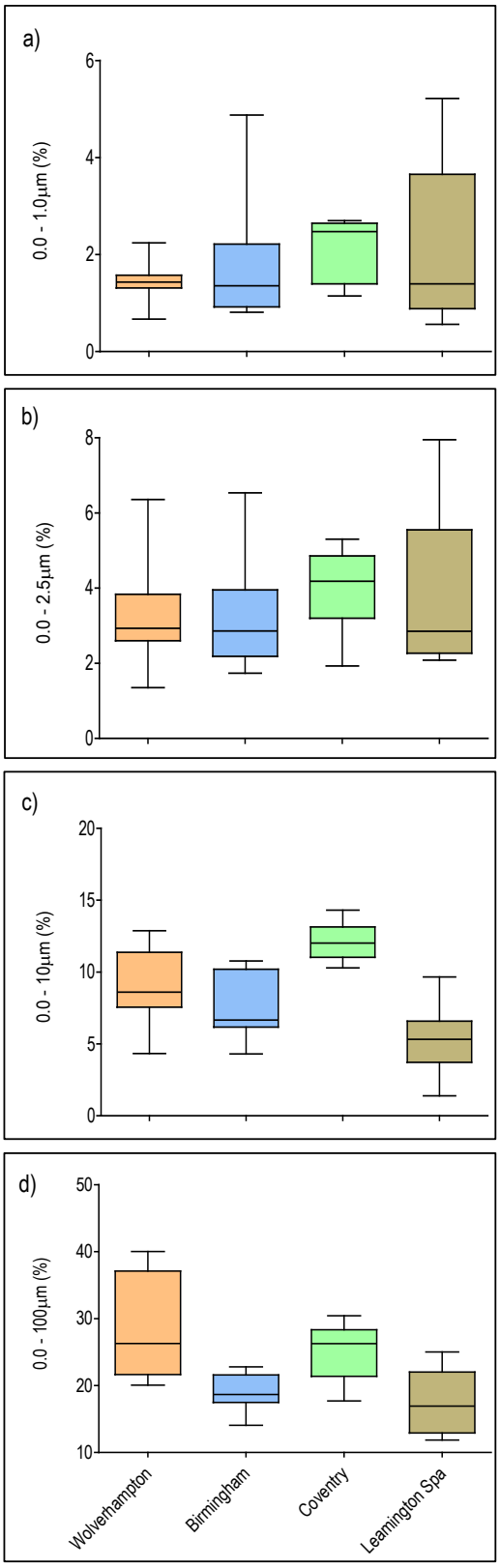

Figure 4.34 Box plots of West Midlands ASU–RDS for selected textural parameters.

Table 4.21 Air pollution bandings and index and the impact on the health of people sensitive to air pollution (Source: UK National Air Quality Archive, 2007)

Banding	Index	Health Descriptor
Low	1, 2, or 3	Effects are unlikely to be noticed, even by individuals who know they are sensitive to air pollutants.
Moderate	4, 5, or 6	Mild effects, unlikely to require action, may be noticed amongst sensitive individuals.
High	7, 8, or 9	Significant effects may be noticed by sensitive individuals and action to avoid or reduce these effects may be needed (e.g. reducing exposure by spending less time in polluted areas outdoors). Asthmatics will find that their 'reliever' inhaler is likely to reverse the effects on lungs.
Very High	10	The effects on sensitive individuals described for 'High' levels of pollution may worsen.

Table 4.22 Air pollution bandings and index guide recommendations for outdoor activities (Source: UK National Air Quality Archive, 2012).

		Health Message	
Banding	Index	At-risk – sensitive individuals*	General population
Low	1, 2, or 3	Enjoy your usual outdoor activities.	Enjoy your usual outdoor activities.
Moderate	4, 5, or 6	Adults and children with lung problems, and adults with heart problems, who experience symptoms, should consider reducing strenuous physical activity, particularly outdoors.	Enjoy your usual outdoor activities.
High	7, 8, or 9	Adults and children with lung problems, and adults with heart problems, should reduce strenuous physical exertion, particularly outdoors, and particularly if they experience symptoms. People with asthma may find they need to use their reliever inhaler more often. Older people should also reduce physical exertion.	Anyone experiencing discomfort such as sore eyes, cough or sore throat should consider reducing activity, particularly outdoors.
Very High	10	Adults and children with lung problems, adults with heart problems, and older people, should avoid strenuous physical activity. People with asthma may find they need to use their reliever inhaler more often.	Reduce physical exertion, particularly outdoors, especially if you experience symptoms such as cough or sore throat.

*Adults and children with heart or lung problems.

4.7.9 Relationships between the mineral magnetic and textural parameters

Table 4.23 summarizes correlation statistics between the mineral magnetic and textural parameters for the West Midlands samples. Almost all mineral magnetic concentration parameters and textural parameters show no significant associations (p <0.05) (Table 4.23). This suggests that the texture of RDS has no influence on mineral magnetic assemblages. The results support the indication that using mineral magnetic methods for proxy purposes are limited and constrained to specific sites.

Table 4.23 Statistical relationships between selected mineral magnetic and textural parameters for West Midlands air sampling units. (**bold** text is significant (*p <0.05; **p <0.01; ***p <0.001)) (n = 208)

χ_{LF}	$PM_{1.0}$	$PM_{2.5}$	PM_{10}	PM_{100}
Wolverhampton	0.364	0.318	0.260	0.108
Birmingham	0.264	0.289	0.247	0.205
Coventry	0.098	0.193	0.101	0.126
Leamington Spa	0.068	0.057	0.085	0.085
SIRM				
Wolverhampton	0.393	0.339	0.339	0.243
Birmingham	0.310	0.293	0.128	0.751
Coventry	0.117	0.293	0.098	0.651
Leamington Spa	0.301	0.235	0.226	0.198

4.7.10 West Midland relationships between the mineral magnetic and PM_{10} (ASU) data

The ASU data were compared with textural and mineral magnetic data. The relationships between the West Midlands ASU and mineral magnetic data (data not presented) was not significant (p <0.05) within all West Midland ASU sites. This suggests that ambient PM_{10} levels do not influence mineral magnetic concentrations. Table 4.24 shows results for mineral magnetic and ASU parameters for Wolverhampton. There are no significant parameter pairings. Results for ASU and mineral magnetic data suggest that such analysis is unsuitable for determining RDS mineral magnetic particle size effects within ASU data sets.

4.7.11 Summary of West Midlands (Regional) sites

Mineral magnetic and textural data for the West Midlands is similar to that investigated within Wolverhampton, suggesting a consistency of magnetic material within RDS. Some differences are found between sites and reflect regional locations and site specific environments. No site has shown any potential for using mineral magnetic methods for PM particle size proxy purposes.

- PM_{10} levels at all the sites are low and are unlikely to be noticed by individuals.
- Mineral magnetic concentrations vary between sites.

Table 4.24 Statistical relationships between the mineral magnetic and PM_{10} parameters for Wolverhampton ASU (WLV 41) (n = 52)

	Parameters	χ_{LF}	$\chi_{FD\%}$	χ_{ARM}	SIRM	Soft $_{IRM20mT}$	Soft $_{IRM40mT}$	Hard $_{IRM300mT}$	Hard $_{IRM500mT}$	S-ratio	ARM/χ	SIRM/ARM	SIRM/χ	χ_{ARM}/SIRM
PM_{10}	Mean 2 Month	0.286	-0.371	0.036	0.214	0.071	-0.321	-0.214	-0.143	0.514	0.286	0.143	-0.071	0.185
	1 Month	0.429	-0.243	0.143	0.464	-0.286	-0.607	-0.143	0.071	0.543	0.321	0.321	0.071	-0.037
	1 Week	0.371	-0.257	-0.143	0.429	-0.429	-0.543	-0.143	0.257	0.547	0.371	0.186	0.143	-0.087
	3 Day	0.371	-0.257	-0.143	0.429	-0.429	-0.543	-0.143	0.257	0.543	0.371	0.186	0.143	-0.087
	2 Day	0.143	0.029	-0.371	0.257	-0.486	-0.314	-0.029	0.200	0.143	0.143	0.371	0.314	-0.290
	1 Day	0.143	0.029	-0.371	0.257	-0.486	-0.314	-0.029	0.200	0.143	0.143	0.371	0.314	-0.290
	Hour	-0.029	0.029	-0.371	-0.086	-0.143	0.029	-0.714	-0.086	0.143	-0.029	-0.143	-0.371	0.406
PM_{10}	Median 2 Month	0.500	-0.143	-0.143	0.393	-0.071	-0.321	0.214	0.286	0.514	0.679	0.136	0.429	0.185
	1 Month	0.321	-0.314	0.000	0.357	-0.107	-0.464	0.143	0.357	0.450	0.429	0.129	0.393	-0.222
	1 Week	0.300	-0.371	0.371	0.371	-0.486	-0.329	0.257	0.543	0.343	0.200	0.214	0.100	-0.174
	3 Day	0.343	-0.257	0.143	0.314	-0.771	-0.571	0.371	0.257	0.486	0.543	0.271	0.257	-0.377
	2 Day	0.371	-0.200	0.086	0.300	-0.714	-0.357	0.543	0.229	0.257	0.371	0.214	0.171	-0.238
	1 Day	0.143	0.029	-0.371	0.257	-0.486	-0.314	-0.029	0.200	0.143	0.143	0.371	0.314	-0.290
	Hour	0.257	-0.143	-0.086	0.200	-0.314	-0.257	-0.600	-0.143	0.429	0.257	0.086	-0.257	0.493

- Coarse grained multi-domain characteristics are apparent at all sites.
- Fine grained ferromagnetic material is also indicated at some sites, indicating a mixture of magnetic material from anthropogenic and natural background sources.
- The sites are unsuitable for mineral magnetic PM size proxy purposes.
- PM_{10} (WMAIR) data shows no association with mineral magnetic-textural data.
- Site location and proximity to roads appear to influence RDS characteristics with increased mineral magnetic concentrations closer to roads.

4.8 Overall summary of Wolverhampton RDS samples

Analysis of RDS collected during January 2008-January 2010 suggests a moderate to high concentration of mineral magnetic parameters. There are indications that magnetic properties of sediments are similar to intermediate igneous rocks, basic/ultra-basic rocks and ferromagnetic minerals.

Results for Wolverhampton RDS indicate low $\chi_{FD\%}$ values, which suggest samples are not dominated by SP ferrimagnets ($\chi_{FD\%}$) and suggest the presence of ultra-fine superparamagnetic ferromagnetic grains (diameter <0.03 μm, (Dunlop,1973)), particularly grains between 0.01-0.025 μm (Dearing *et al*., 1997; Maher, 1988)). This is also reflected in the SIRM/ARM (172.200) and χ_{ARM}/SIRM (0.199 x $10^{-3}Am^2kg^{-1}$) ratios, which indicate the presence of multi-domain grains within samples. SEM analysis supports this indication, with the presence of glassy Fe oxide spheres, which can be attributed to combustion processes. Correlation between $\chi_{FD\%}$ and χ_{ARM} further suggests low concentrations of SP grains within samples.

Results over the sampling period indicate these observations are consistent for all sampling periods in Wolverhampton and suggest that the mineral magnetic signature of Wolverhampton RDS is predominantly due to anthropogenic input. Magnetic signatures when compared to other data sets (traffic, land use), suggest that relationships exist for concentration and anthropogenic activity (Appendix 3.1-3.2.2).

Road types have been identified and results suggest that mineral magnetic techniques could be used to distinguish road environments. The magnetic concentration parameters (χ_{LF}, χ_{ARM} and SIRM) of the Wolverhampton samples showed that they are statistically different over the sampling area and can be categorized into two differing road types. Although mineral magnetic concentration parameters are different, domain size parameters remain fairly consistent between road types. This suggests that the loading of magnetic material is different between road types, but the source of magnetic material is possibly the same. SEM analysis has further supported this, with increased Fe oxide particle counts on arterial road sample points. Textural parameters are consistent throughout the sampling area, with similar $<PM_{100}$ levels in Wolverhampton RDS.

There are few linkages between Wolverhampton RDS parameters. Only when data has been split into individual seasons, months and specific sites can some relationships be identified. The results for Spring months (March-May) have shown strong relationships between mineral magnetic concentration and textural (<PM_{10}) parameters and shows some potential for pollution proxy purposes. Seasonal weather patterns appear to influence the mineral magnetic concentrations and mineral magnetic-particle size proxy potential during warm-dry periods. Individual sites have also shown some potential, with strong correlations between parameters. Isolated sites with limited sediment inputs have shown most potential for these parameter linkages.

Regional variations within the West Midlands are high. RDS characteristics at sites are similar to Wolverhampton. Although magnetic concentrations vary, results suggest the presence of MD ferromagnetic grains within all samples and SSD fine grained material at some sites. The West Midlands site samples are unsuitable for particle size proxy purposes and appear to be influenced by site location and proximity to roads.

Results for the ASU data have shown similar characteristics to Wolverhampton RDS data, but without significant linkages between parameters. This is also the case when collected data is used in conjunction with published monitoring site data. This study did not find any linkages between ASU sites and the collected data and therefore shows no potential for particle size proxy purposes.

In Summary:

- Mineral magnetic properties of RDS in Wolverhampton is predominantly ferromagnetic.
- Mineral magnetic concentration parameters vary over time and display significant relationships for similar time periods.
- Mineral magnetic concentrations vary at specific sites and regional scales.
- Mineral magnetic grain size remains predominantly multi-domain over the study area.
- Several sites contain a mixture of coarse and fine grained magnetic material, indicating a range of sources.
- Road types display clear differences in concentrations but remain multi-domain in nature.
- Land use appears to be an additional factor influencing mineral magnetic concentrations.
- No relationships are evident between PM_{10} (ASU) and analytical data.
- No proxy potential has been found in Wolverhampton over the study period.
- Proxy potential increases during warm dry stable conditions, but relationships are still weak.
- Mineral magnetic methods used as a proxy for PM at city and site specific scales appear to be limited.

Chapter 5

Physico-chemical characteristics of road deposited sediment (RDS) from selected towns and cities in the UK

5.1 Introduction

Chapter 5 further investigates the potential for using mineral magnetic measurements as a PM particle size and pollution (geochemical) proxy. Whereas Chapter 4 illustrated the temporal and spatial linkages, Chapter 5 further investigates spatial characterisation and potential for proxy methods at different spatial scales (UK wide, city, road (Figure 4.1)). Chapter 5 characterizes the mineral magnetic, textural and geochemical properties of eight selected locations in the UK (n = 306) (Figure 3.8). RDS proxy methods will be investigated in Dumfries, Halton, Marylebone Road (London), Norwich, Oswestry, Salford, Scunthorpe and for comparison purposes Wolverhampton (UK).

5.1.2 Mineral magnetic data for the selected towns and cities of the UK

Mineral magnetic data for selected towns and cities in the UK is summarized in Table 5.1. Magnetic concentration-dependent parameters indicate UK RDS contain a moderate to high concentration of magnetic minerals (mean values χ_{LF} 34.590 x $10^{-7}m^3kg^{-1}$; χ_{ARM} 0.217 x $10^{-5}m^3kg^{-1}$; SIRM 545.291 x $10^{-4}Am^2kg^{-1}$). When these results are compared to published values for other environmental materials (Dearing, 1999), they indicate that the magnetic properties of the sediments are similar to intermediate igneous rocks, basic/ultra-basic rocks and ferromagnetic minerals. The χ_{LF} values display high variation between locations (3.377-123.341 x $10^{-7}m^3kg^{-1}$ (Figure 5.1a)). The ARM/χ values range from high to low (0.158-7.111 x $10^{-1}Am^{-1}$ (Figure 5.1b)) indicating a predominately coarse grained magnetic material (mean 0.660 x $10^{-1}Am^{-1}$). SIRM values indicate high variation between sites (37.069-9686.424 x $10^{-4}Am^2kg^{-1}$ (Figure 5.1c)). The SIRM/ARM values range from 17.525-992.035 (mean 228.269) and are high compared to other environmental materials (Yu and Oldfield, 1993). This supports the ARM/χ values, by indicating a coarse magnetic grain size. The SIRM/χ values are also high (Mean 13.415 x $10^{-1}Am^{-1}$ (Figure 5.2b)), with a wide range of values (6.281-45.821 x $10^{-1}Am^{-1}$). The SIRM/χ values suggest a presence of fine-grained magnetic material.

Magnetic properties of the individual towns (Table 5.2) show distinct differences, with relative high and low concentrations of magnetic material when compared to other studies (Table 2.11 (Figure 5.1. and 5.2)). Detailed tables for all selected UK location summary data can be found in Appendix 5.1.1-5.1.8. The magnetic concentration parameters for Dumfries are considered moderate compared to other urban RDS (Table 2.11) (χ_{LF} 21.510 x $10^{-7}m^3kg^{-1}$; and SIRM 298.600 x $10^{-5}Am^2kg^{-1}$ (Soft $_{IRM20mT,}$ 40.419 x $10^{-4}Am^2kg^{-1}$; and Soft $_{IRM40mT,}$ 117.185 x $10^{-4}Am^2kg^{-1}$)). Dumfries RDS contains a mixture of coarse and fine-grained magnetic minerals (SIRM/χ 13.870 x $10^{-1}Am^{-1}$; and SIRM/ARM = 228.160). Results for Halton indicate relatively moderate values of magnetically soft minerals (χ_{LF} 24.910 x $10^{-7}m^3kg^{-1}$; and SIRM 384.000 x $10^{-5}Am^2kg^{-1}$ (Soft $_{IRM20mT,}$ 49.452 x $10^{-4}Am^2kg^{-1}$; and Soft $_{IRM40mT,}$ 143.607 x $10^{-4}Am^2kg^{-1}$).

Table 5.1 Summary RDS analytical data* for the selected towns and cities in the UK (July 2008) (n = 306)

Parameters	Units	Mean	Median	SD	CV (%)	Min	Max	Range
χ_{LF}	$10^{-7}m^3kg^{-1}$	34.950	30.424	21.716	62.134	3.377	123.341	119.964
$\chi_{FD\%}$	%	1.592	1.659	0.917	57.628	0.051	4.549	4.599
χ_{ARM}	$10^{-5}m^3kg^{-1}$	0.217	0.059	0.467	214.948	0.007	2.460	2.454
SIRM	$10^{-4}Am^2kg^{-1}$	545.291	371.773	770.718	141.341	37.069	9686.424	9649.355
S-Ratio	Dimensionless	-0.782	-0.783	0.060	-7.671	-0.980	-0.292	0.688
$Soft\%_{20mT}$	%	16.239	15.392	5.267	32.433	5.702	33.020	27.318
$Soft\%_{40mT}$	%	40.840	40.829	6.107	14.954	12.624	88.508	75.884
$Hard\%_{300mT}$	%	9.243	9.063	3.826	41.393	1.626	25.207	23.581
$Hard\%_{500mT}$	%	4.320	3.835	2.733	63.261	0.310	12.857	12.547
$Soft_{IRM20mT}$	$10^{-4}Am^2kg^{-1}$	78.354	51.316	133.109	169.882	2.617	1833.835	1831.218
$Soft_{IRM40mT}$	$10^{-4}Am^2kg^{-1}$	195.344	137.040	318.172	162.878	10.205	4455.850	4445.646
$Hard_{IRM20mT}$	$10^{-4}Am^2kg^{-1}$	40.707	27.078	46.594	114.461	3.686	542.110	538.424
$Hard_{IRM40mT}$	$10^{-4}Am^2kg^{-1}$	18.908	11.608	20.811	110.065	0.813	142.610	141.797
ARM/χ	$10^{-1}Am^{-1}$	0.660	0.556	0.508	76.944	0.158	7.111	6.953
χ_{ARM}/SIRM	$10^{-3}Am^2kg^{-1}$	0.175	0.151	0.181	103.625	0.032	1.792	1.760
SIRM/ARM	Dimensionless	228.269	217.947	96.014	42.062	17.525	992.035	974.510
SIRM/χ	$10^{-1}Am^{-1}$	13.415	13.157	4.737	35.313	6.281	45.821	39.540
Mean - PS	μm	274.476	273.817	88.341	32.185	88.591	598.063	509.472
Median - PS	μm	350.251	357.051	81.587	23.294	193.200	612.120	418.920
Sorting	σ_1	1.919	1.901	0.334	17.397	1.124	3.239	2.115
Skewness	SK_1	0.358	0.360	0.156	43.546	0.003	0.760	0.757
Kurtosis	K_G	1.321	1.243	0.371	28.112	0.700	3.044	2.344
Sand	%	80.489	81.757	6.821	8.474	53.446	93.875	40.429
Silt	%	17.458	16.177	6.793	38.911	4.450	43.801	39.351
Clay	%	2.053	1.819	1.006	49.011	0.111	8.503	8.392
$PM_{1.0}$	%	1.208	1.059	0.738	61.098	0.000	5.394	5.394
$PM_{2.5}$	%	2.400	2.129	1.118	46.593	0.968	9.818	8.850
PM_{10}	%	5.537	4.969	2.717	49.070	1.718	23.992	22.274
PM_{100}	%	23.104	21.873	7.857	34.008	9.446	51.956	42.510
LOI	%	-1.047	-1.027	0.106	-10.094	-2.000	-0.234	1.766
Mg	mg g^{-1}	7.442	6.600	4.474	60.121	0.990	45.260	44.270
Al	mg g^{-1}	19.167	19.180	6.564	34.247	3.387	49.580	46.193
S	mg g^{-1}	2.545	2.071	1.475	57.978	0.574	7.099	6.525
K	mg g^{-1}	6.410	6.342	1.676	26.146	2.289	11.870	9.581
Ca	mg g^{-1}	29.925	24.735	22.175	74.103	3.808	142.000	138.192
Ti	mg g^{-1}	1.643	1.640	0.515	31.341	0.457	4.439	3.982
V	mg g^{-1}	0.056	0.052	0.027	47.989	0.013	0.193	0.180
Cr	mg g^{-1}	0.146	0.117	0.107	73.602	0.029	0.761	0.732
Mn	mg g^{-1}	0.528	0.359	0.601	113.820	0.116	3.602	3.486
Fe	mg g^{-1}	29.809	27.430	12.917	43.332	10.470	109.100	98.630
Ni	mg g^{-1}	0.021	0.019	0.022	102.031	0.006	0.250	0.244
Cu	mg g^{-1}	0.148	0.093	0.137	92.313	0.011	0.570	0.559
Zn	mg g^{-1}	0.487	0.290	0.458	94.043	0.056	2.078	2.022
Cd	mg g^{-1}	0.008	0.007	0.001	19.412	0.005	0.012	0.006
Sb	mg g^{-1}	0.015	0.013	0.006	42.265	0.006	0.038	0.031
Pb	mg g^{-1}	0.140	0.098	0.135	96.637	0.025	0.999	0.973

*SD = Standard Deviation; CV = Percentage coefficient of variation; Min = Minimum value; Max = maximum value.

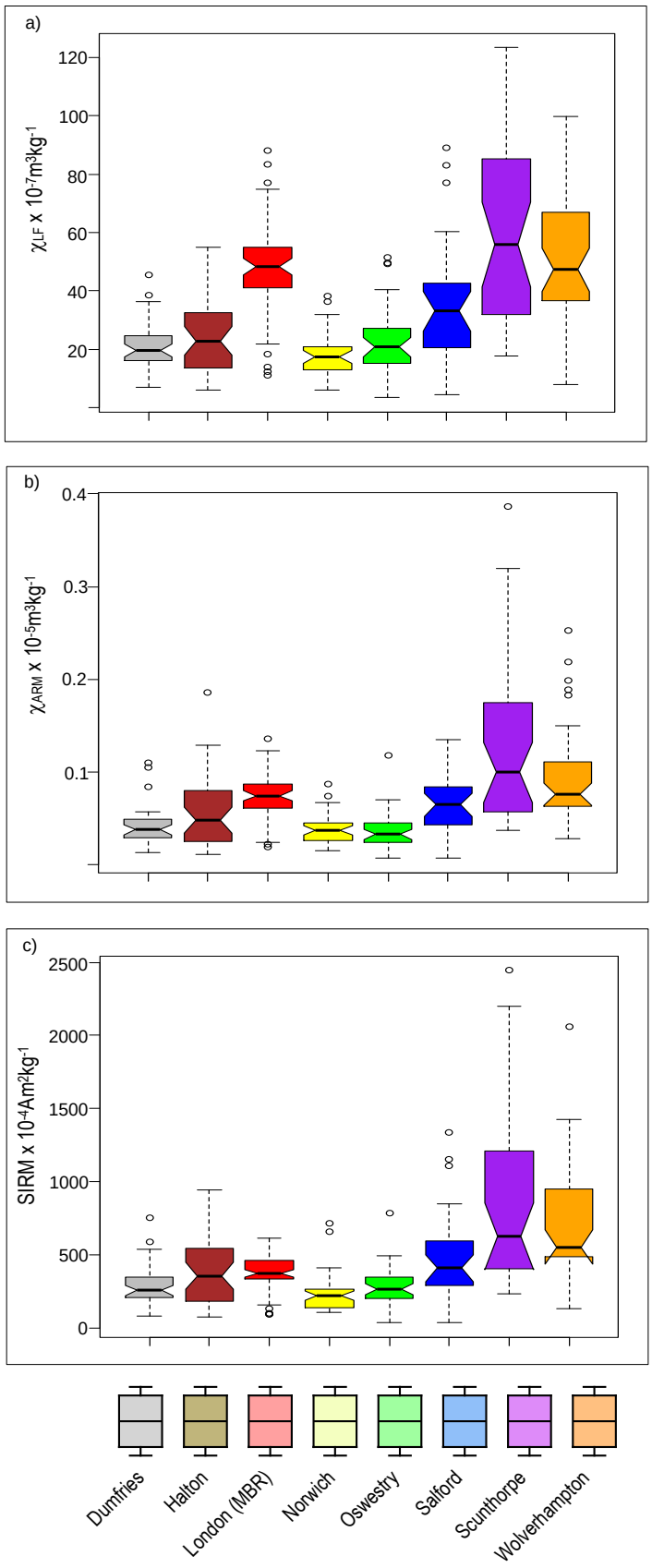

Figure 5.1 Box plots of RDS sample population distributions for selected mineral magnetic parameters for selected towns and cities in the UK

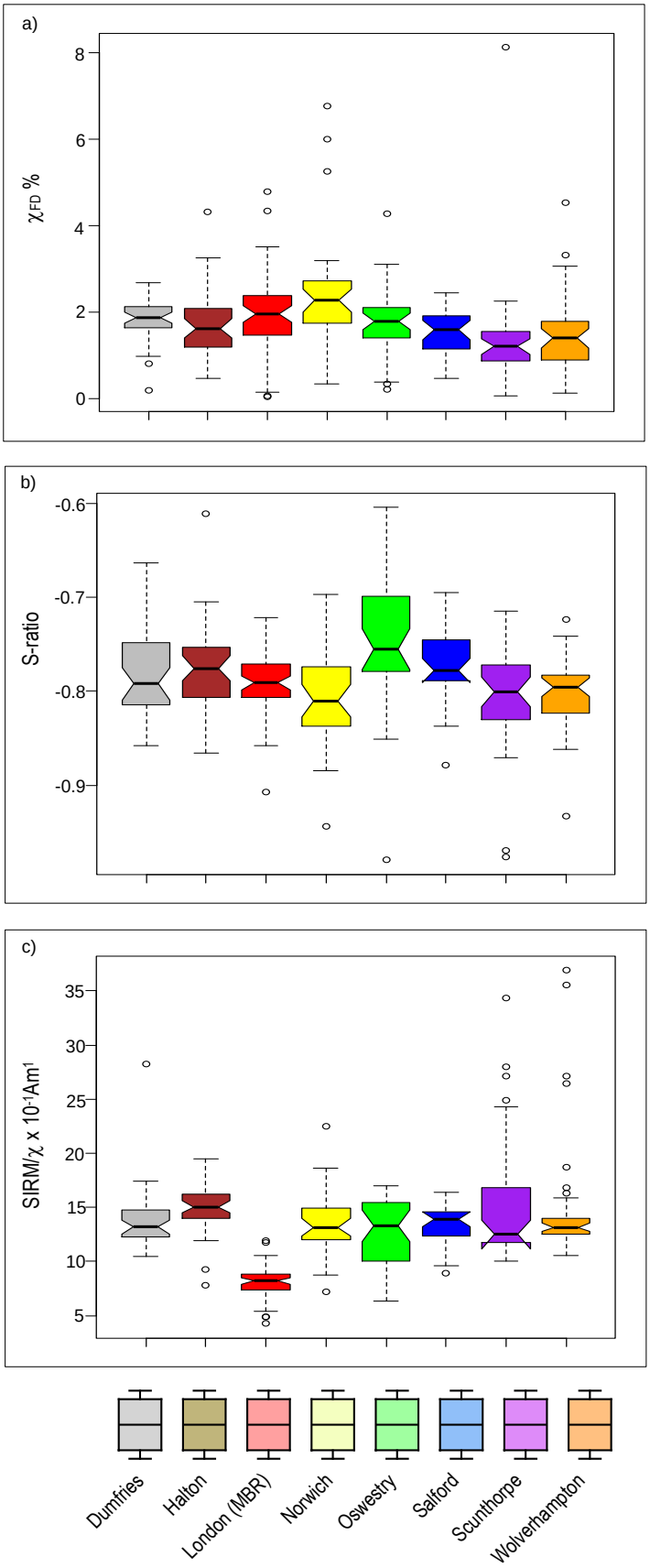

Figure 5.2 Box plots of RDS sample population distributions for selected mineral magnetic parameters for selected towns and cities in the UK

Table 5.2 Selected summary mineral magnetic data for UK samples: χ_{LF} x $10^{-7}m^3kg^{-1}$; $\chi_{FD\%}$; χ_{ARM} x $10^{-5}m^3kg^{-1}$; SIRM x $10^{-4}Am^3kg^{-1}$; ARM/χ x $10^{-1}Am^{-1}$; χ_{ARM}/SIRM x $10^{-3}Am^2kg^{-1}$

Parameters	Wlv	Dum	Hal	MBR	Nor	Osw	Sal	Scu
χ_{LF}	52.410	21.510	24.910	47.880	17.730	22.920	35.570	61.720
$\chi_{FD\%}$	1.510	1.862	1.688	2.183	2.106	1.797	1.565	1.379
χ_{ARM}	0.119	0.042	0.057	0.072	0.040	0.035	0.072	0.183
SIRM	859.000	298.600	384.000	377.900	237.100	248.800	485.700	1286.000
ARM/χ	0.690	0.640	0.853	0.497	0.720	0.496	0.702	0.818
χ_{ARM}/SIRM	0.139	0.150	0.188	0.199	0.173	0.127	0.165	0.143

Norwich results display low values of magnetically soft minerals (χ_{LF} 17.730 x $10^{-7}m^3kg^{-1}$; and SIRM 237.100 x $10^{-5}Am^2kg^{-1}$ (Soft $_{IRM20mT,}$ 29.775 x $10^{-4}Am^2kg^{-1}$; and Soft $_{IRM40mT,}$ 103.506 x $10^{-4}Am^2kg^{-1}$). In Oswestry low values of magnetically soft minerals (χ_{LF} 22.920 x $10^{-7}m^3kg^{-1}$; and SIRM 248.800 x $10^{-5}Am^2kg^{-1}$ (Soft $_{IRM20mT,}$ 49.452 x $10^{-4}Am^2kg^{-1}$; Soft $_{IRM40mT,}$ 143.607 x $10^{-4}Am^2kg^{-1}$) were recorded. Salford results show moderate values of magnetically soft minerals (χ_{LF} 35.570 x $10^{-7}m^3kg^{-1}$; and SIRM 485.700 x $10^{-5}Am^2kg^{-1}$ (Soft $_{IRM20mT,}$ 79.655 x $10^{-4}Am^2kg^{-1}$; Soft $_{IRM40mT,}$ 191.311 x $10^{-4}Am^2kg^{-1}$).

Scunthorpe and Wolverhampton display high mineral magnetic concentrations (mean χ_{LF} 52.410-61.720 x $10^{-7}m^3kg^{-1}$ (Figure 5.1a); χ_{ARM} 0.119-0.183 (Figure 5.1b); SIRM 859.000-1286.000 x $10^{-4}Am^2kg^{-1}$ (Figure 5.1c), compared to the low values of Dumfries, Halton, Norwich and Oswestry (mean χ_{LF} 17.730-24.910 x $10^{-7}m^3kg^{-1}$ (Figure 5.1a); χ_{ARM} 0.035-0.057 (Figure 5.1b); SIRM 237.100–384.000 x $10^{-4}Am^2kg^{-1}$ (Figure 5.1c)). Consistent values of $\chi_{FD\%}$ (Figure 5.2a) in all selected UK towns and cities suggest a relatively uniform magnetic grain size for UK RDS. S-ratio (mean -0.782 (Figure 5.2b)) and SIRM/χ (mean 13.415 (Figure 5.2c)) values indicate concentration parameters are variable when compared. Consistent levels of magnetic mineralogy and grain size suggest a consistent source of magnetic material to RDS over the sampling areas. Mineral magnetic concentration parameters in this case, show the intensity of the source material.

Results show that London, Salford, Scunthorpe and Wolverhampton have the highest concentrations and variability of χ_{LF} (Figure 5.1a, Table 5.2) across the sampling areas (SD 16.120-28.350), compared to the moderate levels in Dumfries, Halton, Norwich and Oswestry (SD 7.90-13.22). Scunthorpe and Wolverhampton display high variability of χ_{ARM} (SD 0.115-0.209 (Figure 5.1b)) and SIRM (SD 737- 1660 (Figure 5.1c)), compared to low levels of variability in Dumfries, Halton, London, Norwich, Oswestry and Salford ($\chi_{ARM,}$ SD 0.019-0.045; SIRM, SD 119.800-310.500). Mineral magnetic results indicate a unique concentration is present for each location, with consistent mineralogy and magnetic grain size.

5.1.3 Textural data for UK towns and locations

Textural data for selected towns and cities of the UK are summarized in Table 5.1. Particle size parameters indicate that RDS contains moderately sorted sediment (1.919 σ_1; mean 274.476 µm), with moderate to high sand concentrations (80.489%), moderate silt concentrations (17.458%), and low clay concentrations (2.053%). The RDS particle size data for the UK also suggests a moderate level of sediment within the PM_{100} boundary (23.104%) with lesser PM_{10} concentrations (5.537%), low concentrations of $PM_{2.5}$ (2.400%) and $PM_{1.0}$ (1.208%). The LOI values are typically low (mean 1.047%; SD 0.106).

The textural data shows the mean particle size as fairly consistent (209.521-336.000µm (Figure 5.3a)) across all selected UK sampling locations. This trend is also evident within the <PM_{100} fractions (Figures 5.3c and Figures 5.4a,b,c). All locations show some mean particle size variability (Figure 5.3a) with Dumfries, Oswestry, Salford and Wolverhampton with the least variation (SD 61.960-71.400) compared to the higher variation of Halton, London, Norwich and Scunthorpe (SD 79.670-97.600). Fine particles <PM_{10} display consistent patterns throughout the selected UK sampling locations, with mean concentrations of $PM_{1.0,}$ $PM_{2.5}$ and PM_{10} steady throughout. Some variation does apply to the selected UK sites and fine particles <$PM_{2.5}$, with London, Norwich, Salford and Scunthorpe showing the highest degree of variation ($PM_{1.0,}$ SD 0.933-1.206; $PM_{2.5,}$ SD 1.418-1.728) compared to lower variation in Dumfries, Halton, Oswestry and Wolverhampton ($PM_{1.0,}$ SD 0.317-0.409; $PM_{2.5}$, SD 0.547-0.612). Textural results for each selected location indicate that RDS particle sizes are relatively consistent spatially, with little variation between sample points.

5.1.4 Geochemical data for UK towns and locations

Geochemical data for selected towns and cities of the UK are summarized in Table 5.1. When compared to other studies (Appendix 2.1), element analysis indicates RDS contains moderate levels of Fe (mean 29.809 mg g^{-1}; SD 12.917) and Al (mean 19.167 mg g^{-1}; SD 6.564) and low levels of Pb (mean 0.140 mg g^{-1}; SD 0.135) and Ni (mean 0.021 mg g^{-1}; SD 0.022). Dumfries RDS contains proportional amounts of Iron, and aluminium, compared to other studies. Moderate levels of Fe (mean 27.258 mg g^{-1}; SD 4.122) and Al (mean 23.316 mg g^{-1}; SD 4.213), K (mean 8.369 mg g^{-1}; SD 1.133), Ca (mean 8.243 mg g^{-1}; SD 2.732) with low levels of Pb (mean 0.115ppm; SD 0.174). Results for Halton indicate that inter-element ratios within RDS were consistent for Fe, Al, Ca, Cu and Pb. Moderate concentrations of Fe (mean 22.630 mg g^{-1}; SD 7.983) and Al (mean 15.704 mg g^{-1}; SD 7.146) and low levels of Pb (mean 0.089 mg g^{-1}; SD 0.085) and Ni (mean 0.022 mg g^{-1}; SD 0.032) were found. Geochemical analysis in London indicates that RDS contains a high amount of Ca (mean 36.430 mg g^{-1}; SD 7.502) and consistent inter-element ratios of Fe, Al, Cu and Pb. Moderate levels of Fe (mean 27.332 mg g^{-1}; SD 5.930), Al (mean 18.053 mg g^{-1}; SD 4.319) and Pb (mean 0.227 mg g^{-1}; SD 0.181) and low levels of Cd (mean 0.012 mg g^{-1}; SD 0.016) were found. Norwich results show RDS contains a moderate amount of Calcium (mean 19.706 mg g^{-1}; SD 7.515) with proportional amounts of Iron (mean 17.183 mg g^{-1}; SD 3.587) and Al (mean 9.312 mg g^{-1}; SD 3.918) and low levels of Pb (mean 0.080 mg g^{-1}; SD 0.016) were found.

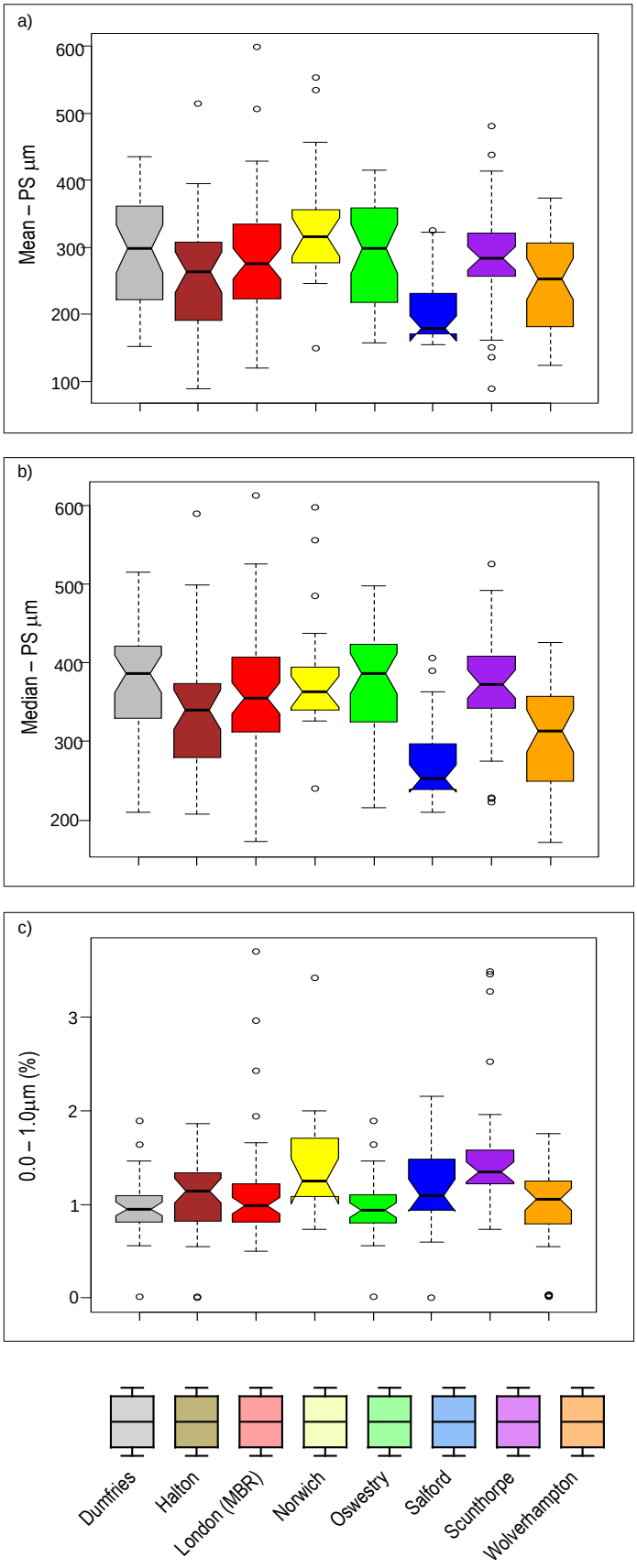

Figure 5.3 Box plots of RDS sample population distributions for selected textural parameters for selected towns and cities in the UK.

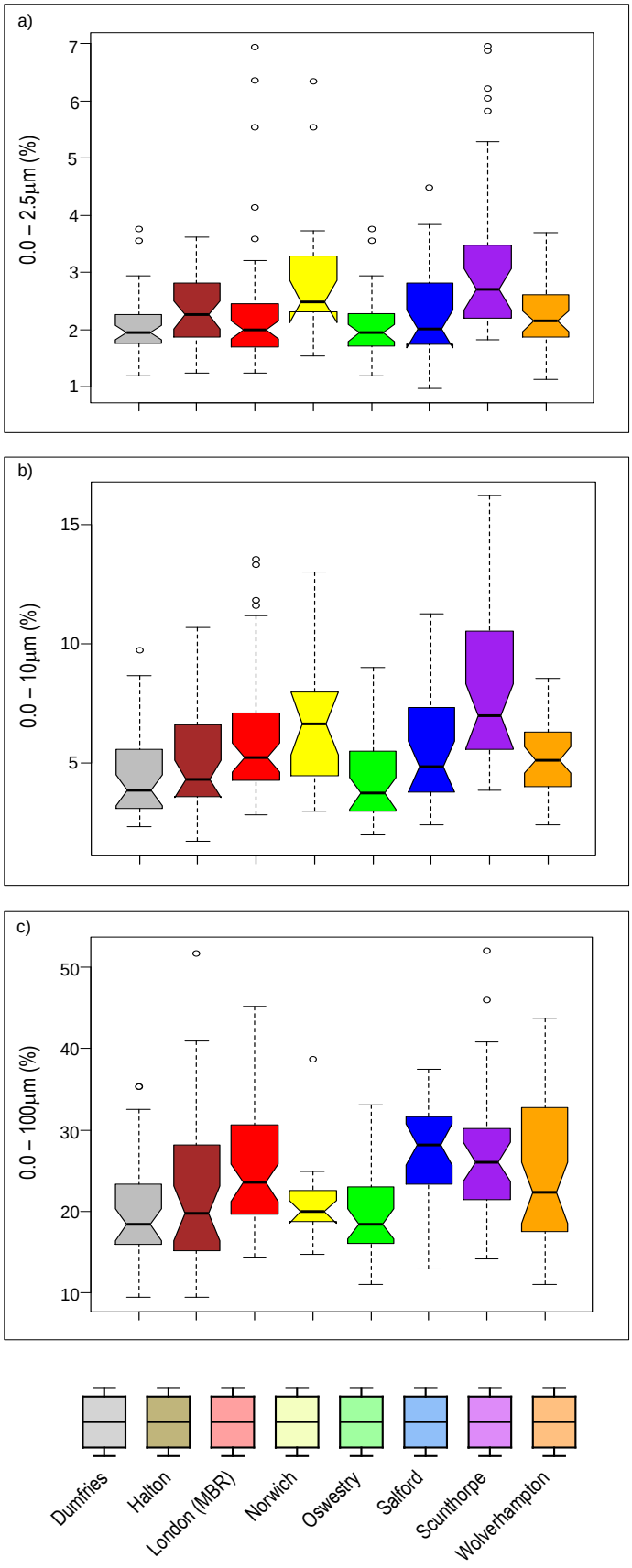

Figure 5.4 Box plots of RDS sample population distributions for selected textural parameters for selected towns and cities in the UK.

Oswestry RDS contains consistent inter-element ratios of Fe, Zn, Cu and Pb compared to other sites. Moderate levels of Fe (mean 29.809 mg g^{-1}; SD 12.917) and Al (mean19.167 mg g^{-1}; SD 6.564) and low levels of Pb (mean 0.140 mg g^{-1}; SD 0.135) and Ni (mean 0.021 mg g^{-1}; SD 0.022) were found. Salford RDS contains a high amount of Fe (mean 34.333 mg g^{-1}; SD 3.830) with consistent inter-element ratios of Al (mean 23.387 mg g^{-1}; SD 3.846), moderate levels of Mg (mean 9.892 mg g^{-1}; SD 2.999). Low levels of Pb (mean 0.085 mg g^{-1}; SD 0.026) were found. Scunthorpe RDS contains very high amounts of Fe (mean 49.704 mg g^{-1}; SD 20.336) and Ca (mean 73.134 mg g^{-1}; SD 20.336) moderate levels of Al and Mg and low levels of Pb (mean 0.085 mg g^{-1}; SD 0.038) and Ni (mean 0.014 mg g^{-1}; SD 0.006) were found.

The selected sample locations appear to display relatively consistent mean values of Fe (28.996 mg g^{-1} (Figure 5.5a)), with the exception of higher values in Scunthorpe (49.704 mg g^{-1}) and the low values in Norwich (17.183 mg g^{-1}). Concentrations of Ni and Cd (Figure 5.5b and c) are consistent, with the greatest variation in London for Ni (SD 0.038) and Oswestry for Cd (SD 0.001), which is minimal. Concentrations of Zn (Figure 5.6a) are consistent throughout most sampling locations, with the exception of Halton which shows much higher readings (0.229 mg g^{-1}; SD 0.138) than the mean (0.487 mg g^{-1}; SD 0.458). High levels of Cu are reported (Figure 5.6b) in London (0.337 mg g^{-1}; SD 0.125) compared to the mean values of all sites (0.148 mg g^{-1}; SD 0.458). All sites appear to display an individual geochemical signature either predominantly anthropogenic, natural back ground, or a mixture of both suggesting differences could be due to environmental factors. These potential differences will be explored further using mineral magnetic and textural parameters. Differences will be statistically investigated using Kruskal Wallis and Mann Whitney tests.

5.1.5 Distinguishing towns using RDS characteristics

The boxplots and summary data for the selected UK samples show the physico-chemical characteristics of Dumfries, Halton, MBR (London), Norwich, Oswestry, Salford, Scunthorpe and Wolverhampton. The null (H_0) and alternative (H_1) hypotheses were tested. Summary data for individual sites are presented in Appendix 5.1.1-5.1.8. Non-parametric Mann-Whitney U tests (Appendix 5.2.1-5.2.5) compare the difference of the medians of each of the sites RDS sample populations for each parameter. The result of the non-parametric Kruskal-Wallis tests (data not presented) show significant differences between the UK town RDS sample populations for each parameter (H_0).

Tested Hypotheses

Null Hypothesis (H_0)	There are significant differences between the towns mineral magnetic characteristics.
Alternative Hypothesis (H_1)	There are no significant differences between the towns mineral magnetic characteristics.

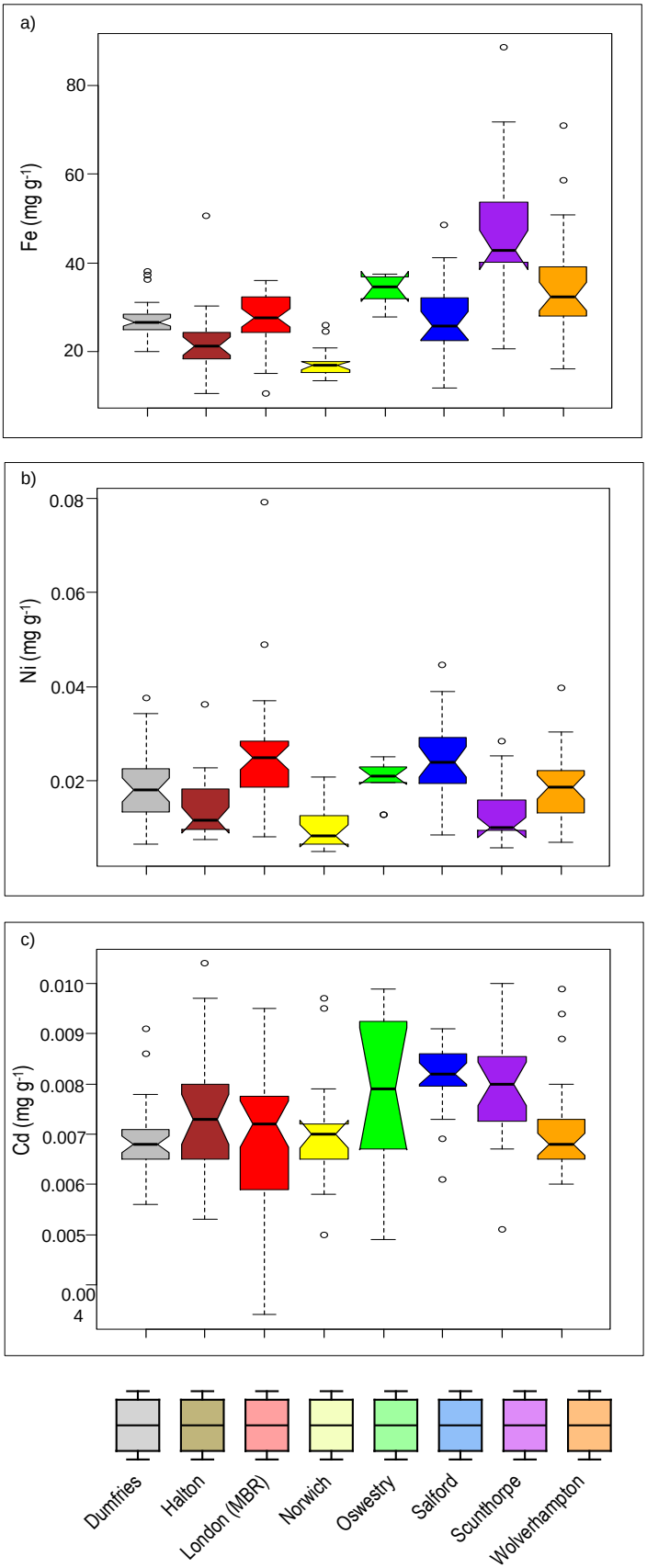

Figure 5.5 Box plots of RDS sample population distributions for selected geochemical parameters for selected towns and cities in the UK.

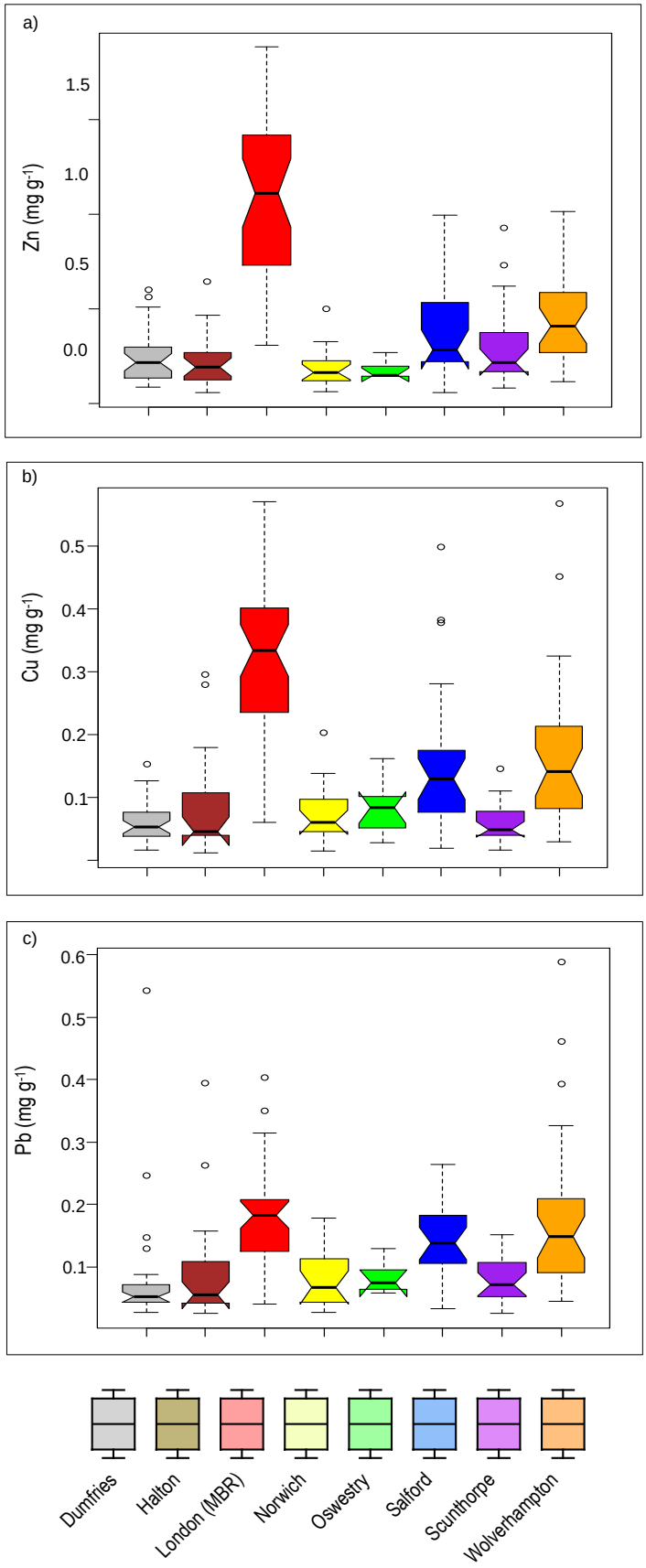

Figure 5.6 Box plots of RDS sample population distributions for selected geochemical parameters for selected towns and cities in the UK.

By comparing boxplots (Figure 5.1–5.6) for each selected mineral magnetic, textural and geochemical parameter, it is clear there is some overlap between the towns. This indicates that the characteristic properties of the towns are in some cases different (H_0). To determine whether variations between the towns are statistically significant, non-parametric Mann Whitney tests were performed on the sites for each of the mineral magnetic and textural parameters (Appendix 5.2.1-5.2.5).

The '*P'* values show that for each of the parameters the null hypothesis can be rejected and therefore, the medians of each of the location populations are significantly different (H_0). Mann Whitney U tests show comparisons between all locations. Selected mineral magnetic parameters of Dumfries, Halton, Marylebone Rd (London), Norwich, Oswestry, Salford, Scunthorpe and Wolverhampton were significantly different (Appendix 5.2.1-5.2.3 (p <0.001)) using Mann Whitney U tests (H_0).

5.1.6 Distinguishing towns using mineral magnetic and textural characteristics

The mineral magnetic characteristics for RDS in Dumfries, Halton, Marylebone Road, Norwich, Oswestry, Salford, Scunthorpe and Wolverhampton display significant differences (Appendix 5.2.1-5.2.3). Mineral magnetic concentration parameters (χ_{LF}, χ_{ARM} and SIRM (Figure 5.1a,c,d)) were significantly different over several towns. χ_{LF} (Appendix 5.2.1a) in Dumfries samples were significantly different (p <0.001) from Marylebone Road, Salford, Scunthorpe and Wolverhampton (H_0) but not significantly different for Halton (p = 0.493), Norwich (p = 0.072) or Oswestry (p = 0.778) (H_1). Halton, Norwich and Oswestry displayed similar characteristics to Dumfries. Scunthorpe and Wolverhampton were significantly different from Dumfries (p <0.001), Halton (p <0.001), Norwich (p <0.001), Oswestry (p <0.001) and Salford (p <0.05), but not significantly different to each other (p = 0.855). Similar relationships were found with χ_{ARM} and SIRM with significant differences between Dumfries, Halton and Oswestry with Marylebone Road, Salford and Scunthorpe. Wolverhampton was significantly different to all other towns except Scunthorpe (p = 0.814-0.919). Soft and Hard mineralogy (Figure 5.4a-d, Appendix 5.2.2a-d) indicates that sites were different, with Scunthorpe and Wolverhampton displaying similarities with each other but significant differences with all other locations. The results suggests linkages and similarities for parameters between the more developed towns, which could be linked to industry, land-use and population. Mineral magnetic grain size parameters indicate a relative consistency of magnetic material (Figure 5.2c, Appendix 5.2.3a). The results display less frequent differences between the towns when compared to mineral magnetic concentration and mineralogical parameters. The most significant differences are found with MBR (Appendix 5.2.3a-d) and display significant differences between all of the other locations and suggests that all other selected UK locations RDS have a common source of magnetic material.

Textural parameters (Appendix 5.2.4-5.2.5) indicate some differences between the selected UK locations with mean particle size (Figure 5.3a) between locations showing differences between Salford and all other locations. Appendix 5.2.4c shows sorting to be significantly different in

Scunthorpe and London (MBR) when compared to other towns, although there are differences it should be noted that all RDS in the selected UK locations are poorly-very poorly sorted (1.00-4.00). Differences in $PM_{1.0}$ (Figure 5.3c) to PM_{10} (Figure 5.4b) shows Wolverhampton significantly different to Scunthorpe (p <0.001). Scunthorpe displays significant differences between most of the other locations through the particle size range (Appendix 5.2.5b-f) but with similarities to Norwich which also has significant differences with other locations (Appendix 5.2.5b-d). Interrogating data via Mann Whitney tests has shown the potential to distinguish differences between sample locations, and identified groups of towns with similar parameter properties.

5.1.7 Relationships between the mineral magnetic and textural parameters

Relationships between the mineral magnetic and textural parameters were further interrogated by correlation statistics and graphically with the aid of bivariate plots. Statistical tests indicate that few weak significant correlations exists (p <0.05) between some mineral magnetic and textural parameters. However, it is only those relationships with the strongest correlation coefficients that have been selected for further examination through bivariate plot analysis. Rather than displaying all possible combinations, selected parameters are presented to reduce the volume of bivariate plots (Figures 5.7–5.8).

Table 5.3 (Figures 5.7 and 5.8) show magnetic concentration dependent parameters versus selected textural parameters with weak correlations (r = ≤0.260, n = 306) between these parameters. Mineral magnetic concentration and textural parameters display weak relationships with $\chi_{FD\%}$ and Clay (r = -0.178; p <0.05), $PM_{2.5}$ (r = -0.162; p <0.05 (Figure 5.7a)), PM_{10} (r = -0.148; p <0.05 (Figure 5.7b)), with negative weak linkages and sand (r = 0.191; p <0.01) with a weak positive relationship and positive linkages to the mean (r = 0.150; p <0.01) and median (r = 0.201; p <0.01) RDS particle size concentration. Other weak relationships exist with χ_{ARM} median (r = -0.205 (Figure 5.7c)) and mean (r = -0.204 (Figure 5.7d) particle size concentrations. This indicates that there is an increase of fine magnetic material as the mean and median particle sizes of RDS decreases. The S-ratio displays weak relationships within the finer fraction of RDS <$PM_{2.5.}$ Figure 5.8a shows S-ratio to decreases when concentrations of clay decrease (r = -0.219; p <0.01), these patterns are concurrent with other fine size fractions of RDS. This relationship suggests that a decrease in hard magnetic minerals is associated with a corresponding decrease in fine PM. Other mineral magnetic concentration parameters have shown very weak or no associations. Figure 5.8b and c shows χ_{LF} versus $PM_{2.5}$ (r = -0.044; p = 0.530) and PM_{10} (r = -0.053; p = 0.440) with no indication of any linkages, a very weak positive relationship does exist between χ_{LF} versus PM_{100} (r = 0.125; p <0.05). None of the SIRM versus textural parameters indicate any linkages.

Mineral magnetic concentration dependent parameters versus selected textural parameters show very few correlations that are significant. Therefore results suggest mineral magnetic measurements have no potential for use as a particle size proxy at the national scale (UK).

Table 5.3 Statistical relationships between the mineral magnetic and textural parameters for the selected towns and cities (**bold** text is significant (*p <0.05; **p <0.01; ***p <0.001)) (n = 306)

Parameters	Median-PS	Mean-PS	Sorting	Skewness	Kurtosis	Sand	Silt	Clay	$PM_{1.0}$	$PM_{2.5}$	PM_{10}	PM_{100}
χ_{LF}	-0.099	-0.059	0.026	-0.034	-0.059	-0.050	0.068	-0.037	-0.010	-0.044	0.053	**0.155***
$\chi_{FD\%}$	**0.150***	**0.201****	-0.087	-0.061	0.036	**0.191****	**-0.166***	**-0.178***	-0.213	**-0.162***	**-0.148***	**-0.154***
χ_{ARM}	**-0.205****	**-0.204****	0.023	-0.037	-0.062	-0.117	0.132	-0.019	0.007	-0.028	0.081	**0.195****
SIRM	-0.131	-0.105	-0.019	-0.061	-0.029	-0.029	0.041	0.025	0.048	0.000	0.045	0.127
Soft $_{\%\ 20mT}$	-0.082	-0.109	**0.158***	0.112	-0.131	**-0.236****	**0.237****	-0.031	-0.025	-0.015	**0.151***	**0.260****
Soft $_{\%\ 40mT}$	0.011	0.014	**0.167***	0.096	-0.092	**-0.213****	**0.205****	0.020	0.051	0.024	0.122	**0.212****
Hard $_{\%\ 300mT}$	**-0.177****	**-0.192****	**-0.152***	-0.110	0.043	0.044	-0.042	0.026	-0.004	-0.002	-0.067	-0.058
Hard $_{\%\ 500mT}$	-0.121	-0.124	-0.022	-0.062	-0.016	-0.056	0.045	0.030	0.080	0.009	-0.013	-0.011
Soft $_{IRM20mt}$	**-0.162****	**-0.148***	0.041	-0.023	-0.090	-0.117	0.131	-0.001	0.022	-0.018	0.087	**0.221*****
Soft $_{IRM40mT}$	**-0.145***	-0.119	0.002	-0.059	-0.047	-0.066	0.077	0.021	0.047	-0.003	0.057	**0.164***
Hard $_{IRM300mT}$	**-0.184****	**-0.173***	-0.103	-0.090	0.033	0.007	-0.002	0.039	0.029	0.004	0.000	0.054
Hard $_{IRM500mT}$	**-0.150***	**-0.137***	0.007	-0.053	-0.027	-0.072	0.067	0.099	0.131	0.060	0.066	0.092
S-ratio	-0.045	-0.030	-0.086	-0.094	-0.069	0.054	-0.003	**-0.219****	**-0.191****	**-0.198****	-0.127	-0.030
ARM/χ	**0.145***	0.090	0.046	**0.163***	0.076	0.034	-0.062	0.178	**0.159***	**0.176***	**0.142***	-0.096
SIRM/ARM	**-0.169***	**-0.148***	-0.082	**-0.155***	0.005	-0.006	0.009	0.047	0.043	0.010	-0.087	0.041
SIRM/χ	-0.029	-0.058	-0.031	-0.005	0.114	0.051	-0.074	0.217	0.188	0.179	0.080	-0.071
χ_{ARM} /SIRM	**0.169***	**0.148***	0.082	0.155	-0.005	0.006	-0.009	-0.047	-0.043	-0.010	0.087	-0.041

The Hypothesis being tested was:-

Null Hypothesis (H_0) — There are no significant relationships between the mineral magnetic parameters.

Alternative Hypothesis (H_1) — There are significant differences between the mineral magnetic parameters.

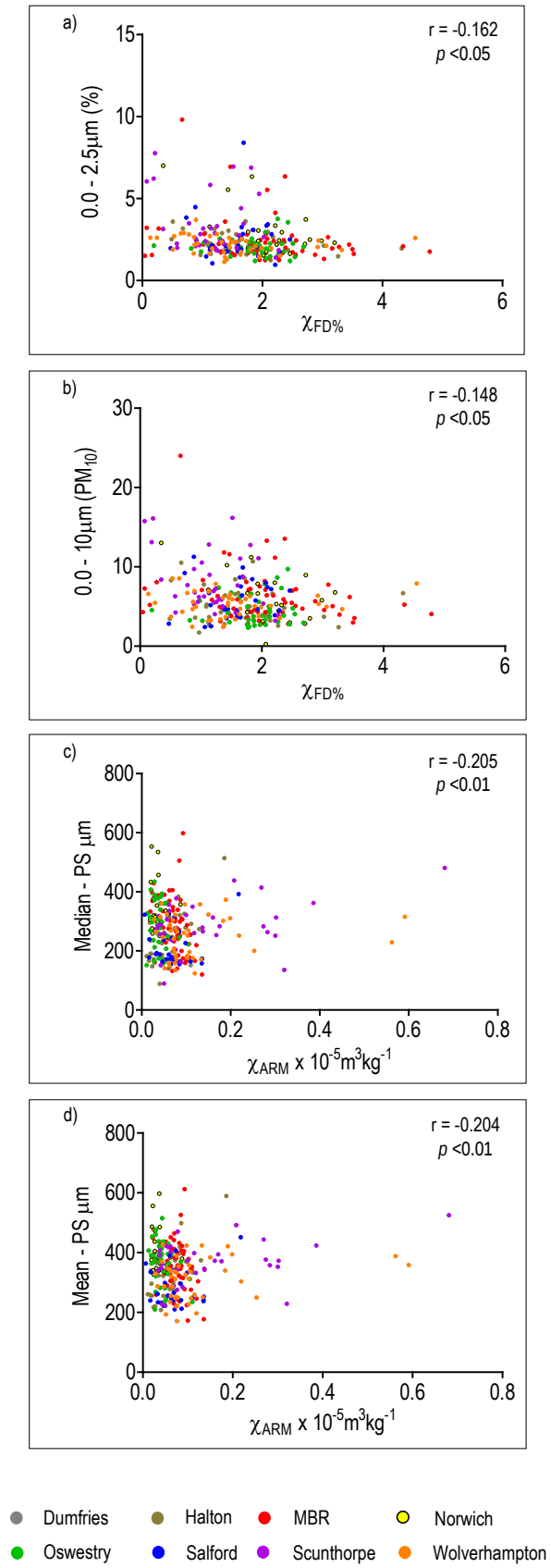

Figure 5.7 Bivariate plots of selected mineral magnetic and textural parameters for selected towns and cities (n = 306).

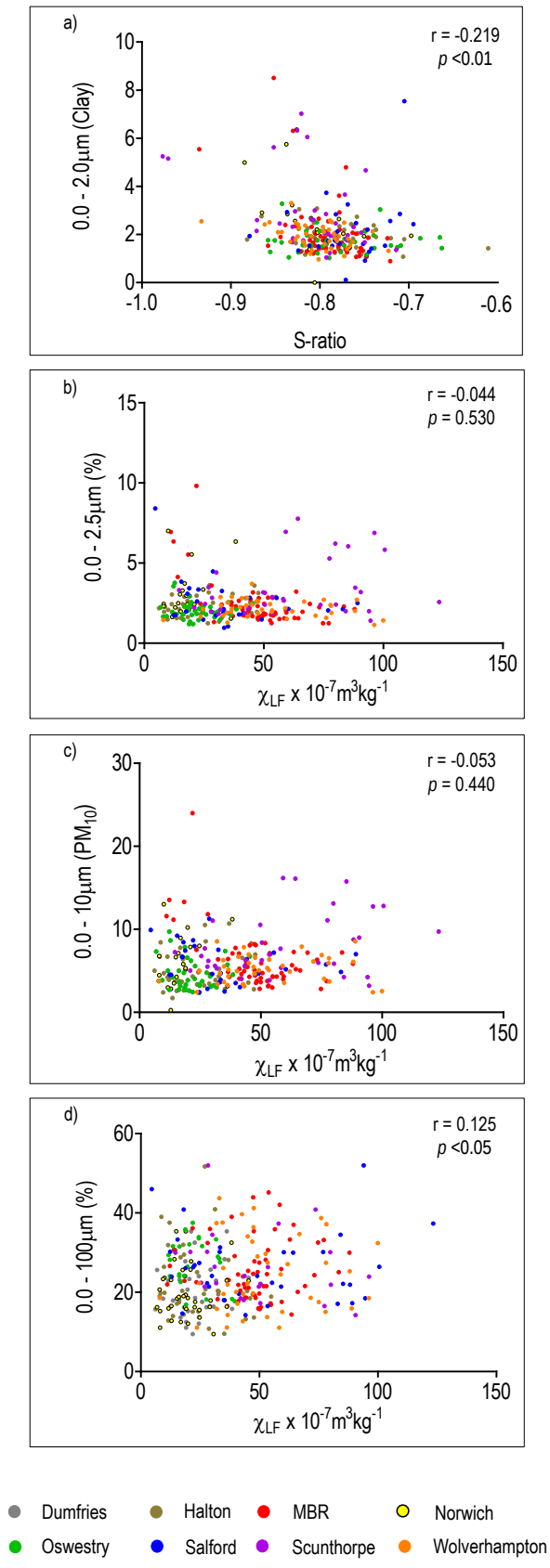

Figure 5.8 Bivariate plots of selected mineral magnetic and textural parameters for selected towns and cities (n = 306).

5.1.8 Relationships between the mineral magnetic parameters

Relationships between the mineral magnetic parameters were interrogated by correlation statistics (Spearman Rank). The results are summarized in Table 5.4. The results show that most mineral magnetic parameters exhibit strong correlation coefficients between each other (p <0.05-<0.001) (Table 5.4). The strongest correlation coefficients exist between each of the magnetic concentration dependent parameters (r = 0.747-0.923; p <0.001), with χ_{LF} and Soft $_{IRM\ 20mT}$ being the strongest (r = 0.923; p <0.001). The weakest correlation coefficient values are associated with correlation between the ARM/χ parameters and most of the other mineral magnetic parameters (r = -0.028-0.056). All other parameters are quite strongly correlated, with most of the correlation coefficient values being *ca*. r = ≤0.3-0.6. The strength of these correlations suggests that the characteristics of the mineral magnetic properties are highly dependent upon each other.

Figure 5.9a shows χ_{LF} versus SIRM, χ_{LF} versus χ_{ARM} (Figure 5.9b) as shown in Table 5.4 an exceptionally strong positive correlation (r = 0.747-0.904; p <0.001, n = 306) exists between these parameters. Any increases in χ_{LF} values are associated with corresponding increases in SIRM values. This indicates that the mineral magnetic signals of all the sediment samples are dominated by remanence type of magnetism (ferrimagnetic and/or canted-antiferromagnetic). Since, none of the data-points have high SIRM values and low χ_{LF} values, canted-antiferromagnetic behaviour is considered to be insignificant in these sediment samples, and the main type of magnetic remanence is ferrimagnetism.

Figure 5.9c shows χ_{ARM} versus SIRM, and as shown in Table 5.4 a strong positive correlation (r = 0.770; p <0.001) exists between these parameters. Any increases in ARM values are associated with corresponding increases in SIRM values. These results suggest that the mineral magnetic signals of the sediment samples in Wolverhampton are dominantly ferrimagnetic and that their magnetic grain sizes are predominantly ultrafine. The indication of χ_{LF} versus $\chi_{FD\%}$ (Figure 5.9d), suggests that the samples are dominated by multi domain magnetic grain sizes.

5.1.9 Relationships between mineral magnetic and geochemical parameters

Bivariate plots of specific geochemical properties have been selected for analysis due to their influence in urban settings with specific significance relating to anthropogenic activity (Table 1.5). Table 5.5 summarizes the correlation statistics between mineral magnetic and elemental parameters for the selected locations. Almost all mineral magnetic and geochemical parameters are correlated (i.e. most correlation of coefficients are *ca*. r = ≤0.221-0.517, p <0.05-<0.001, n = 306). This suggests that the chemistry of RDS has some influence on mineral magnetic assemblages. Those relationships that are statistically significant appear to be related to magnetic mineralogy parameters. Selected significant correlations are presented in Figures 5.10–5.15. Mineral magnetic concentration (χ_{LF}, χ_{ARM} and SIRM) and selected geochemical parameters show some strong positive correlations (p <0.001, n = 306).

Table 5.4 Statistical relationships between the mineral magnetic parameters of the cumulative UK sampled locations (**bold** text is significant (*p <0.05; **p <0.01; ***p <0.001)) (n = 306)

Parameters	χ_{LF}	$\chi_{FD\%}$	χ_{ARM}	SIRM	Soft $_{\% 20mT}$	Soft $_{\% 40mT}$	Hard $_{\% 300mT}$	Hard $_{\% 500mT}$	Soft $_{IRM20mT}$	Soft $_{IRM40mT}$	Hard $_{IRM 300mT}$	Hard $_{IRM 500mT}$	S-ratio	ARM/χ	SIRM/ ARM	SIRM/χ
$\chi_{FD\%}$	-0.243***															
χ_{ARM}	0.747***	-0.385***														
SIRM	0.904***	-0.313***	0.770***													
Soft $_{\% 20mT}$	0.283***	-0.095	0.273***	0.097												
Soft $_{\% 40mT}$	0.322***	-0.039	0.284***	0.184**	0.615***											
Hard $_{\% 300mT}$	-0.165**	-0.200**	0.046	0.026	-0.370***	-0.430***										
Hard $_{\% 500mT}$	-0.174**	-0.243***	0.019	-0.060	-0.194**	-0.263***	0.578***									
Soft $_{IRM20mt}$	0.917***	-0.329***	0.789***	0.898***	0.486***	0.402***	-0.122	-0.126								
Soft $_{IRM40mT}$	0.923***	-0.309***	0.783***	0.979***	0.197**	0.349***	-0.036	-0.096	0.931***							
Hard $_{IRM300mT}$	0.588***	-0.333***	0.598***	0.765***	-0.101	-0.076	0.497***	0.220**	0.616***	0.717***						
Hard $_{IRM500mT}$	0.515***	-0.390***	0.568***	0.664***	-0.036	-0.031	0.421***	0.652***	0.556***	0.626***	0.726***					
S-ratio	-0.266***	0.112	-0.212**	-0.287***	-0.136	-0.297***	0.082	0.153	-0.306***	-0.335***	-0.210**	-0.130*				
ARM/χ	-0.191**	0.056	0.270***	-0.021	-0.051	0.020	0.152*	0.089	-0.066	-0.028	0.055	0.105	-0.084			
SIRM/ARM	0.084	-0.190*	-0.185**	0.252***	-0.290***	-0.264***	0.193**	0.103	0.100	0.197**	0.337***	0.248***	0.000	-0.574***		
SIRM/χ	-0.120	-0.147*	0.104*	0.244**	-0.385***	-0.314***	0.406***	0.234***	0.021	0.167**	0.432***	0.400***	-0.057	0.454***	0.360***	
χ_{ARM}/SIRM	-0.084	0.190**	0.185**	-0.252***	0.290***	0.264***	-0.193**	-0.103	-0.100	-0.197**	-0.337***	-0.248***	0.000	0.574***	-1.000***	-0.360***

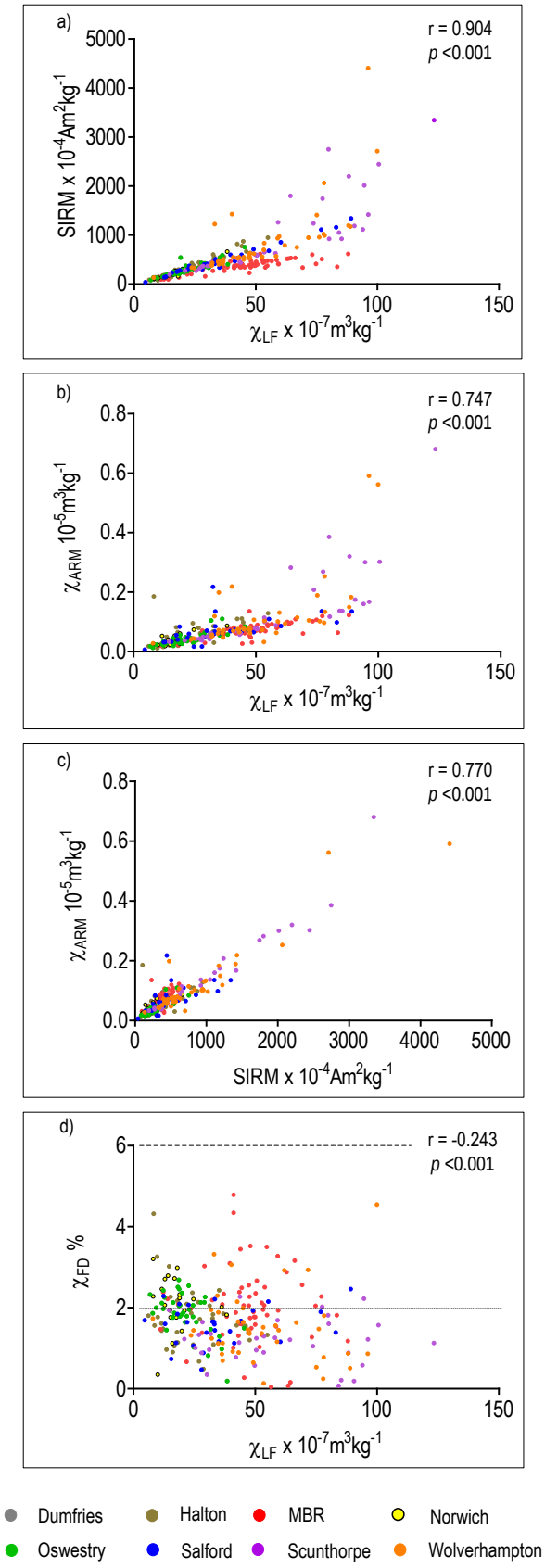

Figure 5.9 Bivariate plots of selected mineral magnetic parameters for the selected towns and cities (n = 306).

Table 5.5 Statistical relationships between the mineral magnetic and geochemical parameters for the sampled locations (**bold** text is significant (*p <0.05; **p <0.01; ***p <0.001)) (n = 306)

Parameters	χ_{LF}	$\chi_{FD\%}$	χ_{ARM}	SIRM	Soft $_{\%\ 20mT}$	Soft $_{\%\ 40mT}$	Hard $_{\%\ 300mT}$	Hard $_{\%\ 500mT}$	Soft $_{IRM20mT}$	Soft $_{IRM40mT}$	Hard $_{IRM\ 300mT}$	Hard $_{IRM\ 500mT}$	S-ratio	χ_{ARM} /χ	SIRM/ $_{ARM}$	SIRM/χ	χ_{ARM} /SIRM
Mg	0.388***	-0.118	0.256***	0.312***	0.162*	0.201**	-0.221**	-0.175*	0.370***	0.344***	0.088	0.086	0.039	-0.242***	0.091	-0.175*	-0.091
Al	0.139*	-0.074	0.046	0.124	0.163*	0.105	-0.108	-0.125	0.194**	0.141*	0.009	-0.017	0.122	-0.164*	0.163*	-0.050	-0.163*
S	0.355***	0.093	0.214**	0.120	0.317***	0.288***	-0.476***	-0.349***	0.263***	0.169*	-0.182*	-0.177*	0.013	-0.306***	0.214**	0.534***	0.213**
K	-0.194**	0.008	-0.181*	-0.099	-0.021	-0.120	0.230**	0.090	-0.093	-0.118	0.058	-0.012	0.204**	-0.025	0.229**	0.163*	-0.230**
Ca	0.474***	-0.174*	0.409***	0.353***	0.313***	0.261***	-0.193**	-0.051	0.449***	0.378***	0.112	0.198**	-0.044	-0.101	-0.162*	0.240***	0.161*
Ti	0.216**	0.019	0.112	0.185**	0.094	0.018	-0.106	-0.109	0.222**	0.191**	0.078	0.054	0.089	-0.209**	0.183**	-0.050	-0.182**
V	0.135	-0.110	0.088	0.165*	0.005	0.085	-0.154*	-0.228**	0.160*	0.175*	0.032	-0.009	0.055	-0.046	0.160*	0.018	-0.157*
Cr	0.626***	-0.080	0.595***	0.565***	0.099	0.081	-0.133	-0.039	0.548***	0.561***	0.300***	0.377***	-0.101	-0.067	-0.051	-0.060	0.050
Mn	0.656***	0.223**	0.551***	0.582***	0.295***	0.272***	-0.197**	-0.202**	0.649***	0.601***	0.294***	0.295***	-0.005	-0.149*	0.054	-0.122	-0.054
Fe	0.673***	-0.162*	0.553***	0.629***	0.146*	0.140*	-0.134	-0.195**	0.637***	0.638***	0.388***	0.333***	-0.019	-0.186**	0.177*	-0.034	-0.176*
Ni	0.394***	0.103	0.284***	0.276***	0.336***	0.099	-0.091	-0.080	0.379***	0.293***	0.171*	0.131	0.019	-0.187**	-0.007	-0.195**	0.007
Cu	0.547***	0.135	0.391***	0.351***	0.341***	0.134	-0.204**	-0.184**	0.459***	0.366***	0.154*	0.094	0.068	0.324***	-0.112	0.414***	0.110
Zn	0.599***	0.119	0.470***	0.379***	0.404***	0.221**	-0.309***	-0.244***	0.517***	0.408***	0.127	0.080	-0.026	-0.276***	0.190**	0.457***	0.189**
Cd	0.033	-0.119	0.059	0.076	0.060	0.003	0.029	0.094	0.088	0.078	0.049	0.126	0.017	0.099	0.053	0.199**	-0.052
Sb	0.099	0.195**	0.003	-0.051	0.156*	-0.021	-0.154*	-0.107	0.031	-0.035	-0.110	-0.124	0.028	-0.174*	-0.069	0.250***	0.070
Pb	0.473***	0.027	0.357***	0.321***	0.272***	0.118	-0.185**	-0.189**	0.411***	0.332***	0.143*	0.073	0.045	0.233***	-0.068	0.288***	0.067

Results for χ_{LF} versus geochemical parameters are shown in Figure 5.10 and 5.11, with the strongest relationship between χ_{LF} versus Fe (r = 0.673 (Figure 5.10a)), Pb (r = 0.473 (Figure 5.10b)), Cr (r = 0.626 (Figure 5.10c)), Ni (r = 0.394 (Figure 5.10d)), Zn (r = 0.599 (Figure 5.11a)), Mn (r = 0.656 (Figure 5.11b)), and Cu (r = 0.347 (Figure 5.11c)). These relationships are replicated within the χ_{ARM} (r = 0.284-0.595 (Figure 5.12 a-d and 5.13 a-c)) and SIRM (r = 0.276-0.629 (Figure 5.14a-d and 5.15a-c)) parameters. These results indicate that mineral magnetic concentration parameters do have potential for proxy purposes as RDS geochemical indicators at the national scale (UK).

5.1.10 Relationships between geochemical parameters

Relationships between geochemical parameters are presented in Table 5.6 and boxplots (Figure 5.16-5.17). Specific geochemical correlations in urban environments can indicate specific sources (Hopke *et al*., 1980; De Miguel *et al* 1997; Robertson *et* al., 2003; Omar and Al-Khashman, 2004; Manno *et al.,* 2006; Christofordis and Stamatis, 2009. The results for the selected locations show that most geochemical parameters exhibit strong correlation values between each other (p <0.05-<0.001) (Table 5.6). The largest correlation coefficients exist between Pb, Fe, Mg, Ti, Ni and Cu, with Mg and Al (r = 0.697; p <0.001, n = 220), Ma and Ca (r = 0.707; p <0.001) being the strongest, suggesting the influence of crustal material. Anthropogenic input is evident with strong correlations of Pb versus Cu (r = 0.659; p <0.001), Pb versus Zn (r = 0.605; p <0.001), Zn versus Cu (r = 0.771; p <0.001) Fe and Pb (r = 0.325; p <0.001 (Figure 5.16a)), Cr (r = 0.379; p <0.001 (Figure 5.16b)), Ni (r = 0.389; p <0.001 (Figure 5.16c)), Zn (r = 0.382; p <0.001 (Figure 5.17a)), Mn (r = 0.731; p <0.001 (Figure 5.17b)), Cu (r = 0.362; p <0.001 (Figure 5.17c)), and Ti respectively. The weakest correlation coefficient values are associated between Sb and most other elemental parameters (r = -0.157–0.315). Other parameters show to display strong relationships, Fe and Mg (r = 0.597), Fe and Ni (r = 0.529; p <0.001) and Fe and Cu (r = 0.522; p <0.001). Other parameters exhibit strong relationships between each other, Mg, Al, Ti, Ni, have correlation coefficients *ca*. r = ≤0.5–0.8 (p <0.001).

5.2 Summary mineral magnetic and textural relationships of selected UK sample locations

The application of mineral magnetic measurements as a proxy for RDS so far, has had limited success with selected UK samples. All eight selected locations have been investigated individually using previous methods discussed. To assess whether relationships exist between the mineral magnetic and textural parameters, the data sets of all eight locations were interrogated by correlation statistics (Spearman Rank). Results are detailed in Appendix 5.3.1-5.3.5 and summarized in Table 5.7. Results for individual UK locations show that most of the mineral magnetic and textural parameters do not exhibit many significant correlations between each other (Table 5.7). No significant relationships exist for Dumfries, Oswestry, Salford and Wolverhampton during the sampling period. Weak relationships exist for Halton and Norwich, strongest correlations exist for Scunthorpe and London.

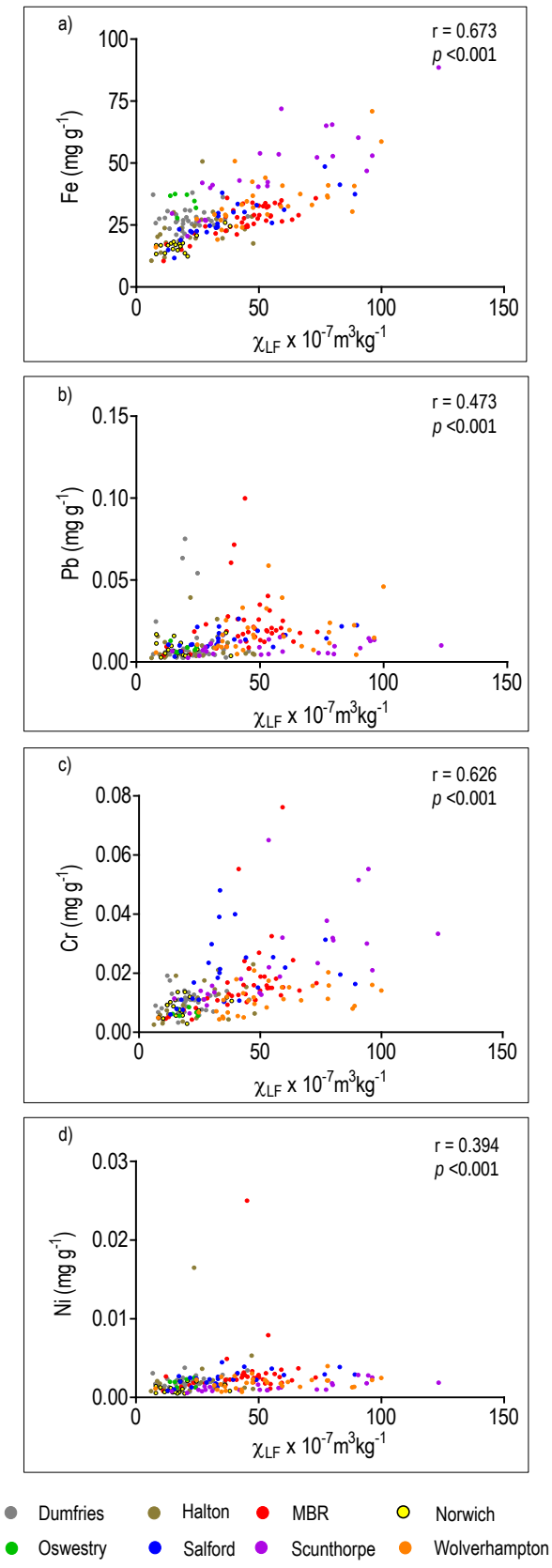

Figure 5.10 Bivariate plots of selected mineral magnetic and geochemical properties for the selected towns and cities (n = 306).

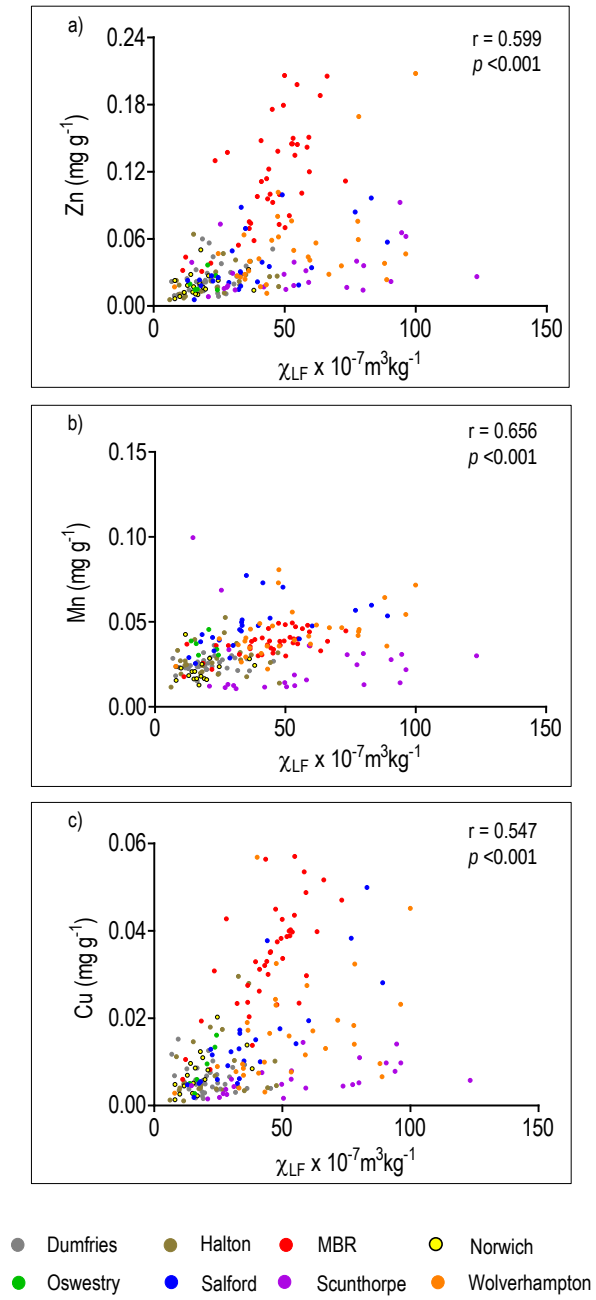

Figure 5.11 Bivariate plots of selected mineral magnetic and geochemical properties for the selected towns and cities (n = 306).

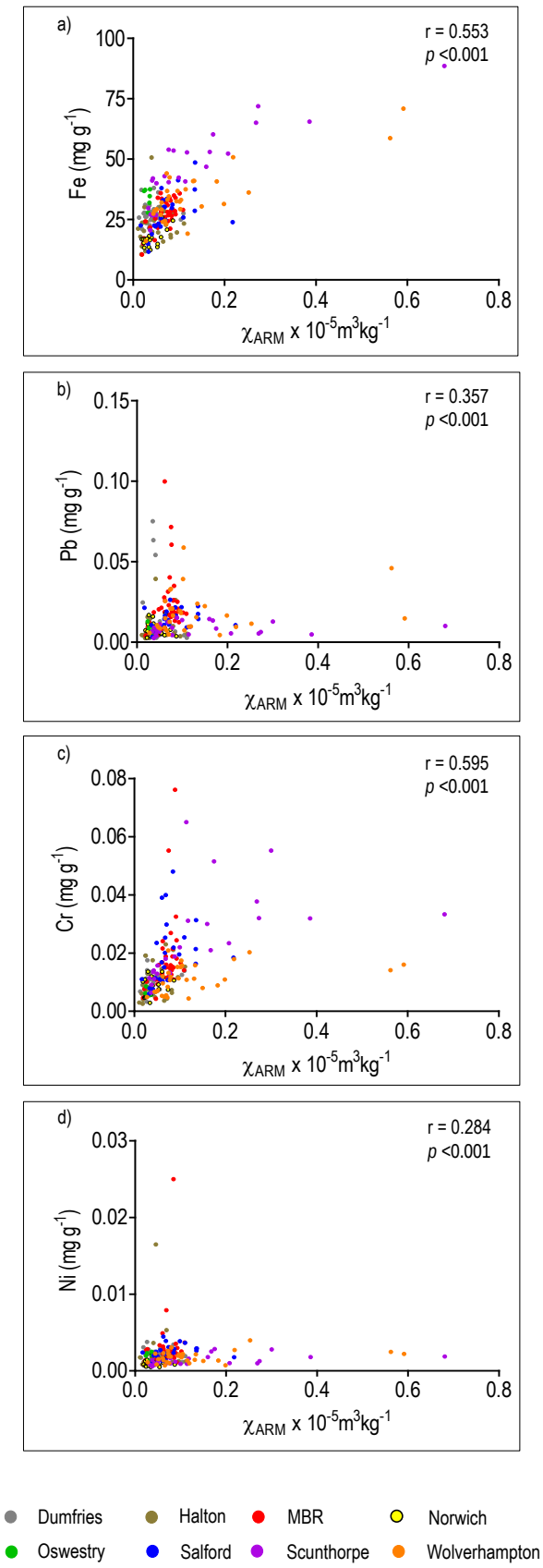

Figure 5.12 Bivariate plots of selected mineral magnetic and geochemical properties for the selected towns and cities (n = 306).

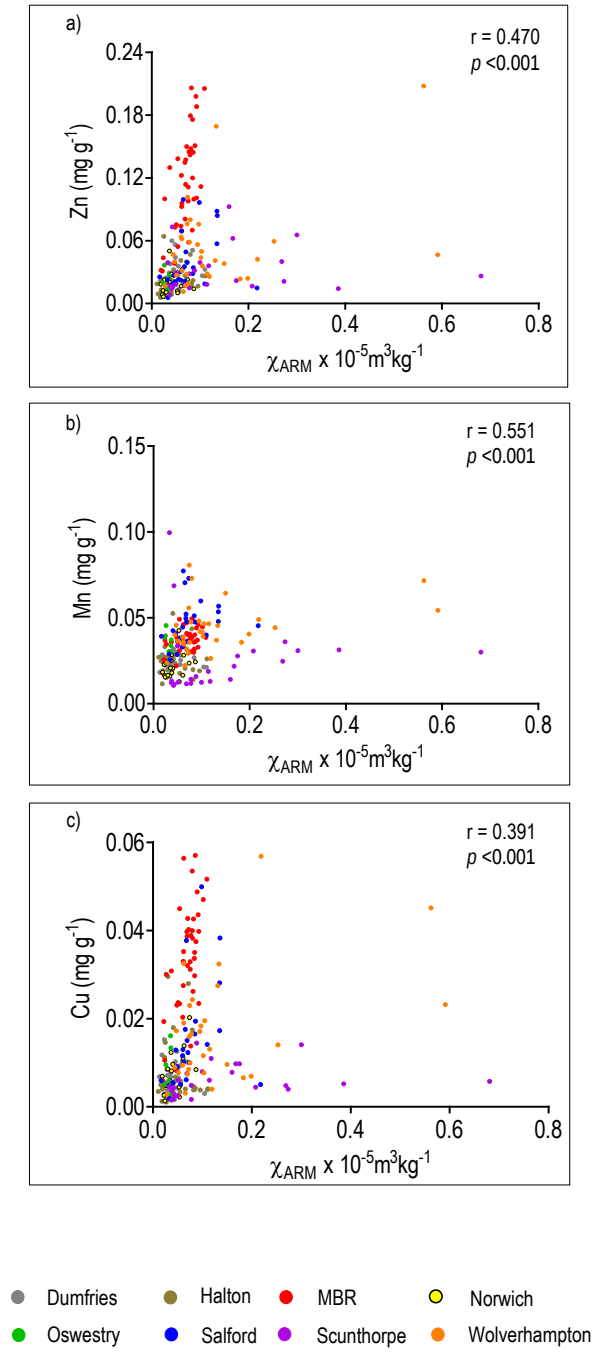

Figure 5.13 Bivariate plots of selected mineral magnetic and geochemical properties for the selected towns and cities (n = 306).

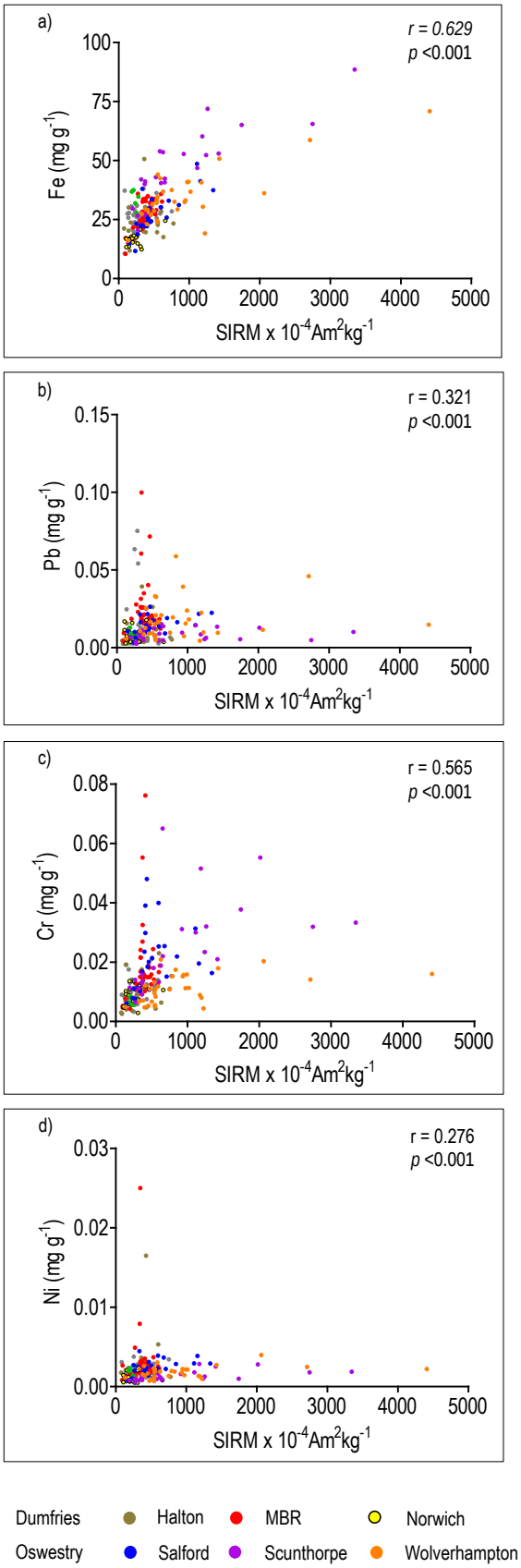

Figure 5.14 Bivariate plots of selected mineral magnetic and geochemical properties for the selected towns and cities (n = 306).

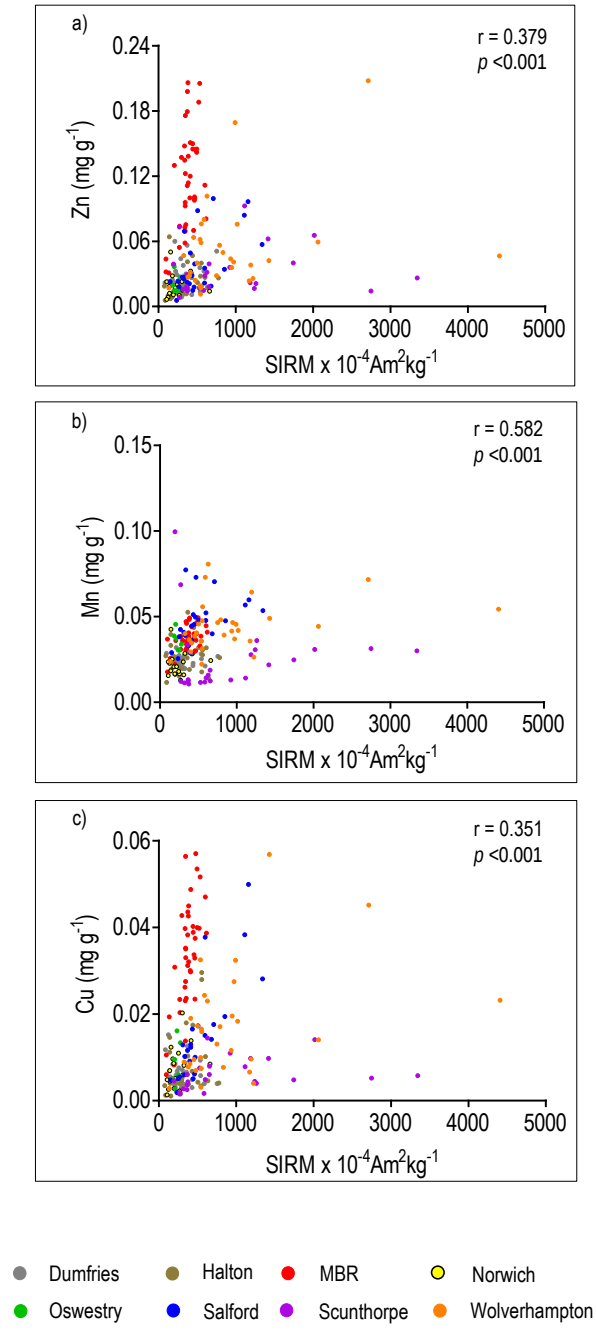

Figure 5.15 Bivariate plots of selected mineral magnetic and geochemical properties for the selected towns and cities (n = 306).

Table 5.6 Statistical relationships between the geochemical parameters for the sampled locations (**bold** text is significant (*p <0.05; **p <0.01; ***p <0.001)) (n = 306)

Parameters	Mg	Al	S	K	Ca	Ti	V	Cr	Mn	Fe	Ni	Cu	Zn	Cd	Sb
Al	0.697***														
S	0.513***	0.258***													
K	0.139	0.587***	-0.171*												
Ca	0.442***	0.004	0.427***	-0.495***											
Ti	0.631***	0.824***	0.321***	0.570***	-0.058										
V	0.514***	0.674***	0.238**	0.366***	-0.112	0.605***									
Cr	0.470***	0.212**	0.307***	-0.195*	0.542***	0.229**	0.096								
Mn	0.626***	0.387***	0.401***	-0.114	0.707***	0.330***	0.336***	0.582***							
Fe	0.680***	0.543***	0.321***	0.049	0.351***	0.567***	0.528***	0.579***	0.731***						
Ni	0.333***	0.392***	0.405***	0.201**	0.122	0.494***	0.169*	0.360***	0.293***	0.389***					
Cu	0.207**	0.061	0.479***	-0.115	0.327***	0.211**	-0.081	0.403***	0.350***	0.362***	0.592***				
Zn	0.208**	0.115	0.585***	-0.104	0.309***	0.244**	0.059	0.388***	0.430***	0.382***	0.571***	0.771***			
Cd	0.026	-0.114	-0.072	-0.228***	0.347***	-0.196*	-0.197	0.116	0.183**	-0.040	-0.102	-0.107	-0.153		
Sb	-0.041	-0.063	0.281***	-0.032	0.004	0.087	-0.108	0.017	-0.070	-0.020	0.257***	0.417***	0.300***	-0.009	
Pb	0.229**	0.130	0.410***	0.006	0.276***	0.259***	0.076	0.287***	0.389***	0.325***	0.435***	0.659***	0.605***	-0.093	0.301***

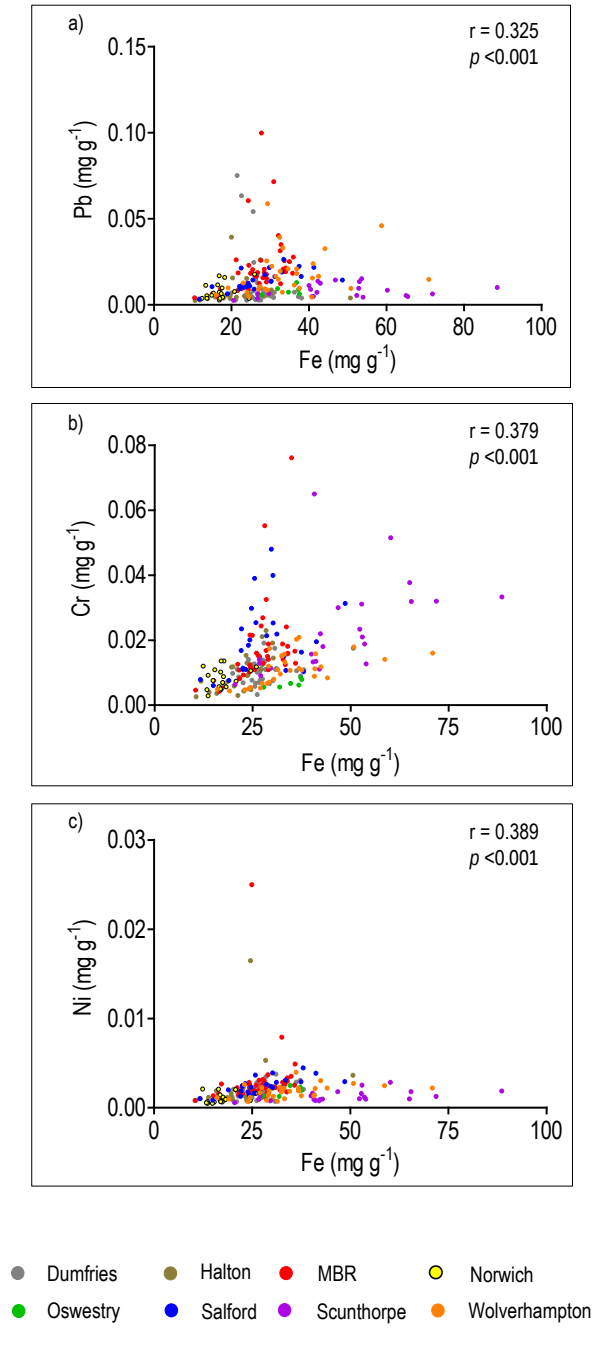

Figure 5.16 Bivariate plots of selected mineral magnetic and geochemical parameters for selected towns and cities (n = 306).

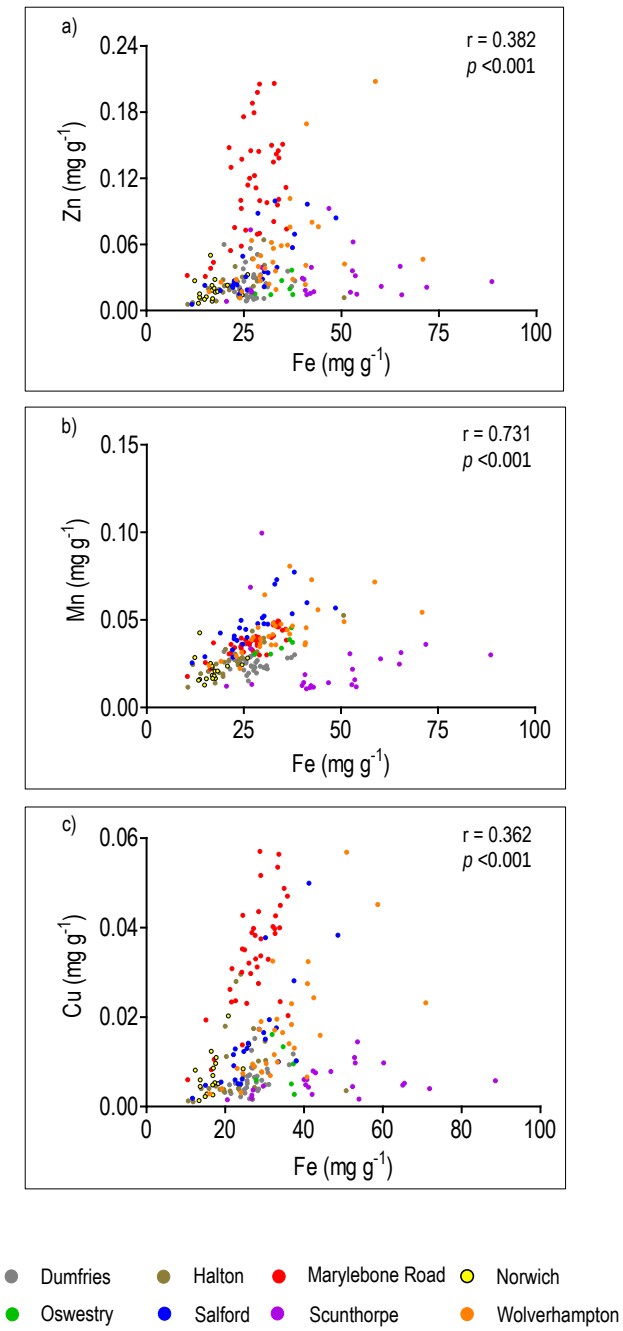

Figure 5.17 Bivariate plots of selected mineral magnetic and geochemical parameters for selected towns and cities (n = 306).

Table 5.7 Summary UK town Spearman rank correlation results for mineral magnetic and textural parameters (**bold** text is significant (*p <0.05; **p <0.01; ***p <0.001))

a) χ_{LF}	Sand	Silt	Clay	$PM_{1.0}$	$PM_{2.5}$	PM_{10}	PM_{100}
Cumulative (n = 306)	-0.050	0.068	-0.037	-0.010	-0.044	0.053	0.155*
Dumfries (n = 38)	-0.173	0.174	-0.057	-0.030	-0.053	0.026	0.230
Halton (n = 36)	0.204	-0.252	0.282*	0.349*	0.258	0.073	-0.231
MBR (n = 61)	0.076	0.010	-0.453***	-0.456***	-0.420**	-0.399**	0.035
Norwich (n =30)	-0.408	0.368	0.227	0.191	0.215	0.335	0.268
Oswestry (n = 32)	-0.095	0.119	0.032	-0.031	0.007	-0.058	0.135
Salford (n = 33)	-0.223	0.254	-0.295	-0.286	-0.308	-0.189	0.305
Scunthorpe (n = 34)	0.024	-0.110	0.053	0.048	0.067	0.120	-0.032
Wolverhampton (n = 42)	0.069	-0.110	0.281	0.149	0.294	0.278	-0.099

b) $\chi_{FD\%}$	Sand	Silt	Clay	$PM_{1.0}$	$PM_{2.5}$	PM_{10}	PM_{100}
Cumulative	0.191**	-0.166*	-0.178*	-0.213	-0.162*	-0.148*	-0.154*
Dumfries	-0.038	0.028	-0.119	-0.030	-0.090	0.032	-0.013
Halton	-0.036	0.062	-0.389**	-0.358***	-0.377*	-0.152	0.027
MBR	0.174	-0.170	-0.166	-0.167	-0.157	-0.180	-0.083
Norwich	0.224	-0.068	-0.382***	-0.459***	-0.356**	-0.211	-0.023
Oswestry	-0.038	0.028	-0.119	-0.030	-0.090	0.032	-0.013
Salford	-0.313	0.275	0.006	0.048	0.011	0.137	0.253
Scunthorpe	0.227	-0.224	-0.162	-0.137	-0.177	-0.275	-0.241
Wolverhampton	-0.333	0.346	-0.183	-0.180	-0.276	0.019	0.416*

c) χ_{ARM}	Sand	Silt	Clay	$PM_{1.0}$	$PM_{2.5}$	PM_{10}	PM_{100}
Cumulative	-0.117	0.132	-0.019	0.007	-0.028	0.081	0.195**
Dumfries	-0.090	0.107	0.074	0.061	0.078	0.066	0.094
Halton	0.225	-0.254	0.216	0.214	0.216	0.180	-0.277
MBR	-0.017	0.109	-0.384**	-0.392**	-0.355**	-0.365**	0.101
Norwich	-0.325	0.329	0.156	0.035	0.191	0.208	0.371
Oswestry	-0.090	0.107	0.074	0.061	0.078	0.066	0.094
Salford	-0.154	0.178	-0.221	-0.215	-0.201	0.012	0.144
Scunthorpe	0.086	-0.198	0.250*	0.146	0.262*	0.295*	-0.132
Wolverhampton	0.123	-0.146	0.274	0.204	0.283	0.169	-0.074

d) SIRM	Sand	Silt	Clay	$PM_{1.0}$	$PM_{2.5}$	PM_{10}	PM_{100}
Cumulative	-0.029	0.041	0.025	0.048	0.000	0.045	0.127
Dumfries	-0.076	0.091	0.127	0.078	0.101	0.021	0.124
Halton	0.203	-0.248	0.264	0.325	0.238	0.066	-0.210
MBR	0.135	-0.049	-0.553***	-0.554***	-0.550***	-0.519***	-0.076
Norwich	-0.474	0.432	0.257	0.205	0.260	0.364	0.374
Oswestry	-0.076	0.091	0.127	0.078	0.101	0.021	0.124
Salford	-0.227	0.251	-0.265	-0.259	-0.274	-0.117	0.305
Scunthorpe	0.109	-0.209	0.678***	0.537***	0.689***	0.609***	-0.145
Wolverhampton	0.082	-0.122	0.360	0.277	0.350	0.235	-0.028

Results for Dumfries, Norwich, Oswestry, Salford, Scunthorpe and Wolverhampton show no significant correlations with χ_{LF} versus all textural fractions (Table 5.7a). Correlations do exist for χ_{LF} versus $<PM_{10}$ in London (r = -0.526 to -0.589; p <0.001, n= 61), and weak correlations (r = 0.282-0.349; p <0.05, n= 36) for χ_{LF} versus $<PM_{2.0}$ in Halton. Table 5.7b summarizes the correlation statistics between $\chi_{FD\%}$ versus $<PM_{100}$ and displays significant relationships for Halton $<PM_{2.5}$ (r = 0.358-0.389; p <0.01). Significant relationships exist between $\chi_{FD\%}$ versus $<PM_{2.5}$ for Norwich (r = -0.356 to -0.459; p <0.001). Wolverhampton displays a moderately weak relationship with $\chi_{FD\%}$ versus $<PM_{100}$ (r = 0.416; p <0.01, n= 42). Results for Scunthorpe and London show that there are moderate relationships between χ_{ARM} versus $PM_{2.0}$ to PM_{10} for Scunthorpe (r = 0.250-0.295; p <0.05, n= 34) and χ_{ARM} versus $PM_{1.0}$ to PM_{10} for London (r = 0.355-0.392; p <0.01 (Table 5.7c)). London and Scunthorpe exhibit moderate relationships with SIRM versus $<PM_{10}$ (r = 0.353-0.413; p <0.01 and 0.537-0.689; p <0.001 (Table 5.7d)). All other mineral magnetic parameters and textural parameters are not strongly related (*ca*. r = ≤-0.050–0.212, p <0.05).

The results show few significant correlations between mineral magnetic and textural parameters. Variation exists between the locations, with most towns having no proxy potential for PM identification. The strongest potential for proxy purposes exist between London and Scunthorpe. To further access the suitability of using mineral magnetic methods as a pollution proxy, these relationships will be further explored in London and Scunthorpe.

5.3 Relationships between the mineral magnetic and textural variables for London (Marylebone Road)

To assess the relationships between the mineral magnetic and textural variables for London, the data set was further interrogated using correlation statistics and bivariate plots. Statistical tests indicate that significant relationship exists between some of the mineral magnetic and textural parameters (p <0.05). However, it is only those relationships with the strongest correlation coefficient values that have been selected for further examination through bivariate plot analysis. These are presented in Figures 5.18–5.20.

Table 5.8 summarizes correlation statistics between the mineral magnetic and textural parameters for London. Strongest correlation coefficients were evident between magnetic concentration dependent parameters χ_{LF} versus PM $_{1.0}$ (r = -0.589; p <0.001, n = 61 (Figure 5.18a)). Mineral magnetic concentration values show strong correlations with the finer fraction of RDS as magnetic concentration parameters show good negative correlation with the smaller textural fractions ($PM_{1.0}$–PM_{10}). However, the weakest correlation coefficients are associated with Hard % parameters (r = 0.050; p = 0.727), suggesting hard mineralogy has no influence. Sand, silt and PM_{100} particles are not significantly correlated to any mineral magnetic parameter. Figure 5.18a-c shows strong negative correlation between χ_{LF} versus textural parameters $<PM_{10,}$ all display significant correlations (r = -0.526 to -0.589; p <0.001).

Table 5.8 Statistical relationships between the mineral magnetic and textural parameters for London (**bold** text is significant (*p <0.05; **p <0.01; ***p <0.001)) (n = 61)

Parameters	Median-PS	Mean-PS	Sorting	Skewness	Kurtosis	Sand	Silt	Clay	$PM_{1.0}$	$PM_{2.5}$	PM_{10}	PM_{100}
χ_{LF}	-0.361*	-0.198	-0.404**	-0.464***	-0.105	0.076	0.010	-0.575***	-0.589***	-0.586***	-0.526***	0.035
$\chi_{FD\%}$	-0.145	-0.121	-0.220	-0.185	0.119	0.174	-0.170	-0.166	-0.167	-0.157	-0.180	-0.083
$\chi/_{ARM}$	-0.399**	-0.284*	-0.388**	-0.421**	-0.169	-0.017	0.109	-0.384**	-0.392**	-0.355**	-0.365**	0.101
SIRM	-0.154	-0.042	-0.357**	-0.248	-0.066	0.135	-0.049	-0.553***	-0.554***	-0.550***	-0.519***	-0.076
Soft $_{\% 20mT}$	0.138	0.119	0.358**	0.308*	-0.061	-0.173	0.159	0.313*	0.317*	0.265*	0.338**	0.100
Soft $_{\% 40mT}$	0.121	0.102	0.290*	0.256*	-0.029	-0.194	0.144	0.267*	0.269*	0.265*	0.308*	0.089
Hard $_{\% 300mT}$	0.013	-0.040	-0.067	0.075	0.113	-0.020	-0.016	0.089	0.089	0.120	0.084	0.000
Hard $_{\% 500mT}$	0.148	0.123	-0.099	0.055	0.191	0.115	-0.167	0.050	0.060	0.056	-0.055	-0.159
Soft $_{IRM20mt}$	-0.163	-0.058	-0.467***	-0.286*	0.049	0.213	-0.129	-0.389**	-0.358**	-0.375**	-0.428**	-0.147
Soft $_{IRM40mT}$	-0.131	-0.013	-0.442***	-0.299*	0.022	0.230	-0.149	-0.404**	-0.374**	-0.406**	-0.473***	-0.172
Hard $_{IRM300mT}$	0.029	0.085	0.049	0.090	-0.065	0.015	0.040	0.011	0.042	-0.030	0.000	-0.030
Hard $_{IRM500mT}$	0.038	0.068	0.098	0.106	-0.128	-0.101	0.124	0.040	0.061	0.041	0.074	0.059
S-ratio	-0.095	-0.030	-0.236	-0.227	-0.071	0.013	0.029	-0.331*	-0.288	-0.331**	-0.261*	0.020
χ_{ARM}/χ	-0.014	-0.119	0.078	0.116	-0.122	-0.116	0.096	0.222	0.215	0.225	0.143	0.072
$SIRM/_{ARM}$	0.218	0.279	0.021	0.144	0.226	0.231	-0.220	0.009	0.038	-0.026	-0.001	-0.242
$SIRM/\chi$	0.333*	0.301	0.173	0.330*	0.065	0.114	-0.119	0.240	0.277*	0.185	0.102	-0.194
χ_{ARM} /SIRM	-0.218	-0.279*	-0.021	-0.144	-0.226	-0.231	0.220	-0.009	-0.038	0.026	0.001	0.242

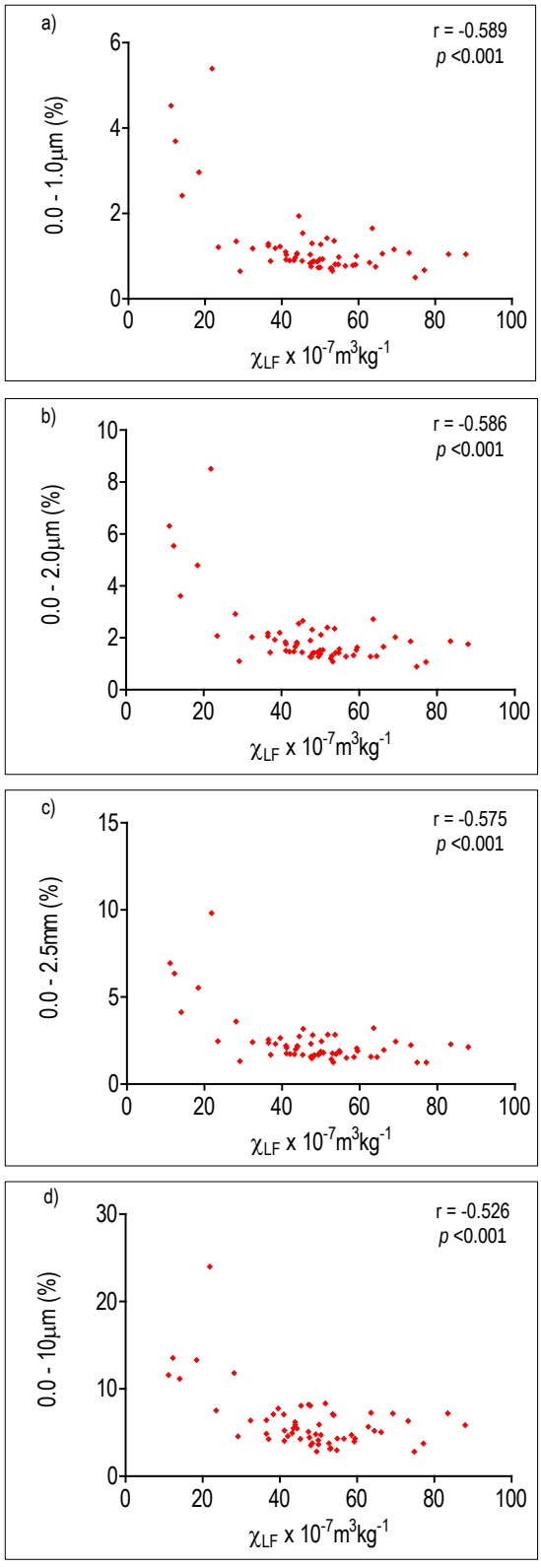

Figure 5.18 Bivariate plots for selected mineral magnetic and textural parameters for London (Marylebone Road) RDS (n = 61).

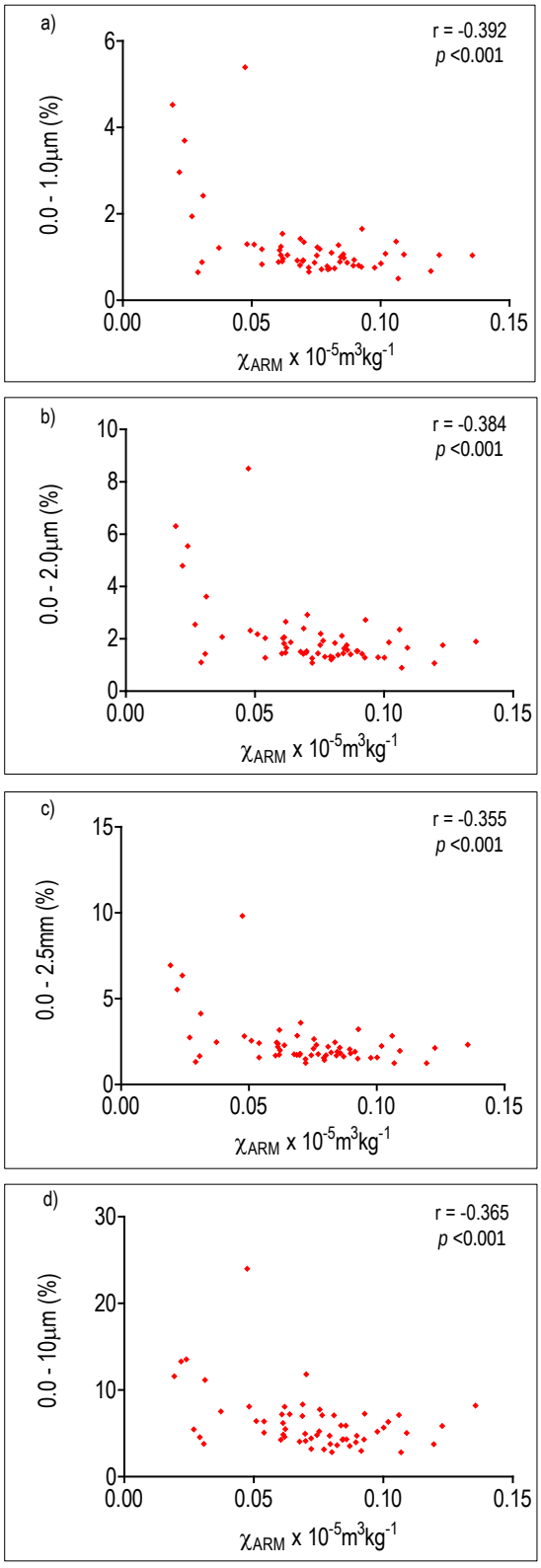

Figure 5.19 Bivariate plots for selected mineral magnetic and textural parameters for London (Marylebone Road) RDS (n = 61).

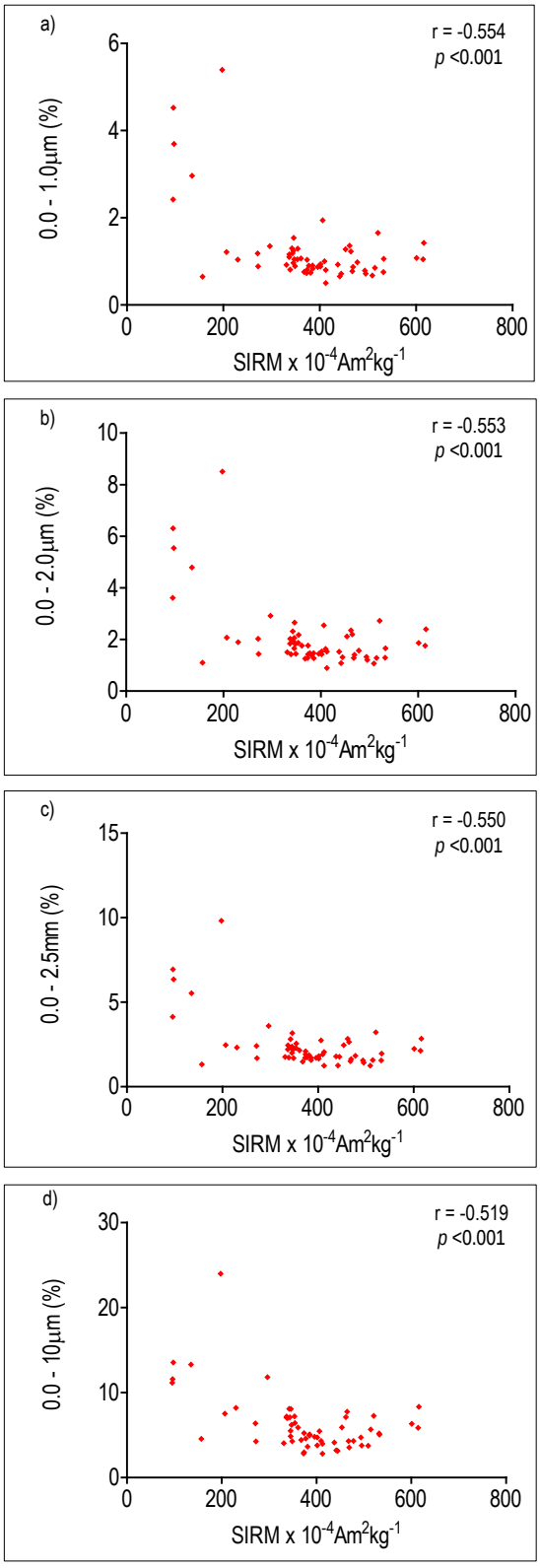

Figure 5.20 Bivariate plots for selected mineral magnetic and textural parameters for London (Marylebone Road) RDS (n = 61).

Figure 5.19a-c shows the bivariate relationships between magnetic concentration parameters χ_{ARM} versus textural parameters $<PM_{10}$, all display significant correlations (r = -0.355 to -0.392; *p* <0.01). Figure 5.20 a-c shows bivariate relationships between magnetic concentration parameters SIRM versus textural parameters $<PM_{10}$, all displaying significant correlations (r = -0.519 to -0.554; *p* <0.001).

The correlations between the mineral magnetic concentration and textural parameters have shown relative consistency. Consistent weakening of the correlation is evident through the particle size range (χ_{LF}, r = 0.589-0.526; χ_{ARM}, r = 0.511-0.402; SIRM, r = 0.554-0.519; *p* <0.001). Mineral magnetic concentration parameters display moderate negative correlations with RDS sorting (*p* <0.01). The strongest correlation is with χ_{LF} versus sorting (r = -0.414; *p* <0.01), with similar correlations with χ_{ARM} (r = -0.388; *p* <0.01), and SIRM (r = -0.357; *p* <0.01). This is a good indication that the greater the concentration of magnetic material the more it is well sorted.

Relationships between magnetic mineralogy dependent parameters $Soft_{\%}$ and $Soft_{IRM}$ versus textural parameters $<PM_{10}$, all display significant correlations (*p* <0.05-<0.01). The weak correlations found between hard and textural parameters suggest that hard mineralogy has no influence on mineral magnetic and textural relationships. Almost all other mineral magnetic and textural parameters are not strongly correlated (i.e. most correlation of coefficient values are *ca*. r = ≤-0.044-0.297). This suggests that the mineral magnetic concentration parameters do have some control on finer fractions of sediments on Marylebone Road.

The strength of the correlations suggests that the characteristics of the mineral magnetic and textural properties could be dependent upon each other. The statistical tests indicate that significant relationships exist between mineral magnetic concentration parameter and fine particle class sizes $<PM_{10}$ (*p* <0.05). These relationships indicate that mineral magnetic methods on Marylebone road could potentially be used as a particle size proxy, with low levels of mineral magnetic concentrations used to estimate higher levels of fine PM (<10 µm). High levels of fine PM on Marylebone Road suggests a dilution effect, which indicates mixing of magnetic and non-magnetic materials.

5.4 Further investigation using Spatial, SEM and factor plot characterization of London physical-characteristics.

Statistical and graphical techniques indicate that significant variations exist in the sedimentological characteristics of the contemporary surface sediments in the sample locations. So far, it has been demonstrated 'how' the samples vary, in terms of their mineral magnetic and textural properties, and that some variation is associated with differences in sedimentary environments. However, the geographical relationships between adjacent samples have not been addressed, nor has an environmental explanation for 'why' these variations exist. These points when addressed may lead to further understanding as to why mineral magnetic and textural relationships exist. Therefore, the mineral magnetic and textural data was used to generate a selection of GIS images and determine the nature of spatial variations.

5.4.1 Spatial characterization of mineral magnetic and geochemical data

Statistical and graphical techniques indicate significant variations in physical characteristics of London (Marylebone Road) RDS. However, bivariate plots and Mann-Whitney U tests failed to show geographical relationships between adjacent samples. Therefore, the mineral magnetic, textural and geochemical data have been used to generate GIS images, determining the nature of spatial variations. Baseline maps were created in Arcview GIS (version 10), forming visual representations of characteristics and patterns. The masked boundary excludes unsampled areas. Spatial variation for other UK locations can be found in Appendix 5.5.1-5.5.5

GIS images are presented of mineral magnetic concentration parameters ($\chi_{LF,}$ χ_{ARM} and SIRM). Both sides of Marylebone Road have been sampled to produce a representation of bi-directional traffic. Figure 5.21 shows χ_{LF} to vary across the sampling area. There are several moderate concentrations of χ_{LF} directly associated with the main road system within the sampling area, these are highlighted in Figure 5.21 (up to χ_{LF} 87.971 x $10^{-7}m^3kg^{-1}$). There are several high and low concentrations along the road. The higher concentrations appear to coincide with stop-start points associated with traffic lights and pedestrian crossings.

High concentrations of magnetic material (χ_{LF} 87.971 x $10^{-7}m^3kg^{-1}$) is found near Marylebone Road ASU (~50 m east of Madame Tussards) and highlights the monitoring importance of this site (Appendix 7.2 shows 'The West Minster Council Air Quality Progress Report 2010'). Figure 5.22a χ_{ARM} shows concentrations also vary across the sample area, with similar patterns of highs and lows associated with traffic stop-start points. This pattern is also evident in Figure 5.22b, with SIRM concentrations varying at these sample points. High SIRM concentrations could be due to being west of the sampling area where there is a convergence of roads into a bottle-neck, which experiences high traffic flows. Figure 5.23a shows concentrations of Cu along Marylebone Road and identifies high concentrations at the road interchange at the west of the road. Highs and lows can also be identified with pedestrian crossings, junctions and traffic lights. High concentrations are at the junctions of Baker Street and Regents Park and also within close proximity of the ASU. Figure 5.23b shows concentrations of Zn to vary across the sampling area, with similar spatial patterns to χ_{ARM} concentrations. Concentrations of Zn show highs and lows across the sampling area, with increased high readings at the junctions of Baker Street, Regents Park and high readings close to Marylebone Road ASU.

5.4.2 Assessing the potential linkages

The GIS images highlighted the variability of parameters over the study area and suggest environmental influences. By investigating variability using GIS it has been possible to identify these potential factors. The main observation is high concentrations of magnetic material associated with junctions, traffic lights and pedestrian crossings. These are areas that are subjected to high volumes of traffic undergoing start-stop manoeuvres, the consequence of such activity is the increase of fuel consumption and CO_2 emissions when pulling away and increased brake wear when stopping.

	Sample	χ		Sample	χ
i	4	83.462	v	21	87.971
ii	8	11.130	vi	23	18.421
iii	47	77.177			
iv	49	28.150			

Figure 5.21 Spatial distribution of χ_{LF} concentrations on Marylebone Road (London).

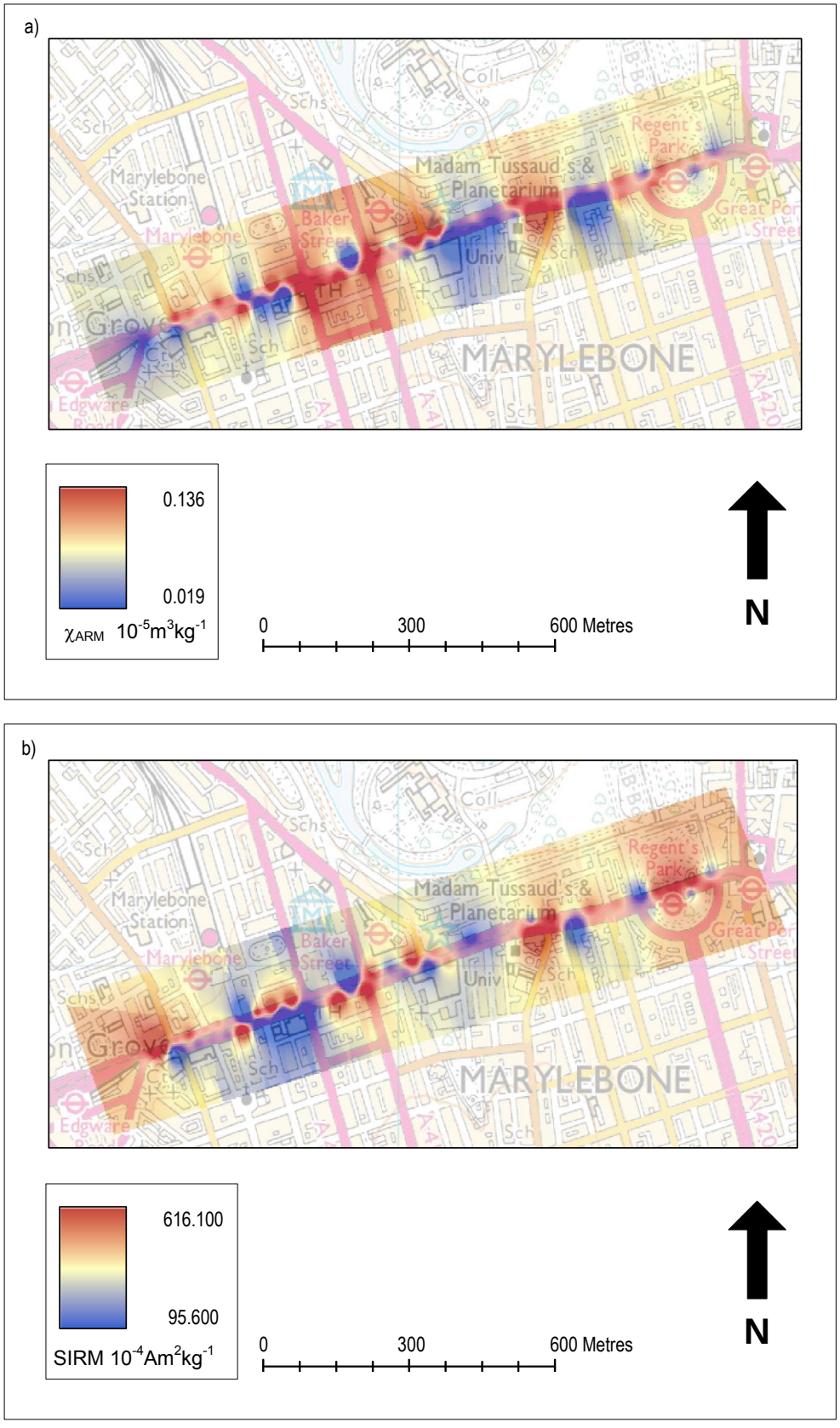

Figure 5.22 Spatial distribution of χ_{ARM} and SIRM concentrations on MBR (London).

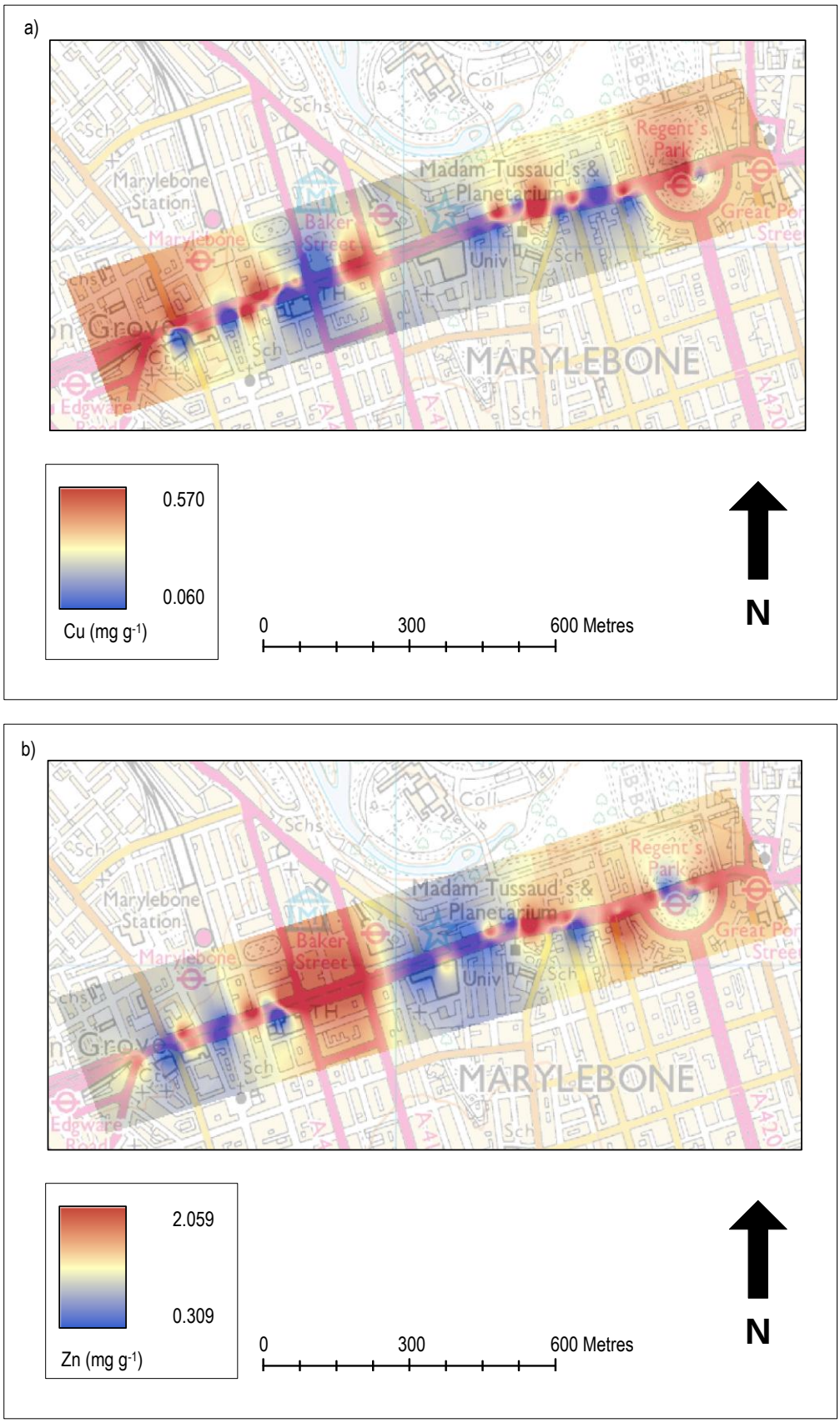

Figure 5.23 Spatial distribution of Cu and Zn concentrations on MBR (London).

Figure 5.24a shows the bivariate relationship between χ_{LF} versus Distance to stopping points (SP). The correlation shows a strong negative relationship which indicates the increase in magnetic material the closer to the SP (r = -0.541; p <0.001). This relationship is also apparent within other mineral magnetic parameters, χ_{ARM} (r = -0.459; p <0.001 (Figure 5.24b)) and SIRM (r = -0.374; p <0.01 (Figure 5.24c)). These correlations show that proximity to SP's are an important factor for mineral magnetic concentrations on Marylebone Road. An assumption based on road proximity can be made from the results found in Wolverhampton and can be applied to this setting with relative confidence. The road experiences dense road traffic and therefore suggests increased concentrations of magnetic material in RDS from this source. To further explore and confirm the source of magnetic material, selected parameters were used to access variability.

The S-ratio confirms that the mineralogy of the samples does not change with distance from SPs (Figure 5.25a). SIRM/χ (Figure 5.25b) values also indicate a consistent source. Figure 5.25c displays no correlation between $\chi_{FD\%}$ versus distance to SP (r = 0.175; p = 0.182) and demonstrates a good indication of a constant source of mineral magnetic material along Marylebone Road. Mineral magnetic and geochemical correlations for all other location can be found in Appendix 5.4.1-5.4.10. Selected geochemical parameters show the relatively consistent concentration of Fe (Figure 5.26a) and Pb (Figure 5.26b) across the sample area. These elements are commonly found in higher concentrations within urban and industrial areas due to being combustion by-products. No significant correlation was found between Fe and SP (r = -0.188; p = 0.243) and Pb and SP (r = -0.159; p = 0.324). The weak relationships found between Fe and Pb could be due to daily street washing, cleaning and the settlement times of combustion particulate (hours - days). Another explanation could be that geochemical analysis cannot distinguish between Fe_2O_3 (haematite) and Fe_3O_4 (magnetite), thus, not obtaining a true indication of the magnetite phase of Fe. χ_{LF} and SP correlations suggest higher concentrations of Fe_3O_4 at the SPs. Figure 5.27a-c shows Zn, Mn and Cu, which can be directly associated with tyre wear, abrasion of vehicles, lubricating oils and brake-linings. Moderate negative correlations exist for Zn and SP (r = -0.384; p <0.01 (Figure 5.27a)), Mn and SP (r = -0.347; p <0.01 (Figure 5.27b)) and CU and SP (r = -0.355; p <0.01 (Figure 5.27c)). These correlation coefficients suggest that SP has some influence on concentrations of Zn, Mn and Cu, with increase of these elements closer to SPs. This association is likely to be a function of vehicles slowing and stopping, due to friction and impact particles as they deposit directly on the road surface. Marylebone Road had the highest concentration of Cu (0.337 mg g^{-1}) out of all the selected towns and cities and reflects the traffic movements in this area.

5.4.3 Relationships between the geochemistry parameters

To further access the likelihood that geochemical composition on Marylebone Road is due to predominantly road traffic, the relationships between elements can be accessed. Previous research found that certain correlations between selected parameters can indicate potential sources.

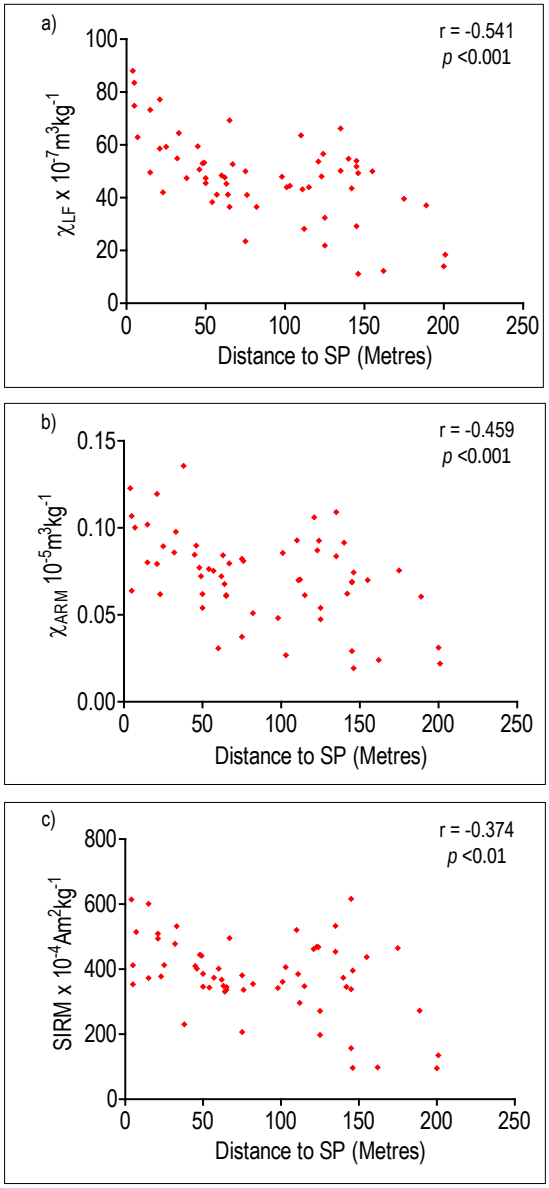

Figure 5.24 Bivariate plots of χ_{LF}, χ_{ARM} and SIRM versus distance to stopping points (SP) on MBR (London).

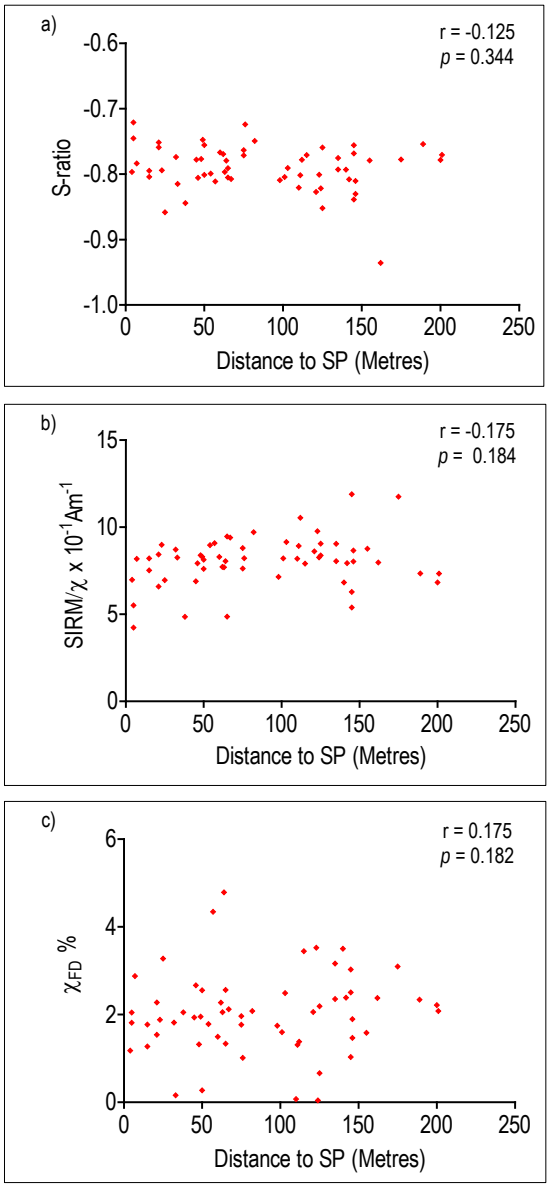

Figure 5.25 Bivariate plots of S-ratio $\chi_{FD\%}$ and SIRM/χ versus distance to stopping points (SP) on MBR (London) (n = 61).

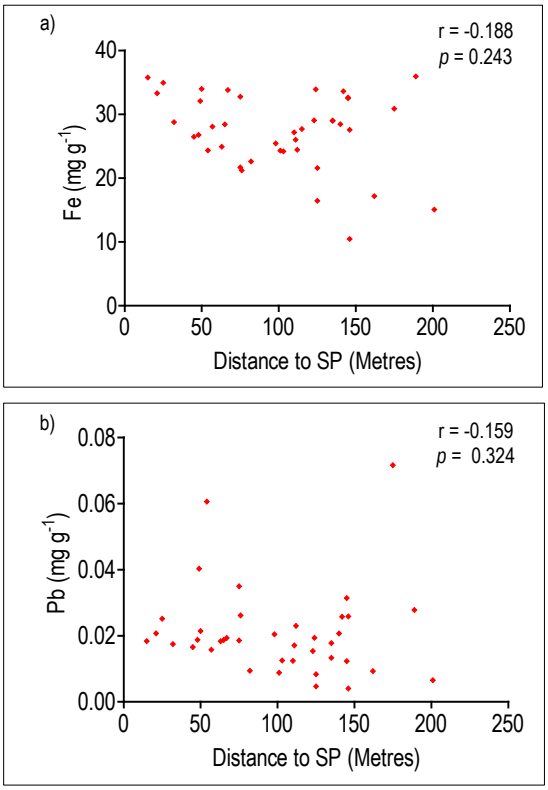

Figure 5.26 Bivariate plots of Fe and Pb versus distance to stopping points (SP) on MBR (London) (n = 61).

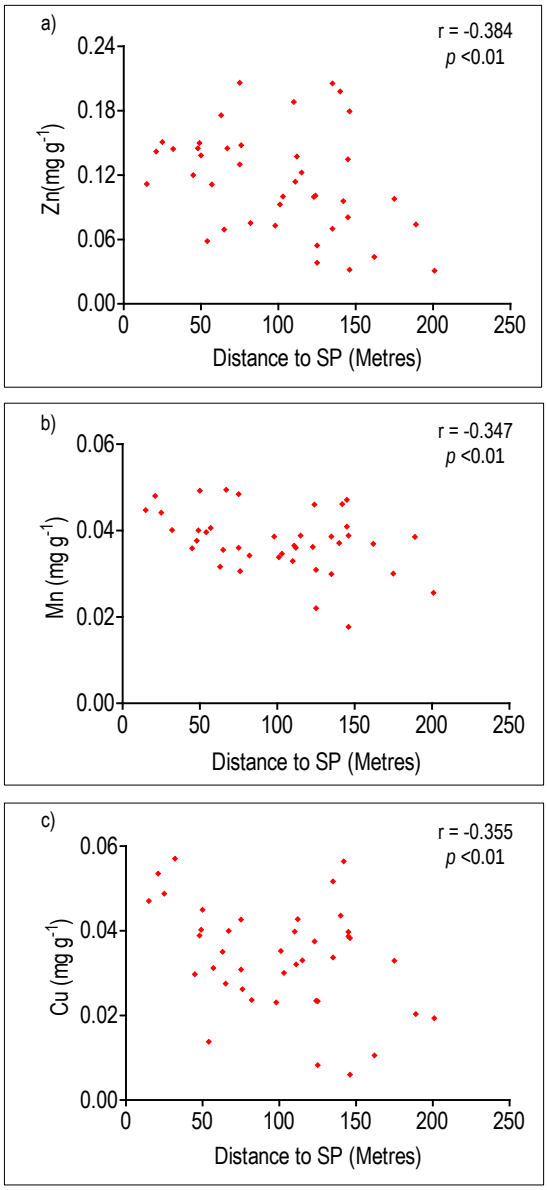

Figure 5.27 Bivariate plots of Zn, Mn and Cu versus distance to stopping points (SP) on MBR (London) (n = 61).

The mineral magnetic measurements identify that mineralogy within RDS on Marylebone Road is likely to be from a single source. As a result, Marylebone Road RDS exhibit strong correlations between specific geochemical parameters (p <0.05-<0.001) (Table 5.9). The strongest correlation coefficients exist between Fe, Mg, Al, Ti, Cu and Zn.

The strongest correlations are between Mg and Al (r = 0.835; p <0.001), Ti and Mn (r = 0.820; p <0.001) and Fe and Mn (r = 0.818; p <0.001). The weakest correlation coefficients are associated with Ca (r = 0.019–0.292), Cd (r = 0.004-0.111) and most other geochemical parameters. Other geochemical parameters show significant correlations. Fe versus Pb shows a relatively weak correlation between (r = 0.299; p <0.05 (Figure 5.28a)), where Cr (Figure 5.28b) and Ni (Figure 5.28c) have strong correlations (r = 0.413-0.526; p <0.01-<0.001). Other significant geochemical correlations include Fe versus Zn (r = 0.742; p <0.001 (Figure 5.29a)), Fe versus Mn (r = 0.818; p <0.001 (Figure 5.29b)), Fe versus Cu (r = 0.695; p <0.001 (Figure 5.29c)) and Fe versus Ti (r = 0.742; p <0.001 (Figure 5.29d)).

Other parameters exhibit strong inter-relationships, Mg, Al, Ti, Cu and Zn, *ca*. r = ≤0.5–0.8. These key parameters (Fe, Pb, Cr, Ni, Zn, Cd, Mn, Ti and Cu), further indicate the main source of elements are from anthropogenic combustion processes. The inter-correlation of Mg, Al, S, K and Fe indicate an additional natural background source (soils) of elements in the RDS cocktail. The geochemical correlation coefficients indicate several sources contributing to the physical properties of RDS with anthropogenic sources dominating the mineral magnetic signal.

5.4.4 Relationships between the mineral magnetic and geochemistry parameters

To further access the source of magnetic material within Marylebone Road RDS, geochemical and mineral magnetic parameters were interrogated by correlation statistics (Spearman Rank). Table 5.10 summarizes correlation statistics between the mineral magnetic and geochemical parameters for Marylebone Road. A large proportion of mineral magnetic concentration parameters and geochemical parameters are strongly related (i.e. most correlation coefficients are *ca*. r = ≤0.382–0.764). This suggests that the chemistry of RDS does have some control on mineral magnetic assemblages on Marylebone Road.

The strongest relationships that are statistically significant appear to be related to mineral magnetic concentration parameters, χ_{LF} versus Fe (r = 0.764; p <0.001) (Figure 5.30a), χ_{ARM} versus Fe (r = 0.740; p <0.001) and SIRM versus Fe (r = 0.651; p <0.001). Figure 5.30b shows a weak correlation between χ_{LF} versus Pb (r = 0.120; p = 0.460), whereas Figure 5.30c,d shows moderate correlation coefficients between χ_{LF} versus Cr (r = 0.382; p <0.01) and χ_{LF} versus Ni (r = 0.313; p <0.05). Figure 5.31 shows strong correlations between significant SP elements. χ_{LF} versus Zn (r = 0.646; p <0.001 (Figure 5.31a)). χ_{LF} versus Mn (r = 0.598; p <0.001 (Figure 5.31b)). A very strong correlation was found between χ_{LF} versus Cu (r = 0.720; p <0.001 (Figure 5.31c)) and a good correlation between χ_{LF} versus Ti (r = 0.604; p <0.001 (Figure 5.31d)).

Table 5.9 Statistical relationships between geochemical parameters for MBR (**bold** text is significant (*p <0.05; **p <0.01; ***p <0.001)) (n = 61)

Parameters	Mg	Al	S	K	Ca	Ti	V	Cr	Mn	Fe	Ni	Cu	Zn	Cd	Sb
Al	0.835***														
S	0.599***	0.378*													
K	0.707***	0.630***	0.572***												
Ca	0.249	0.173	0.019	0.248											
Ti	0.826***	0.877***	0.586***	0.615***	0.069										
V	0.556***	0.685***	0.211	0.393*	0.111	0.709***									
Cr	0.403*	0.192	0.499**	0.197	0.057	0.257	0.052								
Mn	0.753***	0.740***	0.491**	0.529***	0.067	0.820***	0.530***	0.299							
Fe	0.644***	0.677***	0.467**	0.420**	-0.242	0.742***	0.438**	0.413**	0.818***						
Ni	0.204	0.190	0.350*	0.355*	0.134	0.214	0.165	0.102	0.019	0.526***					
Cu	0.460*	0.465**	0.612***	0.289*	-0.263	0.576***	0.282	0.384*	0.627***	0.695***	0.087				
Zn	0.323*	0.239	0.806***	0.329*	-0.158	0.469**	0.184	0.347*	0.464**	0.472**	0.260	0.715***			
Cd	0.056	0.035	-0.262	-0.067	0.034	0.039	0.188	-0.111	0.102	0.057	-0.075	-0.083	-0.111		
Sb	0.093	0.132	-0.160	-0.028	0.057	0.103	0.250	-0.132	0.103	0.083	-0.027	0.047	-0.051	0.703***	
Pb	0.295	0.351*	0.095	0.252	-0.174	0.473**	0.425**	0.042	0.227	0.299	0.033	0.100	0.173	0.100	0.138

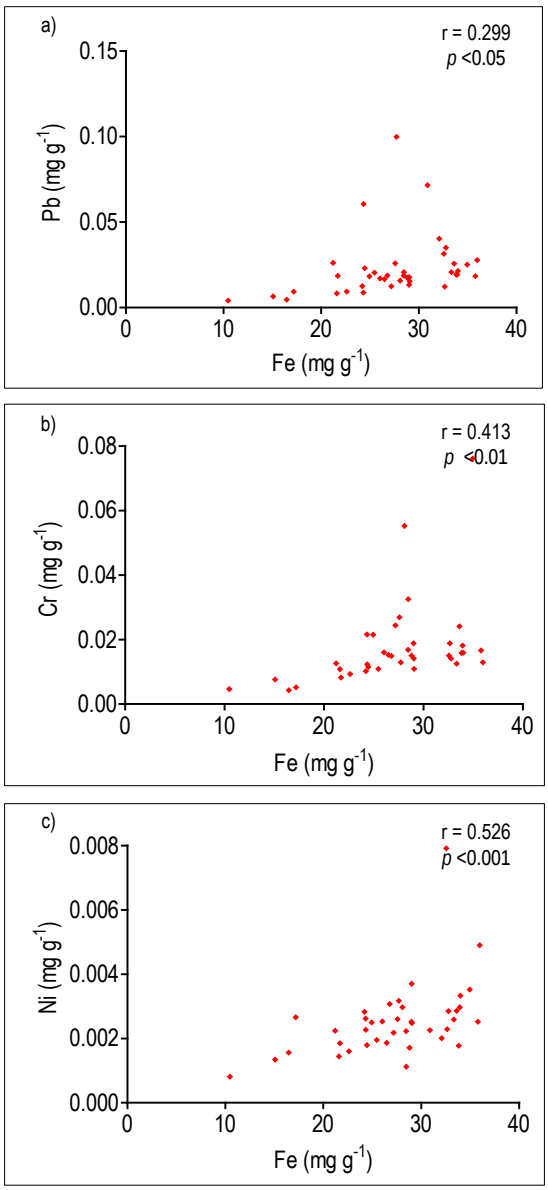

Figure 5.28 Bivariate plots for selected geochemical parameters, Fe versus Pb, Cr and Ni for MBR (London) RDS (n = 61).

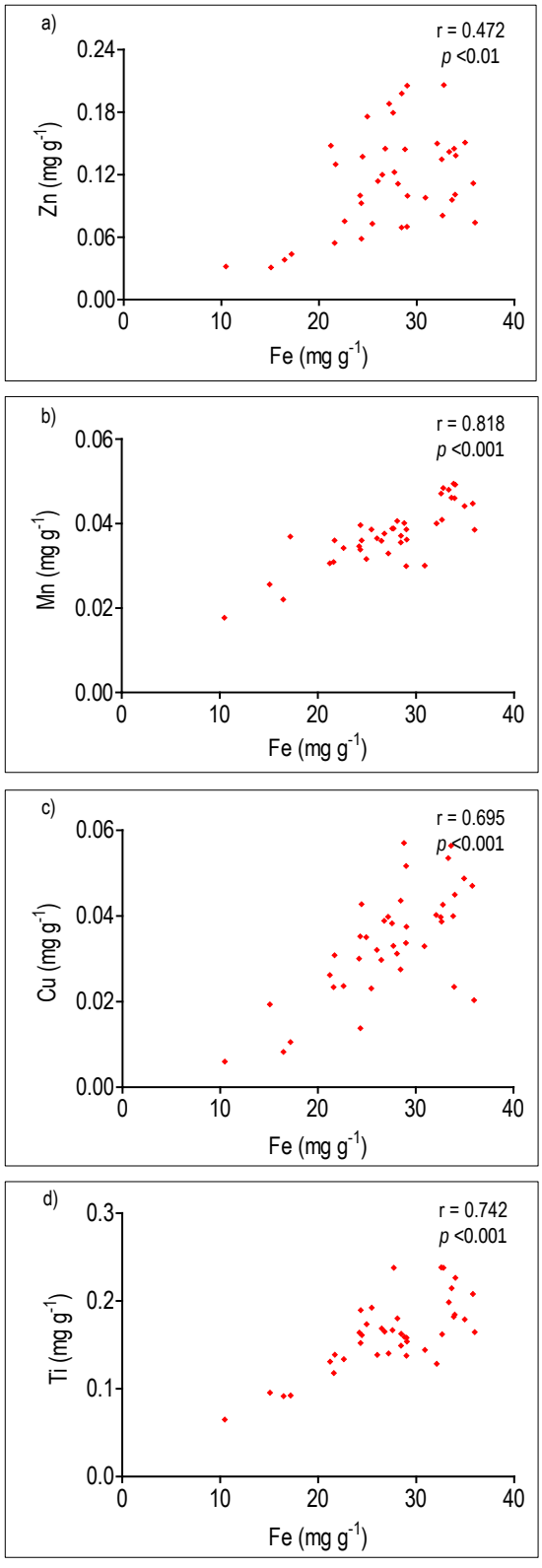

Figure 5.29 Bivariate plots for selected geochemical parameters, Fe Versus Zn, Mn, Cu and Ti for MBR (London) RDS (n = 61).

Table 5.10 Statistical relationships between the mineral magnetic and geochemical parameters for MBR (**bold** text is significant (*p <0.05; **p <0.01; ***p <0.001)) (n =61)

Parameters	χ_{LF}	$\chi_{FD\%}$	χ_{ARM}	SIRM	Soft $_{\%\ 20mT}$	Soft $_{\%\ 40mT}$	Hard $_{\%\ 300mT}$	Hard $_{\%\ 500mT}$	Soft $_{IRM20mT}$	Soft $_{IRM40mT}$	Hard $_{IRM\ 300mT}$	Hard $_{IRM\ 500mT}$	S-ratio	ARM /χ	SIRM/ ARM	SIRM/χ	χ_{ARM} /SIRM
Mg	0.112	0.282	0.134	0.142	-0.069	-0.164	-0.052	-0.223	0.310	0.298	0.151	-0.137	0.162	-0.273	-0.079	**-0.472****	0.044
Al	0.212	0.218	0.243	0.238	-0.181	-0.308	0.150	-0.187	0.276	**0.321***	**0.361***	-0.095	0.178	-0.237	0.057	-0.186	-0.104
S	0.157	0.201	0.172	0.181	0.217	0.198	0.060	-0.279	0.287	0.104	-0.176	-0.201	0.217	-0.152	-0.095	**-0.461****	0.175
K	0.123	0.105	0.176	0.182	-0.080	-0.194	0.100	-0.113	0.205	0.172	0.170	-0.044	0.237	0.028	-0.183	-0.312	0.228
Ca	-0.148	-0.215	-0.091	-0.239	**0.481****	**0.407****	0.107	-0.019	0.054	-0.113	-0.026	-0.050	**-0.515*****	0.120	-0.199	-0.248	0.292
Ti	**0.604*****	0.217	**0.438****	**0.474****	-0.193	-0.256	-0.047	-0.174	**0.353***	**0.410****	0.276	-0.055	0.260	-0.310	0.083	-0.247	-0.143
V	**0.389***	0.138	0.236	0.307	-0.179	**-0.399***	0.069	-0.113	0.197	0.190	0.252	-0.018	0.167	-0.286	0.037	-0.197	-0.174
Cr	**0.382***	0.370	**0.414****	0.275	0.100	0.157	**-0.385***	**-0.517*****	0.316	**0.314****	-0.150	**-0.467****	-0.230	-0.007	-0.145	-0.209	0.152
Mn	**0.598*****	0.151	**0.431****	**0.514*****	-0.238	-0.238	-0.137	-0.193	**0.344***	**0.456****	0.268	-0.021	0.093	-0.295	0.065	-0.179	-0.163
Fe	**0.764*****	0.170	**0.651*****	**0.740*****	**-0.318***	-0.212	-0.063	-0.114	**0.491****	**0.674*****	**0.443****	0.057	0.202	-0.243	0.067	-0.026	-0.191
Ni	**0.313***	0.076	0.171	0.219	0.084	0.095	-0.229	-0.115	0.074	0.043	-0.165	-0.095	0.012	0.072	-0.133	-0.206	0.236
Cu	**0.720*****	0.188	**0.618*****	**0.674*****	-0.139	-0.065	**-0.339*****	-0.070	**0.543*****	**0.648*****	0.152	0.067	0.280	-0.228	0.068	-0.058	-0.179
Zn	**0.646*****	0.119	**0.667*****	**0.496****	0.155	0.159	**-0.540*****	-0.091	**0.575*****	**0.542*****	-0.122	0.008	0.290	-0.029	-0.135	-0.259	0.162
Cd	0.027	0.148	0.159	0.147	-0.227	-0.036	0.220	0.051	-0.031	0.133	0.257	0.076	-0.072	0.174	-0.041	0.229	0.004
Sb	0.021	0.063	0.097	0.157	**-0.355***	-0.107	0.272	0.139	-0.080	0.126	**0.315***	0.184	0.049	0.094	0.094	0.238	-0.080
Pb	0.120	**0.318***	0.183	0.130	**-0.426****	**-0.376***	0.010	-0.073	-0.119	0.017	0.086	-0.039	0.253	0.072	-0.085	0.059	0.032

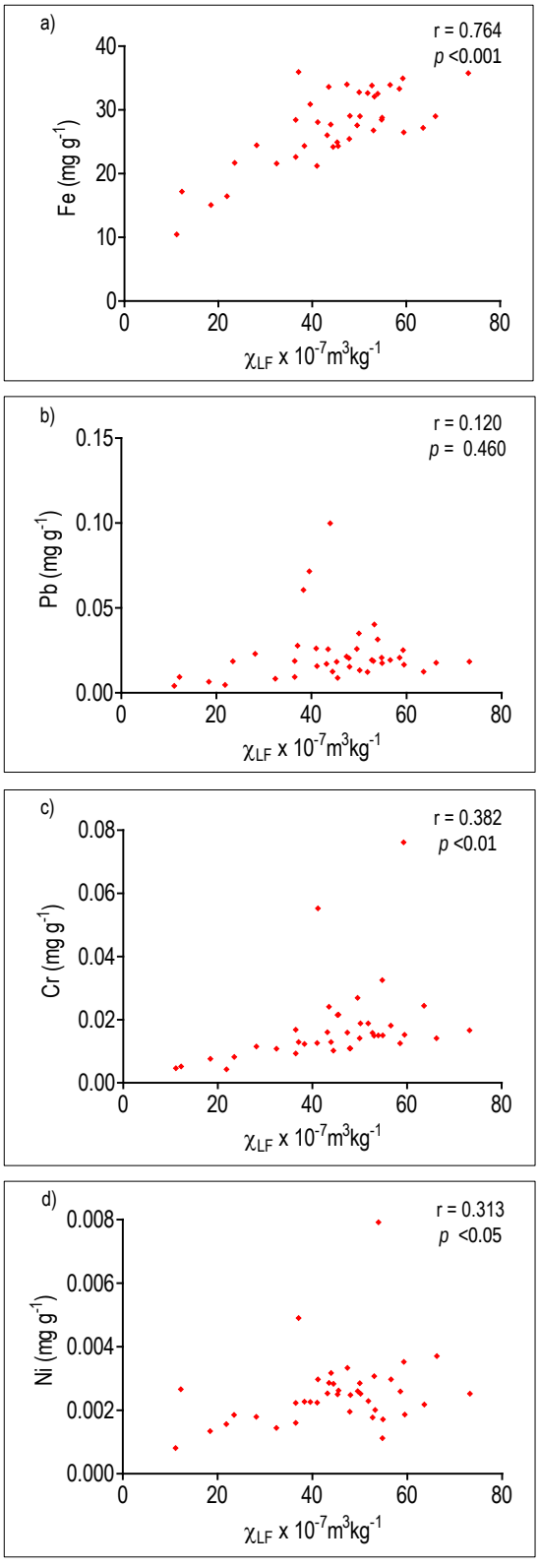

Figure 5.30 Bivariate plots for selected mineral magnetic and geochemical parameters for MBR (London) RDS (n = 61).

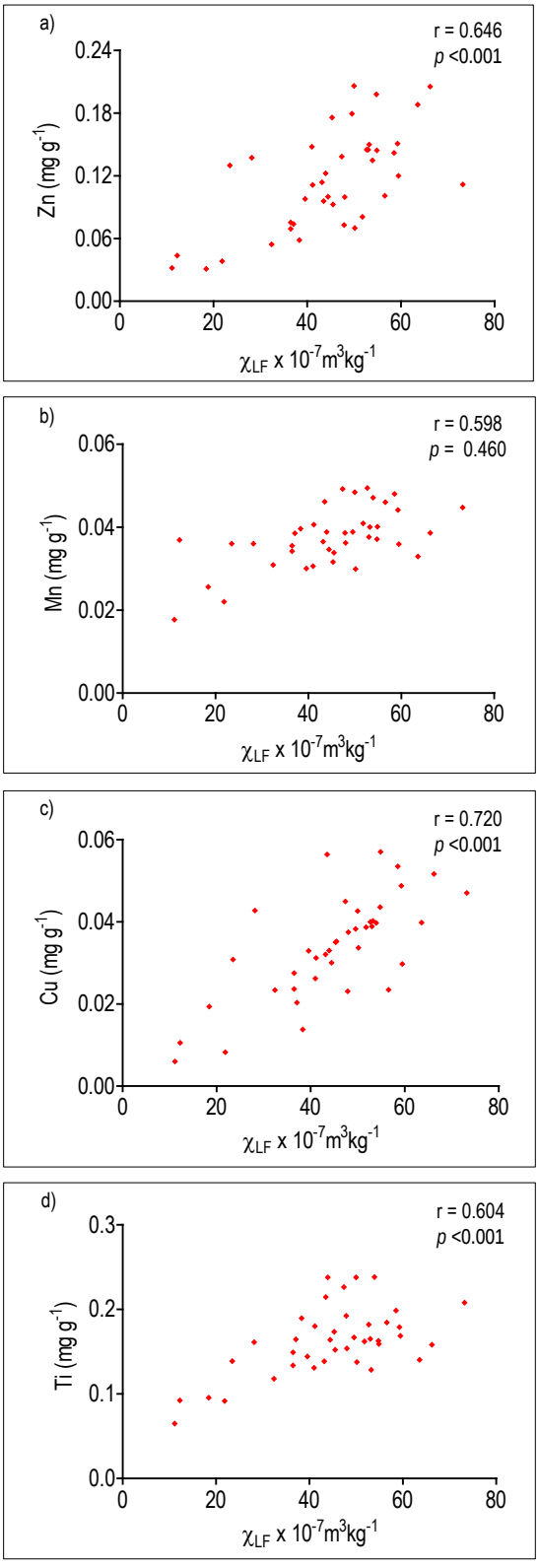

Figure 5.31 Bivariate plots for selected mineral magnetic and geochemical parameters for MBR (London) RDS (n = 61).

Weak relationships are found between χ_{ARM}/SIRM, SIRM/ARM versus all other geochemical parameters and indicate that mineral magnetic grain size is not influenced by the geochemical composition of Marylebone Road RDS. This is further supported by the few linkages found with $\chi_{FD\%,}$ SIRM/χ and most geochemical parameters. $\chi_{LF,}$ χ_{ARM} and SIRM versus Fe correlation suggest an increase in mineral magnetic concentration leads to an increase in the magnetic phase of Fe (Fe_3O_4). However, those relationships with the strongest correlation coefficient values suggest that the magnetic material present in Marylebone Road RDS derives from anthropogenic activity, most notably road traffic.

5.4.5 Further investigation using SEM

A visual comparison of SEM micrographs taken of Marylebone Road RDS illustrates the differences and similarities between the RDS collected at each location and for other studies (Figure 3.16). Figure 5.32a shows spherical Fe oxide particles observed from an SP road sample and has probably been derived from high temperature combustion processes. All other road samples contain almost identical Fe oxide particles and are present in various sizes (<60 µm). Particle counts (Figure 5.33) have shown that samples taken from SP locations are more likely to have higher counts of fine (<20 µm) glassy iron spherules. In some sample locations, SP sample particle counts are two-three times that of other SF location samples. The types and frequency of particles suggest that they derive from traffic and industrial combustion processes. The results are supported by the mineral magnetic data which characterized magnetic particulates of RDS as being of multi-domain ferrimagnetic mineralogy and geochemical data which has shown the inter-relationships of specific geochemical parameters. Figure 5.32b and c shows typical spherical Fe oxide particles found within Marylebone Road RDS. SEM samples display common characteristics and are comparable to combustion particles found in this (Section 4.5.12) and other studies (Figure 3.16). Figure 5.32d and e shows an incomplete cratered sphere with recognisable surface characteristics found in other Fe oxide particles. Figure 5.32f shows two particles combined to produce a binary particle.

5.4.6 Further assessment using factor analysis plots

To further clarify the between-environment and physico-chemical relationships, multivariate factor analysis was used. In each case, parameter and sample loadings extracted from Factors 1 and 2 were used to generate factor plots. Initially all parameters were used to generate factor plots. However the resultant plots (not presented) were chaotic and did not appear to show any clear patterns. Factor analysis was re-applied to various parameter combinations, in some cases excluding some parameters from the data-set, which has then resulted in the factor plots presented in this section.

5.4.7 Factor analysis using mineral magnetic parameters

Simultaneous R- and Q-mode factor analysis was performed by using selected mineral magnetic parameters. Figure 5.34 shows a factor plot created from parameter and sample loadings from Factors 1 and 2. The first two factors explain 57% of variation in 13 parameters, indicating strong positive and negative loadings on both factors.

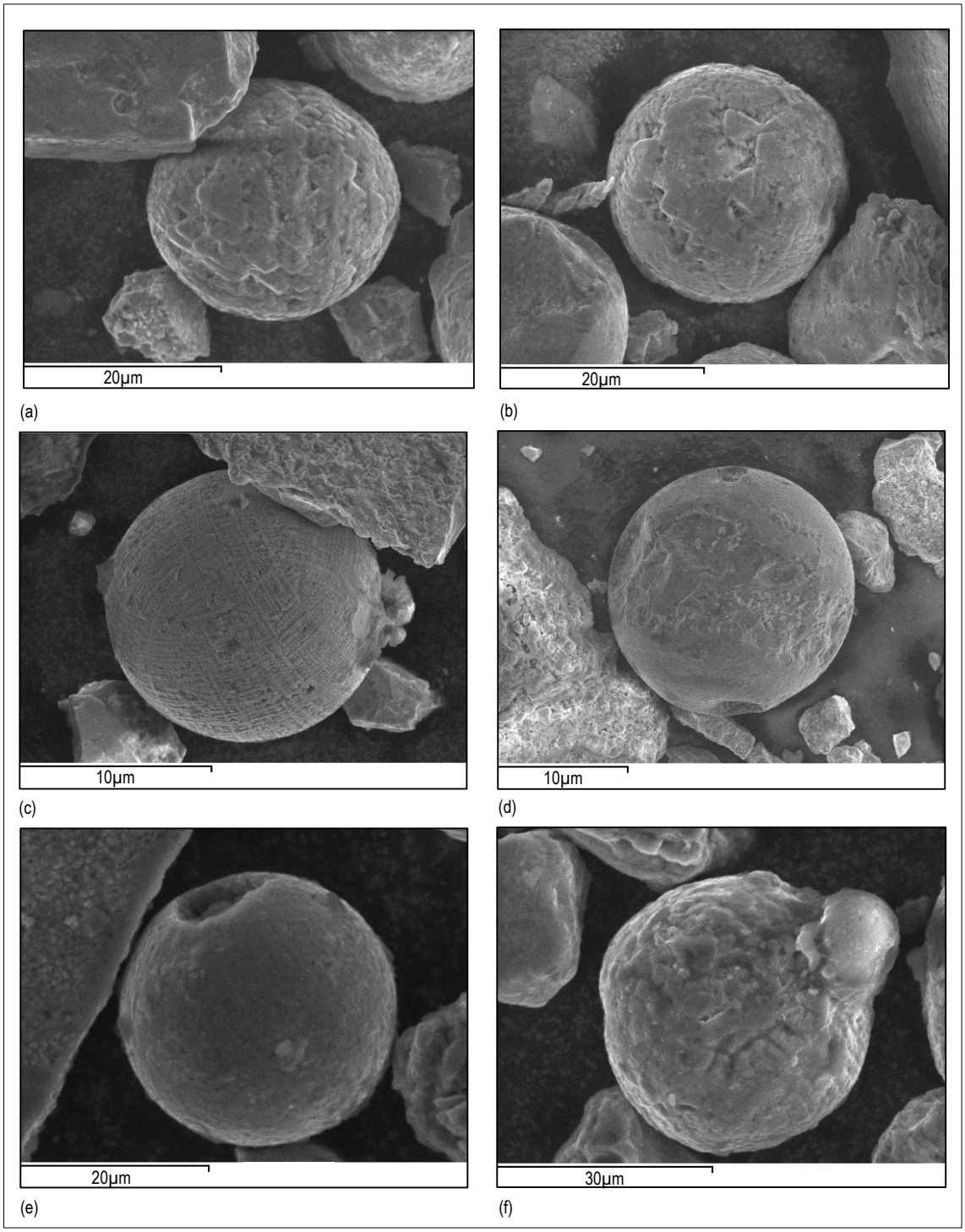

Figure 5.32 SEM micrographs of Fe oxide particles in MBR (London) RDS

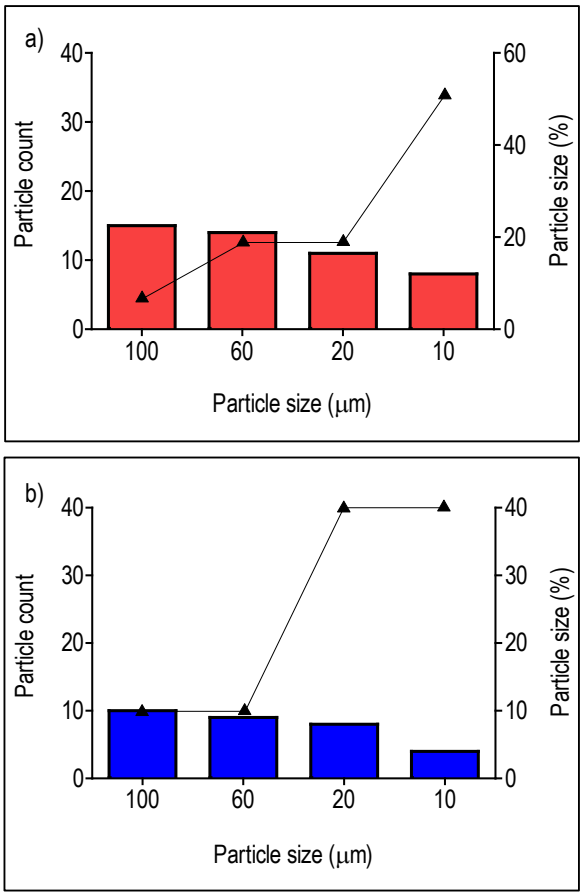

Figure 5.33 SEM particle counts and particle size (%) for MBR (London) (a) SP locations and (b) SF locations.

Loading spread indicates influence by mineral magnetic concentration, mineralogy and magnetic grain size parameters. Factors 1 explains 35% of variation in the parameters, with negative loadings of $\chi_{FD\%}$, $_{ARM}/\chi$ and χ_{ARM}/SIRM, but positive loadings of χ, χ_{ARM}, SIRM,$Soft_{IRM20mT}$, $Soft_{IRM40mT,}$ $Hard_{IRM300mT,}$ $Hard_{IRM500mT}$, S-ratio, $SIRM/_{ARM}$ and SIRM/χ. Factors 2 explains 22% of variation, suggesting a lesser influence than Factor 1. $\chi_{FD\%}$, $_{ARM}/\chi$ and χ_{ARM}/SIRM, $Hard_{IRM300mT,}$ $Hard_{IRM500mT}$ and χ_{ARM} have negative loadings on Factor 1, with all remaining parameters having positive loadings. From the spread of sample loadings, the samples are influenced by both Factors 1 and 2. The distribution of the SP sample points indicates some similarities of magnetic properties between the samples, with positive loadings in line with mineral magnetic concentration parameters along Factor 1. The spread of SF samples indicates a positive and negative across Factor 1, with the influence of concentration, grain size and soft mineral magnetic parameters. The spread of samples across Factor 2 indicates the influence of harder minerals, with an association with grain size and mineral magnetic concentration parameters.

5.4.8 Factor analysis using selected textural parameters

Simultaneous R- and Q-mode factor analysis was performed by using selected particle size and distribution parameters. Figure 5.35a shows a factor plot created from parameter and sample loadings from Factors 1 and 2.

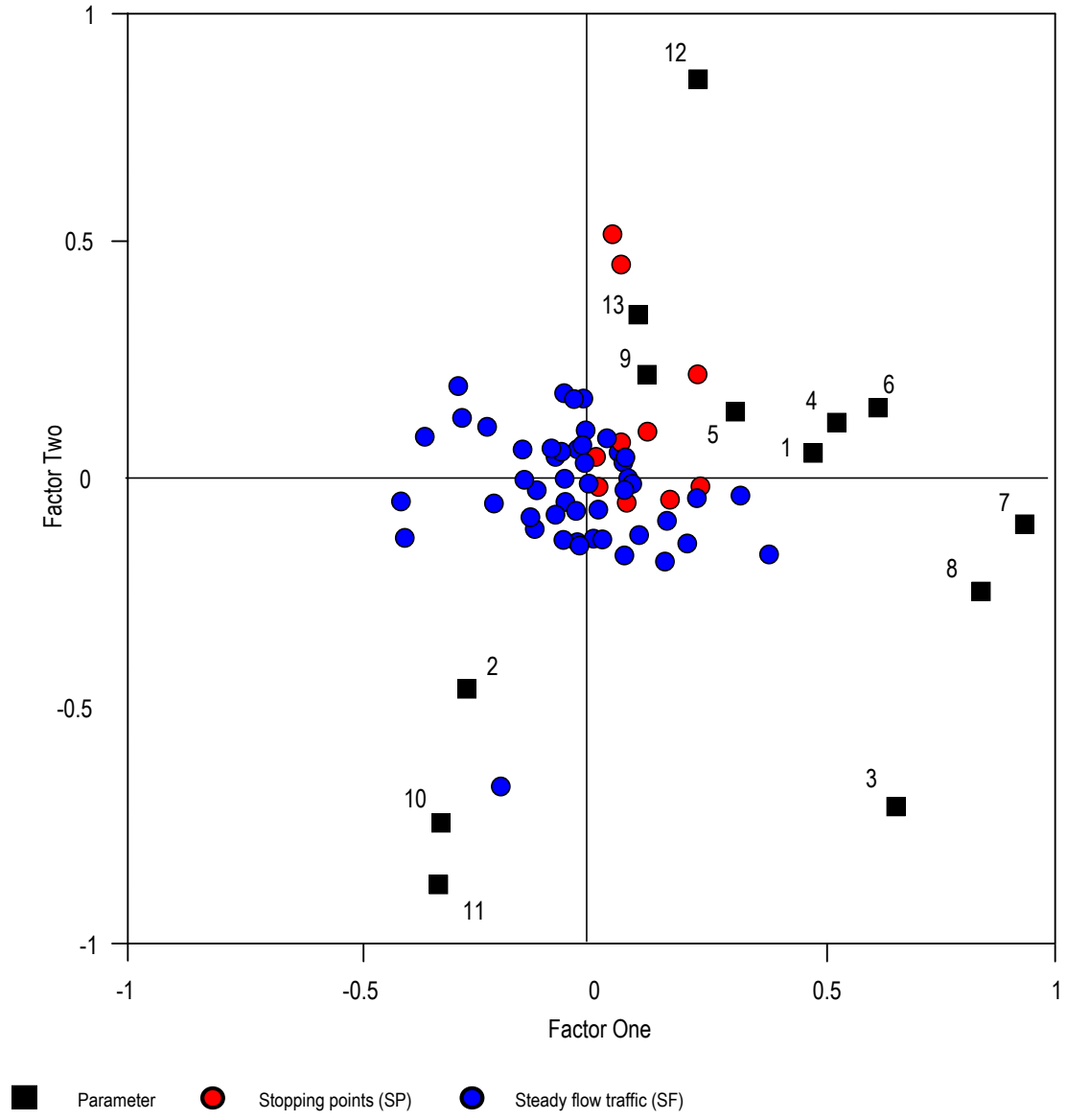

	Parameters				
1	χ_{LF}	6	Soft $_{IRM40mT}$	11	χ_{ARM}/SIRM
2	χ_{FD}	7	Hard $_{IRM20mT}$	12	SIRM/ARM
3	χ_{ARM}	8	Hard $_{IRM40mT}$	13	SIRM/χ
4	SIRM	9	S-ratio		
5	Soft $_{IRM20mT}$	10	ARM/χ		

Figure 5.34 Simultaneous R- and Q mode factor analysis plots of Factor 1 versus Factor 2, based on selected mineral magnetic parameters for MBR (London) RDS.

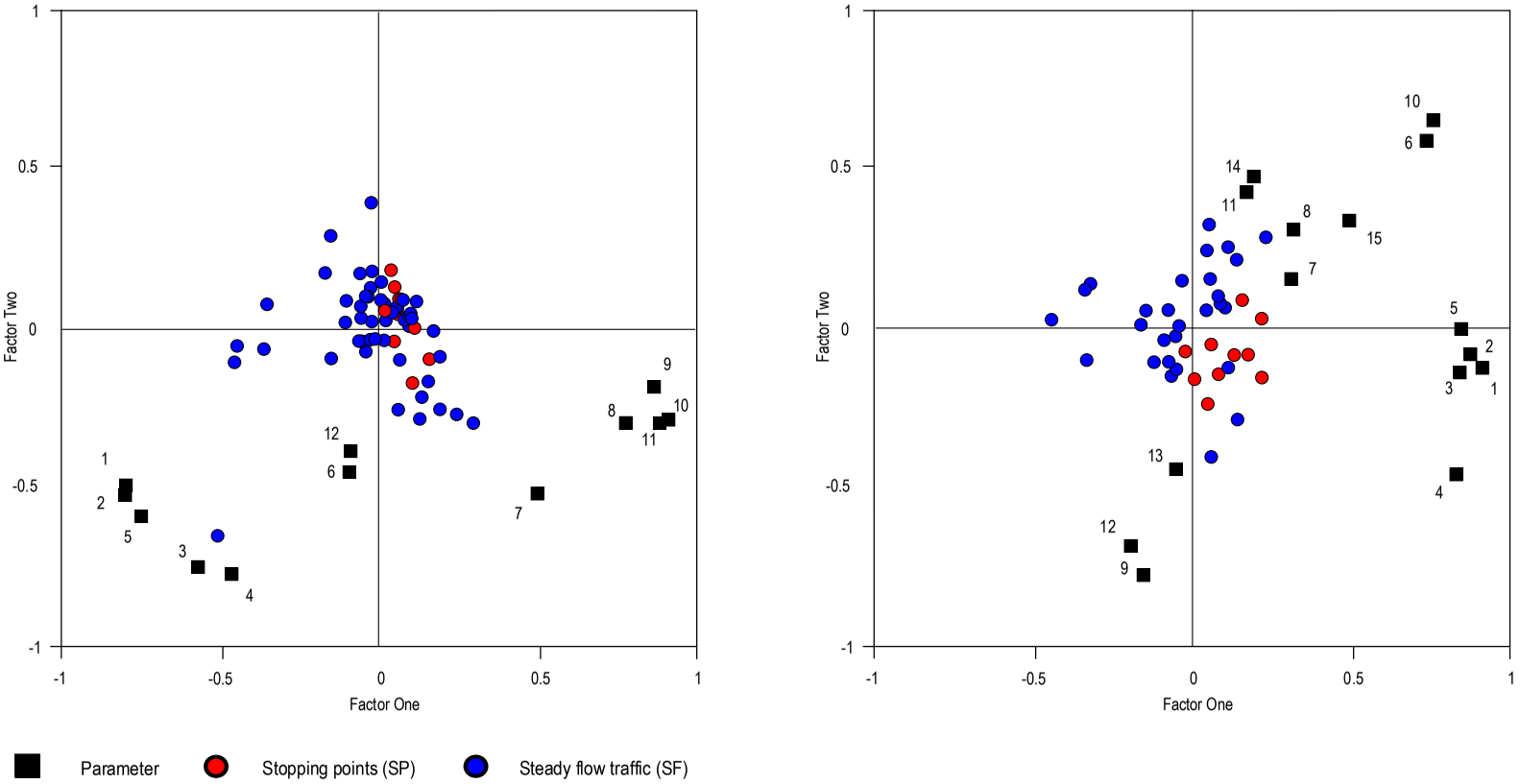

(a)	Parameters				
1	Mean	5	Kurtosis	9	$PM_{1.0}$
2	Median	6	Sand	10	$PM_{2.5}$
3	Sorting	7	Silt	11	PM_{10}
4	Skewness	8	Clay	12	PM_{100}

(b)	Parameters				
1	Mg	6	Ti	11	Ni
2	Al	7	V	12	Cu
3	S	8	Cr	13	Zn
4	K	9	Mn	14	Cd
5	Ca	10	Fe	15	Pb

Figure 5.35 Simultaneous R- and Q mode factor analysis plots of Factor 1 versus Factor 2, based on textural parameters (a) and geochemical parameters (b) for MBR RDS.

The first two factors extracted explain 68% of variation in the 12 parameters, indicating strong positive and negative loadings on both factors. Factors 1 and 2 explain 51% and 17% of the variation in 10 mineral magnetic and textural parameters. The spread of loadings indicates some influences by both particle size and distribution.

Factor 1 explains 51% of variation in parameters, with negative loadings of mean, median, sorting, skewness, kurtosis, sand and $PM_{100,}$ with all other parameters having positive loadings. Factor 2 explains 17% of variation, suggesting limited influence. Particle size classes (<60 µm) are positively loaded on Factor 2 with all remaining parameters being negatively loaded on Factor 2. There is no apparent separation between the loadings of the SP and SF samples due to mixing of samples. The loadings of the SP samples appear to be more influenced by Factor 1 with positive loadings, whereas the SF samples appear to be influenced by Factors 1 and 2. The positive loadings of the SP samples along Factor 1 could indicate that the particle size classes (<60 µm) are the main influencing parameters.

5.4.9 Factor analysis using selected geochemical parameters

Simultaneous R- and Q-mode factor analysis was performed by using selected geochemical parameters. Figure 5.35b shows a factor plot created from parameter and sample loadings from Factors 1 and 2. The first two factors extracted explain 50% of variation in the 15 parameters.

The geochemical parameters have positive and negative loadings on both extracted factors, the spread indicates they are influenced by various chemical association gradients. Factor 1 explains 38% of variation in parameters, with positive loadings of Mg, Al, S, K, Ca, Ti, V, Cr, Fe, Ni, Cd and Pb along Factor 1 and Mn, Cu and Zn negatively loaded along Factor 1. Factor 2 explains 12% of variation suggesting limited influence. Ti, V, Cr, Fe, Ni, Cd and Pb have positive loadings along Factor 2 whereas the remaining parameters are negatively loaded.

The spread of samples indicates influence from both Factors 1 and 2, with sample loadings of SP and SF showing some separation and groupings. The SF sample loadings indicate the main influencing factor being on a positive Factor 1 leading into negative Factor 1. The spread of samples indicates the influence being pulled between Cr, Ni, V, Fe, Cd, Pb (positive Factor 1) and Mn, Cu, Zn (negative Factor 1). The spread of SF samples show loadings on Factors 1 and 2, with the main influencing factor being along a distinct geochemical gradient of Ti, V, Cr, Fe, Ni and Cd positive to Mn, Cu and Zn negative Factor 1 (top right to bottom left). Sample loadings across Factor 1 for SP and SF samples indicate an influence of a predominantly anthropogenic, geochemical cocktail.

5.4.10 Factor analysis using key physico-chemical parameters

Factor analysis was initially performed using the physico-chemical parameters analysed in the previous sections 5.4.7-5.4.9, with selected parameters used to produce an additional plot (Figure 5.36). The first two factors extracted explain 51% of variation in the 18 parameters.

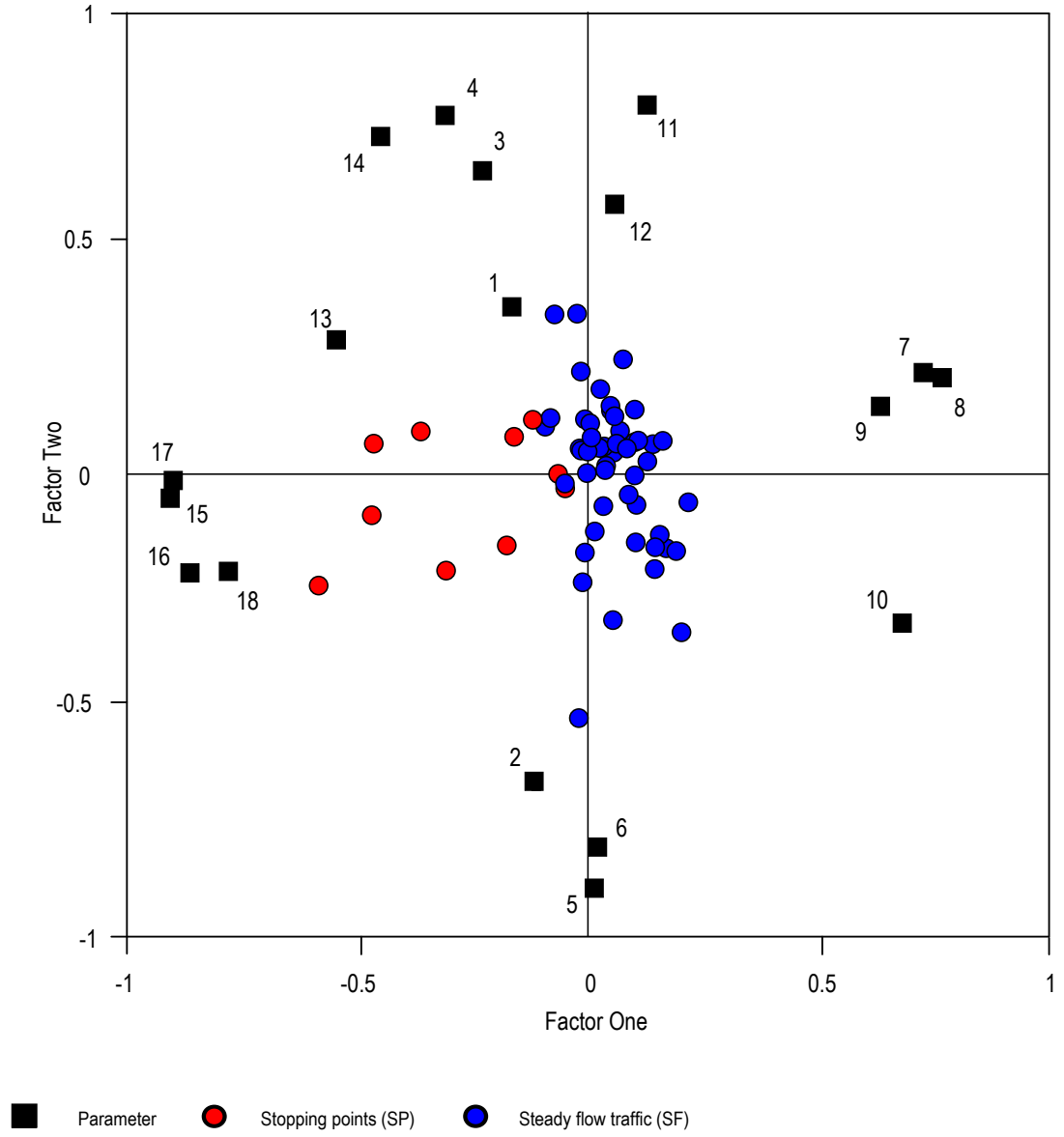

	Parameters						
1	χ_{LF}	6	SIRM/χ	11	Fe	16	Cd
2	χ_{FD}	7	$PM_{1.0}$	12	Pb	17	Mn
3	χ_{ARM}	8	$PM_{2.5}$	13	Cr	18	Cu
4	SIRM	9	PM_{10}	14	Ni		
5	S-ratio	10	PM_{100}	15	Zn		

Figure 5.36 Simultaneous R- and Q mode factor analysis plots of Factor 1 versus Factor 2, based on all selected parameters for MBR (London) RDS.

The physico-chemical parameters have positive and negative loadings on both extracted factors, the spread of which indicated they are influenced by various physico-chemical

association gradients. Factor 1 explains 31% of variation in the parameters, Fe, Pb, $PM_{1.0,}$ $PM_{2.5,}$ $PM_{10,}$ $PM_{100,}$ S-ratio and SIRM/χ and have positive loadings. χ, $\chi_{FD\%}$, χ_{ARM}, SIRM, Cr, Ni, Zn, Cd, Mn and Cu have negative loadings. Factor 2 explains 20% of variation in all 18 parameters, with χ, $\chi_{FD\%}$, χ_{ARM}, SIRM, Fe, Pb, Cr, Ni and particle size classes (<PM_{10}) having positive loadings and Mn, Zn, Cd, Cu, $\chi_{FD\%}$, S-ratio and SIRM/χ having negative loadings.

The spread of samples indicates influence from both Factors 1 and 2, with sample loadings of SP and SF showing some separation and groupings. The SF sample loadings indicate the main influencing factor being on a negative Factor 1. The spread of samples indicates the influence being pulled between mineral magnetic concentration parameters χ, $\chi_{FD\%}$, χ_{ARM}, SIRM and geochemical parameters Zn, Cd, Mn and Cu with the main influencing factors being along a distinct mineral magnetic and geochemical gradient. This grouping of elements suggests the influence of mechanically worn brake and tyre particles from vehicles. The spread of SF samples show loadings being mostly influenced by Factor 1 with the spread of samples concentrated within a negative Factor 1 and positive Factor 2, this indicates a mineral magnetic gradient of concentration and mineralogy – grain size parameters. These groupings suggest an influence from combustion particles, with patterns suggesting high influence of mineral magnetic concentration and mineralogy. The combination of SP and SF samples show a split which indicates samples along positive and negative Factor 2 and suggests a geochemical – particle size gradient. The patterns seen within Figure 5.36 reinforce the findings of Figures 5.24-5.31. The use of factor plots have developed knowledge of the relationships by showing relationship groupings of multiple parameters. This further supports the suggestion that RDS characteristics on Marylebone road is highly influenced by mineral magnetism and geochemistry.

5.4.11 Summary for Marylebone road

The characteristics of Marylebone road RDS show a wide range of variation over the sampling area. Marylebone road shows some potential for mineral magnetic and particle size proxy purposes to work successfully. However, geochemical correlations have given a good indication that mineral magnetic methods can work very well as a geochemical pollution proxy. The characteristics and relationships for Marylebone road RDS can be summarized as:

- Magnetic properties of RDS on Marylebone road are predominantly ferromagnetic.
- Mineral magnetic grain size remains consistently multi-domain within the study area.
- Moderate correlations between χ_{LF}, SIRM and <PM_{10} (p <0.01-0.001)
- No correlations exist between hard minerals and particle class sizes, suggesting soft sources only contributing to significant correlations (soft magnetic material can be directly linked with anthropogenic combustion sources)
- Strong mineral magnetic and geochemical correlations (p <0.01-0.001)

- High mineral magnetic and geochemical concentrations found at specific locations. Locations can be linked to vehicle activity (start-stop points).
- Declining concentrations spatially from start-stop points.
- Specific geochemistry linked with start-stop points (indication of road traffic influence).
- Inter geochemical correlations, SEM and Factor plots further suggest road traffic source.

5.5 Relationships between mineral magnetic and textural parameters for Scunthorpe

To assess the relationships between mineral magnetic and textural variables for Scunthorpe, the data set was further interrogated using all mineral magnetic and textural parameters by correlation statistics (Table 5.11) and graphically with the aid of bivariate plots (Figure 5.37-5.38). Statistical tests indicate that significant (p <0.05) relationships exist between some mineral magnetic and textural parameters. However, it is only those relationships with the strongest correlation coefficients that have been selected for further examination through bivariate plot analysis. These are presented in Figures 5.37–5.38, which show the spread of the sample points in relation to the line of best fit for each set of bivariate data. Table 5.11 summarizes the correlation statistics between the mineral magnetic variables and textural variables for Scunthorpe. The textural fraction of RDS displays a strong positive correlation with SIRM ($PM_{1.0}$–PM_{10}) with consistent weakening of the relationship through the particle size range (r = -0.537 to -0.689; p <0.001, n = 34). Strongest correlation coefficients were evident between magnetic concentration dependent parameters SIRM versus $PM_{2.5}$ (r = 0.689; p <0.001 (Figure 5.37a)). Some mineral magnetic concentrations have strong negative correlations with the finer fraction of RDS ($PM_{1.0}$–PM_{10}).

However, the weakest correlation coefficients were associated with Hard% parameters (r = 0.043; p = 0.805 (NS)), suggesting that hard mineralogy had no influence on the relationships found. Sand, silt and PM_{100} -sized particles were not significantly correlated with any mineral magnetic parameters. Figure 5.37a-c shows strong negative correlations between SIRM versus textural parameters <PM_{10}, all displaying significant correlations (p <0.001). Figure 5.38a shows bivariate relationships between $Soft\%_{20mT}$ and $PM_{2.5}$ which shows a moderate positive correlation (r = 0.346; p <0.01). Figure 5.38b shows strengthened correlation with $Soft\%_{20mT}$ and PM_{10} (r = 0.459; p <0.01). This relationship is also evident with other magnetic mineralogy dependent parameters, $Soft_{IRM20mT}$ and $Soft_{IRM40mT}$ correlate with fine textural parameters (<PM_{10}). The strongest correlation coefficient for $Soft_{IRM20mT}$ is with PM_{10} (r = 0.267; p <0.05) and $Soft_{IRM40mT}$ with $PM_{2.5}$ (r = 0.289; p <0.05).

Figure 5.38c shows the strong negative correlation between the S-ratio and PM_{10} (r = -0.529; p <0.01). The negative correlation is also evident throughout the <PM_{10} size range (r = -0.406 to -0.480; p <0.01) and successively increases in strength with increasing particle size. SIRM/χ displayed some weak correlations with the median (r = 0.223; p <0.05) and mean (r = 0.306; p <0.05) for RDS and also $PM_{1.0}$ (r = 0.234; p <0.05). Almost all other mineral magnetic variables and textural variables are not strongly correlated (i.e. most correlation coefficients are *ca*. r = ≤0.1 to -0.3 and are not statistically significant (p <0.05).

Table 5.11 Statistical relationships between the mineral magnetic and textural parameters for Scunthorpe RDS (**bold** text is significant (*p <0.05; **p <0.01; ***p <0.001)) (n = 34)

Parameters	Median-PS	Mean-PS	Sorting	Skewness	Kurtosis	Sand	Silt	Clay	$PM_{1.0}$	$PM_{2.5}$	PM_{10}	PM_{100}
χ_{LF}	0.150	0.125	0.086	0.253	0.028	0.024	-0.110	0.053	0.048	0.067	0.120	-0.032
$\chi_{FD\%}$	0.113	0.057	-0.241	-0.067	0.152	0.227	-0.224	-0.162	-0.137	-0.177	-0.275	-0.241
χ_{ARM}	0.224	0.204	0.070	0.271	0.146	0.086	-0.198	**0.250***	0.146	**0.262***	**0.295***	-0.132
SIRM	0.234	0.233	0.052	0.261	0.150	0.109	-0.209	**0.678*****	**0.537*****	**0.689*****	**0.609*****	-0.145
Soft $_{\% 20mT}$	0.067	0.075	0.332	0.283	-0.145	-0.243	0.183	**0.309***	0.293	**0.346****	**0.459****	0.156
Soft $_{\% 40mT}$	-0.227	-0.126	0.200	-0.102	-0.340	-0.219	0.254	0.127	0.119	0.159	0.269	0.280
Hard $_{\% 300mT}$	-0.215	-0.243	0.071	-0.057	-0.004	-0.057	0.059	0.080	0.082	0.062	0.120	0.136
Hard $_{\% 500mT}$	0.033	-0.019	0.067	0.057	-0.156	-0.022	0.035	0.047	0.050	0.048	0.081	0.043
Soft $_{IRM20mt}$	0.195	0.216	0.167	0.295	0.082	0.008	-0.109	**0.216***	**0.212***	**0.233***	**0.267***	-0.060
Soft $_{IRM40mT}$	0.216	0.238	0.102	0.252	0.095	0.056	-0.154	**0.225***	**0.189***	**0.289***	**0.251***	-0.096
Hard $_{IRM300mT}$	0.153	0.189	-0.186	0.058	0.169	0.118	**-0.176****	-0.058	-0.023	-0.054	-0.094	-0.297
Hard $_{IRM500mT}$	0.213	0.205	0.175	0.264	-0.009	0.018	-0.118	0.221	0.217	0.230	0.260	-0.051
S-ratio	0.009	-0.032	-0.330	-0.259	0.114	0.289	-0.216	**-0.422****	**-0.406****	**-0.430****	**-0.529*****	-0.213
ARM/χ	0.240	0.242	0.142	0.263	0.064	-0.054	-0.044	0.252	0.284	0.241	0.217	-0.039
SIRM/$_{ARM}$	-0.170	-0.084	0.001	-0.239	-0.222	-0.021	0.107	-0.154	-0.169	-0.149	-0.169	0.139
SIRM/χ	**0.223***	**0.306***	0.098	0.134	0.090	0.042	-0.114	0.184	**0.234***	0.167	0.112	-0.092
χ_{ARM} /SIRM	0.170	0.084	-0.001	0.239	0.222	0.021	-0.107	0.154	0.169	0.149	0.169	-0.139

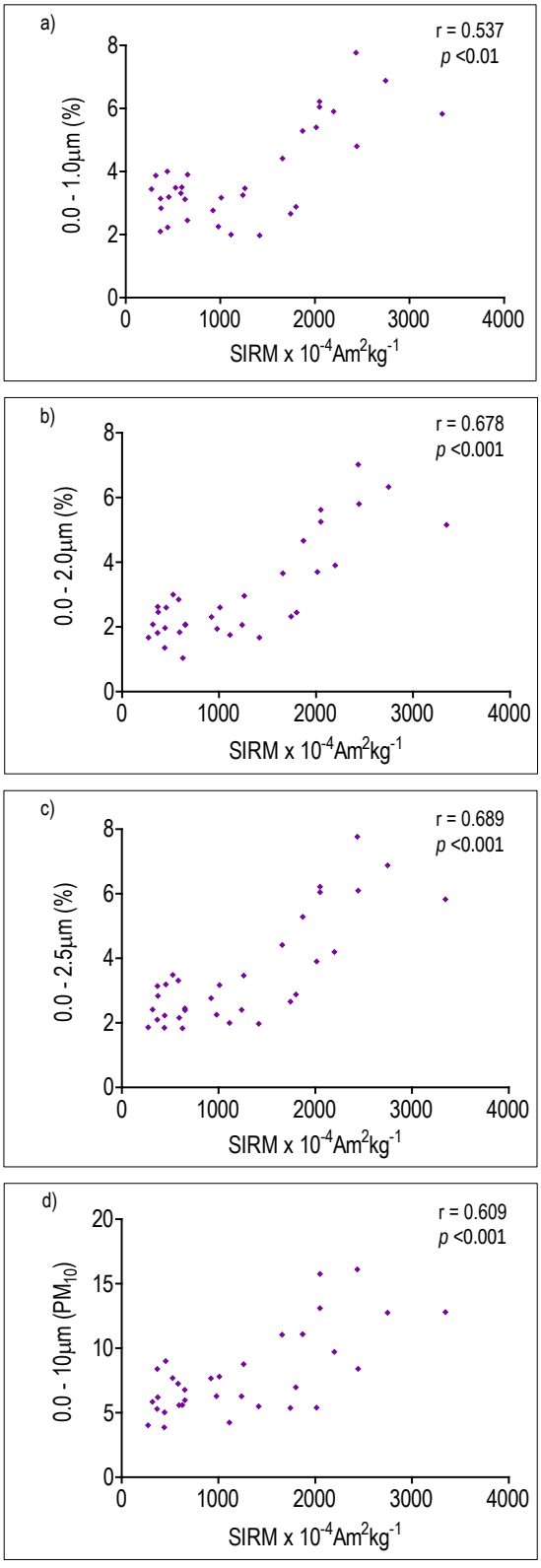

Figure 5.37 Bivariate plots for selected mineral magnetic and textural parameters for Scunthorpe RDS (n = 34).

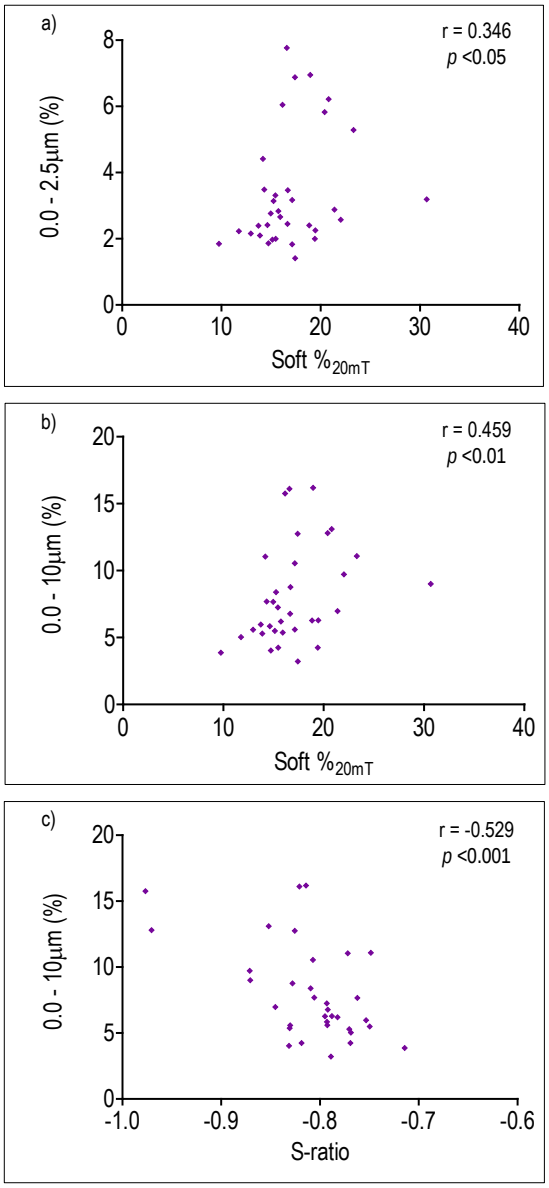

Figure 5.38 Bivariate plots for selected mineral magnetic and textural parameters for Scunthorpe RDS (n = 34).

This suggests that the texture of RDS does not strongly control the mineral magnetic assemblages in Scunthorpe. However, those few relationships that are statistically significant appear to be related to the magnetic mineralogy variables. Mineral magnetic concentration parameter SIRM has shown the greatest potential for particle size relationships. The statistical tests indicate that a low significant relationship exists between all other mineral magnetic and textural variables (p <0.05).

5.6 Further investigation using spatial, SEM and factor plot characterization of Scunthorpe physical-characteristics.

Statistical and graphical techniques indicate that significant variations exist in the sedimentological characteristics of the surface sediments in Scunthorpe. So far, it has been demonstrated 'how' the samples vary, in terms of their mineral magnetic and textural properties, and that some of this variation is associated with differences in sedimentary environments. However, the geographical relationships between adjacent samples have not been addressed, nor has an environmental explanation for 'why' the variations exist been given. Therefore, the mineral magnetic and textural data were used to generate GIS images to determine the nature of any spatial variation.

5.6.1 Spatial characterization of mineral magnetic and textural data

Statistical and graphical techniques indicate significant variations in physical characteristics of Scunthorpe RDS. However, bivariate plots and Mann-Whitney U tests used failed to show geographical relationships between adjacent samples. Therefore, the χ_{LF} data have been used to generate GIS images (Figure 5.39–5.40), determining the nature of spatial variations. Baseline maps were created in Arcview GIS (version 10), forming visual representations of χ_{LF} characteristics and patterns. The masked boundary excludes unsampled areas.

Variation of χ_{LF} is show in Figure 5.39. There are several distinct observations that can be made regarding concentrations of χ_{LF} in the sampling area. There are very high concentrations of magnetic material to the east of the town and this can be distinctly seen by a clear line which divides the east and west of the town. These are highlighted in Table 5.12, with high concentrations to the east (χ_{LF} 123.341 x $10^{-7}m^3kg^{-1}$) and low to the west (χ_{LF} 14.589 x $10^{-7}m^3kg^{-1}$). There are consistently low mineral magnetic concentrations associated with the west of the town with a few exceptions which can be linked to the main road system (viii and ix), which display high χ_{LF} concentrations (90.564-96.259 x $10^{-7}m^3kg^{-1}$). The higher concentrations of magnetic material to the east of the town appear to be widespread and not solely contained to any particular road system, as previously discovered in other towns. The concentrations are also higher than any other found within the sampled towns. The mineral magnetic concentrations within the west side of the town appear to be low to moderate levels compared to other sampled towns. Details of Scunthorpe land use can be seen in Appendix 5.5.6. Figure 5.40 shows how the east of the town is dominated by mineral magnetic and geochemical highs, with the west of the town experiencing relative lows.

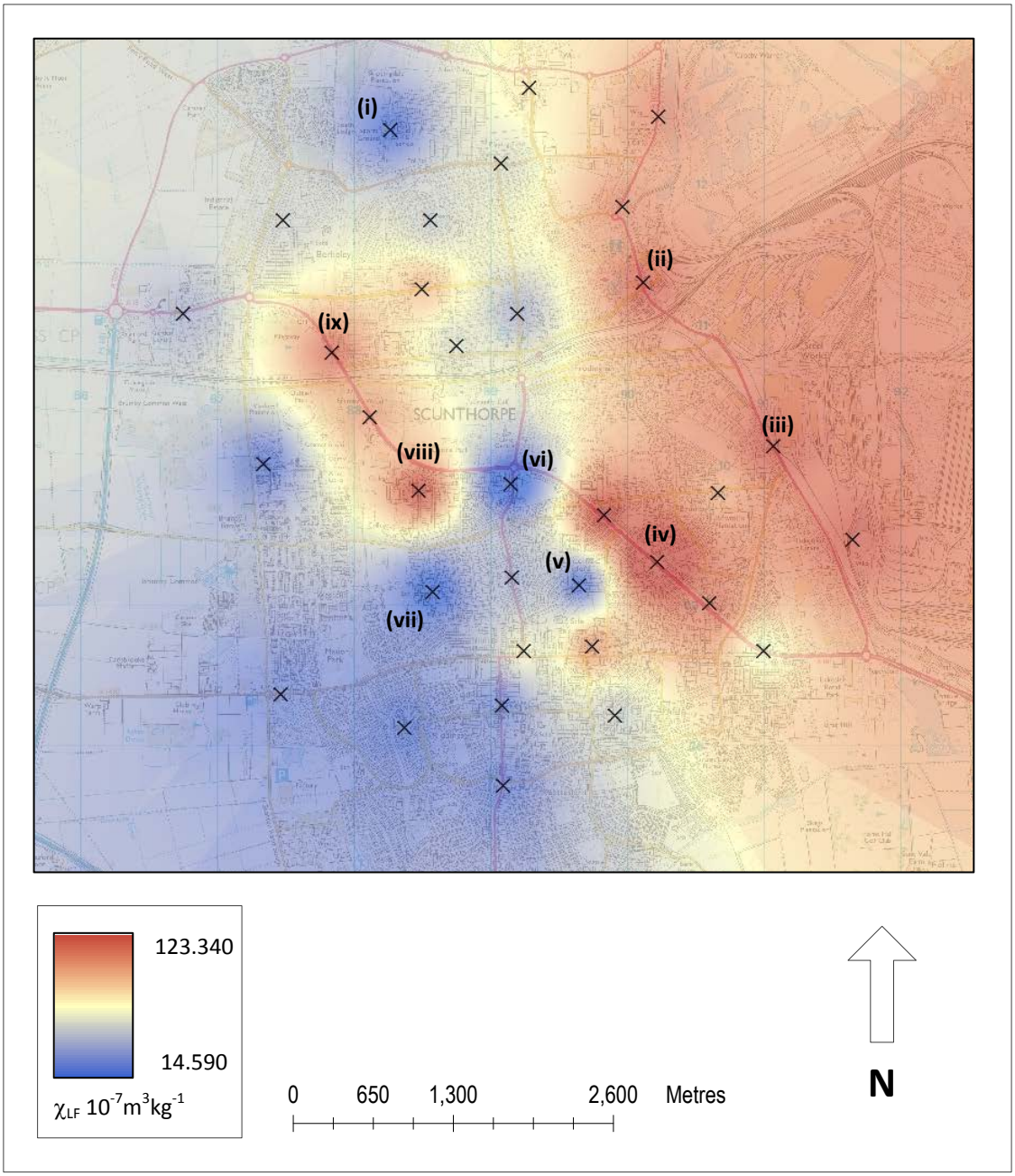

Figure 5.39 Spatial distribution of χ_{LF} concentrations in Scunthorpe RDS.

Table 5.12 χ_{LF} concentrations for specific sites in Scunthorpe

	Sample	χ_{LF}		Sample	χ_{LF}
i	12	25.501	vi	33	14.589
ii	7	94.044	vii	24	20.875
iii	2	95.036	viii	21	96.259
iv	5	123.341	ix	19	90.564
v	26	26.899			

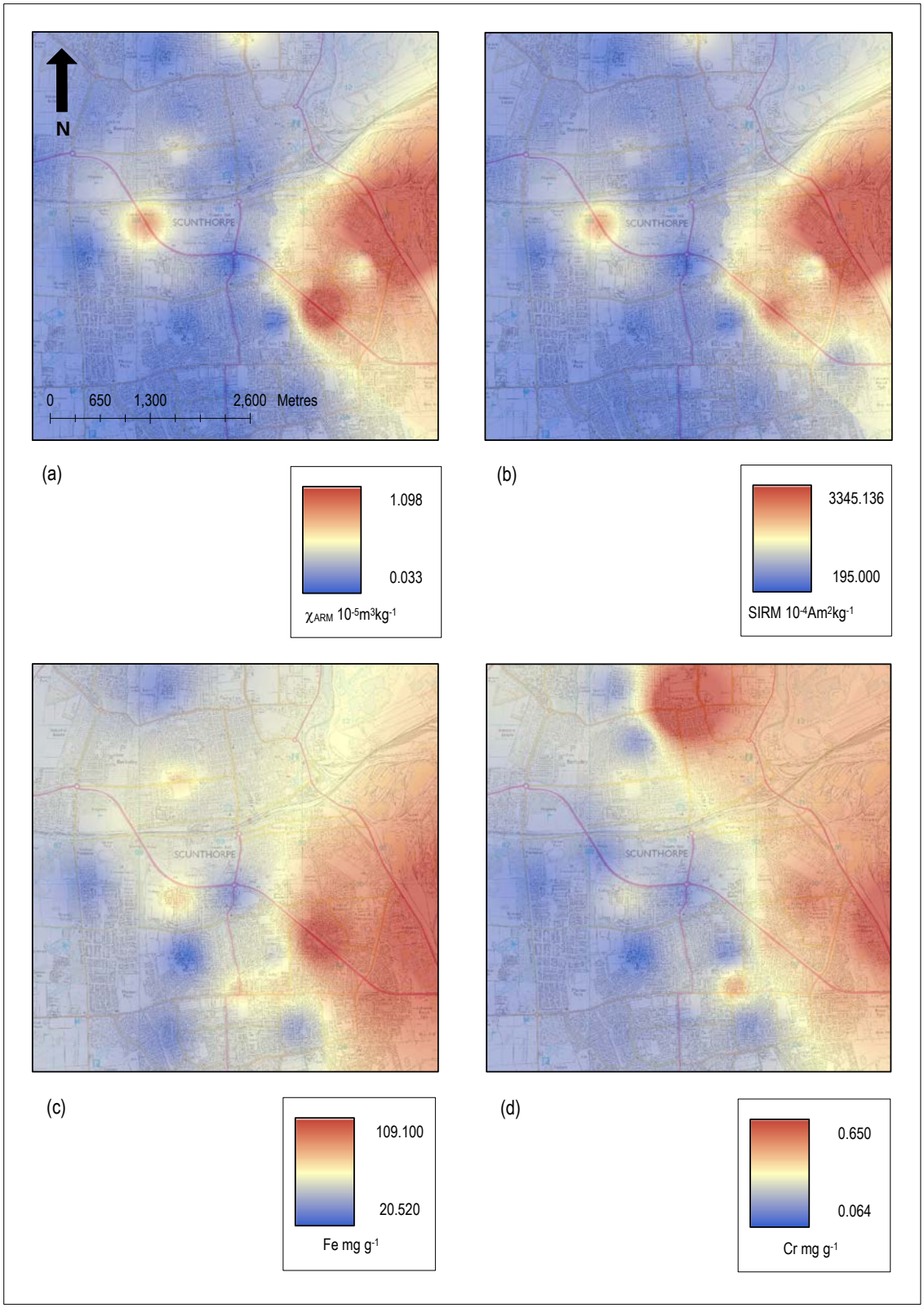

Figure 5.40 Spatial distributions of selected mineral magnetic and geochemical parameters from Scunthorpe RDS.

Figure 5.40a shows the high and low χ_{ARM} concentrations across the sampling area and indicates that most fine mineral magnetic material is located due east, near the steel works and to the south-east of the A18 main carriageway. Figure 5.40b shows a similar GIS image with high concentrations of SIRM directly to the east of the town, a solitary high point can be observed to the west on the A18 main carriageway. This sample point is close to the rail network line which may be an influencing factor. Figure 5.40c shows the high concentrations of Fe to the south-west and the moderate concentrations throughout the central and eastern parts of the town. Figure 5.40d shows high concentrations of Cr north and east of Scunthorpe. The high concentrations of Fe and Cr to the west suggest that the steel works (SW) may be a major influencing factor to the geochemical environment. East of Scunthorpe has major steel industries which are renowned for contributing to poor local air quality which are detailed in the Action Plan for Scunthorpe AQMA (North Lincolnshire Council, 2008, Appendix 7.3). Appendix 5.5.7 shows the Air quality Management Area (AQMA) for Scunthorpe and the coinciding samples which fall within and close to this catchment area. Appendix 5.5.7 also shows the radius from the main foundry stack moving out towards the edge of the AQMA and encompassing a further area to the south west. The eastern side of Scunthorpe has been identified as steelworks (SW) due to the proximity of industry and physico-chemical characteristics (high mineral magnetic and geochemical concentrations). The west is identified as road network (RN) (due to comparable concentrations of mineral magnetic and geochemistry found at other UK road sites) for graphical purposes. In comparison non-combustion geochemistry (Al, Ca, K and Si) displays opposite patterns (Appendix 6.1-6.4) to that of combustion geochemistry, with higher concentrations within the West and South of the town. The concentrations of Al, Ca, K and Si suggest natural background and non-anthropogenic sources and show some mixing into areas of anthropogenic activity. This is also evident in appendix 6.5-6.8 when geochemistry is compared in Wolverhampton.

Figure 5.41a shows the bivariate relationship between χ_{LF} versus Distance to steel works. The correlation shows a moderate negative correlation, which indicates increased magnetic material closer to the SW ($r = -0.462$; $p < 0.01$). This relationship is also apparent within other mineral magnetic parameters, χ_{ARM} ($r = -0.459$; $p < 0.01$ (Figure 5.41b)) and SIRM ($r = -0.447$; $p < 0.01$ (Figure 5.41c)). Figure 5.41b shows a cluster of high values of χ_{ARM} in close proximity to the SW and suggests that higher concentrations of fine magnetic material is deposited close to industry.

Figure 5.42a shows the bivariate plot of the S-ratio versus distance to SW ($r = 0.055$; $p = 0.756$) and indicates a relative uniform dispersion of soft magnetic minerals across the sampling area. This is also seen in Figure 5.42b with SIRM/χ versus distance to SW ($r = -0.252$; $p = 0.157$) with a group of two clusters, which show that samples closer to the SW have higher values. Particle class sizes relative consistency in terms of distance to SW. Figure 5.42c shows the median particle size versus distance to SW and displays no significant correlation ($r = 0.114$; $p = 0.519$). From the bivariate plot it can been seen that the spread of samples is relatively uniform.

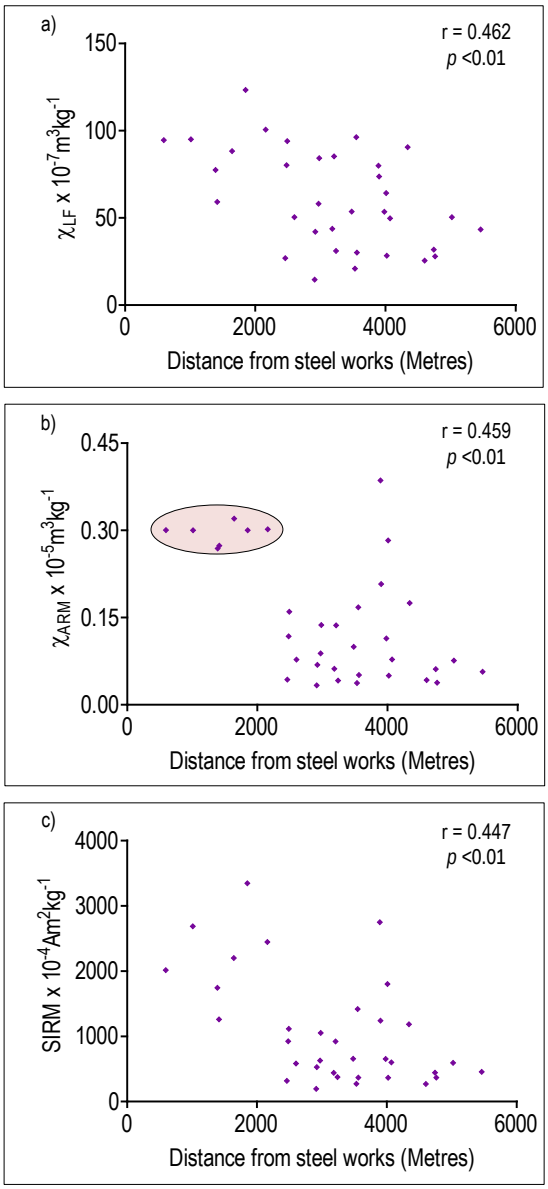

Figure 5.41 Bivariate plots of selected mineral magnetic concentration parameters versus distance from the main Scunthorpe industrial steel works.

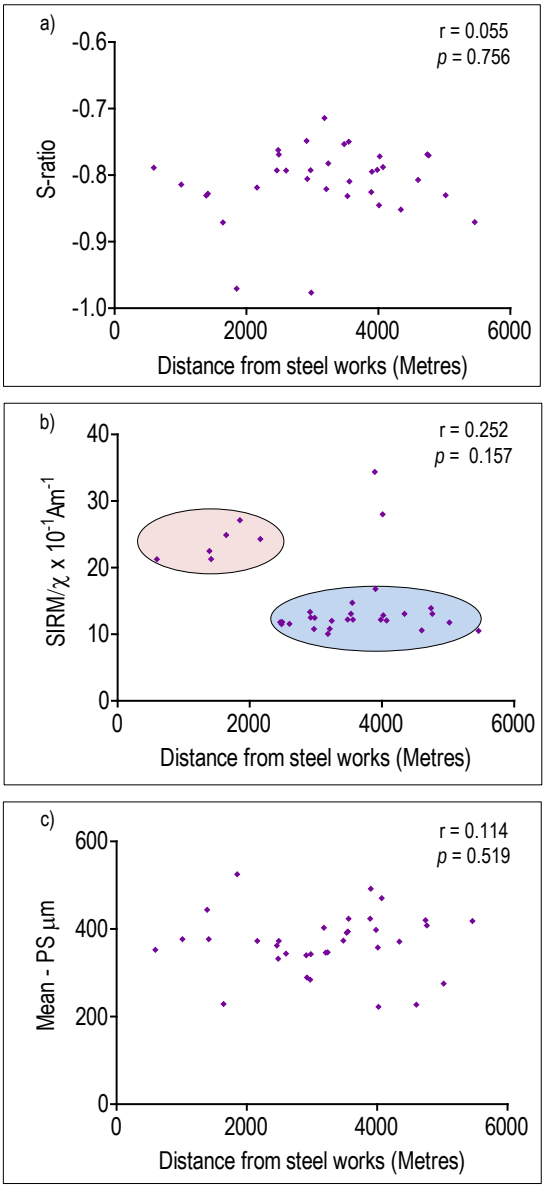

Figure 5.42 Bivariate plots of selected parameters versus distance from the main Scunthorpe industrial steel works.

Figure 5.43a shows the bivariate spread of Fe versus distance to SW, a moderately strong correlation exists (r = -0.584; *p* <0.01) and suggests the concentration of Fe increases closer to the SW. Figure 5.43b shows a similar relationship with Cr versus distance to SW (r = -0.450; *p* <0.01) and further supports the indication that the SW is a major influencing factor in physico-geochemical characteristics of Scunthorpe RDS.

5.6.2 Relationships between geochemical parameters

The results for Scunthorpe samples show some of the geochemical parameters exhibiting strong inter-correlations (*p* <0.05-<0.001) (Table 5.13). The strongest correlation coefficients exist between Al, Ti, V versus Ca, with Al versus V being the strongest (r = 0.850; *p* <0.001), Al and Ti (r = 0.843; *p* = <0.001) and Ti and V (r = 0.821; *p* <0.001). The relationships between Al versus K, Al versus Ca and Mg versus Ca (*p* <0.01-<0.001) suggest some influence from crustal sources to Scunthorpe RDS. The weakest correlation coefficients are associated between Cd and all other geochemical parameters (r = 0.036–0.310; *p* <0.05).

Figure 5.44a shows strong positive correlation of Fe versus Cr (r = 0.636; *p* <0.001), increasing Fe concentrations indicate an increase in Ni (Figure 5.44b) with strong correlation (r = 0.637; *p* <0.001). This is also apparent in Figure 5.44c with additional increase of Fe and Mn (r = 0.630; *p* <0.001) and Figure 5.44d with Fe versus Cu (r = 0.523; *p* <0.001). The results for Figure 5.44 show strong positive correlation between selected geochemical parameters and suggest an influence of combustion–industrial particles on Scunthorpe RDS. The strength of these correlations suggests the characteristics of specific geochemical properties are highly dependent upon each other. The statistical tests indicate that significant relationships exist between groups of geochemical variables (*p* <0.05), most notably crustal and combustion related geochemical combinations.

5.6.3 Relationships between the mineral magnetic and geochemical parameters

Table 5.14 summarizes the correlation statistics between mineral magnetic and geochemical parameters for Scunthorpe. Many mineral magnetic concentration and geochemical parameters are strongly related (i.e. most correlation of coefficient values are *ca*. r = ≤0.382–0.764). Strong positive correlation coefficients exist between χ_{LF} and some geochemical parameters. Figure 5.45a shows the strong positive correlation between χ_{LF} versus Fe (r = 0.789; *p* <0.001), indicating an influence of ferromagnetic grains. Figure 5.45b shows strong positive correlation between χ_{LF} versus Cr (r = 0.637; *p* <0.001) and χ_{LF} versus Ni (r = 0.738; *p* <0.001 (Figure 5.45c)). Strong positive correlations were also found with χ_{LF} versus Mn (r = 0.568; *p* <0.01 (Figure 5.46a)) and χ_{LF} versus Cu (r = 0.533; *p* <0.01 (Figure 5.46b)). These positive relationships are also apparent for other mineral magnetic concentration parameters, χ_{ARM} and SIRM. χ_{ARM} versus Fe (r = 0.791; *p* <0.001), SIRM versus Fe (r = 0.652 *p* <0.001) (Figure 5.46c)). Weak correlations were found between the crustal elements Al, S, Ca and mineral magnetic concentration parameters. Results indicate mineral magnetic concentration parameters identify the soft ferromagnetic phase of anthropogenic particles and suggest the chemistry does influence mineral magnetic assemblages in Scunthorpe RDS.

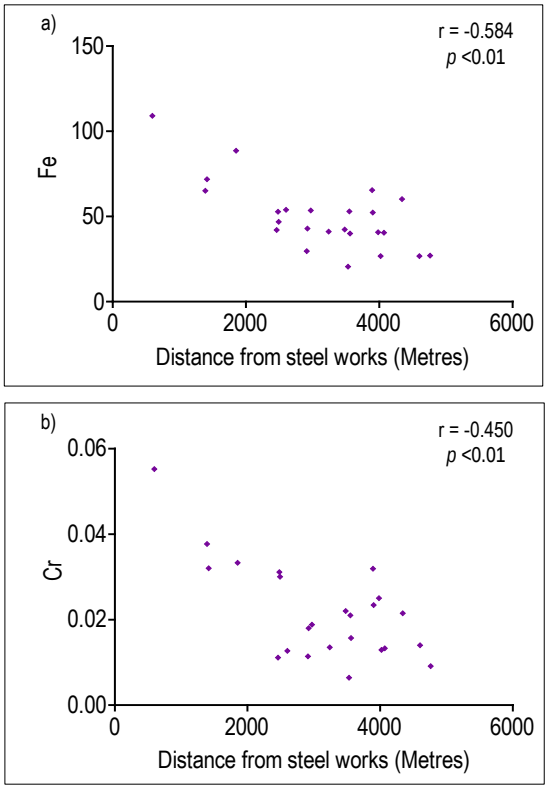

Figure 5.43 Bivariate plots of selected geochemical parameters versus distance from the main Scunthorpe industrial steel works

Table 5.13 Statistical relationships between geochemical parameters for Scunthorpe RDS (**bold** text is significant (*p <0.05; **p <0.01; ***p <0.001)) (n = 34)

Parameters	Mg	Al	S	K	Ca	Ti	V	Cr	Mn	Fe	Ni	Cu	Zn	Cd	Sb
Al	0.020														
S	0.153	**0.590****													
K	-0.324	**0.578****	0.257												
Ca	**0.688*****	**0.536****	**0.583****	-0.192											
Ti	-0.027	**0.843*****	**0.583****	**0.497***	0.429										
V	-0.125	**0.850*****	**0.733*****	**0.502***	**0.446***	**0.821*****									
Cr	-0.175	-0.144	0.013	-0.363	-0.041	-0.053	0.081								
Mn	0.135	0.382	0.304	-0.316	**0.515****	**0.412***	**0.505***	**0.515***							
Fe	-0.153	-0.196	-0.201	**-0.596****	-0.083	-0.072	-0.048	**0.636*****	**0.630*****						
Ni	-0.205	-0.095	0.041	-0.141	-0.176	0.129	0.178	**0.526****	**0.450***	**0.633*****					
Cu	-0.215	-0.134	-0.002	-0.124	-0.210	0.035	0.175	**0.490***	0.149	**0.523****	**0.623*****				
Zn	**-0.454***	-0.261	-0.185	0.104	**-0.455***	-0.152	-0.043	0.180	-0.119	0.185	0.400	0.385			
Cd	0.144	0.061	0.146	-0.132	0.209	0.040	0.095	-0.007	0.310	0.036	-0.117	-0.124	-0.196		
Sb	**0.661*****	-0.157	0.041	-0.248	0.363	-0.251	-0.181	-0.175	0.084	-0.189	-0.263	-0.236	-0.260	0.747	
Pb	-0.334	-0.103	0.060	0.008	-0.213	0.091	0.235	0.102	-0.051	0.284	**0.471***	**0.771*****	**0.477***	-0.218	-0.342

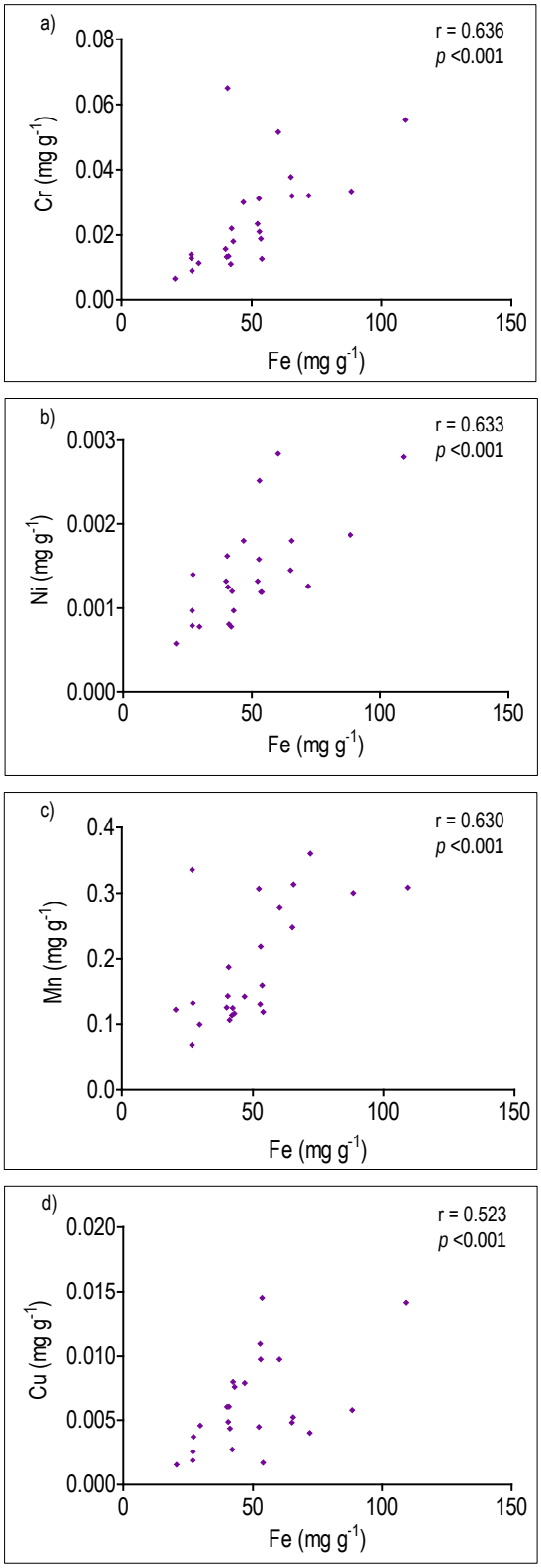

Figure 5.44 Bivariate plots of selected geochemical parameters for Scunthorpe RDS (n = 34).

Table 5.14 Statistical relationships between mineral magnetic and geochemical parameters for Scunthorpe RDS (**bold** text is significant (*p <0.05; **p <0.01; ***p <0.001)) (n = 34)

Parameters	χ	$\chi_{FD\%}$	χ_{ARM}	SIRM	Soft $_{\%\ 20mT}$	Soft $_{\%\ 40mT}$	Hard $_{\%\ 300mT}$	Hard $_{\%\ 500mT}$	Soft $_{IRM\ 20mT}$	Soft $_{IRM\ 40mT}$	Hard $_{IRM\ 300mT}$	Hard $_{IRM\ 500mT}$	S-ratio	χ_{ARM} /χ	SIRM/ $_{ARM}$	SIRM/χ	χ_{ARM} /SIRM
Mg	-0.197	0.126	-0.082	-0.053	-0.338	0.137	-0.020	0.242	-0.077	-0.060	0.097	0.061	-0.078	0.042	0.141	0.140	-0.148
Al	-0.308	0.102	-0.250	-0.253	-0.129	-0.132	0.039	-0.115	-0.261	-0.256	-0.108	-0.144	0.292	-0.080	0.036	-0.083	-0.015
S	-0.040	0.026	-0.166	-0.094	-0.279	-0.164	-0.120	-0.131	-0.133	-0.103	0.212	-0.060	0.405*	-0.161	0.280	-0.046	-0.278
K	**-0.512***	-0.300	**-0.599****	**-0.602****	-0.050	-0.037	0.101	-0.150	**-0.583****	**-0.595****	-0.326	**-0.531****	**0.450***	**-0.548****	0.279	**-0.556****	-0.281
Ca	-0.098	0.243	0.002	0.017	-0.322	0.027	-0.043	0.164	-0.020	0.010	0.088	0.145	0.071	0.174	-0.030	0.222	0.040
Ti	-0.080	0.047	-0.059	0.021	-0.176	-0.210	-0.068	-0.139	-0.018	0.011	0.135	0.100	0.247	0.045	0.185	0.179	-0.172
V	0.031	-0.001	-0.034	-0.018	-0.024	-0.043	0.009	-0.120	-0.024	-0.012	-0.008	0.031	0.207	-0.007	-0.025	-0.010	0.025
Cr	**0.637*****	0.097	**0.495***	**0.526****	0.251	-0.167	-0.262	0.048	**0.510***	**0.523****	0.011	**0.556****	-0.258	**0.410***	**-0.445***	0.362	**0.416***
Mn	**0.568****	0.341	**0.678*****	**0.683*****	0.234	-0.081	-0.218	-0.030	**0.673*****	**0.683*****	0.200	**0.662*****	-0.401	**0.723*****	**-0.453***	**0.692*****	**0.490***
Fe	**0.789*****	0.364	**0.791*****	**0.813*****	0.273	-0.100	-0.060	-0.061	**0.796*****	**0.815*****	0.287	**0.747*****	**-0.452***	**0.678*****	-0.387	**0.652*****	**0.406***
Ni	**0.738*****	-0.088	**0.465***	**0.568****	0.273	0.201	-0.002	0.020	**0.558****	**0.593****	0.074	**0.656*****	-0.173	0.236	0.043	0.319	-0.037
Cu	**0.553***	0.056	0.190	0.279	0.092	0.184	0.142	0.037	0.249	0.294	-0.004	0.356	0.120	-0.027	0.032	0.014	-0.078
Zn	0.346	0.058	0.062	0.120	0.042	0.027	-0.023	-0.050	0.075	0.130	-0.056	0.115	0.247	-0.082	-0.086	-0.095	0.027
Cd	0.120	-0.045	0.103	0.097	0.205	-0.069	**-0.411***	-0.039	0.115	0.091	0.023	0.074	0.000	0.134	-0.197	0.106	0.179
Sb	-0.091	-0.042	-0.057	-0.073	0.002	0.139	-0.257	0.176	-0.056	-0.075	-0.026	-0.031	-0.055	-0.004	-0.079	-0.012	0.048
Pb	0.399	-0.171	0.086	0.127	-0.130	0.305	0.306	0.071	0.101	0.155	0.024	0.198	0.177	-0.151	0.140	-0.147	-0.153

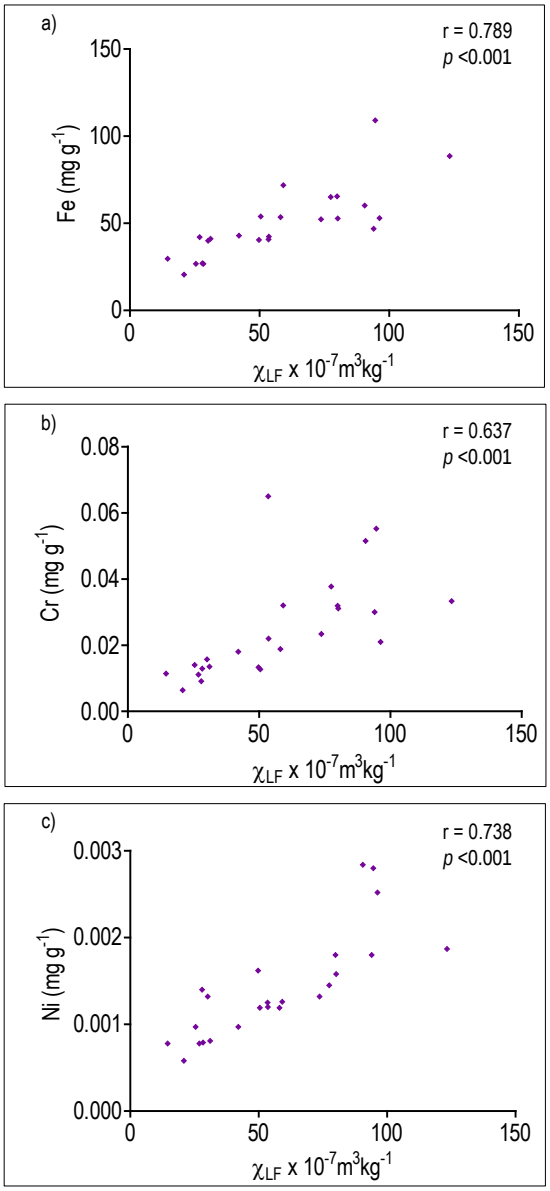

Figure 5.45 Bivariate plots of selected mineral magnetic concentration (χ_{LF}) versus geochemical parameters for Scunthorpe RDS (n = 34).

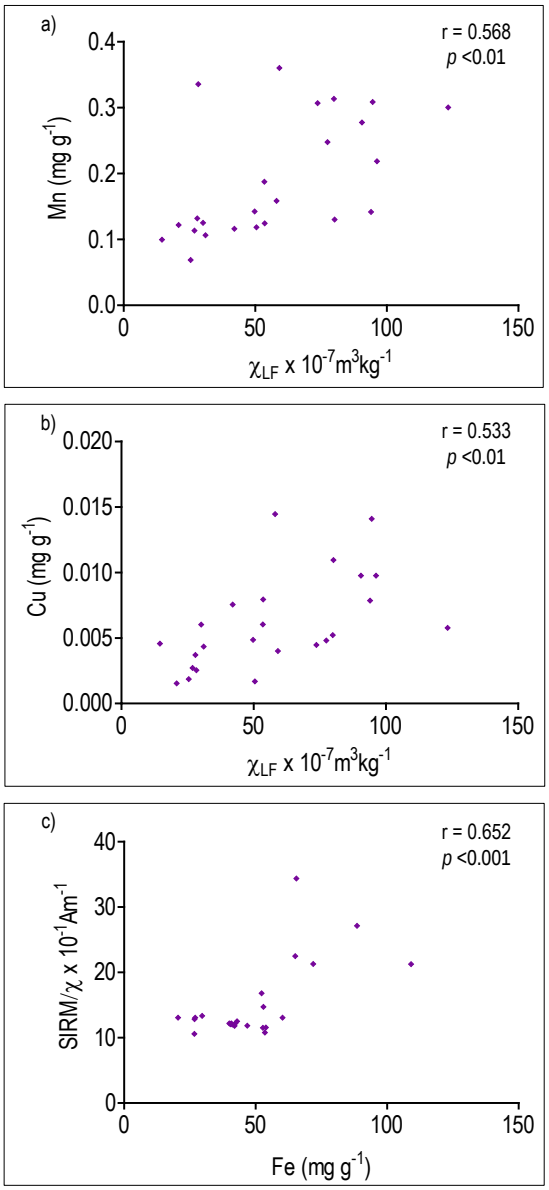

Figure 5.46 Bivariate plots of selected mineral magnetic concentration (χ_{LF}) versus geochemical parameters for Scunthorpe RDS (n = 34).

5.6.4 Further investigation using SEM

Figure 5.47a shows a spherical Fe oxide particle observed from west Scunthorpe RDS samples and is likely to have been derived from high temperature combustion processes. RDS samples contain almost identical Fe oxide particles and ranges (<60 μm). Figure 5.47b shows a typical spherical Fe oxide particle which is comparable to those found in other studies (Figure 3.16). Not all spheres were identical but do display common characteristics. Figure 5.47c shows a typical particle found in Scunthorpe. Particle counts (Figure 5.48) show that samples taken from near the SW tend to have higher counts of glassy iron spherules. Overall, limited differences have been found within the physio-chemical appearance of particles found in and around the sampling area. The main differences are in distinctive sample locations, Fe oxide particles close to the SW are up to five times that of west Scunthorpe. The types and frequency of particles suggest that they derive from traffic and industrial combustion processes. The results support the mineral magnetic and geochemical data, which characterized magnetic particulates of RDS as being of multi-domain soft-ferrimagnetic mineralogy. Figure 5.47d shows an Fe oxide particle which is virtually identical to those found in west Scunthorpe. Figure 5.47e and f show particles observed in west Scunthorpe and display mutated appearance, with droplet shapes and surface characteristics of combustion particles.

5.6.5 Further assessment using factor analysis plots

Initially all parameters were used to generate Factor Plots. However, the resultant plots (not presented) did not show any clear patterns. Factor analysis was re-applied to various parameter combinations, in some cases excluding some parameters from the data-set.

5.6.6 Factor analysis using mineral magnetic parameters

Simultaneous R- and Q-mode factor analysis was performed by using selected mineral magnetic parameters. Figure 5.49 shows a factor plot created from parameter and sample loadings from Factors 1 and 2. The first two factors explain 50% of variation in 13 parameters, indicating strong positive and negative loadings on both factors. The spread of loadings indicates influence by mineral magnetic concentration and mineralogy and magnetic grain size parameters.

Factors 1 explains 32% of variation in the parameters, with negative loadings of S-ratio and SIRM/$_{ARM}$, but positive loadings of χ, $\chi_{FD\%}$, χ_{ARM}, SIRM, Soft$_{IRM20mT}$, Soft$_{IRM40mT,}$ Hard$_{IRM300mT,}$ Hard$_{IRM500mT,\ ARM}$/χ and χ_{ARM}/SIRM, and SIRM/χ. Factors 2 explains 18% of variation, suggesting a lesser influence than Factor 1.S-ratio and SIRM/$_{ARM}$ and χ_{ARM}/SIRM, Hard$_{IRM300mT}$ have negative loadings on Factor 2 with all $\chi_{FD\%}$, $\chi_{ARM,}$ Hard$_{IRM500mT,\ ARM}$/χ, SIRM/χ parameters having positive loadings.

From the spread of sample loadings, the samples are influenced by both Factors 1 and 2. The distribution of the SW sample points indicates a major influence along Factor 1 with some similarities of magnetic properties between the samples and display positive to negative loadings along Factor 1 (top left to bottom left).

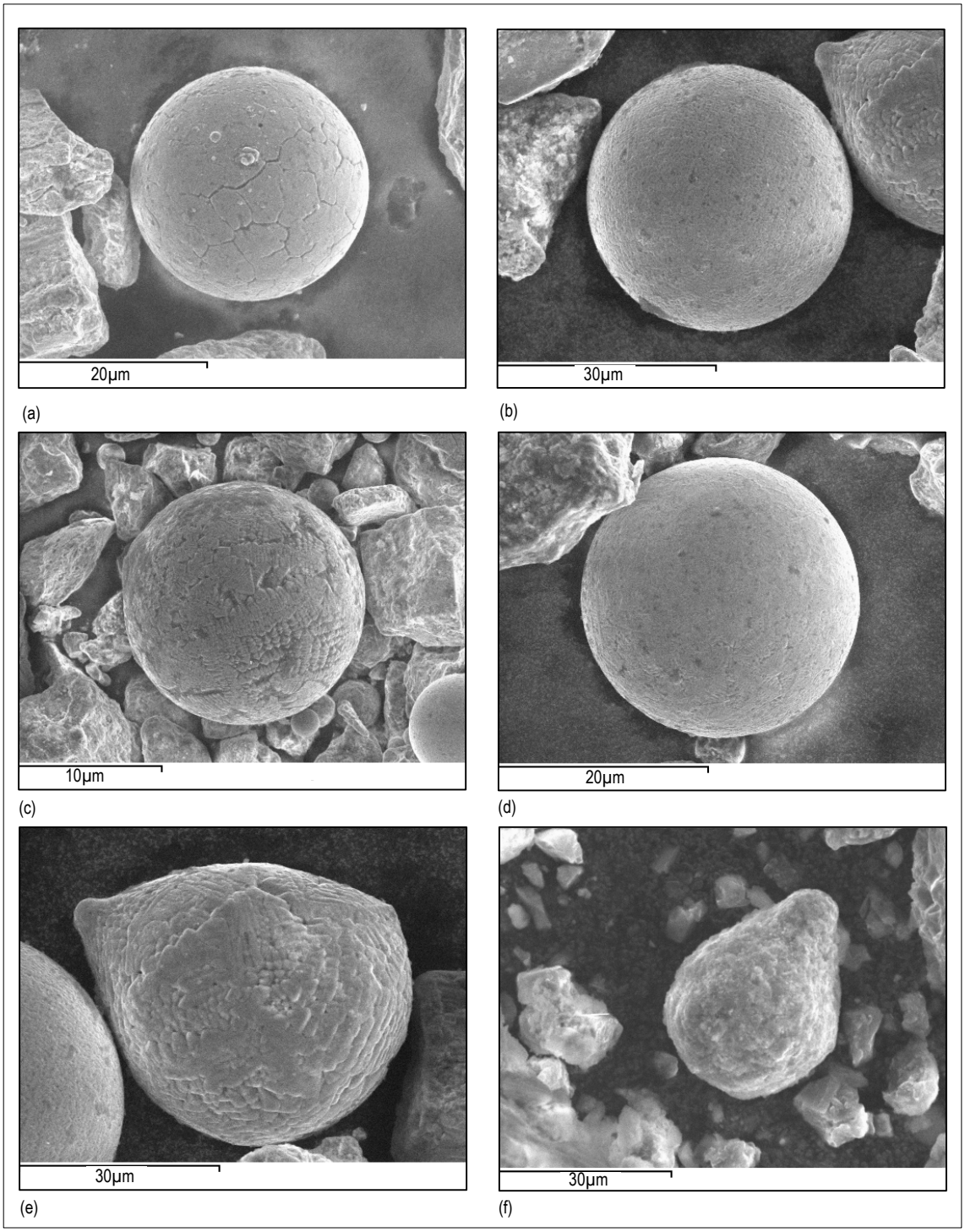

Figure 5.47 SEM micrographs of Fe oxide particles in Scunthorpe RDS

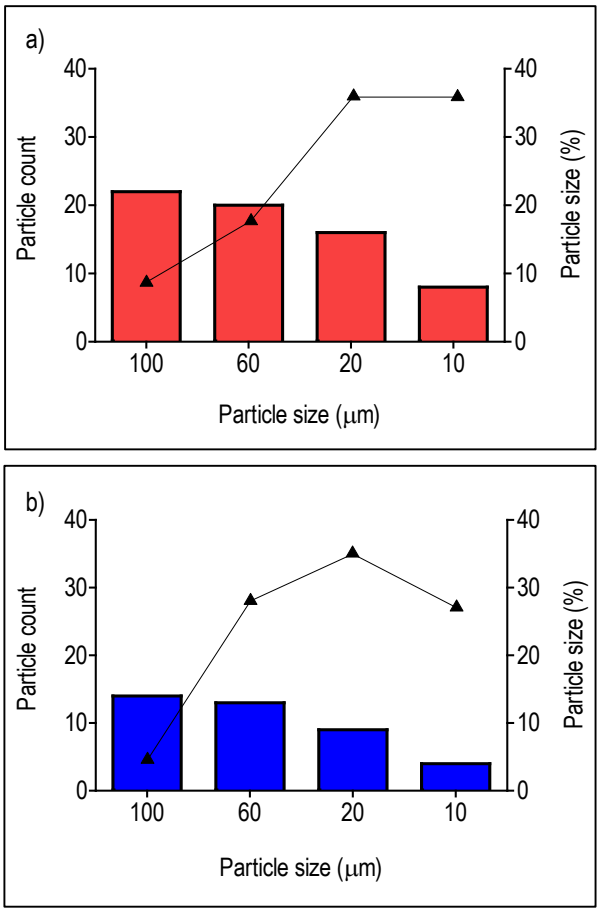

Figure 5.48 SEM particle counts and particle size (%) for a) Steel Works, b) Road Network.

There is an indication of influence from grain size and mineralogy parameters for the SW samples. The spread of samples across the RN samples indicates an influence from Factors 1 and 2. The sample loadings for the RN samples shows a positive to negative influence along Factor 1, suggesting some mineral magnetic concentration, magnetic grain size and mineralogy influence.

5.6.7 Factor analysis using selected textural parameters

Simultaneous R- and Q-mode factor analysis was performed using selected particle size and distribution parameters. Figure 5.50a shows a factor plot created from parameter and sample loadings from Factors 1 and 2. The first two factors extracted explain 73% of variation in the 12 parameters, indicating strong positive and negative loadings on both factors. Factors 1 and 2 explain 58% and 15% of the variation in 10 mineral magnetic and textural parameters used. The spread of loadings indicate some influences by both particle size and distribution. Factor 1 explains 58% of variation in parameters, with positive loadings of all parameters mean, median, sorting, skewness, kurtosis, sand, silt clay, $PM_{100,}$ $PM_{10,}$ $PM_{2.5}$ and $PM_{1.0,}$ Factor 2 explains 15% of variation, suggesting limited influence. Distribution parameters include, mean, median, skewness, sorting, kurtosis and PM_{100}. Sample loadings are influenced by Factors 1 and 2 appearing more influenced by Factor 1. Sample groupings show separation with SW samples (positively-negatively loaded along Factor 1) and display no influence on any parameter.

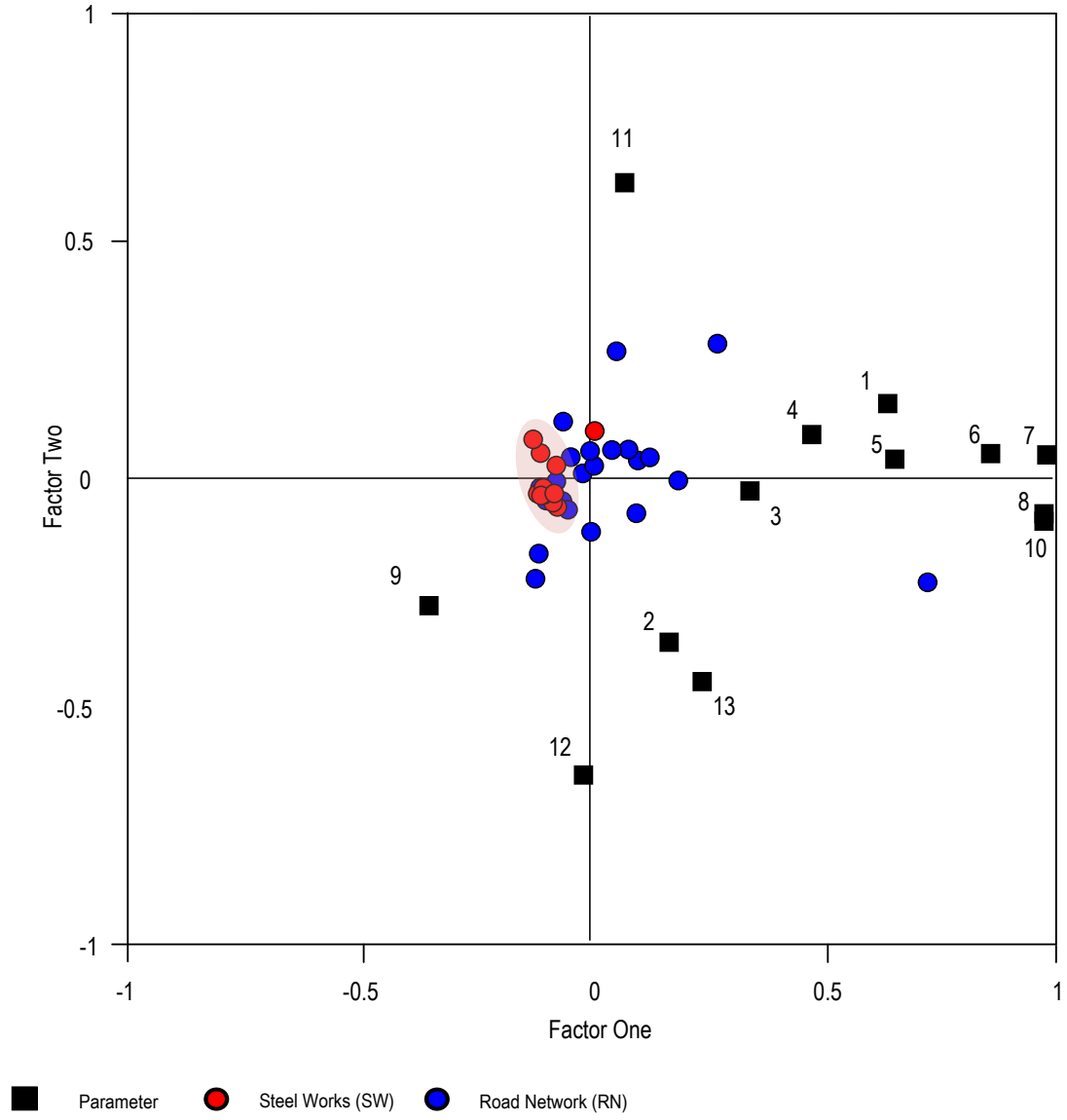

	Parameters				
1	χ_{LF}	6	Soft $_{IRM40mT}$	11	χ_{ARM}/SIRM
2	χ_{FD}	7	Hard $_{IRM20mT}$	12	SIRM/ARM
3	χ_{ARM}	8	Hard $_{IRM40mT}$	13	SIRM/χ
4	SIRM	9	S-ratio		
5	Soft $_{IRM20mT}$	10	ARM/χ		

Figure 5.49 Simultaneous R- and Q mode factor analysis plots of Factor 1 versus Factor 2, based on selected mineral magnetic for parameters Scunthorpe RDS.

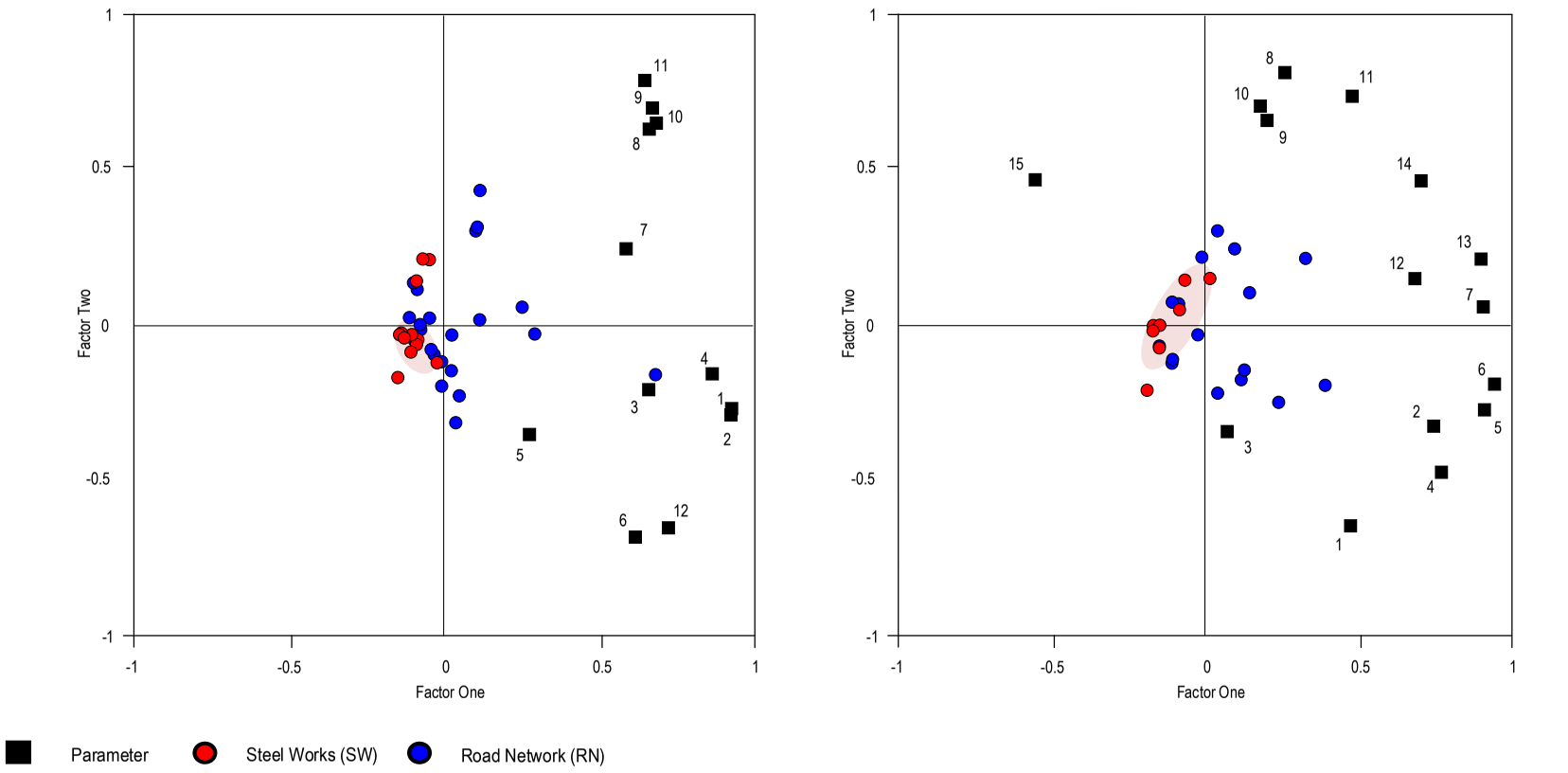

(a)	Parameters				
1	Mean	5	Kurtosis	9	$PM_{1.0}$
2	Median	6	Sand	10	$PM_{2.5}$
3	Sorting	7	Silt	11	PM_{10}
4	Skewness	8	Clay	12	PM_{100}

(b)	Parameters				
1	Mg	6	Ti	11	Ni
2	Al	7	V	12	Cu
3	S	8	Cr	13	Zn
4	K	9	Mn	14	Cd
5	Ca	10	Fe	15	Pb

Figure 5.50 Simultaneous R- and Q mode factor analysis plots of Factor 1 versus Factor 2, based on (a) selected textural and (b) selected geochemical parameters for Scunthorpe RDS.

RN sample loadings show a positive sample loading along Factor 1, with some positive influence along Factor 2. RN sample loadings display weak influences from distribution and particle size parameters.

5.6.8 Factor analysis using selected geochemical parameters

Simultaneous R- and Q-mode factor analysis was performed using selected geochemical parameters. Figure 5.50b shows a factor plot created from parameter and sample loadings from Factors 1 and 2. The first two factors extracted explain 53% of variation in the 15 parameters. The geochemical parameters have positive and negative loadings on both extracted factors, the spread of which indicated they are influenced by various chemical association gradients.

Factor 1 explains 36% of variation in parameters, with positive loadings of Mg, Al, S, K, Ca, Ti, V, Cr, Fe, Ni, Cd, Mn, Cu and Zn along Factor 1 with no parameters negatively loaded along Factor 1. Factor 2 explains 17% of variation, suggesting limited influence Fe, Mn, Cr, Ni, Cd, Zn V and Pb. These all have positive loadings along Factor 2, with no parameters negatively loaded. The spread of samples indicates influence from both Factors 1 and 2, with sample loadings of SW and RN showing some separation and groupings. The SW sample loadings indicate the main influencing factor as positive Factor 1, leading into negative Factor 1. Sample spread indicates the influence of anthropogenic geochemical influences (Cr, Me, Ni and Fe). The RN sample loadings indicate a similar influence along Factor 1, but also negative-positive Factor 2, with indication of natural background (Al, Ca, K and S) influences.

5.6.9 Factor analysis using key physico-chemical parameters

Factor analysis was initially performed using the physico-chemical parameters analysed in the previous plots (Sections 5.6.6–5.6.8). The first two factors extracted explain 58% of variation in the 18 parameters. Figure 5.51 shows a factor plot created from parameter and sample loadings from Factors 1 and 2. The physico-chemical parameters have positive and negative loadings on both extracted factors. Factor 1 explains 37% of variation in the parameters: χ, χ_{ARM}, SIRM, $PM_{1.0,}$ $PM_{2.5,}$ $PM_{10,}$ $PM_{100,}$ Fe, Zn, Ni, Mn, Cd, Pb and Cu, where all have positive loadings. However $\chi_{FD\%}$, S-ratio, SIRM/χ and Cr have negative loadings. Factor 2 explains 21% of the variation in all 18 parameters, with χ, χ_{ARM}, SIRM, Fe, Zn, Ni, Mn, Cd, Pb and Cu having positive loadings and the S-ratio having negative loadings.

The spread of samples indicates influence from both Factors 1 and 2, with sample loadings of SW and RN showing some separation and groupings. The SW sample loadings indicate the main influencing factor being positive leading into a negative Factor 1 (top right to bottom left). The spread of samples indicates the influence being pulled between mineral magnetic concentration parameters χ, χ_{ARM}, SIRM, geochemical parameters Fe, Zn, Ni, Mn, Cd, Pb and Cu and the S-ratio. The spread of RN samples show loadings mostly influenced by a positive-negative Factor 1 with main influencing parameters indicating a mineral magnetic gradient of mineralogy and grain size parameters. None of the particle size parameters appear to have detectable influencing factors.

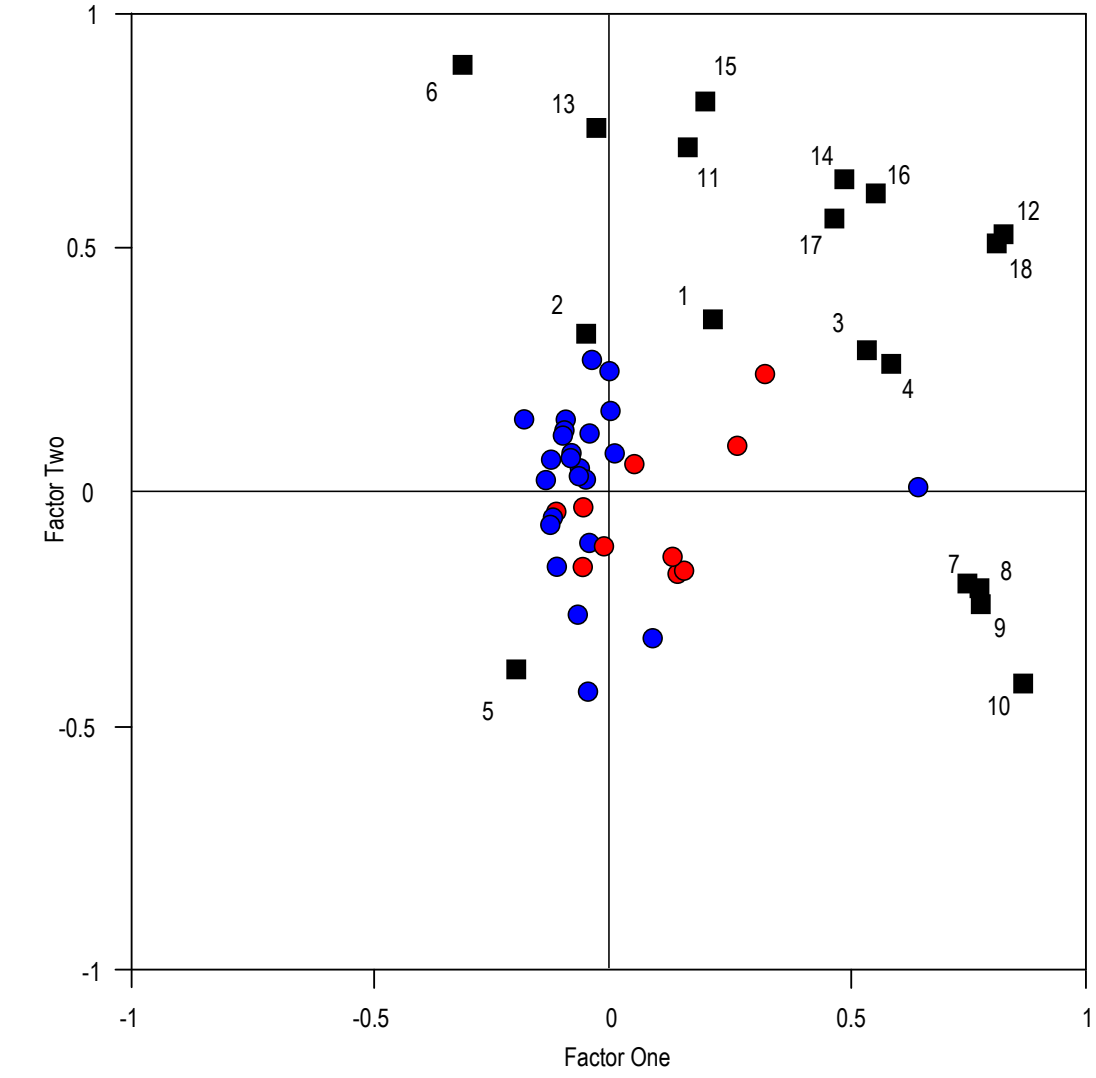

	Parameters						
1	χ_{LF}	6	SIRM/χ	11	Fe	16	Cd
2	χ_{FD}	7	$PM_{1.0}$	12	Pb	17	Mn
3	χ_{ARM}	8	$PM_{2.5}$	13	Cr	18	Cu
4	SIRM	9	PM_{10}	14	Ni		
5	S-ratio	10	PM_{100}	15	Zn		

Figure 5.51 Simultaneous R- and Q mode factor analysis plots of Factor 1 versus Factor 2, based on characteristics for selected parameters for Scunthorpe RDS.

5.6.10 Summary for Scunthorpe

The characteristics of Scunthorpe RDS show a wide range of variation over the sampling area. Scunthorpe shows some potential for a mineral magnetic - particle size proxy. Geochemical correlations give a good indication that mineral magnetic methods can work very well as a geochemical pollution proxy in this area. The characteristics and relationships for Scunthorpe RDS can be summarized as:

- Magnetic properties of RDS in Scunthorpe are predominantly ferromagnetic.
- High concentrations of magnetic minerals found (Highest within UK samples).
- Mineral magnetic grain size remains consistently multi-domain within the study area.
- Good correlations between SIRM and $<PM_{10}$ (p <0.001).
- No Hard minerals correlate with particle class sizes, suggesting soft sources contributing to significant correlations (soft magnetic material can be directly linked with anthropogenic combustion sources).
- Strong mineral magnetic and geochemical correlations (p <0.01-0.001).
- High mineral magnetic and geochemical concentrations found at specific locations (found within the Scunthorpe AQMA).
- East-west concentration boundary, with high concentrations of magnetic material found within close proximity to industry.
- Specific geochemistry linked with east side and industry. GIS and statistical analysis of geochemistry show a combination of natural background and anthropogenic sources which suggest mixing in areas.
- Inter geochemical correlations, SEM and Factor plots further suggest road traffic and industrial sources.

5.7 Selected towns and cities of the UK sample summary

All town samples indicate a large proportion of coarse grained particles ($\chi_{FD\%}$ mean 1.379-2.183) with relatively high χ_{LF} (17.730-61.720 x $10^{-7}m^3kg^{-1}$) and soft behaviour, with low concentrations of hard minerals. Levels of χ_{ARM}/SIRM suggest the dominant magnetic component comprises multi-domain (MD) grains of ferromagnetic minerals, with superparamagnetic (SP) and stable single domain (SSD) ferromagnetic grains and non-ferrimagnetic minerals present in low concentrations. The RDS in the selected UK towns and cities is an admixture of natural and anthropogenic components, both contain magnetic mineral fractions with specific magnetic properties. Results suggested a low to high level of mineral magnetic parameter concentrations, with an indication that the magnetic properties of the sediments are similar to intermediate igneous rocks, basic/ultra-basic rocks and ferromagnetic minerals with moderate to high concentrations of magnetically soft minerals. Organic matter content was low in all samples. Due to the low values the diluting effect on the magnetic concentrations was not significant.

Few mineral magnetic and particle size linkages have been found in the selected towns and cities. Those locations which have shown potential show that geochemical parameters and the environment could be influencing factors for mineral magnetic and particle size relationships. By further investigating the potential proxy locations (London and Scunthorpe), it has been demonstrated that mineral magnetic concentration parameters can be used with confidence to identify potential sites of specific anthropogenic pollution. Sample analysis of London (MBR) has shown the potential for mineral magnetic measurements to identify 'start-stop' vehicle locations, via increased concentrations of Zn, Mn and Cu. Mineral magnetic concentration parameters have also shown the potential to identify relationships with other anthropogenic geochemical influences, notably from combustion (Fe, Pb). Investigation of the geochemical relationships have suggested the presence of crustal and predominantly anthropogenic sources of elements.

Spatial analysis for Scunthorpe displayed a distinct difference in mineral magnetic concentrations between the east and west. Mineral magnetic concentration parameters, when used in conjunction with geochemical parameters, have successfully determined specific environmental magneto-physico signatures. Scunthorpe has been identified as a sink for anthropogenic combustion and industrial particles, due to local steel works. Mineral magnetic concentration parameters identified high concentrations of magnetic material with an associated particle size linkage.

The geochemical compositions for both locations are mainly anthropogenic, but do posses differing signatures due to location activity. The resulting correlations found within London and Scunthorpe suggests that unique environments, which are dominant and relatively isolated, have large influences on mineral magnetic and particle size associations.

SEM micrographs and multivariate techniques supported some of the assumptions that the samples are influenced by mineral magnetic and geochemical parameters, but have also shown the limited influence particle size has on RDS and the other parameters.

The use of mineral magnetic techniques in the analysis of RDS for selected towns and cities has shown good potential for identifying sites of localized geochemical pollution, but very limited potential for mineral magnetic concentration parameters to be used as a particle size proxy. This has been shown through analysis of all parameters which have displayed weak or no relationships. It is only sites with a dominant anthropogenic activity that have shown some potential. The results show that there are complex linkages between particle size, mineral magnetic and geochemical parameters that differ, depending on location and environmental circumstances.

In Summary:

- Magnetic properties of RDS in UK towns are predominantly ferromagnetic.
- Mineral magnetic concentrations vary spatially and appear to reflect anthropogenic activity in the locality.
- Mineral magnetic grain size remains predominantly multi-domain within the study areas
- Several sites contain a mixture of coarse and fine grained magnetic material suggesting a number of influences.
- The predominantly coarse / multi domain magnetic material appears to be related to higher mineral magnetic concentrations and anthropogenic sources.
- Results suggest linkages and similarities for parameters between the more developed towns, which could be linked to industry, land-use and population.
- Few correlations have been found within the study areas and are not suitable for particle size proxy purposes.
- Correlations that are evident appear to relate to the direct environmental conditions of the location and justify further investigation to establish if suitable for proxy purposes.
- Specific geochemistry linked with locations. Anthropogenic and crustal geochemistry showing distinct areas of dominance and some mixing.
- Results suggest mixing of geochemical sources, shown within the GIS of Scunthorpe and Wolverhampton.
- Strong mineral magnetic and geochemical correlations (p <0.01-0.001) have been found at various sites and suggest the suitability of mineral magnetic measurements as a geochemical pollution proxy.
- Inter geochemical correlations, SEM and Factor plots further suggest road traffic and industrial sources at most locations.

Chapter 6

Mineral magnetic measurements as a proxy for evaluating pollution and sediment texture

6.1 Introduction

Chapter 6 collates the findings of Chapters 4 and 5 and contextualises the information within the framework of existing knowledge. Moreover, factors influencing sediment relationships and proxy reliability are further examined to create a means of determining whether users can be certain of relationships between RDS and mineral magnetic properties. This is achieved through: (i) examining spatial and temporal patterns to provide linkages to urban sediment systems; (ii) exploring magnetic–textural proxy relationships to reveal insights into sediment dynamics; and (iii) investigating the factors that influence the reliability of mineral magnetics as a texture proxy, so as to create a conceptual appreciation for its application.

6.2 Insight from spatial and temporal patterns

This Section compares the findings of Wolverhampton, the West Midlands air monitoring stations and the selected towns and cities with those of other UK and global studies, which facilitates linkages to built environment sediment systems.

Concentrations of magnetic material in this study are notably high compared to other Wolverhampton data sets (Booth *et al.,* 2006; Power *et al*., 2006), double those of Manchester (Robertson *et al*., 2003), yet similar to Liverpool (Xie *et al*., 2001). Compared to global studies, Wolverhampton values are similar to other large cities, such as Kathmandu (Gautam *et al.*, 2005), Madrid, (McIntosh *et al*., 2007), Seoul (Kim *et al*., 2007), Shanghai (Tanner *et al*., 2008), Beijing (Zheng and Zhang, 2008) Lanzhou (Wang *et al*., 2012) and Loudi (Zhang *et al*., 2012).

Spatial data comparisons have highlighted distinct concentration anomalies, which may be associated with intensities of traffic volume and industrial land use. Moreno *et al*. (2003) and Sheng-Gao *et al.* (2008) indicated high magnetic concentrations and relatively larger domain sizes of magnetic particles alongside roads with high volumes of vehicle traffic. The same relationships are evident at Wolverhampton sites, with highest concentration values associated with high volume traffic roads and near railways. Moreno *et al.* (2003) also found a decrease in concentration and grain size of magnetic particles with distance from roadsides, which supported the inference of particulate pollution linked to vehicle emissions. Applying the same analogy, lowest concentration values are associated with residential roads with low volumes of traffic, which illustrate mineral magnetic methods could be used as a potential pollution proxy. However, this would necessitate a further study, separate from the aims and objectives of this study.

Concentrations of magnetic material for some Wolverhampton sites illustrate low intra-site variability with time and can be mostly predicted (e.g. site 15 always contained low concentrations). Similarly, high inter-site variability can also be predicted (e.g. site 15 always has lower concentrations than sites 27 and 29). This evidence suggests there is minimal wider

source ingress or loss of RDS at the sites and/or source volumes are kept relatively constant with time. Based on the earlier pollution assumption, this indicates minimal differences in levels of anthropogenic activity with time (i.e. traffic levels are not seasonal dependent-residential roads (e.g. site 15) do not get any busier than corresponding arterial roads (e.g. site 29) during specific seasons.

Trends within intra-site variability reveal possible seasonal influences, which appear to be associated with specific weather conditions (Appendix 4.3). For instance, there are increases in magnetic material during the warmer drier months, compared to decreases in magnetic material during the cooler wetter months. Ideally, a longer study would be needed to verify this statement. However, this observation is supported by Xie *et al.* (2001), who found χ_{LF} concentrations were higher during summer months (χ_{LF} 74.5 x $10^{-7}m^3kg^{-1}$) than winter months (χ_{LF} 55.8 x $10^{-7}m^3kg^{-1}$) in Liverpool. Conversely, Kim *et al*. (2009) found highs of magnetic material during cooler months (SIRM 596.25 x $10^{-4}Am^2kg^{-1}$) than warmer months (SIRM 283.85 x $10^{-4}Am^2kg^{-1}$) Seoul has a monsoonal climate: dry cool winters; warm wet summers. So, in winter in Seoul, RDS would accumulate and not be washed much. Wolverhampton has rainfall all year round. Either way, in line with other studies, this indicates weather conditions may play important roles in the build-up and dilution effect of RDS (Figure 2.13); whereby, rainfall can dilute or washout particulates, via surface runoff to gully pots and other drainage systems (Lee *et al.,* 2005; Kim *et al*., 2009). Davis and Birch (2010) identified significant pollutants in storm-water runoff associated with busy urban roads. Similarly, prolonged dry spells influence residence times of ground-level street dusts (Akhter and Madany, 1993).

Concentration of ASU magnetic material in this study is relatively consistent between sites (Birmingham (mean χ_{LF} 11.376 x $10^{-7}m^3kg^{-1}$), Leamington Spa (mean χ_{LF} 22.592 x $10^{-7}m^3kg^{-1}$) and Coventry (mean χ_{LF} 16.193 x $10^{-7}m^3kg^{-1}$) are similar), with the exception of Wolverhampton (mean χ_{LF} 41.880 x $10^{-7}m^3kg^{-1}$). This is probably because the Wolverhampton ASU site is located within a busy city centre; whereas, the other sites are adjacent to car parks, urban back streets and parks. Therefore, site proximity to busy arterial roads is a probable influencing factor. Similar results have been found in other major cities, Kim *et al.* (2009) and Yang *et* al. (2010) reported high χ_{LF} concentrations in RDS near main roads and lower concentrations near green open park areas, which allowed the inference of anthropogenic sources from vehicles.

Mineral magnetic concentrations of the selected towns and cities in this study show a wide range of values (Scunthorpe, mean χ_{LF} 61.720 x $10^{-7}m^3kg^{-1}$ and Norwich, mean χ_{LF} 17.730 x $10^{-7}m^3kg^{-1}$), but the range is comparable to other UK studies. For instance, χ_{LF} values range from 16.8-116.6 x $10^{-7}m^3kg^{-1}$ for Liverpool (Xie *et al.,* 2001), range from 14.33-27.95 x $10^{-7}m^3kg^{-1}$ for Southport (Booth *et al.,* 2007) and range from 14.91-111.21 x $10^{-7}m^3kg^{-1}$ for Wolverhampton (Shilton *et al.,* 2005). This is further supported by the similarity of the Salford values (mean 35.570 x $10^{-7}m^3kg^{-1}$) of this study compared to those of a nearby study (χ_{LF} 27.8 x $10^{-7}m^3kg^{-1}$) conducted by Robertson *et al.* (2003), who proposed vehicle-derived particles as the principal sediment source.

Despite the towns and cities having comparable values to other UK places, the range of values for individual places reveals unique signatures that indicate discrete characteristics, which may reflect particular sources and distinct environmental surroundings. For instance, Scunthorpe is a predominantly industrial town and has exceptionally high values (mean 61.720 x $10^{-7}m^3kg^{-1}$); Salford is a densely populated city with high volume major transport routes and moderate to high values (mean 35.570 x $10^{-7}m^3kg^{-1}$). In contrast, Oswestry and Dumfries are small towns situated away from major transport routes, have no sizeable industry and have low values (means 21.510, 22.920 x $10^{-7}m^3kg^{-1}$, respectively).

Charlesworth *et al*. (2003) studied RDS in Birmingham and Coventry and found high concentrations of magnetic material associated with industrial and high traffic volume areas, and low mineral magnetic concentrations associated with residential and park areas. Despite both cities having similar variability, their concentrations were notably different. Elsewhere, Yang *et al*. (2010) showed park areas with low mineral magnetic concentrations (SIRM 112.91 x $10^{-4}Am^2kg^{-1}$) compared to industrial areas (SIRM 162.60 x $10^{-4}Am^2kg^{-1}$). Kim *et al*. (2009) found high variability (χ_{LF}) in Seoul (South Korea) when traffic flow into the City exceeded an estimated 90,000 vehicles per day. The size of urban areas appears to elevate concentrations, with Charlesworth *et al*. (2003) demonstrating linkages between population size and potential input of heavy metals to RDS in urban areas.

To surmise the spatial and temporal patterns section, it has been shown that this study has comparable values to previous studies, which suggest specific sediment sources may play significant roles in the magnetic signatures of individual places and their site-related variability. Furthermore, both natural and built environment processes influence RDS properties and their dynamics within the urban sediment system.

6.3 Magnetic-textural proxy relationships

This Section compares the proxy findings of Wolverhampton, the West Midlands air monitoring stations and the selected towns and cities with those of other UK and global studies. These comparisons may reveal insights into urban sediment transport dynamics that may influence the potential use of magnetic measurements as a pollution and/or texture proxy.

With the exception of a few relatively weak significant correlations between mineral magnetic and textural parameters (χ_{LF} versus clay r = 0.125; p <0.01), no significant strong relationships are evident from the Wolverhampton data sets. Detailed analysis of the seasonal data set revealed the spring months exhibited the strongest correlations (χ_{LF} versus PM_{10} r = 0.376; p <0.001), but the all year round reliability of using mineral magnetic as a proxy tool is doubtful because the autumn and winter months display insignificant relationships. Unfortunately, there are no previous published studies to compare with these findings. However, given the nature of the sampling periods, it is assumed that differences maybe reflect weather conditions, which accords with the findings of Xie *et al.* (2001) and Kim *et al.* (2009).

West Midlands (ASU) sites show no significant correlations between mineral magnetics-RDS and air-borne PM sizes. However, this may be a reflection of the difference between samples collected directly from the ground compared with those measured by the ASU above the ground. For instance, Saragnses *et al*. (2011) collected material derived from filters directly linked to the positioning of above-ground analytical instruments. They found significant correlations between magnetic particles, which were dominated by ferromagnetic minerals, and NO_x emissions, which were derived from vehicles. ASU data and filters also had significant associations with PM_{10}. Muxworthy *et al.* (2003) also used filters and revealed mineral magnetic and particle size linkages (<100 nm), with the main source believed to be from vehicles.

Several studies (Matzka and Maher, 1999; Power *et al*., 2006; McIntosh *et al.,* 2007; Maher *et al.,* 2008) have identified tree leaves as effective receiver-surfaces of anthropogenic magnetic material and could be used as natural filter media for airborne particles. Power *et al*. (2006) found that by using tree leaves as a settlement medium for urban particulates, particle size and mineral magnetic associations could be determined. These studies provide valuable insights into the potential for the techniques to be used in localised settings to determine nearby contaminant conditions, particularly where direct access to ASUs is unavailable. Thus, it may be possible to sample tree leaves at similar heights to ASU monitoring devices. However, tree leaf particle deposition does experience environmental changes, due to precipitation and washing of leaves (McIntosh *et al.,* 2007).

Very few of the towns and cities in this study have shown significant correlations between mineral magnetic and particle size parameters. However, Marylebone Road demonstrates the greatest proxy potential (χ_{LF} versus $PM_{1.0}$ r = 0.589; p <0.001; χ_{ARM} versus $PM_{1.0}$ r = 0.392; p <0.01; SIRM versus $PM_{1.0}$ r = 0.554; p <0.001). When compared to the other UK sample sites, Marylebone Road represents a much smaller sample area with a limited diversity of land uses. Unlike the other towns and cities, Marylebone Road represents a semi-secluded catchment, where sediment sources are likely to be derived from a limited number of sources that are presumably derived locally. In contrast, given the larger size of the sampling areas, the towns and cities are likely to contain a range of sediment sources derived from various land uses over the sampling areas.

Previous research has demonstrated significant relationships between mineral magnetic and particle size data. Oldfield *et al.* (1993) and Clifton *et al.* (1999) found χ_{LF} versus silt and sand held the greatest proxy for their site study, whereas Booth *et al*. (2005) demonstrated that χ_{LF} χ_{ARM} and SIRM could show significant proxy potential over a series of textural classes in one environmental setting, but no potential in another. Zhang *et al.* (2007) found χ_{ARM} and SIRM to work well with a range of textural classes (clay, silt, sand), but χ_{LF} had limited proxy potential within the silt textural fraction. Booth *et al.* (2007) had further success with χ_{LF} versus PM classes (PM_{10}, $PM_{2.5}$ and $PM_{1.0}$), whereas χ_{ARM} and SIRM were found to only correspond with the finer fraction of PM ($PM_{2.5}$ and $PM_{1.0}$). These studies have explored the relationships between mineral magnetic methods and particle size, with a variety of inconclusive results

which show that the methods are unreliable. Booth *et al*. (2008) further demonstrated this by identifying differing sedimentary systems for those areas that do and do not work. Furthermore, the strength and significance of χ_{LF}, χ_{ARM} and SIRM parameter associations with sand, silt and clay content can be different for specific environments within an individual setting (Booth *et al*., 2005).

To surmise the magnetic textural proxy section, it has been shown that significant correlations are rarely evident for large towns and cities, plus ASU sites, but there may be opportunities to utilise the kinship during particular times of the year. Furthermore, the size of the sampling area is an important factor influencing the significance of magnetic-textural relationships, which is presumed to be linked to the number of sediment sources contributing to RDS at each site.

6.4 Magnetic-geochemical proxy relationships

This Section compares the proxy findings of geochemical and mineral magnetic measurements for the selected towns and cities with those of other UK and global studies. Insights are revealed into urban sediment transport dynamics that may influence the potential use of magnetic measurements as a proxy.

Strong associations (p <0.01-0.001) have been found between specific geochemical and mineral magnetic parameters over various scales (national, town, road). Associations have been found between specific geochemical and mineral magnetic parameters.

Previous research has demonstrated significant associations between specific geochemical parameters. Robertson *et al.* (2003) found associations between Pb, Fe, Mn and Cu in Manchester, which were attributed to vehicular sources (Table 2.8). A similar study in Jordan found urban sediments on an industrial estate with strong associations between Cu, Pb and Fe from anthropogenic sources (Al-Khashman, 2004). Lopez (2005) and Apeagyei *et al.* (2011) also attributed the linkages of Zn, Pb, Fe and Cu to combustion and vehicles. The geochemical proxy associations with the UK locations are similar to those in other urban sediment studies. These associations add to the evidence and support the view that anthropogenic input is a major influencing factor influencing RDS characteristics.

Detailed analysis of the UK town data reveal significant associations between Fe, Ni, Cu, Zn and Pb (r = 0.325-0.771; p <0.001). When individual towns are investigated, results reveal that these associations do not apply to all towns and cities. The strongest associations exist in London (MBR) (r = 0.472-0.717; p <0.01-0.001); Salford (r = 0.652-0.767; p <0.001); and Wolverhampton (r = 0.436-0.677; p <0.05-0.01). Due to activities occurring in these towns (busy commercial and industrial areas) results support the assumption that associations between these geochemical elements are related to anthropogenic sources, probably combustion particles (Robertson *et al*., 2003; Harrison *et al*., 2004). The geochemical results for the UK sample locations show distinct relationships within their environmental setting and spatial analysis of geochemistry data show distinct patterns across the sampling areas. Both

anthropogenic and 'natural' background source materials are proposed to influence these trends and sediment source mixing is probable throughout the different locations. Marylebone Road shows significant correlations between Fe, Zn and Cu, amongst other associations, which can be attributed to vehicular contributions (Ti, Mn and Cr). Table 2.8 indicates that the sources of contaminants to RDS may be directly related to traffic conditions and activity. The presence of Fe, Zn and Cu indicate sources from vehicle tyres, brakes and combustion particles. Scunthorpe geochemical properties possibly show different signatures, which reflect the main industrial activity, with associations between Fe, Cr, Mn and Ni. The geochemical indicators successfully show that source can be linked with specific element ratios, which are evident in other studies.

Several studies have identified mineral magnetic and geochemical linkages (Beckwith *et al.,* 1986; Hay *et al*., 1997; Georgeaud *et al*., 1997; Schmidt *et al*., 2005; Lu and Bai, 2006; Sheng-Gao *et al.,* 2008). Strong associations have been found with anthropogenically-produced particles (Mn, Cu, Fe, Ni, Zn and Pb) (Beckwith *et al*., 1986; Schmidt *et al*., 2005; Lu and Bai, 2006; Sheng-Gao *et al.,* 2008). Wang *et al*. (2012) found strong correlations (p <0.01) between heavy metals (Fe, r = 0.770; Zn, r = 0.481; Cu, r = 0.464; Mn, r = 0.546; Pb, r = 0.458) and χ_{LF}. Schmidt *et al*. (2005) found strong correlations between χ_{LF} and heavy metals, when χ_{LF} was >17.6 x $10^{-7}m^3kg^{-1}$. Beckwith *et al*. (1986) and Schmidt *et al*. (2005) found this association was due to the enhanced magnetic signature of the samples, which indicated anthropogenic sources. Varied results have shown linkages between mineral magnetics and geochemical composition in the environment. For example, Charlesworth and Lees (2001) failed to find any linkages between heavy metals and mineral magnetic properties, but did find other linkages. Mixing of contaminants contributed to weak correlations of mineral magnetic and geochemical parameters. Wang *et al.* (2012) showed that the strongest correlations occurred within areas of anthropogenic activity, with high magnetic and geochemical signatures attributed to combustion particles.

The results from the UK locations in this study reveal moderately strong correlations with selected geochemical parameters (Fe, Ni, Cu, Zn and Pb) and χ_{LF} (r = 0.394-0.673; p <0.001). When individual towns are investigated, results reveal that these associations do not apply to all towns and cities. The strongest correlations exist in London (MBR) (r = 0.313-0.764; p <0.05-0.001); Salford (r = 0.565-0.817; p <0.01-0.001); and Wolverhampton (r = 0.467-0.686; p <0.01-0.001). These results support Beckwith *et al.* (1986) and Schmidt *et al.,* (2005) and reveal similar patterns, with correlations between magnetic susceptibility and selected geochemical properties (Mn, Fe, Cu, Ni and Zn) only in towns with mean χ_{LF} concentrations >35.57 x $10^{-7}m^3kg^{-1}$ (MBR, Salford, Scunthorpe and Wolverhampton). Results suggest that towns with associated high anthropogenic activity have better proxy potential than those with relatively limited anthropogenic input. Sites deemed to comprise chiefly of 'natural' source materials showed very weak associations with mineral magnetic measurements. For instance, those towns (such as Dumfries and Oswestry) with a likelihood of minimal anthropogenic sources of activity will be masked or diluted by natural sources. This also probably explains why Booth *et al*.

(2008) found that proxy relationships were problematic for soils, but were clearly apparent in places with high activity (Charlesworth *et al*., 1997; Shilton *et al.,* 2006).

To surmise, the magnetic-geochemical proxy section has shown strong correlations in towns and cities dominated by anthropogenic inputs and geochemical kinships may indicate specific environmental activity. Towns and cities with high values of magnetic material appear to be associated with anthropogenic and combustion particles and is a plausible reason for their proxy potential.

6.5 Linking observations to urban sediment sources and sinks

This Section investigates the factors that may influence the reliability of mineral magnetic as a proxy. Charlesworth and Lees (2001) suggested disturbance (weather events) of catchments and complexity of the urban environment, create a 'pulsing effect' over time from environmental changes (Wolman, 1967, 1975; Douglas, 1985). Surfaces are subjected to erosion, sediment transport, removal of atmospheric dusts and particulates from wash-out; thus, removing contaminants from road surfaces. Seasonal variations alter concentrations of magnetic particulates, but also weather and topographical conditions transport magnetic particles from industries (Kim *et al*., 2009). Concentrations during high rainfall seasons suggest only a fraction of particulates are removed-deposited to storm sewers/gully pots (Figure 2.8). This also supports the findings of Butler and Clark (1995) with the input-output state of RDS; that is not all sediment is removed by fluvial or aeolian action during weather events but is 'moved' rather than 'removed.' Figure 6.1 suggests how this could potentially affect the sediment loads of RDS, with influencing factors being attributed to site-specific conditions and the external influence of weather events.

Figure 6.1 is a modified version of the urban sediment cascade (Figure 2.8) and suggests the importance of changes that RDS experience within its environment. The cascade has been developed into a theoretical sediment cycle, which undergoes continual change; whereby, RDS is trapped in this cycle after primary source ingredients are input into the system (sources: mixing and deposition). Once primary source material integrate and deposit, the material undergoes a continual process of change and recycling. RDS is continually under the influence of gravity and weather conditions. Sediment is eventually deposited in a sink, where it undergoes deposition processes, continual change in other systems (rivers, canals, lake, atmosphere), or recycled back into the cycle via re-suspension and deposition.

Detailed examination of the data reveals several Wolverhampton sites may be subject to recycling and mixing, due to location and environmental conditions. The mixing of soil, building material, historical pollution and sources could be attributed to the urban sediment cycle, resulting in the continual mixing of various materials. Constant changing of sediment properties, as it is modified by physico-geochemical conditions in large urban areas, makes the ability to find inter-parameter relationships unlikely.

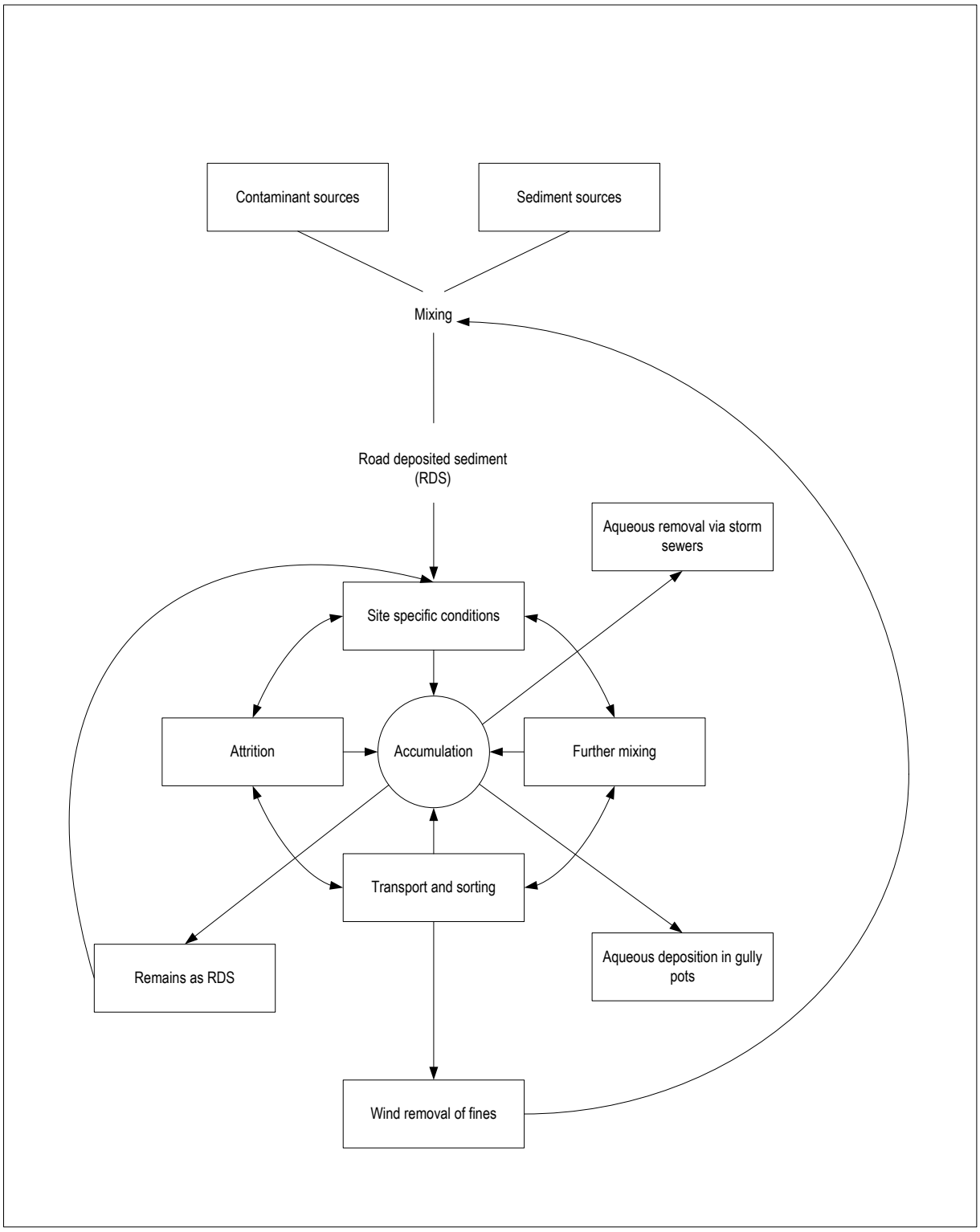

Figure 6.1 The urban sediment cycle showing potential pathways of, and changes in, road deposited sediments from sources to sinks (modified from the 'urban sediment cascade' (Charlesworth and Lees, 1999; Perry and Taylor, 2007)).

Compared to previous studies, where mineral magnetic-textural properties showed significant correlations, it is apparent that sampling area size; landscape and land use, together with several potential sources and mixing, are factors that influence the likely success of the application of mineral magnetic as a proxy. For instance, Oldfield *et al*. (1993) used a small flat sample site with minimal diversity of land use and sediment sources. Muxworthy *et al*. (2003), Power *et al*. (2006) and Booth *et al*. (2007) also had small sample sites with minimal land uses and sediment sources (Figure 6.2).

Based on the characteristics outlined in these cited works, when the places used in this study are scrutinised in the same manner, it highlights potential reasons for both the success and failure of mineral magnetics as a proxy instrument. For instance, Marylebone Road can be described as having similar characteristics to those of Muxworthy *et al*. (2003), Power *et al*. (2006) and Booth *et al.* (2007). Whereas, those sites with large sample areas and variable topography, together with variable land uses and multiple sediment sources, are unlikely to exhibit significant correlations between mineral magnetic and particle size parameters. This is highlighted in Figure 6.2. To further support this proposal, when individual sites (such as some Wolverhampton sites) are examined on an individual seasonal basis, the correlation significantly improves. Charlesworth and Lees (1999) identified that time was an important factor in the speciation of urban sediments, due to the stability of Fe and Mn over time (Forstner and Wittman, 1981).

It is postulated that in environments where sediments are in continual flux (Figure 6.1) the mineral magnetic-particle size proxy potential is weaker, due to continual changes in sediment properties (large catchment area + mores sources + time (weather conditions) = mixing). Booth *et al*. (2008) found magnetic measurements were not always suitable for particle proxy purposes. Observations from this and other studies (Figure 6.2) suggest that physical environmental differences influence the potential mineral magnetic-textural associations. Sample area size appears to be an important factor when investigating mineral magnetic–textural associations. The greater the sampling area, the greater sediment mixing potential; this also appears to be true for time-frames used for sampling.

This work has highlighted the methods do not work:

- Over large areas (due to the high potential of sample mixing and samples having different provenances).

- Over time periods at large and small scales (Figure 6.2-6.3) (due to factors attributed to Figure 6.1, mixing and weather conditions contributing to RDS movement).

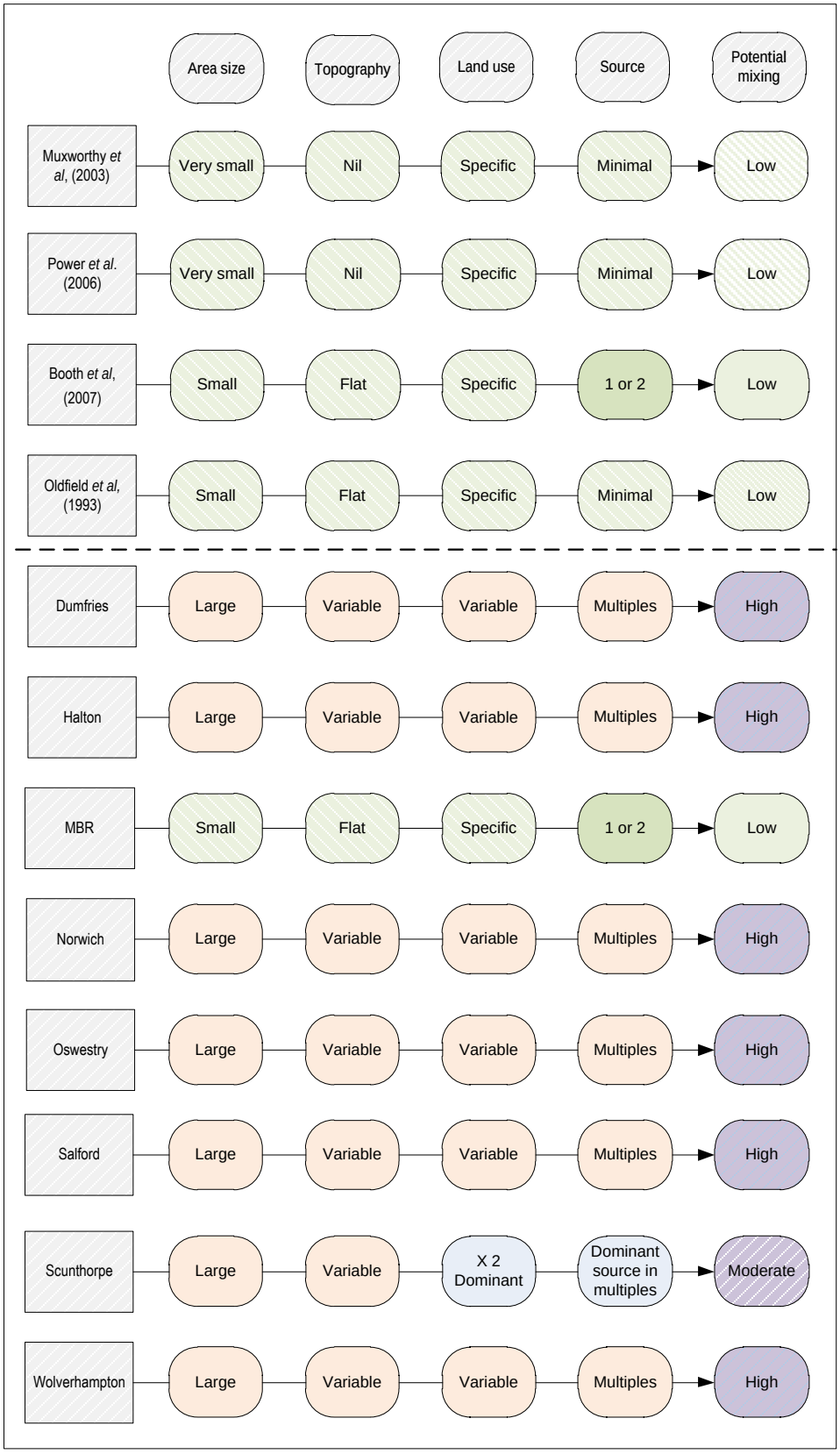

Figure 6.2 Comparisons of **c**haracteristics for this and previous studies, detailing area characteristics and RDS particle mixing potential for sample locations. Muxworthy *et al*. (2003); Power *et al*. (2006); Booth *et al*. (2007) and Oldfield *et al*. (1993) all showed some particle size proxy potential. (Green = few variables (<2) and little mixing potential; Blue = 2-3 variables; Orange = multiple variables (>3); Purple = high mixing potential).

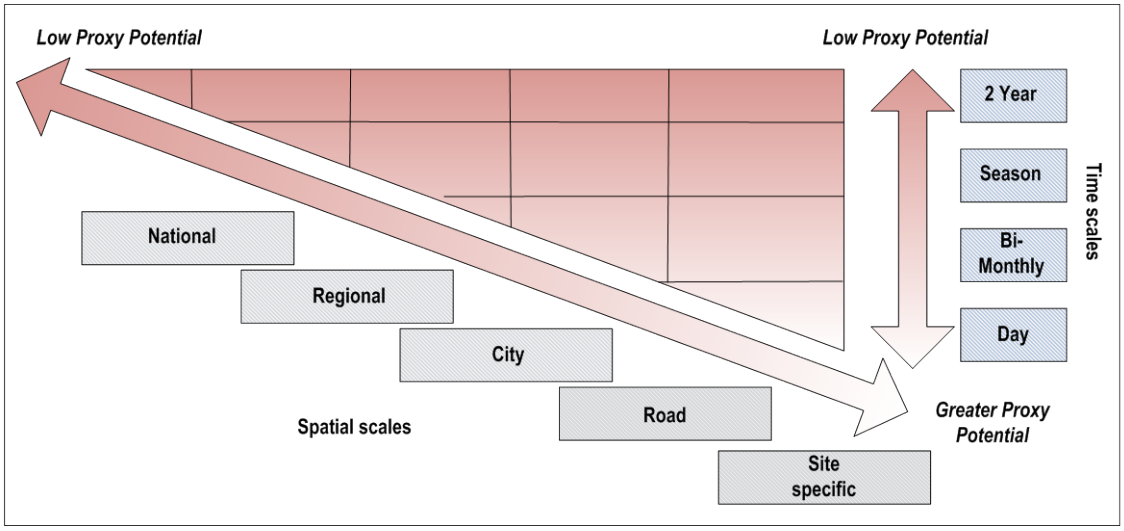

Figure 6.3 The affects of spatial and time scales on the mineral magnetic-textural proxy potential.

The methods do show some potential when sampling small areas and in a brief time-frame (hours and day) (Figure 6.3), as there is less chance of mixing, and samples are relatively homogenous.

Table 6.1 establishes the site size index, which could be considered when assessing the potential sample sites for particle mixing and mineral magnetic-particle size associations. Road, city, regional and national scales have been assessed in this study and appear to show the strength of mineral magnetic-particle size associations decreasing in that order. Micro-environments have been included, due to the strong correlations reported by Muxworthy *et al*. (2003) and Power *et al.* (2006). Although the material of Muxworthy *et al*. (2003) and Power *et al.* (2006) is not RDS specific, as collected in this study, it is a constituent of RDS particulates and consists of PM collected at road sides. The smaller sample area sites appear to be a major influencing factor when investigating mineral magnetic-textural associations.

Land use appears to be another influencing factor. Identified land use of Marylebone Road is predominantly commercial, and Scunthorpe is mostly industry and residential. These environments have been identified as the dominant land use activities of an area, and with activity, a coinciding source can be estimated. Table 6.2 lists the four main sources of RDS input.

Each source can be identified as a main contributor to airborne PM_{10}, which have negative effects on air quality (AQEG, 2005). Land use of sampled areas display predictable characteristics (residential = low mineral magnetic concentrations; industrial and commercial = moderate-high mineral magnetic concentrations (Table 6.3)). Because of the linkages observed, results reveal the importance of identifying these areas when evaluating the particle mixing potential of a specific site.

Table 6.1 Area size index categories used to establish area size for site RDS particle mixing potential

Area	Area size	Index Score
Point	Micro-environment	0.5
Road	Small	1
Small town	Medium	2
City	Medium-Large	3
Region	Large	4
National	Very Large	5

Table 6.2 Four sources of sediment input used to evaluate RDS particle mixing potential

Soil and vegetation*(s_i)*	Parks, embankments or rural locations, potential high levels of soil and vegetation eroded and added to RDS.
Building wear/ Construction material*(s_{ii})*	Commercial locations with urbanised street canyons or areas undergoing construction activities.
Atmospheric input*(s_{iii})*	Industrial locations with the potential to input particulates (steel mills, power plants, incinerators, solid fuel burning systems).
Vehicle particulates*(s_{iv})*	Locations with high traffic density, arterial road networks or road systems with slow moving, 'stop-start' traffic.

Table 6.3 Land use types used in evaluating site RDS particle mixing potential

Industrial	Areas of industrial activity, steel, oil, power industries.
Commercial	Commercial locations with urbanised street canyons.
Residential	Residential areas, with dense housing and park areas

To support this interpretation Figure 6.4a shows a theoretical particulate arrangement for particle size-mineral magnetic relationships. This example shows how potentially, a single source magnetic material with high magnetic concentrations corresponds with particle sizes. The bivariate plot indicates a strong positive correlation between these two parameters (p <0.001). When a secondary source (Figure 6.4b) with a negative mineral magnetic correlation is added, the correlation coefficient becomes insignificant. However, although the concentration and mineralogy can be specifically identified through the methods used in this study, the mineral magnetic-particle size correlations cannot be retrieved when there is mixing of particulates.

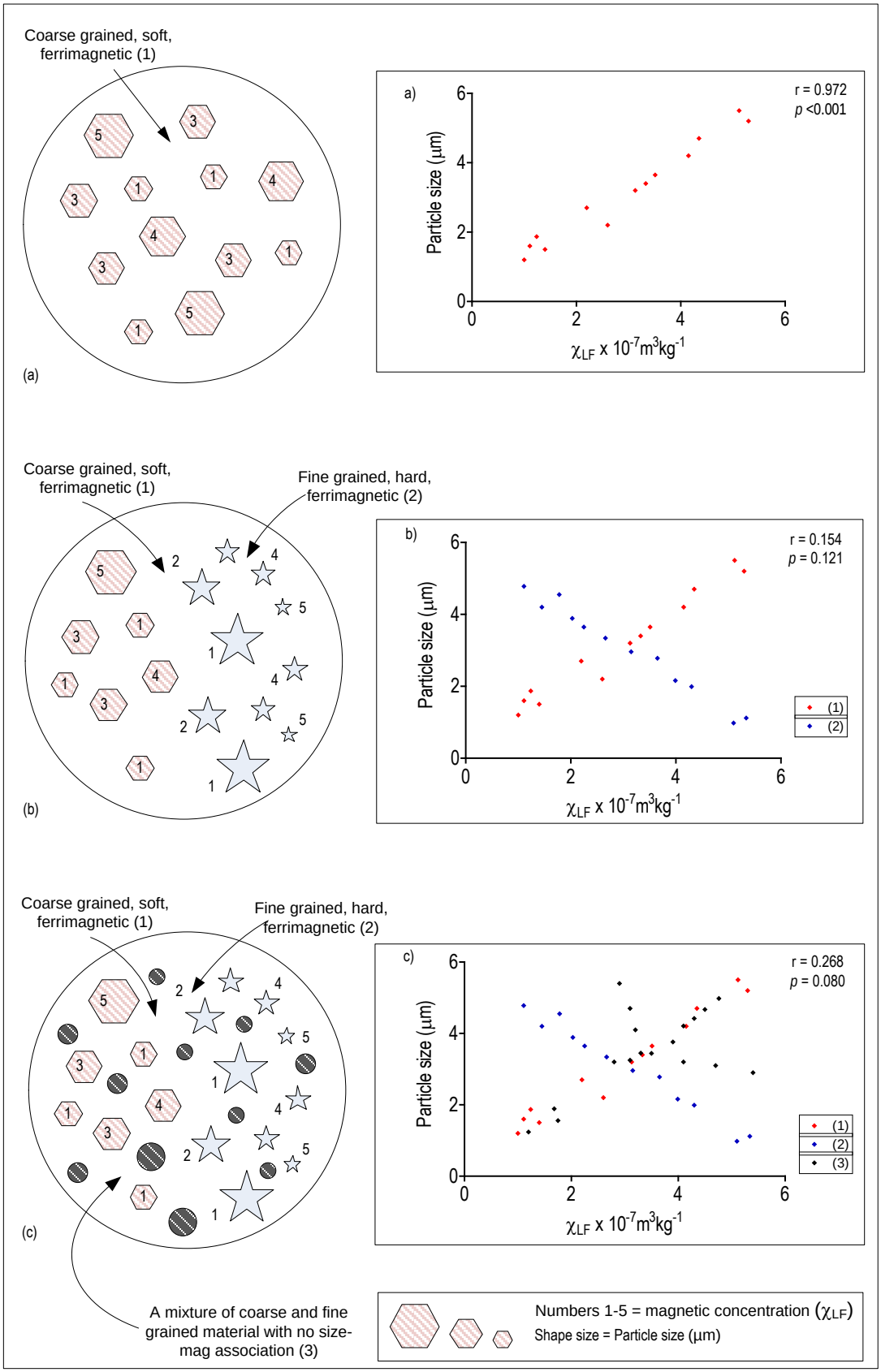

Figure 6.4 Theoretical potential particle mixing conditions and mineral magnetic-particle size effects: (a) single source with strong positive correlation (b) two contrasting sources mixed, with weak correlation (c) multiple sources with weak correlation.

Figure 6.4a-b could potentially be found in environments where there are dominant sources of particulates and little to no mixing (MBR). The results in this study suggest that RDS is made up from several sources of magnetic material. Results show the dominance of ferromagnetic multi-domain, soft mineralogy, with an indication of fine, super-paramagnetic and hard mineralogy in RDS. This is illustrated in Figure 6.4c where several sources of magnetic material (anthropogenic and natural) potentially dilute the textural-mineral magnetic correlations. Figure 6.4 is based on the theoretical assumption that there are universal relationships in regards to separate source mineral magnetic concentrations and particle size in urban RDS. Further work could make a more accurate assessment of the source particle size-mineral magnetic relationships, where particles directly from sources are analysed to determine individual relationships.

To surmise, several factors are proposed to influence proxy relationships. Large catchment areas are potential sinks for multiple sources of particulates, because of the likelihood to have mixed land uses. The larger areas provide seasonal weather conditions opportunities to disturb RDS where it is subject to transport, mixing and deposition. This mixing dilutes mineral magnetic material and results in a heterogeneous cocktail of sources. The smaller areas are likely to have fewer sources, less seasonal influence, less mixing and more homogenous source(s) of RDS.

6.6 Predicting the likelihood of proxy success

This Section discusses a conceptual model which attempts to reveal the likelihood of proxy success at sample sites based on those of this and previous studies. The consistent and accurate prediction of RDS movement has proved elusive. Modelling has focused on the transport of sediment into drainage and affects on storm-water quality. Reviews of available models have consistently stated that no model is best for every situation, complex models are difficult to verify and calibrate, and that even the most physically-based models contain much uncertainty (Huber and Heaney, 1980; Bertrand-Krajewski *et al*., 1993, 2007; Ahyerre *et al*., 1998). Consequently, there are a variety of approaches to predict the quality of urban runoff, with the choice of approach being largely based on the reason for modelling.

Descriptions of the processes involved can be grouped into atmospheric deposition (wet and dry), interception by plants and buildings, build up, wash-off and transport (Duncan, 1995; Charlesworth and Lees 1999; Zheng *et al*., 2012). Of course, these processes are intimately related to the cycling of pollutants throughout the environment and, in turn, affected by the production of atmospheric pollution and the capacity of the urban environment to assimilate pollutants. Many authors have divided models into groups based on the modelling approach (Huber, 1992; Bertrand-Krajewski *et al*., 1993; Zoppou, 2001). Models are generally grouped according to their level of complexity; physical representation attempted or planned use, with numerous sediment models developed in recent decades utilising different scientific methods and modelling approaches. In general, three different kinds of model exist:

- Empirical models are a simplified representation of natural processes based on empirical observations. They are based on observations of the environment and thus, are often of statistical relevance (Nearing *et al*., 1998). Empirical models are frequently utilised for modelling complex processes and, in the context of erosion and soil erosion, are particularly useful for identifying sediment sources (Walden *et al*., 1997; Merritt *et al*., 2003).

- Physically-based models represent natural processes by describing each individual physical process of the system and combining them into a complex model. Physical equations describe natural processes, such as sediment transport (Merritt *et al*., 2003). This complex approach requires high resolution spatial and temporal input data. Physically-based models are therefore often developed for specific applications, and are typically not intended for universal utilisation. Physically-based models are able to explain the spatial variability of most important land surface characteristics (such as topography, slope, aspect, vegetation and soil) and climate parameters (including precipitation, temperature and evaporation) (Legesse *et al*., 2003).

- Conceptual models are a mixture of empirical and physically-based models and their application is therefore more applicable to answer general questions (Beck, 1987). These models usually incorporate general descriptions of catchment processes without specifying process interactions that would require very detailed catchment information (Merritt *et al*., 2003).These models therefore provide an indication of quantitative and qualitative processes within an urban catchment.

To establish linkages at sample sites it would be useful to assess the likelihood of a working PM identification method at the site. Pre-testing of the potential of a specific site would reduce the cost and time of sampling, by only testing areas or methods of greater potential. Modelling of the established influences could predict areas sensitive to proxy methods. Figure 6.1 suggests the influence of the mixing of material on the physical properties of RDS. A pre-testing model could provide an initial assessment of a location's potential for mineral magnetic-textural relationships, due to land use, size and source influences on RDS.

Due to the continual flux of RDS (Figure 6.1), it is inappropriate to apply a mixing model using mineral magnetic, geochemical or textural data. Walden *et al*. (1997) stated that the magnetic parameters used in any numerical un-mixing model ideally need to meet fixed criteria. Primarily, all parameters should be linearly additive (i.e. mineral magnetic mass specific parameters only, and not mineral magnetic ratio parameters).That is, if two source sediments have values for a particular magnetic variable of x_1 and x_2, respectively, and are subsequently mixed in known proportions of p_1 and p_2, the resultant sediment mixture should have a value of this variable (x_r) (Eq. 6.1). Due to the many parameters and unknowns due to constant mixing and adding of new material that apply to urban RDS, this was not a suitable approach.

Eq. 6.1: $x_r = p_1 x_1 + p_2 x_2$

Studies have shown some mineral magnetic-particle size associations but have not demonstrated why the associations are present. Power *et al.* (2006) found significant (p <0.001) particle size (PM_{10}) and mineral magnetic (χ_{LF}, χ_{ARM}, SIRM) associations on tree leaves. The micro-environment studied by Power *et al.* (2006) is illustrated in Figure 6.2a. This example shows how associations could be due to settled particles from dominant sources with little to no mixing with other particles. At a slightly larger scale, Booth *et al.* (2007) found similar associations within RDS along short lengths of roads, suggesting low mixing potential over small areas.

To surmise, by incorporating the findings and influences to mineral magnetic-particle size proxy methods, a pre-testing model could be used to assess the potential for RDS mixing in sample areas.

6.7 Sediment mixing factors

Eq. 6.2 illustrates the culmination of findings in this study, which has produced a site mixing model (m) (Figure 6.5). Factors 1 (l_1), Factors 2 (s_1) and Factors 3 (a_1) are presented as the main influencing factors for RDS mixing. Land use (l_1) is estimated by investigating the study area and calculating the land use total (industrial, commercial and residential (Table 6.3)). If any of the three land uses are present, the number is then added together (one land use = 1, two land uses = 2, three land uses = 3).

Eq. 6.2 $m = (l_1)+(s_1)+(a_1)$

s_1 represents the total estimated input of particulates from the four main sources (Table 6.3; soil, construction-building material, atmospheric input and vehicle particulates). By estimating the input types for a sampling area, the input can be calculated into a total source score (s_1) (one source = 1, two sources = 2, three sources = 3, four sources = 4). To distinguish the size (a_1) of the sample area the area size index is used as a guide ((Table 6.2). Size 0.5 = micro-environment, 1 = small scale (road), 2 = medium (small town), 3 = medium-large (city), 4 = large (regional) 5 = very large (national)).

The resultant l_1, s_1 and a_1 are added to produce m. The result (m) scores the risk of a site to particulate mixing and shows potential for a location to provide mineral magnetic and particle size associations. The index shows high m scores, as highly complex systems, with high mixing potential and offering little to no proxy potential.

Low m scores are simple systems, with little mixing and better chances for proxy methods to work successfully. Table 6.4 illustrates this and is based upon typical values found at different area size classifications. These classifications are examples of typical characteristics found at the listed locations. For example, a typical road would be expected to cross either 1 or 2 land uses, which would reflect the sources of magnetic material deposited (Zhang *et al.,* 2012).

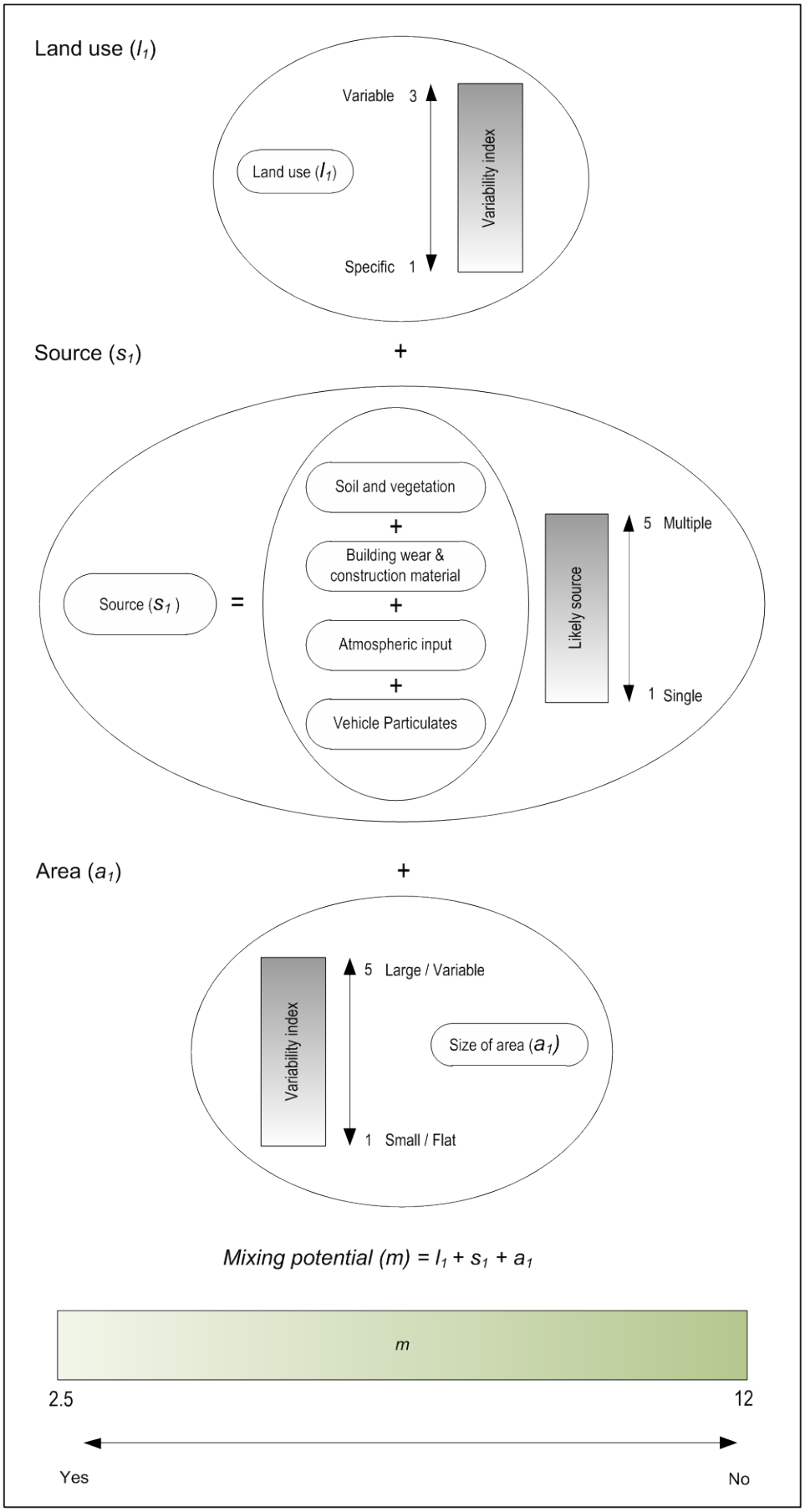

Figure 6.5 Site mixing model, shows the potential of a specific location to particle mixing, based on source inputs, area size and land use characteristics.

When compared to a small town, the larger area size would indicate several areas incorporating differing land uses and more input sources.

To surmise, city, regional and national area sizes indicate the maximum potential for numbers of source inputs and land uses, producing high mixing potential (*m*) values. This model only takes into account physical properties of a location and deems the less input, use and limited variability of physical characteristics better chances of establishing a mineral magnetic-particle size proxy. This model does not take into account other parameters, such as environmental conditions and RDS residence time, this is a strand of potential further work identified by Charlesworth and Lees (1999) (Figures 2.8 and 6.1).

6.8 Validating the conceptual model

To validate the model, it has been applied to the UK locations in this study (Table 6.5). Towns showing the most promising potential have low *m* values. The results also suggest that Marylebone Road is the most likely location to display mineral magnetic-particle size associations. This result is due to the location's specific characteristics, with the area being dominated by a specific land use source and small size.

The results for Scunthorpe have shown that a larger area with more potential inputs of sources due to land use has reduced the likelihood of detecting mineral magnetic-particle size associations, because of the high mixing potential of RDS particulates. The other selected UK locations show high levels of potential mixing, which are due to large areas, number of land uses and potential sources. When compared to the mineral magnetic and particle size results of this study, Marylebone Road and Scunthorpe are the most probable candidates to find associations due to dominant anthropogenic activity.

The proposed model cannot be used exclusively to predict trends, as the factors are open to individual estimation and interpretation (number of land uses and sources), but as a guide the model does show some potential use as a tool for study area identification. The more dominant the environmental factor and the smaller the area, the more likely a mineral magnetic–particle size association could be evident. Figure 6.5 is based on fixed sources and physical conditions to predict the potential of determining particle size associations. To further understand possible linkages of urban sedimentary particles, the model could be used in conjunction with the sedimentary cycle, with the addition of physical parameters (weather conditions and time factors), as described in Figure 6.1.

To surmise, the site mixing model has shown some potential to predict likely areas of proxy potential based on findings in this and other studies relating to environmental factors within study areas. By using the environmental characteristics of an area, the model can potentially determine the potential for RDS mixing and mineral magnetic-textural associations. Figure 6.6 displays how a simple flow diagram using the results from this investigation can predict the particle mixing potential of a sample area.

Table 6.4 Score classification for specific area types (Table 6.1 (**Bold** * = potential site with low mixing rate))

Location	Land use *(l_1)*	Source *(s_1)*	*Area (a_1)*	*m*
Point (Power *et al*., 2006)	1	1	0.5	2.5*
Road (Booth *et al*., 2007)	2	2	1	5*
Small town	3	3	2	8
City	3	4	3	10
Regional	3	4	4	11
National	3	4	5	12

Table 6.5 Mixing model results for the UK selected locations sampled in this study (**Bold *** indicates some partial success found in this study)

Location	Land use *(l_1)*	Source *(s_1)*	*Area (a_1)*	*m*
Dumfries	3	4	3	10
Halton	3	4	3	10
MBR	1	2	1-2	4-5*
Norwich	3	4	3	10
Oswestry	3	4	3	10
Salford	3	4	3	10
Scunthorpe	3	3	3	9*
Wolverhampton	3	4	3	10
Regional	3	4	4	11
National	3	4	5	12

6.9 Chapter summary

The use of mineral magnetic methods as a particle size proxy is a complex problem. Few significant correlations have been found and this indicates that the use of mineral magnetic methods as a proxy is unsuitable at most places and scales investigated in this study. However, the study has identified factors which affect the likelihood of associations at different scales. The methods work best with few identified influencing factors. The methods also appear to work best when sampling in short time periods with potentially less impacts from weather conditions which influence particle transport.

Results clarify that further work should attempt to identify the effectiveness of the methods at the micro-scale. RDS is perhaps not the best medium for determining PM using mineral magnetic methods, whereas, tree leaf and micro-environments potentially have the right conditions (small scale, influenced by direct source) for PM identification.

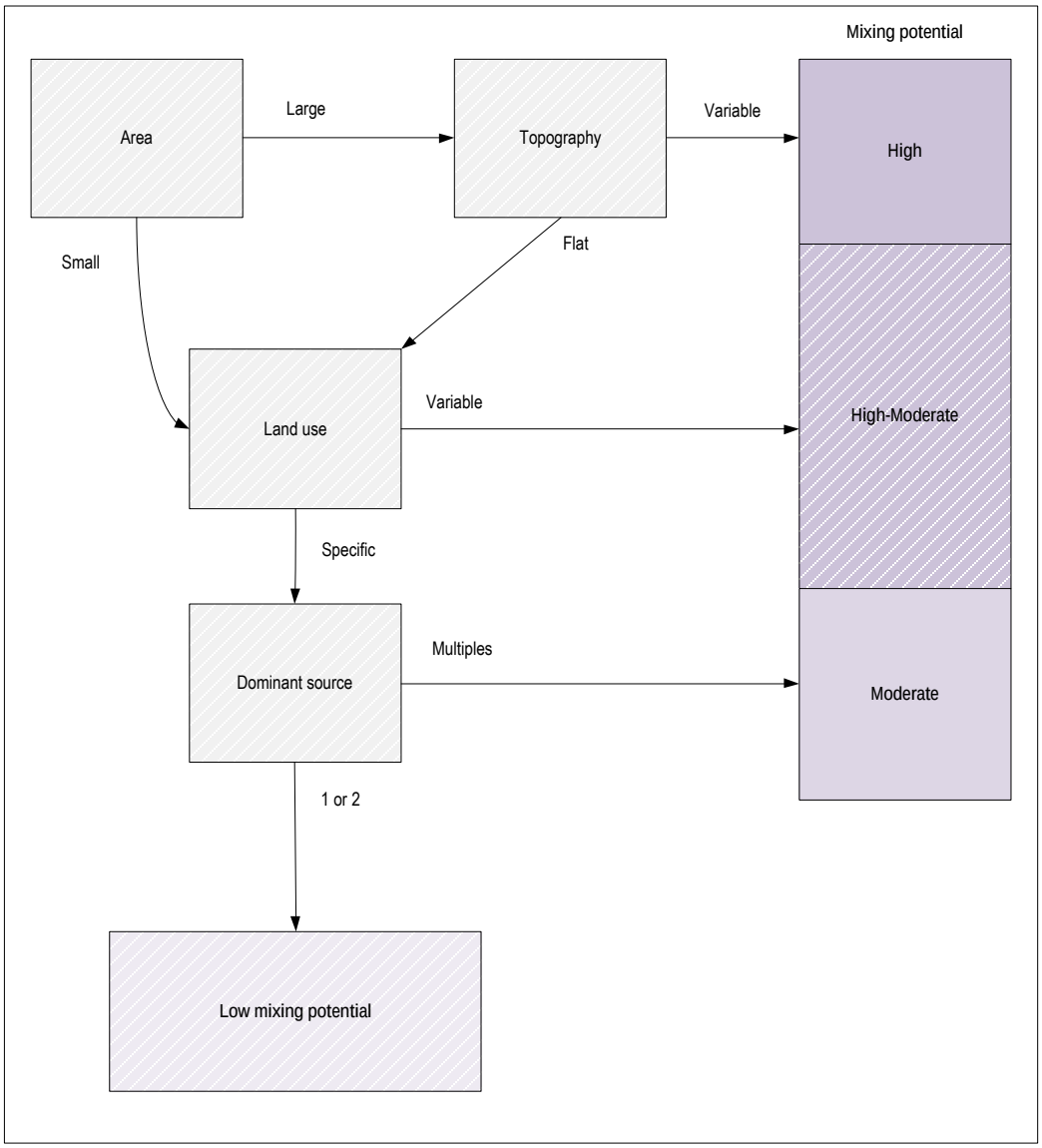

Figure 6.6 Theoretical flow diagram to establish potential mineral magnetic-particle size proxy sites, based upon low RDS particle mixing rates.

At the scales shown in this study (road, city, region, national) mineral magnetic methods as a particle size proxy cannot be used reliably and should be investigated further using the mixing model (Figure 6.5-6.6) to identify likely areas of study. Once areas are identified, the use of mineral magnetic-textural methods should be re-applied. In-addition, steps should be considered to identify specific particle sources, by use of additional geochemical methods (such as XRD). If separate mineral magnetic sources can be identified, then mixing models could be applied to identify sediment transport and mixing.

Spatial variability found with individual towns show that using mineral magnetic methods for PM monitoring is unlikely to produce reliable results. It is because of this variability that point sampling is not appropriate for establishing a towns PM concentrations, nor is it appropriate for indicating single point PM concentrations. Ideally, monitoring techniques need to show results that represent a specific sampled area.

The advantages of pursuing alternative techniques to detect health related PM is clear. It would be appropriate to apply further research of PM monitoring techniques to small homogenous land use areas to establish likely PM-Mineral magnetic links and PM concentrations. For example Appendix 3.1 shows the land use for Wolverhampton, future studies could potentially segregate the land uses identified (polygons) on the map and sample within the areas. Alternatively, traffic data (Appendix 3.2.1) could be used to target areas of interest and sampled in a similar manner to that of Marylebone Road. This study has shown that traffic data can indicate areas with high concentrations of mineral magnetic material and reveal mineral magnetic methods to have potential which need to be fully explored.

Mineral magnetic methods are mainly an unreliable indicator of PM particle size for RDS over time or at national, regional, city, road or site scales. However, mineral magnetic methods have shown strong correlations with geochemical parameters and suggest that these methods could be used reliably as a pollution indicator in RDS studies. The results show areas with distinct geochemical concentration which can be attributed to specific sources. The application of a geochemical proxy would prove useful in identifying high-risk concentration areas within the urban environment. These high concentration areas could be easily, quickly and cheaply monitored using mineral magnetic methods. The resultant data could aid health, urban studies and urban planning.

Mineral magnetic methods are a reliable tool for anthropogenic geochemical indication:

- Operates effectively at large and small scales.
- Works very well using established RDS collection methods.
- Recommended for use in RDS, health and urban studies.

Advantages of using mineral magnetic methods for RDS investigations include ease of collection and availability of RDS throughout the year. In environmental studies, using RDS is distinctly advantageous due to its interactions with human health. This makes mineral magnetic investigations best suited for effective geochemical pollution monitoring in urban areas.

Chapter 7
Conclusions

This Chapter restates the aims and objectives of this research project in relation to the main findings. The scientific contribution to the research is evaluated. Limitations of the study are discussed and suggestions made for further research.

PM (particle size) was the primary interest of this study, due to health implications associated with size, shape, surface area and number of particles potentially inhaled into the lungs and triggering respiratory problems. Mineral magnetic and textural linkages have proven complex, as results for Wolverhampton and UK sample locations show some weak associations between mineral magnetic and textural properties. Spatial and temporal patterns have also been identified using mineral magnetic parameters. The research can conclude that mineral magnetic methods are unreliable indicators of particle size for urban PM RDS studies over time or at differing spatial scales.

As a secondary objective, geochemical composition has also been investigated and adds additional findings which enable further understanding of the behaviour of RDS. The geochemical composition reveals the close relationship an area has with its activity and provides insights into sources of particulates, the inter-geochemical–mineral magnetic associations and concentrations which appear to influence the PM proxy potential. As a proxy, geochemical and mineral magnetic analyses appear to be reliable indicators of pollution at the investigated scales and when compared to other studies.

7.1 Research findings

From the results discussed in previous chapters, several conclusions can be drawn:

1) Mineral magnetic methods do not indicate any potential for linkages between ground or airborne PM and ASU data.
2) Geochemical analysis indicates distinct associations between geochemical groups and is a good indicator of both anthropogenic and natural sources.
3) Mineral magnetic methods are a good indicator of urban anthropogenic pollution at small and large spatial scales.
4) The associations are influenced by the direct environment. Land use, size of area and potential sources are primary influences. Differing weather patterns can lead to disturbance, dilution and mixing of RDS and magnetic material. The conceptual model integrates these factors and identifies areas where sampling strategies could be improved when investigating mineral magnetic-particle size associations. To successfully apply these methods, this research suggests sampling of RDS should occur within small, specific land use areas, where urban activity is a significant factor (e.g. Marylebone Road and Scunthorpe illustrate this).

5) The use of mineral magnetic techniques has shown great potential in the analysis of urban environments. Specific road systems have shown strong magnetic signatures. Mineral magnetic concentrations on arterial roads were nearly double the concentration of residential roads. The PM loadings on arterial and residential roads have been well documented, along with the effects on the health of individuals living near busy arterial roads (Oosterlee *et al.,* 1996; Edwards *et al*., 1994; Duran-Tauleria and Rona, 1999). The use of mineral magnetic techniques as an RDS particle size proxy clearly merits further investigation, but the potential for a pollution proxy is evident. These methods have the potential to be used in relation to PM problems, with the identification of highly polluted areas, which could then be used in urban planning.
6) The mineral magnetic approach used in this work has proved reasonably successful. It could be employed in other urban contexts as a geochemical pollution proxy, but has limitations for a particle size proxy.

7.2 Regional, national and international implications

Air sampling monitoring stations have proved a useful asset in the analysis of urban pollutants, but only provide data for the station location. Currently the AURN techniques are not versatile, due to static constraints, cost and no ability to determine PM size fractions. Given scientific and public concerns regarding the effects of particulate matter, the analysis of polluted roads via mineral magnetic investigations appear to be limited in investigations of PM pedestrian exposure. The use of mineral magnetic techniques could alternatively be employed as an indicator tool for anthropogenic pollution, which is flexible and non-site specific. It is possible for mineral magnetic techniques to identify potential pollution 'hotspots' and could, in theory, be used in conjunction with air monitoring data. If these methods were employed in areas where air monitoring stations cannot be situated, mineral magnetic testing could give indications of areas meriting further investigation. These methods are non-destructive, rapid and efficient in any location, with low cost and high sensitivity of measurements.

7.3 Application of the mineral magnetic approach

The reported research contributes to further understanding and has developed from previous research in the following ways:

- By establishing that mineral magnetic measurements over time and at varying spatial scales (road, city, regional and national) are an unreliable indicator of PM size at the roadside or compared to ASU data.
- Determined influences on the reliability for mineral magnetic methods as a particle size proxy, concluding that sample area size, land use and source are contributing factors to proxy potential.
- Establishes specific geochemical parameters linked to source and mixing of RDS at small – large spatial scales, in addition to identifying factors that influence the dynamics.
- Establishing mineral magnetic measurements as a reliable indicator of anthropogenic pollution within RDS at several spatial scales.

This work further emphasises the potential for applying mineral magnetic measurements and addressing potential environmental problems. In doing so, it highlights the limitations of using mineral magnetic methods as an indicator of PM particle size, but does provide an alternative or complementary approach to studies of urban and atmospheric depositional environments, such as predicting pollution loads in sediments. It also demonstrates that the mineral magnetic technique permits sediment transport theories to be inferred for urban roadside environments. It also shows that when utilised in conjunction with other data, the techniques could be used to help validate urban sediment models.

7.4 Limitations of the study

1) The analysis of large scale sampling areas has shown limited potential for investigating mineral magnetic-particle size associations. To further understanding of potential relationships, small-scale sampling areas could provide insights into the micro-environments of RDS.
2) The bi-monthly sampling of Wolverhampton and other locations could have been improved with daily-weekly sampling. This is also an apparent weakness of the UK study, where only a 'snap-shot' was investigated. Sampling at shorter intervals and over longer periods would provide more information on seasonal changes in RDS. Nevertheless, this was not possible within the restrictions of time and resources.
3) Mineral magnetic material and geochemical associations suggest a mix of anthropogenic sources. The use of more detailed chemical analysis could be employed to determine specific sources. The use of XRD and ICP-MS could identify organic compounds, such as Polycyclic Aromatic Hydrocarbons (PAH) and distinguish between Fe_2O_3 and Fe_3O_4, which could be used to identify significant sources of anthropogenic emissions.
4) Monitoring several specific environmental variables at a site over a prolonged period of time is recommended. Important variables include weather conditions, pedestrian and vehicle volumes, vegetation density, plant species and building densities.

7.5 Suggestions for further research

The complex nature of RDS requires further investigation. Future research should include investigations into:

- RDS magnetic minerals and sources, the individual sources of mineral magnetic materials and their textural and geochemical characteristics.
- RDS transport and flow modelling.
- RDS mixing and interaction of source particulates.
- Further testing and development of the mixing model at the spatial scales identified.
- Incorporate individual source, transport and mixing into a complex physically-based model which uses seasonal conditions and the framework of Charlesworth and Lees (1999).

In light of the findings and limitations in this work, these recommendations could be deployed in the following ways:

1) The collection of magnetic particles from air sampling unit filter papers proved successful in investigating RDS pollution. Marylebone Road is renowned for its large traffic volumes and high particle counts, making it an ideal site for magnetic particle filter collection and long-term study.
2) Considerable inter-site magneto-geochemical variation has been shown. Concentrations of mineral magnetic material could be analysed by collecting RDS from various locations within the road vicinity. The results could provide truly representative values for RDS at that location. This could include collection of RDS from gully-pots, kerbs, pavements, other depositional catchments, and road surfaces, to determine magneto-geochemical concentrations.
3) Magnetic extract analysis (Hounslow and Maher, 1999) is becoming a relatively routine aspect of mineral magnetic studies. Therefore, it would also be appropriate to extract bacterial magnetite from road sediment samples and characterise their magnetic properties. These characteristics could then be used to further identify sediment sources (Stolz *et al*., 1989).
4) The additional use of other mineral magnetic detection equipment has considerable research potential. This could include hand-held susceptibility meters to quickly identify urban pollution.
5) It would be appropriate to re-apply this research to other regional, national and international urban RDS, to investigate the broader applicability of the work.
6) Mineral magnetic methods could be used to develop a national and international urban RDS database. This could encourage an international effort to map mineral magnetic concentrations of RDS.
7) To further validate the site mixing model, random locations should be tested and scored, with a full site investigation carried out to further establish the reliability of predicting sites with magneto-particle size trends. This approach should focus on long-term study areas.
8) Accumulate long-term daily data for specific land use areas and size, this could include methods applied in this work, used in conjunction with ASU data. Apply detailed physical (DTM, infrastructure), social (traffic and movement) and environmental (weather, vegetation) characteristics to develop urban sediment flow models within a GIS.

References

Abu-Allaban, M., Gillies, J.A., Gertler, A.W., Clayton, R. and Proffitt, D. (2003) Tailpipe, resuspended road dust, and brake-wear emission factors from on-road vehicles. *Atmospheric Environment*, **37**(37), 5283-5293.

Ackermann, F. (1980) A procedure for correcting the grain size effects in heavy metal analyses of estuarine and coastal sediments. *Environ Technology Letters*, **1**, 518–527.

Ackermann, F., Bergmann, H., Schleichert, U. (1983) Monitoring of heavy metals in coastal and estuarine sediments—a question of grain size: b20 Am versus b60 Am. *Environment Technology Letters*, **4**, 317–328.

Adams, M.J. and Allen, J.R. (1998) Variable selection and multivariate calibration models for x-ray fluorescence spectrometry. *Journal of Analytical Atomic Spectrometry*, **13**, 119-124.

Adgate, J.L., Ramachandran, G., Pratt, G.C., Waller, L.A. and Sexton, K. (2002) Spatial and temporal variability in outdoor, indoor, and personal PM2.5 exposure. *Atmospheric Environment*, **36(**20), 3255-3265.

Aea. (2008) *UK Air Quality Archive*. Department for Environment, Food & Rural Affairs.

AEAT/NETC. (2004) UK Emissions of Air Pollutants 1970 to 2002 [online], London: Available at <http://www.naei.org.uk>.

Ahyerre, M., Chebbo, G., Tassin, B. and Gaume, E. (1998) Storm water quality modelling, an ambitious objective? *Water Science & Technology*, **37**, 205–213.

Air Quality Expert Group (AQEG) (2005) Particulate Matter in the United Kingdom. London: DEFRA.

Air Quality Expert Group (AQEG) (2011) Understanding PM_{10} in Port Talbot. London: DEFRA.

Akhter, M.S. and Madany, I.M. (1993) Heavy metals in street and house dust in Bahrain. *Water Air and Soil Pollution*, **66**, 111-119.

Al-Khashman, O. (2004) Heavy metal distribution in dust, street dust and soils from the work placein Karak industrial estate, Jordan. *Atmospheric Environment*, **38**, 6803-6812.

Al-Khashman, O. (2007) Determination of metal accumulation in deposited street dusts in Amman Jordan. *Environmental Geochemistry and Health*, **29**, 1-10.

Allen, G.P., Castaing, P., and Klingebiel, A. (1972) Distinction of elementary sand populations in the Gironde Estuary (France) by R-mode factor analysis of grain size data, *Sedimentology*, **19**, 21-35.

Allen, J.R.L. and Rae, J.E. (1986) Time sequence of metal pollution, Severn Estuary, southwestern UK. *Marine Pollution Bulletin*, **17**(9), 427-431.

Allen, A.G., Nemitz, E., Shi, J.P., Harrison, R.M. and Greenwood, J.C (2001) Size distributions of trace metals in atmospheric aerosols in the United Kingdom. *Atmospheric Environment*, **35(**27), 4581-4591

Al-Merey, R., Karajou, J. and Issa, H. (2005) X-ray fluorescence analysis of geological samples: exploring the effect of sample thickness on the accuracy of results. *Applied Radiation and Isotopes*, **62**(3), 501-508.

Allott, R.W., Hewitt, C.N., and Kelly, M.R. (1990) The environmental half-lives and mean residence times of contaminants in dust for an urban environment: Barrow-in-Furness. *Science of The Total Environment*, ***93***, 403-410.

Alloway, B.J. and Ayres, D.C. (1997) *Chemical Principles of Environmental Pollution.* London: Blackie Academic and Professional.

Amato, F., Pandolfi, M., Viana, M., Querol, X., Alastuey, A. and Moreno, T. (2009) Spatial and chemical patterns of PM10 in road dust deposited in urban environment. *Atmospheric Environment*, **43**(9), 1650-1659.

Anagnostopoulou, M.A. and Day, J.P. (2006) Lead concentrations and isotope ratios in street dust in major cities in Greece in relation to the use of lead in petrol. *Science of The Total Environment*, **367**(2-3), 791-799.

Apeagyei, E., Bank, M.S. and Spengler, J.D. (2011) Distribution of heavy metals in road dust along an urban-rural gradient in Massachusetts. *Atmospheric Environment*, **45**(13), 2310-2323.

ApSimon, H.M., Gonzalez del Campo, M.T., Adams, H.S. (2001) Modelling long-range transport of primary particulate material over Europe. *Atmospheric Environment*, **35**(2), 343-352.

Araujo, M., Fatima, D., Bernard, P.C. and Van Grieken, R.E. (1988) Heavy metal contamination in sediments from the Belgian coast and Scheldt Estuary. *Maritime Pollution Bulletin*, **19**, 269–273.

Armistead G. and Brunekreef, B. (2009) A Focus on Particulate Matter and Health. *Environmental Science & Technology,* **43**(13), 4620-4625.

Artiola, J.F. and Warrick, A.W. (2004) Sampling and Data Quality Objectives for Environmental Monitoring, In: Janick F., Artiola, I. L. and Brusseau, M.L. (Editors), *Environmental Monitoring and Characterization,* Academic Press, Burlington, 11-27.

Aston, S.R., and D.A. Stanners. (1982) Local variability in the distribution of windscale fission products in estuarine sediments. *Estuarine Coastal Shelf Science*, **14**, 167-174.

Ball, D.F. (1964) Loss-on-ignition as an estimate of organic matter and organic carbon in non-calcareous soils. *European Journal of Soil Science*, **15**(1), 84-92.

Banerjee, A.D.K. (2003) Heavy metal levels and solid phase speciation in street dusts of Delhi, India. *Environmental Pollution*, **123**(1), 95-105.

Bari, A., Ferraro, V., Wilson, L.R., Luttinger, D. and Husain L. (2003) Measurements of gaseous HONO, HNO_3, SO_2, HCl, NH_3, particulate sulphate and $PM_{2.5}$ in New York, NY. *Atmospheric Environment*, **37**(20), 2825-2835.

Barrett, P.J. (1980) *The shape of particles, a critical review*. Sedimentology . **27**, 291-303.

Bartington Instruments (2012) MS2/MS3 Magnetic Susceptibility Equipment [online]. Witney: Bartington Instruments Ltd. Available at: < http://www.bartington.com/ms3.html>

Bartington Instruments (2011) *Bartington Price List*. Email from M. Tracey, 20 October 2011.

Bartlett, C.J.S., Betts, W.E., Booth, M., Giavazzi, F., Guttman, H., Heinze, R., Mayers, R.F. and Roberts, D. (1992) *CONCAWE Report no 92/51 - the chemical composition of diesel particulate emissions*. Automotive Emissions Management Group.

Bazylinski, D.A. (1996) Controlled biomineralization of magnetic minerals by magnetotactic bacteria. *Chemical Geology*, **132**(1-4), 191-198.

Beck, M.B. (1987) Water Quality Modelling: A Review of Uncertainty. *Water Resources Res*, **23**(8), 1393-1442.

Beckwith, P.R., Ellis, J.B., Revitt, D.M. and Oldfield, F. (1986) Heavy metal and magnetic relationships for urban source sediments. *Physics of The Earth and Planetary Interiors*, **42**(1-2), 67-75.

Bertrand-Krajewski, J.L., Briat, P. and Scrivener, O. (1993). Sewer sediment production and transport modelling: a literature review. *JHR*, **31**(4), 435–460.

Bertrand-Krajewski, J. L. (2007) Stormwater pollutant loads modelling: epistemological aspects and case studies on the influence of field data sets on calibration and verification. *Water Science & Technology,* **55**(4), 1–17.

Berubé, K.A., Jones, T.P. and Williamson, B.J. (1997) Electron Microscopy of urban particulate matter. *Microscopy and Analysis,* **Sept**, 11-13.

Bigazzi, A.Y. and Figliozzi, M.A. (2012) Congestion and emissions mitigation: A comparison of capacity, demand, and vehicle based strategies, Transportation Research Part D: *Transport and Environment,* **17**(7), 538-547.

Blundell, A., Hannam, J.A., Dearing, J.A. and Boyle, J.F. (2009) Detecting atmospheric pollution in surface soils using magnetic measurements: A reappraisal using an England and Wales database. *Environmental Pollution*, **157**(10), 2878-2890.

Bockhorn, H. (1995) A short introduction to the problem - structure of the following parts. In Bockhorn H (Ed) *Soot formation in combustion,* Berlin: Springer Verlag, 3-7.

Bohren, C.F. and Huffman, D.R. (1988) *Absorption and scattering of light by small particles.* New York: John Wiley & Sons.

Bonnett, P.J.P., Appleby, P.G., and Oldfield, F. (1988) Radionuclides in coastal and estuarine sediments from Wirral and Lancashire, *The Science of the Total Environment*, **70**, 215-236.

Booth, C.A., Walden, J., Neal, A., Smith, J.P. and Morgan, E. (2004) A Comparison of Inter-Site, Intra-Site, Intra-Sample and Instrument Variability in Environmental Magnetic Data: An Example Based on the Gwendraeth Estuary, South Wales, U.K. *Journal of Coastal Research*, **20**(3), 808–813.

Booth, C.A., Fullen, M.A., Walden, J., Smith, J.P., Hallett, M.D., Harris, J. and Holland, K. (2005a). Magnetic properties of agricultural topsoils of the Isle of Man: their characterization and classification by factor analysis. *Communications in Soil Science and Plant Analysis*, **36**, 1241-1262.

Booth, C.A., Walden, J., Neal, A. and Smith, J.P. (2005b) Use of mineral magnetic concentration data as a particle size proxy: A case study using marine, estuarine and fluvial sediments in the Carmarthen Bay area, South Wales, U.K. *Science of the Total Environment*, **347**, 241-253.

Booth, C.A., Shilton, V., Fullen, M.A., Walden, J., Worsley, A.T. and Power, A.L. (2006). Environmental magnetism: measuring, monitoring and modelling urban street dust pollution, p. 333-342 In: J.W.S. Longhurst and C.A. Brebbia (Eds) *Air Pollution XIV*. Wessex Institute of Technology (WIT) Press, Southampton.

Booth, C.A., Winspear, C.M., Fullen, M.A., Worsley, A.T., Power, A.L. and Holden, V.J. (2007) A pilot investigation into the potential of mineral magnetic measurements as a proxy for urban roadside particulate pollution. *Air Pollution XV*, **101**, 391-400.

Booth, C.,A., Fullen, M.A., Walden, J., Worlsey, A., Marcinkonis, S. and Coker, A.O. (2008) Problems and potential of mineral magnetic measurements as a soil particle size proxy. *Journal of Environmental Engineering and Landscape Management*, **16**(3), 151-158.

Bowman, E.T., Soga, K. and Drummond T.W. (2000): *Particle shape characterization using Fourier analysis*. CUED/D-Soils/TR315.

Boyle. J.F. (2000) Rapid elemental analysis of sediment samples by isotope source XRF. *Journal of Palaeolimnology*, **200**(23), 213-221.

Brimblecombe, P. (2011) Air Pollution Episodes, In: Jerome O. Nriagu, (Editors), *Encyclopedia of Environmental Health*, Elsevier, Burlington, 39-45.

Brüggeman, E., Gerwig, H., Gnauk, Th., Muller, K. and Herrmann, H. (2009) Influence of seasons, air mass origin and day of the week on size-segregated chemical composition of aerosol particles at a kerbside. *Atmospheric Environment*, **43**, 2456-2463

Brunekreef, B. and Forsberg, B. (2005) Epidemiological evidence of effects of coarse airborne particles on health. *European Respiratory Journal,* 309-318.

Bucko, M.S., Magiera, T., Johanson, B., Petrovský, E. and Pesonen, L.J. (2011) Identification of magnetic particulates in road dust accumulated on roadside snow using magnetic, geochemical and micro-morphological analyses. *Environmental Pollution*,

Butler, R.F. (1992) *Palaeomagnetism: magnetic domains to geologic terranes*, Blackwell Scientific Publications, Oxford.

Butler, D. and Clark, P. *(*1995*) Sediment Management in Urban Drainage Catchments.* CIRIA, London.

Canbay, M., Aydin, A. and Kurtulus, C. (2010) Magnetic susceptibility and heavy-metal contamination in topsoils along the Izmit Gulf coastal area and Izaytas (Turkey). *Journal of Applied Geophysics*, **70**, 46–57.

Canepari, S., Perrino, C., Astolfi, M. L., Catrambone, M. and Perret, D. (2009) Determination of soluble ions and elements in ambient air suspended particulate matter: Inter-technique comparison of XRF, IC and ICP for sample-by-sample quality control. *Talanta*, **77**(5), 1821-1829.

Celis, J.E., Morales, J.R., Zaror, C.A. and Inzunza, J.C. (2004) A study of the particulate matter PM_{10} composition in the atmosphere of Chillán, Chile. *Chemosphere*, **54**(4), 541-550.

Chameides, W.L., Yu, H., Liu, S.C., Bergin, M.N., Zhou, X., Mearns, L., Wang, G., Kiang, C.S., Saylor, R.D., Luo, C., Huang, Y., Steiner, A. and Giorgi, F. (1999) Case study of the effects of atmospheric aerosols and regional haze on agriculture: An opportunity to enhance crop yields in China through emission controls?" *In Proceedings of the National Academy of Sciences of the United States of America*, **96**(24).

Chan, L.S., Ng, S.L., Davis, A.M., Yim, W.W.S. and Yeung, C.H. (2001) Magnetic Properties and Heavy-metal Contents of Contaminated Seabed Sediments of Penny's Bay, Hong Kong. *Marine Pollution Bulletin*, **42**(7),569-583,

Chaparro, M.A.E., Marinelli, C., Sinito, A.M. (2008) Multivariate techniques as alternative statistical tools applied to magnetic proxies for pollution: a case study from Argentina and Antarctica. *Environmental Geology*, **54**, 365-371.

Charlesworth, S.M. and Lees, J.A. (1999) Particulate-associated heavy metals in the urban environment: their transport from source to deposit, Coventry, UK. *Chemosphere*, **39**, 833-848.

Charlesworth, S.M. and Lees, J.A. (2001) The application of some mineral magnetic measurements and heavy metal analysis for characterising fine sediments in an urban catchment, Coventry, UK. *Journal of Applied Geophysics*, **48**, 113-125

Charlesworth, S.M, Everett, M., Mccarthy, R., Ordonez, A. and De Miguel, E. (2003) A comparative study of heavy metal concentration and distribution in deposited street dusts in a large and a small urban area: Birmingham and Coventry, West Midlands, UK. *Environment International*, **29**(5), 563-573.

Charron, A., Harrison, R.M., Quincey, P. (2007) What are the sources and conditions responsible for exceedences of the 24h PM_{10} limit value at a heavily trafficked London site?. *Atmospheric Environment*, **41**(9), 1960-1975,

Chatterjee, A. and Banerjee, R.N. (1999) Determination of lead and other metals in a residential area of greater Calcutta. *Science of the Total Environment*, **227**, 175-185.

Chen, T., Gokhale, J., Shofer, S. and Kuschner, W. (2007) Outdoor Air Pollution: Particulate Matter Health Effects. *The American Journal of the Medical sciences*, **333**(4), 235 - 243.

Chen, X., Xia, X., Zhao, Y. and Zhang, P. (2010) Heavy metal concentrations in roadside soils and correlation with urban traffic in Beijing, China. *Journal of Hazardous Materials*, **181**, 640-646.

Chen, Y. and Xie, S. (2012) Temporal and spatial visibility trends in the Sichuan Basin, China, 1973 to 2010. *Atmospheric Research*, **112**, 25-34.

Chow, J.C., Watson, J.G., Fujita, E.M., Lu, Z., Lawson, D.R. and Ashbaugh, L.L. (1994) Temporal and spatial variations of $PM_{2.5}$ and PM_{10} aerosol in the Southern California air quality study. *Atmospheric Environment*, **28**(12), 2061-2080.

Chow, J.C., Watson, J.G., Edgerton, S.A. and Vega, E. (2002) Chemical composition of $PM_{2.5}$ and PM_{10} in Mexico City during winter 1997. *Science of The Total Environment*, **287(**3), 177-201.

Christoforidis, A. and Stamatis, N. (2009) Heavy metal contamination in street dust and roadside soil along the major national road in Kavala's region, Greece. *Geoderma*, **151**, 257-263.

Claiborn, C.S., Larson F.D. and Koenig, J.Q. (2000) Windblown dust contributes to high PM2.5 concentrations. *Journal of Air Waste Management Association*, **50,** 1440-1445.

Clifton, R.J., and Hamilton, E.I. (1982) The application of radioisotopes in the study of estuarine sedimentary processes. *Estuarine Coastal Shelf Science*, **14**, 433-446.

Clifton, J., McDonald, P., Plater, A., and Oldfield, F. (1997) Relationships between radionuclide content and textural properties in Irish Sea intertidal sediments, *Water Air and Soil Pollution*, **99**, 209-216.

Clifton, J., Mcdonald, P., Plater, A. and Oldfield, F. (1999) Derivation of a grain-size proxy to aid the modelling and prediction of radionuclide activity in salt marshes and mud flats of the Eastern Irish Sea. *Estuarine, Coastal and Shelf Science*, **48**(5), 511-518.

Committee on the Medical Effects of Air Pollutants (COMEAP) (2001) Long-term effects of particles on mortality. Oxford: Health Protection Agency Chemical Hazards and Poisons Division.

Committee on the Medical Effects of Air Pollutants (COMEAP) (2009) Long-Term Exposure to Air Pollution: Effect on Mortality. Oxford: Health Protection Agency Chemical Hazards and Poisons Division.

Committee on the Medical Effects of Air Pollutants (COMEAP) (2010) The Mortality Effects of Long-term exposure to particulate air pollution in the United Kingdom. Oxford: Health Protection Agency Chemical Hazards and Poisons Division.

Committee on the Medical Effects of Air Pollutants (COMEAP) (2012) Particles [online]. Oxford: COMEAP. Available at <http://comeap.org.uk/introduction-to-air-pollution/126-particles.html>

Corn, M., Montgomery, T.L. and Esmen, N.A. (1971) Suspended particulate matter: Seasonal variation in specific areas and densities. *Environmental Science and Technology*, **5(**2).

Covelli, S. and Fontolan, G. (1997) Application of a normalisation procedure in determining regional geochemical baselines. *Environmental Geology*, **30**, 34–45.

Curtis, L., Rea, W., Smith-Wallis, P., Fenyves, E. and Pan, Y. (2006) Adverse health effects of outdoor air pollutants. *Environmental International*, **32**, 815-830.

Cyrys, J., Stölzel, M., Heinrich, J., Kreyling, W.G., Menzel, N., Wittmaack, K., Tuch, T. and Wichmann, H.E. (2003) Elemental composition and sources of fine and ultrafine ambient particles in Erfurt, Germany. *The Science of The Total Environment*, **305**(1-3), 143-156.

Dahl, A., Gharibi, A., Swietlicki, E., Gudmunsson, A., Bohgard, M., Ljungman, A., Blomqvist, G. and Gustafsson, M. (2006) Traffic-generated emissions of ultrafine particles from pavement-tire interface. *Atmospheric Environment*, **40**(7), 1314-1323.

D'alessandro, A., Lucarelli, F., Mandò, P.A., Marcazzan, G., Nava, S., Prati, P., Valli, G., Vecchi, R. and Zucchiatti, A. (2003) Hourly elemental composition and sources identification of fine and coarse PM_{10} particulate matter in four Italian towns. *Journal of Aerosol Science*, **34**(2), 243-259.

Dao, L., Morrison, L. and Zhang, C. (2010) Spatial variation of urban soil geochemistry in a roadside sports ground in Galway, Ireland. *Science of The Total Environment*, **408**(5), 1076-1084.

Davies, D.J.A., Watt, J.M. and Thornton, I. (1987) Lead levels in Birmingham dusts and soils. *Science of the Total Environment*, **67**, 177-185.

Davis, J.C. (1986) *Statistics and Data Analysis in Geology.* 2nd. Edition, John Wiley & Sons, Chichester.

Davis, J.C. (2002) *Statistics and Data Analysis in Geology.* 3rd. Edition, John Wiley & Sons, Chichester.

Davis, B. and Birch, G. (2010) Comparison of heavy metal loads in stormwater runoff from major and minor urban roads using pollutant yield rating curves. *Environmental Pollution*, **158**(8), 2541-2545.

Davis, H. T., Marjorie Aelion, C., Mcdermott, S. and Lawson, A. B. (2009) Identifying natural and anthropogenic sources of metals in urban and rural soils using GIS-based data, PCA, and spatial interpolation. *Environmental Pollution*, **157**(8-9), 2378-2385.

Day, J.P., Hart, M. and Robinson, M.S. (1975) Lead in urban street dusts. *Nature*, **253**, 343-345.

Deacon, A.R., Derwent, R.G., Harrison, R.M., Middleton, D.R. and Moorcrott, S. (1997) Analysis and interpretation of measurements of suspended particulate matter at urban background sites in the United Kingdom. *Science of The Total Environment*, **203**(1), pp.17-36.

Dean, W. E. (1974) Determination of carbonate and organic matter in calcareous sediments and sedimentary rocks by loss on ignition: Comparison with other methods. *J. Sed. Petrol*, **44**, 242-248.

Dearing, J.A., Dann, R.J.L., Hay, K., Lees, J.A., Loveland, P.J., Maher, B.A. and O'Grady, K. (1996) Frequency-dependant susceptibility measurements of environmental materials. *Geophysics Journal International*, **124**, 228-240.

Dearing J. (1999) Magnetic susceptibility. In: Walden J, Smith JP, Oldfield F, (Editors). *Environmental Magnetism: a practical guide,* Quaternary Research Association. London. Technical Guide, No. 6, 35–62.

Dearing, J.A. and Jones, R.T. (2003) Coupling temporal and spatial dimensions of global sediment flux through lake and marine sediment records. *Global and Planetary Change*, **39**(1-2), 147-168.

DeCarlo, P.F., Slowik, J.G., Worsnop, D.R., Davidovits, P. and Jimenez, J.L. (2004) Particle morphology and density characterization by combined mobility and aerodynamic diameter measurements. Part 1: Theory. *Aerosol Science and Technology*, **38**, 1185-1205.

de Groot, A.J., Zschuppe, K.H., Salomons, W. (1982) Standardisation of methods of analysis for heavy metals in sediments. *Hydrobiologia,* **92**, 689–695.

de Kok, T.M.C.M., Driece, H.A.L., Hogervorst, J.G.F. and Briedé, J.J. (2006) Toxicological assessment of ambient and traffic-related particulate matter: A review of recent studies. *Mutation Research,* **613**, 103-122.

Dekkers, M.J. (1997) Environmental magnetism: an introduction. *Geologie en Mijnbouw*, **76**, 163-182.

De Miguel, E., Llamas, J., Chacon, E., Berg, T., Larssen, S., Royset, O. and Vadset, M. (1997) Origin and patterns of distribution of trace elements in street dust: unleaded petrol and urban lead. *Atmospheric Environment*, **31**(17), 2733 - 2740.

Department for Environment Food and Rural Affairs (DEFRA) (2009) UK and EU Air Quality Policy Context [online]. London: DEFRA. Available at: <http://uk-air.defra.gov.uk/air-pollution/uk-eu-policy-context>

Department for Environment Food and Rural Affairs (DEFRA) (2012) What are the effects of air pollution? [online]. London: DEFRA. Available at: <http://uk-air.defra.gov.uk/air-pollution/effects>

Department of the Environment. (1997) The United Kingdom National Air Quality Strategy. *Department of the Environment*. London.

Dinarès-Turell, J., Hoogakker, B.A.A., Roberts, A.P., Rohling, E.J. and Sagnotti, L. (2003) Quaternary climatic control of biogenic magnetite production and eolian dust input in cores from the Mediterranean Sea. *Palaeogeography, Palaeoclimatology, Palaeoecology*, **190**, 195-209.

Dockery, D.W., Pope, C.A., Xu, X., Spengler, J.D., Ware, J.H., Fay, M.E., Ferris, B.G. and Speizer, F.E. (1993) An association between air pollution and mortality in six U.S. cities. *The New England Journal of Medicine*, **329**(24), 1743-1759.

Dodds, J. (2003) *Particle shape and stiffness – effects on soil behavior.* Unpublished Master of Science Thesis, Georgia Institute of Technology.

Donaldson, K. and Borm, P.J.A. (1998) The quartz hazard: a variable entity. *The Annals of Occupational Hygiene*, **42**(5), 287-294.

Donaldson, K., Li, X.Y., MacNee, W. (1998) Ultrafine (nanometre) particle mediated lung injury. *Journal of Aerosol Science*, **29**(5–6), 553-560.

Donaldson, K. and Tran, C.L. (2002) Inflammation caused by particles and fibres. *Inhalation Toxicology*, 14:5-27.

Donaldson, K., MacNee, W., Stone, V. (2006) ENVIRONMENTAL POLLUTANTS | Particulate Matter, Ultrafine Particles, In: Geoffrey J. Laurent and Steven D. Shapiro, (Editors), *Encyclopedia of Respiratory Medicine*, Academic Press, Oxford.

Donaldson, K. and Borm, P. (2010) Particle Toxicology. Boca Raton: Tailor and Francis Group.

Douglas, I. (1985) Urban sedimentology. *Progress in Physical Geography,* **9**(2), 255–280.

Droppo, I.G., Irvine, K.N., Murphy, T.P. and Jaskot, C. (1998) Fractional metals in street dust of a mixed land use sewershed, Hamilton, Ontario. *Hydrology in a Changing Environment III*, 384-393.

Duan, X.M., Hu, S.Y., Yan, H.T., Blaha, U., Roesler, W., Appel, E. and Sun, W.H. (2009) Relationship between magnetic parameters and heavy element contents of arable soil around a steel company, Nanjing, China. *Earth Science*, **10**, 241-249.

Duncan, H.P. (1995) A Bibliography of Urban Stormwater Quality. *Cooperative Research Centre for Catchment Hydrology*, Report 95/8.

Dunlop, D.J., and Özdemir, Ö. (1997) *Rock Magnetism: Fundamentals and Frontiers*, Cambridge University Press, 573.

Duong, T.T.T. and Lee, B. (2011) Determining contamination level of heavy metals in road dust from busy traffic areas with different characteristics. *Journal of Environmental Management*, **92**, 554-562.

Duran-Tauleria, E. and Rona, R.J. (1999) Geographical and socioeconomic variation in the prevalence of asthma symptoms in English and Scottish children. *Thorax*, **54**, 476-481.

Dybing, E. and Totlandsdal, A. I. (eds.) (2005) *Air pollution and the risk to human health – a toxicological perspective*. AIRNET A Thematic Network on Air Pollution and Health, Work Group 3 – Toxicology.

Ebdon, D. (1978) *Statistics in Geography: A Practical Approach*, Basil Blackwell, Oxford.

Edwards, J., Walters, S. and Griffiths, R. (1994) Hospital admissions for asthma in preschool children: relationship to major roads in Birmingham, United Kingdom. *Archives of Environmental Health*, **49,** 223-225.

Ellis, J.B. and Revitt, D.M. (1982) Incidence of heavy metals in street surface sediments: solubility and grain size studies. *Water, Air and Soil pollution,* **17**, 87-100.

Ergin, M., Kazan, B., Ediger, V. (1996) Source and depositional controls on heavy metal distribution in marine sediments of the Gulf of Iskenderun, East Mediterranean. *Maritime Geology*, **133**, 223–239.

European Commission (2012) Review of the EU AIR policy. Brussells: European Union.

Fergusson, J.E. and Ryan, D.E. (1984) The elemental composition of street dust from large and small urban areas related to city type, source and particle size. *The Science of The Total Environment*, **34**(1-2), 101-116.

Ferreira-Baptista, L. and De Miguel, E. (2005) Geochemistry and risk assessment of street dust in Luanda, Angola: A tropical urban environment. *Atmospheric Environment*, **39**(25), 4501-4512.

Flanders, P.J. (1994) Collection, measurement, analysis of airborne magnetic particulates from pollution in the environment. *Journal of Applied Physics*, **75**, 5931-5936.

Folk, R.L., and Ward, W.C. (1957) Brazos River bar: a study in the significance of grain size parameters, *Journal of Sedimentary Petrology*, **27**, 3-26.

Förstner, U. and. Wittmann, G. T. W (1979) *Metal Pollution in the aquatic Environment. Berlin, Heidelberg*. Springer-Verlag, New York.

Friedman, G.M., and Sanders, J.E. (1978) *Principles of Sedimentology*, Wiley, New York.

Fubini, B. (1997) Surface reactivity in the pathogenic response to particulates. *Environmental Health Perspectives*, **105**, 1013-1020.

Fubini, B. and Areán, C.O. (1999) Chemical aspects of the toxicity of inhaled mineral dusts. *Chemical Society Review*, 28, 373-381.

Fujiwara, F., Rebagliati, R.J., Dawidowski, L., Gómez, D., Polla, G., Pereyra, V. and Smichowski, P. (2011) Spatial and chemical patterns of size fractionated road dust collected in a megacitiy. *Atmospheric Environment*, **45**(8), 1497-1505.

Fuller, G.W. and Green, D. (2006) Evidence for increasing concentrations of primary PM_{10} in London. *Atmospheric Environment*, **40**, 6134-6145.

Gautam, P., Blaha, U. and Appel, E. (2005) Magnetic susceptibility of dust-loaded leaves as a proxy of traffic-related heavy metal pollution in Kathmandu City, Nepal. *Atmospheric Environment*, **39**(12), 2201-2211.

Georgeaud, V.M., Rochette, P., Ambrosi, J.P., Vandamme, D.and Williamson, D. (1997) Relationship between heavy metals and magnetic properties in a large polluted catchment: the Etang de Berre (south of France). *Physics and Chemistry of the Earth,* **22**, 211-214.

Giugliano, M., Lonati, G., Butelli, P., Romele, L., Tardivo, R. and Grosso, M. (2005) Fine particulate ($PM_{2.5}$-PM_1) at urban sites with different traffic exposure. *Atmospheric Environment*, **39**(13), 2421-2431.

Goddu, S.R., Appel, E., Jordanova, D. and Wehland, F. (2004) Magnetic properties of road dust from Visakhapatnam (India) - relationship to industrial pollution and road traffic. *Physics and Chemistry of the Earth, Parts A/B/C*, **29**(13-14), 985-995.

Gold, D.R., Litonjua, A., Schwartz, J., Lovett, E., Larson, A., Nearing, B., Allen, G., Verrier, M., Cherry, R. and Verrier, R. (2000) Ambient pollution and heart rate variability. *Circulation*, **101**, 1267-1273.

Goldacre, M., Yeates, D., Gill, L., McGuinness, H. and Meddings, D. (2005) *Asthma in England 1998/9 to 2002/3. A Geographical Profile of Hospital Admissions.* Oxford: Oxford University.

Gomes, C.D.S.F. and Silva, J.B.P. (2007) Minerals and clay minerals in medical geology. *Applied Clay Science*, **36**(1-3), 4-21.

González, C.M. and Aristizábal, B.H. (2012) Acid rain and particulate matter dynamics in a mid-sized Andean city: The effect of rain intensity on ion scavenging. *Atmospheric Environment*, **60**, 164-171.

Granum, B., Gaarder, P.I., Groeng, E.-C., Leikvold, R.-B., Namork, E. and Løvik, M. (2001) Fine fraction of widely different composition have an adjuvant effect on the production of allergen-specific antibodies. *Toxicology Letters,* **115**, 171-181.

Greenwood, N.N. (1996). *Chemistry of the Elements*: Butterworth Heinemann Ltd., Akademic Press: Berjing, p. 248.

Haberle, S.G. and Lumley, S.H. (1998) Age and origin of tephras recorded in postglacial lake sediments to the west of the southern Andes, 44°S to 47°S. *Journal of Volcanology and Geothermal Research*, **84**(3-4), *239-256.*

Hallett, D.J., Mathewes, R.W. and Foit Jr. F.F. (2001) Mid-Holocene Glacier Peak and Mount St Helens. tephra layers detected in lake sediments from Southern British Columbia using high-resolution techniques.*Quaternary Research*, **55**,(3), 284-292.

Hamilton, R.S., Revitt, D.M. and Warren, R.S. (1984) Levels and physico-chemical associations of Cd, Cu, Pb, and Zn in road sediments. *Science of the Total Environment*, **33**, 59-74.

Han, Y., Du. J., Cao, E. and Posmentier, E. (2006) Multivariate analysis of heavy metal contamination in urban dusts of Xi'an, Central China. *Science of the Total Environment*, **355**, 176-186.

Han, Y., Cao, J., Posmentier, E. S., Fung, K., Tian, H. and An, Z. (2008) Particulate-associated potentially harmful elements in urban road dusts in Xi'an, China. *Applied Geochemistry*, **23**(4), 835-845.

Hanesch, M., Scholger, R. and Rey, D. (2003) Mapping dust distribution around an industrial site by measuring magnetic parameters of tree leaves. *Atmospheric Environment*, **37**(36), 5125-5133.

Harrison, R.M. (1979) Toxic metals in street and household dusts. *The Science of the Total Environment*, **11**, 89-97.

Harrison, R.M., Laxen, D. and Wilson, S. (1981) Chemical associations of lead, cadmium, copper, and zinc in street dusts and roadside soils. *Environmental Science and Technology*, **15**(11), 1378-1383.

Harrison, R.M. and Jones, M. (1995) The chemical composition of airborne particles in the UK atmosphere. *Science of The Total Environment*, **168**(3), 195-214.

Harrison, R. M., Brimblecombe, P. and Dervent, R. G. (1996) Health effects of non-biological particles. In: *Airborne Particulate Matter in the United Kingdom: Third Report of the Quality of Urban Air Review Group.* Department of Environment, London.

Harrison, R.M., Deacon, A.R., Jones, M.R. and Appleby, R.S. (1997) Sources and processes affecting concentrations of PM_{10} and $PM_{2.5}$ particulate matter in Birmingham (U.K.). *Atmospheric Environment*, **31**(24), 4103-4117.

Harrison, R.M. and van Greiken, R. (1998) *Atmospheric particulates, IUPAC Series on Analytical and Physical Chemistry of Environmental Systems*. John Wiley and Sons, Chichester UK.

Harrison, R.M. and Yin, J. (2000) Particulate matter in the atmosphere: which particle properties are important for its effects on health? *The Science of the Total Environment*, **249**, 85-101.

Harrison, R.M., Tilling, R., Callén Romero, R.M., Harrad, S. and Jarvis, K. (2003) A study of trace metals and polycyclic aromatic hydrocarbons in the roadside environment. *Atmospheric Environment*, **37**(17), 2391-2402.

Harrison, R.M. (2004) Key pollutants--airborne particles. *Science of The Total Environment*, **334-335**, pp.3-8.

Harrison, R.M., Jones, A.M. and Lawrence, R.G. (2004) Major component composition of PM_{10} and $PM_{2.5}$ from roadside and urban background sites. *Atmospheric Environment*, **38**(27), 4531-4538.

Haugland, T., Ottesen, R.T. and Volden, T. (2007) Lead and polycyclic aromatic hydrocarbons (PAHs) in surface soil from day care centres in the city of Bergen, Norway. *Environmental Pollution*, **153**(2), 266-272.

Hay, K.L., Dearing, J.A., Baban, S.M.J. and Loveland, P. (1997) A preliminary attempt to identify atmospherically-derived pollution particles in English topsoils from magnetic susceptibility measurements. *Physics and Chemistry of the Earth*, **22**(1-2), 207-210.

Hays, M.D., Cho, S., Baldauf, R., Schauer, J.J. and Shafer, M. (2011) Particle size distributions of metal and non-metal elements in an urban near-highway environment. *Atmospheric Environment*, **45**, 925-934.

Haywood, J.B. (1988) *Internal Combustion Engine Fundamentals*; McGraw Hill: New York.

Heinrich, J., Pitz, M., Bischof, W., Krug, N. and Borm, P.J.A. (2003) Endotoxin in fine ($PM_{2.5}$) and coarse ($PM_{2.5-10}$) particle mass of ambient aerosols. A temporospatial analysis*. Atmospheric Environment,* **37**, 3659-3667.

Heinrich, J. and Slama, R. (2007) Fine particles, a major threat to children. *International Journal of Hygiene and Environmental Health*, **210**, 617-622.

Heiri, O., Lotter, A. F. and Lemcke, G. (2001) Loss on ignition as a method for estimating organic and carbonate content in sediments: reproducibility and comparability of results. *Journal of Paleolimnology*, **25**, 101-110.

Herngren, L., Goonetilleke, A. and Ayoko, G. (2006) Analysis of heavy metals in road-deposited sediments. *Analytica Chemica Acta*, **571**, 270-278.

Hetland, R.B., Refsnes, M., Myran, T., Johansen, B.V., Uthus, N. and Schwarze P.E. (2000) Mineral and/or metal content as critical determinants of particle-induced release of IL-6 and IL-8 from A549 Cells. *Journal of Toxicology and Environmental Health, Part A,* **60**, 47-65.

Hetland, R.B., Schwarze, P.E., Johansen, B.V., Myran, T., Uthus, N. and Refsnes, M. (2001) Silica-induced cytokine release from A549 cells: importance of surface area versus size. *Human and Experimental Toxicology*, **20**, 46-55.

Hetland, R.B., Schwarze, P.E., Johansen, B.V., Myran, T., Uthus, N. and Refsnes, M. (2001) Silica-induced cytokine release from A549 cells: importance of surface area versus size. *Human and Experimental Toxicology*, **20**, 46-55.

Hilton, J. and Lishman, J.P. (1985) The effects of redox changes on the magnetic susceptibility of sediments from a seasonally anoxic lake. *Limnology and Oceanography*, **30**, 907-909.

Hinds, W.C. (1999) *Aerosol Technology. Properties, Behavior, and Measurement of Airborne Particles*. Second edition, Wiley-Interscience Publication, John Wiley & Sons Inc.

Hoffmann, V., Knab, M. and Appel, E. (1999) Magnetic susceptibility mapping of roadside pollution. *Journal of Geochemical Exploration*, **66**(1-2), 313-326.

Hopke, P.K., Lamb, R.E. and Natusch, D.F.S. (1980) Multielemental characterization of urban roadway dust. *Environmental Science and Technology*, **14**(2), 164-172.

Hornung, H., Krum, M.D., Cohen, Y. (1989) Trace metal distribution in sediments and benthic fauna of Haifa Bay, Israel. *Estuarine Coastal Shelf Science*, **29,** 43–56.

Hosiokangas, J., Pekkanen, J., Ruuskanen, J. (1996) Sources of PM_{10} particles in urban air; effects of co-combustion of different fuels and soil dust episodes, In: Kulmala, M. and Wagner, P.E. (Editors), *Nucleation and Atmospheric Aerosols*, Pergamon, Amsterdam, 635-638.

Hu, X. F., Su, Y., Ye, R., Li, X.Q., and Zhang, G.L. (2007) Magnetic properties of the urban soils in Shanghai and their environmental implications. *Catena*, **70**(3), 428-436.

Huber, W.C. and Heaney, J.P. (1980) Operational Models for Stormwater Quality Management, In: Overcash, M.R. and Daidson, J.M, (Editors), *Environmental Impact of Nonpoint Source Pollution*, Ann Arbor Science Publisher, Ann Arbor, Michigan.

Huber, W.C. (1992) *Prediction of* urban *nonpoint source water quality methods and models*. International Symposium on Urban Stormwater Management, The Institution of Engineers, Sydney, Australia.

Hunt, A., Jones, J. and Oldfield, F. (1984) Magnetic measurements and heavy metals in atmospheric particulates of anthropogenic origin. *The Science of The Total Environment*, **33**, 129-139.

Husain, L., Dutkiewicz, V.A., Khan, A.J. and Ghauri, B.M. (2007) Characterization of caronaceous aerosols in urban air. *Atmospheric Environment*,

Hutchinson, S.M., and Prandle, D. (1994) Siltation in the saltmarsh of the Dee Estuary derived from Cs-137 analysis of shallow cores, *Estuarine Coastal and Shelf Science*, **38**, 471-478.

International Organization for Standardization (ISO) (2008) ISO 13320-1 - *Particle size analysis - laser diffraction methods*. Switzerland: ISO.

Ito, M., Mitchell, M.J., Driscoll, C.T. (2002) Spatial patterns of precipitation quantity and chemistry and air temperature in the Adirondack region of New York. *Atmospheric Environment*, **36**(6), 1051-1062.

Jacobson, M.Z. (1997) Development and application of a new air pollution modeling system—II. Aerosol module structure and design. *Atmospheric Environment*, **31**(2), 131-144,

Jiles, D. (1991) *Introduction to Magnetism and Magnetic Materials*, Chapman & Hall, London.

Johansson, C., Norman, M. and Gidhagen, L. (2007): Spatial and temporal variations of PM_{10} and particle number concentrations in urban air. *Environ Monitoring Assessment*, **127**, 477-487.

Johnson, R.J. (1980) *Multivariate Statistical Analysis in Geography*, Longman, London.

Johnson, J.P., Kittelson, D.B., Watts, W.F. (2005) Source apportionment of diesel and spark ignition exhaust aerosol using on-road data from the Minneapolis metropolitan area. *Atmospheric Environment*, **39**(11), 2111-2121.

Jones, B. and Turki, A. (1997) Distribution and speciation of heavy metals in surficial sediments from the Tees Estuary, North-east England. *Maritime Pollution Bulletin*, **34**, 768–779.

Joshi, U.M., Vijayaraghavan, K. and Balasubramanian, R. (2009) Elemental composition of urban street dusts and their dissolution characteristics in various aqueous media. *Chemosphere*, **77**, 526-533

Kampa, M. and Castanas, E. (2008) Human health effects of air pollution. *Environmental Pollution*, **151**(2), 362-367.

Kartal, S., Aydin, Z. and Tokalioglu, S. (2006) Fractionation of metals in street sediment samples by using the BCR sequential extraction procedure and multivariate statistical elucidation of the data. *Journal of Hazardous Materials*, **132**(1), 80-89.

Katsouyanni, K. (ed.), Hoek, G. (ed.) (2005): *Air pollution and the risk to human health – Epidemiology*. AIRNET A Thematic Network on Air Pollution and Health, Work Group 2 Epidemiology.

Kaur, S., Nieuwenhuijsen, M. J. and Colvile, R. N. (2005) Pedestrian exposure to air pollution along a major road in Central London, UK. *Atmospheric Environment*, **39**(38), 7307-7320.

Kaur, S., Nieuwenhuijsen, M.J. and Colvile, R.N. (2007) Fine particulate matter and carbon monoxide exposure concentrations in urban street transport microenvironments. *Atmospheric Environment*, **41**, 4781-4810.

Keeling, P.S. (1962) Some experiments in the low-temperature removal of cabonaceous material from clay. *Clay Mineral Bulletin*, **28**, 155-158.

Kelly, F.J. and Fussell, J.C. (2012) Size, source and chemical composition as determinants of toxicity attributable to ambient particulate matter. *Atmospheric Environment*, **60**, 504-526.

Ken Versteeg, J., Morris, W. A. and Rukavina, N. A. (1995) The utility of magnetic properties as a proxy for mapping contamination in Hamilton Harbour sediment. *Journal of Great Lakes Research*, **21**(1), pp.71-83.

Ketzel, M., Omstedt, G., Johansson, C., Düring, I., Pohjola, M., Oettl, D., Gidhagen, L., Wåhlin, P., Lohmeyer, A., Haakana, M. and Berkowicz, R. (2007) Estimation and validation of $PM_{2.5}/PM_{10}$ exhaust and non-exhaust emission factors for practical street pollution modelling. *Atmospheric Environment*, **41**(40), 9370-9385.

Kim, J.Y., Myung, J.H., Ahn, J.S. and Chon, H.T. (1998) Heavy metal speciation in dusts and stream sediments in the Taejon area, Korea. *Journal of Geochemical Exploration*, **64**, 409-419.

Kim, W., Doh, S.J., Park, Y.H. and Yun, S.T. (2007) Two-year magnetic monitoring in conjunction with geochemical and electron microscopic data of roadside dust in Seoul, Korea. *Atmospheric Environment*, **41**(35), 7627-7641.

Kim, W., Doh, S. and Yu, Y. (2009) Anthropogenic contribution of magnetic particulates in urban roadside dust. *Atmospheric Environment*, **43**, 3137-3144.

Kittelson, D. B. (1998) Engines and nanoparticles: a review. *Journal of Aerosol Science*, **29**(5-6), 575-588.

Kittleson, D.B., Watts, W.F., Johnson, J.P., Schauer, J.J. and Lawson, D.R. (2006) On-road and laboratory evaluation of combustion aerosols - Part 2: Summary of spark ignition engine results. *Aerosol Science*, **37**, 931-949.

Klamer, J.C., Hegeman, W.J.M., Smedes, F. (1990) Comparison of grain size correction procedures for organic micropollutants and heavy metals in marine sediments. *Hydrobiologia*, **208**, 213–219.

Kleeman, M.J., Schauer, J.J. and Cass, G.R. (2000) Size and composition distribution of fine particulate matter emitted from motor vehicles. *Environmental Science & Technology*, **34**(7), 1132-1142.

Klemm, R.J., Mason Jr., R.M., Heilig, C.M., Neas, L.M. and Dockery, D.W. (2000) Is daily mortality associated specifically with fine particles? Data reconstruction and replication of analyses. *Journal of Air and Waste Management Association,* **50**, 1215-1222.

Klovan, J.E. (1966) The use of factor analysis in determining depositional environments from grain size distributions, *Journal of Sedimentary Petrology*, **36**, 115-125.

Kovach, W.L. (1995) Multivariate data analysis. In: D. Maddy. and J.S. Brew. (Eds) *Statistical Modelling of Quaternary Science Data*, Technical Guide Series No. 5, Quaternary Research Association, Cambridge.

Kukier, U., Ishak, C.F., Sumner, M.E. and Miller, W.P. (2003) Composition and element solubility of magnetic and non-magnetic fly ash fractions. *Environmental Pollution*, **123**(2), 255-266.

Kulshrestha, A., Satsangi, G., Masih, J. and Taneja, A. (2009) Metal concentration of $PM_{2.5}$ and PM_{10} particles and seasonal variations in urban and rural environment of Agra, India. *Science of the Total Environment*. **407**, 6196–6204

Kumar, P. and Britter, R. (2005) *Particulate Matter: Importance, regulations and its historical perspective.* University of Cambridge, UK.

Kumar, P., Fennell, P. and Britter, R. (2008) Effect of wind direction and speed on the dispersion of nucleation and accumulation mode particles in an urban street canyon. *Science of the Total Environment*, **402**(1), 82-94.

Langston, W.J. (1986) Metals in sediments and benthic organisms in the Mersey Estuary. *Estuarine Coast Shelf Science*,**23**, 239–261.

Lapp, B. and Balzer, W. (1993) Early diagenesis of trace metals used as an indicator of past productivity changes in coastal sediments. *Geochimica et* Cosmochimica Acta, **57**, 4639–52.

Lee, S.V. and Cundy, A.B. (2001) Heavy metal contamination and mixing processes in sediments from the Humber Estuary, Eastern England. *Estuarine, Coastal and Shelf Science*, **53**(5), 619-636.

Lees, J.A. (1994) *Modelling the magnetic properties of natural and environmental materials,* Unpublished Ph.D. thesis, Coventry University.

Lees, J.A. (1999) Evaluating magnetic parameters for use in source identification, classification and modelling of natural and environmental materials, In: Walden, J., Oldfield, F., and Smith, J.P., (Editors), *Environmental Magnetism: a Practical Guide*, Quaternary Research Association,London. Technical Guide No. 6, 113-138.

Legesse, D., Vallett-Coulomb, C., Gasse, F. (2003) Hydrological response of a catchment to climate and land use changes in Tropical Africa: a case study South Central Ethiopia. *Journal of Hydrology*, **275**, 67-85.

Leharne, S., Charlesworth, D. and Chowdhry, B. (1992) A survey of metal levels in street dusts in an inner London neighbourhood. *Environment International*, **18**(3), 263-270.

Lehndorff, E. and Schwark, L. (2004) Biomonitoring of air quality in the Cologne conurbation using pine needles as a passive sampler-Part II: polycyclic aromatic hydrocarbons (PAH). *Atmospheric Environment*, **38**(23), 3793-3808.

Lehner, D., Kellner, G., Schnablegger, H. and Glatter, O. (1998) Static light scattering on dense colloidal systems: new instrumentation and experimental results. *Journal of Colloid and Interface Science*, **201**, 34-47.

Leong, L.S. and Tanner, P.A. (1999) Comparison of Methods for Determination of Organic Carbon in Marine Sediment. *Marine Pollution Bulletin*, **38**(10), 875-879.

Lepland, A., and Stevens, R.L. (1996) Mineral magnetic and textural interpretations of sedimentation in the Skagerrak, eastern North Sea, *Marine Geology*, **135**, 51-64.

Li, Z., Hopke, P.K., Husain, L., Qureshi, S., Dutkiewicz, V.A., Schwab, J.J., Drewnick, F. and Demerjian, K.L. (2004) Sources of fine particle composition in New York city *Atmospheric Environment*, **38**(38), 6521-6529.

Lipman, M. (2010) Targeting the Components Most Responsible for Airborne Particulate Matter Health Risks. *Journal of Exposure Science and Environmental Epidemiology*. **20**, 117–118.

Locke, G. and Bertine, K.K. (1986) Magnetite in sediments as an indicator of coal combustion. *Applied Geochemistry*, **1**, 345-356.

Lu, S.G. and Bai, S.Q. (2006) Study on the correlation of magnetic properties and heavy metals content in urban soils of Hangzhou City, China. *Journal of applied Geophysics*, **60**, 1-12.

Lu, S.G., Bai, S.Q. and Fu, L.X. (2008) Magnetic properties as indicators of Cu and Zn contamination in soils. *Pedosphere*, **18**(4), 479-485.

Lu, X., Wang, L., Lei, K., Huang, J. and Zhai, Y. (2009) Contamination assessment of copper, lead, zinc, manganese and nickel in street dust of Baoji, NW China. *Journal of Hazardous Materials*, **161**(2-3), 1058-1062.

Lu, X., Wang, L., Li, L.Y., Lei, K., Huang, L. and Kang, D. (2010) Multivariate statistical analysis of heavy metals in street dust of Baoji, NW China. *Journal of Hazardous Materials*, **173**, 744-749.

Luo, D., Corey, R., Propper, R., Collins, J., Komorniczak, A., Davis, M., Berger, N., Lum, S. (2011) Comprehensive environmental impact assessment of exempt volatile organic compounds in California. *Environmental Science & Policy*, **14**(6), 585-593,

Luo, X., Yu, S., Li, X. (2011) Distribution, availability, and sources of trace metals in different particle size fractions of urban soils in Hong Kong: Implications for assessing the risk to human health. *Environmental Pollution*, **159**(5), 1317-1326.

Maher, B.A. (1986) Characterisation of soils by mineral magnetic measurements. *Physics of the Planetary Interiors*, **42** 76-92.

Maher, B. A. and Thompson. R. (1999) *Quaternary Climates, Environments and Magnetism*. Cambridge University Press. Cambridge

Maher, B. A., Moore, C. and Matzka, J. (2008) Spatial variation in vehicle-derived metal pollution identified by magnetic and elemental analysis of roadside tree leaves. *Atmospheric Environment*, **42**(2), 364-373.

Malvern Instruments Ltd (2008) *Laser diffraction particle sizing* [online]. Malvern: [Accessed 12 November 2008]. Available at <http://www.malverncom/labeng/technology/laser_diffraction/ particlesizing.htm>.

Manno, E., Varrica, D. and Dongarra, G. (2006) Metal distribution in road dust samples collected in an urban area close to a petrochemical plant at Gela, Sicily. *Atmospheric Environment*, **40**, 5929-5941.

Martuzevicius, D., Kliucininkas, L., Prasauskas, T., Krugly, E., Kauneliene, V. and Strandberg, B. (2011) Resuspension of particulate matter and PAHs from street dust. *Atmospheric Environment*, **45**(2), 310-317.

Matsuyama, T. and Yamamoto, H. (2004) Particle shape and laser diffraction: A discussion of the particle shape problem. *Journal of Dispersion Science and Technology,* **25**, (4) 409-416.

Matzka, J. and Maher, B.A. (1999) Magnetic biomonitoring of roadside tree leaves: identification of spatial and temporal variations in vehicle-derived particulates. *Atmospheric Environment*, **33**(28), 4565-4569.

McClellan, R. (1989) Health effects of exposure to diesel exhaust particles. *Pharmacology and Toxicology*, **27**, 279-300.

McElhinny, M.W. (1973) *Palaeomagnetism and Plate Tectonics*, Cambridge University Press.

McGill, R., Tukey, J.W., and Larsen, W.A. (1978) Variations on box plots, *The American Statistician*, **32**, 12-16.

Mckenzie, E.R., Wong, C.M., Green, P.G., Kayhanian, M. and Young, T.M. (2008) Size dependent elemental composition of road-associated particles. *Science of the Total Environment*, **398**(1-3), 145-153.

Mckenzie, E.R., Money, J.E., Green, P.G. and Young, T.M. (2009) Metals associated with stormwater-relevant brake and tire samples. *Science of The Total Environment*, **407**(22), 5855-5860.

Meena, N.K., Maiti, S. and Shrivastava, A. (2011) Discrimination between anthropogenic (pollution) and lithogenic magnetic fraction in urban soils (Delhi, India) using environmental magnetism. *Journal of Applied Geophysics*, **73**(2), 121-129.

Merritt, W.S., Letcher, R.A., Jakeman, A.J. (2003) A review of erosion and sediment transport models. *Environmental Modelling & Software*, **18**(8–9), 761-799.

McIntosh, G., Gomez-Paccard, M. and Osete, M. L. (2007) The magnetic properties of particles deposited on *Platanus xhispanica* leaves in Madrid, Spain, and their temporal and spatial variations. *Science of The Total Environment*, **382**(1), 135-146.

Middleton, R. and Grant, A. (1990) Heavy metals in the Humber Estuary: Scrobicularia clay as a pre-industrial datum. *Proccedings of the Yorkshire Geological Society*,**48**,75–80.

Mitra, A.P., Sharma, C. (2002) Indian aerosols: present status. *Chemosphere*, **49**(9), 1175-1190.

Molfino, N.A., Wright, S.C., Katz, I., Tarlo, S., Silverman, F., McClean, P.A., Slutsky, A.S., Zamel, N., Szalai, J.P. and Raizenne, M. (1991) Effect of low concentrations of ozone on inhaled allergen responses in asthmatic subjects. *The Lancet*, **338**(8761), 199-203.

Monn, C. (2001) Exposure assessment of air pollutants: a review on spatial heterogeneity and indoor/outdoor/personal exposure to suspended particulate matter, nitrogen dioxide and ozone,. *Atmospheric Environment*, **35**(1), 1-32.

Morawska, L. and Zhang, J. (2002) Combustion sources of particles. 1. Health relevance and source signatures. *Chemosphere*, **49**(9), 1045-1058.

Moreno, E., Sagnotti, L., Dinarès-Turell, J., Winkler, A. and Cascella, A. (2003) Biomonitoring of traffic air pollution in Rome using magnetic properties of tree leaves. *Atmospheric Environment*, **37**(21), 2967-2977.

Moreno, T., Jones, T.P. and Richards, R.J. (2004) Characterization of aerosol particulate matter from urban and industrial environments: examples from Cardiff and Port Talbot, South Wales, UK. *Science of the Total Environment*, **334-335**, 337-346.

Mugica, V., Ortiz, E., Molina, L., De Vizcaya-Ruiz, A., Nebot,A., Quintana, R., Aguilar, J. and Alcántara, E. (2009) PM composition and source reconciliation in Mexico City. *Atmospheric Environment*, **43**(32), 5068-5074.

Muhle, H. and Mangelsdorf, I. (2003) Inhalation toxicity of mineral particles: critical appraisal of endpoints and study design. *Toxicology Letters,* **140-141**, 223-228.

Murakami, M., Nakajima, F., Furumai, H., Tomiyasu, B. and Owari, M. (2007) Identification of particles containing chromium and lead in road dust and soakaway sediment by electron probe microanalyser. *Chemosphere*, **67**(10), 2000-2010.

Muxworthy, A.R., Matzka, J. and Petersen, N. (2001) Comparison of magnetic parameters of urban atmospheric particulate matter with pollution and meteorological data. *Atmospheric Environment*, **35**(26), 4379-4386.

Muxworthy, A.R., Matzka, J., Davila, A.F. and Petersen, N. (2003) Magnetic signature of daily sampled urban atmospheric particles. *Atmospheric Environment*, **37**(29), 4163-4169.

Næss, Ø., Nafstad, P., Aamodt, G., Claussen, B. and Rosland, P. (2006) Relation between concentration of air pollution and cause-specific mortality: four-year exposures to nitrogen dioxide and particulate matter pollutants in 470 neighborhoods in Oslo, Norway. *American Journal of Epidemiology,* **165**(4) 435-443.

Nagata, T. (1961) *Rock Magnetism*, Maruzen, Tokyo.

Nageotte, S.M. and Day, J.P. (1998) Lead concentrations and isotope ratios in street dust determined by electrothermal atomic absorption spectrometry and inductively coupled plasma mass spectrometry. *Analyst* **123**, 59–62.

Namdeo, A.K. and Colls, J.J. (1996) Development and evaluation of SBLINE, a suite of models for the prediction of pollution concentrations from vehicles in urban areas. *Science of The Total Environment*, **189**(28) 311-320.

National Health Service (NHS) (2009) *Causes of asthma* [online]. London: Directgov. Available at <http://www.nhs.uk/conditions/asthma/pages/causes.aspx>.

Nearing, M.A. (1998) Why soil erosion models over-predict small soil losses and under-predict large soil losses. *CATENA*, **32**(1), 15-22.

Nicholson. (2000) Re-suspension from roads: Initial estimate of emission factors. *AEAT internal report, Vienna.*

Nygaard, U.C., Samuelsen, M., Aase, A. and Løvik, M. (2004) The capacity of particles to increase allergic sensitization is predicted by particle number and surface area, not by particle mass. *Toxicological Sciences,* **82**, 515-524.

Oberdörster, G., Ferin, J. and Lehnert, B.E. (1994) Correlation between particle size, in vivo particle persistence, and lung injury. *Environmental Health Perspect*ives, **102,**173-179.

Oberdörster, G., Gelein, R., Ferin, J. and Weiss, B. (1995) Association of particulate air pollution and acute mortality: Involvement of ultrafine particles. *Inhalation Toxicology*, **7**(1), 111-124.

Oldfield, F., Barnosky, C., Leopold, E.B. and Smith, J.P. (1983) Mineral magnetic studies of lake sediments - a brief review. *Proceedings of the 3rd International Symposium on Paleolimnology.*

Oldfield, F. and Richardson, N. (1990) Lake sediment magnetism and atmospheric deposition. Philosophical Transactions of the Royal Society. London, **B327**, 325-330.

Oldfield, F., and Clark, R.L. (1990) Lake sediment-based studies of soil erosion, In: Boardman, J., Foster, I.D.L., and Dearing, J.A., (Editors), *Soil Erosion on Agricultural Land*, Wiley, 201-230.

Oldfield, F. (1991) Environmental magnetism - A personal perspective. *Quaternary Science Reviews*, **10**, 73-85.

Oldfield, F., Darnley, I., Yates, G., France, D.E. and Hilton, J. (1992) Storage diagenesis versus sulphide authigenesis: possible implications in environmental magnetism. *Journal of Palaeolimnology*, **7**, 179-189.

Oldfield, F., Richardson, N., Appleby, P.G. and Yu, L. (1993) ^{241}Am and ^{137}Cs activity in fine grained saltmarsh sediments from parts of the N.E. Irish sea shoreline. *Journal of Environmental Radioactivity*, **19**(1), 1-24.

Oldfield, F., and Yu, L., (1994) The influence of particle size variations on the magnetic properties of sediments from the north-eastern Irish Sea, *Sedimentology*, **41**, 1093-1108.

Oldfield, F. (1999a) Environmental magnetism; the range of applications, In: Walden, J., Oldfield, F., and Smith, J.P., (Editors), *Environmental Magnetism: A Practical Guide*, Quaternary Research Association, London. Technical Guide No. 6, 212-222.

Oldfield, F. (1999b) The rock magnetic identification of magnetic mineral and grain size assemblages, In: Walden, J., Oldfield, F., and Smith, J.P., (Editors), *Environmental Magnetism: A Practical Guide*, Quaternary Research Association, Technical Guide No. 6, 98-112.

Oldfield, F. (2007) Sources of fine-grained magnetic minerals in sediments: a problem revisited. *The Holocene*, **17**(8), 1265-1271.

Oosterlee, A., Drijver, M., Lebret, E. and Brunekreef, B. (1996) Chronic respiratory symptoms in children and adults living along streets with high traffic density. *Occupational and Environmental Medicine*. **53**(4), 241-247.

O'Reilly, W. (1976) Magnetic Minerals in the crust of the Earth, *Reports of Progress in Physics*, **39**, 857-908.

O'Reilly, W. (1984) *Rock and Mineral Magnetism*, Blackie, Glasgow.

Ovrevik, J. and Schwarze, P.E. (2006) Chemical composition and not only total surface area is important for the effects of ultrafine particles. *Mutation Research/Fundamental and Molecular Mechanisms of Mutagenesis*, **594**(1–2), 201-202.

Parekh, P.P., Khwaja, H.A., Khan, A.R., Naqvi, R.R., Malik, A., Shah, S.A., Khan, K. and Hussain, G. (2001) Ambient air quality of two metropolitan cities of Pakistan and its health implications. *Atmospheric Environment,* **35**, 5971-5978.

Patashnick, H. and Rupprecht, E.G. (1991) Continuous PM_{10} Measurements Using the Tapered Element Oscillating Microbalance. *Journal of the Air and Waste Management Association*, **41**,(8).

Perera, F.P. (2008) Children are likely to suffer from our fossil fuel addiction. *Environmental Health Perspectives*, **116**(8) 987-990.

Perry, C. and Taylor, K. (2007) *Environmental Sedimentology*. Blackwell Publishing, Oxford.

Peters, N.E., Meyers, T.P., Aulenbach, B.T. (2002) Status and trends in atmospheric deposition and emissions near Atlanta, Georgia, 1986–99. *Atmospheric Environment*, **36**(10) 1577-1588,

Petrovský, E., Kapička, A., Jordanova, N., Knab, M. and Hoffmann, V. (2000) Low-field magnetic susceptibility: a proxy method of estimating increased pollution of different environmental systems. *Environmental Geology*, **39**(3), 312-318.

Petrovský, E. and Ellwood, B.B. (1999) Magnetic monitoring of air-land and water-pollution. In: B.A. Maher and R. Thompson (Editors), *Quaternary Climates, Environments and Magnetism*, Cambridge University Press.

Phalen, R. F. (2002) *The Particulate Air Pollution Controversy: A Case Study and Lessons Learned*. Kluwer Academic Publishers. Boston. 81–94.

Pope, C. A., Thun, M., Namboodiri, M., Dockery, D., Evans, J., Speizer, F., and Heath, C. (1995) Particulate air pollution as a predictor of mortality in a prospective study of U.S. adults. *American Journal Respiratory Critical Care Medicine*, **151**,669 -674.

Pope, C.A. and Dockery, D.W. (2006) Health effects of fine particulate air pollution: Lines that connect. *Journal of Air and Waste Management Association*. **56,** 709-742.

Power, A.,L., Worsley, A.,T., Booth, C., A. and Farr, K.,M. (2006) Preliminary insights into magneto-biomonitoring (*Tilia europaea* and *Acer pseudoplatanus*) as an alternative roadside particulate air pollution technology. *Air Pollution XIV*, **86**, 525-534.

Pye, K., Blott, S.J., Croft, D.J. and Witton, S.J. (2007) Discrimination between sediment and soil samples for forensic purposes using elemental data: An investigation of particle size effects. *Forensic Science International*, **167**, 30-42.

QUARG (1996) *Airborne Particulate Matter in the United Kingdom*. Third Report of the Quality of Urban Air Review Group. Institute of Public and Environmental Health, University of Birmingham. May 1996.

Raabe, O.G. and Yeh, H. (1976) Principles for inhalation exposure systems using concurrent flow spirometry. *Journal of Aerosol Science*, **7**(3), 233-238.

Rae, J. E. (1997) Trace metals in deposited intertidal sediments. In: Jickells T. D and Rae, J.E. (Editors), *Biogeochemistry of Intertidal Sediments,* Cambridge Environmental Chemistry Series 9, Cambridge University Press, Cambridge.

Ricci, P.F., Catalano, J.A., Kelsh, M.D. (1996) Time series (1963–1991) of mortality and ambient air pollution in California: an assessment with annual data. *Inhalation Toxicology,* **9**, 95–106.

Riddle, S.G., Jakober, C.A., Robert, M.A., Cahill, T.M., Charles, M.J. and Kleeman, M.J. (2007) Large PAHs detected in fine particulate matter emitted from light-duty gasoline vehicles. *Atmospheric Environment*, **41**(38), 8658-8668.

Robertson, D.J., Taylor, K.G. and Hoon, S.R. (2003) Geochemical and mineral magnetic characterisation of urban sediment particulates, Manchester, UK. *Applied Geochemistry*, **18**, 269-282.

Robinson M, Boardman J, Evans R, Heppell K, Packman J, Leeks G. (2000) Land use change. In: Acreman M, (editor). The Hydrology of the UK. Routledge Publishers, London. 30– 54.

Rose, N.L., Boyle, J.F., Du, Y., Yi, C., Dai, X., Appleby, P.G., Bennion, H., Cai, S. and Yu, L. (2004) Sedimentary evidence for changes in the pollution status of Taihu in the Jiangsu region of eastern China. *Journal of Paleolimnology*. **32**, 41-51.

Ryu, H. J. and Saito, F. (1991) Single particle crushing of nonmetallic inorganic brittle materials. *Solid State Ionics*, **47**,(1-2), 35-50.

Sadovska, V. (2012) Health risk assessment of heavy metals absorbed in particulates. *World Academy of Science: Engineering and Technology*, **68**, 211-214.

Sagai, M. and Ichinose, T. (1994) Asthma and lung cancer by diesel exhaust. *Japanese Journal of Toxicology and Environmental Health.* **40**(5), 399-413.

Sagnotti, L., Macrì, P., Egil, R. and Mondolino, M. (2006) Magnetic properties of atmospheric particulate matter from automatic air sampler stations in Latium (Italy): toward a definition of magnetic fingerprints for natural and anthropogenic PM_{10} sources. *Journal of Geophysical Research*. **111**.

Salvi, S., Blomberg, A., Rudell, B., Kelly, F., Sandström, T., Holgate, S.T. and Frew, A. (1999) Acute inflammatory responses in the airways and peripheral blood after short-term exposure to diesel exhaust in healthy human volunteers. *American Journal of Respiratory and Critical Care Medicine*, **159**, 702-709.

Sandström, T. (1995) Respiratory effects of air pollutants: experimental studies in humans. *European Respiratory Journal*, **8**, 976–995.

Saragnese, F., Lanci, L. and Lanza, R. (2011) Nanometric-sized atmospheric particulate studies by magnetic analyses. *Atmospheric Environment*, **45**, 450-459.

Schmeling, M. (2004) Characterization of urban air pollution by total reflection X-ray fluorescence, Spectrochimica Acta Part B. *Atomic Spectroscopy*, **59**(8), 1165-1171.

Schmidt, A., Yarnold, R., Hill, M. and Ashmore, M. (2005) Magnetic susceptibility as proxy for heavy metal pollution: a site study. *Journal of Geochemical Exploration*, **85**, 109-117.

Schneeweiss, H., and Mathes, H. (1995) Factor analysis and principal components, *Journal of Multivariate Analysis*, **55**, 105-124.

Schwar, M.J.R., Moorcroft, J.S., Laxen, D.P.H., Thompson, M. and Armorgie, C. (1988) Baseline metal-in-dust concentrations in Greater London. *Science of The Total Environment*, **68**, 25-43.

Schwartz, J., Dockery, D. W. and Neas, L. M. (1996) Is daily mortality associated specifically with fine particles? Journal of Air and Waste Management Association, **46,** 927-939.

Schwartz, J. (2004) Air pollution and children's health. *Pediatrics*, **113**, 1037-1043.

Schwarze, P.E., Hetland, R.B., Refsnes, M., Låg, M. and Becher, R. (2002) Mineral composition other than quartz is a critical determinant of the particle inflammatory potential. *International Journal of Hygiene and Environmental Health*, **204**(5-6), 327-331.

Seaton, A., Macnee, W., Donaldson, K. and Godden, D. (1995) Particulate pollution and acute health effects. *The Lancet*, **345**, 176-178.

Seinfeld, J. and Pandis, H. (1998) *Atmospheric Chemistry and Physics: From Air Pollution to Climate Change.* New York: J Wiley.

Seinfeld, J.H. and Pandis, S.N. (2006) *Atmospheric Chemistry and Physics. From Air Pollution to Climate Change*. Second edition, Wiley-Interscience Publication, John Wiley & Sons, New York.

Shah, M.H., Shaheen, N., Jaffar, M. and Saqib, M. (2004) Distribution of lead in relation to size of airborne particulate matter in Islamabad, Pakistan. *Journal of Environmental Management*, **70**(2), 95-100.

Shah, M.H. and Shaheen, N. (2007) Statistical analysis of atmospheric trace metals and particulate fractions in Islamabad, Pakistan. *Journal of Hazardous Materials*, **147**(3), 759-767.

Shaw, G., and Wheeler, D. (1985) *Statistical Techniques in Geographical Analysis*, Wiley.

Sheng-Gao, L., Shi-Qiang, B. and Li-Xia, F. (2008) Magnetic properties as indicators of Cu and Zn contamination in soils. *Pedosphere*, **18**(4), 479-485.

Shi, G., Chen, Z., Xu, S., Zhang, J., Wang, L., Bi, C. and Teng, J. (2008) Potentially toxic metal contamination of urban soils and roadside dust in Shanghai, China. *Environmental Pollution*, **156**(2), 251-260.

Shilton, V.F., Booth, C.A., Smith, J.P., Giess, P., Mitchell, D.J. and Williams, C. (2005) Magnetic properties of urban street dust and their relationship with organicmatter content in the West Midlands, UK. *Atmospheric Environment*, **39**(20), 3651-3659.

Shilton, V.F., Booth, C.A., Fullen, M.A., Walden, J., Worsley, A.T. and Power, A.L. (2006) Environmental magnetism: measuring, monitoring and modelling urban street dust pollution. *Air Pollution*, **86**, 333-342.

Shu, J., Dearing, J.A., Morse, A.P., Yu, L. and Yuan, N. (2001) Determining the sources of atmospheric particles in Shanghai, China, from magnetic and geochemical properties. *Atmospheric Environment*, **35**(15), 2615-2625.

Skaug, V. (2001) *Exposure to particles and lung disease*. Occupational exposure limits – approaches and criteria. Proceedings from a NIVA course held in Uppsala, Sweden, 24-28 September 2001.

Smith, J.P. (1999) An introduction to the magnetic properties of natural materials, In: Walden, J., Oldfield, F., and Smith, J.P., (Editors) *Environmental Magnetism: A Practical Guide*, Quaternary Research Association, London. Technical Guide No. 6, 5-25.

Smith, S., Stribley, F.T., Milligan, P. and Barratt, B. (2001) Factors influencing measurements of PM_{10} during 1995–1997 in London. *Atmospheric Environment*, **35**(27), 4651-4662.

Snowball, I.F. and Thompson, R. (1988) The occurrence of greigite in sediments from Loch Lomond. *Journal of Quaternary Science*, **3**, 121-125.

Snowball, I.F. (1994) Bacterial magnetite and the magnetic properties of sediments in a Swedish lake. *Earth and Planetary Science Letters*, **126**(1-3), 129-142.

Solomon, C., Poole, J., Jarup, L., Palmer, K. and Coggon, D. (2003) Cardio-respiratory and long-term exposure to particulate air pollution. *International Journal of environmental Health Research*, **13**(4), 327-335.

Sørensen, M., Autrup, H., Møller, P., Hertel, O., Jensen, S. S., Vinzents, P., Knudsen, L. E. and Loft, S. (2003) Linking exposure to environmental pollutants with biological effects. *Mutation Research,* **544,** 255-271.

Stacey, F.D., and Banerjee, S.K. (1974) *The Physical Principles of Rock Magnetism*, Elsevier, Amsterdam.

Stein, F., Esmen, N.A. and Corn, M. (1969) The shape of atmospheric particles in Pittsburg air. *Atmospheric Environment,* **3**, 443-453.

Sternbeck, J., Sjödin, Å. and Andréasson, K. (2002) Metal emission from road traffic and the influence of resuspension – results from two tunnel studies. *Atmospheric Environment,* **36,** 4735-4744.

Stuttard, R. (1994) *Data Collection, Presentation, Exploration and Analysis*. Third Edition, Erithacus Press, Wolverhampton.

Sutherland, R.A. and Tolosa, C.A. (2000) Multi-element analysis of road-deposited sediment in an urban drainage basin, Honolulu, Hawaii. *Environmental Pollution*, **110**(3), 483-495.

Syvitski, J. P. M. (1991) *Principles, Methods and Application of Particle Size Analysis.* Cambridge: Cambridge University Press.

Szava-Kovats, R.C. (2002) Outlier-resistant errors-in-variables regression: anomaly recognition and grain-size correction in stream sediments. *Applied Geochemistry*, **17**, 1149– 57.

Tahri, M., Benyaich, M., Bounakhla, E., Bilal, E., Gruffat, J., Moutte, J. and Garcia, D. (2005) Multivariate analysis of heavy metal contents in soils. Sediments and water in the region of Meknes (central Morocco). *Environmental Monitoring and Assessment*, **102**, 405-417.

Tanner, P.A., Ma, H., Yu, P.K.N. (2008) Fingerprinting metals in urban street dust of Beijing, Shanghai, and Hong Kong. *Environmental Science & Technology,* 42.

Taylor, P.I., Nusbaum, R.L., Fronabarger, A.K., Katuna, M.P. and Summer, N. (1996) Magnetic sediments in coastal plain sediments, Sullivan's Island, South Carolina, USA. *Meteoritics and Planetary Science,* **31**, 77-80

Taylor, K.G. and Robertson, D.J. (2009) Electron microbeam analysis of urban road-deposited sediment, Manchester, UK: Improved source discrimination and metal speciation assessment. *Applied Geochemistry*, **24**(7), 1261-1269.

Temple, J.T. (1978) The use of factor analysis in Geology, *Mathematical Geology*, **10**, 379-387.

Tessier A, Cambell PGC and Bisson, M. (1979), Sequential extraction procedure for the speciation of particulate trace metals. *Analytical Chemistry*, **51**, 844-851.

Thorpe, A. and Harrison, R.M. (2008) Sources and properties of non-exhaust particulate matter from road traffic: A review. *Science of The Total Environment*, **400**(1–3), Pages 270-282.

Thompson, R., Bloemendal, J., Dearing, J.A., Oldfield, F., Rummery, T.A., Stober, J.C. and Turner, G.M. (1980) Environmental applications of magnetic minerals. *Science*, **207**, 481-485.

Thompson, R. and Oldfield, F. (1986) *Environmental Magnetism.* London: Allen & Unwin.

Tokahoğlu, Ş. and Kartal, Ş. (2006) Multivariate analysis of the data and speciation of heavy metals in street dust samples from the organized industrial district in Kayseri (Turkey), *Atmospheric Environment*, **40**, 2797-2805.

Tomlin, C.D. (1990) *Geographic Information Systems and Cartographic Modelling*, Prentice-Hall, New Jersey, 249.

Trang T.T. Duong, Byeong-Kyu Lee. (2011) Determining contamination level of heavy metals in road dust from busy traffic areas with different characteristics. *Journal of Environmental Management*, **92** (3), 554-562.

Tucker, M. (1991) *Techniques in Sedimentology.* Oxford: Blackwell Scientific Publications.

Tukey, J.W. (1977) *Exploratory Data Analysis*, Reading, Mass., Addison-Wesley Publishing.

UK National Air Quality Archive (2007) UK-AIR: information resource [online]. London: DEFRA. Available at: <http://uk-air.defra.gov.uk/>

UK National Air Quality Archive (2012) Daily air quality index [online]. London: DEFRA. Available at: <http://uk-air.defra.gov.uk/ air-pollution/daqi>

Vardoulakis, S. and Kassomenos, P. (2008) Sources and factors affecting PM_{10} levels in two European cities: Implications for local air quality management. *Atmospheric Environment*, **42**(17), 3949-3963.

Veritas, B. (2008) *Automatic urban and rural network (AURN) site*. Department for Environment, Food and Rural Affairs, London.

Versteeg, J.K., Morris, W.A., Rukavina, N.A. (1995) The Utility of Magnetic Properties as a Proxy for Mapping Contamination in Hamilton Harbour Sediment. *Journal of Great Lakes Research*, **21**(1), 71-83.

Virtanen, A.K., Ristimaki, J., Keskinen, J. and Lappi, M.K. (2002): *Effective density of diesel exhaust particles as a function of size*. SAE 2002 World Congress & Exhibition, Detroit, MI, USA.

Walden, J. (1990) *The use of magnetic analysis in the study of glacial diamicts*, Unpublished Ph.D. thesis, University of Wolverhampton.

Walden, J., Smith, J.P. and Dackombe, R.V. (1992) The use of simultaneous R- and Q-mode factor analysis as a tool for assisting interpretation of mineral magnetic data. *Mathematical Geology*, **24**(3), 227-247.

Walden, J., and Smith, J.P. (1995) Factor analysis: a practical application, *In*: Maddy,D., & Brew, J.S., (Editors): *Statistical Modelling of Quaternary Science Data*, Technical Guide Series No. 5, Quaternary Research Association, Cambridge, 39-64.

Walden, J. , Slattery, M. C., Burt, T. P. (1997) Use of mineral magnetic measurements to fingerprint suspended sediment sources: approaches and techniques for data analysis. *Journal of Hydrology,* **202**, 353-372.

Walden, J., Oldfield, F. and Smith, J. P. (1999) *Environmental Magnetism: A Practical Guide.* Quaternary Research Association, London.

Wang, J., Xie, Z., Zhang, Y., Shao, M., Zeng, L., Cheng, C., Xu, X., Zhao, X. and Meng, Y. (2004) Study on the characteristics of mass concentration of atmospheric fine particles in Beijing. *Acta Meteorologica Sinica,* **62**(1), 104–111.

Wang, X. S. and Qin, Y. (2006) Comparison of magnetic parameters with vehicular Br levels in urban roadside soils. *Environmental Geology*, **50**,787–791.

Wang, G., Oldfield, F., Xia, D., Chen, F., Liu, X. and Zhang, W. (2012) Magnetic properties and correlation with heavy metals in urban street dust: A case study from the city of Lanzhou, China. *Atmospheric Environment*, **46**, 289-298.

Watson, J.G., Chow, J.C., Lu, Z., Fujita, E.M., Lowenthal, D.H., Lawson, D.R. and Ashbaugh, L.L. (1994) Chemical mass balance source apportionment of PM_{10} during the Southern California Air Quality Study. *Aerosol Science and Technology*, **21**, 1-36.

Webb, B.W., (Editor), (1995) *Sediment and Water Quality in River Catchments*, John Wiley & Sons, Chichester. 353-362.

West Midlands Air Quality Group (2007) Air Quality [online]. Birmingham: Birmingham City Council. Available at: < http://www.wmair.org/>

Wessa, P. (2011) Notched Boxplots (v1.0.5) in Free Statistics Software (v1.1.23-r7), Office for Research Development and Education. Leuven: Available at <http://www.wessa.net/rwasp_notchedbox1.wasp/>

Williams, S.C., Simpson, H.J., Olsen, C.R. and Bopp, R.F. (1978) Sources of heavy metals in sediments of the Hudson River Estuary. *Maritime Chemistry*, **6**, 195–213.

World Health Organization (WHO) (2007) Health risks of heavy metals from long-range transboundary air pollution. Copenhagen. WHO.

World Health Organization (WHO) (2007) *The WHO's fight against cancer, strategies to prevent cure and care.* [online]. Switzerland: WHO. [Assessed 8 November 2007]. Available at <http://www.who.int/cancer/.../whocancerbrochure2007.finalweb.pdf>.

Wilkinson, P., Elliott, P., Grundy, C., Shaddick, G., Thakar, B., Wallis, P. and Falconer, S. (1999) Case-control study of hospital admission with asthma in children aged 5-14years: relation with road traffic in north west London. *Thorak*, **54**, 1070-1074.

Wilson, W.E. and Suh, H.H. (1997): Fine particles and coarse particles: concentration relationships relevant to epidemiologic studies. *Journal of Air and Waste Management Association*, **47,** 1238-1249.

Wilson, J.G., Kingham, S., Pearce, J. and Sturman, A.P. (2005) A review of intraurban variations in particulate air pollution: Implications for epidemiological research. *Atmospheric Environment*, **39**, 6444-6462.

Wolfgang, R.F., Hidemann, L.M., Mazurek, M.A. and Cass, G.R. (1993) Sources of fine organic aerosol iii: road dust, tyre debris, and organometallic brake lining dust: roads as sources and sinks. *Environmental Science and Technology*. **27**, 1892-1904

Wolman, M.G. (1967) A cycle of sedimentation and erosion in urban river channels. *Geografiska Annaler* **49**, 385–395.

Wolman, M.G., 1975. Erosion in the urban environment. Hyd*rological Sciences Bulletin*, **20**(1), 117–125.

Wu, Y., Fang, G., Chen, J., Lin, C., Huang, S., Rau, J. and Lin, J. (2006) Ambient air particulate dry deposition, concentrations and metallic elements at Taichung Harbor near Taiwan Strait. *Atmospheric Research*, **79**(1), 52-66.

Xie, S., Dearing, J.A., Bloemendal, J. and Boyle, J.F. (1999a) Association between the organic matter content and magnetic properties in street dust, Liverpool, UK. *Science of The Total Environment*, **241**(1-3), 205-214.

Xie, S., Dearing, J., A. and Bloemendal, J. (1999b) A partial susceptibility approach to analysing the magnetic properties of environmental materials: a case study. *Geophysics Journal International*, **138**, 851-856.

Xie, S., Dearing, J.A. and Bloemendal, J. (2000) The organic matter content of street dust in Liverpool, UK, and its association with dust magnetic properties. *Atmospheric Environment*, **34**(2), 269-275.

Xie, S., Dearing, J.A., Boyle, J.F., Bloemendal, J. and Morse, A.P. (2001) Association between magnetic properties and element concentrations of Liverpool street dust and its implications. *Journal of Applied Geophysics*, **48**(2), 83-92.

Yang, T., Liu, Q.S., Chan, L.S. and Gao, G.D. (2007) Magnetic investigation of heavy metals contamination in urban topsoils around the East Lake, Wuhan, China. *Geophysics Journal International*, **171**, 603-612.

Yang, T., Liu, Q., Li, H., Zeng, Q. and Chan, L. (2010) Anthropogenic magnetic particles and heavy metals in the road dust: Magnetic identification and its implications. *Atmospheric Environment*, **44**(9), 1175-1185.

Yin, J., Allen, A.G., Harrison, R.M., Jennings, S.G., Wright, E., Fitzpatrick, M., Healy, T., Barry, E., Ceburnis, D. and McCusker, D. (2005) Major component composition of urban PM10 and PM2.5 in Ireland. *Atmospheric Research*, **78**(3-4), 149-165.

Yu, M. (2001) Environmental Toxicology: Impact of Environmental Toxicants on Living Systems, Boca Raton: CRS Press LLC

Zanobetti, A. and Schwartz, J. (2007) Particulate air pollution, progression and survival after myocardial infarction. *Environmental Health Perspectives*. **115**(5), 769-775.

Zhang, W., Yu, L., Lu, M., Hutchinson, S.M. and Feng, H. (2007) Magnetic approach to normalizing heavy metal concentrations for particle size effects in intertidal sediments in the Yangtze Estuary, China. *Environmental Pollution*, **147**(1), 238-244.

Zhang, C. Qiao, Q. Appel, E. Huang, B. (2012) Discriminating sources of anthropogenic heavy metals in urban street dusts using magnetic and chemical methods. *Journal of Geochemical Exploration*, **119–120**, 60-75,

Zhao, X., Zhang, X., Xu, X., Xu, J., Meng, W. and Pu, W. (2009) Seasonal and diurnal variations of ambient PM2.5 concentration in urban and rural environments in Beijing. *Atmospheric Environment,* **43**, 2893–2900.

Zhao, H., Li, X., Wang, X. and Tian, D. (2010) Grain size distribution of road-deposited sediment and its contribution to heavy metal pollution in urban runoff in Beijing, China. *Journal of Hazardous Materials*, **183**(1–3), 203-210.

Zheng, L., Hopke, P.K., Husain, L., Qureshi, S., Dutkiewicz, V.A., Schwab, J.J., Drewnick, F. and Demerjian, K.L. (2004) Sources of fine particle composition in New York city. *Atmospheric Environment*, **38**, 6521-6529.

Zheng, Y. and Zhang, S. (2008) Magnetic properties of street dust and topsoil in Beijing and its environmental implications. *Chinese Science Bulletin,* **53**, 408-417.

Zheng, X., Chen, D., Liu, X., Zhou, Q., Liu, Y., Yang, W. and Jiang, G. (2010) Spatial and seasonal variations of organochlorine compounds in air on an urban–rural transect across Tianjin, China. *Chemosphere*, **78**(2), Pages 92-98.

Zheng, Y., Luo, X., Zhang, W., Wu, B., Han, F., Lin, Z. and Wang, X. (2012) Enrichment behaviour and transport mechanism of soil-bound PAHs during rainfall-runoff events. *Environmental Pollution*, **171**, 85-92.

Zhou, D., Chang, T., and Davis, J.C. (1983) Dual extraction of R-mode and Q-mode factor solutions, *Mathematical Geology*, **15**, 581-606.

Zoppou, C. (2001) Review of urban storm water models. *Environmental Modelling & amp; Software*, **16**(3), 195-231.